ELSEVIER

World Journal of Gastroenterology®

Supported by NSFC 2005-2006

Volume 11 Number 16
April 28, 2005

National Journal Award 2005

Contents

World Journal of Gastroenterology®
Volume 11 **Number** 16 **April** 28, 2005

Contents

World Journal of Gastroenterology®
Volume 11 **Number** 16 **April** 28, 2005

Contents

Editorial Coordinator for this issue: Umayal Rajarathinam

World Journal of Gastroenterology (*World J Gastroenterol , WJG*), a leading international journal in gastroenterology and hepatology, has an established reputation for publishing first class research on esophageal cancer, gastric cancer, liver cancer, viral hepatitis, colorectal cancer, and *Helicobacter pylori* infection, providing a forum for both clinicians and scientists, and has been indexed and abstracted in Index Medicus, MEDLINE, PubMed, Chemical Abstracts, EMBASE, Abstracts Journals, Nature Clinical Practice Gastroenterology and Hepatology, CAB Abstracts and Global Health. Impact factor of ISI JCR during 2000-2003 is 0.993, 1.445, 2.532 and 3.318 respectively. *WJG* is a weekly journal published jointly by The *WJG* Press and Elsevier Inc. The publication date is on 7th, 14th, 21st, and 28th every month. The *WJG* is supported by The National Natural Science Foundation of China, No. 30224801 and No.30424812, which was founded with a name of *China National Journal of New Gastroenterology* on October 1,1995, and renamed as *WJG* on January 25, 1998.

PUBLISHED JOINTLY BY
The WJG Press and Elsevier Inc

PRINTING GROUP
Printed in Beijing on acid-free paper by Beijing Kexin Printing House

 Print ISSN 1007-9327
CN 14-1219/R.

SPECIAL STATEMENT
All articles published in this journal represent the viewpoints of the authors except where indicated otherwise.

EDITORIAL OFFICE
Editor: *World Journal of Gastroenterology*,
The WJG Press, Apartment 1066 Yishou Garden, 58 North Langxinzhuang Road, PO Box 2345, Beijing 100023, China
Telephone: +86-(0)10-85381901-1023
Fax:+86-10-85381893
E-mail: wjg@wjgnet.com
http://www.wjgnet.com

Public Relationship Manager
Shi-Yu Guo
The WJG Press, Apartment 1066 Yishou Garden, 58 North Langxinzhuang Road, PO Box 2345, Beijing 100023, China
Telephone: +86-(0)10-85381901-1023
Fax: +86-10-8538 1893
E-mail: s.y.guo@wjgnet.com
http://www.wjgnet.com

SUBSCRIPTION INFORMATION
Foreign
Elsevier (Singapore) Pte Ltd, 3 Killiney Road #08-01, Winsland House I, Singapore 239519
Telephone: +65-6349 0200
Fax: +65-6733 1817
E-mail: r.garcia@elsevier.com
http://asia.elsevierhealth.com
Institutional Rates Print-2005 rates: USD1 500.00
Personal Rates Print-2005 rates: USD700.00

Domestic
Local Post Offices Code No. BM 82-261

Author Reprints and Commercial Reprints
The WJG Press, Apartment 1066 Yishou Garden, 58 North Langxinzhuang Road, PO Box 2345, Beijing 100023, China
Telephone: +86-(0)10-85381901-1023
Fax:+86-10-85381893
E-mail: wjg@wjgnet.com
http://www.wjgnet.com

ADVERTISING
Rosalia Da Carcia
Elsevier Science
Journals Marketing & Society Relations Health Science Asia
3 Killiney Road #08-01, Winsland House 1
Singapore 239519
Telephone: +65-6349 0200
Fax +65- 6733 1817
E-mail: r.garcia@elsevier.com
http://asia.elsevierhealth.com

INSTRUCTIONS TO AUTHORS
Full instructions are available online at http://www.wjgnet.com/wjg/help/instructions.jsp If you do not have web access please contact the editorial office.

World Journal of Gastroenterology®

Editorial Board

2004-2006

Published by The WJG Press and Elsevier Inc., PO Box 2345, Beijing 100023, China
Fax: +86-(0)10-85381893 E-mail: wjg@wjgnet.com http://www.wjgnet.com

Bulgaria
Zahariy Alexandrov Krastev, *Sofia*

Canada
Wang-Xue Chen, *Ottawa*
Richard N Fedorak, *Edmonton*
Hugh James Freeman, *Vancouver*
Samuel S Lee, *Calgary*
Philip Martin Sherman, *Toronto*
Alan BR Thomson, *Edmonton*
Eric M Yoshida, *Vancouver*

China
Francis KL Chan, *Hong Kong*
Xiao-Ping Chen, *Wuhan*
Jun Cheng, *Beijing*
Chi-Hin Cho, *Hong Kong*
Zong-Jie Cui, *Beijing*
Da-Jun Deng, *Beijing*
Er-Dan Dong, *Beijing*
Sheung-Tat Fan, *Hong Kong*
Xue-Gong Fan, *Changsha*
Jin Gu, *Beijing*
De-Wu Han, *Taiyuan*
Shao-Heng He, *Shantou*
Fu-Lian Hu, *Beijing*
Wayne HC Hu, *Hong Kong*
Ching Lung Lai, *Hong Kong*
Kam Chuen Lai, *Hong Kong*
Wai-Keung Leung, *Hong Kong*
Zhi-Hua Liu, *Beijing*
Ai- Ping Lu, *Beijing*
Jing-Yun Ma, *Beijing*
Lun-Xiu Qin, *Shanghai*
Yu-Gang Song, *Guangzhou*
Peng Shang, *Xi'an*
Qin Su, *Beijing*
Yuan Wang, *Shanghai*
Benjamin Wong, *Hong Kong*
Wai-Man Wong, *Hong Kong*
Hong Xiao, *Shanghai*
Dong-Liang Yang, *Wuhan*
Xue-Biao Yao, *Hefei*
Yuan Yuan, *Shenyang*
Man-Fung Yuen, *Hong Kong*
Jian-Zhong Zhang, *Beijing*
Zhi-Rong Zhang, *Chengdu*
Xiao-Hang Zhao, *Beijing*
Shu Zheng, *Hangzhou*

Costa Rica
Edgar M Izquierdo, *San José*

Croatia
Marko Duvnjak, *Zagreb*

Denmark
Flemming Burcharth, *Herlev*
Peter Bytzer, *Copenhagen*
Hans Gregersen, *Aalborg*
Jens H Henriksen, *Hvidovre*
Fin Stolze Larsen, *Copenhagen*
Søren Møller, *Hvidovre*

Egypt
Abdel-Rahman El-Zayadi, *Giza*

Finland
Pentti Sipponen, *Espoo*

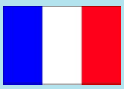

France
Charles Paul Balabaud, *Bordeaux*
Jacques Belghiti, *Clichy*
Pierre Brissot, *Rennes*
Franck Carbonnel, *Besancon*
Bruno Clément, *Rennes*
Jacques Cosnes, *Paris*
Francoise Degos, *Clichy*
Francoise Lunel Fabian, *Angers*
Gérard Feldmann, *Paris*
Jean Fioramonti, *Toulouse*
Rene Lambert, *Lyon*
Didier Lebrec, *Clichy*
Francis Mégraud, *Bordeaux*
Richard Moreau, *Clichy*
Jose Sahel, *Marseille*
Jean-Yves Scoazec, *Lyon*
Jean-Pierre Henri Zarski, *Grenoble*

Germany
HD Allescher, *Garmisch-Partenkirchen*
Rudolf Arnold, *Marburg*
Hubert Blum, *Freiburg*
Peter Born, *Muchen*
Heinz J Buhr, *Berlin*
Haussinger Dieter, *Düsseldorf*
Dietrich CF, *Bad Mergentheim*
Wolfram W Domschke, *Muenster*
Ulrich Robert Fölsch, *Kiel*
Peter R Galle, *Mainz*
Burkhard Göke, *Munich*
Axel M Gressner, *Aachen*
Eckhart Georg Hahn, *Erlangen*
Werner Hohenberger, *Erlangen*
RG Jakobs, *Ludwigshafen*
Joachim Labenz, *Siegen*
Ansgar W Lohse, *Hamburg*
Peter Malfertheiner, *Magdeburg*
Andrea Dinah May, *Wiesbaden*
Stephan Miehlke, *Dresden*
Gustav Paumgartner, *Munich*
Ulrich Ks Peitz, *Magdeburg*
Giuliano Ramadori, *Göttingen*
Tilman Sauerbruch, *Bonn*
Hans Seifert, *Oldenburg*
J Ruediger Siewert, *Munich*
Manfred V Singer, *Mannheim*
Jurgen M Stein, *Frankfurt*
Manfred Stolte, *Bayreuth*
Wolfgang R Stremmel, *Heidelberg*
Hans Ludger Tillmann, *Leipzig*
Siegfried Wagner, *Deggendorf*
Bertram Wiedenmann, *Berlin*

Greece
Arvanitakis C, *Thessaloniki*
Elias A Kouroumalis, *Heraklion*

Hungary
Simon A László, *Szekszárd*
János Papp, *Budapest*

Iceland
Hallgrimur Gudjonsson, *Reykjavik*

India
Sujit Kumar Bhattacharya, *Kolkata*
Chawla YK, *Chandigarh*
Radha Dhiman K, *Chandigarh*
Sri Prakash Misra, *Allahabad*
Kartar Singh, *Lucknow*

Iran
Reza Malekzadeh, *Tehran*

Israel
Abraham Rami Eliakim, *Haifa*
Yaron Niv, *Pardesia*

Italy
Giovanni Addolorato, *Roma*
Alfredo Alberti, *Padova*
Annese V, *San Giovanni Rotondo*
Giovanni Barbara, *Bologna*
Gabrio Bassotti, *Perugia*
Franco Bazzoli, *Bologna*
Adolfo Francesco Attili, *Roma*
Antomio Benedetti, *Ancona*
Giovanni Cammarota, *Roma*
Antonino Cavallari, *Bologna*
Dario Conte, *Milano*
Gino Roberto Corazza, *Pavia*
Guido Costamagua, *Roma*
Antonio Craxi, *Palermo*
Fabio Farinati, *Padua*
Giovanni Gasbarrini, *Roma*
Paolo Gentilini, *Florence*
Edoardo G Giannini, *Genoa*

Paolo Gionchetti, *Bologna*
Roberto De Giorgio, Bologna
Mario Guslandi, *Milano*
Giovanni Maconi, *Milan*
Giulio Marchesini, *Bologna*
Giuseppe Montalto, *Palermo*
Luisi Pagliaro, *Palermo*
Fabrizio R Parente, *Milan*
Perri F, *San Giovanni Rotondo*
Raffaele Pezzilli, *Bologna*
Pilotto A, *San Giovanni Rotondo*
Massimo Pinzani, *Firenze*
Gabriele Bianchi Porro, *Milano*
Piero Portincasa, *Bari*
Giacomo Laffi, *Firenze*
Enrico Roda, *Bologna*
Massimo Rugge, *Padova*
Vincenzo Savarino, *Genova*
Vincenzo Stanghellini, *Bologna*
Calogero Surrenti, *Florence*
Roberto Testa, *Genoa*
Dino Vaira, *Bologna*

Japan

Kyoichi Adachi, *Izumo*
Takashi Aikou, *Kagoshima*
Taiji Akamatsu, *Matsumoto*
Takafumi Ando, *Nagoya*
Akira Andoh, *Otsu*
Taku Aoki, *Tokyo*
Masahiro Arai, *Tokyo*
Tetsuo Arakawa, *Osaka*
Yasuji Arase, *Tokyo*
Masahiro Asaka, *Sapporo*
Hitoshi Asakura, *Tokyo*
Yutaka Atomi, *Tokyo*
Takeshi Azuma, *Fukui*
Nobuyuki Enomoto, *Yamanashi*
Kazuma Fujimoto, *Saga*
Toshio Fujioka, *Oita*
Yoshihide Fujiyama, *Otsu*
Hiroyuki Hanai, *Hamamatsu*
Kazuhiro Hanazaki, *Nagano*
Naohiko Harada, *Fukuoka*
Makoto Hashizume, *Fukuoka,*
Tetsuo Hayakawa, *Nagoya*
Kazuhide Higuchi, *Osaka*
Ichiro Hirata, *Osaka*
Keiji Hirata, *Kitakyushu*
Takafumi Ichida, *Shizuoka*
Kenji Ikeda, *Tokyo*
Kohzoh Imai, *Sapporo*
Fumio Imazeki, *Chiba*
Masayasu Inoue, *Osaka*
Hiromi Ishibashi, *Nagasaki*
Shunji Ishihara, *Izumo*
Toru Ishikawa, *Niigata*
Kei Ito, *Sendai*
Masayoshi Ito, *Tokyo*
Hiroaki Itoh, *Akita*
Hiroshi Kaneko, *Aichi-Gun*
Shuichi Kaneko, *Kanazawa*
Takashi Kanematsu, *Nagasaki*
Junji Kato, *Sapporo*
Mototsugu Kato, *Sapporo*
Shinzo Kato, *Tokyo*
Sunao Kawano, *Osaka*
Yoshikazu Kinoshita, *Izumo*
Masaki Kitajima, *Tokyo*
Tsuneo Kitamura, *Chiba*
Seigo Kitano, *Oita*
Hironori Koga, *Kurume*
Satoshi Kondo, *Sapporo*
Shoji Kubo, *Osaka*
Shigeki Kuriyama, *Kagawa*
Masato Kusunoki, *Mie*
Takashi Maeda, *Fukuoka*
Shin Maeda, *Tokyo*
Osamu Matsui, *Kanazawa*
Yasushi Matsuzaki, *Tsukuba*
Hiroto Miwa, *Hyogo*
Masashi Mizokami, *Nagoya*
Motowo Mizuno, *Hiroshima*
Morito Monden, *Suita*
Hisataka S Moriwaki, *Gifu*
Yoshiharu Motoo, *Kanazawa*
Akihiro Munakata, *Hirosaki*
Kazunari Murakami, *Oita*
Kunihiko Murase, *Tusima*
Masato Nagino, *Nagoya*
Yujl Naito, *Kyoto*
Hisato Nakajima, *Tokyo*
Hiroki Nakamura, *Yamaguchi*
Shotaro Nakamura, *Fukuoka*
Akimasa Nakao, *Nagoya*
Mikio Nishioka, *Niihama*
Susumu Ohmada, *Maebashi*
Masayuki Ohta, *Oita*
Tetsuo Ohta, *Kanazawa*
Susumu Okabe, *Kyoto*
Katsuhisa Omagari, *Nagasaki*
Saburo Onishi, *Nankoku*
Morikazu Onji, *Ehime*
Hiromitsu Saisho, *Chiba*
Hidetsugu Saito, *Tokyo*
Takafumi Saito, *Yamagata*
Isao Sakaida, *Yamaguchi*
Michiie Sakamoto, *Tokyo*
Iwao Sasaki, *Sendai*
Motoko Sasaki, *Kanazawa*
Chifumi Sato, *Tokyo*
Shuichi Seki, *Osaka*
Hiroshi Shimada, *Yokohama*
Mitsuo Shimada, *Tokushima*
Hiroaki Shimizu, *Chiba*
Tooru Shimosegawa, *Sendai*
Tadashi Shimoyama, *Hirosaki*
Ken Shirabe, *Iizuka City*
Yoshio Shirai, *Niigata*
Katsuya Shiraki, *Mie*
Yasushi Shiratori, *Okayama*
Yasuhiko Sugawara, *Tokyo*
Toshiro Sugiyama, *Toyama*
Kazuyuki Suzuki, *Morioka*
Hidekazu Suzuki, *Tokyo*
Tadatoshi Takayama, *Tokyo*
Tadashi Takeda, *Osaka*
Koji Takeuchi, *Kyoto*
Kiichi Tamada, *Tochigi*
Akira Tanaka, *Kyoto*
Eiji Tanaka, *Matsumoto*
Noriaki Tanaka, *Okayama*
Shinji Tanaka, *Hiroshima*
Kyuichi Tanikawa, *Kurume*
Tadashi Terada, *Shizuoka*
Akira Terano, *Shimotsugagun*
Kazunari Tominaga, *Osaka*
Hidenori Toyoda, *Ogaki*
Akihito Tsubota, *Chiba*
Shingo Tsuji, *Osaka*
Takato Ueno, *Kurume*
Shinichi Wada, *Tochigi*
Hiroyuki Watanabe, *Kanazawa*
Sumio Watanabe, *Akita*
Toshio Watanabe, *Osaka*
Yuji Watanabe, *Ehime*
Chun-Yang Wen, *Nagasaki*
Koji Yamaguchi, *Fukuoka*
Takayuki Yamamoto, *Yokkaichi*
Takashi Yao, *Fukuoka*
Hiroshi Yoshida, *Tokyo*
Masashi Yoshida, *Tokyo*
Norimasa Yoshida, *Kyoto*
Kentaro Yoshika, *Toyoake*
Masahide Yoshikawa, *Kashihara*

Lithuania

Sasa Markovic, *Japljeva*

Macedonia

Vladimir Cirko Serafimoski, *Skopje*

Malaysia

Andrew Seng Boon Chua, *Ipoh*
Jayaram Menon, *Sabah*
Khean-Lee Goh, *Kuala Lumpur*

Monaco

Patrick Rampal, *Monaco*

Netherlands

Louis MA Akkermans, *Utrecht*
Karel Van Erpecum, *Utrecht*
Albert K Groen, *Amsterdam*
Dirk Joan Gouma, *Amsterdam*
Jan BMJ Jansen, *Nijmegen*
Evan Anthony Jones, *Abcoude*
Ernst Johan Kuipers, *Rotterdam*
Chris JJ Mulder, *Amsterdam*
Michael Müller, *Wageningen*

Pena AS, *Amsterdam*
Andreas Smout, *Utrecht*
RW Stockbrugger, *Maastricht*
GP Vanberge-Henegouwen, *Utrecht*

New Zealand
Ian David Wallace, *Auckland*

Norway
Trond Berg, *Oslo*
Helge Lyder Waldum, *Trondheim*

Pakistan
Muhammad S Khokhar, *Lahore*

Philippines
Eulenia Rasco Nolasco, *Manila*

Poland
Tomasz Brzozowski, *Cracow*
Andrzej Nowak, *Katowice*

Portugal
Miguel Carneiro De Moura, *Lisbon*

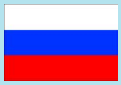

Russia
Vladimir T Ivashkin, *Moscow*
Leonid Lazebnik, *Moscow*
Vasiliy I Reshetnyak, *Moscow*

Singapore
Bow Ho, *Kent Ridge*
Francis Seow-Choen, *Singapore*

Slovakia
Anton Vavrecka, *Bratislava*

South Africa
Michael C Kew, *Parktown*

South Korea
Jin-Hong Kim, *Suwon*
Myung-Hwan Kim, *Seoul*
Yun-Soo Kim, *Seoul*
Yung-Il Min, *Seoul*
Jae-Gahb Park, *Seoul*
Dong Wan Seo, *Seoul*

Spain
Abraldes JG, *Barcelona*
Fernando Azpiroz, *Barcelona*
Ramon Bataller, *Barcelona*
Josep M Bordas, *Barcelona*
Maria Buti, *Barcelon*
Xavier Calvet, *Sabadell*
Antoni Castells, *Barcelona*
Manuel Daz-Rubio, *Madrid*
Juan C Garcia-Pagán, *Barcelona*
Genover JB, *Barcelona*
Javier P Gisbert, *Madrid*
Jaime Guardia, *Barcelona*
Angel Lanas, *Zaragoza*
Ricardo Moreno-Otero, *Madrid*
Julian Panes, *Barcelona*
Miguel Perez-Mateo, *Alicante*
Josep M Pique, *Barcelona*
Jesus Prieto, *Pamplona*
Luis Rodrigo, *Oviedo*

Sri Lanka
Janaka De Silva, *Ragama*

Swaziland
Gerd Kullak-Ublick, *Zurich*

Sweden
Lars Christer Olbe, *Molndal*
Curt Einarsson, *Huddinge*
Lars R Lundell, *Stockholm*
Xiao-Feng Sun, *Linkoping*

Switzerland
Christoph Beglinger, *Basel*
Michael W Fried, *Zurich*
Bruno Stieger, *Zurich*
Arthur Zimmermann, *Berne*

Turkey
Yusuf Bayraktar, *Ankara*
Figen Gurakan, *Ankara*
Cihan Yurdaydin, *Ankara*

United Kingdom
Axon ATR, *Leeds*
Paul Jonathan Ciclitira, *London*
Amar Paul Dhillon, *London*
Stuarts Forbes
Subrata Ghosh, *London*
Brian T Johnston, *Belfast*
David EJ Jones, *Newcastle*
Michael A Kamm, *Harrow*
Hong-Xiang Liu, Cambridge
Giorgina Mieli-Vergani, *London*
Nikolai V Naoumov, *London*
John P Neoptolemos, *Liverpool*
James Neuberger, *Birmingham*
Colm Antoine O'Morain, *Dublin*
Simon D Taylor-Robinson, *London*
Frank Ivor Tovey, *Basingstoke*
Min Zhao, *Foresterhill*

United States
Firas H Ac-Kawas, *Washington*
Gianfranco D Alpini, *Temple*
Paul Angulo, *Rochester*
Jamie S Barkin, *Miami Beach*
Todd Baron, *Rochester*
Kim Elaine Barrett, *San Diego*
Jennifer D Black, *Buffalo*
Xu Cao, *Birmingham*
David L Carr-Locke, *Boston*
Marc F Catalano, *Milwaukee*
Xian-Ming Chen, *Rochester*
James M Church, *Cleveland*
Vincent Coghlan, *Beaverton*
James R Connor, *Hershey*
Pelayo Correa, *New Orleans*
John Cuppoletti, *Cincinnati*
Peter V Danenberg, *Los Angeles*
Kiron Moy Das, *New Brunswick*
Hala El-Zimaity, *Houston*
Ronnie Fass, *Tucson*
Emma E Furth, *Pennsylvania*
John Geibel, *New Haven*
Graham DY, *Houston*
Joel S Greenberger, *Pittsburgh*
Anna S Gukovskaya, *Los Angeles*
Gavin Harewood, *Rochester*
Atif Iqbal, *Omaha*
Hajime Isomoto, *Rochester*
Dennis M Jensen, *Los Angeles*
Leonard R Johnson, *Memphis*
Peter James Kahrilas, *Chicago*
Anthony Nicholas Kalloo, *Baltimore*
Neil Kaplowitz, *Los Angeles*
Emmet B Keeffe, *Palo Alto*
Joseph B Kirsner, *Chicago*
Burton I Korelitz, *New York*
Robert J Korst, *New York*
Richard A Kozarek, *Seattle*
Shiu-Ming Kuo, *Buffalo*
Frederick H Leibach, *Augusta*
Andreas Leodolter, *La Jolla*
Ming Li, *New Orleans*
Lenard M Lichtenberger, *Houston*
Gary R Lichtenstein, *Philadelphia*
Josep M Llovet, *New York*
Martin Lipkin, *New York*

Manuscript reviewers of *World Journal of Gastroenterology*

PO Box 2345, Beijing 100023, China
www.wjgnet.com
wjg@wjgnet.com

ELSEVIER

World J Gastroenterol 2005;11(16):2371-2384
World Journal of Gastroenterology ISSN 1007-9327

• *REVIEW* •

Radical induction theory of ulcerative colitis

Jay Pravda

Jay Pravda, PO Box 142181, Gainesville, FL 32614, USA
Correspondence to: Jay Pravda, MD, PO Box 142181, Gainesville, FL 32614, USA. jaypravda@yahoo.com
Telephone: +1-352-598-8866
Received: 2004-06-30 Accepted: 2004-07-15

Abstract

To propose a new pathogenesis called Radical Induction to explain the genesis and progression of ulcerative colitis (UC). UC is an inflammatory bowel disease. Colonic inflammation in UC is mediated by a buildup of white blood cells (WBCs) within the colonic mucosal lining; however, to date there is no answer for why WBCs initially enter the colonic mucosa to begin with. A new pathogenesis termed "Radical Induction Theory" is proposed to explain this and states that excess un-neutralized hydrogen peroxide, produced within colonic epithelial cells as a result of aberrant cellular metabolism, diffuses through cell membranes to the extracellular space where it is converted to the highly damaging hydroxyl radical resulting in oxidative damage to structures comprising the colonic epithelial barrier. Once damaged, the barrier is unable to exclude highly immunogenic fecal bacterial antigens from invading the normally sterile submucosa. This antigenic exposure provokes an *initial* immune response of WBC infiltration into the colonic mucosa. Once present in the mucosa, WBCs are stimulated to secrete toxins by direct exposure to fecal bacteria leading to mucosal ulceration and bloody diarrhea characteristic of this disease.

Key words: Ulcerative colitis; Radical induction; Oxidative stress; Hydrogen peroxide

Pravda J. Radical induction theory of ulcerative colitis. *World J Gastroenterol* 2005; 11(16): 2371-2384
http://www.wjgnet.com/1007-9327/11/2371.asp

INTRODUCTION

Ulcerative colitis (UC) is an inflammatory bowel disease characterized by infiltration of white blood cells (WBCs) into the colonic mucosa resulting in tissue destruction and recurrent bouts of bloody diarrhea. The initial inflammatory reaction begins in the rectal mucosa in over 95% of cases and may extend in a contiguous fashion to involve the whole colon[1]. Often, young individuals in the prime of life are struck with this disease whose course can be severely debilitating, unpredictable and unrelenting. Treatment modalities are few and unsatisfactory with total colectomy being the only option for individuals unresponsive to the limited medical therapy currently available.

Since the history of medically treated UC is characterized by lifelong repeated episodes of this disease, it appears that no currently available medical therapeutic modality is capable of addressing the fundamental disorder present and therefore unable to alter the natural history of this condition.

Several immunologically oriented hypotheses regarding the etiology and pathogenesis of UC have been advanced[1]. All remain ill defined, fall short of promoting a clear understanding of this illness and lack predictive value for therapeutic development. These postulates provide no basis for individual risk factor profiling and are unable to explain the known histological, biochemical, immunological and epidemiological abnormalities associated with this disease.

WBCs found within the colonic mucosal lining mediate the tissue injury in active UC; however, to date there is no satisfactory answer for why these WBCs accumulate within the colonic mucosa to begin with. It is the purpose of this paper to propose a new evidenced based pathogenesis termed "Radical Induction Theory" to explain the genesis of this initial influx of WBCs which leads to UC.

The Radical Induction Theory of UC states that excess un-neutralized hydrogen peroxide, produced within colonic epithelial cells as a consequence of aberrant cellular metabolism, diffuses through cell membranes to the extracellular space where it is converted to the highly damaging hydroxyl radical, which is capable of causing extensive oxidative damage to structures responsible for maintaining the colonic epithelial barrier function.

Once damaged, the epithelial barrier is no longer able to exclude highly immunogenic fecal bacterial antigens from invading the normally sterile submucosal tissue. This antigenic exposure provokes an *initial* immune response consisting of WBC infiltration into the colonic mucosal surface in an attempt to "plug the hole" and prevent systemic bacterial invasion and fatal sepsis. Once present within the mucosa, WBCs are stimulated to secrete toxic substances by direct exposure to high concentrations of fecal bacteria leading to mucosal ulceration and bloody diarrhea characteristic of this disease.

BACKGROUND

It is perhaps among the greatest physiological wonders of evolution that the most highly evolved immune system ever engendered can remain unperturbed while surrounding the highest concentration of bacteria on the planet, separated only by a tenuous sheet of tissue one cell thick.

This unlikely truce describes the living conditions of the normal human colon where the luminal concentration

of potentially pathogenic bacteria is estimated to be 10^{12} (one trillion) colony-forming units (viable bacterial cells) per gram of colonic contents[2].

Previous attempts at creating an animal model of UC have met with limited success. No current animal model is perfect[3] and experimental attempts to create an animal model of human UC using rectal instillation of toxic chemicals are inherently limited in their ability to faithfully reproduce the disease due to complex psychological, physiological, genetic, environmental and immunological interactions that antecede and contribute to the pathogenesis of this condition in humans[2].

What is clear from animal studies is that the integrity of the colonic epithelial surface barrier is paramount in maintaining immune quiescence within the colonic tissues and preventing the colonic immune system from mounting an immune response to the high concentration of bacterial antigen that is poised to invade the normally sterile sub-epithelial environment.

Cellular mechanisms involved in maintaining the integrity of the colonic surface barrier function may therefore be compromised early on in the pathogenesis of UC. Dysfunction of a vital process required to maintain mucosal integrity must therefore be an early and necessary part of a sequential series of events ultimately leading to deterioration of epithelial barrier function with subsequent mucosal immune activation secondary to antigenic penetration into the normally sterile colonic sub-mucosal tissues.

In other words, the additive effects of abnormal cellular stressors focused on a common biochemical pathway are acting in concert to disrupt an intracellular biochemical process that contributes a required function necessary for maintaining colonic surface barrier integrity.

The high incidence (over 50%) of spontaneous improvement and relapse seen in UC[4] suggests a reversible disruption and the possibility of a self-replenishing depletion syndrome affecting a crucial element required for mucosal integrity.

In 1951 Science published an article entitled "A New Concept of the Pathogenesis of Ulcerative Colitis"[5]. In this seminal publication, the authors demonstrated that patients with UC have either completely absent or severely damaged colonic epithelial basement membranes (BMs). An important observation was that total destruction of BM was seen in the absence of any mucosal inflammation (no WBCs present) and in many areas the BM was noted to be "thinned out". The authors ascribed an important pathogenetic role to the BM destruction seen in colonic biopsy samples of their patients with UC.

The first real clue came from initial observations that BM was destroyed in areas uninvolved in active inflammation[5,6]. It was already known that UC was an inflammatory condition with infiltration of WBCs (neutrophils) into the mucosal lining of the colon and that these WBCs were capable of causing inflammation and tissue damage. However, the presence of damaged BM in tissue areas without inflammation suggested that a prior process anteceded the WBC involvement.

The presence of "thinned out" BM suggested that a gradual, non-immune mediated, erosion had taken place. The authors also noted sections of epithelium which had "sloughed" away from seemingly intact BM. This suggested that the epithelial cells themselves played a role in the process that led to the BM alterations and their own (epithelial cell) detachment from the BM. It also suggested that this process began in the interface between the BM and epithelium. Since BM regeneration was noted after successful treatment, it appeared that the process could be halted and reversed. What this process was and what effector molecules, if any, were involved could not be determined from histological studies alone, and in 1951 there was no animal model of UC to experiment with. However, there was a human model of this disease readily available for study which provides a second clue.

The second clue came from a series of case reports from dedicated clinicians over the span of several decades. For many years during the 20th century, hydrogen peroxide (H_2O_2) enemas were routinely employed and recommended by physicians for the evacuation of fecal impactions. However, in the 1930s reports began to surface regarding the development of rectal bleeding and colitis subsequent to the use of hydrogen peroxide enemas[7]. A fatal case of UC subsequent to hydrogen peroxide enema was first recorded in 1948[8]. In 1951, Pumphery reports severe ulcerative proctosigmoiditis following hydrogen peroxide enemas in two patients[9].

In 1960 Sheenan and Brynjolfsson[8] were able to reproduce acute and chronic UC by rectal injection of rats with a 3% solution of H_2O_2. This was the first animal model of UC and it mirrored the effects of human UC. Microscopic examination of killed rats revealed colonic mucosal ulceration and WBC (neutrophilic) infiltration, which was "sharply delineated from adjacent normal mucosa". The mucosal inflammation extended proximally over time.

It was noted that, in surviving rats, most of the mucosal ulcerations were healed by 10 wk with the exception of some ulcers which "were located almost always in the left colon a few centimeters above the anus". These three observations (sharp inflammatory tissue delineation from normal tissue, rectal inflammatory persistence and contiguous proximal extension) are also characteristic of human UC.

Despite the demonstrated adverse effects of hydrogen peroxide it continued to be used as an enema and, in 1981, Meyer reported three cases of acute UC after administration of hydrogen peroxide enema and stated that "acute ulcerative colitis appears to be a fairly predictable occurrence after hydrogen peroxide enemas"[10]. Even small amounts of hydrogen peroxide could cause human UC as was reported by Bilotta and Waye in 1989[11] after experiencing an epidemic of hydrogen peroxide-induced colitis in the GI endoscopy unit at their institution due to the inadvertent instillation of hydrogen peroxide during colonoscopy. These results indicate that, when in contact with the colonic mucosa, small amounts of hydrogen peroxide can, in predisposed individuals, produce a clinical and histological picture, which is indistinguishable from spontaneously occurring primary idiopathic human UC.

The data presented thus far reveals that epithelial cell "sloughing" (detachment) from BM and BM erosion (in non-inflamed areas only populated by colonic epithelial

cells) are fairly characteristic histological findings in UC suggesting that epithelial cells play a role both in their own detachment and in BM erosion. Additionally, clinical reports and experimental results reveal that UC is a "fairly predictable" occurrence when hydrogen peroxide comes in contact with rectal epithelium.

The third and final clue tying histological observations of Levine and Kirsner with the adverse clinical effects of hydrogen peroxide enemas came by way of biochemical studies undertaken by investigators in the early 1970s, which demonstrated that mammalian cells are constantly generating hydrogen peroxide as a byproduct of normal aerobic metabolism[12].

WHAT IS HYDROGEN PEROXIDE?

Hydrogen peroxide is a colorless, highly damaging oxidizing agent, a powerful bleaching agent; used for wastewater treatment, and as an oxidant in rocket fuels. H_2O_2 has a ubiquitous presence in cells and is continuously being generated by the plasma membrane, cytosol and several different sub-cellular organelles including peroxisomes, endoplasmic reticulum, nucleus and by almost 100 enzyme systems[12-15]. Under normal conditions, 90% of H_2O_2 is generated as a toxic by-product of mitochondrial electron transport chain (ETC) respiratory activity[14,16]. The mitochondrial ETC is a series of proteins that channel the flow of electrons derived from ingested food into the synthesis of adenosine triphosphate (ATP), which is used as a chemical energy source for all energy requiring cellular processes.

The transfer of electrons through the ETC, however, is not perfect. Up to 5% of electrons do not make it all the way through the chain and fail to combine with oxygen to produce water[17-19]. These "leaked" electrons combine directly with molecular oxygen in the immediate vicinity, instead of the next carrier in the chain, to form the superoxide ($O_2^-\cdot$) radical[20]. It is estimated that under normal conditions 2% of available oxygen is converted to superoxide by ETC "leakage"[21].

Superoxide spontaneously dismutates to H_2O_2 or undergoes enzymatic conversion to H_2O_2 at the site of production within mitochondria by the enzyme superoxide dismutase (SOD) (EC 1.15.1.1)[12,14,17]. Complex I and III, of the ETC, are the source of electron leakage leading to the eventual intracellular generation of hydrogen peroxide[22,23].

H_2O_2 is long lived and highly biomembrane permeable and must be immediately neutralized at the site of production to prevent diffusion throughout the cell or to the extracellular space[12]. Sophisticated enzyme systems exist expressly for this purpose. These H_2O_2 neutralizing anti-oxidant enzymes are catalase (E.C. 1.11.1.6) and glutathione peroxidase (GPx, E.C. 1.11.1.9) with GPx responsible for 91% of H_2O_2 consumption[24]. If allowed to accumulate H_2O_2 will diffuse from its site of production and generate hydroxyl radical ($\cdot OH$), which is the most damaging and chemically reactive radical formed in cellular metabolism. Hydroxyl will indiscriminately destroy everything it encounters[17,25,26]. The hydroxyl radical is principally responsible for the cytotoxic effects of oxygen in animals[25].

The iron catalyzed Haber-Weiss reaction ($O_2^-\cdot + Fe^{+3} \rightarrow O_2 + Fe^{+2}$), followed by ($Fe^{+2} + H_2O_2 \rightarrow Fe^{+3} + HO^- + HO\cdot$), is considered to be the major mechanism by which the highly reactive hydroxyl radical is generated[27]. Molecules interacting with hydroxyl radicals sustain severe damage to the extent that the hydroxyl radical is able to crack polysaccharides; nucleic acids and proteins[25]. H_2O_2 is also able to peroxidize and destroy lipids that make up cell biomembranes[28]. Detoxification of hydrogen peroxide, the immediate precursor to hydroxyl radical, therefore is crucial to normal cellular function and survival.

MECHANISM OF DISEASE

The above data suggests a link between intracellular hydrogen peroxide production and UC. Since exogenously applied hydrogen peroxide can cause UC in humans, and colonic epithelial cells produce hydrogen peroxide, is it reasonable to speculate that excess hydrogen peroxide generated by colonic epithelial cells may be causing UC? How this may come about is suggested by the histological work of Levine and Kirsner (above) which hints of an extracellular process in the epithelial cell/BM interface causing epithelial cell detachment by erosion of subjacent anchoring BM and destruction of apical intercellular tight junctions (TJs). Together, these two bits of data suggest that colonic epithelial cells produce excess hydrogen peroxide, which exits the cell causing oxidative damage to BMs and TJs, which are structures responsible for physical epithelial integrity and barrier function. The resulting destruction of the epithelial barrier allows luminal bacterial antigens to enter the normally sterile submucosal layers of the colonic wall itself initiating an immune response leading to UC.

For hydrogen peroxide to be considered a primary etiologic agent in the pathogenesis of UC, a logical pathogenetic chain of events should be demonstrable starting from the generation of H_2O_2 within sub-cellular organelles to the eventual development of UC. H_2O_2 should possess distinct physicochemical attributes that render it uniquely qualified, to the exclusion of other agents, to induce UC.

In effect it must be demonstrated that H_2O_2 can be produced in excess in colonic epithelial cells and this leads to UC. H_2O_2 must also be capable of exiting colonic epithelial cells and be the source of damage to colonic barrier function structures (BMs and TJs), whose disintegration is important in the development of UC. Finally, in order to have clinical relevance it follows that conditions associated with UC must lead to excessive hydrogen peroxide within colonic epithelial cells. UC associated intracellular abnormalities such as impaired beta oxidation and neoplastic transformation should also be readily explainable. The following sections address these concerns.

1. Can H_2O_2 be produced in excess within colonic epithelial cells and does this cause UC? The answer came by way of genetic studies of knockout mice. These are mice that are genetically engineered with a deletion of a certain gene in order to isolate and study its effects. Knockout mice rendered genetically devoid of GPx (the main hydrogen peroxide neutralizing enzyme) spontaneously develop a crypt destructive colitis (mucosal inflammation -

similar to human UC) as early as 11 d of age with extension to the proximal colon by d 15[29]. This indicates that, when the biological enzyme system needed to neutralize hydrogen peroxide is hindered, the resulting increase in un-neutralized colonic epithelial intracellular hydrogen peroxide can lead to UC.

2. Can hydrogen peroxide egress from the cell? This is important since H_2O_2would need to exit the cell in order to cause the severe BM damage seen during histological examination of affected colonic tissue. It turns out that hydrogen peroxide is freely and highly permeable through biological membranes[12] enabling its diffusion out of the cell from any site of excess production within the cell. H_2O_2 therefore is capable of reaching both the extracellular BMs and TJs from any intracellular location. H_2O_2's proportionately variable production as a coupled consequence of fundamental cellular metabolic processes plus its ability to pass through biomembranes and produce damaging oxygen radicals far from its site of generation is a unique combination of properties not possessed by any other substance.

3. Can hydrogen peroxide damage BMs and TJs? It has been reported that extracellular hydrogen peroxide can severely damage BMs, TJs and colonic epithelial cell membranes by producing hydroxyl radical via a metal catalyzed Haber-Weiss reaction. Hydroxyl radical is able to damage proteins in BMs and TJs by cleavage of peptide bonds, formation of intra- and inter-molecular cross-linkages and oxidation of amino acids[14,30,31]. The mechanism has been identified as a site-specific metal ion catalyzed oxidative damage and cleavage of amino acids and peptide bonds by hydroxyl radical. The *in vivo* source of all hydroxyl radical was identified as endogenously generated hydrogen peroxide[32]. H_2O_2 can therefore disintegrate the micro-anatomical GI barrier structures that maintain epithelial integrity (BMs and TJs). Hydroxyl radical oxidizes and destroys everything it encounters resulting in microscopic alterations, which increase mucosal permeability allowing penetration of luminal proteins and antigens[31,33-38].

Using a well-characterized model of BM, Riedle and Kerjaschki[31] evaluated the *in vitro* effects of hydrogen peroxide induced changes on interstitial matrix proteins and the consequences for the integrity of the BM/matrix network.

The authors documented significant disintegration of matrix structure with 15% of matrix proteins being released into the incubation medium. This corresponded to seven times that was seen in control conditions without hydrogen peroxide. Importantly, extensive oxidative damage of individual amino acid residues (tryptophan) was noted without any morphological change to the BM/matrix network. The hydrogen peroxide-derived hydroxyl radical was found to be the main reactive oxygen species responsible for matrix protein disintegration. Laminin, a major BM structural protein, was also released from BM when incubated with low concentrations of hydrogen peroxide.

Hydrogen peroxide infused into rat renal artery produced local H_2O_2-derived oxygen radicals and subsequent marked glomerular protein leak suggesting an increased porosity of the glomerular BM secondary to oxidative damage of its constituent proteins[35].

In addition to BM damage, hydrogen peroxide-derived oxygen radicals are also able to disrupt colonic epithelial TJs. TJs are composed of thin bands of plasma-membrane proteins that completely encircle the apical (luminal) region of colonic epithelial cells and are in contact with similar thin bands on adjacent cells. These intercellular protein junctions fasten adjacent epithelial cells together forming a sealing gasket, which prevents the passage of most dissolved molecules and bacterial antigens from one side of the epithelial sheet to the other.

Since only a single layer of colonic epithelial cells separates the bacterial laden luminal contents from the subjacent lamina propria, the epithelial TJ constitutes the major primary barrier that prevents luminal bacterial antigens from gaining access to the effector immune cells and vasculature in the normally sterile lamina propria[39]. Thus, the intestinal barrier function relies primarily on the tightness of the epithelial layer to maintain impermeability with sub-epithelial layers contributing a minor function[37].

Hydrogen peroxide, at a low concentration of 0.2 mmol/L, was reported to increase *in vitro* epithelial monolayer permeability by disrupting paracellular junctional complexes[37]. In experiments to assess the effect of hydrogen peroxide on intestinal permeability, Grisham *et al*[38] found a significant increase in mucosal permeability after *in vivo* perfusion of rat intestine with hydrogen peroxide. Altered epithelial permeability is also a consistent effect of hydrogen peroxide in other tissues including endothelial and renal cell lines[33].

In studies to determine the *in vitro* effect of oxidative stress on TJ integrity, Parrish *et al*[36] studied the effect of chemically induced oxidative stress on the E-cadherin/catenin protein complex, which is the principal intercellular TJ (zonula adherens) anchoring protein. The authors bathed precision cut rat liver slices with non-lethal concentrations of oxidant chemicals (diamide and *t*-butylhydroperoxide), which penetrate the hepatocytes and oxidize both intracellular-reduced glutathione and NADPH. This depletes available glutathione stores and prevents the regeneration of reduced glutathione. This causes oxidation from both these added chemicals and any endogenously generated hydrogen peroxide. The authors found that this level of oxidative stress disrupted the E-cadherin/catenin cell-adhesion protein complex of the TJ.

4. Are BMs and TJs important in the pathogenesis of UC? BMs together with colonic epithelial cells and the TJs that bind them together are the micro-anatomical structures that comprise the gastrointestinal barrier, which prevents fecal bacteria from entering the sterile deeper layers of the colonic tissue and gaining entrance to the blood stream.

In an early study, BMs were found to be absent or severely damaged in UC[5]. In a subsequent report of 29 patients with UC, Jacobson and Kirsner[6] reported either completely destroyed or fragmented BM in all subjects. Of note was the observation of "thinned" out sections of BM consistent with a diffusible agent such as H_2O_2 causing membrane dissolution.

The authors also point out that destruction of BM was noted in the absence of leukocytic infiltration, which is also consistent with a diffusible agent of non-leukocytic (i.e., colonic epithelial cell) origin.

Colonic epithelial BM structure and function was also

found to be seriously disturbed in active cases of UC. In a study to determine the integrity of BM in active UC, Schmehl *et al*, found no positive immunoreactivity for BM laminin in affected colonic tissue. The authors concluded that the three-dimensional network of colonic epithelial BM and its function is seriously disturbed in active UC[40].

Using alternating current impedance analysis Schmitz *et al* [34] found that epithelial resistance in UC is strongly impaired and that this barrier defect was paralleled by a decrease in TJ strand count.

Employing immunostaining with anti-human E-cadherin and catenin antibodies, Karayiannakis[41] determined that E-cadherin expression was reduced in all cases of active UC but in none of the inactive cases. (The E-cadherin/catenin protein complex is the primary intercellular TJ (zonula adherens) anchoring protein.).

Altered a-catenin was also seen in all cases of active UC but was not altered in any case with inactive disease. Importantly, epithelial cells adjacent to mucosal ulcers showed loss of E-cadherin and a-catenin, while epithelial cells distant from the mucosal margin revealed normal E-cadherin and a-catenin expression. The authors found that altered E-cadherin always coexisted with abnormal a-catenin. This is consistent with an advancing margin of a diffusible agent which is disrupting the E-cadherin/catenin complex within the TJ.

TJ disruption was also found to correlate with the progression of UC. In studies employing immuno-cytochemistry, Western blotting and *in situ* hybridization, Jankowski found a strong correlation between E-cadherin disruption and the progression of UC[42]. The authors showed that as disease activity progresses both cytoplasmic and membranous E-cadherin expression are lost. The authors propose that normal E-cadherin function is essential for the maintenance of normal colorectal epithelium.

In agreement with the above studies, results are obtained with genetically engineered chimeric mice expressing enterocytes with either normal or non-functional cadherin. Mice expressing non-functional cadherin developed an inflammatory bowel disease with histological similarities to human UC, including cryptitis, crypt abscesses and a neutrophilic infiltrate.

These inflammatory changes were confined to foci of epithelium expressing non-functional cadherin, confirming the absence of an autoimmune response[43,44].

If extracellular hydrogen peroxide, originating from intracellular sources, is a causative factor in the breakdown of colonic barrier (TJ) function, then an increase in epithelial permeability should be an early manifestation in UC. Furthermore, these early permeability lesions should be macroscopically normal and occur in intact epithelium since the neutrophilic inflammatory process has not yet begun.

Gitter *et al*[45] found such early permeability increases in colonic tissue obtained from individuals with early (Truelove I) UC. The authors found that in seemingly intact epithelium there was a 35% increase in conductivity (ionic permeability) in early/mild (Truelove I) UC tissue samples with a 300% permeability increase in tissue samples showing a moderate to severe inflammation. These areas of early permeability increases correlated with foci of colonic epithelial apoptosis. Both of these effects (i.e., increase in epithelial permeability and induction of apoptosis) are known consequences of tissue exposure to hydrogen peroxide[33]. This is in agreement with permeability studies in animal models of UC, which demonstrated an increase in colonic mucosal permeability to tracer molecules prior to the appearance of a visible inflammatory process[46].

5. Are conditions that enhance production of hydrogen peroxide also associated with UC? Elevated levels of intracellular hydrogen peroxide can result from increased production or decreased neutralization. H_2O_2 originates from two main intracellular sources. One is the mitochondrial ETC and the other is the total sum metabolic activity of nearly 100 oxidase enzymes distributed within most sub-cellular organelles and cytosol[12-15,17,47,48]. H_2O_2 neutralization is mainly accomplished via the enzymatic action of GPx (E.C. 1.11.1.9) in conjunction with the anti-oxidant tri-peptide co-factor glutathione (GSH-reduced). Selenium is a required active-site co-factor for GPx enzymatic function. Oxidized glutathione (glutathione disulfide, GSSG) is converted back to the cytoprotective reduced state via the enzymatic activity of glutathione-disulfide reductase (GDR) (E.C. 1.8.1.7-formally E.C. 1.6.4.2.), with electrons supplied by NADPH which itself is generated by the pentose phosphate pathway (PPP). The chemical equation for H_2O_2 neutralization and glutathione regeneration is as follows:

Cytoprotective (reduced) intracellular glutathione is the main reducing agent available to colonic epithelial cells to neutralize hydrogen peroxide. Although other redox couples such as cysteine:cystine, NAD^+:NADH, $NADP^+$:NADPH and reduced:oxidized thioredoxin participate in the maintenance of the required intracellular reduction state critical to metabolic function, the glutathione redox couple (GSH:GSSG) is a two to four orders of magnitude more abundant than any other redox couple[49].

Glutathione also serves as a common reducing agent for other redox couples[49] and accounts for over 90% of intracellular H_2O_2 neutralization (catalase contributes a small amount to overall H_2O_2 neutralization). Glutathione is therefore the main supplier of reducing equivalents and a reliable indicator of the redox state of cells.

Intracellular H_2O_2 can thus be abnormally elevated secondary to increased production or impairment of any element or action required for its neutralization. The following sections illustrate this concept.

INCREASED H_2O_2 PRODUCTION

Increased oxidase enzyme activity

Oxidase enzymes utilize molecular oxygen as an electron accepting co-factor necessary for the enzymatic reaction to proceed. H_2O_2 is produced as an end by-product of these reactions. Thus, increased oxidase enzymatic activity can contribute to the generation of intracellular hydrogen peroxide. UC has been reported subsequent to the administration of certain xenobiotics (i.e., vitamin B-6)[50].

Vitamin B-6 is metabolized by pyridoxine 4-oxidase (EC 1.1.3.12), which generates H_2O_2 as a by-product.

Increased electron transport activity

UC can develop subsequent to hyperthyroidism[51-55]. Hyperthyroidism is known to enhance ETC activity, which increases hydrogen peroxide generation. On the other hand, cigarette smoking, which inhibits ETC activity, is protective. Studies quantifying the effect of cigarette tar on mitochondrial electron transport activity report an 82% inhibition rate on whole chain respiration[56], whereas cessation of cigarette smoking (which releases ETC inhibition) is a powerful risk factor for the development of UC[2,57-59].

Colonocyte ETC activity can become a source of excess H_2O_2 if subjected to hypoxia and sudden re-oxygenation[60]. This process of hypoxia and re-oxygenation increases the activity of the ETC due to the interim accumulation of reducing substrate resulting in increased production of hydrogen peroxide. Local colonic hypoxia/reoxygenation can be caused by stress. The following section reviews mechanisms of stress-related increases in colonocyte H_2O_2.

Psychological stress

Psychological stress has long been recognized as an exacerbating factor for UC. Dr. Burrill Crohn was well aware of the psychological effects of stress on UC when, in the first issue of Gastroenterology in January 1943, he reported the appearance of acute UC in a 16-year-old girl following a criminal rape, noting that "the psycho-somatic aspect of this case was particularly significant"[61].

During the 1950s, practitioners noticed the onset and/or exacerbation of UC commonly occurring subsequent to emotional disturbances[62-64]. Early observations of severely emotionally disturbed individuals with UC reported resolution of the latter when the former was treated[65,66].

More recently an association has been reported between stress and UC disease activity[2,67]. Up to 40% of patients with UC report psychological stress as an exacerbating factor[68]. Life stress has been reported to be associated with both objective and subjective aspects of activity in UC[67] and high long-term stress was found to triple the risk of disease exacerbation[69]. The importance of stress as an initiating factor can be seen in the cotton-top tamarin, a small monkey found only in northwest Columbia that spontaneously develops colitis when deprived of its native habitat while in captivity. Affected animals will enter remission when transferred to natural conditions indicating that the effects of stress can be reversed[70].

The molecular basis of stress-induced exacerbation of UC can be correlated to both increased H_2O_2 production and decrease H_2O_2 neutralization secondary to the effect of stress on electron transport activity and cellular enzyme systems. These mechanisms may find expression either through systemic or local effects of stress on the colon as discussed below.

1. Acute systemic psychological stress increases the amount of systemic circulating biogenic amines (catecholamines), such as serotonin, epinephrine, nor-epinephrine and dopamine[71]. Mono-amine oxidase (EC#1.4.3.4), an enzyme present on the outer surface of mitochondria within colonic epithelial cells, catalyzes the oxidative deamination of both exogenous xenobiotic amines (i.e., medications) as well as endogenous catecholamine stress hormones and in the process reduces molecular oxygen to hydrogen peroxide[20].

The reaction catalyzed is $RCH_2+H_2O+O_2 \rightarrow RCHO+NH_3+H_2O_2$.

Stress therefore may increase H_2O_2 levels by providing additional metabolic substrate (endogenous catecholamines) for mono-amine oxidase. Thus, individuals with genetically diminished anti-oxidant (reductive, H_2O_2 neutralizing) capacity are at greater risk of developing UC when exposed to acute stressful events.

2. Chronic systemic psychological stress, such as depression, has been associated with circulating increased nor-epinephrine levels[71]. Depression has been reported to precede the onset of UC significantly more often than expected[72]. Depressive stress and anxiety, however, were found to be significantly more common after the appearance of Crohn's disease[73]. This suggests that physiological alterations present in depression contribute to the appearance of UC in contrast to Crohn's disease where depression may be a psychological reaction to the appearance of the disease.

Chronic depression, therefore, may result in significant long-term increases in circulating endogenous catecholamine levels, which may elevate intracellular colonocyte H_2O_2 when metabolized via mono-amine oxidase. Chronically depressed individuals with marginal anti-oxidant capacity needed to neutralize this excess H_2O_2 are at increased risk for development of UC.

3. Local colonic perfusion/reperfusion (hypoxia/reoxygenation) can result from the effects of psychological stress on the colon. Stress-induced colonic spasm may result in local hypoxia and re-oxygenation, which can lead to oxygen deprivation of dozens of oxidase enzymes such as xanthine oxidase (XO)[74-76]. In a seminal study, Almy and Tulin[77] directly observed the effects of stress on the colonic mucosa of seven healthy volunteer medical students.

The students were fitted with a metal helmet containing 18 large screws that could be tightened against the head to produce a painful distressing headache lasting 30 min during which time visual colonoscopic evaluation of the sigmoid colon was recorded. In each case the authors visualized severe colonic spasm, which was sufficient to occlude the lumen. Marked mucosal hyperemia and engorgement with intermittent blanching and flushing (perfusion/reperfusion) was also noted. During periods of maximum engorgement, gentle movement of the proctoscope caused a superficial injury with hemorrhage. Nausea often accompanied visualized episodes of colonic spasm. This study indicates that stress can cause severe alterations in colonic function and predispose to colonic hypoxia and reoxygenation (perfusion/reperfusion) injury (sequential blanching and hyperemia with mucosal engorgement). Thus, local stress-induced colonic spasm is mediated via the enteric nervous system, which results in spastic contraction of colonic smooth muscle leading to transient local tissue hypoxemia with subsequent reoxygenation upon colonic smooth muscle relaxation.

XO is a prototypical example of an oxidase enzyme that is affected by perfusion/reperfusion-induced oxygen deprivation. XO catalyzes the conversion of hypoxanthine

to uric acid and in the process reduces molecular oxygen to hydrogen peroxide. During hypoxia, XO activity is significantly reduced due to unavailability of oxygen needed as an electron-accepting co-factor for the enzymatic conversion (oxidation) of hypoxanthine to uric acid. When oxygen is reintroduced (re-perfusion), an increased substrate load leads to increased hypoxanthine metabolism and hydrogen peroxide production. Stress-induced perfusion/re-perfusion, therefore, results in additional H_2O_2 due to increased metabolism of oxidase enzyme substrate which, after having accumulated during hypoxemia, undergoes amplified metabolism upon re-oxygenation with concomitant increases in hydrogen peroxide. Pre-treatment of mice with allopurinol (XO inhibitor) prior to experimentally induced colonic ischemia/reperfusion significantly attenuated leukocyte adhesion to colonic submucosal endothelium[78]. Thus, in this model of murine colitis, inhibition of XO significantly reduces WBC endothelial adhesion, a crucial early step which is likewise present in the development of human UC[79].

Stress-induced colonic smooth muscle spasm with hypoxia/re-oxygenation can also increase colonocyte electron transport activity with concomitant increases in H_2O_2. Rectal epithelial cells possess an ETC, which can become a source of excess H_2O_2 if subjected to hypoxia and sudden re-oxygenation[60].

DECREASED HYDROGEN PEROXIDE NEUTRALIZATION

Decreased glutathione peroxidase activity

Hydrogen peroxide is metabolized via the enzymatic action of GPx, a selenium containing enzyme, which utilizes the anti-oxidant tri-peptide co-factor glutathione to neutralize intracellular H_2O_2. Genetic conditions which inhibit GPx or decrease glutathione availability will lead to increased hydrogen peroxide levels. Genetic research by Cho uncovered the existence of a "pathophysiologically crucial IBD susceptibility gene" located on the small arm of human chromosome 1 (1p36)[80,81]. This genetic locus codes for two enzymes that exert control on intracellular H_2O_2.

One is methylenetetrahydrofolate reductase (MTHFR, EC 1.5.1.20), which is a main regulatory enzyme of homocysteine metabolism[82,83]. Molloy has reported that 17.5% of individuals with UC possess a polymorphic variant of the MTHFR gene *vs* 7.3% of controls[84]. Polymorphic variants of MTHFR result in an elevation of serum homocysteine levels[83]. Nagano has shown that children with UC have elevated serum homocysteine levels and concludes that elevated homocysteine may be associated with the underlying basic pathophysiology of the disease[85]. Markedly elevated levels of tissue homocysteine have also been reported in colonic mucosa of individuals with UC[86]. Elevated homocysteine will increase hydrogen peroxide production by several mechanisms.

Hydrogen peroxide is generated during the oxidation of homocysteine to homocystine[82,87]. Homocysteine also increases levels of the enzyme SOD[88]. SOD catalyzes the conversion of superoxide anion to hydrogen peroxide and increased activity of this enzyme will result in greater hydrogen peroxide generation. Homocysteine has been reported to inhibit GPx activity[87] by 10-fold. This epistatic inactivation of GPx will increase hydrogen peroxide levels and inhibition of GPx was shown to occur at physiologic (9 μmol/L) concentrations of free homocysteine[89].

Decreased 6-phosphogluconate dehydrogenase activity

A second enzyme located at this locus (1p36.3) is 6-phosphogluconate dehydrogenase (PGD) (EC 1.1.1.44). PGD is one of only two enzymes in the PPP, which are responsible for production of NADPH, which is crucial for the reduction of glutathione disulfide (GSSG) back to reduced glutathione (GSH) in order to neutralize the continuous production of H_2O_2 being generated within the cell. Without NADPH to regenerate reduced glutathione, intracellular enzymes would suffer irreversible oxidative damage from excess hydrogen peroxide and cellular function would cease in minutes as apoptosis is triggered. The PPP is the engine that drives H_2O_2 neutralization and there is no backup system. PGD exists in several polymorphic forms with decreased activity ranging from 22% to 79% of normal[90-94]. Decreased levels of glutathione have been reported as a result of a PGD polymorphic enzyme[95].

The phenotypic expression of both these genes supports Cho's conclusion of a pathophysiologically crucial IBD susceptibility gene located at 1p36. PGD activity is also lowered by exogenous factors, i.e., antibiotics, dietary fat and ageing[96-98]. Studies of normal appearing colonic mucosa report significant inter-individual variation of enzymes involved in glutathione synthesis and metabolism[99]. Individual variation was considerable at 8-fold for glutathione-*S*-transferase, 10 fold for GPx, 14-fold for gamma-glutamyl-transpeptidase and 5 fold for gamma-glutamylcysteine synthetase.

These large enzyme variations directly or indirectly affect intracellular glutathione concentrations which itself shows a 16-fold variation between individuals placing certain individuals at the very lowest range of H_2O_2 neutralizing capability.

Decreased glucose-6-phosphate dehydrogenase activity

Epinephrine has been shown to stimulate H_2O_2 release by macrophages and to inhibit glucose-6-phosphate dehydrogenase (G-6-PD, EC 1.1.1.49)[100]. G-6-PD is a crucial enzyme in the PPP, which produces NADPH needed to regenerate reduced glutathione, which is crucial in order to neutralize (reduce) H_2O_2. Inhibition of this enzyme by circulating epinephrine during stressful events reduces the amount of NADPH generated by the PPP, which may lead to increased intracellular H_2O_2 levels. Therefore, conditions of sustained stress can increase the concentration of circulating endogenous catecholamines and boost production of hydrogen peroxide by rectal epithelial cells by either direct production of H_2O_2 or reduction in NADPH needed for H_2O_2 neutralization.

Increased cytochrome P450 enzyme activity

The cytochrome P450 enzyme system is responsible for the majority of oxidation reactions of drugs and other xenobiotics[101]. One study reports that 56% of over 300

drugs tested are metabolized via the cytochrome P450 (CYP) family of oxygenase enzymes present in the endoplasmic reticulum[102]. CYP is mostly found in the liver but is also present in the intestine. A typical CYP catalyzed reaction is as follows:

$NADPH+H^+ + O_2 + RH \rightarrow NADP^+ + H_2O + R\text{-}OH$.

This reaction consumes NADPH, which is also used in regeneration of reduced glutathione required to neutralize H_2O_2. Excessive NADPH utilization in predisposed individuals with marginal anti-oxidant capacity may contribute to increased H_2O_2 levels and the development of colitis associated with certain drugs.

In a prospective cohort study, Jowett[103] found that individuals who consumed the most alcohol tripled their risk of UC relapse compared to those who drank the least. After ingestion, alcohol is distributed to all cells of the body including the rectal epithelial cells. Alcohol is enzymatically converted to acetaldehyde by alcohol dehydrogenase. The acetaldehyde is enzymatically converted to acetic acid by aldehyde dehydrogenase. Both of these cytosolic enzymes utilize NAD^+ to oxidize their respective substrates and generate NADH that normally serves as an electron donor to the ETC. The increased availability of NADH can activate the ETC and generate excess hydrogen peroxide[104,105].

Alcohol can also be metabolized in the endoplasmic reticulum by cytochrome P450 2E1 depleting NADPH needed for glutathione regeneration. Alcohol, thus, generates H_2O_2 and decreases production of glutathione needed for neutralization of hydrogen peroxide.

Alcohol inhibits GPx, a crucial enzyme that neutralizes H_2O_2, and depletes mitochondrial glutathione[104]. Glutathione is not synthesized within mitochondria and must be transported from the cytosol into mitochondria through mitochondrial membranes. Alcohol inhibits active transport of glutathione into mitochondria[106,107] leading to mitochondrial depletion of glutathione and H_2O_2 accumulation.

A relationship exists, therefore, between UC and conditions that enhance H_2O_2 production. Furthermore, significant genetic variability in H_2O_2 neutralizing capacity confers greatest risk of developing UC to those individuals with genetically low H_2O_2 neutralizing capacity and co-existence of any of several conditions provoking increased production of H_2O_2. Figure 1 illustrates this concept.

6. Is impaired beta oxidation and neoplastic transformation a consequence of excess H_2O_2? The preferred energy source for colonic epithelial cells is a short chain 4-carbon fatty acid known as butyrate (SCFA). Most butyrate is derived from colonic bacterial fermentation of unabsorbed dietary fiber[113]. SCFAs are metabolized rapidly by beta oxidation and are the major respiratory fuels of colonocytes[113]. Beta-oxidation is the anapleurotic process occurring within mitochondria by which fats are broken down into two carbon units to form acyl-CoA, which is the entry molecule for the Krebs (tricarboxylic acid) cycle. The Krebs cycle generates NADH, which is used as a fuel for ETC activity resulting in ATP production.

Inhibition studies carried out on beta oxidation led Roediger and Nance[114], to conclude that "a suitable inhibitor of beta-oxidation would have unimpeded entry into mitochondria of colonic epithelial cells". Hydrogen peroxide

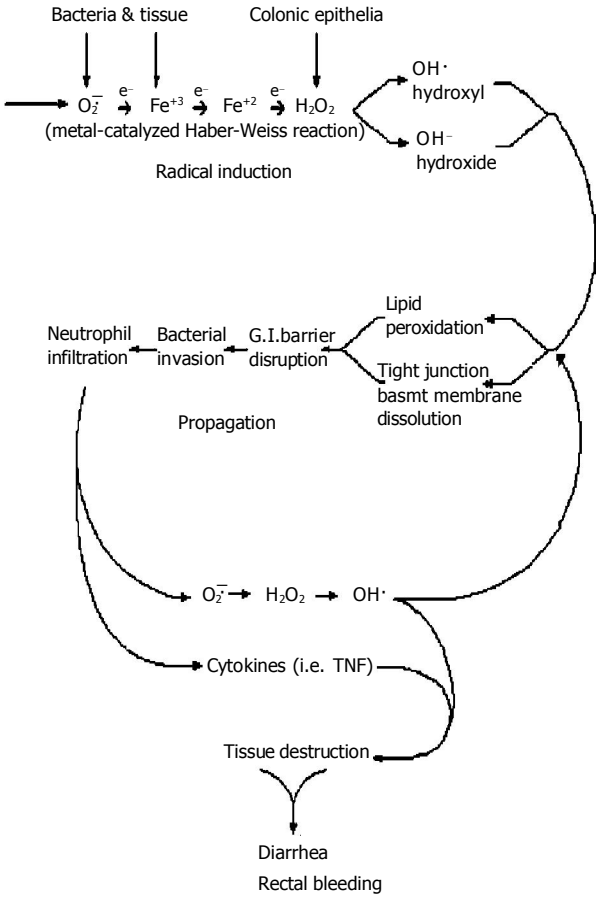

Figure 1 Pathogenesis of UC: Individuals with UC are basically normal. Polymorphic genes (MTHFR and PGD) and significant inter-individual variability in anti-oxidant capacity places certain individuals at the lower threshold of their physiological hydrogen peroxide reducing capability for any given environmental oxidant stress level. Oxygen radical production is induced by environmental oxidant stressors (xenobiotics, stress, smoking cessation, hypermetabolic states) interacting with cellular metabolism. This process is called "Radical Induction". Excess un-neutralized hydrogen peroxide generated during the radical induction phase diffuses from intracellular compartments of colonic epithelial cells, through the plasma membrane, to the extracellular space. Free extracellular hydrogen peroxide reacts with superoxide ($O_2\cdot$) in a transition metal catalyzed Haber-Weiss reaction to form hydroxyl radical ($HO\cdot$) and hydroxide (HO^-) as follows: $*O_2^-\cdot + Fe^{+3}$ (or Cu) $\rightarrow O_2 + Fe^{+2}$ (followed by) $Fe^{+2} + H_2O_2 \rightarrow Fe^{+3} + HO^- + HO\cdot$. Hydroxyl radical initiates oxidative damage to structures that comprise the gastrointestinal barrier (epithelial TJs, BM and epithelial lipid peroxidation) resulting in transient immune activation, which ceases when the damage is repaired. Intermittent immune activation by colonic bacterial antigens can lead to antibody formation (p-anca) and extra-intestinal manifestations. When oxidative damage to the GI barrier cannot be repaired in time to prevent subjacent endothelial adhesion molecule expression, WBCs (neutrophils) begin infiltrating into the damaged colonic epithelium in an effort to prevent systemic bacteremia, which would otherwise result in fatal sepsis. Resident mucosal neutrophils produce additional large quantities of diffusible H_2O_2 which causes oxidative tissue damage in adjacent colonic epithelial cells whose anti-oxidant (GSH) levels have already been previously compromised by radical induction. This results in a proximal "advancing edge" of oxidative tissue damage, TJ disruption and lipid peroxidation extending proximally from the rectum, a unique tissue with high oxidant exposure secondary to fecal generated oxygen radicals, maximum bacterial antigenic load and least anti-oxidant defense as compared to the rest of the GI tract. The accompanying intense neutrophilic diapedesis in a restricted area of epithelial TJ disruption is followed initially by microscopic erythrocyte extravasation eventually leading to frank hemorrhage as endothelial junctions fail to close leading to bloody diarrhea and further neutrophil infiltration characteristic of this disease. The process is only temporarily halted when sufficient anti-oxidant (GSH) capacity is encountered producing a clear line of demarcation between diseased and normal tissue. This self-perpetuating and auto-stimulating cycle is called propagation. *Both iron (Fe) and superoxide ($O_2^-\cdot$) are plentiful within the colonic lumen[108-110]. UC has been reported subsequent to oral iron supplementation for the treatment of anemia[111] and in association with conditions of copper overload (i.e. Wilson's disease)[112].

is permeable through biomembranes including the cell membrane and both the inner and outer mitochondrial membranes. Hydrogen peroxide has been shown to inhibit the beta-oxidation enzyme system of enzymes[115].

The last enzyme in the mitochondrial beta-oxidation process is acetyl-CoA C-acyltransferase (EC 2.3.1.16)(ACT) also known as 3-ketoacyl-CoA thiolase or thiolase I[116]. This enzyme contains two active binding sites each of which includes a conserved cysteine residue, which is crucial for enzymatic activity[117]. Cysteine is an amino acid which has a thiol (hydrosulfide or sulfhydril) group. The thiol group is a univalent radical (-SH) which must be maintained in a reduced state in order for ACT to be functional. H_2O_2 is capable of oxidizing these cysteine residues and inactivating ACT.

Inhibition of beta-oxidation has been reported in macroscopically normal and clinically quiescent UC[118]. Studies have shown that impairment of beta-oxidation is significantly associated with increased colonic permeability followed by clinical relapse to active UC within a few weeks. Remission was associated with normal beta-oxidation[119].

This supports a separate and distinct diffusible intracellular oxidizing agent (i.e., H_2O_2) as the vehicle for both impaired beta-oxidation and subsequent increase in colonic permeability. Appearance of diffusible intracellular H_2O_2 explains the abnormalities of butyrate metabolism during active UC, which may resolve during remission and reappear prior to subsequent activation of the disease since H_2O_2 would accumulate within mitochondria and other sub-cellular organelles prior to extracellular diffusion and destruction of BMs and TJs.

NEOPLASTIC TRANSFORMATION

Patients with UC have an incidence of colorectal cancer (CRC) which is up to 20 fold higher and 20 years younger than CRC in the general population[120]. UC associated CRC originates from dysplastic colonic epithelial cells[121]. The mechanism of neoplastic transformation involves nuclear DNA damage within colonic epithelial cells[122,123]. H_2O_2 is known to cause oxidative DNA damage and treatment of colonic epithelial cells with low concentrations of H_2O_2 has been shown to cause oxidative nuclear DNA damage[124-126]. Cells whose nuclear DNA is damaged by H_2O_2 generated free radicals can undergo neoplastic transformation[127,128]. Thus, active colonic inflammation will lead to cancer due to the high amount of H_2O_2 generated by infiltrating neutrophils; however, studies have shown that individuals with quiescent disease in "remission" have the same risk of developing CRC as those with a more active disease course[129] suggesting an intracellular mechanism (i.e., excessive H_2O_2) which is present during "remission". In fact, studies demonstrate that CRC in the setting of UC increases the risk of CRC in non-colitic relatives by 80%[130] suggesting the anteceding presence of a genetically predisposing genotoxic mechanism or agent such as H_2O_2.

5-Aminosalicylic acid (5-ASA) has been proposed as a maintenance therapy for the prevention of CRC[131-133]. However, results are conflicting and recent studies show that maintenance with 5-ASA does not protect against the development of colonic cancer[134]. Once dissolved in the near neutral pH of colonic fluids 5-ASA becomes a zwitterion with a positive charge on the protonated amino group at one end and a negative charge on the dissociated carboxylic group at the other end of the molecule. This promotes attraction between the positively charged amino terminal of 5-ASA and negatively charged surface membrane proteins favoring retention of 5-ASA on the exterior surface of colonic epithelial cells[135,136]. *In vitro* studies of 5-ASA have shown that the site of action of 5-ASA is extracellular[137]. Its mode of action is that of an extracellular tetravalent reducing agent capable of donating four electrons per molecule for H_2O_2 and oxygen radical neutralization[138]. 5-ASA also sequesters ferrous ions (Fe^{+2})[139] possibly by electrostatic attraction to its (5-ASAs) negatively charged terminal thereby inhibiting the hydroxyl generating extracellular Haber-Weiss reaction.

5-ASA's extracellular site and mode of action precludes it from affecting the intracellular pathogenetic mechanisms leading to neoplastic transformation during disease quiescence. While in "remission" H_2O_2 generated during the radical induction phase and exiting the cell will be neutralized by luminal 5-ASA reducing the incidence of clinical reactivation; however, excessive intracellular H_2O_2 is free to diffuse into the nucleus causing oxidative DNA damage resulting in CRC in this clinically quiescent stage of disease.

CONCLUSION

The evidence presented in this paper points to excess hydrogen peroxide diffusing out of colonic epithelial cells as the initiating etiology of UC. Hydrogen peroxide (H_2O_2), a highly toxic oxidizing agent and by-product of normal aerobic cellular metabolism, is constantly being generated within all cells including colonic epithelial cells and must be immediately neutralized in order for the cells to survive.

The intracellular generation of H_2O_2 is determined by the metabolic and respiratory activity of the cell; however, the anti-oxidant capacity required to neutralize H_2O_2 resides within a genetically determined fixed range for each individual with significant inter-individual variability being expressed. This places a sub-group of individuals at the lowest end of anti-oxidant (H_2O_2 neutralizing) capacity. It is this sub-group of individuals that have the highest risk of developing UC when exposed to oxidant stressors.

Under appropriate conditions excess H_2O_2 generated due to the effect of oxidant stressors on cellular metabolism may overwhelm the genetically predetermined anti-oxidant/reducing capacity available within the cell resulting in intracellular H_2O_2 accumulation. This process is called "Radical Induction". Radical induction will initially manifest in the rectum which has the lowest anti-oxidant defense (H_2O_2 neutralizing) capacity of the entire GI tract coupled with the highest bacterial exposure[140-143]. This makes rectal epithelium especially vulnerable to oxidant injury.

Hydrogen peroxide is freely permeable through cell membranes and essentially forms one intracellular compartment. H_2O_2 generation is biochemically coupled to fundamental metabolic processes such as ATP (energy) production and ETC activity in addition to the enzymatic activity of nearly 100 intracellular enzyme systems. H_2O_2

production is therefore very sensitive to and will fluctuate with environmental influences that affect respiratory activity (tobacco use, stress, hyperthyroidism) and availability of specific enzyme substrate (i.e., xenobiotics, alcohol, vitamin B-6). Excess un-neutralized H_2O_2 will diffuse from any intracellular location to the extracellular space where it can be converted to the highly destructive hydroxyl radical via a metal catalyzed Haber-Weiss reaction causing significant oxidative damage to colonic epithelial TJs, BM and epithelial biomembranes, which are micro-anatomical structures that comprise the colonic barrier function. This in turn increases colonic mucosal permeability to luminal antigens resulting in the *initial* influx of WBCs (neutrophils) from the subjacent vasculature to the mucosal surface. This is a normal and expected immune response to antigenic exposure; a normal response to normal colonic flora.

Once present on the colonic mucosal surface, exposure to high concentrations of fecal bacterial antigens stimulates neutrophils to secrete their own tissue damaging oxygen radicals. Neutrophil mediated tissue damage attracts additional neutrophils from the subjacent intravascular compartment to the mucosal surface. This process is repeated until sufficient tissue anti-oxidant (glutathione) levels are encountered to temporarily halt its progression, sharply delineating diseased from normal tissue.

This self-perpetuating process of tissue destruction is called propagation and results in a proximally advancing edge of contiguous oxidative tissue destruction in adjacent epithelium whose anti-oxidant defense capacity has already been previously compromised during the radical induction phase. Continued inflammatory tissue destruction results in rectal bleeding and bloody diarrhea characteristic of this disease.

SUMMARY

Since Hale-White first coined the term "ulcerative colitis" in 1888[144] we have learnt that the clinical phase of this disease which begins with rectal bleeding is characterized by colonic mucosal inflammation mediated by the accumulation of WBCs (mainly neutrophils) within the colonic epithelium. Based on the histological findings in this phase, UC is classified as an inflammatory bowel disease. The mechanism of neutrophil-mediated tissue injury responsible for colonic bleeding has been well described[145].

To date however there is no satisfactory answer for why neutrophils accumulate within the colonic mucosa to begin with. The Radical Induction Theory of UC provides an explanation for this initial influx of neutrophils.

Radical Induction Theory states that H_2O_2 originating from colonic epithelial cells diffuses to the extracellular space resulting in oxidative damage and dissolution of intercellular TJs and BM, which are micro-anatomical structures that maintain the GI barrier function. Once compromised, the GI barrier can no longer exclude highly antigenic bacterial antigens from invading the normally sterile deeper layers of the colonic wall resulting in the initial influx of neutrophils to the mucosal surface. Continued accumulation of neutrophils results in extensive tissue damage and bleeding characteristic of this disease.

Radical Induction Theory implies two distinct phases of UC. The first phase is operational prior to any colonic bleeding. During this initial preclinical "Radical Induction" phase colonocytes are induced to generate excessive un-neutralized H_2O_2 due to effects of oxidant stressors upon cellular metabolism. Hydroxyl radical and H_2O_2 have very short half lives (nanoseconds and seconds to minutes respectively) which limits their destructive activity to intracellular molecules (i.e., DNA, enzymes) and local extracellular structures immediately adjacent to the cell (i. e., TJs and BM). Pro-inflammatory cytokines, however, may be carried to distal sites to exert their effect. Thus, initial intermittent extracellular diffusion of H_2O_2 from epithelial cells causes short lived local barrier compromise and transient immune activation resulting in cytokine production and distal extra-intestinal manifestations such as arthritis, uveitis, skin manifestations (i.e., pyoderma gangrenosum) and p-anca type antibodies. Continued oxidative insult to colonic barrier function culminates in neutrophilic infiltration.

A second (clinical) phase begins with rectal bleeding and signals further destructive GI barrier compromise secondary to neutrophil-mediated tissue damage. Continued stimulation of mucosal neutrophils by fecal bacteria converts the condition into an auto-stimulating/self-perpetuating process termed propagation.

Patients will normally present for treatment during the propagation phase, which will continue inexorably to the inflammatory destruction of the colon without outside intervention. Although clinical remission (cessation of rectal bleeding), endoscopic remission (normal macroscopic mucosal appearance) and histologic remission (no mucosal neutrophils) are important milestones, the lack of metabolic remission precludes complete reversal of this condition and predisposes to future reactivation and neoplastic transformation.

Fifty years of research has not demonstrated any antecedent immune vulnerability in patients with UC[146]. However, rather than a local mucosal immune dysfunction, high levels of H_2O_2 found in other cell lines in individuals with UC[147] suggests that this condition is a systemic disease of oxidant stress whose primary pathological manifestation is in the rectum, a unique body site with minimal anti-oxidant defense, high continuous oxidant stress and maximum bacterial antigenic exposure.

Thus, the crucial element required for mucosal integrity mentioned earlier consists of the biochemical machinery needed to detoxify hydrogen peroxide which, if allowed to accumulate, can oxidize and disintegrate TJ proteins leading to dissolution of barrier integrity and UC. Neutralization of intracellular hydrogen peroxide, therefore, constitutes a vital process whose dysfunction results in physical disintegration of gastrointestinal barrier function.

GPx (E.C. 1.11.1.9) in conjunction with co-factor glutathione, a self-replenishing tripeptide reducing agent, is responsible for 91% of H_2O_2 neutralization. Factors that decrease the activity of GPx or decrease the amount of available reduced glutathione will lead to increases in intracellular hydrogen peroxide which upon diffusion to the extracellular space will result in oxidative disruption of TJs and BM whose integrity is required for GI barrier function.

The oxidative stress to which UC patients are exposed

has exceeded their physiological antioxidant defense mechanisms. The significant inter-individual variability in oxidant neutralizing capacity places certain individuals at the lower threshold of their physiological (H_2O_2) reducing capability for any given environmental oxidant stress level. As the environment becomes increasingly toxic more individuals will succumb to its effects. UC, a purely descriptive term, may be more accurately described by its pathophysiology as oxidative colitis.

ACKNOWLEDGEMENTS

I wish to thank Drs. William W. Taylor and Charles E. Reed for their continued encouragement and support. I am deeply indebted to Kimberly D. Shepherd whose courageous existence made this work possible.

REFERENCES

1 **Hendrickson BA**, Gokhale R, Cho JH. Clinical aspects and pathophysiology of inflammatory bowel disease. *Clin Microbiol Rev* 2002; **15**: 79-94
2 **Farrell RJ,** Peppercorn MA. Ulcerative colitis. *Lancet* 2002; **359**: 331-340
3 **Hoffmann JC**, Pawlowski NN, Kuhl AA, Hohne W, Zeitz M. Animal models of inflammatory bowel disease: an overview. *Pathobiology* 2003; **70**: 121-130
4 **Meyers S**, Janowitz HD. The "natural history" of ulcerative colitis: an analysis of the placebo response. *J Clin Gastroenterol* 1989; **11**: 33-37
5 **Levine MD**, Kirsner JB, Klotz AP. A new concept of the pathogenesis of ulcerative colitis. *Science* 1951; **114**: 552-553
6 **Jacobson MA**, Kirsner JB. The basement membranes of the epithelium of the colon and rectum in ulcerative colitis and other diseases. *Gastroenterology* 1956; **30**: 279-285
7 **Benson K**, Bargen J. Fecal impaction. *Am J M Sc* 1939; **198**: 541-545
8 **Sheenan JF,** Brynjolfsson G. Ulcerative colitis following hydrogen peroxide enema: case report and experimental production with transient emphysema of colonic wall and gas embolism. *Lab Invest* 1960; **9**: 150-168
9 **Pumphery RE**. Hydrogen peroxide proctitis. *Am J Surg* 1951; **81**: 60-62
10 **Meyer CT**, Brand M, DeLuca VA, Spiro HM. Hydrogen peroxide colitis: a report of three patients. *J Clin Gastroenterol* 1981; **3**: 31-35
11 **Bilotta JJ**, Waye JD. Hydrogen peroxide enteritis: the "snow white" sign. *Gastrointest Endosc* 1989; **35**: 428-430
12 **Chance B**, Sies H, Boveris A. Hydroperoxide metabolism in mammalian organs. *Physiol Rev* 1979; **59**: 527-605
13 Enzyme Nomenclature Database [database on the internet]. Geneva Switzerland: Swiss Institute of Bioinformatics, Expert Protein Analysis System [cited 2003 Sept 14]. Search term: H(2) 0(2). Available from URL: http://us.expasy.org/enzyme
14 **Thannickal VJ**, Fanburg BL. Reactive oxygen species in cell signaling. *Am J Physiol Lung Cell Mol Physiol* 2000; **279**: L1005-L1028
15 **Parks DA**. Oxygen radicals: mediators of gastrointestinal pathophysiology. *Gut* 1989; **30**: 293-298
16 **Eaton JW**, Qian M. Molecular bases of cellular iron toxicity. *Free Radic Biol Med* 2002; **32**: 833-840
17 **Eberhardt MK**. Reactive Oxygen Metabolites: Chemistry and Medical Consequences. CRC Press 2001: the whole book. (Crucial reading for understanding oxygen radicals)
18 **Liu SS**. Generating, partitioning, targeting and functioning of superoxide in mitochondria. *Biosci Rep* 1997; **17**: 259-272
19 **Turrens JF**. Superoxide production by the mitochondrial respiratory chain. *Biosci Rep* 1997; **17**: 3-8
20 **Cadenas E**, Davies KJ. Mitochondrial free radical generation, oxidative stress, and aging. *Free Radic Biol Med* 2000; **29**: 222-230
21 **Boveris A**, Chance B. The mitochondrial generation of hydrogen peroxide. General properties and effect of hyperbaric oxygen. *Biochem J* 1973; **134**: 707-716
22 **Lemasters J**, Nieminen A. Mitochondria in Pathogenesis. *Kluwer Academic/Plenum Publishers* 2001: 281-286
23 **St-Pierre J**, Buckingham JA, Roebuck SJ, Brand MD. Topology of superoxide production from different sites in the mitochondrial electron transport chain. *J Biol Chem* 2002; **277**: 44784-44790
24 **Boveris A**, Cadenas E. Mitochondrial production of hydrogen peroxide regulation by nitric oxide and the role of ubisemiquinone. *IUBMB Life* 2000; **50**: 245-250
25 **Chen SX,** Schopfer P. Hydroxyl-radical production in physiological reactions. A novel function of peroxidase. *Eur J Biochem* 1999; **260**: 726-735
26 **Fridovich I**. Oxygen toxicity: a radical explanation. *J Exp Biol* 1998; **201**: 1203-1209
27 **Kehrer JP**. The Haber-Weiss reaction and mechanisms of toxicity. *Toxicology* 2000; **149**: 43-50
28 **Sheridan AM**, Fitzpatrick S, Wang C, Wheeler DC, Lieberthal W. Lipid peroxidation contributes to hydrogen peroxide induced cytotoxicity in renal epithelial cells. *Kidney Int* 1996; **49**: 88-93
29 **Esworthy RS**, Aranda R, Martin MG, Doroshow JH, Binder SW, Chu FF. Mice with combined disruption of Gpx1 and Gpx2 genes have colitis. *Am J Physiol Gastrointest Liver Physiol* 2001; **281**: G848-G855
30 **Moskovitz J**, Yim MB, Chock PB. Free radicals and disease. *Arch Biochem Biophys* 2002; **397**: 354-359
31 **Riedle B**, Kerjaschki D. Reactive oxygen species cause direct damage of Engelbreth-Holm-Swarm matrix. *Am J Pathol* 1997; **151**: 215-231
32 **Stadtman ER**. Metal ion-catalyzed oxidation of proteins: biochemical mechanism and biological consequences. *Free Radic Biol Med* 1990; **9**: 315-325
33 **Meyer TN**, Schwesinger C, Ye J, Denker BM, Nigam SK. Reassembly of the tight junction after oxidative stress depends on tyrosine kinase activity. *J Biol Chem* 2001; **276**: 22048-22055
34 **Schmitz H**, Barmeyer C, Gitter AH, Wullstein F, Bentzel CJ, Fromm M, Riecken EO, Schulzke JD. Epithelial barrier and transport function of the colon in ulcerative colitis. *Ann N Y Acad Sci* 2000; **915**: 312-326
35 **Kalluri R**, Cantley LG, Kerjaschki D, Neilson EG. Reactive oxygen species expose cryptic epitopes associated with autoimmune goodpasture syndrome. *J Biol Chem* 2000; **275**: 20027-20032
36 **Parrish AR**, Catania JM, Orozco J, Gandolfi AJ. Chemically induced oxidative stress disrupts the E-cadherin/catenin cell adhesion complex. *Toxicol Sci* 1999; **51**: 80-86
37 **Rao RK**, Baker RD, Baker SS, Gupta A, Holycross M. Oxidant induced disruption of intestinal epithelial barrier function: role of protein tyrosine phosphorylation. *Am J Physio* 1997; **273**: G812-G823
38 **Grisham MB**, Gaginella TS, von Ritter C, Tamai H, Be RM, Granger DN. Effects of neutrophil-derived oxidants on intestinal permeability, electrolyte transport, and epithelial cell viability. *Inflammation* 1990; **14**: 531-542
39 **Lodish H**, Berk A, Zirpursky L, Matsuaira P, Baltimore D, Darnell J. Molecular Cell Biology 5th ed. *W.H Freeman Co* 2004: 201-208
40 **Schmehl K**, Florian S, Jacobasch G, Salomon A, Korber J. Deficiency of epithelial basement membrane laminin in ulcerative colitis affected human colonic mucosa. *Int J Colorectal Dis* 2000; **15**: 39-48
41 **Karayiannakis AJ**, Syrigos KN, Efstathiou J, Valizadeh A, Noda M, Playford RJ, Kmiot W, Pignatelli M. Expression of catenins and E-cadherin during epithelial restitution in inflammatory bowel disease. *J Pathol* 1998; **185**: 413-418
42 **Jankowski JA**, Bedford FK, Boulton RA, Cruickshank N, Hall

C, Elder J, Allan R, Forbes A, Kim YS, Wright NA, Sanders DS. Alterations in classical cadherins associated with progression in ulcerative and Crohn's colitis. *Lab Invest* 1998; **78**: 1155-1167

43 **Hermiston ML**, Gordon JI. *In vivo* analysis of cadherin function in the mouse intestinal epithelium: essential roles in adhesion, maintenance of differentiation, and regulation of programmed cell death. *J Cell Biol* 1995; **129**: 489-506

44 **Hermiston ML**, Gordon JI. Inflammatory bowel disease and adenomas in mice expressing a dominant negative N-cadherin. *Science* 1995; **270**: 1203-1207

45 **Gitter AH**, Wullstein F, Fromm M, Schulzke JD. Epithelial barrier defects in ulcerative colitis: characterization and quantification by electrophysiological imaging. *Gastroenterology* 2001; **121**: 1320-1328

46 **Kitajima S**, Takuma S, Morimoto M. Changes in colonic mucosal permeability in mouse colitis induced with dextran sulfate sodium. *Exp Anim* 1999; **48**: 137-143

47 **Han D**, Williams E, Cadenas E. Mitochondrial respiratory chain-dependent generation of superoxide anion and its release into the intermembrane space. *Biochem J* 2001; **353**: 411-416

48 **Boveris A**, Oshino N, Chance B. The cellular production of hydrogen peroxide. *Biochem J* 1972; **128**: 617-630

49 **Rebrin I**, Kamzalov S, Sohal RS. Effects of age and caloric restriction on glutathione redox state in mice. *Free Radic Biol Med* 2003; **35**: 626-635

50 **Geerling BJ**, Dagnelie PC, Badart-Smook A, Russel MG, Stockbrugger RW, Brummer RJ. Diet as a risk factor for the development of ulcerative colitis. *Am J Gastroenterol* 2000; **95**: 1008-1013

51 **Jarnerot G**, Azad Khan AK, Truelove SC. The thyroid in ulverative colitis and Crohn's disease. II. Thyroid enlargement and hyperthyroidism in ulcerative colitis. *Acta Med Scand* 1975;**197**: 83-87

52 **Modebe O**. Autoimmune thyroid disease with ulcerative colitis. *Postgrad Med J* 1986; **62**: 475-476

53 **Venditti P**, Balestrieri M, Di Meo S, De Leo T. Effect of thyroid state on lipid peroxidation, antioxidant defences, and susceptibility to oxidative stress in rat tissues. *J Endocrinol* 1997; **155**: 151-157

54 **Goglia F**, Silvestri E, Lanni A. Thyroid hormones and mitochondria. *Biosci Rep* 2002; **22**: 17-32

55 **Venditti P**, Puca A, Di Meo S. Effects of thyroid state on H_2O_2 production by rat heart mitochondria: sites of production with complex I- and complex II-linked substrates. *Horm Metab Res* 2003; **35**: 55-61

56 **Pryor WA**, Arbour NC, Upham B, Church DF. The inhibitory effect of extracts of cigarette tar on electron transport of mitochondria and submitochondrial particles. *Free Radic Biol Med* 1992; **12**: 365-372

57 **Case records of the Massachusetts General Hospital**. Weekly clinicopathological exercises. Case 36-1997. A 58-year-old man with recurrent ulcerative colitis, bloody diarrhea, and abdominal distention. *N Engl J Med* 1997; **337**: 1532-1540

58 **Odes HS**, Fich A, Reif S, Halak A, Lavy A, Keter D, Eliakim R, Paz J, Broide E, Niv Y, Ron Y, Villa Y, Arber N, Gilat T. Effects of current cigarette smoking on clinical course of Crohn's disease and ulcerative colitis. *Dig Dis Sci* 2001; **46**: 1717-1721

59 **Abraham N**, Selby W, Lazarus R, Solomon M. Is smoking an indirect risk factor for the development of ulcerative colitis? An age-and sex-matched case-control study. *J Gastroenterol Hepatol* 2003; **18**: 139-146

60 **Li C**, Jackson RM. Reactive species mechanisms of cellular hypoxia-reoxygenation injury. *Am J Physiol Cell Physiol* 2002; **282**: C227-C241

61 **Crohn Burril B**. The clinical use of succinyl sulfathiazole (Sulfasuxidine). *Gastroenterology* 1943; **1**: 140-146

62 **Kirsner JB**, Palmer WL. Therapeutic problems in ulcerative colitis. *Med Clin North Am* 1953; **1**: 247-259

63 **Brown CH**. The treatment of acute and chronic ulcerative colitis. *Am Pract Dig Treat* 1958; **9**: 405-411

64 **Kirsner JB**. Ulcerative colitis-a challenge. *AMA Arch Intern Med* 1958; **101**: 3-8

65 **Tyndel M**, Forester W. Chronic ulcerative colitis: recovery after leukotomy. *Can Med Assoc J* 1956; **74**: 455-457

66 **Levy RW**, Wilkins H, Herrmann JD, Lisle AC, Rix A. Experiences with prefrontal lobotomy for intractable ulcerative colitis; preliminary report. *J Am Med Assoc* 1956; **160**: 1277-1280

67 **Levenstein S**, Prantera C, Varvo V, Scribano ML, Berto E, Andreoli A, Luzi C. Psychological stress and disease activity in ulcerative colitis: a multidimensional cross-sectional study. *Am J Gastroenterol* 1994; **89**: 1219-1225

68 **Theis MK**, Boyko EJ. Patient perceptions of causes of inflammatory bowel disease. *Am J Gastroenterol* 1994; **89**: 1920

69 **Levenstein S**, Prantera C, Varvo V, Scribano ML, Andreoli A, Luzi C, Arca M, Berto E, Milite G, Marcheggiano A. Stress and exacerbation in ulcerative colitis: a prospective study of patients enrolled in remission. *Am J Gastroenterol* 2000; **95**: 1213-1220

70 **Wood JD**, Peck OC, Tefend KS, Stonerook MJ, Caniano DA, Mutabagani KH, Lhotak S, Sharma HM. Evidence that colitis is initiated by environmental stress and sustained by fecal factors in the cotton-top tamarin (Saguinus oedipus). *Dig Dis Sci* 2000; **45**: 385-393

71 **Lechin F**, Van der Dijs B, Benaim M. Stress versus depression. Prog Neuropsychopharm. *Prog Neuropsychopharmacol Biol Psychiatry* 1996; **20**: 899-950

72 **Kurina LM**, Goldacre MJ, Yeates D, Gill LE. Depression and anxiety in people with inflammatory bowel disease. *J Epidemiol Community Health* 2001; **55**: 716-720

73 **Andrews H**, Barczak P, Allan RN. Psychiatric illness in patients with inflammatory bowel disease. *Gut* 1987; **28**: 1600-1604

74 **Granger DN, Parks DA**. Role of oxygen radicals in the pathogenesis of intestinal ischemia. *Physiologist* 1983; **26**: 159-164

75 **Parks DA**, Shah AK, Granger DN. Oxygen radicals: effects on intestinal vascular permeability. *Am J Physiol* 1984; **247**: G167-G170

76 **Parks DA**, Granger DN. Contributions of ischemia and reperfusion to mucosal lesion formation. *Am J Physiol* 1986; **250**: G749-G753

77 **Almy TP**, Tulin M. Alterations in colonic function in man under stress. *Gastroenetrology* 1947; **8**: 616-626

78 **Riaz AA**, Wan MX, Schafer T, Dawson P, Menger MD, Jeppsson B, Thorlacius H. Allopurinol and superoxide dismutase protect against leucocyte-endothelium interactions in a novel model of colonic ischaemia-reperfusion. *Br J Surg* 2002; **89**: 1572-1580

79 **Laroux FS**, Grisham MB. Immunological basis of inflammatory bowel disease: role of the microcirculation. *Microcirculation* 2001; **8**: 283-301

80 **Cho JH**, Nicolae DL, Ramos R, Fields CT, Rabenau K, Corradino S, Brant SR, Espinosa R, LeBeau M, Hanauer SB, Bodzin J, Bonen DK. Linkage and linkage disequilibrium in chromosome band 1p36 in American Chaldeans with inflammatory bowel disease. *Hum Mol Genet* 2000; **9**: 1425-1432

81 **Cho JH**, Nicolae DL, Gold LH, Fields CT, LaBuda MC, Rohal PM, Pickles MR, Qin L, Fu Y, Mann JS, Kirschner BS, Jabs EW, Weber J, Hanauer SB, Bayless TM, Brant SR. Identification of novel susceptibility loci for inflammatory bowel disease on chromosomes 1p, 3q, and 4q:evidence for epistasis between 1p and IBD1. *Proc Natl Acad Sci USA* 1998; **95**: 7502-7507

82 **Friedman G**, Goldschmidt N, Friedlander Y, Ben-Yehuda A, Selhub J, Babaey S, Mendel M, Kidron M, Bar-On H. A common mutation A1298C in human methylenetetrahydrofolate reductase gene: association with plasma total homocysteine and folate concentrations. *J Nutr* 1999; **129**: 1656-1661

83 **Goyette P**, Pai A, Milos R, Frosst P, Tran P, Chen Z, Chan M, Rozen R. Gene structure of human and mouse methylenetetrahydrofolate reductase (MTHFR). *Mamm Ge-*

nome 1998; **9**: 652-656
84 **Mahmud N**, Molloy A, McPartlin J, Corbally R, Whitehead AS, Scott JM, Weir DG. Increased prevalence of methylenetetrahydrofolate reductase C677T variant in patients with inflammatory bowel disease, and its clinical implications. *Gut* 1999; **45**: 389-394
85 **Nagano M**, Nakamura T, Niimi S, Fujino T, Nishimura T, Murayama N, Ishida S, Ozawa S, Saito Y, Sawada J. Substitution of arginine for cysteine 643 of the glucocorticoid receptor reduces its steroid-binding affinity and transcriptional activity. *Cancer Lett* 2002; **181**: 109-114
86 **Morgenstern I**, Raijmakers MT, Peters WH, Hoensch H, Kirch W. Homocysteine, cysteine, and glutathione in human colonic mucosa: elevated levels of homocysteine in patients with inflammatory bowel disease. *Dig Dis Sci* 2003; **48**: 2083-2090
87 **Upchurch GR**, Welch GN, Fabian AJ, Freedman JE, Johnson JL, Keaney JF, Loscalzo J. Homocyst(e)ine decreases bioavailable nitric oxide by a mechanism involving glutathione peroxidase. *J Biol Chem* 1997; **272**: 17012-17017
88 **Wilcken DE**, Wang XL, Adachi T, Hara H, Duarte N, Green K, Wilcken B. Relationship between homocysteine and superoxide dismutase in homocystinuria: possible relevance to cardiovascular risk. *Arterioscler Thromb Vasc Biol* 2000; **20**: 1199-1202
89 **Chen N**, Liu Y, Greiner CD, Holtzman JL. Physiologic concentrations of homocysteine inhibit the human plasma GSH peroxidase that reduces organic hydroperoxides. *J Lab Clin Med* 2000; **136**: 58-65
90 **Davidson RG**. Electrophoretic variants of human 6-phosphogluconate dehydrogenase: population and family studies and description of a new variant. *Ann Hum Genet* 1967; **30**: 355-361
91 **Parr CW**. Erythrocyte phosphogluconate dehydrogenase polymorphism. *Nature* 1966; **210**: 487-489
92 **Parr CW**, Fitch LI. Inherited quantitative variations of human phosphogluconate dehydrogenase. *Ann Hum Genet* 1967; **30**: 339-353
93 **Dern RJ**, Brewer GJ, Tashian RE, Shows TB. Hereditary variation of erythrocytic 6-phosphogluconate dehydrogenase. *J Lab Clin Med* 1966; **67**: 255-264
94 **Nelson MS**. Biochemical and genetic characterization of the Lowell variant. A new phenotype of 6-phosphogluconate dehydrogenase. *Hum Genet* 1982; **62**: 333-336
95 **Caprari P**, Caforio MP, Cianciulli P, Maffi D, Pasquino MT, Tarzia A, Amadori S, Salvati AM. 6-Phosphogluconate dehydrogenase deficiency in an Italian family. *Ann Hematol* 2001; **80**: 41-44
96 **Ciftci M**, Beydemir S, Yilmaz H, Bakan E. Effects of some drugs on rat erythrocyte 6-phosphogluconate dehydrogenase: an in vitro and in vivo study. *Pol J Pharmacol* 2002; **54**: 275-280
97 **Tomlinson JE**, Nakayama R, Holten D. Repression of pentose phosphate pathway dehydrogenase synthesis and mRNA by dietary fat in rats. *J Nutr* 1998; **118**: 408-415
98 **Gordillo E**, Machado A. Implication of lysine residues in the loss of 6-phosphogluconate dehydrogenase activity in aging human erythrocytes. *Mech Ageing Dev* 1991; **59**: 291-297
99 **Batist G**, Mekhail-Ishak K, Hudson N, DeMuys JM. Interindividual variation in phase II detoxification enzymes in normal human colon mucosa. *Biochem Pharmacol* 1988; **37**: 4241-4243
100 **Costa Rosa LF**, Curi R, Murphy C, Newsholme P. Effect of adrenaline and phorbol myristate acetate or bacterial lipopolysaccharide on stimulation of pathways of macrophage glucose, glutamine and O2 metabolism. Evidence for cyclic AMP-dependent protein kinase mediated inhibition of glucose-6-phosphate dehydrogenase and activation of NADP+-dependent 'malic' enzyme. *Biochem J* 1995; **310 (Pt 2)**: 709-714
101 **Snawder JE**, Lipscomb JC. Interindividual variance of cytochrome P450 forms in human hepatic microsomes: correlation of individual forms with xenobiotic metabolism and implications in risk assessment. *Regul Toxicol Pharmacol* 2000; **32**: 200-209
102 **Bertz RJ**, Granneman GR. Use of *in vitro* and *in vivo* data to estimate the likelihood of metabolic pharmacokinetic interactions. *Clin Pharmacokinet* 1997; **32**: 210-258
103 **Jowett SL**, Seal CJ, Pearce MS, Phillips E, Gregory W, Barton JR, Welfare MR. Influence of dietary factors on the clinical course of ulcerative colitis: a prospective cohort study. *Gut* 2004; **53**: 1479-1484
104 **Hoek JB**, Cahill A, Pastorino JG. Alcohol and mitochondria: a dysfunctional relationship. *Gastroenterology* 2002; **122**: 2049-2063
105 **Bailey SM**, Pietsch EC, Cunningham CC. Ethanol stimulates the production of reactive oxygen species at mitochondrial complexes I and III. *Free Radic Biol Med* 1999; **27**: 891-900
106 **Maher JJ**. Exploring alcohol's effects on liver function. *Alcohol Health Res World* 1997; **21**: 5-12
107 **Fernandez-Checa JC**, Kaplowitz N, Garcia-Ruiz C, Colell A, Miranda M, Mari M, Ardite E, Morales A. GSH transport in mitochondria: defense against TNF-induced oxidative stress and alcohol-induced defect. *Am J Physiol* 1997; **273**: G7-G17
108 **Huycke MM**, Abrams V, Moore DR. Enterococcus faecalis produces extracellular superoxide and hydrogen peroxide that damages colonic epithelial cell DNA. *Carcinogenesis* 2002; **23**: 529-536
109 **Liochev SI**, Fridovich I. Superoxide and iron: partners in crime. *IUBMB Life* 1999; **48**: 157-161
110 **Owen RW**, Spiegelhalder B, Bartsch H. Generation of reactive oxygen species by the faecal matrix. *Gut* 2000; **46**: 225-232
111 **Kawai M**, Sumimoto S, Kasajima Y, Hamamoto T. A case of ulcerative colitis induced by oral ferrous sulfate. *Acta Paediatr Jpn* 1992; **34**: 476-478
112 **Torisu T**, Esaki M, Matsumoto T, Nakamura S, Azuma K, Okada M, Tsuji H, Yao T, Iida M. A rare case of ulcerative colitis complicating Wilson's disease: possible association between the two diseases. *J Clin Gastroenterol* 2002; **35**: 43-45
113 **Topping DL**, Clifton PM. Short-chain fatty acids and human colonic function: roles of resistant starch and nonstarch polysaccharides. *Physiol Rev* 2001; **81**: 1031-1064
114 **Roediger WE**, Nance S. Metabolic induction of experimental ulcerative colitis by inhibition of fatty acid oxidation. *Br J Exp Pathol* 1986; **67**: 773-782
115 **Gulati S**, Ainol L, Orak J, Singh AK, Singh I. Alterations of peroxisomal function in ischemia-reperfusion injury of rat kidney. *Biochim Biophys Acta* 1993; **1182**: 291-298
116 **Bartlett K**, Eaton S. Mitochondrial beta-oxidation. *Eur J Biochem* 2004; **271**: 462-469
117 Database of protein families and domains [database on the internet]. Geneva Switzerland: Swiss Institute of Bioinformatics, Expert Protein Analysis System [cited 2003 Dec 27]. Search term: Thiolase. Available from: URL: http://us.expasy.org/prosite
118 **Chapman MA**, Grahn MF, Boyle MA, Hutton M, Rogers J, Williams NS. Butyrate oxidation is impaired in the colonic mucosa of sufferers of quiescent ulcerative colitis. *Gut* 1994; **35**: 73-76
119 **Den Hond E**, Hiele M, Evenepoel P, Peeters M, Ghoos Y, Rutgeerts P. *In vivo* butyrate metabolism and colonic permeability in extensive ulcerative colitis. *Gastroenterology* 1998; **115**: 584-590
120 **Harpaz N**, Talbot IC. Colorectal cancer in idiopathic inflammatory bowel disease. *Semin Diagn* 1996; **13**: 339-357
121 **Hussain SP**, Amstad P, Raja K, Ambs S, Nagashima M, Bennett WP, Shields PG, Ham AJ, Swenberg JA, Marrogi AJ, Harris CC. Increased p53 mutation load in noncancerous colon tissue from ulcerative colitis: a cancer-prone chronic inflammatory disease. *Cancer Res* 2000; **60**: 3333-3337
122 **Olinski R**, Gackowski D, Rozalski R, Foksinski M, Bialkowski K. Oxidative DNA damage in cancer patients: a cause or a consequence of the disease development? *Mutat Res* 2003; **531**: 177-190
123 **Alberts B**, Johnson A, Lewis J, Raff M, Roberts K, Walter P. Molecular Biology of the Cell. 4th ed. *Taylor Francis Group* 2002:

1313-1362
124 **Nakamura J**, Purvis ER, Swenberg JA. Micromolar concentrations of hydrogen peroxide induce oxidative DNA lesions more efficiently than millimolar concentrations in mammalian cells. *Nucleic Acids Res* 2003; **31**: 1790-1795
125 **Rosignoli P**, Fabiani R, De Bartolomeo A, Spinozzi F, Agea E, Pelli MA, Morozzi G. Protective activity of butyrate on hydrogen peroxide-induced DNA damage in isolated human colonocytes and HT29 tumour cells. *Carcinogenesis* 2001; **22**: 1675-1680
126 **Henle ES,** Linn S. Formation, prevention, and repair of DNA damage by iron/hydrogen peroxide. *J Biol Chem* 1997; **272**: 19095-19098
127 **Dreher D**, Junod AF. Role of oxygen free radicals in cancer development. *Eur J Cancer* 1996; **32A**: 30-38
128 **Hu JJ**, Dubin N, Kurland D, Ma BL, Roush GC. The effects of hydrogen peroxide on DNA repair activities. *Mutat Res* 1995; **336**: 193-201
129 **Munkholm P**. Review article: the incidence and prevalence of colorectal cancer in inflammatory bowel disease. *Aliment Pharmacol Ther* 2003; **18** Suppl 2: 1-5
130 **Askling J**, Dickman PW, Karlen P, Brostrom O, Lapidus A, Lofberg R, Ekbom A. Colorectal cancer rates among first-degree relatives of patients with inflammatory bowel disease: a population-based cohort study. *Lancet* 2001; **357**: 262-266
131 **Eaden J**. Review article: the data supporting a role for aminosalicylates in the chemoprevention of colorectal cancer in patients with inflammatory bowel disease. *Aliment Pharmacol Ther* 2003; **18** Suppl 2: 15-21
132 **Allgayer H**. Review article: mechanisms of action of mesalazine in preventing colorectal carcinoma in inflammatory bowel disease. *Aliment Pharmacol Ther* 2003; **18** Suppl 2: 10-14
133 **Eaden J**, Abrams K, Ekbom A, Jackson E, Mayberry J. Colorectal cancer prevention in ulcerative colitis: a case-control study. *Aliment Pharmacol Ther* 2000; **14**: 145-153
134 **Bernstein CN**, Blanchard JF, Metge C, Yogendran M. Does the use of 5-aminosalicylates in inflammatory bowel disease prevent the development of colorectal cancer? *Am J Gastroenterol* 2003; **98**: 2784-2788
135 **Pearson DC**, Jourd'heuil D, Meddings JB. The anti-oxidant properties of 5-aminosalicylic acid. *Free Radic Biol Med* 1996; **21**: 367-373
136 **Dull BJ**, Salata K, Van Langenhove A, Goldman P. 5-Aminosalicylate: oxidation by activated leukocytes and protection of cultured cells from oxidative damage. *Biochem Pharmacol* 1987; **36**: 2467-2472
137 **Williams JG,** Hallett MB. Effect of sulphasalazine and its active metabolite, 5-amino-salicylic acid, on toxic oxygen metabolite production by neutrophils. *Gut* 1989; **30**: 1581-1587
138 **Ahnfelt-Ronne I,** Nielsen OH. The antiinflammatory moiety of sulfasalazine, 5-aminosalicylic acid, is a radical scavenger. *Agents Actions* 1987; **21**: 191-194
139 **Yamada T**, Volkmer C, Grisham MB. The effects of sulfasalazine metabolites on hemoglobin-catalyzed lipid peroxidation. *Free Radic Biol Med* 1991; **10**: 41-49
140 **Roediger WE,** Babidge W. Human colonocyte detoxification. *Gut* 1997; **41**: 731-734
141 **Grisham MB**, MacDermott RP, Deitch EA. Oxidant defense mechanisms in the human colon. *Inflammation* 1990; **14**: 669-680
142 **Bourlioux Pierre**. Intestinal flora: role in colonization, resistance and other effects. [monograph on the Internet]. Châtenay-Malabry (France): University of Paris South, Dept of Microbiology [cited 2003 Jan 7] Available from URL: http://h0.web.u-psud.fr/microfun/ch1.html
143 **Guyton A**. Human Physiology and Mechanisms of Disease. 6th ed. W.B Saunders 1997: 3-4
144 **Baron JH**. Inflammatory bowel disease up to 1932. *Mt Sinai J Med* 2000; **67**: 174-189
145 **Grisham MB**. Oxidants and free radicals in inflammatory bowel disease. *Lancet* 1994; **344**: 859-861
146 **Kirsner JB**. Historical origins of current IBD concepts. *World J Gastroenterol* 2001; **7**: 175-184
147 **Cao W**, Vrees MD, Kirber MT, Fiocchi C, Pricolo VE. Hydrogen peroxide contributes to motor dysfunction in ulcerative colitis. *Am J Physiol Gastrointest Liver Physiol* 2004; **286**: G833-G843

Science Editor Guo SY **Language Editor** Elsevier HK

PO Box 2345, Beijing 100023, China
www.wjgnet.com
wjg@wjgnet.com

ELSEVIER

World J Gastroenterol 2005;11(16):2385-2389
World Journal of Gastroenterology ISSN 1007-9327

No association of the *matrix metalloproteinase 1* promoter polymorphism with susceptibility to esophageal squamous cell carcinoma and gastric cardiac adenocarcinoma in northern China

Xia Jin, Gang Kuang, Li-Zhen Wei, Yan Li, Rui Wang, Wei Guo, Na Wang, Shu-Mei Fang, Deng-Gui Wen, Zhi-Feng Chen, Jian-Hui Zhang

Xia Jin, Gang Kuang, Li-Zhen Wei, Yan Li, Wei Guo, Na Wang, Deng-Gui Wen, Zhi-Feng Chen, Shu-Mei Fang, Jian-Hui Zhang, Hebei Cancer Institute, Hebei Medical University, Shijiazhuang 050011, Hebei Province, China
Rui Wang, The Fourth Affiliated Hospital, Hebei Medical University, Shijiazhuang 050011, Hebei Province, China
Supported by the Grant from the Natural Science Foundation of China, No. 30371591, and Grant from Natural Science Foundation of Hebei Province, China, No. C200400062
Correspondence to: Professor Jian-Hui Zhang, Hebei Cancer Institute, Hebei Medical University, Jiankanglu 12, Shijiazhuang 050011, Hebei Province, China. jianhuizh@hotmail.com
Telephone: +86-311-6093338 Fax: +86-311-6077634
Received: 2004-03-20 Accepted: 2004-04-14

Abstract

AIM: To investigate association of the *2G* or *1G* single nucleotide polymorphism (SNP) in *matrix metalloproteinase 1* (*MMP1*) promoter with susceptibility to esophageal squam-ous cell carcinoma (ESCC) and gastric cardiac adenocarcinoma (GCA) in a population of North China.

METHODS: *MMP1* promoter SNP was genotyped by polymerase-chain reaction (PCR)-restriction fragment length polymorphism (RFLP) analysis in 417 cancer patients (234 ESCC and 183 GCA) and 350 healthy controls.

RESULTS: The genotype frequencies of the *MMP1* promoter SNP in healthy controls were 55.4% (*2G/2G*), 30% (*1G/2G*) and 14.6% (*1G/1G*), respectively. The genotype and allelotype distribution in ESCC and GCA patients was not significantly different from that in healthy controls (all *P* values were above 0.05). Compared with the *1G/1G* genotype, neither the *2G/2G* nor in combination with the *1G/2G* genotype significantly modified the risk of developing ESCC and GCA, the adjusted odds ratio was 1.28 (95%CI = 0.78-2.09), 1.23 (95%CI = 0.38-2.05) in ESCC and 1.39 (95%CI = 0.80-2.41), 1.34 (95%CI = 0.74-2.40) in GCA, respectively. When stratified by smoking status and family history of upper gastrointestinal cancer, the *2G/2G* genotype alone or in combination with the *1G/2G* genotype also did not show any significant influence on the risk of ESCC and GCA development. In addition, influence of the *MMP1* SNP on lymphatic metastasis in ESCC and GCA was also not obs-erved.

CONCLUSION: The *2G* or *1G* SNP in the *MMP1* promoter might not modify the risk of ESCC and GCA development and might not be used as a stratification marker to predict the potential of lymphatic metastasis in these two tumor types.

Key words: SNP; ESCC; GCA

Jin X, Kuang G, Wei LZ, Li Y, Wang R, Guo W, Wang N, Fang SM, Wen DG, Chen ZF, Zhang JH. No association of the *matrix metalloproteinase 1* promoter polymorphism with susceptibility to esophageal squamous cell carcinoma and gastric cardiac adenocarcinoma in northern China. *World J Gastroenterol* 2005; 11(16): 2385-2389
http://www.wjgnet.com/1007-9327/11/2385.asp

INTRODUCTION

Matrix metalloproteinases (MMPs) are a family of enzymes that degrade the extracellular matrix and have been implicated in invasion and metastasis of tumor cells. Twenty-six human MMPs have been identified currently and these enzymes are classified according to their substrate specificity and structural similarities[1]. MMP1 belongs to interstitial collagenase, a subfamily of MMPs that cleaves stromal collagens. *MMP1* gene is localized on 11q22 and expressed in a wide variety of normal cells, e.g., stromal fibroblasts, macrophages, endothelial cells and epithelial cells, and in various tumor cells[1]. The level of MMP1 expression, and its potential to mediate connective tissue degradation and tumor progression, can be influenced by a genetic variation in *MMP1* promoter[2]. This variation is a single nucleotide polymorphism (SNP) located at-1 607 bp, where an insertion of a guanine base (G) creates the sequence of 5'-GGAT-3', the core binding site for members of the EST family of transcription factors[2]. The *MMP1* SNP has been correlated to the risk of renal cell carcinoma[3], lung cancer[4] and colorectal cancer[5]. This polymorphism has also been associated with the invasiveness of cutaneous malignant melanoma[6], ovarian cancer[7] and colorectal cancer[8].

China is a country with high incidence regions of esophageal squamous cell carcinoma (ESCC) and gastric cardiac adeno-carcinoma (GCA). Although the expression of MMP1 was associated with local invasion and poor prognosis in ESCC[9] and gastric cancer[10], the role of the *MMP1* promoter SNP in the development and progression of ESCC and GCA is

still unknown. Since *in vitro* study suggested that the *MMP1* SNP might modify MMP1 expression by increasing its binding with transcription factors[2,11], we hypothesize that the genotype which leads to higher MMP1 expression (i.e., *2G/2G*) might increase the susceptibility to ESCC and GCA and enhance the potential of lymphatic metastasis of these two tumor types. Therefore, in the present study, we conducted a hospital-based case control study to explore the role of the *MMP1* promoter SNP in the development and lymphatic metastasis of ESCC and GCA in a population of north China.

MATERIALS AND METHODS

Subjects

This study included 417 patients (234 with ESCC and 183 with CAC) and 350 healthy individuals without overt cancer. The cases were outpatients for endoscopic biopsy or inpatients for tumor resection in the Fourth Affiliated Hospital, Hebei Medical University between 2001 and 2003. Histological tumor typing was carried out on basis of the biopsy or resection specimens in the Department of Pathology of the same hospital. The esophageal carcinomas were all squamous cell carcinomas. The gastric cardiac carcinomas were all adenocarcinomas with their epicenters at the gastroesophageal junction, i.e., from 1 cm above until 2 cm below the junction between the end of tubular esophagus and the beginning of the saccular stomach[12]. The healthy subjects, who had no history of cancer and genetic diseases, visited the same hospital for physical examination between 2001 and 2003. All of the cancer patients and control subjects were unrelated Han nationality and from Shijiazhuang city or its surrounding regions. Information on TNM staging was available from 131 ESCC and 94 GCA patients from hospital records and pathological diagnosis. Information on sex, age, smoking habit and family history was obtained from cancer patients and healthy controls by interview following sampling. Smokers were defined as formerly or currently smoking five cigarettes per day for at least 2 years. Individuals with at least one first-degree relative or at least two second-degree relatives having esophageal/cardiac/gastric cancer were defined as having a family history of upper gastrointestinal cancers (UGIC). The smoking status and family history were only available from a subset of cancer patients and healthy controls (Table 1). The study was approved by the Ethics Committee of Hebei Cancer Institute and informed consent was obtained from all recruited subjects.

DNA extraction

Five milliliters of venous blood from each subject was drawn in Vacutainer tubes containing EDTA and stored at 4 ℃. Genomic DNA was extracted within 1 wk after sampling by using proteinase K (Merck, Darmstadt, Germany) digestion followed by a salting out procedure according to the method published by Miller *et al*[13].

MMP1 promoter SNP genotyping

The *MMP1* genotyping was determined by PCR-RFLP assay. The PCR primers used for amplifying the *MMP-1* polymorphism were: forward 5'-TGACTTTTAAAACATAGTCTATGTTCA-3' and reverse 5'-TCTTGGATTGATTTGAGATAAGTCATAGC-3'[4]. The reverse primer was specially designed to introduce a recognition site of restriction enzyme *Alu*I (AGCT) by replacing a T with a G at the second position close to the 3' end of the primer. The *1G* allele has this recognition site, whereas the *2G* allele destroys the recognition site by inserting a guanine. The PCR was performed in a 20-μL volume containing 100 ng of DNA template, 2.0 μL of 10× PCR buffer, 1.5 mmoL of $MgCl_2$, 1 unit of *Taq*-DNA-polymerase (BioDev-Tech., Beijing, China), 200 μmoL of dNTPs and 200 nmoL of sense and antisense primers. The PCR cycling conditions were 5 min at 94 ℃ followed by 35 cycles of 30 s at 94 ℃, 30 s at 58 ℃, and 30 s at 72 ℃, with a final step at 72 ℃ for 5 min to allow for the complete extension of all PCR fragments. An 8 μL aliquot of PCR product was digested overnight at 37 ℃ in a 10-μL reaction containing 10 units of *Alu*I (TakaRa Biotechnology Co., Ltd, Dalian, China) and 1× reaction buffer. After overnight digestion, the products were resolved and separated on a 4% agarose gel stained with ethidium bromide. After electrophoresis, homozygous *2G* alleles were represented by a DNA band with a size of 269 bp, homozygous *1G* alleles were represented by DNA bands with sizes of 241 and 28 bp, whereas heterozygotes displayed a combination of both alleles (269, 241, and 28 bp). For a negative control, each PCR reaction used distilled water instead of DNA in the reaction system. For 10% of the samples, the reaction was repeated once for *MMP1* genotyping and all of the genotypes matched with the original results.

Statistical analysis

Statistical analysis was performed using SPSS10.0 software package (SPSS Company, Chicago, IL, USA). Comparison of the *MMP1* genotype distribution in the study groups was performed by means of two-sided contingency tables using χ^2 test. A probability level of 5% was considered significant. The odds ratio (OR) and 95%CI were calculated using an unconditional logistic regression model and adjusted according to age and sex.

RESULTS

The mean age of all ESCC cases was 54.1±10.2 years (range 34-76 years), of all GCA cases was 55.0±10.5 (range 37-76 years) and of controls was 51.7±10.7 years (range 30-68 years). The gender distribution in ESCC and GCA patients (72.2% and 73.2% men) was comparable to that in healthy controls (65.4% men) ($P = 0.08$ and 0.07, respectively). The proportion of smokers in ESCC patients (50.5%) was not significantly different from that in healthy controls (42.9%) ($\chi^2 = 2.79$, $P = 0.10$). However, smokers in GCA patients (55.4%) were more frequently seen than in healthy controls ($\chi^2 = 6.78$, $P = 0.01$). Therefore, smoking significantly increased the risk for GCA development (the age and sex adjusted OR = 1.64, 95%CI = 1.12-2.38). In addition, the frequency of a positive family history of UGIC in ESCC (30.4%) and GCA (39.7%) patients was significantly higher than that in healthy controls (4.7%) ($\chi^2 = 31.74$ and 47.87, respectively, $P<0.0001$). Thus, a family history of UGIC significantly increased the risk to develop ESCC (the age and sex adjusted OR = 7.89, 95%CI = 3.25-15.49) and GCA (the age and

sex adjusted OR = 13.24, 95%CI = 5.98-26.40). Among 131 ESCC patients with tumor resection, lymphatic metastasis was reported in 59 cases and the rest (72 cases) were diagnosed as lymph node negativity, whereas among 94 GCA patients with operation, positive and negative lymphatic metastases were reported in 46 and 48 cases, respectively. The demographic distribution of ESCC and GCA patients as well as healthy controls is shown in Table 1.

Table 1 Characteristics of ESCC, GCA patients, and healthy individuals

Groups	Control *n* (%)	ESCC*n* (%)	*P*[1]	GCA *n* (%)	*P*[1]
Sex					
Male	229 (65.4)	169 (72.2)	0.08	134 (73.2)	0.07
Female	121 (34.6)	65 (27.8)		49 (26.8)	
Mean age in yr (SD)	51.7 (10.7)	54.1 (10.2)	0.06[1]	55.0 (10.5)	0.06[2]
Smoking status[3]					
Ex-or current smoker	120 (42.9)	96 (50.5)	0.10	92 (55.4)	0.01[5]
Non-smoker	160 (57.1)	94 (49.5)		74 (44.6)	
Family history of UGIC[4]					
Positive	6 (4.7)	56 (30.4)	<0.0001[6]	62 (39.7)	<0.0001[6]
Negative	123 (95.3)	128 (69.6)		96 (60.3)	
MMP-1 SNP genotype					
2G/2G	194 (55.4)	130 (55.6)	0.611	12 (61.2)	0.35
1G/2G	105 (30.0)	76 (32.5)		51 (27.3)	
1G/1G	51 (14.6)	28 (11.9)		20 (10.9)	
MMP-1 SNP allelotype					
2G	493 (70.4)	336 (71.8)	0.61	275(75.1)	0.10
1G	207 (29.6)	132 (28.2)		91 (24.9)	

ESCC: esophageal squamous cell carcinoma; GCA: gastric cardiac adenocarcinoma; UGIC: upper gastrointestinal cancer. [1]*P* value for χ^2 test; [2]*P* value for *t* test; [3,4]information of smoking status and family history was available from a subset of subjects; [5]smoking significantly increased the risk for GCA development (the age and sex adjusted OR = 1.64, 95%CI = 1.12-2.38); [6]positive family history of UGIC significantly increased the risk of developing ESCC (the age and sex adjusted OR = 7.89, 95%CI = 3.25–15.49) and GCA (the age and sex adjusted OR = 13.24, 95%CI = 5.98-26.40).

MMP1 SNP genotyping was successfully performed in all study subjects. The SNP genotype distribution was not correlated with gender, age and smoking status both in healthy controls and in ESCC and GCA patients (data not shown). In healthy controls, the frequencies of the *2G/2G, 1G/2G* and *1G/1G* genotypes were 55.4%, 30.0% and 14.6% while the distribution of the *2G* and *1G* allele was 70.4% and 29.6%, respectively. The genotype distribution in healthy controls was not in Hardy-Weinberg equilibrium ($P = 0.002$). In contrast, the genotype frequencies in ESCC and GCA patients were consistent with Hardy-Weinberg equilibrium ($P = 0.10$ and 0.09, respectively).

As shown in Table 1, there was no statistic difference in allele distribution between ESCC, GCA patients and healthy controls ($\chi^2 = 0.25$ and 2.65, $P = 0.61$ and 0.10, respectively). The overall *MMP1* genotype distribution in ESCC and GCA patients was also not significantly different from that in healthy controls ($\chi^2 = 0.98$ and 2.08, $P = 0.61$ and 0.35, respectively). By using *1G/1G*, the genotype with a lower MMP1 expression as reference, neither the *2G/2G* genotype alone nor in combination with the *1G/2G* significantly modified the risk of ESCC and GCA, the adjusted OR for ESCC was 1.28 (95% CI = 0.78-2.09) and 1.23 (95% CI = 0.38-2.05), for GCA it was 1.39 (95% CI = 0.80-2.41) and 1.34 (95% CI = 0.74-2.40), respectively. When stratified by smoking status and family history of upper gastrointestinal cancer, the frequencies of the *MMP1* genotypes in ESCC and GCA patients were also not significantly different from that in healthy controls. Consistently, the *2G/2G* genotype, alone or in combination with the *1G/2G*, did not show any significant influence on the risk of ESCC and GCA in the stratification groups (Table 2), when compared with the *1G/1G* genotype.

Furthermore, we tried to identify that if *MMP1* genotyping played a role in predicting lymphatic metastasis in ESCC and GCA in the study subjects. As shown in Table 3, in both ESCC and GCA groups, the distribution of the *MMP1* genotypes was not significantly different between patients with

Table 2 Association analysis of the *MMP1* SNP with the risk of ESCC and GCA development

	1G/1G	2G/2G	2G/1G+2G/2G	aOR (95%CI)[3]	aOR (95%CI)[4]
Overall					
Normal	51 (14.9)	194 (55.4)	299 (85.4)		
ESCC	28 (12.0)	130 (55.6)	206 (88.0)	1.28 (0.78-2.09)	1.23 (0.38-2.05)
GCA	20 (10.9)	112 (61.2)	163 (89.1)	1.39 (0.80-2.41)	1.34 (0.74-2.40)
Non-smoker[1]					
Normal	25 (15.6)	89 (55.6)	135 (84.4)		
ESCC	10 (10.6)	58 (61.7)	84 (89.4)	1.55 (0.65-3.46)	1.54 (0.68-3.48)
GCA	10 (13.5)	40 (54.1)	64 (86.5)	1.12 (0.49-2.58)	1.20 (0.38-3.82)
Smoker					
Normal	18 (15.0)	64 (53.3)	102 (85.0)		
ESCC	14 (14.6)	46 (47.9)	82 (85.4)	1.03 (0.48-2.19)	0.93 (0.42-2.06)
GCA	8 (8.7)	59 (64.1)	84 (91.3)	1.80 (0.74-4.37)	1.36 (0.46-4.05)
Negative family history[2]					
ESCC	16 (12.5)	73 (57.0)	112 (87.5)	1.19 (0.65-2.18)	1.18 (0.63-2.20)
GCA	7 (7.3)	54 (56.2)	89 (92.7)	1.19 (0.56-2.51)	0.42 (0.16-1.04)
Positive family history[3]					
ESCC	8 (14.3)	29 (51.8)	48 (85.7)	1.02 (0.46-2.29)	0.95 (0.41-2.21)
GCA	10 (16.1)	38 (61.3)	52 (83.9)	0.95 (0.59-1.53)	0.72 (0.31-1.70)

ESCC: esophageal squamous cell carcinoma; GCA: gastric cardiac adenocarcinoma; [1,2]information of smoking status and family history was available from a subset of subjects; [3,4]the age and sex adjusted odds ratio of the *2G/2G* (c) and *1G/2G*+*2G/2G* genotype (d) against the *1G/1G* genotype.

or without lymphatic metastasis. Compared to the *1G/1G* genotype, neither the *2G/2G* nor the *1G/2G+2G/2G* genotype showed modification in the potential of lymphatic metastasis, with age and sex adjusted OR of 1.72 and 1.73 (95%CI = 0.58-5.33 and 0.60-4.97) in ESCC, and of 3.80 and 3.66 (95%CI = 0.71-20.41 and 0.71-18.87) in GCA, respectively.

Table 3 Influence of the *MMP-1* SNP on lymphatic metastasis in ESCC and GCA[1]

Groups	LM negative cases (%)	LM positive cases (%)	aOR (95%CI)[2]
ESCC			
1G/1G	12 (16.7)	6 (10.2)	1.0 (ref.)
2G/2G	31 (43.0)	29 (49.2)	1.72 (0.58-5.33)
1G/2G+2G/2G	60 (83.3)	53 (89.8)	1.73 (0.60-4.97)
GCA			
1G/1G	7 (14.6)	2 (4.4)	1.0 (ref.)
2G/2G	25 (52.1)	28 (60.9)	3.80 (0.71-20.41)
1G/2G+2G/2G	41 (85.4)	44 (95.6)	3.66 (0.71-18.87)

ESCC: esophageal squamous cell carcinoma; GCA: gastric cardiac adenocarcinoma; LM: lymphatic metastasis, [1]all of the 131 ESCC (53 LM positive and 60 negative) and 96 GCA patients (46 LM positive and 48 negative) with available related data were considered; [2]the age and sex adjusted odds ratio of the *2G/2G* and *2G/1G+1G/1G* genotype against the *1G/1G* genotype.

DISCUSSION

Several exogenous factors were correlated to the development of ESCC and GCA in China[14-18]. However, genetic background has been suggested to play important roles in cancer occurrence, as displayed in this study which showed that a family history of UGIC significantly increased the risk of ESCC and GCA. In addition, some polymorphic genes encoding metabolic enzymes, cell cycle regulators and mismatch repair enzymes, such as aldehyde dehydrogenase-2 (ALDH2)[19], cytochrome P450(CYP)[20], glutathione S-transferase (GST)[20], methylenetetrahydrofolate reductase (MTHFR)[21], NAD(P)H: quinone oxidoreductase 1 (NQO1)[22] , cyclin D1[23], X-ray repair cross-complementing group 1(XRCC1) and xeroderma pigmentosum group D (XPD)[24], have been found to be able to modify the susceptibility to chemically induced cancers including esophageal and gastric cardiac cancer. Therefore, these polymorphic genes, alone or in combination with each other or through interaction with exogenous risk factors, may be used as predicative parameters for screening individuals at a high risk of ESCC and GCA.

Carcinogenesis is a multicellular and multistage process in which destruction of the microenvironment is required for the conversion of normal tissue to tumor. Molecular analysis of the microenvironment and its deregulation during neoplasia is an essential step to understand the mechanism of malignant conversion process. Given the fact that MMPs, produced by both tumor and normal cells, influence the microenvironment by degrading extracellular matrix and altering cellular signals[25], they may be also involved in the initial stages of tumor development. MMP1 is the most highly expressed interstitial collagenase degrading fibrillar collagens, the most abundant protein in human body. Expression of MMP1 is partially regulated by the upstream promoter sequence in which the *2G* or *1G* SNP site is located. The *MMP1 2G/2G* genotype, which leads to higher expression of MMP1, has been reported to increase the susceptibility to renal cell carcinoma[3], lung cancer[4] and colorectal cancer[5]. The *2G/2G* genotype or the *2G* allele has also been correlated to poorer prognosis of cutaneous malignant melanoma[6], ovarian cancer[7] and colorectal cancer[8].

Since MMP1 overexpression was an independent factor for tumor invasion and prognosis in ESCC[9], we presently conducted a case control study to explore the role of the *MMP1* SNP in the development and lymphatic metastasis of ESCC as well as of GCA, another common carcinoma with similar geographic epidemic regions to ESCC. In line with the results from Caucasian[4] and Japanese[18] populations, the genotype distribution of the *MMP1* promoter SNP in our healthy controls was not in Hardy-Weinberg equilibrium. Although the underlying reason is unknown, the random recruitment of healthy controls and reproducible genotyping method used in this study should not influence the feasibility of control group.

In contrary to our expectation, the *MMP1* genotype distribution difference was not found between the two cancer groups and healthy controls, as well as in the stratification comparisons according to smoking status (never smoking or currently and previously smoking) and family history of UGIC. The result suggests that although the *MMP1* promoter SNP is correlated with some cancer types, this genetic alteration may not be associated with the susceptibility to ESCC and GCA in a population of north China. In addition, lymphatic metastasis, which is one of the main factors to influence prognosis and survival of upper gastrointestinal tumors, is also not correlated with this *MMP1* promoter polymorphism, suggesting that MMP1 expression might influence ESCC progress via mechanisms other than regulation by the promoter SNP. Our result is consistent with a recent study on gastric cancer in Japan, which showed that the genotype distribution of the *MMP1* promoter SNP in cancer patients was similar to that in healthy controls, and the SNP showed no influence on tumor invasion, lymph node metastasis and clinical stage of gastric cancer[26].

In summary, the result from gastric cancer[26], together with the finding in this study, indicate that the *MMP1* promoter SNP might not be used as a stratification marker to predict the susceptibility to upper gastrointestinal carcinoma and the potential of lymphatic metastasis in these tumor types, at least in Asian population.

ACKNOWLEDGMENTS

We greatly acknowledge Mr. Li-Wei Zhang, Mr. Xiao-Qing Guo, Mr. Ming He, and Mr. Ming-Li Wu in the Fourth Affiliated Hospital of Hebei Medical University, China, for their assistance in recruiting study subjects.

REFERENCES

1 **Brinckerhoff CE,** Rutter JL, Benbow U. Interstitial collagenases as markers of tumor progression. *Clin Cancer Res* 2000; **6**: 4823-4830

2 **Rutter JL,** Mitchell TI, Buttice G, Meyers J, Gusella JF, Ozelius LJ, Brinckerhoff CE. A single nucleotide polymorphism in the

matrix metalloproteinase-1 promoter creates an Ets binding site and augments transcription. *Cancer Res* 1998; **58**: 5321-5325

3 **Hirata H,** Naito K, Yoshihiro S, Matsuyama H, Suehiro Y, Hinoda Y. A single nucleotide polymorphism in the matrix metalloproteinase-1 promoter is associated with conventional renal cell carcinoma. *Int J Cancer* 2003; **106**: 372-374

4 **Zhu Y,** Spitz MR, Lei L, Mills GB, Wu X. A single nucleotide polymorphism in the matrix metalloproteinase-1 promoter enhances lung cancer susceptibility. *Cancer Res* 2001; **61**: 7825-7829

5 **Hinoda Y,** Okayama N, Takano N, Fujimura K, Suehiro Y, Hamanaka Y, Hazama S, Kitamura Y, Kamatani N, Oka M. Association of functional polymorphisms of matrix metalloproteinase (MMP)-1 and MMP-3 genes with colorectal cancer. *Int J Cancer* 2002; **102**: 526-529

6 **Ye S,** Dhillon S, Turner SJ, Bateman AC, Theaker JM, Pickering RM, Day I, Howell WM. Invasiveness of cutaneous malignant melanoma is influenced by matrix metalloproteinase 1 gene polymorphism. *Cancer Res* 2001; **61**: 1296-1298

7 **Kanamori Y,** Matsushima M, Minaguchi T, Kobayashi K, Sagae S, Kudo R, Terakawa N, Nakamura Y. Correlation between expression of the matrix metalloproteinase-1 gene in ovarian cancers and an insertion/deletion polymorphism in its promoter region. *Cancer Res* 1999; **59**: 4225-4227

8 **Ghilardi G,** Biondi ML, Mangoni J, Leviti S, DeMonti M, Guagnellini E, Scorza R. Matrix metalloproteinase-1 promoter polymorphism 1G/2G is correlated with colorectal cancer invasiveness. *Clin Cancer Res* 2001; **7**: 2344-2346

9 **Murray GI,** Duncan ME, O'Neil P, McKay JA, Melvin WT, Fothergill JE. Matrix metalloproteinase-1 is associated with poor prognosis in oesophageal cancer. *J Pathol* 1998; **185**: 256-261

10 **Inoue T,** Yashiro M, Nishimura S, Maeda K, Sawada T, Ogawa Y, Sowa M, Chung KH. Matrix metalloproteinase-1 expression is a prognostic factor for patients with advanced gastric cancer. *Int J Mol Med* 1999; **4**: 73-77

11 **Wyatt CA,** Coon CI, Gibson JJ, Brinckerhoff CE. Potential for the 2G single nucleotide polymorphism in the promoter of matrix metalloproteinase to enhance gene expression in normal stromal cells. *Cancer Res* 2002; **62**: 7200-7202

12 **Siewert JR,** Stein HJ. Classification of adenocarcinoma of the oesophagogastric junction. *Br J Surg* 1998; **85:** 1457-1459

13 **Miller SA,** Dykes DD, Polesky HF. A simple salting out procedure for extracting DNA from human nucleated cells. *Nucleic Acids Res* 1988; **16**: 1215

14 **Yokokawa Y,** Ohta S, Hou J, Zhang XL, Li SS, Ping YM, Nakajima T. Ecological study on the risks of esophageal cancer in Ci-Xian, China: the importance of nutritional status and the use of well water. *Int J Cancer* 1999; **83**: 620-624

15 **van Gijssel HE,** Divi RL, Olivero OA, Roth MJ, Wang GQ, Dawsey SM, Albert PS, Qiao YL, Taylor PR, Dong ZW, Schrager JA, Kleiner DE, Poirier MC. Semiquantitation of polycyclic aromatic hydrocarbon-DNA adducts in human esophagus by immunohistochemistry and the automated cellular imaging system. *Cancer Epidemiol Biomarkers Prev* 2002; **11**: 1622-1629

16 **Guo W,** Blot WJ, Li JY, Taylor PR, Liu BQ, Wang W, Wu YP, Zheng W, Dawsey SM, Li B. A nested case-control study of oesophageal and stomach cancers in the Linxian nutrition intervention trial. *Int J Epidemiol* 1994; **23**: 444-450

17 **Ji BT,** Chow WH, Yang G, McLaughlin JK, Gao RN, Zheng W, Shu XO, Jin F, Fraumeni JF, Gao YT. The influence of cigarette smoking, alcohol, and green tea consumption on the risk of carcinoma of the cardia and distal stomach in Shanghai, China. *Cancer* 1996; **77**: 2449-2457

18 **Matsha T**, Erasmus R, Kafuko AB, Mugwanya D, Stepien A, Parker MI. Human papillomavirus associated with oesophageal cancer. *J Clin Pathol* 2002; **55**: 587-590

19 **Matsuo K,** Hamajima N, Shinoda M, Hatooka S, Inoue M, Takezaki T, Tajima K. Gene-environment interaction between an aldehyde dehydrogenase-2 (ALDH2) polymorphism and alcohol consumption for the risk of esophageal cancer. *Carcinogenesis* 2001; **22**: 913-916

20 **Tan W,** Song N, Wang GQ, Liu Q, Tang HJ, Kadlubar FF, Lin DX. Impact of genetic polymorphisms in cytochrome P450 2E1 and glutathione S-transferases M1, T1, and P1 on susceptibility to esophageal cancer among high risk individuals in China. *Cancer Epidemiol Biomarkers Prev* 2000; **9**: 551-556

21 **Song C,** Xing D, Tan W, Wei Q, Lin D. Methylenetetrahydrofolate reductase polymorphisms increase risk of esophageal squamous cell carcinoma in a Chinese population. *Cancer Res* 2001; **61**: 3272-3275

22 **Zhang J,** Schulz WA, Li Y, Wang R, Zotz R, Wen D, Siegel D, Ross D, Gabbert HE, Sarbia M. Association of NAD(P)H: quinone oxidoreductase 1 (NQO1) C609T polymorphism with esophageal squamous cell carcinoma in a German Caucasian and a northern Chinese population. *Carcinogenesis* 2003; **24**: 905-909

23 **Zhang J,** Li Y, Wang R, Wen D, Sarbia M, Kuang G, Wu M, Wei L, He M, Zhang L, Wang S. Association of cyclin D1 (G870A) polymorphism with susceptibility to esophageal and gastric cardiac carcinoma in a northern Chinese population. *Int J Cancer* 2003; **105**: 281-284

24 **Xing D,** Qi J, Miao X, Lu W, Tan W, Lin D. Polymorphisms of DNA repair genes XRCC1 and XPD and their associations with risk of esophageal squamous cell carcinoma in a Chinese population. *Int J Cancer* 2002; **100**: 600-605

25 **Lukashev ME,** Werb Z. ECM signalling: orchestrating cell behaviour and misbehaviour. *Trends Cell Biol* 1998; **8**: 437-441

26 **Matsumura S,** Oue N, Kitadai Y, Chayama K, Yoshida K, Yamaguchi Y, Toge T, Imai K, Nakachi K, Yasui W. A single nucleotide polymorphism in the MMP-1 promoter is correlated with histological differentiation of gastric cancer. *J Cancer Res Clin Oncol* 2004; **130**: 259-265

Science Editor Zhu LH **Language Editor** Elsevier HK

PO Box 2345, Beijing 100023, China
www.wjgnet.com
wjg@wjgnet.com

ELSEVIER

World J Gastroenterol 2005;11(16):2390-2397
World Journal of Gastroenterology ISSN 1007-9327

• *GASTRIC CANCER* •

Gene expression profile differences in gastric cancer, pericancerous epithelium and normal gastric mucosa by gene chip

Chuan-Ding Yu, Shen-Hua Xu, Hang-Zhou Mou, Zhi-Ming Jiang, Chi-Hong Zhu, Xiang-Lin Liu

Chuan-Ding Yu, Shen-Hua Xu, Hang-Zhou Mou, Zhi-Ming Jiang, Chi-Hong Zhu, Xiang-Lin Liu, Zhejiang Cancer Research Institute, Hangzhou 310022, Zhejiang Province, China
Co-first-authors: Chuan-Ding Yu and Shen-Hua Xu
Correspondence to: Dr. Chuan-Ding Yu, Zhejiang Cancer Research Institute, No. 38 Guangji Road, Hangzhou 310022, Zhejiang Province, China. yuchuanding@hotmail.com
Telephone: +86-571-88122588 Fax: +86-571-88122508
Received: 2004-04-28 Accepted: 2004-06-28

Abstract

AIM: To study the difference of gene expression in gastric cancer (T), pericancerous epithelium (P) and normal tissue of gastric mucosa (C), and to screen an associated novel gene in early gastric carcinogenesis by oligonucleotide microarray.

METHODS: U133A (Affymetrix, Santa Clara, CA) gene chip was used to detect the gene expression profile difference in T, P and C, respectively. Bioinformatics was used to analyze the detected results.

RESULTS: When gastric cancer was compared with normal gastric mucosa, 766 genes were found, with a difference of more than four times in expression levels. Of the 766 genes, 530 were up-regulated (Signal Log Ratio [SLR]>2), and 236 were down-regulated (SLR<-2). When pericancerous epithelium was compared with normal gastric mucosa, 64 genes were found, with a difference of more than four times in expression levels. Of the 64 genes, 50 were up-regulated (SLR>2), and 14 were down-regulated (SLR<-2). Compared with normal gastric mucosa, a total of 143 genes with a difference in expression levels (more than four times, either in cancer or in pericancerous epithelium) were found in gastric cancer (T) and pericancerous epithelium (P). Of the 143 genes, 108 were up-regulated (SLR>2), and 35 were down-regulated (SLR<-2).

CONCLUSION: To apply a gene chip could find 143 genes associated with the genes of gastric cancer in pericancerous epithelium, although there were no pathological changes in the tissue slices. More interesting, six genes of pericancerous epithelium were up-regulated in comparison with genes of gastric cancer and three genes were down-regulated in comparison with genes of gastric cancer. It is suggested that these genes may be related to the carcinogenesis and development of early gastric cancer.

Key words: Gastric cancer; Pericancerous epithelium; Gene expression profile; Gene chip

Yu CD, Xu SH, Mou HZ, Jiang ZM, Zhu CH, Liu XL. Gene expression profile differences in gastric cancer, pericancerous epithelium and normal gastric mucosa by gene chip. *World J Gastroenterol* 2005; 11(16): 2390-2397
http://www.wjgnet.com/1007-9327/11/2390.asp

INTRODUCTION

Differentially expressed genes from different specimens may be detected with parallel analysis by gene chips. This technique possesses many advantages, of which the greatest is to improve traditional experiments by allowing a single or several gene expression differences to be observed in a single test. More and more cDNA microarray methods are applied in the study of gene expression. In the paper, a gene chip technique was used to analyze the different gene expression patterns in gastric cancer, its pericancerous epithelium tissue and normal tissue of gastric mucosa. Exploring tumor-associated gene-clusters and their role in the process of carcinogenesis and development of gastric cancer is helpful in gaining a comprehensive understanding of the molecular mechanisms in cell transformation. This may also provide molecular markers and target genes for clinical diagnosis and prevention, and treatment of gastric cancer.

MATERIALS AND METHODS

Materials

Gastric cancer tissues and pericancerous epithelial tissues as well as normal gastric mucosa tissues were obtained from five patients who underwent gastrectomy at our hospital. For each specimen one part was immediately snap-frozen in liquid nitrogen and the other was used for histopathological examination to ensure all the pericancerous and control gastric mucosa without cancer cells but with their corresponding histological appearance. The clinical and pathological data of these patients are shown in Table 1.

Oligonucleotide microarray gene chip

Human full-length genome U133A (Affymetrix, Santa Clara, CA) contained about 18 000 full-length genes from the unigene GenBank.

Sample preparation

Total RNA was extracted by a single step method[1]. Briefly, after T, P and C tissues were taken out from liquid nitrogen, specimens were ground completely into tiny powders while liquid nitrogen was added into a ceramic mortar. TRIzol was used to extract total RNA. A QIAGEN reagent kit was used to purify the total RNA. A spectrophotometer was

Table 1 Clinical and pathological data of five patients with gastric cancer

Number of In-P	Name	Sex	Age (yr)	Pathological diagnosis	Lymph metastasis	Clinical stage
113702	Jiang	F	45	Lesser curvature of stomach invasion ulcer type moderate differentiation adenocarcinoma invasion serosa	1/35	III
123730	Xu	M	48	Anterior wall in body of stomach moderate differentiation adenocarcinoma invasion muscular layers and nerve	1/17	III
123673	Tang	F	57	Lesser curvature in cardia of stomach invasion ulcer type moderate differentiation adenocarcinoma invasion serosa	1/14	III
123808	Yu	F	49	Anterior wall in cardia of stomach poor-moderate differentiation adenocarcinoma, a part of mucinous adenocarcinoma and esophagus of extremities inferior	0/35	II
123733	Huang	M	60	Cardia of stomach node type moderate differentiation adenocarcinoma invasion muscular layer esophagus	5/22	III

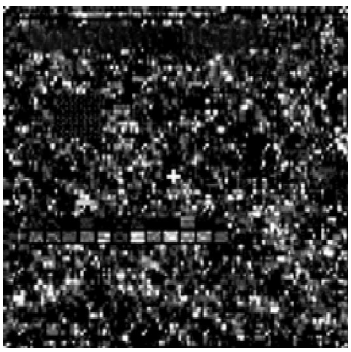

Figure 1 Control cRNA *vs* test chip post-hybridization.

used to calculate the total RNA concentration on the basis of optical density of A_{260}. Total RNA was taken out from the T, P and C tissues and mixed, respectively. T7-(dT)24 was made for a primer, the first strand of cDNA was synthesized through retro-transcription on the base of the first strand as a template to synthesize the second strand. After the double stranded DNA was purified, a high yield RNA transcript labeling kit was used to transcribe synthetic cRNA directly. Then the transcribed cRNA was purified and treated at high temperature to produce fragments of 35-200 bp cRNA.

Hybridization and washing

The fragments of cRNA were mixed with other control agents to prepare a hybridization solution, the hybridization solution was injected into the chip. The three chips (T, P, C) were put into the hybridization oven (640 type) for 16 h to finish the hybridization procedure. The chips were taken out from the hybridization oven to recover the hybridization solution, then each composition elution and staining were automatically completed in the Fluidics Station 400.

Fluorescence scanning and result analysis

The chip was scanned with a GeneChip scanner. The intensity value of a fluorescent signal was obtained by expressing those genes. An internal reference gene (housekeeping gene) was chosen in advance. With regard to the primary signals, data were normalized and corrected. The acquired image was analyzed by Microarray suit software using a digital computer, and the intensity of fluorescence signals and its ratio were calculated.

RESULTS

Quantity judgment of the test chip

Each scanning profile was shown after hybridization with the test chip (Figure 1). A clearly printed character "GeneChip test" was on the upper of the profile. A lot of spots and well-distributed lines were around the profile. Some spots were on the four corners and the character "+" was clear. There was a good quantity between the gene chip and the samples of RNA. So this was a complete and reliable result of the detecting gene chip. Then, the samples from three groups were hybridized with U133A gene chip and scanned, respectively.

Hybridization result of the sample chip

A scanning profile was obtained from the samples of three

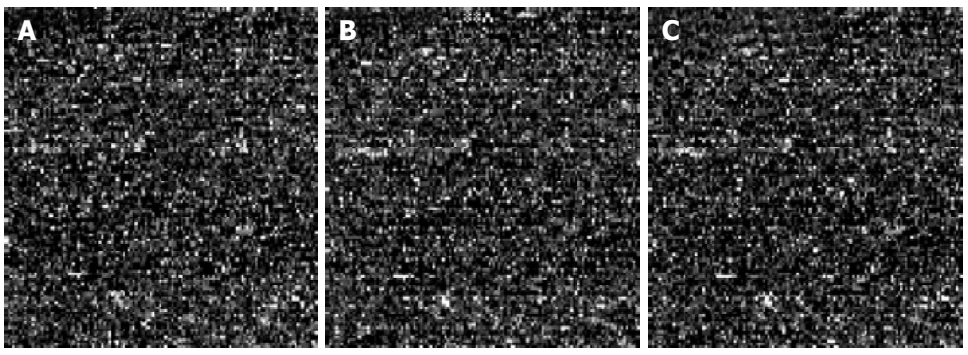

Figure 2 Hybridization results of the sample chip of scanning results. **A**: Post-hybridization of scanning results in control cRNA *vs* U133A chip; **B**: Post-hybridization of scanning results in gastric cancer group cRNA *vs* U133A chip; **C**: Post-hybridization of scanning results in pericancerous group cRNA *vs* U133A chip.

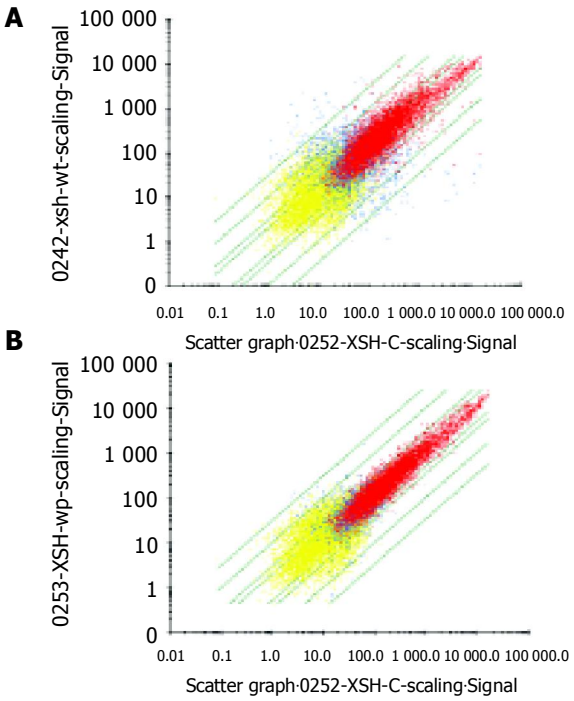

Figure 3 Scatter plots in gastric cancer and pericancerous tissues **A**: Scatter plots in gastric cancer tissue *vs* control **B**: Scatter plots in pericancerous tissue *vs* control.

groups after being hybridized with U133A gene chip (Figure 2). The scatter plots are shown in Figure 3.

Bioinformatics was used to detect and analyze the number of differentially expressed genes in gastric cancer (T) or pericancerous tissues (P). The results were compared to the normal gastric mucosa as shown in Table 2.

Table 2 Differentially expressed gene number in T, P and C

Numbers of genes	Up-regulated		Down-regulated	
	SLR>2	SLR>3	SLR <-2	SLR <-3
T *vs* C	530	157	236	113
P *vs* C	50	17	14	7
T and P *vs* C	108	21	35	17

Although there were no pathological changes in the tissue slices, 143 genes were found. More interesting, six genes of pericancerous epithelium were up-regulated compared to gastric cancer and three genes were down-regulated compared to gastric cancer. Their functions were related to the activity of a number of factors such as lipid transporter factor, electron transporter, receptor of signal protein, growth factor, ATP dependent RNA helicase (Table 3).

T and P were compared with C. The gene molecular function of a simultaneous expression difference belonged to nucleic acid binding activity (including RNA, DNA), protein binding activity (calcium, growth factor, cellular skeleton), enzyme activity. The functions of 34 genes were unknown (Table 4).

Genes with a difference of more than eight times are listed in Tables 5 and 6.

DISCUSSION

Gastric cancer is one of the most common malignant tumors in China. At present, its treatment has been greatly improved,

Table 3 Up-regulated and down-regulated genes

Probe Set ID	T *vs* C SLR	P *vs* C SLR	Name	GO molecular function
202580-x-at	2	2.4	Forkhead box M1	GO:3702; RNA polymerase II transcription factor activity; traceable author statement GO:3700; transcription factor activity; traceable author statement
203098-at	2.3	2.4	Chromodomain protein, Y chromosome-like	GO:3682; chromatin binding; inferred from electronic annotation GO:3824; enzyme activity; inferred from electronic annotation
203334-at	3.1	3.8	DEAD/H (Asp-Glu-Ala-Asp/His) box polypeptide 8 (RNA helicase)	GO:3723; RNA binding; inferred from electronic annotation GO:8248; pre-mRNA splicing factor activity; traceable author statement GO:5524; ATP binding; inferred from electronic annotation GO:4004; ATP dependent RNA helicase activity; traceable author statement
208152-s-at	1.9	2.1	DEAD/H (Asp-Glu-Ala-Asp/His) box polypeptide 21	GO:3723; RNA binding; inferred from electronic annotation GO:5524; ATP binding; inferred from electronic annotation GO:4004; ATP dependent RNA helicase activity; traceable author statemen
209820-s-at	2.2	2.3	Transducin (beta)-like 3	GO:5057; receptor signaling protein activity; predicted/computed
217173-s-at	3.4	3.6	Low density lipoprotein receptor (familial hypercholesterolemia)	GO:5041; low-density lipoprotein receptor activity; traceable author statement GO:5509; calcium ion binding; inferred from electronic annotation GO:8034; lipoprotein binding; traceable author statement GO:5319; lipid transporter activity; inferred from electronic
207102-at	-2.4	-3.6	Aldo-keto reductase family 1, member D1 (delta 4-3-ketosteroid-5-beta-reductase)	GO:5489; electron transporter activity; experimental evidence
208580-x-at	-2.7	-3	H4 histone family, member E (H4FE)	Unknown
218730-s-at	-2.5	-3.3	Osteoglycin (osteoinductive factor, mimecan)	GO:8083; growth factor activity; inferred from electronic annotation

Table 4 Comparison between gene molecular functions of T, P and C

Molecular function	Up-regulated (SLR> 2)	Down-regulated (SLR <-2)
Enzyme activity	15	4
Enzyme regular activity	4	0
Structural molecule activity	3	1
Transcription factor activity	3	0
Nucleic acid binding (RNA, DNA)	16	5
Protein binding activity (Ca , GF, cell skeleton)	14	7
Carbohydrate binding activity	3	0
Metal ion binding activity	1	0
Signal transduction activity (receptor, GF)	7	3
Sport activity	2	1
Transporter activity (electron, ion, protein)	7	6
Tumor antigen	2	0
Tumor suppressor	3	0
Apoptosis suppressor	1	0
Fibrinogen	0	1
Unknown	27	7
Total	108	35

but it still is one of the principal diseases to seriously hurt people's health. To explore its etiology and to seek the ideal and early molecular markers, and to develop a new method of gene therapy are a new direction against cancers. Carcinogenesis is a series of molecular changes caused by abnormal expression of tumor-associated genes or inactivation of tumor suppression genes. The gene chip has been widely used to detect gene expression differences in various specimens by parallel analysis. The largest advantage of this technique is that it changes the traditional experiment where only a single or several gene expression differences could be observed in one procedure. Therefore, more and more cDNA microarrays have been applied to the study of gene expression. For example, gene chip was used to study the relationship between *Helicobacter pylori* and gastric malignancy[2-6], to research the multidrug-resistance to chemotherapy[7-9], to establish carcinogensis models of gastric carcinoma[10], to find gastric cancer and its metastasis associated genes[11-14], to analyse gastric carcinoma and its prognosis and to compare gastric carcinoma with its normal gastric mucosa[15-29].

We used the oligonucleotide of gene chip technique to analyze the gene expression profile difference in gastric cancer, pericancerous epithelium and normal mucosa. When gastric cancer was compared with normal gastric mucosa, a total of 766 genes were found with a difference of more than four times in expression levels. Of the 766 genes, 530 were up-regulated (SLR>2), and 236 were down-regulated (SLR>-2), suggesting that these genes are associated with the occurrence and development of gastric cancer. When pericancerous epithelium was compared with normal gastric mucosa, a total of 64 genes were found, with a difference of more than four times in expression levels. Of the 64 genes, 50 were up-regulated (SLR>2) and 14 were down-regulated (SLR>-2). Compared with normal gastric mucosa, a total of 143 genes with a difference in expression levels (more than four times, either in cancer or in pericancerous epithelium) were found in gastric cancer (T) and pericancerous epithelium (P). Of the 143 genes, 108 were up-regulated (SLR>2) and 35 were down-regulated (SLR>-2). Although an abnormal appearance of pericancerous epithelium was not found in pathological examination, but the 143 genes were shown to have differences in gene expression levels. A more interesting finding was that six genes of pericancerous epithelium were up-regulated compared to gastric cancer and three genes were down-regulated compared to gastric cancer. All but one gene's function was unknown, the function of other genes was related to the transporter activity of lipid and electrons, transcription factor activity, growth factor activity and ATP dependent RNA helicase activity, suggesting that these genes are probably related to the promotion and progression of carcinogensis at the early stage of gastric cancer. To seek for the expression products of these genes would be very useful in early diagnosis of gastric cancer.

CEA is a soluble glycoprotein with a complex structure. Its molecular weight is about 200 000, CEA presents in gastrointestinal tract, pancreas and liver at embryonic development stage, and would increase in gastrointestinal malignant tumors. In other tumors such as breast and lung cancer, it was increased in the serum. Therefore, CEA is a broad-spectrum tumor marker, although it does not act as a specific marker for some malignant tumors, but it still has an important clinical value in differential diagnosis. In the present study, we found that CEA associated cell adhesion molecule 5 (CAM-5) (SLR cancer was 4.6, pericancerous epithelium was 2.1) and CAM-6 (SLR cancer was 5.6, pericancerous epithelium was 2.1) were up-regulated. Sakakura[12] reported that CEA gene expression was up-regulated in metastatic gastric cancer. Oue reported that CEA CAM-6 gene expression was up-regulated in 50% patients with gastric cancer, suggesting that carcino-embryonic antigen associated genes are up-regulated to produce a soluble glycoprotein which could secrete into the blood, increasing the amount of CEA in serum. It could be a molecular mechanism of CEA appearance in serum of patients with gastric cancer. It is a useful tumor marker for gastric cancer.

Na^+/K^+-ATPase widely distributed on cell membranes is a key enzyme for keeping Na^+, K^+ ion gradients of cells. Such an enzyme not only attends the ion and protein translocation and keeps the ion self-balance of stabilization, but also has an important role in embryogenesis of vertebrate, neuronal recognition, development of central nervous system, cell morphogenesis, cell adhesion, *etc*. Lee[24] reported that

Table 5 Comparison between molecular functions of 21 genes in T, P and C

Probe Set ID	T *vs* C SLR	P *vs* C SLR	Name	GO molecular function
201655-s-at	3.1	2.6	Heparan sulfate proteoglycan 2 (perlecan)	GO:5198; structural molecule activity; inferred from electronic annotation GO:5206; heparin sulfate proteoglycan; traceable author statement
201890-at	3.1	1.6	Ribonucleotide reductase M2 polypeptide	GO:4748; ribonucleoside-diphosphate reductase activity;non-traceable author statement GO:16491; oxidoreductase activity; inferred from electronic annotation
201926-s-at	3.1	1	Decay accelerating factor for complement (CD55, Cromer blood group system)	Unknown
203334-at	3.1	3.8	DEAD/H (Asp-Glu-Ala--Asp/His) box polypeptide 8 (RNA helicase)	GO:3723; RNA binding; inferred from electronic annotation GO:8248; pre-mRNA splicing factor activity; traceable author statement GO:5524; ATP binding;inferred from electronic annotation GO:4004; ATP dependent RNA helicase activity; traceable author statement
202870-s-at	3.3	1.5	CDC20 cell division cycle 20 homolog (S. cerevisiae)	Unknown
209035-at	3.3	1.6	Midkine (neurite growth-promoting factor 2)	GO:8201; heparin binding; not recorded GO:8083; growth factor activity; not recorded GO:5125; cytokine activity; not recorded
209803-s-at	3.4	1.8	Tumor suppressing subtransferable candidate 3	Unknown
212444-at	3.4	1.2	*Homo sapiens*, clone IMAGE:4471726, mRNA	Unknown
217173-s-at	3.4	3.6	Low density lipoprotein receptor (familial hypercholesterolemia)	GO:5041; low-density lipoprotein receptor activity; traceable author statement GO:5509; calcium ion binding; inferred from electronic annotation GO:8034; lipoprotein binding; traceable author statement GO:5319; lipid transporter activity; inferred from electronic
217221-x-at	3.5	2.2	RNA binding motif protein 10	GO:3676; rrm; nucleic acid binding activity; 8.4e-05; extended: inferred from electronic annotation GO:3676; rrm; nucleic acid binding activity; 0.76; extended: inferred from electronic annotation
202855-s-at	3.6	1.2	Solute carrier family 16 (monocarboxylic acid transporters), member 3	GO:8028; monocarboxylic acid transporter activity; traceable author statement GO:15355; monocarboxylate porter activity; inferred from electronic annotation GO:15293; symporter activity; inferred from electronic annotation
203559-s-at	3.6	1.2	Amiloride binding protein 1(amine oxidase (copper-containing))	GO:8144; drug binding;not recorded GO:8201; heparin binding; inferred from electronic annotation GO:8122; amine oxidase (copper-containing) activity; inferred from electronic annotation GO:16491; oxidoreductase activity; inferred from electronic annotation
209373-at	3.8	1.6	BENE protein	Unknown
203108-at	4.2	1.5	Retinoic acid induced 3	GO:8067; metabotropic glutamate, GABA-B-like receptor activity; inferred from electronic annotation GO:4872; receptor activity; inferred from electronic annotation
202067-s-at	4.5	3.8	Low density lipoprotein receptor (familial hypercholesterolemia)	GO:5041; low-density lipoprotein receptor activity; traceable author statement GO:5509; calcium ion binding; inferred from electronic annotation GO:8034; lipoprotein binding; traceable author statement GO:5319; lipid transporter activity; inferred from electronic
218900-at	4.5	3.7	Cyclin M4	Unknown
201884-at	4.6	2.1	Carcinoembryonic antigen-related cell adhesion molecule 5	GO:8222; tumor antigen; traceable author statement
211657-at	5.9	2.1	Carcinoembryonic antigen-related cell adhesion molecule 6	GO:8222; tumor antigen; traceable author statement
212768-s-at	4.7	1.3	Differentially expressed in hematopoietic lineages	Unknown
208250-s-at	6.3	1.7	Deleted in malignant brain tumors 1	GO:8181; tumor suppressor; predicted/computed GO:5044; SRCR; scavenger receptor activity; 3.7e-42;extended: unknown
204855-at	7.7	4.2	Serine (or cysteine) proteinase inhibitor, clade B (ovalbumin) member 5	GO:4868; serpin; not recorded GO:4867; serine protease nhibitor activity; inferred from electronic annotation GO:8181; tumor suppressor; traceable author statement serp

Na+/K+-ATPase expression levels were up-regulated in intestinal type of gastric cancer. In our study, ATPase, Na^+/K^+ transporting, alpha 1 polypeptide were found (SLR cancer was 2.4, pericancerous was 1.4).

Alcohol dehydrogenase and aldehyde dehydrogenase are two key enzymes in ethanol metabolism and its metabolic products. Aldehyde dehydrogenase and its gene polymorphism (aldehyde dehydrogenase) are related to liver cancer, gastric cancer and esophageal cancer. Abe[10] reported that aldehyde dehydrogenase expression level was obviously down-regulated in tissues of gastric cancer. In the present study, we also found that alcohol dehydrogenase IB expression levels were

Table 6 Comparison between molecular functions of 17 genes in T, P and C

Probe Set ID	T *vs* C SLR	P *vs* C SLR	Name	GO molecular function
207102-at	-2.4	-3.6	Aldo-keto reductase family 1, member D1 (delta 4-3-ketosteroid-5-beta-reductase)	GO:5489; electron transporter activity; experimental evidence
218730-s-at	-2.5	-3.3	Osteoglycin (osteoinductive factor, mimecan)	GO:8083; growth factor activity; inferred from electronic annotation
204940-at	-3.3	-1.3	Phospholamban	GO:42030; ATPase inhibitor activity; inferred from electronic annotation GO:5246; calcium channel regulator activity; not recorded
208281-x-at	-3.3	-1.1	Deleted in azoospermia 3	GO:3676; nucleic acid binding; inferred from electronic annotation
216351-x-at	-3.3	-1.6	Deleted in azoospermia 4	Unknown
209894-at	-3.7	-1.5	Leptin receptor	GO:4896; hematopoietin/interferon-class (D200-domain) cytokine receptor activity; inferred from electronic annotation
214723-x-at	-3.7	-1.5	KIAA1641 protein	Unknown
208282-x-at	-4.3	-1.2	Deleted in azoospermia 2	GO:3676; nucleic acid binding; inferred from electronic annotation
219564-at	-4.3	-1.2	Potassium inwardly-rectifying channel, subfamily J, member 16	GO:5242; inward rectifier potassium channel activity; inferred from electronic annotation GO:5244; voltage-gated ion channel activity; inferred from electronic annotation GO:5267; potassium channel activity; inferred from electronic annotation
203571-s-at	-4.8	-1.6	Adipose specific 2	Unknown
218087-s-at	-5	-1.3	Sorbin and SH3 domain containing 1	GO:8092; cytoskeletal protein binding; experimental evidence GO:3779; actin binding; experimental evidence
207909-x-at	-5.2	-1.2	Deleted in azoospermia	GO:3676; rrm; nucleic acid binding activity; 4.3e-10; extended:inferred from electronic annotation GO:3723; RNA binding; predicted/computed
213071-at	-5.3	-1.3	Dermatopontin	GO:5515; protein binding; traceable author statement GO:5194; cell adhesion molecule activity; inferred from electronic annotation
201497-x-at	-5.4	-1	Myosin, heavy polypeptide 11, smooth muscle	GO:3779; actin binding; inferred from electronic annotation GO:5516; calmodulin binding; inferred from electronic annotatio GO:5524; ATP binding; inferred from electronic annotation GO:3774; motor activity; inferred from electronic annotation
207912-s-at	-5.9	-1.3	Deleted in azoospermia	GO:3676; rrm; nucleic acid binding activity; 4.3e-10;extended:inferred from electronic annotation GO:3723; RNA binding;predicted/computed
220630-s-at	-6.3	-1.8	Eosinophil chemotactic cytokine	GO:16787; Glyco_hydro_18; hydrolase activity; 2.7e-81; extended:Unknown GO:16798; hydrolase activity, acting on glycosyl bonds;inferred from electronic annotation GO:8061; chitin binding;inferred from electronic annotation GO:8843; endochitinase activity; inferred from electronic annotation
209612-s-at	-6.9	-1.4	Alcohol dehydrogenase IB (class I), beta polypeptide	GO:4024; alcohol dehydrogenase activity, zinc-dependent;traceable author statement GO:4327; 1.2.1.1; formaldehyde dehydrogenase (glutathione) activity; 3.69e-120; extended: inferred from electronic annotation GO:4023; alcohol dehydrogenase activity, metal ion-independent; inferred from electronic annotation GO:4025; alcohol dehydrogenase activity, iron-dependent;inferred from electronic annotation GO:8270; zinc ion binding; traceable author statement GO:4552; 1.1.1.73; octanol dehydrogenase activity; 4.76e-120; extended: non-traceable author statement GO:16491; oxidoreductase activity; inferred from electronic annotation GO: 5489; electron transporter activity; traceable author statement

obviously down-regulated (SLR cancer was-6.9, pericancerous was-1.4).

Serine protein kinase takes part in translocation and localization, as well as signal transfer of cells. Oien[20] reported that serine protein kinase expression levels were obviously up-regulated in human gastric cancer tissues. In the present study, we also found that serine protein kinase inhibitor expression level was obviously up-regulated (SLR cancer was 7.7, pericancerous was 4.2).

It has been demonstrated that the activity of topoisomerase II (Topo II) was rapidly increased in proliferating cells from S phase to G2/M phase, suggesting that this enzyme activity might be related to the malignant transformation of tumor cells. So Topo II expression levels (high or low) might be a parameters for cell proliferation. It also could be used as a marker for judging the sensitivity and tolerance of antitumor

drugs. Varis *et al*[30], reported that Topo II expression level was obviously up-regulated in human gastric cancer tissues. Skotheim[31] reported that Topo II expression level was obviously up-regulated in malignant peripheral nerve sheath tumors. In our study the Topo II expression was also up-regulated in gastric cancer and pericancerous epithelium (SLR cancer was 2.3, pericancerous was 1.4). It might be related to a degree of malignancy and resistance. In the present study, we found that the cell cycle protein M4 (SLR cancer was 4.5, pericancerous was 3.7) was highly expressed. It might indicate that tumor cells had a high proliferation ratio.

In our study, the expression of E-cadherin (SLR cancer was 2.3, pericancerous was 1.8) and integrin β 4 (SLR cancer was 2.7, pericancerous was 2.0) was significantly increased in gastric cancer as reported by Mori *et al*[16], Hippo *et al*[25] and Oue *et al*[34].

Cell skeleton tissues and formation of external matrix of cells play an important role in the invasion of tumors. In the present study we found a number of genes were involved in cell skeleton and matrix such as keratin protein 19 (SLR cancer was 2.5, pericancerous was 1.6), microtubule protein β 4 (SLR cancer was 2.4, pericancerous was 1.4), microtubule protein β 2 (SLR cancer was 2.1, pericancerous was 1.4), reticuloprotein 1, and interzonal fiber binding protein 500 ku (SLR cancer was 2.1, pericancerous was 1.8). Bae *et al*[32] reported that cell skeleton protein was up-regulated in gastric cancer. Inhibitor 3 of proteins belongs to external matrix of cells (SLR cancer was 2.3, pericancerous was 1.7). Wang *et al*[33] reported that external matrix of gastric cancer cells was up-regulated. We found that 4/5 patients had a lymph-node metastasis, and related metastatic genes had a higher expression, further suggesting that the overexpression of cell skeleton tissues and external matrix is associated with tumor invasion and metastasis.

The application of gene chip technique is a revolution in life science. This kind of study models will produce a great effect on researches in life science. Gene chip might provide a new direction for diagnosis, therapy and prevention of human gastric carcinoma.

REFERENCES

1 **Peng XL,** Yuan HY, Xie Y, Wang HH. Experimental technique of gene engineering. *Huna Science Technique Issue Agency Second* 1998: 197-199

2 **Yoshida N,** Ishikawa T, Ichiishi E, Yoshida Y, Hanashiro K, Kuchide M, Uchiyama K, Kokura S, Ichikawa H, Naito Y, Yamamura Y, Okanoue T, Yoshikawa T. The effect of rebamipide on *Helicobacter pylori* extract-mediated changes of gene expression in gastric epithelial cells. *Aliment Pharmacol Ther* 2003; **18** Suppl 1: 63-75

3 **Nardone G,** Morgner A. *Helicobacter pylori* and gastric malignancies. *Helicobacter* 2003; **8** Suppl 1: 44-52

4 **Nilsson C,** Sillen A, Eriksson L, Strand ML, Enroth H, Normark S, Falk P, Engstrand L. Correlation between cag pathogenicity island composition and *Helicobacter pylori*-associated gastroduodenal disease. *Infect Immun* 2003; **71**: 6573-6581

5 **Sepulveda AR,** Tao H, Carloni E, Sepulveda J, Graham DY, Peterson LE. Screening of gene expression profiles in gastric epithelial cells induced by *Helicobacter pylori* using microarray analysis. *Aliment Pharmacol Ther* 2002; **16** Suppl 2: 145-157

6 **Maeda S,** Otsuka M, Hirata Y, Mitsuno Y, Yoshida H, Shiratori Y, Masuho Y, Muramatsu M, Seki N, Omata M. cDNA microarray analysis of *Helicobacter pylori*-mediated alteration of gene expression in gastric cancer cells. *Biochem Biophys Res Commun* 2001; **284**: 443-449

7 **Kang HC,** Kim IJ, Park JH, Shin Y, Ku JL, Jung MS, Yoo BC, Kim HK, Park JG. Identification of genes with differential expression in acquired drug-resistant gastric cancer cells using high-density oligonucleotide microarrays. *Clin Cancer Res* 2004; **10**: 272-284

8 **Suganuma K,** Kubota T, Saikawa Y, Abe S, Otani Y, Furukawa T, Kumai K, Hasegawa H, Watanabe M, Kitajima M, Nakayama H, Okabe H. Possible chemoresistance-related genes for gastric cancer detected by cDNA microarray. *Cancer Sci* 2003; **94**:355-359

9 **Ludwig A,** Dietel M, Lage H. Identification of differentially expressed genes in classical and atypical multidrug-resistant gastric carcinoma cells. *Anticancer Res* 2002; **22**: 3213-3221

10 **Abe M,** Yamashita S, Kuramoto T, Hirayama Y, Tsukamoto T, Ohta T, Tatematsu M, Ohki M, Takato T, Sugimura T, Ushijima T. Global expression analysis of N-methyl-N'-nitro-N-nitrosoguanidine-induced rat stomach carcinomas using oligonucleotide microarrays. *Carcinogenesis* 2003; **24**: 861-867

11 **Weiss MM,** Kuipers EJ, Postma C, Snijders AM, Siccama I, Pinkel D, Westerga J, Meuwissen SG, Albertson DG, Meijer GA. Genomic profiling of gastric cancer predicts lymph node status and survival. *Oncogene* 2003: **22**: 1872-1879

12 **Sakakura C,** Simomura K, Shuichi K, Nakase Y, Fukuda K, Takagi T, Hagiwara A, Ichikawa Y, Nishizuka I, Ishikawa T, Okazaki Y, Yamagishi H. Screening of novel biomarkers for the detection of intraperitoneally disseminated cancer cells using human cDNA microarray. *Gan To Kagaku Ryoho* 2002; **29**: 2271-2274

13 **Wang JH,** Chen SS. Screening and identification of gastric adenocarcinoma metastasis-related genes by using cDNA microarray coupled to FDD-PCR. *Shengwu Huaxue Yu Shengwu Wuli Xuebao (Shanghai)* 2002; **34**: 475-481

14 **Hippo Y,** Yashiro M, Ishii M, Taniguchi H, Tsutsumi S, Hirakawa K, Kodama T, Aburatani H. Differential gene expression profiles of scirrhous gastric cancer cells with high metastatic potential to peritoneum or lymph nodes. *Cancer Res* 2001; **61**: 889-895

15 **Meireles SI,** Carvalho AF, Hirata R, Montagnini AL, Martins WK, Runza FB, Stolf BS, Termini L, Neto CE, Silva RL, Soares FA, Neves EJ, Reis LF. Differentially expressed genes in gastric tumors identified by cDNA array. *Cancer Lett* 2003; **190**: 199-211

16 **Mori M,** Mimori K, Yoshikawa Y, Shibuta K, Utsunomiya T, Sadanaga N, Tanaka F, Matsuyama A, Inoue H, Sugimachi K. Analysis of the gene-expression profile regarding the progression of human gastric carcinoma. *Surgery* 2002; **131**: S39-S47

17 **Hasegawa S,** Furukawa Y, Li M, Satoh S, Kato T, Watanabe T, Katagiri T, Tsunoda T, Yamaoka Y, Nakamura Y. Genome-wide analysis of gene expression in intestinal-type gastric cancers using a complementary DNA microarray representing 23 040 genes. *Cancer Res* 2002; **62**: 7012-7017

18 **Inoue H,** Matsuyama A, Mimori K, Ueo H, Mori M. Prognostic score of gastric cancer determined by cDNA microarray. *Clin Cancer Res* 2002; **8**: 3475-3479

19 **Ji J,** Chen X, Leung SY, Chi JT, Chu KM, Yuen ST, Li R, Chan AS, Li J, Dunphy N, So S. Comprehensive analysis of the gene expression profiles in human gastric cancer cell lines. *Oncogene* 2002; **21**: 6549-6556

20 **Oien KA,** Vass JK, Downie I, Fullarton G, Keith WN. Profiling, comparison and validation of gene expression in gastric carcinoma and normal stomach. *Oncogene* 2003; **22**: 4287-4300

21 **Stephen RL,** Crabtree JE, Yoshimura T, Clayton CL, Dixon MF, Robinson PA. Increased zinc finger protein zFOC1 transcripts in gastric cancer compared with normal gastric tissue. *Mol Pathol* 2003; **56**: 167-171

22 **Boussioutas A,** Li H, Liu J, Waring P, Lade S, Holloway AJ, Taupin D, Gorringe K, Haviv I, Desmond PV, Bowtell DD. Distinctive patterns of gene expression in premalignant gastric mucosa and gastric cancer. *Cancer Res* 2003; **63**: 2569-2577

23 **Askari MD,** Miller GH, Vo-Dinh T. Simultaneous detection

of the tumor suppressor FHIT gene and protein using the multi-functional biochip. *Cancer Detect Prev* 2002; **26**: 331-342

24 **Lee S,** Baek M, Yang H, Bang YJ, Kim WH, Ha JH, Kim DK, Jeoung DI. Identification of genes differentially expressed between gastric cancers and normal gastric mucosa with cDNA microarrays. *Cancer Lett* 2002; **184**: 197-206

25 **Hippo Y,** Taniguchi H, Tsutsumi S, Machida N, Chong JM, Fukayama M, Kodama T, Aburatani H. Global gene expression analysis of gastric cancer by oligonucleotide microarrays. *Cancer Res* 2002; **62**: 233-240

26 **El-Rifai W,** Frierson HF, Harper JC, Powell SM, Knuutila S. Expression profiling of gastric adenocarcinoma using cDNA array. *Int J Cancer* 2001; **92**: 832-838

27 **Kim B,** Bang S, Lee S, Kim S, Jung Y, Lee C, Choi K, Lee SG, Lee K, Lee Y, Kim SS, Yeom YI, Kim YS, Yoo HS, Song K, Lee I. Expression profiling and subtype-specific expression of stomach cancer. *Cancer Res* 2003; **63**: 8248-8255

28 **Chen X,** Leung SY, Yuen ST, Chu KM, Ji J, Li R, Chan AS, Law S, Troyanskaya OG, Wong J, So S, Botstein D, Brown PO. Variation in gene expression patterns in human gastric cancers. *Mol Biol Cell* 2003; **14**: 3208-3215

29 **Tay ST,** Leong SH, Yu K, Aggarwal A, Tan SY, Lee CH, Wong K, Visvanathan J, Lim D, Wong WK, Soo KC, Kon OL, Tan P. A combined comparative genomic hybridization and expression microarray analysis of gastric cancer reveals novel molecular subtypes. *Cancer Res* 2003; **63**: 3309-3316

30 **Varis A,** Wolf M, Monni O, Vakkari ML, Kokkola A, Moskaluk C, Frierson H, Powell SM, Knuutila S, Kallioniemi A, El-Rifai W. Targets of gene amplification and overexpression at 17q in gastric cancer. *Cancer Res* 2002; **62**: 2625-2629

31 **Skotheim RI,** Kallioniemi A, Bjerkhagen B, Mertens F, Brekke HR, Monni O, Mousses S, Mandahl N, Soeter G, Nesland JM, Smeland S, Kallioniemi OP, Lothe RA. Topoisomerase-II alpha is upregulated in malignant peripheral nerve sheath tumors and associated with clinical outcome. *J Clin Oncol* 2003;**21**: 4586-4591

32 **Bae CD,** Sung YS, Jeon SM, Suh Y, Yang HK, Kim YI, Park KH, Choi J, Ahn G, Park J. Up-regulation of cytoskeletal-associated protein 2 in primary human gastric adenocarcinomas. *J Cancer Res Clin Oncol* 2003; **129**: 621-630

33 **Wang YM,** Xu SM, Huang QH. Analysis of human gastric cancer associated genes expression by gene chip. *J Tongji Univ* 2003; **24**: 932-934

34 **Oue N,** Hamai Y, Mitani Y, Matsumura S, Oshimo Y, Aung PP, Kuraoka K, Nakayama H, Yasui W. Gene expression profile of gastric carcinoma: identification of genes and tags potentially involved in invasion, metastasis, and carcinogenesis by serial analysis of gene expression. *Cancer Res* 2004; **64**: 2397-2405

Science Editor Wang XL and Guo SY **Language Editor** Elsevier HK

PO Box 2345, Beijing 100023, China
www.wjgnet.com
wjg@wjgnet.com

ELSEVIER

World J Gastroenterol 2005;11(16):2398-2401
World Journal of Gastroenterology ISSN 1007-9327

Expression of β-catenin in hepatocellular carcinoma

Liem Thanh Tien, Masahiro Ito, Mikiko Nakao, Daisuke Niino, Meirmanov Serik, Masahiro Nakashima, Chun-Yang Wen, Hiroshi Yatsuhashi, Hiromi Ishibashi

Liem Thanh Tien, Masahiro Ito, Mikiko Nakao, Department of Pathology, National Nagasaki Medical Center, 2-1001-1 Kubara, Omura, Nagasaki 856-8562, Japan
Daisuke Niino, Meirmanov Serik, Chun Yang Wen, Department of Molecular Pathology, Atomic Bomb Disease Institute, Nagasaki University Graduate School of Biomedical Science, 1-12-4 Sakamoto, Nagasaki 852-8523, Japan
Masahiro Nakashima, Tissue and Histopathology Section Division of Scientific Data Registry, Atomic Bomb Disease Institute, Nagasaki University Graduate School of Biomedical Science, 1-12-4 Sakamoto, Nagasaki 852-8523, Japan
Chun-Yang Wen, Department of Digestive Disease, Nanjing Drum Tower Hospital, Medical School of Nanjing University, Nanjing 210008, Jiangsu Province, China
Hiroshi Yatsuhashi, Hiromi Ishibashi, Clinical Research Center, National Nagasaki Medical Center, 2-1001-1 Kubara, Omura, Nagasaki 856-8562, Japan
Correspondence to: Masahiro Ito, MD, Department of Pathology, National Nagasaki Medical Center, 2-1001-1 Kubara, Omura, Nagasaki 856-8562, Japan. itohm@nmc.hosp.go.jp
Telephone: +81-957-52-3128 Fax: +81-957-54-0292
Received: 2004-06-08 Accepted: 2004-08-12

Abstract

AIM: The β-catenin has been recognized as a critical member of the Wnt signaling pathway and plays an important role in the generation/differentiation of many tissues. Inappropriate activation of this pathway has been implicated in carcinogenesis. The mechanism underlying the development as well as its prognosis of hepatocellular carcinoma (HCC) has remained unclear. The purpose of this study is to analyze the expression of β-catenin in HCC in relation to histological grades and viral hepatitis backgrounds.

METHODS: Thirty-two sections were selected at random from autopsy and surgical cases of HCC. Immuohistologically, the location and positivity of β-catenin expression in HCC was examined.

RESULTS: Normal hepatocytes did not express β-catenin. In 78% of HCC β-catenin was expressed at the membrane of the cells, with or without cytoplasmic and/or nuclear expression. The tumor cells with well- and moderately-differentiated grades expressed frequently at the membrane and cytoplasm compared with poorly-differentiated type. Nuclear expression of β-catenin was prone to occur in the tumor cells of poorly-differentiated grade. There were 15% of hepatitis C virus (HCV) backgrounds with nuclear expression. In contrast, there was 38% with nuclear expression in hepatitis B virus (HBV) backgrounds. In nonB-nonC hepatitis, no case expressed nuclear β-catenin.

CONCLUSION: The β-catenin expression in HCC cells was heterogenous among types of hepatitis viral infection. Wnt signaling pathway might be deeply involved in less-differentiated HCC and HBV background.

Key words: Hepatocellular carcinoma; β-Catenin; Immunohistochemistry

Tien TL, Ito M, Nakao M, Niino D, Serik M, Nakashima M, Wen CY, Yatsuhashi H, Ishibashi H. Expression of β-catenin in hepatocellular carcinoma. *World J Gastroenterol* 2005; 11(16): 2398-2401
http://www.wjgnet.com/1007-9327/11/2398.asp

INTRODUCTION

Hepatocellular carcinoma (HCC) is a major type of primary liver cancer and one of the rare human neoplasms etiologically linked to viral factors. Chronic infections with the hepatitis B virus (HBV) and the hepatitis C virus (HCV) have been implicated in about 80% of cases worldwide. However, the molecular mechanisms underlying their development are still poorly understood.

HCCs display gross genomic alterations, including DNA rearrangements associated with HBV DNA integration, loss of heterozygosity, and, less importantly, chromosomal amplifications and loss of imprinting[1]. Many genes with somatic mutations have been identified in these tumors. Most frequently involved genes are tumor suppressor genes such as p53, β-catenin, and retinoblastoma genes[2-4].

β-Catenin is a structure protein in the cadherin mediated cell-cell adhesive system as a regulator[5], and plays an important role in the generation/differentiation of tissues as well as in the repair of normal tissues. It is also known to act as a mediator in the Wingless/Wnt signal transduction pathway[6]. In HCC, accumulation of β-catenin was present in the early stage of HCC[7,8]. The previous studies investigated the correlation between β-catenin expression and the differentiation grades of HCC, and prognostic roles of β-catenin expression in HCC[9-11].

The purpose of this study is to investigate the expression of β-catenin in HCC in relation to histological grades and to viral hepatitis backgrounds.

MATERIALS AND METHODS

Liver tissue sections were obtained at random of 32 sections from 15 autopsy cases and 13 surgical cases. They consisted of 20 males and 8 females. Age ranged from 36 to 86

years with an average of 64. The diagnosis was confirmed histopathologically in all cases, based mainly on examination of sections stained with H&E.

Immunohistochemistry

The sections were stained immunohistochemically by the avidin-biotin complex method for β-catenin antibody (Mouse IgG1, BD Transduction Laboratories - BD Biosciences, SanJose, California, USA) with dilution of 1:200. For immunostaining, the sections were deparaffinized, washed with phosphate-buffered saline (PBS, pH 7.4) in 10 min, soaked in sodium citrate buffer (pH 6.0) and heated in microwave at 97 ℃ in 15 min for antigen retrieval. It was then allowed to cool at room temperature before being immersed into 0.3% H_2O_2/methanol to block endogenous peroxidase activity. The sections were pre-incubated with 10% normal bovine serum to prevent non-specific binding. Primary antibodies were incubated for 2 h at room temperature. Secondary antibodies, anti-mouse IgG was applied for 30 min, followed by incubation with avidin-peroxidase for 10 min and visualized with diaminobenzidine (DAB), rinsed and soaked in PBS for 3-5 min, thrice after each step. They were counterstained with Mayer hematoxylin.

For the evaluation of immunohistochemical staining of β-catenin, the constitutional expression on the cell membrane of bile duct at non-cancerous area was used as positive control (Figure 1). The membranous expression (Figure 2) was evaluated as (+) when at least one-third section of it was expressed or strong expression if less than one-third and (-) when it was unexpressed or less than one-third section was weakly expressed. The cytoplasmic expression was evaluated as + when it was stronger than the expression in non-cancerous areas, and (-) when the expression was the same as in non-cancerous area. In the nucleus, the expression (Figure 3) was evaluated as + when it was found clearly in any portion. All the results were observed and agreed by two pathologists (Dr. Ito and Dr. Wen).

RESULTS

Relation between histological grade and hepatitis background

There were 20 sections with hepatitis C virus background, eight with hepatitis B virus, three with nonB-nonC viral hepatitis, and one section with non-hepatitis infection. Eleven sections were well-differentiated type, 17 were moderately-differentiated type, and four sections were poorly-differentiated type. In well-differentiated cases, their backgrounds consisted of two with viral hepatitis B, six with viral hepatitis C, and three with nonB-nonC viral hepatitis. In moderately-differentiated sections, their backgrounds were three sections with viral hepatitis B, 13 sections with viral hepatitis C, and one section with nonB-nonC viral hepatitis. In poorly-differentiated cases, their backgrounds were three with viral hepatitis B and one section with viral hepatitis C.

Immunocytochemical expression of β-catenin

Most sections (25 of 32 sections: 78%) expressed at the membrane of the cells. Among them, 17 of 32 sections (53%) were only expressed at the membrane (Figure 2). For cytoplasmic expression, there were 9 of 32 cases (28%), but 7 of 32 sections (22%) were only expressed at the cytoplasm and two cases were associated with membranous and/or nuclear expression. There were 7 of 32 (22%) sections with nuclear expression (Figure 3) and there were no cases with nuclear expression alone. Figure 4 shows percentages of immunocytochemical expression pattern in the tumor cells.

Relation between hepatitis background and β-catenin expression (Table 1)

There were eight sections with HBV background which were mainly β-catenin expression of membranous type, in which three sections were both membranous and nuclear expressions. There were 20 sections with HCV background in which six sections were cytoplasmic. Two sections were membranous and nuclear type. One section was membranous and cytoplasmic expression. One section was membrano-cytoplasm-nuclear expression and 10 sections were membranous expression of β-catenin. The sections with nonB-nonC expressed only membranous type. Overall the nuclear localization of β-catenin was highly encountered in HBV background.

Relation with the grade of HCC histology of β-catenin expression (Table 2)

For well-differentiated grade, there were five sections with membranous expression, three sections with cytoplasmic expression, two sections with membrano-nuclear expression, and one section with membrano-cytoplasmic expression. For

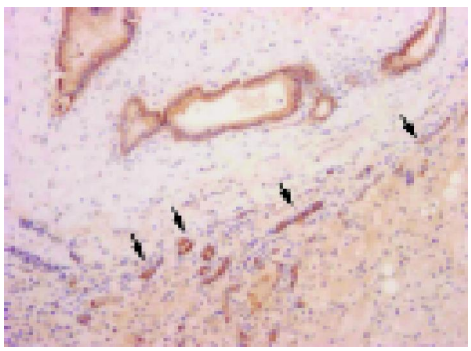

Figure 1 Constitutive expression of β-catenin in normal bile ducts. Membranous expression is conspicuous in normal bile ducts and newly formed bile ducts (arrow heads), but no expression is observed in normal hepatocytes.

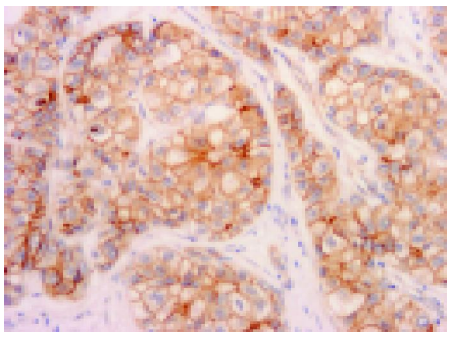

Figure 2 Membranous expression. Membranous expression is conspicuous in tumor cell membranes. This case is moderately-differentiated HCC.

moderately-differentiated grade, there were 11 sections with membranous expression, four sections with cytoplasmic expression, and two sections with membrano-nuclear expressions. For poorly-differentiated grade, there was one section with membranous expression, two sections with membrano-nuclear expression, and one section with membrano-cytoplasm-nuclear expression.

There were 7 of 32 sections (22%) which expressed the nuclear type, in which three sections were encountered in poorly-differentiated grade, two sections in moderately-differentiated grade, and two sections in well-differentiated grade. In each differentiation grade, nuclear expression was highly detected in poorly-differentiated type (3 of 4 sections, 75%) compared with well (2 of 11 sections, 18%) and moderately-differentiated types (2 of 17 sections, 12%).

Table 1 β-Catenin expression and viral hepatitis background

	M (%)	M+N (%)	M+C (%)	M+N+C (%)	C(%)
HBV	49 (4/8)	38 (3/8)	13 (1/8)		
HCV	50 (10/20)	10 (2/20)	5 (1/20)	5 (1/20)	30 (6/20)
NonB-nonC	100 (3/3)				

M: membranous, M+N: membranous and nuclear, M+C: membranous and cytoplasmic, M+C+N: membranous, cytoplasmic, and nuclear, C: cytoplasmic.

Table 2 β-Catenin expression and histological grade

	M (%)	M+N (%)	M+C (%)	M+N+C (%)	C (%)
Well	46 (5/11)	18 (2/11)	9 (1/11)		27 (3/11)
Moderate	65 (11/17)	12 (2/17)			23 (4/17)
Poor	25 (1/4)	50 (2/4)		25 (1/4)	

M: membranous, M+N: membranous and nuclear, M+C: membranous and cytoplasmic, M+C+N: membranous, cytoplasmic, and nuclear, C: cytoplasmic.

DISCUSSION

Prevalence and localization of β-catenin nuclear expression and mutation varies among previous reports[7,9-15]. Also prognostic implication of β-catenin expression in hepatocarcinogenesis is inconsistent[9-11,14,15,]. Some reports suggest better prognosis in cases with nuclear expression and mutation[10,16], but most reports indicate tumor progression and tumor cell proliferation[9,11,15].

In HCC, accumulation of β-catenin was present in the early stage of HCC. Most authors have described that β-catenin is strongly expressed on the membrane of HCC cells[7,9-11]. Suzuki *et al*[7] showed that β-catenin expression in nodule-in-nodule HCC is 41.7% at the membrane and 41.7% in the cytoplasm of the cells. Inagawa *et al*[9] noted that about 61% exhibited increased membranous and/or cytoplasmic expression. Hey-Chi Hsu *et al*[10] examined 366 cases of multifocal HCCs and stained 282 cases immunochemically for β-catenin, in which 212 cases (57.9%) expressed at the cell membrane alone and 70 cases (19.1%) expressed scattered nuclear expressions. We have documented 78% β-catenin expression at the membrane with or without cytoplasmic and/or nuclear expression, in which 53% of them expressed only at the membrane of the cells. The tumor cells with well- and moderately-differentiated grade expressed at the membrane and cytoplasm for β-catenin. Nuclear expression of β-catenin occurred in moderately- and poorly-differentiated grades, although having no section with nuclear expression alone. In viral infection background, HBV-infected HCC expressed nuclear translocation in high prevalence. These findings suggest that nuclear expression of β-catenin is likely to be induced in less-differentiated type and HBV backgroud. Nuclear expression of β-catenin implies more important roles in view of tumor progression than membranous and cytoplasmic expression. β-catenin can enter the nucleus by binding the T-cell factor and lymphoid-enhancer factor family of DNA binding proteins, and regulates transcription of target genes, such as cyclin D1 and c-myc. Both c-mys and cyclin D1 are involved in the transition between the G1-S check-point of the cell cycle and do so by influencing the activity of retinoblastoma tumor-suppressor pRB[17,18].

Cyclin D1 is a major regulator of the progressing of cells into proliferation stage of the cell cycle. Increased β-catenin levels may promote neoplastic conversion by triggering cyclin D1 gene expression and consequently uncontrolled progression into the cell cycle. Activation of cyclin D1 and disruption of the Rb pathway are also commonly involved in liver tumorigenesis[18]. In our cases cyclin D1 was expressed only in poorly-differentiated HCCs (data not shown). In less-differentiated HCCs, cell proliferation might be induced via β-catenin/cyclin D1 signal pathway[10,19]. But the prevalent type of HCC, well- and moderately-differentiated type, does not seem to be involved

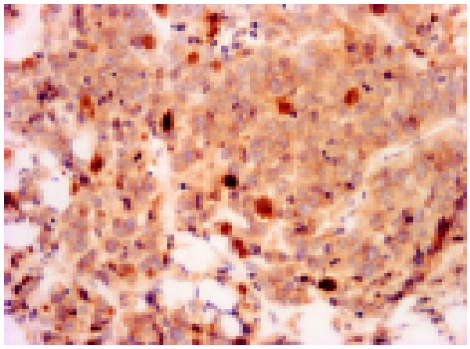

Figure 3 Nuclear expression. Nuclear expression is encountered in the poorly-differentiated HCC (arrows). Most cells co-expressed β-catenin in the cytoplasm.

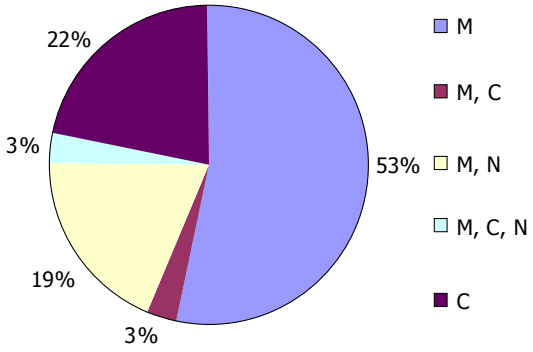

Figure 4 Localization of β-catenin expression in cell level. M: membranous, M+C: membranous and cytoplasmic, M+N: membranous and nuclear, M+N+C: membranous, cytoplasmic, and nuclear, C: cytoplasmic.

in cyclin D1 overexpression. One study suggests that without cyclin D1 activation the β-catenin-related cell proliferation exists in hepatocarcinogenesis[9,20]. And the study on embryonic development indicated that β-catenin might not regulate cyclin D1 during liver development[21].

Statistical analysis clearly showed a distinction between the gene expression profiles of HCV and HBV-related HCC[22]. HBV-associated HCC exhibited involvement of different cellular pathways, those controlling apoptosis, p53 signaling and G1/S transition. In HCV-related HCC a more heterogenous pattern with an over-expression of the TGF-beta induced gene was identified. It is still unclear as to whether the gene expression profile in HCV or HBV-related HCC exhibits a degree of specificity[22].

By mutational analysis of β-catenin gene, Hey-Chi Hsu *et al*[10] indicated that mutation plays a more important role in the tumorigenesis of non-HBV-related HCC than in HBV-related HCC and different types of β-catenin mutations reflect different etiologies of carcinogenesis in specific tissue. In this study, viral hepatitis backgrounds were 63% of HCV and 25% of HBV. This prevalence is similar to that of previous studies. There are differences of expression pattern for β-catenin between B and C viral hepatitis backgrounds. Nuclear translocation was highly observed in HBV background. These results suggest that the expression of β-catenin is influenced by virus infections and carcinogenesis of HBV and HCV infections are different. Integrated hepatitis B virus (HBV) DNA is present in many HCC, suggesting that HBV has a direct oncogenic effect through interaction with transformation-associated genes. The HBX protein of hepatitis B virus is thought to contribute to the development of carcinoma by disruption of intercellular adhesion. β-catenin was tyrosine-phosphorylated in a Src-dependent manner in HBX-expressing cells. Tyrosine phosphorylation of β-catenin by Src kinase results in an increase in its free cytosolic pool. Recent study suggests that HBX induces the stabilization and subsequent nuclear translocation of β-catenin by activating Src kinase and GSK3β suppression.

The overall cytological expression pattern was not consistent with previous reports, suggesting that ethnical and district differences are significant in Wnt signaling pathway in hepatocarcinogenesis. More studies are warranted to understand the expression of β-catenin which effects histological grade and viral hepatitis background in HCC better.

REFERENCES

1 **Calvisi DF**, Factor VM, Ladu S, Conner EA, Thorgeirsson SS. Disruption of beta-catenin pathway or genomic instability define two distinct categories of liver cancer in transgenic mice. *Gastroenterology* 2004; **126**: 1374-1386

2 **Ozturk M**. Genetic aspects of hepatocellular carcinogenesis. *Semin Liver Dis* 1999; **19**: 235-242

3 **Prange W**, Breuhahn K, Fischer F, Zilkens C, Pietsch T, Petmecky K, Eilers R, Dienes HP, Schirmacher P. Beta-catenin accumulation in the progression of human hepatocarcinogenesis correlates with loss of E-cadherin and accumulation of p53, but not with expression of conventional WNT-1 target genes. *J Pathol* 2003; **201**: 250-259

4 **Torbenson M**, Kannangai R, Abraham S, Sahin F, Choti M, Wang J. Concurrent evaluation of p53, beta-catenin, and alpha-fetoprotein expression in human hepatocellular carcinoma. *Am J Clin Pathol* 2004; **122**: 377-382

5 **Wei Y**, Van Nhieu JT, Prigent S, Srivatanakul P, Tiollais P, Buendia MA. Altered expression of E-cadherin in hepatocellular carcinoma: correlations with genetic alterations, beta-catenin expression, and clinical features. *Hepatology* 2002; **36**: 692-701

6 **Cui J**, Zhou X, Liu Y, Tang Z, Romeih M. Wnt signaling in hepatocellular carcinoma: analysis of mutation and expression of beta-catenin, T-cell factor-4 and glycogen synthase kinase 3-beta genes. *J Gastroenterol Hepatol* 2003; **18**: 280-287

7 **Suzuki T**, Yano H, Nakashima Y, Nakashima O, Kojiro M. Beta-catenin expression in hepatocellular carcinoma: a possible participation of beta-catenin in the dedifferentiation process. *J Gastroenterol Hepatol* 2002; **17**: 994-1000

8 **Harada N**, Oshima H, Katoh M, Tamai Y, Oshima M, Taketo MM. Hepatocarcinogenesis in mice with beta-catenin and Ha-ras gene mutations. *Cancer Res* 2004; **64**: 48-54

9 **Inagawa S**, Itabashi M, Adachi S, Kawamoto T, Hori M, Shimazaki J, Yoshimi F, Fukao K. Expression and prognostic roles of beta-catenin in hepatocellular carcinoma: correlation with tumor progression and postoperative survival. *Clin Cancer Res* 2002; **8**: 450-456

10 **Hsu HC**, Jeng YM, Mao TL, Chu JS, Lai PL, Peng SY. Beta-catenin mutations are associated with a subset of low-stage hepatocellular carcinoma negative for hepatitis B virus and with favorable prognosis. *Am J Pathol* 2000; **157**: 763-770

11 **Buendia MA**. Genetics of hepatocellular carcinoma. *Semin Cancer Biol* 2000; **10**: 185-200

12 **Nhieu JT**, Renard CA, Wei Y, Cherqui D, Zafrani ES, Buendia MA. Nuclear accumulation of mutated beta-catenin in hepatocellular carcinoma is associated with increased cell proliferation. *Am J Pathol* 1999; **155**: 703-710

13 **Huang H**, Fujii H, Sankila A, Mahler-Araujo BM, Matsuda M, Cathomas G, Ohgaki H. Beta-catenin mutations are frequent in human hepatocellular carcinomas associated with hepatitis C virus infection. *Am J Pathol* 1999; **155**: 1795-1801

14 **Wong CM**, Fan ST, Ng IO. beta-Catenin mutation and overexpression in hepatocellular carcinoma: clinicopathologic and prognostic significance. *Cancer* 2001; **92**: 136-145

15 **Kondo Y**, Kanai Y, Sakamoto M, Genda T, Mizokami M, Ueda R, Hirohashi S. Beta-catenin accumulation and mutation of exon 3 of the beta-catenin gene in hepatocellular carcinoma. *Jpn J Cancer Res* 1999; **90**: 1301-1309

16 **Fujito T**, Sasaki Y, Iwao K, Miyoshi Y, Yamada T, Ohigashi H, Ishikawa O, Imaoka S. Prognostic significance of beta-catenin nuclear expression in hepatocellular carcinoma. *Hepatogastroenterology* 2004; **51**: 921-924

17 **Edamoto Y**, Hara A, Biernat W, Terracciano L, Cathomas G, Riehle HM, Matsuda M, Fujii H, Scoazec JY, Ohgaki H. Alterations of RB1, p53 and Wnt pathways in hepatocellular carcinomas associated with hepatitis C, hepatitis B and alcoholic liver cirrhosis. *Int J Cancer* 2003; **106**: 334-341

18 **Levy L**, Renard CA, Wei Y, Buendia MA. Genetic alterations and oncogenic pathways in hepatocellular carcinoma. *Ann N Y Acad Sci* 2002; **963**: 21-36

19 **Shtutman M**, Zhurinsky J, Simcha I, Albanese C, D'Amico M, Pestell R, Ben-Ze'ev A. The cyclin D1 gene is a target of the beta-catenin/ LEF-1 pathway. *Proc Natl Acad Sci USA* 1999; **96**: 5222-5227

20 **Shang XZ**, Zhu H, Lin K, Tu Z, Chen J, Nelson DR, Liu C. Stabilized beta-catenin promotes hepatocyte proliferation and inhibits TNFalpha-induced apoptosis. *Lab Invest* 2004; **84**: 332-341

21 **Monga SP**, Monga HK, Tan X, Mule K, Pediaditakis P, Michalopoulos GK. Beta-catenin antisense studies in embryonic liver cultures: role in proliferation, apoptosis, and lineage specification. *Gastroenterology* 2003; **124**: 202-216

22 **Delpuech O**, Trabut JB, Carnot F, Feuillard J, Brechot C, Kremsdorf D. Identification, using cDNA macroarray analysis, of distinct gene expression profiles associated with pathological and virological features of hepatocellular carcinoma. *Oncogene* 2002; **21**: 2926-2937

Science Editor Guo SY **Language Editor** Elsevier HK

PO Box 2345, Beijing 100023, China
www.wjgnet.com
wjg@wjgnet.com

ELSEVIER

World J Gastroenterol 2005;11(16):2402-2407
World Journal of Gastroenterology ISSN 1007-9327

Differentiation between malignant and benign nodules in the liver: Use of contrast C³-MODE technology

Bao-Ming Luo, Yan-Ling Wen, Hai-Yun Yang, Hui Zhi, Bing Ou, Jian-Hong Ma, Jing-Sheng Pan, Xiao-Ning Dai

Bao-Ming Luo, Yan-Ling Wen, Hai-Yun Yang, Hui Zhi, Bing Ou, Jian-Hong Ma, Jing-Sheng Pan, Xiao-Ning Dai, Department of Ultrasound, the Second Affiliated Hospital, Sun Yat-Sen University, 107 Yanjiangxi Road, Guangzhou 510120, Guangdong Province, China
Supported by the Science Foundation of the Department of Science and Technology of Guangdong Province, No. 2002C30315
Co-first-authors: Bao-Ming Luo and Yan-Ling Wen
Correspondence to: Dr. Yan-Ling Wen, Department of Ultrasound, the Second Affiliated Hospital, Sun Yat-Sen University, 107 Yanjiangxi Rd, Guangzhou 510120, Guangdong Province, China. yanlingwen20@hotmail.com
Telephone: +86-20-8133-2516
Received: 2004-07-09 Accepted: 2004-09-19

Abstract

AIM: To investigate the value of contrast-enhanced C³-MODE technology in differentiating malignant nodules of liver from the benign ones.

METHODS: Forty-six nodules in 36 patients (29 men and 7 women) were studied by contrast-enhanced C³-MODE technology and contrast-enhanced CT in 1 wk before the biopsy or operation. A low MI monitor and a high MI flash imaging were intermittently performed. After the injection of contrast agent, the period from 10 to 30 s and the time later than 100 s were respectively defined as early arterial phase and the late phase. The vascularities of the liver nodules in the two phases were combined for differential diagnosis. Corresponding to the pathological diagnosis, the accuracy, sensitivity and specificity of contrast-enhanced C³-MODE technology were compared to those of contrast-enhanced CT.

RESULTS: By C³-MODE technology, 33 of the 46 liver nodules were demonstrated as defected area in the late phase and were diagnosed as malignant tumors. Of them, 28 with hypervascularity in the early arterial phase were assessed as hepatocellular carcinoma, the other five nodules with rim-like enhancement in the early arterial phase were diagnosed as metastatic tumors. Thirteen nodules were shown as iso or hypervascularity in the late phase as well as centripetal filling in the early arterial phase and we made a diagnosis of hemangioma. Corresponding to the pathological results, the sensitivity, specificity and accuracy of contrast-enhanced C³-MODE technology in differentiating malignant and benign nodules in the liver were 97.0%, 92.3% and 95.7%, respectively. With comparison to those of contrast CT (sensitivity, 94.1%; specificity, 91.7%; accuracy, 93.5%), the difference was not significant.

CONCLUSION: Contrast-enhanced C³-MODE technology can effectively differentiate malignant liver tumors from the benign nodules. It highly agrees diagnostically with the pathology. We suggest that it provides a new approach for differential diagnosis of liver nodules in addition to contrast-enhanced CT.

Key words: Contrast medium; Harmonic imaging; Hepatic nodule; Ultrasound

Luo BM, Wen YL, Yang HY, Zhi H, Ou B, Ma JH, Pan JS, Dai XN. Differentiation between malignant and benign nodules in the liver: Use of contrast C³-MODE technology. *World J Gastroenterol* 2005; 11(16): 2402-2407
http://www.wjgnet.com/1007-9327/11/2402.asp

INTRODUCTION

With the development of ultrasonography, small lesions in liver can be sensitively detected[1]. However, because of the similar appearance in B-mode image, it is difficult for B-mode ultrasonography to differentiate the malignant from the benign ones.

The intranodular blood supply is the base of differential diagnosis of hepatic nodules. Color Doppler imaging (CDI) and power Doppler imaging (PDI) are quite useful in some settings for detecting the intranodular blood signals[2,3]. Unfortunately, the ability is not satisfying due to the low sensitivity of CDI and PDI to weak blood signals, and the differential diagnosis of nodular hepatic lesions should be on the basis of other imaging approaches, such as three-phase dynamic CT, MRI or digital subtraction angiography[4,5]. As ultrasonography is often the first choice of scanning in assessment of nodular hepatic lesions because of its noninvasiveness and cheapness, new technologies of ultrasound do great effort for revealing the difference between malignant and benign lesions. Contrast-enhanced ultrasound is one of those newly developed technologies. With use of contrast agent and some special contrast-enhanced technique, the ability of differentiation on ultrasound has been greatly developed[6-14].

Combined Contrast Chain procession (C³-MODE technology) has been developed in recent years. Based on the delayed transmission and the technology that modify the signals of different phase and frequency in different ways, C³-MODE technology can use not only the sub-harmonic, second harmonic and ultra-harmonic signals, but also the

fundamental signals which come from the microbubbles. As a result, C^3-MODE technology theoretically has high sensitivity and specificity to the signals produced by microbubbles. This study was planned to investigate the detectability of contrast-enhanced C^3-MODE technology on intranodular blood signals of nodular hepatic lesions, and its ability in differentiating malignant from benign nodular lesions of liver.

MATERIALS AND METHODS

Materials

From March to October 2002, 36 patients with 46 nodular lesions of liver were enrolled into this study. Oral informed consent from each patient was obtained by explaining the purpose of the study before contrast-enhanced ultrasonography was performed. Of the patients, 29 were men and 7 were women. The ages ranged from 29 to 76 years (mean±SD, 52±12 years). Fifteen of them had B type hepatitis and the others did not have any type of hepatitis. Twenty of the patients had single lesion and the other ten had double lesions in the liver. The maximal diameter of the lesion was recorded according to ultrasonography and ranged from 0.49 cm to 5.72 cm (mean±SD, 2.67±1.26 cm). Thirty-three of the lesions were less than 3.0 cm in maximal diameter (mean±SD, 1.96±0.74 cm). The depths of the lesions (the distance from the surface of the skin to the far edge of the lesions) were from 3.6 cm to 12 cm (mean±SD, 7.6±2.37 cm). All patients were diagnosed with C^3-MODE technology, contrast-enhanced CT, MRI and/or DSA. The final diagnosis for each nodule was confirmed by ultrasound-guided biopsy or pathological examination after operation.

C^3-MODE technology

Ultrasonography was performed a week before biopsy or operation. The used machine was Esaote Technos DU6 (Esaote Co., Italy). A convex-arrayed transducer was used with the frequency of 2.5 MHz. Before contrast-enhanced C^3-MODE technology was performed, the lesions were scanned with fundamental B-mode and CDI to choose a good plane and posture for researching. During this time, the size, echo type and the depth of the lesion were recorded. C^3-MODE technology was started with a low MI of 0.2-0.3. After administration of contrast agent, flash imaging was emitted intermittently with a high MI of 1.0-1.2. Focus was located in the deep level of the lesion. From the time about 10 s after the bolus injection of Levovist (early arterial phase), the flash imaging was performed 3-5 times with an interval of about 5 s. Then low MI C^3-MODE technology was scanned to monitor the lesion. In the late phase (after 100 s from the administration of the contrast agent), flash imaging was emitted twice with an interval of 10 s. All ultrasonography were performed by the same sonographer to minimize the bias. The information of ultrasound examination was stored on magnetic optical disks and digital videotapes.

Contrast agent

Levovist was used with a concentration of 300 mg/mL, which was obtained by adding 7 mL sterile water into 2.5 g Levovist microparticles. Eight milliliters of the contrast agent was injected as a bolus via an antecubital venous with the speed of 1 mL/s, then, flash with 5 mL of normal saline. If there were two nodules in the liver, two vials of Levovist were used. Each of the contrast agents was injected separated by an interval of more than 10 min.

All the contrast-enhanced C^3-MODE technology studies were performed by the same operators for decreasing the variation. The contrast-enhanced patterns were assessed by three experienced sonographers who did not know the results from contrast-enhanced CT and pathological diagnosis. The contrast-enhanced pattern of the lesions in early arterial phase and late phase were assessed with comparison to the liver parenchyma around the lesions. After administration of Levovist, compared with peripheral liver tissue, hyperechoic or iso-echoic pattern was considered to be positive enhancement. In contrast, hypoechoic pattern was defined as negative enhancement.

Contrast-enhanced CT

Contrast-enhanced CT was performed a week before biopsy or operation. Siemens Somatom AR. T (Siemens, Berlin, German) was used. A plain scanning was obtained before contrast agent was used. The used contrast agent was 100 mL of Iopromide 300 (Schering, Guangzhou, China). About 25 s after the administration of the contrast agent, contrast-enhanced CT scanning was obtained. On contrast-enhanced CT scanning, a high attenuation or iso-attenuation of the hepatic nodule was assessed as positive intranodular vascularity. A low attenuation of the nodule was considered to be negative intranodular vascularity. All CT scanning were reviewed by two experienced radiologists who did not know the results on contrast-enhanced C^3-MODE technology.

Statistical analysis

The sensitivity, specificity and accuracy of each approach for differentiating malignant and benign lesions were assessed corresponding to pathological diagnosis. When the ability of contrast-enhanced C^3-MODE technology in differentiating malignant and benign lesions was compared to that of contrast-enhanced CT, the χ^2-square test was used. When P value was less than 0.05, the difference was considered to be significant.

RESULTS

The diagnosis made by contrast-enhanced C^3-MODE

Table 1 Appearance of the 46 hepatic lesions on contrast-enhanced C^3-MODE technology: corresponding to the pathological diagnosis

C^3-MODE	Pathological diagnosis			
	HCC	Metastatic tumor	Hemangioma	Lipid degeneration
HCC	27	0	1	0
Metastatic tumor	0	5	0	0
Hemangioma	0	1	9	3

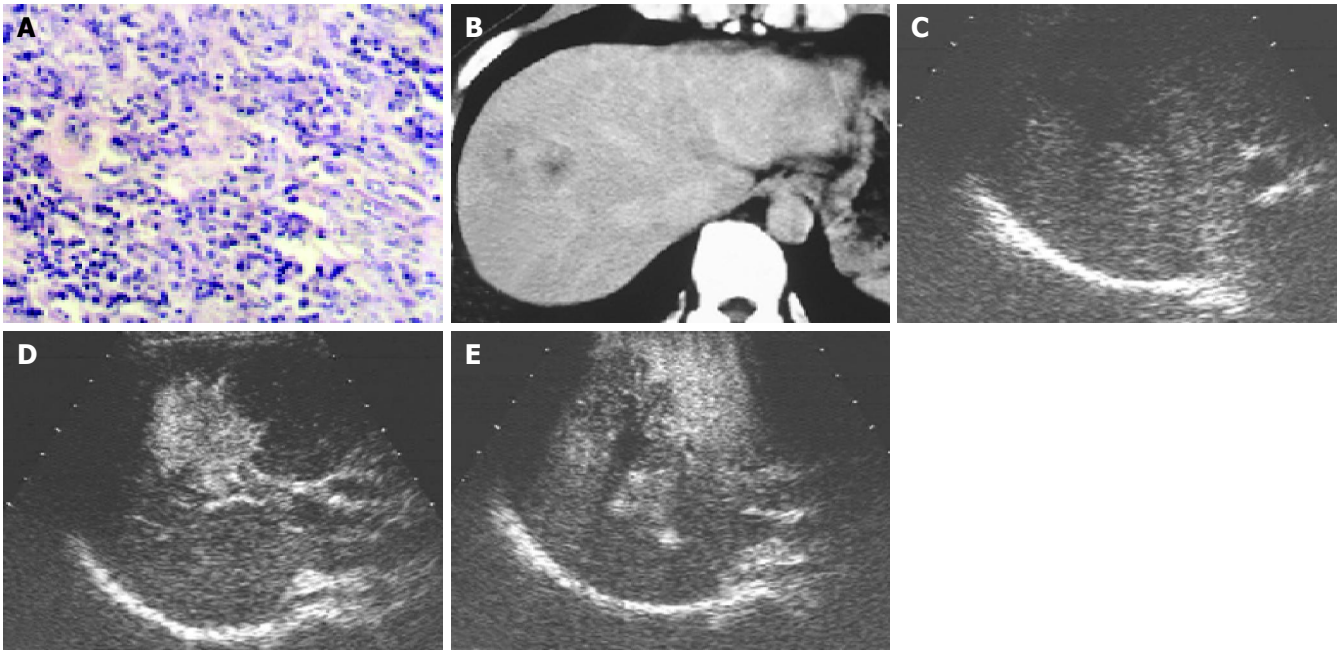

Figure 1 **A**: hepatocellular carcinoma; **B**: heterogenous high attenuation on contrast-enhanced CT; **C**: low echo on B-mode image; **D**: the hypervascularity in early arterial phase on contrast-enhanced C^3-MODE technology; **E**: perfusion defect in the late phase on contrast-enhanced C^3-MODE technology.

technology and pathological diagnoses are shown in Table 1.

On contrast-enhanced C^3-MODE technology, 33 of the 46 nodules were demonstrated as defected area in the late phase and were assessed to be malignant tumors. Of them, 28 nodules showed intranodular vascularity, which appeared from the edge to the center of the nodules, and assessed to be hypervascular tumors in the early arterial phase and HCC was diagnosed (Figure 1). The other five nodules showed rim-like enhancement in the early arterial phase and the diagnosis of metastasis was made (Figure 2). Corresponding to the pathological diagnosis, the positive and negative predictive value to hepatic malignant tumor of contrast-enhanced C^3-MODE technology was 97.0% (32/33) and 92.3% (12/13), respectively.

Using contrast-enhanced C^3-MODE technology, 13 nodules were found with spot-like or wool-cotton enhancement and centripetal filling in the early arterial phase followed by long-time enhancement which lasted till the late phase. All of them were assessed to be hemangioma (Figure 3). According to the pathological diagnosis, the three fatty degenerative nodules (Figure 4) and one metastatic tumor were falsely diagnosed.

Corresponding to the results of pathological diagnosis, the sensitivity, specificity and accuracy of contrast-enhanced C^3-MODE technology on malignant hepatic tumors were 97.0%, 92.3% and 95.7%, respectively (Table 2).

The diagnosis made by adopting contrast-enhanced CT is shown in Table 2. One HCC was falsely diagnosed to be cystic change on the basis of its low attenuation on contrast-enhanced CT. In addition, two of the fatty degenerative nodules were assessed to be HCC by contrast-enhanced CT. Hence, the diagnostic sensitivity, specificity and accuracy of contrast-enhanced CT to malignant hepatic tumors was 94.1%, 91.7% and 93.5%, respectively (Table 2). There was no significant difference between the ability of contrast-enhanced C^3-MODE technology and contrast-enhanced CT on differential diagnosis of nodular hepatic nodules.

Table 2 Ability of differential diagnosis of malignant or benign lesions in liver: comparison between contrast-enhanced C^3-MODE technology and contrast-enhanced CT

		Pathological diagnosis		Sensitivity	Specificity	Accuracy
		Malignant	Benign			
C^3-MODE	Malignant	32	1	97.0%	92.3%	95.7%
	Benign	1	12			
CT	Malignant	32	2	94.1%	91.7%	93.5%
	Benign	1	11			
Total		33	13			

DISCUSSION

Contrast-enhanced ultrasonography has been developed rapidly in recent years. From fundamental CDI to second harmonic imaging, the detectability of contrast-enhanced ultrasound to the intratumoral vascularity of hepatic tumors increased significantly[6,7]. However, the relatively low sensitivity to contrast-enhanced signals of second harmonic imaging limited its use in clinical settings. Many kinds of new technologies were developed for higher detection of intratumoral vascularities of hepatic tumors for differential diagnosis[10,11]. Unfortunately, as the contrast agent was being injected via a peripheral venous, the concentration of the contrast agent decreased to 5% of the primary one when it reached the target organs because of the dilution of blood, attached by tissue or destroyed en route[15,16]. To increase the efficiency in utilization of the signals from microbubbles may be an effective way to increase the sensitivity of ultrasound. As reported, many new harmonic technologies greatly increased the detectability to harmonic signals by

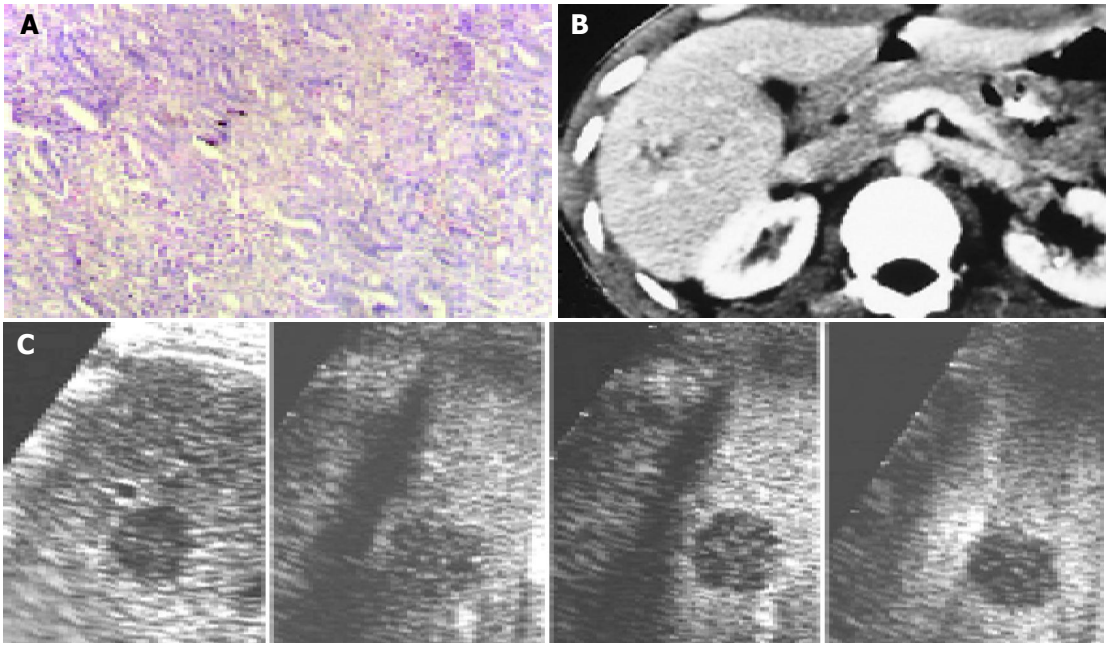

Figure 2 **A**: a 1.5 cm-sized metastatic adenocacinoma in liver; **B**: low attenuation on contrast-enhanced CT; **C**: rim-like enhancement in early arterial phase (28 s) and perfusion defect (46–130 s) on contrast-enhanced C^3-MODE technology.

different mechanisms[17,18]. However, they ignore the fundamental signals scattered from microbubbles, which is the strongest part of the signals from the microbubbles. To effectively use this part of the signals may be a useful way to increase the sensitivity of ultrasound to the contrast-enhanced signals. On the basis of the techniques of delayed emission method, time and dimension double manager technique and contrast moving scan (low MI monitor and high MI flash), C^3-MODE technology was recently developed. When it receives the signals from the contrast agent, C^3-MODE technology catches not only the second harmonic signals, but also the sub-harmonic, ultra-harmonic and fundamental signals from the microbubbles. As a result, more signals scattered by microbubbles were used. Theoretically, a higher resolution and sensitivity could be obtained.

In this study, C^3-MODE technology was performed with double mode, a low and a high MI mode. It is convenient to change the mode by pushing a small button. Low MI image can observe the lesion continuously without destroying

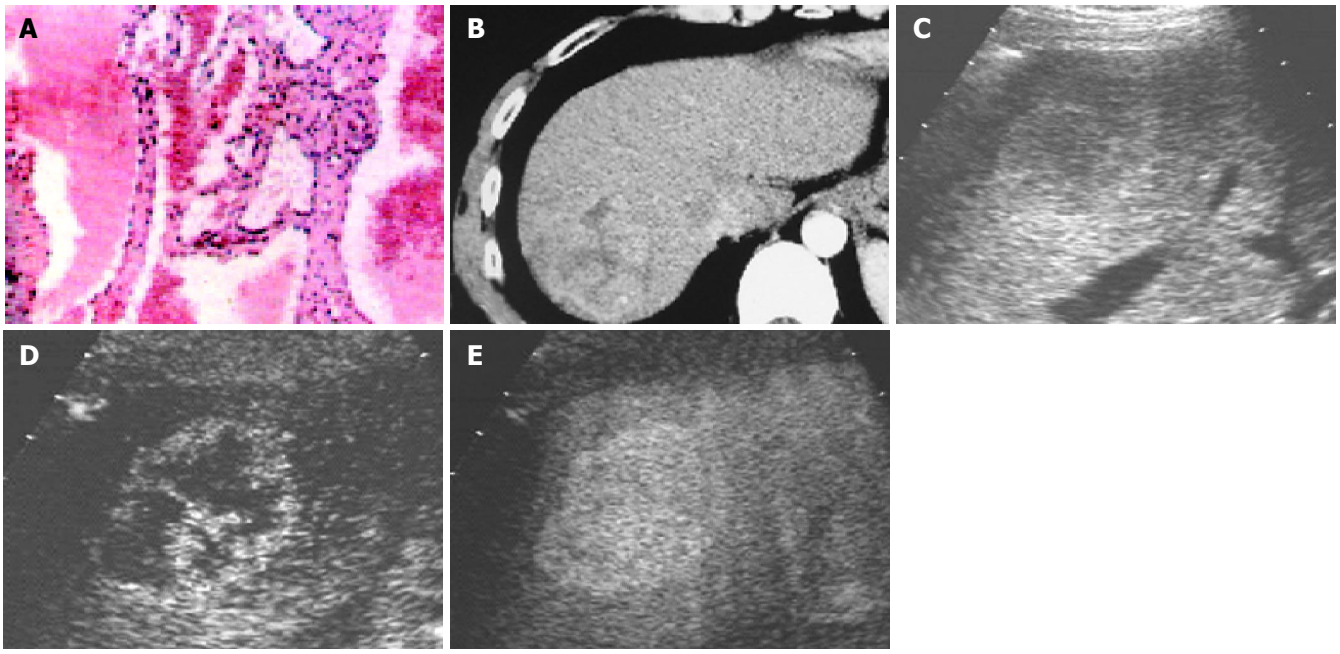

Figure 3 **A**: a 4.1 cm-sized hemangioma; **B**: heterogenous high attenuation on contrast-enhanced CT; **C**: hypoechoic lesion on B-mode image; **D**: the spot-like enhancement in early arterial phase on contrast-enhanced C^3-MODE technology; **E**: centripetal filling in late phase (e) on contrast-enhanced C^3-MODE technology.

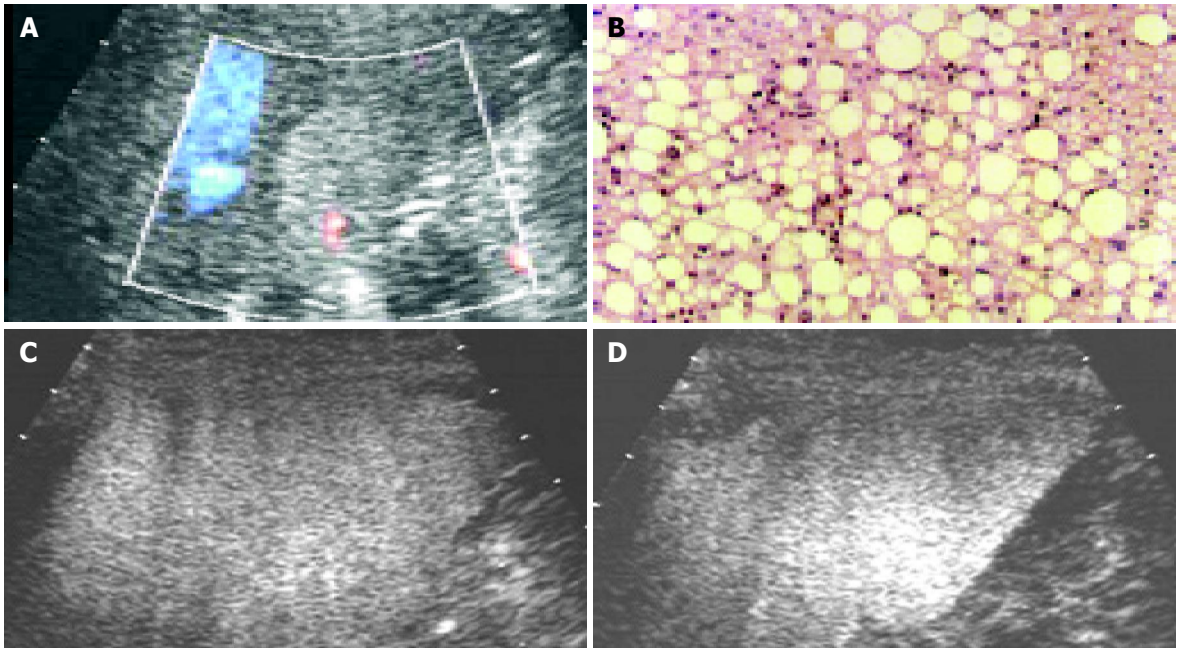

Figure 4 **A**: a hyperechoic lesion; **B**: pathological diagnosis of fatty degeneration; **C**: the intranodular enhancement on contrast-enhanced C^3-MODE technology in the early arterial phase; **D**: the intranodular enhancement in the late phase on contrast-enhanced C^3-MODE technology.

the microbubbles of the contrast agent, and high MI image can demonstrate the flash image by destroying the microbubbles. So we can monitor the lesion on low MI image which helps us from not losing the target, and observe the contrast-enhanced effect on high MI image.

In this study, we differentiate malignant tumors from benign ones according to the perfusion defect in the late phase on contrast-enhanced C^3-MODE technology. Thirty-two (69.6%) of the 46 nodules that showed perfusion defect in the late phase were proved to be malignant tumors, in this study. The specificity was as high as 97.0% and sensitivity was 92.3%. In contrast, those that showed high echo or iso-echo in the late phase were considered to be benign nodules. The diagnostic sensitivity and specificity were comparable to those of contrast-enhanced CT. With the help of the appearance in the early arterial phase, C^3-MODE technology can effectively differentiate HCC from metastatic tumors. The diagnoses were highly agreeable with the pathological diagnosis.

On C^3-MODE technology, one metastatic tumor was falsely diagnosed to be hemangioma and one hemangioma was falsely assessed to be HCC. This may be due to the high echo appearance of them on B-mode image, which disturbed the assessment of contrast-enhanced image. Other metastatic tumors were shown with rim-like enhancement in the early arterial phase and perfusion defect in the late phase. It may due to hypovascularity of these tumors which originated from the rectum.

In 13 benign nodules, three nodules of lipid degeneration were diagnosed to be hemangioma on C^3-MODE technology. It may be due to the high echo of the nodules and the loss of experience of its hemodynamics. By reviewing the video, we found that homogenous enhancement of the nodules occurred in the early arterial phase but not in the cotton-wool pattern.

The relatively small group and fewer kinds of the nodules are limitations of this study. In addition, C^3-MODE technology is still a high MI contrast-enhanced technology. It observes the contrast-enhanced effect mainly on the basis of high MI flash imaging. As the flash image is obtained, the microbubbles were destroyed rapidly. As a result, we cannot observe the contrast-enhancement continuously.

In conclusion, C^3-MODE technology can effectively depict the blood supply of hepatic nodules in the early arterial phase and the late phase by using a double mode system. It gets a high diagnostic agreement with pathological diagnosis in differential diagnosis of nodular hepatic lesions. We suggest that it provides a new approach for differentiating the malignant tumors from the benign lesions in the liver.

REFERENCES

1 **Menu Y**. Hepatocellular carcinoma-radiological findings. *Hepatogastroenterology* 1998; **45 Suppl 3**: 1232-1235
2 **Tanaka S**, Kitamura T, Fujita M, Nakanishi K, Okuda S. Color Doppler flow imaging of liver tumors. *AJR Am J Roentgenol* 1990; **154**: 509-514
3 **Kawasaki T**, Itani T, Nakase H, Mimura J, Komori H, Sugimoto K. Power Doppler imaging of hepatic tumours: differential diagnosis between hepatocellular carcinoma and metastatic adenocarcinoma. *J Gastroenterol Hepatol* 1998; **13**: 1152-1160
4 **Kudo M**. Imaging diagnosis of hepatocellular carcinoma and premalignant/borderline lesions. *Semin Liver Dis* 1999; **19**: 297-309
5 **Takayasu K**, Muramatsu Y, Furukawa H, Wakao F, Moriyama N, Takayama T, Yamasaki S, Sakamoto M, Hirohashi S. Early hepatocellular carcinoma: appearance at CT during arterial portography and CT arteriography with pathologic correlation. *Radiology* 1995; **194**: 101-105
6 **Fujimoto M**, Moriyasu F, Nishikawa K, Nada T, Okuma M. Color Doppler sonography of hepatic tumors with a galactose-based contrast agent: correlation with angiographic findings. *AJR Am J Roentgenol* 1994; **163**: 1099-1104
7 **Wen YL**, Kudo M, Minami Y, Chung H, Suetomi Y, Onda H,

Kitano M, Kawasaki T, Maekawa K. Value of new contrast harmonic technique for detecting tumor vascularity in hepatocellular carcinoma: preliminary results. *J Med Ultrasonics* 2003; **30**: 85-92

8 **Wen YL**, Kudo M, Minami Y, Chung H, Suetomi Y, Onda H, Kitano M, Kawasaki T, Maekawa K. Contrast-enhanced agent detection imaging: early experience in hepatocellular carcinoma. *J Med Ultrasonics* 2003; **30**: 77-84

9 **Wen YL**, Kudo M, Maekawa K, Minami Y, Chung H, Suetomi Y, Onda H, Kitano M, Kawasaki T. Contrast advanced dynamic flow imaging and contrast pulse subtraction imaging: preliminary results in hepatic tumors. *J Med Ultrasonics* 2002; **29**: 195-204

10 **Wen YL**, Kudo M, Zheng RQ, Ding H, Zhou P, Minami Y, Chung H, Kitano M, Kawasaki T, Maekawa K. Characterization of hepatic tumors: value of contrast-enhanced coded phase-inversion harmonic angio. *AJR Am J Roentgenol* 2004; **182**: 1019-1026

11 **Yücel C**, Ozdemir H, Gurel S, Ozer S, Arac M. Detection and differential diagnosis of hepatic masses using pulse inversion harmonic imaging during the liver-specific late phase of contrast enhancement with Levovist. *J Clin Ultrasound* 2002; **30**: 203-212

12 **Skjoldbye B**, Pedersen MH, Struckmann J, Burcharth F, Larsen T. Improved detection and biopsy of solid liver lesions using pulse-inversion ultrasound scanning and contrast agent infusion. *Ultrasound Med Biol* 2002; **28**: 439-444

13 **Forsberg F**, Piccoli CW, Liu JB, Rawool NM, Merton DA, Mitchell DG, Goldberg BB. Hepatic tumor detection: MR imaging and conventional US versus pulse-inversion harmonic US of NC100100 during its reticuloendothelial system-specific phase. *Radiology* 2002; **222**: 824-829

14 **Kim JH**, Kim TK Kim BS, Eun HW, Kim PN, Lee MG, Ha HK. Enhancement of hepatic hemangiomas with levovist on coded harmonic angiographic ultrasonography. *J Ultrasound Med* 2002; **21**: 141-148

15 **Kaul S**. Myocardial contrast echocardiography. *Curr Probl Cardiol* 1997; **22**: 549-635

16 **Maresca G**, Summaria V, Colagrande C, Manfredi R, Calliada F. New prospects for ultrasound contrast agents. *Eur J Radiol* 1998; **27 Suppl 2**: S171-S178

17 **Quaia E**, Bertolotto M, Dalla Palma L. Characterization of liver hemangiomas with pulse inversion harmonic imaging. *Eur Radiol* 2002; **12**: 537-544

18 **von Herbay A**, Vogt C, Häussinger D. Late-phase pulse-inversion sonography using the contrast agent levovist: differentiation between benign and malignant focal lesions of the liver. *AJR Am J Roentgenol* 2002; **179**: 1273-1279

Science Editor Guo SY **Language Editor** Elsevier HK

PO Box 2345, Beijing 100023, China
www.wjgnet.com
wjg@wjgnet.com

ELSEVIER

World J Gastroenterol 2005;11(16):2408-2412
World Journal of Gastroenterology ISSN 1007-9327

Hepatic artery infusion of antisense oligodeoxynucleotide and lipiodol mixture transfect liver cancer in rats

Han-Ping Wu, Gan-Sheng Feng, Yuan Tian

Han-Ping Wu, Gan-Sheng Feng, Department of Interventional Radiology, Union Hospital, Tongji Medical College, Huazhong University of Science and Technology, Wuhan 430022, Hubei Province, China
Yuan Tian, Laboratory of General Surgery, Union Hospital, Tongji Medical College, Huazhong University of Science and Technology, Wuhan 430022, Hubei Province, China
Correspondence to: Dr. Han-Ping Wu, Department of Interventional Radiology, Union Hospital, Tongji Medical College, Huazhong University of Science and Technology, Wuhan 430022, Hubei Province, China. shhwhp@public.wh.hb.cn
Telephone: +86-27-85726432 Fax: +86-27-85727002
Received: 2004-08-31 Accepted: 2004-12-16

Abstract

AIM: To study the distribution and stability of antisense oligodeoxynucleotide (ASODN) in Walker-256 cells and their distribution in liver, lung and kidney tissues after being infused alone or mixed with lipiodol via hepatic artery in a rat liver tumor model.

METHODS: 5′-Isothiocyananate (FITC)-labeled vascular endothelial growth factor (VEGF) ASODN was added into Walker-256 cell culture media. Its distribution in cells was observed by fluorescence microscope at different time points. Walker-256 carcinosarcoma was transplanted into Wistar rat liver to establish a liver cancer model. 5′-FITC-labeled VEGF ASODN mixed with (mixed group, $n = 6$) or without (TAI group, $n = 6$) ultra-fluid lipiodol was administrated via hepatic artery. Frozen samples of liver, lung and kidney tissue were taken from rats after 1, 3 and 6 d, respectively. The distribution of ASODN was observed under fluorescent microscope.

RESULTS: ASODN could enter cytoplasm within 2 h and nuclei within 6 h. Accumulation of ASODN reached the peak point in nuclei at 12 h, and then disappeared gradually. No fluorescence could be seen in cells at 48 h. *In vivo* experiment, on d 1 and 3 the fluorescence staining in liver was stronger in mixed group than in TAI group and more fluorescence could be detected in lung and kidney in TAI group than in mixed group. On d 6, no fluorescence could be detected in TAI group, but faint fluorescence could be seen in mixed group. ASODN could be seen in cancer cells and normal hepatic cells. In mixed group, ASODN was mainly distributed in liver tumor tissues.

CONCLUSION: ASODN can transfect Walker-256 cells. ASODN mixed with lipiodol infusion via hepatic artery can be used in the treatment of HCC.

Key words: Antisense oligodeoxynucleotide; VEGF; Lipiodol; Liver cancer model; Transhepatic artery infusion

Wu HP, Feng GS, Tian Y. Hepatic artery infusion of antisense oligodeoxynucleotide and lipiodol mixture transfect liver cancer in rats. *World J Gastroenterol* 2005; 11(16): 2408-2412
http://www.wjgnet.com/1007-9327/11/2408.asp

INTRODUCTION

Angiogenesis plays an important role in tumor progression and metastasis. One of the key mediators of angiogenesis is vascular endothelial growth factor (VEGF)[1-4]. It is overexpressed and secreted by the majority of human and animal tumors. Hepatocellular carcinoma (HCC) is one of the most common cancers in China. It is a hypervascular cancer and easy to metastasize. Recent studies indicate that VEGF is overexpressed in HCC tissues and positively related with progression and metastasis[5-7].

Antisense oligodeoxynucleotides (ASODNs) are short synthetic DNA molecules, their sequences are complementary to those present in specific target mRNA within cells. They can bind to target mRNA and block gene expression. They are becoming the focus of attention as a tool for down-regulation of gene expression that contributes to disease states[8]. It was reported that VEGF ASODN inhibits VEGF expression of cultured tumor cells and growth of implanted tumors in nude mice and is a potential drug to inhibit angiogenesis, prevent recurrence and metastasis of HCC[9-11]. However, there is no satisfactory method to deliver ASODN into the target tumor tissue and cells. Systemic administration of ASODN needs a high dosage, causes many side effects, and has no organ specificity for gene transfection[12-15]. Hepatic artery infusion (HAI) of ASODN can result in transfection organ or tumor tissue specificity; reduce the dosage and side effects. However, the time of ASODN action with tumor cells is transient and the transfection efficiency is still low.

Lipiodol is a common liquid embolic agent for transcatheter hepatic artery embolization for HCC. It stays in tumor tissue for a long period of time (several months), is absorbed by tumor cells[16,17], and acts as a carrier of chemotherapeutic agents to maximize the concentration and exposure time in

the tumor. We assumed that ASODN and lipiodol mixture infused via hepatic artery could enhance its transfection efficiency. In this study, we compared the different distributions of ASODN in Walker-256 carcinosarcoma liver transplantation model after infusion of ASODN alone or mixed with lipiodol via hepatic artery.

MATERIALS AND METHODS

Oligodeoxynucleotides (ODN)

Phosphorothioate ASODN with 5' end labeled with fluorescein isothiocyanate (FITC) was synthesized by Shanghai Sangon Biological Engineering Technology and Service Co., Ltd. Its sequence is 5'-GCA GTA GCT GCG CTG ATA GCG C-3', complementary to the exon 3 area of VEGF mRNA.

Cellular experiments

Walker-256 carcinosarcoma cells were purchased from China Center for Type Culture Collection. After recovery, the cells were inoculated into the abdominal cavity of male pathogen-free Wistar rats, weighing 100-120 g (Department of Experimental Animals, Tongji Medical College). Three days later, 0.2 mL of cancerous ascites was aspirated and cultured in RPMI-1640 containing 5 mL/L fetal calf serum (FCS) (Gibco, Grand Island, NY) and equilibrated with 950 mL/L air and 50 mL/L CO_2. Cells were passaged every 2 d. After the 3rd passage, cells were seeded into a 24-well plate at 1×10^3/well (100 μL/well), cultured with 33 μg (20 μL) FITC-ASODN at 37 ℃ in a humidified atmosphere containing 950 mL/L air and 50 mL/L CO_2. At 2, 6, 12, 24, 36 and 48 h, the cells were harvested, washed with non-serum medium thrice, dropped onto a slide, and then the FITC-ASODN cellular distribution was observed under a fluorescence microscope (Olympus, Japan).

Transplantation liver cancer model in rats

Tumor implantation was performed using a technique described by Li *et al*. Briefly, Walker-256 carcinosarcoma cells were inoculated subcutaneously into the right flank of Wistar rats with 1×10^7 tumor cells in approximately 0.1 mL of cell suspension. The tumor was palpable 7 d after inoculation. Fresh tumor tissue was isolated and cut into 1-mm^3 sections. The recipient animal was laparotomized through a midline abdominal incision under intraperitoneal anesthesia with 1% pentobarbital sodium (30 mg/kg body weight). The left lateral lobe of the liver was protruded out of the abdominal cavity and a subcapsular tunnel about 3-5 mm in depth was made by a fine-point tweezers. Then a solid tumor fragment was inserted into the subcapsular tunnel and fixed with a small piece of gelfoam on the liver surface. The abdominal cavity was closed, and the rat was bred. One week later, a transplanted tumor 0.5-1 cm in diameter grew in the left lobe of liver.

Catheterization of hepatic artery

Ten days after the implantation, another midline abdominal incision was made under intraperitoneal anesthesia. The common hepatic artery, gastroduodenal artery and right hepatic artery were isolated under a binocular operative microscope (Suzhou Medical Instruments Factory, Jiangsu, China). Through an arteriotomy of the gastroduodenal artery, the gastroduodenal artery was catheterized retrograde for drug infusion with a Portex PE10 tube (inner diameter 0.28 mm, external diameter 0.61 mm, Neolab, Germany) and temporarily fixed by a suture.

Animal group and ASODN infusion

Twelve tumor-bearing rats were divided into TAI group and mixed group, six rats each. TAI group received 165 μg FITC-ASODN diluted with 0.2 mL PBS and mixed group received 165 μg FITC-ASODN mixed with 0.2 mL lipiodol (Lipiodol UltraFluid, Andre Guerbet, Aulnay-sous-Bois, France). The drugs were infused retrograde into the gastroduodenal artery through the PE10 tube, while the common hepatic artery and right hepatic artery were temporarily ligated. Ten minutes after drug infusion, the tube was pulled out, the gastroduodenal artery was ligated, the common hepatic artery and right hepatic artery were untied and the abdominal wall was closed.

ASODN distribution

On d 1, 3 and 6 after drug administration, two animals in each group were killed at each time point. The liver tumor tissue, adjacent normal liver tissue, lung and kidney tissue samples were excised and frozen in liquid nitrogen and stored at -70 ℃. Frozen sections (5 μm in thickness) were cut and observed under a fluorescence microscope.

RESULTS

Cellular uptake and distribution of FITC-ASODN

At 2 h after Walker-256 cells were cultured with FITC-ASODN, granular fluorescence was detected in cytoplasm, and no fluorescences were detected in nuclei. At 6 h fluorescences in cytoplasm became denser and granular fluorescences were seen in nuclei. At 12 h fluorescences in cytoplasm and nuclei reached the peak. Then fluorescences disappeared gradually. No fluorescences could be seen in cells at 48 h (Figure 1).

Distribution of FITC-ASODN in rat liver tumor model

In mixed group, on d 1, fluorescences were detected mainly in liver tumor tissues and heavily stained with deep-yellow color. The delimitation of cells was hard to identify. Some peri-tumor zone also contained fluorescences. In lung and kidney tissues, the fluorescence was stained lightly. Piece-like fluorescence stain could be detected in some small areas of the lung tissues. On d 3, fluorescences in tumor and peri-tumor tissues became less, were mainly distributed in tumor tissue and could be found in most tumor cells. On d 6, fluorescences in tumor and peri-tumor tissues became further less, but fluorescences were still seen. Faint fluorescences were seen in lung and kidney on d 3 and 6 (Figure 2A).

In TAI group, fluorescences were dense in liver tumor and peri-tumor tissue, lung and kidney tissues on d 1, and then decreased gradually. No fluorescence was seen on d 6. The fluorescences in liver tumor and peri-tumor tissue in TAI group were much less than those in mixed group at each time point (Figure 2B).

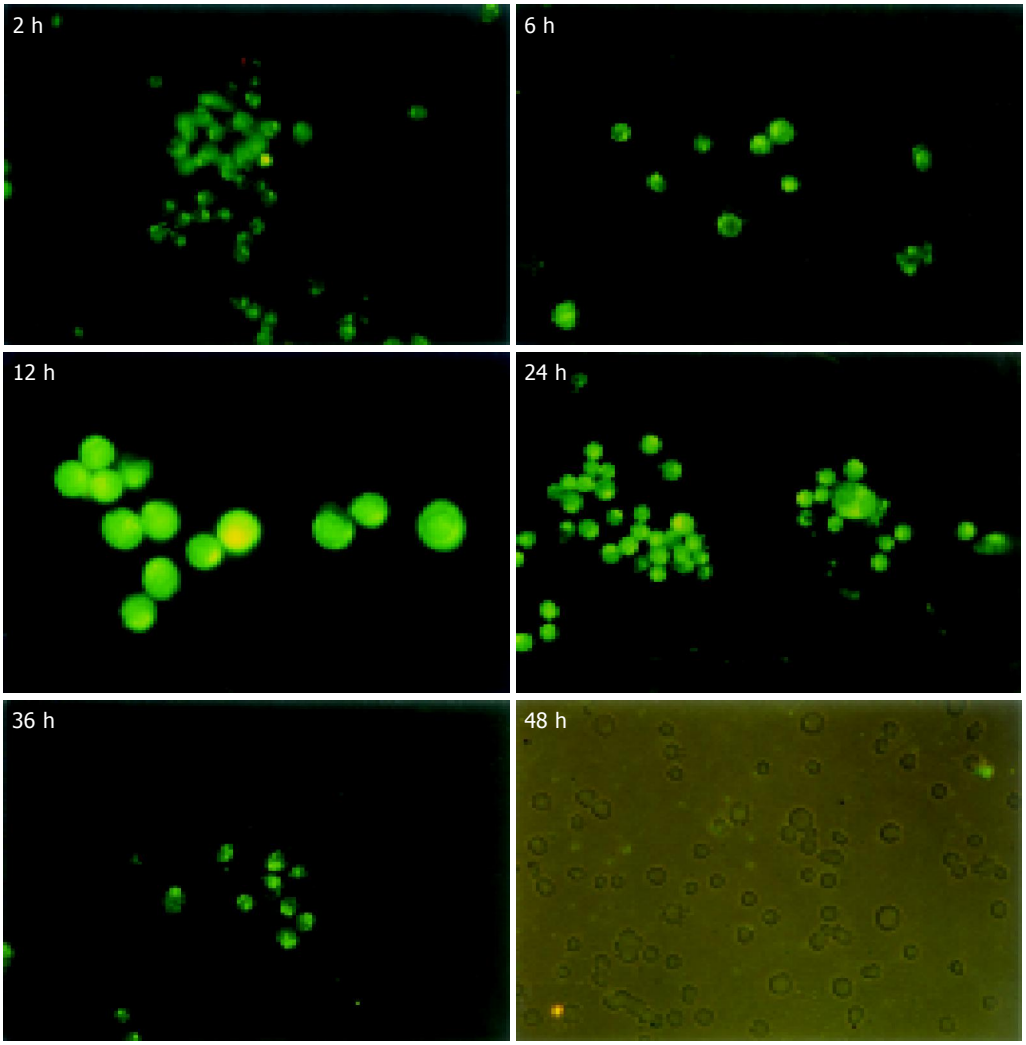

Figure 1 Distribution of FITC-ASODN in Walker-256 cells.

DISCUSSION

ASODN is a new therapeutic agent for HCC treatment. It binds specifically to mRNA via Watson-Crick base pair interaction and blocks the translation of corresponding proteins[9]. It can penetrate cell membrane and achieve appropriate concentration in the correct intracellular compartment (cytoplasm or nucleus)[18]. Tumor cell is the target cell of most designed ASODNs, such as VEGF ASODN. How to efficiently deliver ASODN to liver tumor cells remains to be solved[19]. Systemic intravenous injection is the routine route for ASODN administration. Studies of the distribution and metabolism of ASODN revealed that ASODN delivery has no organ specificity, ASODN stays in liver transiently, and high dose is required for transfection of hepatic cells[20-23]. Graham *et al*[24,25] reported that after a 10 mg/kg ASODN bolus, intracellular drug levels in liver reached the peak at 8 h and diminished significantly thereafter. Nonparenchymal (Kupffer and endothelial) cells contain approximately 80% of the total organ cellular dose, while the remaining 20% is associated with hepatocytes. At doses lower than 25 mg/kg, hepatocytes contain significantly less drug with no detectable ASODN in nuclei. Doses at or above 25 mg/kg appear to saturate nonparenchymal cell types, whereas hepatocytes continue to accumulate drugs in all cellular compartments, including nuclei. A higher dose of ODN may result in more side effects such as dose-dependent hypotension, complement activation, and transient prolongation of thromboplastin time[12-15]. Transcatheter artery infusion (TAI) can enhance the concentration of therapeutic gene, realize gene transfection in target organ selectively, and reduce dose and side effects. This administration route has been widely used in experimental and clinical gene therapies for brain tumor[26], coronary artery occlusive diseases[27], *etc*. However, as for the liver tumor treatment, the action ASODN on HCC cells is still transient, the transfection efficiency is still low, and the *in vivo* distribution of ASODN in liver and other organs after HAI has not been reported.

Most HCCs are hypervascular tumors. Their blood supply mainly comes from hepatic artery. Lipiodol can selectively accumulate in HCC when it is injected into the hepatic artery. The mechanism of selective retention of lipiodol in HCC includes the "siphoning effect" of tumor vessels resulting in lipiodol flowing into tumor vessels, the electrostatic difference between lipiodol and cancerous endothelia, transcapillary leak coupled with lack of lymphatic and Kupffer cell's clearance of lipiodol in HCC, membranous attachment of lipiodol to tumor cells, pinocytosis of lipiodol

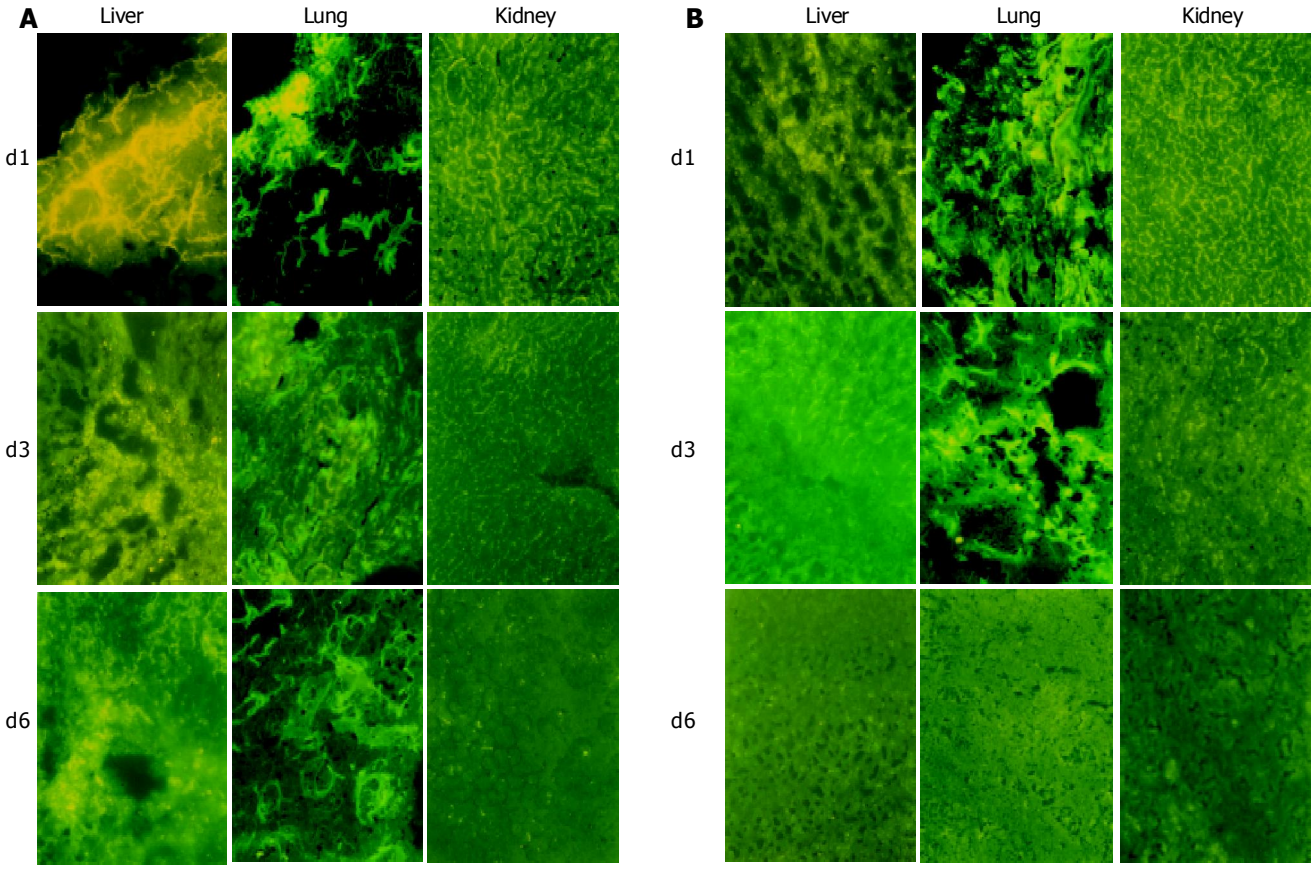

Figure 2 Cellular distribution of FITC-ASODN in liver, lung and kidney tissue in mixed group (**A**) and TAI group (**B**).

by tumor cells[18]. Lipiodol is a common liquid embolic agent and used as a carrier of chemotherapeutic agents for transcatheter artery chemoembolization of HCC.

In this study, ex vivo cell culture experiment indicated that ASODN could enter the cytoplasm and nuclei of Walker-256 cell and stay in a short period of time (about 36 h). In *in vivo* animal experiment, we found that ASODN mixed with lipiodol could transfect and enter into tumor cells and adjacent normal hepatic cells, mainly in tumor cells, and stay for more than 5 d. However, in TAI group, the distribution of ASODN in tumor and adjacent tissues showed no difference, and the retention of ASODN in liver tissue was less and shorter (about 3 d) than that in mixed group. The concentration of ASODN in lung and kidney tissue in mixed group was lower than that in TAI group on d 1. These findings indicate that ASODN can transfect normal hepatic cells and tumor cells without specificity, lipiodol can act as a carrier of ASODN to make it mainly distribute in tumor tissue, ASODN mixed with lipiodol can slowly diffuse into tumor tissue, act a longer period of time with tumor cells, thus enhancing the transfection rate and minimizing the distribution of ASODN in organs outside the liver.

In mixed group, piece-like fluorescence stained areas were seen in liver tissue on d 1. This is because FITC-ASODN does not release from lipiodol at that time. We also found piece-like fluorescence stain in some area of the lung on d 1. This is because the mixed ASODN and lipiodol enter the pulmonary artery and stay there.

ASODN mixed with lipiodol can enter tumor cells, but its mechanism is not clear. It may be due to the following points: (1) ASODN can release from lipiodol; (2) tumor vessels are immature, lack tunica media, and the gaps between endothelial cells are wide, leading to leak of ASODN and lipiodol into extracellular space easily; (3) lipiodol and ASODN can be absorbed by tumor cells.

In conclusion, ASODN mixed with lipiodol infusion via hepatic artery can be used in the treatment of HCC.

REFERENCES

1 **Giavazzi R,** Sennino B, Coltrini D, Garofalo A, Dossi R, Ronca R, Tosatti MP, Presta M. Distinct role of fibroblast growth factor-2 and vascular endothelial growth factor on tumor growth and angiogenesis. *Am J Pathol* 2003; **162**: 1913-1926
2 **Ferrara N**. Role of vascular endothelial growth factor in physiologic and pathologic angiogenesis: therapeutic implications. *Semin Oncol* 2002; **29**: 10-14
3 **Ziemer LS,** Koch CJ, Maity A, Magarelli DP, Horan AM, Evans SM. Hypoxia and VEGF mRNA expression in human tumors. *Neoplasia* 2001; **3**: 500-508
4 **Salgado R,** Benoy I, Bogers J, Weytjens R, Vermeulen P, Dirix L, Van Marck E. Platelets and vascular endothelial growth factor (VEGF): a morphological and functional study. *Angiogenesis* 2001; **4**: 37-43
5 **Cascinu S,** Graziano F, Catalano V, Staccioli MP, Barni S, Giordani P, Rossi MC, Baldelli AM, Muretto P, Valenti A, Catalano G. Differences of vascular endothelial growth factor (VEGF) expression between liver and abdominal metastases from colon cancer. Implications for the treatment with VEGF inhibitors. *Clin Exp Metastasis* 2000; **18**: 651-655
6 **Hirohashi K,** Yamamoto T, Uenishi T, Ogawa M, Sakabe K,

Takemura S, Shuto T, Tanaka H, Kubo S, Kinoshita H. CD44 and VEGF expression in extrahepatic metastasis of human hepatocellular carcinoma. *Hepatogastroenterology* 2004; **51**: 1121-1123

7 **Zhao J,** Hu J, Cai J, Yang X, Yang Z. Vascular endothelial growth factor expression in serum of patients with hepatocellular carcinoma. *Chin Med J (Engl)* 2003; **116**: 772-776

8 **Narayanan R,** Akhtar S. Antisense therapy. *Curr Opin Oncol* 1996; **8**: 509-515

9 **Yang PY,** Rui YC, Jin YX, Li TJ, Qiu Y, Zhang L, Wang JS. Antisense oligodeoxynucleotide inhibits vascular endothelial growth factor expression in U937 foam cells. *Acta Pharmacol Sin* 2003; **24**: 610-614

10 **Gong BD,** Luo W, Du FT, Ye RM, Liu JM, Yu CG, Zou YQ, Zhang JX. Inhibitory effects of antisense oligonucleotides on VEGF gene expression by human hepatocellular carcinoma cells. *Zhonghua Ganzangbing Zazhi* 2004; **12**: 35-37

11 **Zhu J,** Huang J, Chen Y. Effect of PCNA antisense oligooxynucleotides and VEGF antisense oligoxynucleotides on growth of hepatocellular carcinoma transplanted in nude mice. *Zhonghua Waike Zazhi* 2001; **39**: 875-877

12 **Iversen PL**, Copple BL, Tewary HK. Pharmacology and toxicology of phosphorothioate oligonucleotides in the mouse, rat, monkey and man. *Toxicol Lett* 1995; **82-83**: 425-430

13 **Leeds JM,** Henry SP, Bistner S, Scherrill S, Williams K, Levin AA. Pharmacokinetics of an antisense oligonucleotide injected intravitreally in monkeys. *Drug Metab Dispos* 1998; **26**: 670-675

14 **Tolcher AW,** Reyno L, Venner PM, Ernst SD, Moore M, Geary RS, Chi K, Hall S, Walsh W, Dorr A, Eisenhauer E. A randomized phase II and pharmacokinetic study of the antisense oligonucleotides ISIS 3521 and ISIS 5132 in patients with hormone-refractory prostate cancer. *Clin Cancer Res* 2002; **8**: 2530-2535

15 **Webb MS,** Tortora N, Cremese M, Kozlowska H, Blaquiere M, Devine DV, Kornbrust DJ. Toxicity and toxicokinetics of a phosphorothioate oligonucleotide against the c-myc oncogene in cynomolgus monkeys. *Antisense Nucleic Acid Drug Dev* 2001; **11**: 155-163

16 **Han GH,** Guo QL, Huang GS, Guo YL. Distribution of lipiodol in hepatocellular carcinoma after hepatic arterial injection and its significance. *Zhonghua Fangshexue Zazhi* 1993; **27**: 828-831

17 **Kan Z,** Sato M, Ivancev K, Uchida B, Hedgpeth P, Lunderquist A, Rosch J, Yamada R. Distribution and effect of iodized poppyseed oil in the liver after hepatic artery embolization: experimental study in several animal species. *Radiology* 1993; **186**: 861-866

18 **Butler M,** Stecker K, Bennett CF. Cellular distribution of phosphorothioate oligodeoxynucleotides in normal rodent tissues. *Lab Invest* 1997; **77**: 379-388

19 **Lappalainen K,** Miettinen R, Kellokoski J, Jaaskelainen I, Syrjanen S. Intracellular distribution of oligonucleotides delivered by cationic liposomes: light and electron microscopic study. *J Histochem Cytochem* 1997; **45**: 265-274

20 **Geary RS,** Yu RZ, Watanabe T, Henry SP, Hardee GE, Chappell A, Matson J, Sasmor H, Cummins L, Levin AA. Pharmacokinetics of a tumor necrosis factor-alpha phosphorothioate 2′-O-(2-methoxyethyl) modified antisense oligonucleotide: comparison across species. *Drug Metab Dispos* 2003; **31**: 1419-1428

21 **Bijsterbosch MK,** Manoharan M, Dorland R, Van Veghel R, Biessen EA, Van Berkel TJ. bis-Cholesteryl-conjugated phosphorothioate oligodeoxynucleotides are highly selectively taken up by the liver. *J Pharmacol Exp Ther* 2002; **302**: 619-626

22 **Ponnappa BC,** Dey I, Tu GC, Zhou F, Aini M, Cao QN, Israel Y. *In vivo* delivery of antisense oligonucleotides in pH-sensitive liposomes inhibits lipopolysaccharide-induced production of tumor necrosis factor-alpha in rats. *J Pharmacol Exp Ther* 2001; **297**: 1129-1136

23 **Zhang R,** Iyer RP, Yu D, Tan W, Zhang X, Lu Z, Zhao H, Agrawal S. Pharmacokinetics and tissue disposition of a chimeric oligodeoxynucleoside phosphorothioate in rats after intravenous administration. *J Pharmacol Exp Ther* 1996; **278**: 971-979

24 **Graham MJ,** Crooke ST, Monteith DK, Cooper SR, Lemonidis KM, Stecker KK, Martin MJ, Crooke RM. *In vivo* distribution and metabolism of a phosphorothioate oligonucleotide within rat liver after intravenous administration. *J Pharmacol Exp Ther* 1998; **286**: 447-458

25 **Graham MJ,** Crooke ST, Lemonidis KM, Gaus HJ, Templin MV, Crooke RM. Hepatic distribution of a phosphorothioate oligodeoxynucleotide within rodents following intravenous administration. *Biochem Pharmacol* 2001; **62**: 297-306

26 **Koga H,** Inamura T, Ikezaki K, Samoto K, Matsukado K, Fukui M. Selective transvascular delivery of oligodeoxynucleotides to experimental brain tumors. *J Neurooncol* 1999; **43**: 143-151

27 **Matsushita H,** Morishita R, Aoki M, Tomita N, Taniyama Y, Nakagami H, Shimozato T, Higaki J, Kaneda Y, Ogihara T. Transfection of antisense p53 tumor suppressor gene oligodeoxynucleotides into rat carotid artery results in abnormal growth of vascular smooth muscle cells. *Circulation* 2000; **101**: 1447-1452

Science Editor Wang XL **Language Editor** Elsevier HK

PO Box 2345, Beijing 100023, China
www.wjgnet.com
wjg@wjgnet.com

ELSEVIER

World J Gastroenterol 2005;11(16):2413-2419
World Journal of Gastroenterology ISSN 1007-9327

Determination of optical properties of normal and adenomatous human colon tissues *in vitro* using integrating sphere techniques

Hua-Jiang Wei, Da Xing, Jian-Jun Lu, Huai-Min Gu, Guo-Yong Wu, Ying Jin

Hua-Jiang Wei, Da Xing, Huai-Min Gu, Ying Jin, Institute of Laser Life Science, South China Normal University, Guangzhou 510631, Guangdong Province, China
Jian-Jun Lu, Guo-Yong Wu, Department of Surgery, the First Affiliated Hospital, Sun Yat-Sen Medical University, Guangzhou 510080, Guangdong Province, China
Supported by the National Major Fundamental Research Project of China 2002CCC00400 and the Team Project of Natural Science Foundation of Guangdong Province 015012
Correspondence to: Da Xing, Institute of Laser Life Science, South China Normal University, Guangzhou 510631, Guangdong Province, China. xingda@hsut.scnu.edu.cn
Telephone: +86-20-85210089 Fax: +86-20-85216052
Received: 2004-06-08 Accepted: 2004-08-21

Abstract

AIM: The purpose of the present study is to compare the optical properties of normal human colon mucosa/submucosa and muscle layer/chorion, and adenomatous human colon mucosa/submucosa and muscle layer/chorion *in vitro* at 476.5, 488, 496.5, 514.5 and 532 nm. We believe these differences in optical properties should help differential diagnosis of human colon tissues by using optical methods.

METHODS: *In vitro* optical properties were investigated for four kinds of tissues: normal human colon mucosa/submucosa and muscle layer/chorion, and adenomatous human colon mucosa/submucosa and muscle layer/chorion. Tissue samples were taken from 13 human colons (13 adenomatous, 13 normal). From the normal human colons a total of 26 tissue samples, with a mean thickness of 0.40 mm, were used (13 from mucosa/submucosa and 13 from muscle layer/chorion), and from the adenomatous human bladders a total of 26 tissue samples, with a mean thickness of 0.40 mm, were used (13 from mucosa/submucosa and 13 from muscle layer/chorion). The measurements were performed using a double-integrating-sphere setup and the optical properties were assessed from these measurements using the adding-doubling method that was considered reliable.

RESULTS: The results of measurement showed that there were significant differences in the absorption coefficients and scattering coefficients between normal and adenomatous human colon mucosa/submucosa at the same wavelength, and there were also significant differences in the two optical parameters between both colon muscle layer/chorion at the same wavelength. And there were large differences in the anisotropy factors between both colon mucosa/submucosa at the same wavelength, there were also large differences in the anisotropy factors between both colon muscle layer/chorion at the same wavelength. There were large differences in the value ranges of the absorption coefficients, scattering coefficients and anisotropy factors between both colon mucosa/submucosa, and there were also large differences in these value ranges between both colon muscle layer/chorion. There are the same orders of magnitude in the absorption coefficients for four kinds of colon tissues. The scattering coefficients of these tissues exceed the absorption coefficients by at least two orders of magnitude.

CONCLUSION: There were large differences in the three optical parameters between normal and adenomatous human colon mucosa/submucosa at the same laser wavelength, and there were also large differences in these parameters between both colon muscle layer/chorion at the same laser wavelength. Large differences in optical parameters indicate that there were large differences in compositions and structures between both colon mucosa/submucosa, and between both colon muscle layer/chorion. Optical parameters for four kinds of colon tissues are wavelength dependent, and these differences would be useful and helpful in clinical applications of laser and tumors photodynamic therapy (PDT).

Key words: Optical properties; Laser; Normal and adenomatous human colon tissues; Integrating sphere

Wei HJ, Xing D, Lu JJ, Gu HM, Wu GY, Jin Y. Determination of optical properties of normal and adenomatous human colon tissues *in vitro* using integrating sphere techniques. *World J Gastroenterol* 2005; 11(16): 2413-2419
http://www.wjgnet.com/1007-9327/11/2413.asp

INTRODUCTION

In the field of biomedical optics, determination of the optical properties of various biological materials is essential and important for many diagnostic and therapeutic applications of light in medicine[1-12]. Clinical protocols are usually based on clinical experience and optical properties of tissues[13-15]. For example, photodynamic therapy (PDT) is a relatively new cancer therapy, it is a superficial treatment characterized by a depth of necrosis, which depends on several parameters including delivered light dose, photosensitizer concentration and tissue optical properties[16]. The tumors of many kinds seems ideally suited to PDT, for example,

colon, bladder, *etc.* tumors are suited to PDT, as it is readily accessible using an endoscope and the entire mucosa can be easily treated simultaneously via a diffusing light fiber. Multifocal superficial disease and occult carcinoma *in situ* do not have to be localized precisely for PDT to be effective[17-19], and yet PDT treatment effectiveness is greatly influenced by photosensitizer content and light distribution in the irradiated tumor tissue[20-27], and an accurate evaluation of energy fluence in depth should allow an estimate of whether the whole tumor mass will be properly irradiated[28-31]. Consequently tissue optical properties, absorption coefficients (μ_a), scattering coefficients (μ_s) and anisotropy factors (g) of thin slabs of human colon and diseased colon tissue are important for medical applications in diagnosis and therapy[27]. The purpose of the present study is to compare the optical properties of normal human colon mucosa/submucosa and muscle layer/chorion, and adenomatous human colon mucosa/submucosa and muscle layer/chorion *in vitro* at 476.5, 488, 496.5, 514.5 and 532 nm, i.e., μ_a, μ_s and *g*. The results of the experiment were analyzed and compared, and experimental results were obtained.

MATERIALS AND METHODS

Materials

Experimental materials *In vitro* optical properties were investigated for four kinds of tissues: normal human colon mucosa/submucosa and muscle layer/chorion, and adenomatous human colon mucosa/submucosa and muscle layer/chorion. Tissue samples were taken from 13 human colons (13 adenomatous, 13 normal), immediately after excision of the tissues. Each removed colon sample was immediately rinsed briefly in saline to remove surface excess blood and peeled off surface fats, and was put into bottles with saline as soon as possible, was stored in a refrigerator at 0 ℃, was sectioned by microtome before measurement. All tissue samples were respectively clamped between two glass slides of 1.03 mm thickness, and then were respectively placed between the two integrating spheres before tissue samples were measured. From the normal human colons a total of 26 tissue samples, with a mean thickness of 0.40 mm, were used (13 from mucosa/submucosa and 13 from muscle layer/chorion), and from the adenomatous human bladders a total of 26 tissue samples, with a mean thickness of 0.40 mm, were used (13 from mucosa/submucosa and 13 from muscle layer/chorion). Tissue samples were prepared and measurements were taken within at most 17 h after removal.

Methods

Measurement of tissue optical parameters An established method for measuring the optical parameters of turbid materials is the integrating-sphere technique. This technique is widely used for the determination of the optical properties of biological tissues *in vitro* and for the verification of the optical techniques intended for use *in vivo*[32-38]. The experimental set-up is schematically shown in Figure 1. The colon samples were placed between two identical integrating spheres (Anhui Institute of Optics and Fine Mechanics, Academia Sinica, China, model: F4) of 50 mm diameter with a circular sample port of 12 mm diameter and illuminated with collimated light from (1) a 2.2 mm beam diameter, 532 nm laser (LBO double-frequency, COHERENT, USA, model: Verdi-V10) operating at 0-10 W, (2) a 2.7 mm beam diameter, 476.5, 488, 496.5, 514.5 nm argon ion laser (COHERENT, USA, model: INNOVA 70) operating at 0-1.5 W. The output of all laser were collimated and attenuated (to a power at most 10 mW) by 2 mm pinhole and light attenuators, respectively. The light fluences within each sphere (the diffuse reflectance in the first sphere, the diffuse transmission in the second sphere), and the collimated transmission (at a distance of 80 cm beyond the second sphere) were measured using standard light measuring techniques[39]. The input light beams to form an intersection with light axis was approximately 1.5° were chopped mechanically at 500 Hz by using light chopper (SRS, USA, model: SR540). The collimated transmitted light signals, the diffuse reflectance R_d, and the diffuse transmittance T_d were measured by using photodiode detectors (APP, Hamamatsu, Japan, model: C5460) at 476.5, 488, 496.5, 514.5 and 532 nm. The signals were amplified using a lock-in-amplifier (SRS, USA, model: SR830) and processed by a personal computer. All measurements within the spheres were made relative to the signal when a 99% reflecting plate (Anhui Institute of Optics and Fine Mechanics, Academia Sinica, China, model: F4) was placed at the sample aperture, and the collimated transmission measurement was made relative to a measurement with no sample. For a more detailed description of the measurement method of a double-integrating-sphere set-up see Pickering *et al*[40-42], and van van Hillegersberg *et al*[43]. The optical properties, μ_a, μ_s and *g*, of thin slabs of colon tissue were determined by measuring the collimated transmission, diffuse reflectance and transmission in the aforesaid set-up. The inverse adding-doubling algorithm was used to determine the optical parameters from these measurements[44]. The algorithm accounts for the refractive index of the glass slides (n = 1.55) and of tissue (n = 1.4)[45].

Statistical analysis

Optical parameters of biological tissue samples were expressed as the mean±SD, were demonstrated by Student's

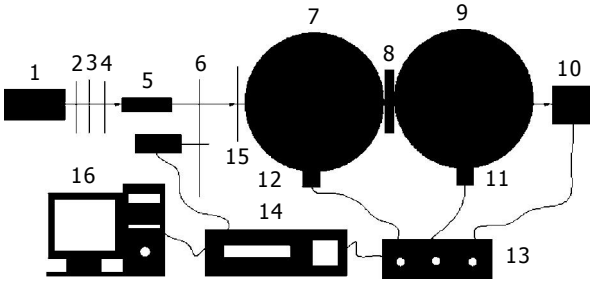

Figure 1 Experimental set-up consisting of double- integrating-sphere with an intervening sample. 1. Laser 2. Attenuator 3. Attenuator 4. 2 mm pinhole 5. Beam expander 6. 6 mm pinhole 7. Integrating sphere 8. Sample 9. Integrating sphere 10. Photodiode detector 11. Photodiode detector 12. Photodiode detector 13. Switch box 14. Lock-in-amplifier 15. Light chopper 16. PC.

t-test, and were considered significant at P values <0.01. The SPSS10 was used for the statistical analysis.

RESULTS

In this experiment, five different wavelengths of laser were respectively used for radiating the two incision areas of tissue slices, each of the measured value at each wavelength of laser in the same condition of experimentation was the mean arithmetical value that was gained by 24 measurements repeatedly at each kind of tissue sample of a total of 13 tissue samples at the same wavelength of laser, and per tissue sample was measured twice for each incision area of the tissue slice, respectively. The position of luminous spot of incident light radiation on the sample was changed after each measured datum was obtained. The two incision areas of the same kind of all samples were respectively radiated at each one wavelength of laser respectively, the measured results were reproducible for a specific sample at specific wavelength. There were no significant differences in the measured values R_d or T_d and or T_c of the two incision areas of the same kind of all samples at the same wavelength. Consequently, the collimated transmittance, diffuse reflectance and transmittance of the two incision areas of the same kind of all samples at the same wavelength were estimated with arithmetical average. By the inverse adding-doubling algorithm, we gained the wavelength dependence of the absorption coefficients, the scattering coefficients and the scattering anisotropy factors of these tissues from these measurements. Tables 1 and 2 summarize the results of our measurements for four kinds of tissues at the five wavelengths. The optical properties are expressed as the mean±SD for all measurements within one group of samples (e.g., normal human colon mucosa/submucosa at 488 nm).

DISCUSSION

In vitro optical properties of both normal and adenomatous human colon mucosa/submucosa and muscle layer/chorion were determined at 476.5, 488, 496.5, 514.5 and 532 nm, the measurements were performed using a double-integrating-sphere setup and the optical properties were assessed from these measurements using the adding-doubling method that was considered reliable[42,44,46]. In our study, it is interesting to note the differences in optical properties measured between these tissues at five different laser wavelengths. We believe these differences in optical properties should help the differential diagnosis of human colon tissues by using optical methods.

Absorption coefficients

Table 1 shows that the absorption coefficient for normal human colon mucosa/submucosa is 2.32/cm at 476.5 nm but increases to 3.27/cm at 488 nm and drops to 2.58/cm at 496.5 nm but increases to 3.12/cm at 514.5 nm and to 3.33/cm at 532 nm, and that for adenomatous human colon mucosa/submucosa is 5.27/cm at 476.5 nm but increases to 5.34/cm at 488 nm and drops to 4.87/cm at

Table 1 Anisotropy factors, absorption and scattering coefficients of normal and adenomatous human colon mucosa/submucosa at five different wavelengths of laser irradiation by the inverse adding-doubling method

Tissue	λ (nm)	μ_a (/cm)	μ_s (/cm)	g
Normal human colon mucosa/submucosa	476.5	2.32±0.09	214±5.35	0.885±0.019
	488.0	3.27±0.13	228±5.69	0.891±0.021
	496.5	2.58±0.10	212±5.27	0.897±0.024
	514.5	3.12±0.12	216±5.38	0.902±0.026
	532.0	3.33±0.14	208±5.16	0.908±0.029
Adenomatous human colon mucosa/submucosa	476.5	5.27±0.21	233±5.72	0.897±0.023
	488.0	5.34±0.22	238±5.84	0.903±0.027
	496.5	4.87±0.19	228±5.67	0.907±0.028
	514.5	4.37±0.17	231±5.69	0.917±0.033
	532.0	5.16±0.20	223±5.63	0.913±0.031

Table 2 Anisotropy factors, absorption and scattering coefficients of normal adenomatous human colon muscle layer/chorion at five different wavelengths of laser irradiation by the inverse adding-doubling method

Tissue	λ (nm)	μ_a (/cm)	μ_s (/cm)	g
Normal human colon muscle layer/chorion	476.5	1.31±0.05	221±5.61	0.923±0.037
	488.0	1.73±0.07	215±5.33	0.932±0.044
	496.5	1.27±0.05	200±5.08	0.927±0.041
	514.5	1.14±0.04	189±5.03	0.933±0.045
	532.0	1.53±0.06	193±5.05	0.941±0.048
Adenomatous human colon muscle layer/chorion	476.5	3.17±0.12	233±5.71	0.927±0.042
	488.0	3.51±0.14	223±5.62	0.935±0.046
	496.5	2.90±0.11	216±5.36	0.933±0.044
	514.5	2.57±0.09	198±5.07	0.936±0.047
	532.0	2.75±0.10	208±5.14	0.945±0.049

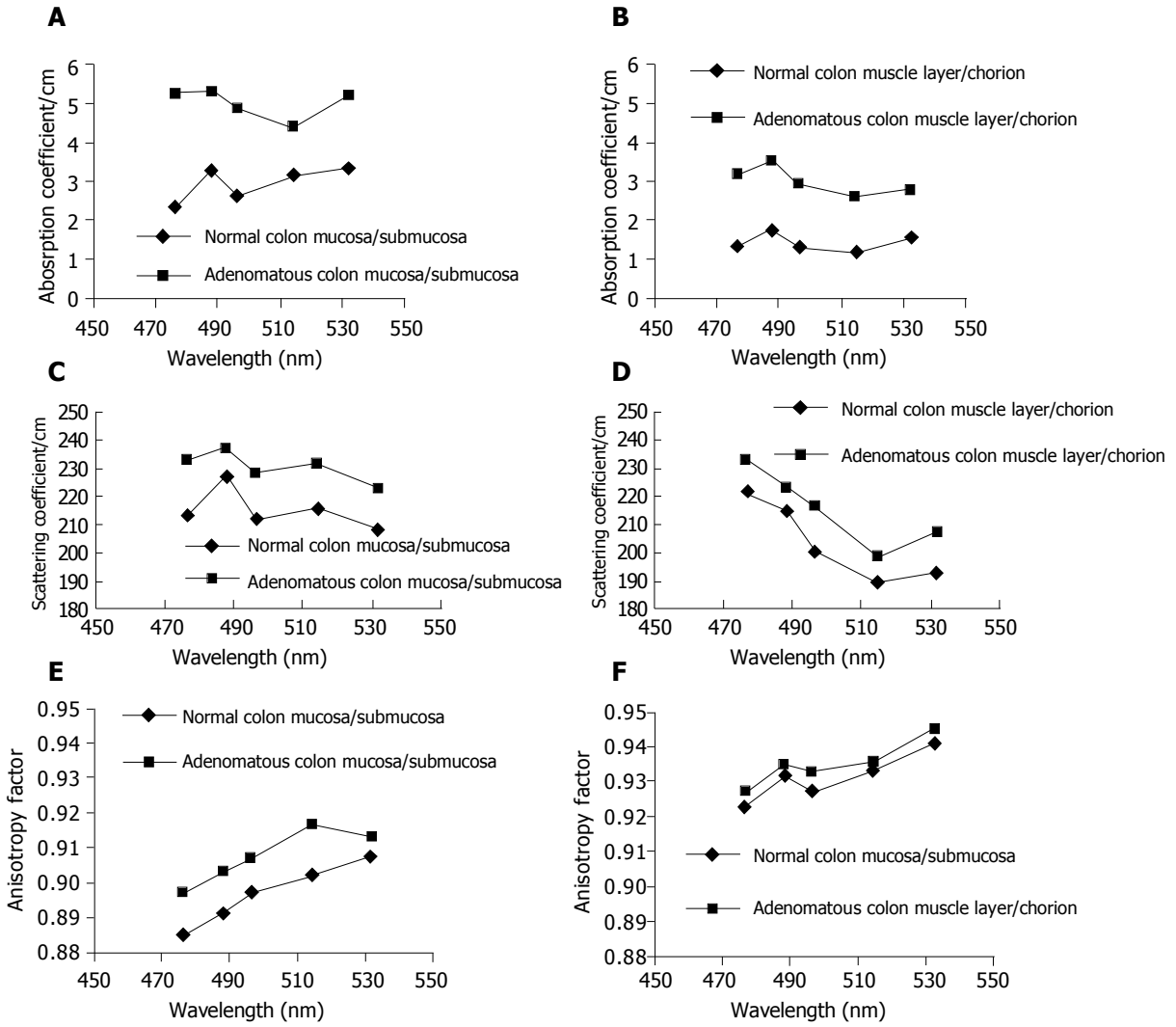

Figure 2 Optical properties of normal and adenomatous human colon mucosa/submucosa *in vitro* vary with a change of laser wavelength *in vitro*. **A**: Plots of the absorption coefficients measured *in vitro vs* wavelength of normal and adenomatous human colon mucosa/submucosa; **B**: Plots of the absorption coefficients measured *in vitro vs* wavelength of normal and adenomatous human colon muscle layer/chorion; **C**: Plots of the scattering coefficients measured *in vitro vs* wavelength of normal and adenomatous human colon mucosa/submucosa; **D**: Plots of the scattering coefficients measured *in vitro vs* wavelength of normal and adenomatous human colon muscle layer/chorion; **E**: Plots of the anisotropy factors measured *in vitro vs* wavelength of normal and adenomatous human colon mucosa/submucosa; **F**: Plots of the anisotropy factors measured *in vitro vs* wavelength of normal and adenomatous human colon muscle layer/chorion.

496.5 nm and to 4.37/cm at 514.5 nm but increases to 5.16/cm at 532 nm. It is obvious that there were significant differences in the absorption coefficients between both colon mucosa/submucosa at the same wavelength ($P<0.01$). The minimum value of the absorption coefficients for normal colon mucosa/submucosa is 2.32/cm at 476.5 nm and the maximum value is 3.33/cm at 532 nm, it is obvious that the values lie in the range between 2.32 and 3.33/cm. And the minimum value for adenomatous colon mucosa/submucosa is 4.37/cm at 514.5 nm and the maximum value is 5.34/cm at 488 nm, the values lie in the range between 4.37 and 5.34/cm, obviously there are large differences in the value range of the absorption coefficients between both tissues. Table 2 shows that the absorption coefficient for normal colon muscle layer/chorion is 1.31/cm at 476.5 nm but increases to 1.73/cm at 488 nm and drops to 1.27/cm at 496.5 nm and to 1.14/cm at 514.5 nm but increases to 1.53/cm at 532 nm, and that for adenomatous colon muscle layer/chorion is 3.17/cm at 476.5 nm but increases to 3.51/cm at 488 nm and drops to 2.90/cm at 496.5 nm and to 2.57/cm at 514.5 nm but increases to 2.75/cm at 532 nm. It is obvious that there were also significant differences in the absorption coefficients between both colon muscle layer/chorion at the same wavelength ($P<0.01$). The minimum value of the absorption coefficients for normal colon muscle layer/chorion is 1.14/cm at 514.5 nm and the maximum value is 1.73/cm at 488 nm, it is obvious that the values lie in the range between 1.14 and 1.73/cm. And the minimum value for adenomatous colon muscle layer/chorion is 2.75/cm at 532 nm and the maximum value is 3.51/cm at 488 nm, the values lie in the range between 2.75 and 3.51/cm, obviously there are large differences in the value range of the absorption coefficients between both tissues. Figure 2A,B show respectively the wavelength dependence of the absorption coefficients of both tissues obtained from the measurements, the shape of the two curves in Figure 1 is not similar, and the shape of the two curves in Figure 2A is similar, and large differences

of the absolute values of two curves in Figures 2A and B, respectively indicate that there were large differences in compositions and structures between two tissues, and just large differences in compositions and structures induce large differences in absorption characteristics between both tissues.

The scattering coefficients

Table 1 shows that the scattering coefficient for normal human colon mucosa/submucosa is 214/cm at 476.5 nm but increases to 228/cm at 488 nm and drops to 212/cm at 496.5 nm but increases to 216/cm at 514.5 nm and drops to 208/cm at 532 nm, and that for adenomatous human colon mucosa/submucosa is 233/cm at 476.5 nm but increases to 238/cm at 488 nm and drops to 228/cm at 496.5 nm but increases to 231/cm at 514.5 nm drops to 223/cm at 532 nm. It is obvious that there were also significant differences in the scattering coefficients between both colon mucosa/submucosa at the same wavelength ($P<0.01$). The minimum value of the scattering coefficients for normal colon mucosa/submucosa is 208/cm at 532 nm and the maximum value is 228/cm at 488 nm, it is obvious that the values lie in the range between 208 and 228/cm. And the minimum value for adenomatous colon mucosa/submucosa is 223/cm at 532 nm and the maximum value is 238/cm at 488 nm, the values lie in the range between 223 and 238/cm, obviously there are large differences in the value range of the scattering coefficients between both tissues. Table 2 shows that the scattering coefficient for normal colon muscle layer/chorion is 221/cm at 476.5 nm and drops to 215/cm at 488 nm and to 200/cm at 496.5 nm and to 189/cm at 514.5 nm but increases to 193/cm at 532 nm, and that for adenomatous colon muscle layer/chorion is 233/cm at 476.5 nm and drops to 223/cm at 488 nm and to 216/cm at 496.5 nm and to 198/cm at 514.5 nm but increases to 208/cm at 532 nm. It is obvious that there were also significant differences in the scattering coefficients between both colon muscle layer/chorion at the same wavelength ($P<0.01$). The minimum value of the scattering coefficients for normal colon muscle layer/chorion is 189/cm at 514.5 nm and the maximum value is 221/cm at 476.5 nm, obviously the values lie in the range between 189 and 221/cm. And the minimum value for adenomatous colon muscle layer/chorion is 198/cm at 514.5 nm and the maximum value is 233/cm at 476.5 nm, the values lie in the range between 198 and 233/cm, obviously there are also large differences in the value range of the scattering coefficients between both tissues. Figures 2C and D show respectively the wavelength dependence of the scattering coefficients of both tissues obtained from the measurements, the shape of the two curves in Figure 2B is similar, and the shape of the two curves in Figure 2C is also similar, and large differences of the absolute values of two curves in Figures 2C and D respectively indicate that there were also large differences in compositions and structures between two tissues, and just large differences in compositions and structures induce large differences in scattering characteristics between both tissues.

Anisotropy factors

Table 1 shows that the anisotropy factors for normal human colon mucosa/submucosa is 0.885 at 476.5 nm but increases to 0.891 at 488 nm and to 0.897 at 496.5 nm and to 0.902 at 514.5 nm and to 0.908 at 532 nm, and that for adenomatous human colon mucosa/submucosa is 0.897 at 476.5 nm but increases to 0.903 at 488 nm and to 0.907 at 496.5 nm and to 0.917 at 514.5 nm and drops to 0.913 at 532 nm. It is obvious that there were large differences in the anisotropy factors between both colon mucosa/submucosa at the same wavelength. The minimum value of the anisotropy factors for normal colon mucosa/submucosa is 0.885 at 476.5 nm and the maximum value is 0.908 at 532 nm, obviously the values lie in the range between 0.885 and 0.908. And the minimum value for adenomatous colon mucosa/submucosa is 0.897 at 476.5 nm and the maximum value is 0.917 at 514.5 nm, the values lie in the range between 0.897 and 0.917, obviously there are large differences in the value range of the anisotropy factors between both tissues. Table 2 shows that the anisotropy factors for normal colon muscle layer/chorion is 0.923 at 476.5 nm but increases to 0.932 at 488 nm and drops to 0.927 at 496.5 nm but increases to 0.933 at 514.5 nm and to 0.941 at 532 nm, and that for adenomatous colon muscle layer/chorion is 0.927 at 476.5 nm but increases to 0.935 at 488 nm and drops to 0.933 at 496.5 nm but increases to 0.936 at 514.5 nm and to 0.945 at 532 nm. It is obvious that there were large differences in the anisotropy factors between both colon muscle layer/chorion at the same wavelength. The minimum value of the anisotropy factors for normal colon muscle layer/chorion is 0.923 at 476.5 nm and the maximum value is 0.941 at 532 nm, it is obvious that the values lie in the range between 0.923 and 0.941. And the minimum value for adenomatous colon muscle layer/chorion is 0.927 at 476.5 nm and the maximum value is 0.945 at 532 nm, the values lie in the range between 0.927 and 0.945, it is obvious that there are obvious differences in the value range of the anisotropy factors between both tissues. Figures 2E and F show respectively the wavelength dependence of the anisotropy factors of both tissues obtained from the measurements, the shape of the two curves in Figure 2E is not similar, and the shape of the two curves in Figure 2F is similar, and obvious differences of the absolute values of two curves in Figures 2E andF, respectively indicate also that there were obvious differences in compositions and structures between two tissues, and just obvious differences in compositions and structures induce obvious differences in anisotropy characteristics between both tissues.

Researching the results indicate that there were obvious differences in tissue optical properties between both colon mucosa/submucosa and between both colon muscle layer/chorion at the same laser wavelength. The same orders of magnitude exist in the absorption coefficients for four kinds of colon tissues. The scattering coefficients of these tissues exceed the absorption coefficients by at least two orders of magnitude. The absorption coefficients are strongly affected by the presence of blood, particularly at wavelengths below 600 nm. Tissues of various pathologies have differing absorption coefficients and scattering properties and these differences are wavelength dependent, and these differences would be useful and helpful in clinical applications of laser and tumors PDT.

ACKNOWLEDGMENTS

We gratefully acknowledge the development of the inverse adding-doubling program by Dr. S.A.

REFERENCES

1 **Kienle A**, Forster FK, Hibst R. Influence of the phase function on determination of the optical properties of biological tissue by spatially resolved reflectance. *Opt Lett* 2001; **26**: 1571-1573
2 **Tunnell JW**, Wang LV, Anvari B. Optimum pulse duration and radiant exposure for vascular laser therapy of dark port-wine skin: a theoretical study. *Appl Opt* 2003; **42**: 1367-1378
3 **Fabbri F**, Franceschini MA, Fantini S. Characterization of spatial and temporal variations in the optical properties of tissuelike media with diffuse reflectance imaging. *Appl Opt* 2003; **42**: 3063-3072
4 **Dam JS**, Dalgaard T, Fabricius PE, Andersson-Engels S. Multiple polynomial regression method for determination of biomedical optical properties from integrating sphere measurements. *Appl Opt* 2000; **39**: 1202-1209
5 **Wang LV**, Jacques SL. Source of error in calculation of optical diffuse reflectance from turbid media using diffusion theory. *Comput Methods Programs Biomed* 2000; **61**: 163-170
6 **Qian Z,** Victor S, Gu Y, Giller C, Liu H. Look-Ahead Distance of a fiber probe used to assist neurosurgery: Phantom and Monte Carlo study. *Opt Express* 2003; **11**: 1844-1855
7 **Ghosh N**, Patel H, Gupta P. Depolarization of light in tissue phantoms-effect of a distribution in the size of scatterers. *Opt Express* 2003; **11**: 2198-2205
8 **Hadley KC**, Vitkin IA. Optical rotation and linear and circular depolarization rates in diffusively scattered light from chiral, racemic, and achiral turbid media. *J Biomed Opt* 2002; **7**: 291-299
9 **Pogue BW**, White EA, Osterberg UL, Paulsen KD. Absorbance of opaque microstructures in optically diffuse media. *Appl Opt* 2001; **40**: 4616-4621
10 **Mehrubeoglu M**, Kehtarnavaz N, Marquez G, Duvic M, Wang LV. Skin lesion classification using oblique-incidence diffuse reflectance spectroscopic imaging. *Appl Opt* 2002; **41**: 182-192
11 **Kokhanovsky AA**. Reflection and transmission of polarized light by optically thick weakly absorbing random media. *J Opt Soc Am A* 2001; **18**: 883-887
12 **Jarry G**, Henry F, Kaiser R. Anisotropy and multiple scattering in thick mammalian tissues. *J Opt Soc Am A Opt Image Sci Vis* 2000; **17**: 149-153
13 **Tunnell JW**, Wang LV, Anvari B. Optimum pulse duration and radiant exposure for vascular laser therapy of dark port-wine skin: a theoretical study. *Appl Opt* 2003; **42**: 1367-1378
14 **Choi J**, Wolf M, Toronov V, Wolf U, Polzonetti C, Hueber D, Safonova LP, Gupta R, Michalos A, Mantulin W, Gratton E. Noninvasive determination of the optical properties of adult brain: near-infrared spectroscopy approach. *J Biomed Opt* 2004; **9**: 221-229
15 **Fantini S**, Walker SA, Franceschini MA, Kaschke M, Schlag PM, Moesta KT. Assessment of the size, position, and optical properties of breast tumors *in vivo* by noninvasive optical methods. *Appl Opt* 1998; **37**: 1982-1989
16 **Solonenko M**, Cheung R, Busch TM, Kachur A, Griffin GM, Vulcan T, Zhu TC, Wang HW, Hahn SM, Yodh AG. *In vivo* reflectance measurement of optical properties, blood oxygenation and motexafin lutetium uptake in canine large bowels, kidneys and prostates. *Phys Med Biol* 2002; **47**: 857-873
17 **Roche JVE**, Whitehurst C, Watt P, Moore JV, Krasner N. Photodynamic therapy (PDT) of gastrointestinal tumours: a new light delivery system. *Lasers Med Sci* 1998; **13**: 137-142
18 **Barr H**, Kendall C, Reyes-Goddard J, Stone N. Clinical aspects of photodynamic therapy. *Sci Prog* 2002; **85**: 131-150
19 **van Veen P,** Schouwink JH, Star WM, Sterenborg HJ, van der Sijp JR, Stewart FA, Baas P. Wedge-shaped applicator for additional light delivery and dosimetry in the diaphragmal sinus during photodynamic therapy for malignant pleural mesothelioma. *Phys Med Biol* 2001; **46**: 1873-1883
20 **Masumoto K**, Yamada I, Tanaka H, Fujise Y, Hashimoto K. Tissue distribution of a new photosensitizer ATX-S10Na(II) and effect of a diode laser (670nm) in photodynamic therapy. *Lasers Med Sci* 2003; **18**: 134-138
21 **Jiang F**, Robin AM, Katakowski M, Tong L, Espiritu M, Singh G, Chopp M. Photodynamic therapy with photofrin in combination with Buthionine Sulfoximine (BSO) of human glioma in the nude rat. *Lasers Med Sci* 2003; **18**: 128-133
22 **Hammer-Wilson MJ**, Cao D, Kimel S, Berns MW. Photodynamic parameters in the chick chorioallantoic membrane (CAM) bioassay for photosensitizers administered intraperitoneally (IP) into the chick embryo. *Photochem Photobiol Sci* 2002; **1**: 721-728
23 **Theodossiou T**, Hothersall JS, Woods EA, Okkenhaug K, Jacobson J, MacRobert AJ. Firefly luciferin-activated rose bengal: *in vitro* photodynamic therapy by intracellular chemiluminescence in transgenic NIH 3T3 cells. *Cancer Res* 2003; **63**: 1818-1821
24 **Kawauchi S**, Morimoto Y, Sato S, Arai T, Seguchi K, Asanuma H, Kikuchi M. Differences between cytotoxicity in photodynamic therapy using a pulsed laser and a continuous wave laser: study of oxygen consumption and photobleaching. *Lasers Med Sci* 2004; **18**: 179-183
25 **Tsutsui H**, MacRobert AJ, Curnow A, Rogowska A, Buonaccorsi G, Kato H, Bown SG. Optimisation of illumination for photodynamic therapy with mTHPC on normal colon and a transplantable tumour in rats. *Lasers Med Sci* 2002; **17**: 101-109
26 **Whitacre CM**, Feyes DK, Satoh T, Grossmann J, Mulvihill JW, Mukhtar H, Oleinick NL. Photodynamic therapy with the phthalocyanine photosensitizer Pc4 of SW480 human colon cancer xenografts in athymic mice. *Clin Cancer Res* 2000; **6**: 2021-2027
27 **Pitris C**, Jesser C, Boppart SA, Stamper D, Brezinski ME, Fujimoto JG. Feasibility of optical coherence tomography for high-resolution imaging of human gastrointestinal tract malignancies. *J Gastroenterol* 2000; **35**: 87-92
28 **De Jode ML.** Monte carlo simulations of light distributions in an embedded tumour model: studies of selectivity in photodynamic therapy. *Lasers Med Sci* 2000; **15**: 49-56
29 **Rezzoug H**, Bezdetnaya L, Aamar O, Merlin JL, Guillemin F. Parameters affecting photodynamic activity of foscan or Metatetra (hydroxyphenyl) chlorin (mTHPC) *in vitro* and *in vivo*. *Lasers Med Sci* 1998; **13**: 119-125
30 **Kelty CJ**, Ackroyd R, Brown NJ, Brown SB, Reed MW. Comparison of high-vs low-dose 5-aminolevulinic acid for photodynamic therapy of Barrett's esophagus. *Surg Endosc* 2004; **18**: 452-458
31 **van den Boogert J**, van Staveren HJ, de Bruin RW, Siersema PD, van Hillegersberg R. Fractionated illumination for oesophageal ALA-PDT: effect on blood flow and PpIX formation. *Lasers Med Sci* 2001; **16**: 16-25
32 **Skinner MG**, Everts S, Reid AD, Vitkin IA, Lilge L, Sherar MD. Changes in optical properties of ex vivo rat prostate due to heating. *Phys Med Biol* 2000; **45**: 1375-1386
33 **Du Y**, Hu XH, Cariveau M, Ma X, Kalmus GW, Lu JQ. Optical properties of porcine skin dermis between 900nm and 1500nm. *Phys Med Biol* 2001; **46**: 167-181
34 **Shah RK**, Nemati B, Wang LV, Shapshay SM. Optical-thermal simulation of tonsillar tissue irradiation. *Lasers Surg Med* 2001; **28**: 313-319
35 **Ritz JP**, Roggan A, Isbert C, Muller G, Buhr HJ, Germer CT. Optical properties of native and coagulated porcine liver tissue between 400 and 2400nm. *Lasers Surg Med* 2001; **29**: 205-212
36 **Zhu D**, Luo Q, Cen J. Effects of dehydration on the optical properties of *in vitro* porcine liver. *Lasers Surg Med* 2003; **33**:

226-231

37 **Lualdi M**, Colombo A, Farina B, Tomatis S, Marchesini R. A phantom with tissue-like optical properties in the visible and near infrared for use in photomedicine. *Lasers Surg Med* 2001; **28**: 237-243

38 **Ugryumova N**, Matcher SJ, Attenburrow DP. Measurement of bone mineral density via light scattering. *Phys Med Biol* 2004; **49**: 469-483

39 **Beek JF**, Blokland P, Posthumus P, Aalders M, Pickering JW, Sterenborg HJ, van Gemert MJ. *In vitro* double-integrating-sphere optical properties of tissues between 630 and 1064nm. *Phys Med Biol* 1997; **42**: 2255-2261

40 **Pickering JW**, Moes CJM, Sterenborg HJCM, Prahl SA, van Gemert MJC. Two integrating spheres with an intervening scattering sample. *J Opt Soc Am A* 1992; **9**: 621-631

41 **Pickering JW**, Bosman S, Posthumus P, Blokland P, Beek JF, van Gemert MJ. Changes in the optical properties (at 632.8 nm) of slowly heated myocardium. *Appl Opt* 1993; **32**: 367-371

42 **Pickering JW**, Prahl SA, van Wieringen N, Beek JF, Sterenborg HJ, van Gemert MJ. Double-integrating-sphere system for measuring the optical properties of tissue. *Appl Opt* 1993; **32**: 399-410

43 **van Hillegersberg R**, Pickering JW, Aalders M, Beek JF. Optical properties of rat liver and tumor at 633nm and 1064nm: photofrin enhances scattering. *Lasers Surg Med* 1993; **13**: 31-39

44 **Prahl SA**, van Gemert MJ, Welch AJ. Determining the optical properties of turbid mediaby using the adding-doubling method. *Appl Opt* 1993; **32**: 559-568

45 **Bolin FP**, Preuss LE, Taylor RC, Ference RJ. Refractive index of some mammalian tissues using a fiber optic cladding method. *Appl Opt* 1989; **28**: 2297-2303

46 **Prahl SA**. Light transport in tissue. *phD Thesis University of Austin, Texas* (1988)

Science Editor Guo SY **Language Editor** Elsevier HK

PO Box 2345, Beijing 100023, China
www.wjgnet.com
wjg@wjgnet.com

ELSEVIER

World J Gastroenterol 2005;11(16):2420-2425
World Journal of Gastroenterology ISSN 1007-9327

• *COLORECTAL CANCER* •

Two-dimensional polyacrylamide gel electrophoresis analysis of indomethacin-treated human colon cancer cells

Yan-Li Cheng, Gui-Ying Zhang, Zhi-Qiang Xiao, Fa-Qing Tang

Yan-Li Cheng, Gui-Ying Zhang, Department of Gastroenterology, Xiangya Hospital, Central South University, Changsha 410008, Hunan Province, China
Zhi-Qiang Xiao, Key Laboratory of Cancer Proteomics of Chinese Ministry of Health, Xiangya Hospital, Central South University, Changsha 410008, Hunan Province, China
Fa-Qing Tang, Department of Clinical Laboratory, Xiangya Hospital, Central South University, Changsha 410008, Hunan Province, China
Supported by the National Natural Science Foundation of China, No. 30271516
Correspondence to: Gui-Ying Zhang, Department of Gastroenterology, Xiangya Hospital, Central South University, Xiangya Road, Changsha 410008, Hunan Province, China. guiyingzhang@hotmail.com
Telephone: +86-731-4327249
Received: 2004-06-11 Accepted: 2004-07-22

Abstract

AIM: To establish the two-dimensional gel electrophoresis (2-DE) profiles of indomethacin (IN)-treated human colon cancer cell line HCT116, and to provide a new way to study its anti-tumor molecular mechanism through analyzing a variety of protein maps.

METHODS: Two-DE profiles of HCT116 were established in IN-treated and untreated groups. Total proteins were separated by immobilized pH gradient-based 2-DE. The gels were stained by silver, scanned by ImageScanner, and analyzed with Image Master software.

RESULTS: Clear background, well-resolved and reproducible 2-DE patterns of HCT116 cells were acquired in IN-treated and untreated group. The average deviation of spot position was 0.896±0.177 mm in IEF direction and 1.106±0.289 mm in SDS-PAGE direction respectively. In IN-treated group, 1 169±36 spots were detected and 1 061±32 spots were matched, the average matching rate was 90.6% in three gels. In untreated group, 1 256±50 spots were detected and 1 168±46 spots were matched, the average matching rate was 93.0% in three gels. Forty-five differential protein spots were displayed between IN-treated and untreated groups. Of which, 34 protein spots decreased and 9 showed higher expression in IN-treated group, and only two protein spots showed an expression in untreated cells.

CONCLUSION: Two-DE profiles of IN-treated and untreated HCT116 cells were established. Apparent 45 different protein spots were detected in IN-treated and untreated HCT116 cells. The analysis on differential protein spots may serve as a new way to study the molecule mechanism of IN-treated colon cancer.

Key words: Gel electrophoresis; Indomethacin; Colon cancer

Cheng YL, Zhang GY, Xiao ZQ, Tang FQ. Two-dimensional polyacrylamide gel electrophoresis analysis of indomethacin-treated human colon cancer cells. *World J Gastroenterol* 2005; 11(16): 2420-2425
http://www.wjgnet.com/1007-9327/11/2420.asp

INTRODUCTION

Colorectal cancer is one of the most common malignant tumors in the world. It has a high 5-year mortality rate and a low early stage diagnosis rate. It still has a poor prognosis, because 50% of the cases are incurable at the time of diagnosis. It is crucial to find the drugs which have a lower toxicity and a higher effect in treating colorectal cancer. Indomethacin (IN) belongs to nonsteroidal anti-inflammatory drugs (NSAIDs). NSAIDs including IN have many functions such as anti-inflammation, anti-rheumatism, decreasing cerebral thrombosis, and abroad anti-tumor. In addition, using NSAIDs may prevent adenoma occurrence or progression and may lead to a lower incidence of colorectal cancer[1,2]. Several studies have reported a 40-50% decrease in mortality from colorectal cancer with prolonged use of NSAIDs[3-6]. The well-documented pharmacological action of NSAIDs is to inhibit COX[7-9], but NSAIDs in general have numerous targets other than COX by which they may inhibit tumor cell growth and induce apoptosis, such as modulation of Ras signal transduction, p53 point mutation and activation, of the transcription factor nuclear factor κB[10-15]. But the molecular mechanism by which IN exerts its effects is not well understood. Proteome technology is a useful tool for the identification of new cancer markers and treatment-related changes in cancer. Comparative analysis of protein alterations between pre-treated and treated cells or tissues using high-throughput proteome technology has allowed us to find the special treatment-related proteins and develop new molecular-based therapies. Two-dimensional gel electrophoresis (2-DE) has become the most widely used method for separating and quantifying many types of proteins including those from whole cell lysates, tissue extracts, and subcellular fractions (including membrane proteins). Indeed, 2-DE is regarded as the most powerful separation method for resolving complex mixtures of proteins, and has provided a new way to study the molecular mechanism of IN-treated colon cancer. In this work, 2-DE, followed by ImageMaster analysis was used to study a

variety of protein maps on IN-treated and untreated HCT116 cells. It will provide a new method to look for the correlated proteins of IN-treated colon cancer.

MATERIALS AND METHODS

Materials

IN, urea, iodoacetamide, acetic acid, DTT and second-dimension SDS-PAGE standard proteins were obtained from Sigma. RPMI1640 and 10% FBS were purchased from Xiangya Medical Collage, Central South University. Acrylamide, agarose, glycerol, bromophenol blue, Tris, CHAPS, SDS, IPG buffer, and the linear immobiline dry strips, pH gradients 3-10 (24 cm long) were obtained from Amersham Pharmacia Biotech. Glycine and ammonium persulfate were from Bio-Rad, MTT from Fluk.

Cell culture

Human colon cancer cell line HCT116 was obtained from ATCC of USA. The cell line was cultured in RPMI1640 medium supplemented with 10% fetal calf serum at 37 ℃, 50 mL/L CO_2 environment.

Assay of growth-inhibitory effect and IC_{50} on HCT116 cells

Growth-inhibitory effect on HCT116 cells was determined by MTT. Cells were planted on 96-well cell culture plates (2×10^4 cells/well). After being cultured for 24 h, the cells adhered to the plates. IN was added at 100, 200, 400 and 800 μmol/L for HCT116 cells and cultured for 48 h. IN was dissolved in DMSO such that the final concentration of DMSO was less than 0.2%. One line treated by the complete medium without IN served as a control. According to MTT method, the absorbance of each well was determined by a spectrophotometer at 490 nm wavelength. The percentage of all viability was calculated by multiplying the absorbance ratio of the sample *vs* the control by 100. IN IC_{50} was determined as IN concentration showing 50% cell growth inhibition as compared with control cell growth. The experiments were repeated in triplicate, and the percentage of cell viability was expressed as mean±SD.

Time-dependent growth-inhibitory effect of IN (316 μmol/L)

HCT116 cells were seeded in 96-well plates (2×10^4 cells/well) in RPMI1640 medium with 10% FBS. After 24 h, media were replaced with fresh standard media or media containing 316 μmol/L IN. According to MTT method, at the appropriate time points, the absorbance of each well was determined by a spectrophotometer at 490 nm wavelength. The percentage of all viability was calculated by multiplying the absorbance ratio of the sample *vs* the control by 100.

Sample preparation

HCT116 cells were seeded in 75-cm^2 tissue culture flasks, grown for 1-2 d prior to use. When 50% confluent growth was reached, the media were changed to fresh standard media or media containing 316 μmol/L IN. The cells were harvested 48 h after treatment, rinsed with PBS (0.8 g/L NaCl, 0.2 g/L KCl, 1.44 g/L NaH_2PO_4, 0.24 g/L KH_2PO_4), and trypsinized with a solution of 2.5 g/L trypsin and 0.2 g/L EDTA. After 1 min, media containing FBS were added to terminate the action of trypsin. The resulting suspension was centrifuged at 1 000 r/min for 7 min at 4 ℃. After the supernatant was discarded, the cells were resuspended in ice-cold 1× PBS and centrifuged at 1 500 r/min for 10 min at 4 ℃ and the supernatant was removed. This wash-step was repeated thrice and stored at -80 ℃ until further use.

Protein extraction from cells untreated and treated with IN was performed with lysis buffer. The harvested IN-treated and untreated HCT116 cells were left in lysis buffer (7 mol/L urea, 2 mol/L thiourea, 4% CHAPS, 40 mmol/L Tris and 1 mmol/L PMSF) for 30 min in ice. The resulting cell lysates were then vortexed. The sample was incubated at room temperature for 10 min. After centrifugation at 15 000 *g* at 4 ℃, for removal of particulate materials, the protein solution was collected and stored at -80 ℃ until use.

Protein concentrations were determined using the Bio-Rad protein assay kit (Bio-Rad) with BSA (Sigma) as the standard.

IPG-2D PAGE[16-20]

IPG-IEF was run on an IPGphor isoelectric focusing (IEF) system (Amersham Pharmacia Biotech). Twenty-four centimeter pH 3-10 immobilized pH gradient strips were rehydrated for 14 h with 450 μL of 2-D solubilizing solution (8 mol/L urea, 2% CHAPS, 0.5% IPG buffer, pH 3-10, 3% DTT and a trace of bromophenol blue) containing 260 μg of total proteins for analytical runs, and mixed with a rehydrated solution to a total volume of 450 μL. The mixtures were pipetted into IPG strip holder channels. IPG dry strips were lowered into the mixtures with the gel side down, and overlayered with the dry-strip fluid covered. The holders were placed onto the electrode plates of the IPGphor platform. After rehydration for 14 h, IEF was carried out with a low initial voltage (500-1 000 V) during the first 2 h and then the voltage gradient up to 8 000 V with a limiting current of 15 μA/strip. The total product time×voltage applied was 69 920 V·h for analytical runs. The temperature was maintained at 20 ℃. Following IEF separation, the gel strips were equilibrated for 2×15 min in an equilibration buffer containing 50 mmol/L Tris-HCl, pH 8.8, 6 mol/L urea, 30% glycerol, 2% SDS and a trace of bromophenol blue. One percent DTT was added to the first equilibration buffer, and 2.5% iodoacetamide was added in the second equilibration buffer. The equilibrated gel strips were then applied onto 0.75-mm thick 12.5% SDS linear polyacrylamide gradient vertical slab gels, and sealed with 0.5% agarose. SDS-PAGE was run in a Bio-Rad Protean II electrophoresis apparatus for 30 min at constant current of 10 mA/gel, and then switched to 25 mA/gel until the bromophenol blue frontier reached the bottom of the gels. During the whole run the temperature was set at 15 ℃. To determine the isoelectric point (pI) and molecular weight (M_r) of separated proteins, 2-D standards were added to the protein samples as internal markers. After 2-DE, the protein spots were visualized by silver-based staining technique with the protein silver stain kit (Amersham Biosciences).

Image analysis

The stained 2-DE gels were scanned with LabScan software

on ImageScanner (Amersham Pharmacia Biotech). The spot-intensity calibration, spot detection, background abstraction, matching, 1-D calibration, and the establishment of average-gel were performed with ImageMaster 2D Elite 4.01 analysis software (Amersham Pharmacia Biotech). Intensity of each spot was quantified by calculation of spot volume after normalization of the image using the total spot volume normalization method multiplied by the total area of all the spots. The reproducibility of spot position was calculated according to Corbett's method[21].

Statistical analysis

Data were expressed as mean±SD with the exception of 2-DE data, which were expressed as mean only. Data were analyzed using parametric Student's *t* test. Statistical analysis was carried out with SPSS for Windows 11.0. $P<0.05$ was considered statistically significant.

RESULTS

Effect of IN on HCT116 cells

MTT assay demonstrated that HCT116 cells were sensitive to IN. Dose-dependent growth-inhibitory effect of IN on HCT116 cells was found at the concentrations of 0, 100, 200, 400, 800 μmol/L (Figure 1A). From the growth-inhibition curve figure, we got IC_{50} = 316±1.2 μmol/L. This analysis revealed an increase in toxicity with increasing IN concentration. Cells were exposed to 316 μmol/L of IN for varying times (12, 24, 36, 72 h) at which the IN-containing medium was replaced and/or the proliferation assay was performed. There was time-dependent growth-inhibitory effect of IN that showed a significant growth inhibition (Figure 1B).

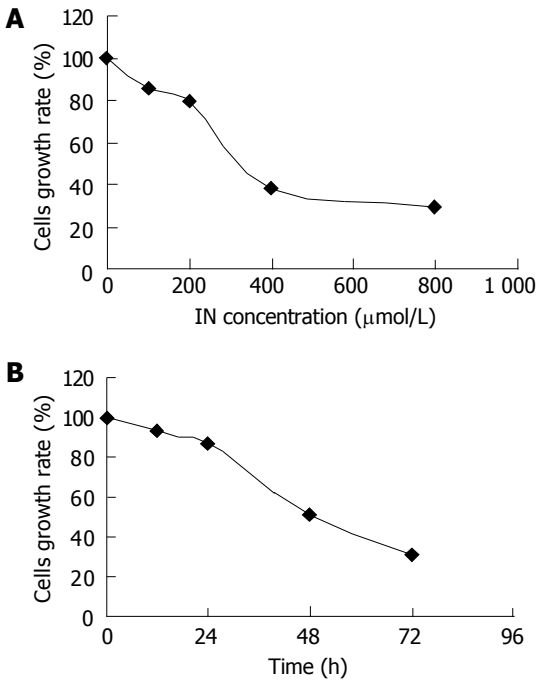

Figure 1 Dose-dependent grow-inhibitory effect (**A**) and time-dependent growth-inhibitory effect (**B**) of IN on HCT116 cells.

Result of 2-DE and ImageMaster analysis

Resolving power Total cell lysate was isolated from IN-treated and untreated HCT116 cells and analyzed by high-resolution 2-DE. IEF was first conducted on a 24 cm, pH 3-10 nonlinear immobilized pH gradient (IPG) strip. For colon cancer HCT116 cells, 1213±58 spots were detected.

Reproducibility and expression of 2-DE profiles on IN-treated and untreated HCT116 cells With the same condition and parameters, the experiment was repeated thrice from cell culture to 2-DE respectively. For IN-treated and untreated HCT 116 cells, the clear background, well-resolved and reproducible 2-DE pattern were attained (Figure 2). Through Image Master 2D Elite 4.01, we found that the separation was better in the lower molecular weight range and towards the acidic pH. Horizontal streaks were apparent for proteins in the higher molecular weight range. Three silver-stained 2-DE profiles of each sample were very similar. The image analysis showed that these 2-DE maps were reproducible. For IN-treated HCT116 cells, the average spots were 1 169±36 in three gels, 1 061±32 spots were matched with an average matching rate of 90.6%. For untreated HCT116 cells, the average spots were 1 256±50 in three gels, and 1 168±46 spots were matched with an average matching rate of 93.0%. A total of 100 well-resolved and matched spots among three untreated cells were chosen randomly to calculate the deviation of the spot positions. The spot positional deviation was 0.896±0.177 mm in IEF direction and 1.106±0.289 mm in SDS-PAGE direction. A total of 1 058±47 spots were matched in IN-treated-2-DE and untreated-2-DE maps. Compared with untreated maps, average spots decreased 6.9% in IN-treated group.

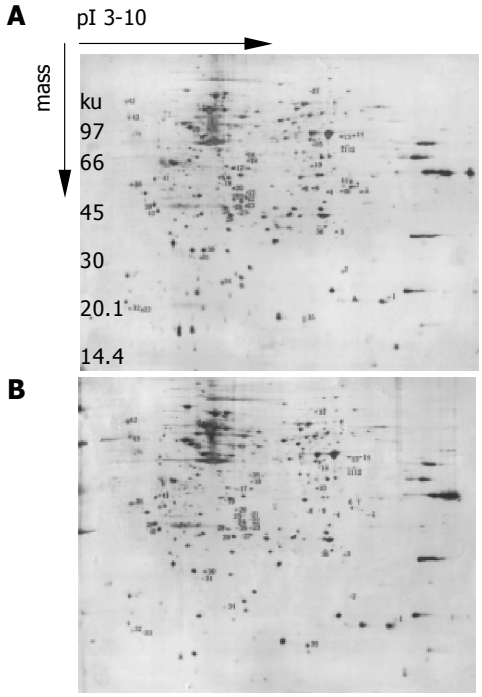

Figure 2 Two-dimensional electrophoretic maps of human colon cancer HCT116 cells untreated (**A**) and treated with IN (**B**). + stands for differential protein spots. 1-34 means decreasing spots and 35-43 increasing spots in IN-treated cells. Forty-four and 45 spots were expressed in untreated cells.

Table 1 Characteristics differentially expressed protein alterations of HCT116 between IN-treated and untreated groups (mean±SD)

Spotnumber	pI	M_r(ku)	Relative volume of spots in untreated group (%)	Relative volume of spots in IN-treated group (%)	*P*
1	8.611	19.869	0.181±0.019	0.106±0.024	0.040
2	7.736	22.956	0.769±0.044	0.119±0.069	0.036
3	7.619	27.827	0.238±0.043	0.136±0.041	0.043
4	7.441	38.143	0.236±0.019	0.077±0.027	0.027
5	8.079	38.304	0.319±0.029	0.122±0.035	0.034
6	7.872	40.125	0.334±0.037	0.193±0.007	0.026
7	7.946	40.232	0.117±0.007	0.020±0.009	0.002
8	6.978	39.321	0.236±0.014	0.071±0.012	0.017
9	7.166	39.536	0.233±0.023	0.070±0.014	0.010
10	7.136	48.279	0.276±0.014	0.121±0.008	0.010
11	7.719	56.079	0.227±0.040	0.065±0.027	0.006
12	7.198	56.856	0.181±0.041	0.088±0.026	0.010
13	7.692	57.936	0.314±0.031	0.146±0.023	0.044
14	7.924	58.023	0.225±0.006	0.017±0.001	0.001
15	7.163	57.003	0.166±0.005	0.017±0.001	0.002
16	5.897	52.261	0.194±0.006	0.030±0.019	0.020
17	5.648	45.818	0.415±0.024	0.110±0.009	0.004
18	5.899	47.261	0.211±0.018	0.091±0.004	0.014
19	5.471	42.589	0.150±0.088	0.058±0.008	0.011
20	5.657	39.161	0.234±0.054	0.080±0.029	0.017
21	5.913	37.714	0.209±0.038	0.094±0.042	0.005
22	5.902	35.732	0.252±0.017	0.075±0.016	0.012
23	5.894	32.625	0.278±0.057	0.104±0.035	0.021
24	5.804	34.339	0.320±0.011	0.128±0.015	0.001
25	5.665	34.768	0.212±0.030	0.057±0.015	0.042
26	5.670	32.411	0.172±0.004	0.063±0.004	0.003
27	5.749	29.912	0.100±0.011	0.005±0.002	0.014
28	5.507	32.036	0.404±0.021	0.249±0.036	0.049
29	5.605	29.737	0.529±0.076	0.309±0.047	0.038
30	5.098	25.374	0.516±0.107	0.093±0.072	0.039
31	5.044	24.428	0.293±0.009	0.077±0.016	0.002
32	3.719	18.436	0.173±0.006	0.046±0.009	0.004
33	3.943	18.306	0.239±0.021	0.049±0.009	0.005
34	5.450	21.449	0.278±0.046	0.030±0.009	0.022
35	7.019	17.438	0.137±0.003	0.446±0.023	0.006
36	7.297	28.441	0.070±0.003	0.197±0.012	0.007
37	7.104	96.008	0.094±0.005	0.186±0.008	0.020
38	3.719	40.179	0.182±0.012	0.450±0.028	0.006
39	4.185	32.786	0.343±0.042	0.512±0.063	0.029
40	4.228	30.536	0.261±0.047	0.446±0.042	0.021
41	4.274	44.732	0.055±0.004	0.193±0.012	0.004
42	3.621	85.344	0.135±0.058	0.350±0.075	0.019
43	3.665	71.952	0.133±0.034	0.342±0.032	0.010
44	7.698	38.411	0.177±0.036		
45	7.752	40.500	0.121±0.032		

In this study, the 2-DE protein patterns of IN-treated and untreated pairs were quantified and matched mutually. Furthermore, the differentially detected protein spots between IN-treated and untreated group in three experiments must accord with a significant difference in relative volume ($P<0.05$, Table 1). Forty-five differential protein spots were displayed between IN-treated and untreated groups. Of which, 34 protein spots decreased and 9 showed higher expression in IN-treated group, and only 2 protein spots showed an expression in untreated cells.

DISCUSSION

It is a hot point of using IN in anti-neoplastic therapy, but the molecular mechanism by which IN exerts its effects is not well understood. Subbegowda and Frommel[22] found in flow cytometric analysis, an increase of cells and subdiploid nuclei in S and G2/M phases in cultures treated with high dose of aspirin. The results suggested that aspirin could induce cell cycle arrest and cause necrosis at high concentrations *in vitro*, but not apoptosis. In our previous study, IN altered the cell cycle phase distribution of HCT116 cells, and

increased the proportion of cells in the G_0/G_1 phase and reduced the proportion in the S phase of the cell cycle. In addition, we proved that IN could induce apoptosis and found that the anti-tumor activity of IN through P53-$P21^{WAF1/CIP1}$ depended on pathways to inhibit cell proliferation and induce cell apoptosis[23,24]. Compared with untreated maps, the average spots decreased 6.9% in IN-treated group in our study. According to MTT experiments, we confirmed that IN could inhibit the proliferation of HCT116 cells.

The expression of proteins is different in different tissues, cells, and stage of upgrowth, physiology or pathology. The basic challenges are to find the proteins and to predict their functions. This would contribute to a new understanding of human biology and to the design of new molecular structures as potential novel diagnostic or drug discovery target[25]. In order to further explore the molecular mechanism of IN in treating colon cancer, we used high-throughput proteomics technique to address the molecular basis of this effect through analyzing protein expression profiles of HCT116 cells in treated and untreated groups. In our experiment, IPG-IEF was run on an IEF system. For the sample swung in with hydration fluid and rehydrated and isoelectrically focused in the same chamber, we avoided the use of sample cups, eliminated precipitations at the sample application site, thus improving resolution over the entire pH range of the gels. It also allowed precise control of protein amounts and sample volumes loaded onto the IPG gels, and also enlarged the reproducibility of 2-DE[16,26]. In addition, we used the newest Pharmacia software, ImageMaster, to analyze our protein maps. Compared with Bio-Rad PDQuest, ImageMaster 2-D gel analysis software (4.01 version) demonstrated a higher sensitivity. From the ImageMaster, we found that most of protein spots distribute pI: 3-8 and M_r: 20.1-66 ku. We also found that the separation was better in the lower molecular weight range and towards the acidic pH. Horizontal streaks were apparent for protein in the higher molecular weight range. This seems to be a common feature of 2-DE, seen in most gels[27-31].

Clear background, well resolved and reproducible 2-DE patterns of IN-treated and untreated HCT116 cells were acquired. Three silver-stained 2-DE profiles of each sample were very similar. The image analysis showed that the 2-DE maps were reproducible. A total of 1 256±50 protein spots were resolved in untreated group and the match rate was 93.0%. A total of 1 169±36 protein spots were resolved in IN-treated group and the match rate was 90.6%. In order to further identify our experiment that was reproducible, a total of 100 well-resolved and matched spots in the IN-treated group were chosen randomly to calculate the deviation of the spot positions. The spot positional deviation was 0.896±0.177 mm in IEF direction and 1.106±0.289 mm in SDS-PAGE direction. Analyzing the 2-DE profiles of IN-treated and untreated groups, 45 differential protein spots displayed quantitative changes in expression after IN treated. Of which, 34 decreased in abundance, 9 showed a higher expression, and only 2 were expressed in untreated cells. The results indicated that there were many pathways of IN in colon cancer. Most of pI values distributed pH 3-8 in our gels. Molecular weight distributed 21-61 ku. Comparison of the differential protein spots between IN-treated and untreated groups could contribute to study the molecular mechanisms of the anti-tumor effect of IN. Some differential protein spots between IN-treated and untreated cells should be further identified with amino acid sequence analysis and mass spectrometry analysis.

REFERENCES

1 **Giovannucci E,** Rimm EB, Stampfer MJ, Colditz GA, Ascherio A, Willett WC. Aspirin use and the risk for colorectal cancer and adenoma in male health professionals. *Ann Intern Med* 1994; **121**: 241-246

2 **Garcia-Rodriguez LA,** Huerta-Alvarez C. Reduced risk of colorectal cancer among long-term users of aspirin and nonaspirin nonsteroidal antiinflammatory drugs. *Epidemiology* 2001; **12**: 88-93

3 **Kune GA,** Kune S, Watson LF. Colorectal cancer risk, chronic illnesses, operations, and medications: case control results from the Melbourne Colorectal Cancer Study. *Cancer Res* 1988; **48**: 4399-4404

4 **Rosenberg L,** Palmer JR, Zauber AG, Warshauer ME, Stolley PD, Shapiro S. A hypothesis: nonsteroidal anti-inflammatory drugs reduce the incidence of large-bowel cancer. *J Natl Cancer Inst* 1991; **83**: 355-358

5 **Baron JA,** Cole BF, Sandler RS, Haile RW, Ahnen D, Bresalier R, McKeown-Eyssen G, Summers RW, Rothstein R, Burke CA, Snover DC, Church TR, Allen JI, Beach M, Beck GJ, Bond JH, Byers T, Greenberg ER, Mandel JS, Marcon N, Mott LA, Pearson L, Saibil F, van Stolk RU. A randomized trial of aspirin to prevent colorectal adenomas. *N Engl J Med* 2003; **348**: 891-899

6 **Liu Y,** Eu W, Seow-Choen F, Cheah Y. Differential cytostatic effect of sodium salicylate in human colorectal cancers using an individualized histoculture system. *Cancer Chemother Pharmacol* 2002; **49**: 473-478

7 **Elder DJ,** Halton DE, Crew TE, Paraskeva C. Apoptosis induction and cyclooxygenase-2 regulation in human colorectal adenoma and carcinoma cell lines by the cyclooxygenase-2-selective non-steroidal anti-inflammatory drug NS-398. *Int J Cancer* 2000; **86**: 553-560

8 **Elder DJ,** Halton DE, Playle LC, Paraskeva C. The MEK/ERK pathway mediates COX-2-selective NSAID-induced apoptosis and induced COX-2 protein expression in colorectal carcinoma cells. *Int J Cancer* 2002; **99**: 323-327

9 **Nishihara H,** Kizaka-Kondoh S, Insel PA, Eckmann L. Inhibition of apoptosis in normal and transformed intestinal epithelial cells by cAMP through induction of inhibitor of apoptosis protein (IAP)-2. *Proc Natl Acad Sci USA* 2003; **100**: 8921-8926

10 **Boudreau MD,** Sohn KH, Rhee SH, Lee SW, Hunt JD, Hwang DH. Suppression of tumor cell growth both in nude mice and in culture by n-3 polyunsaturated fatty acids: mediation through cyclooxygenase-independent pathways. *Cancer Res* 2001; **61**: 1386-1391

11 **Lonnroth C,** Andersson M, Lundholm K. Indomethacin and telomerase activity in tumor growth retardation. *Int J Oncol* 2001; **18**: 929-937

12 **Piazza GA,** Rahm AK, Finn TS, Fryer BH, Li H, Stoumen AL, Pamukcu R, Ahnen DJ. Apoptosis primarily accounts for the growth-inhibitory properties of sulindac metabolites and involves a mechanism that is independent of cyclooxygenase inhibition, cell cycle arrest, and p53 induction. *Cancer Res* 1997; **57**: 2452-2459

13 **Taylor MT,** Lawson KR, Ignatenko NA, Marek SE, Stringer DE, Skovan BA, Gerner EW. Sulindac sulfone inhibits K-ras-dependent cyclooxygenase-2 expression in human colon cancer cells. *Cancer Res* 2000; **60**: 6607-6610

14 **Yamamoto Y,** Yin MJ, Lin KM, Gaynor RB. Sulindac inhibits activation of the NF-kappaB pathway. *J Biol Chem* 1999; **274**: 27307-27314

15 **Shureiqi I,** Jiang W, Zuo X, Wu Y, Stimmel JB, Leesnitzer

LM, Morris JS, Fan HZ, Fischer SM, Lippman SM. The 15-lipoxygenase-1 product 13-S-hydroxyoctadecadienoic acid down-regulates PPAR-delta to induce apoptosis in colorectal cancer cells. *Proc Natl Acad Sci USA* 2003; **100**: 9968-9973

16 **Sanchez JC,** Rouge V, Pisteur M, Ravier F, Tonella L, Moosmayer M, Wilkins MR, Hochstrasser DF. Improved and simplified in-gel sample application using reswelling of dry immobilized pH gradients. *Electrophoresis* 1997; **18**: 324-327

17 **Seow TK,** Ong SE, Liang RC, Ren EC, Chan L, Ou K, Chung MC. Two-dimensional electrophoresis map of the human hepatocellular carcinoma cell line, HCC-M, and identification of the separated proteins by mass spectrometry. *Electrophoresis* 2000;**21**: 1787-1813

18 **Issaq HJ.** The role of separation science in proteomics research. *Electrophoresis* 2001; **22**: 3629-3638

19 **Gorg A,** Obermaier C, Boguth G, Harder A, Scheibe B, Wildgruber R, Weiss W. The current state of two-dimensional electrophoresis with immobilized pH gradients. *Electrophoresis* 2000; **21**: 1037-1053

20 **Li C,** Chen Z, Xiao Z, Wu X, Zhan X, Zhang X, Li M, Li J, Feng X, Liang S, Chen P, Xie JY. Comparative proteomics analysis of human lung squamous carcinoma. *Biochem Biophys Res Commun* 2003; **309**: 253-260

21 **Corbett JM,** Dunn MJ, Posch A, Gorg A. Positional reproducibility of protein spots in two-dimensional polyacrylamide gel electrophoresis using immobilised pH gradient isoelectric focusing in the first dimension: an interlaboratory comparison. *Electrophoresis* 1994; **15**: 1205-1211

22 **Subbegowda R,** Frommel TO. Aspirin toxicity for human colonic tumor cells results from necrosis and is accompanied by cell cycle arrest. *Cancer Res* 1998; **58**: 2772-2776

23 **Zhang G,** Duan C, Shi J, Leng A. Neoplasm-inhibiting effect and sensitivity-promoting effect of indomethacin in vitro. *Hunan Yike Daxue Xuebao* 1997; **22**: 478-482

24 **Xu MH,** Zhang GY, Xie ZX, He CM. The effects of Indomethacin on the expression of CDK_2, CDK_4, Bcl-2, Bax and P21 $^{WAF1/CIP1}$ Protein in the human colon adenocarcinoma cell line. *Zhonghua Xiaohua Zazhi* 2002; **22**: 605-607

25 **Haberkorn U,** Altmann A, Eisenhut M. Functional genomics and proteomics-the role of nuclear medicine. *Eur J Nucl Med Mol Imaging* 2002; **29**: 115-132

26 **Rabilloud T,** Valette C, Lawrence JJ. Sample application by in-gel rehydration improves the resolution of two-dimensional electrophoresis with immobilized pH gradients in the first dimension. *Electrophoresis* 1994; **15**: 1552-1558

27 **Reymond MA,** Sanchez JC, Hughes GJ, Gunther K, Riese J, Tortola S, Peinado MA, Kirchner T, Hohenberger W, Hochstrasser DF, Kockerling F. Standardized characterization of gene expression in human colorectal epithelium by two-dimensional electrophoresis. *Electrophoresis* 1997; **18**: 2842-2848

28 **Antonucci F,** Chilosi M, Parolini C, Hamdan M, Astner H, Righetti PG. Two-dimensional molecular profiling of mantle cell lymphoma. *Electrophoresis* 2003; **24**: 2376-2385

29 **Gharib TG,** Chen G, Wang H, Huang CC, Prescott MS, Shedden K, Misek DE, Thomas DG, Giordano TJ, Taylor JM, Kardia S, Yee J, Orringer MB, Hanash S, Beer DG. Proteomic analysis of cytokeratin isoforms uncovers association with survival in lung adenocarcinoma. *Neoplasia* 2002; **4**: 440-448

30 **Shekouh AR,** Thompson CC, Prime W, Campbell F, Hamlett J, Herrington CS, Lemoine NR, Crnogorac-Jurcevic T, Buechler MW, Friess H, Neoptolemos JP, Pennington SR, Costello E. Application of laser capture microdissection combined with two-dimensional electrophoresis for the discovery of differentially regulated proteins in pancreatic ductal adenocarcinoma. *Proteomics* 2003; **3**: 1988-2001

31 **Swiss-2D Page Map: colorectal adenocarcinoma cell line (DL-1)**. http://expasy. Proteome.org. au/cgi-bin/map2/def?DLD1-HUMAN

Science Editor Wang XL and Li WZ **Language Editor** Elsevier HK

PO Box 2345, Beijing 100023, China
www.wjgnet.com
wjg@wjgnet.com

ELSEVIER

World J Gastroenterol 2005;11(16):2426-2430
World Journal of Gastroenterology ISSN 1007-9327

Effects and possible anti-tumor immunity of electrochemotherapy with bleomycin on human colon cancer xenografts in nude mice

Min-Hua Zheng, Bo Feng, Jian-Wen Li, Ai-Guo Lu, Ming-Liang Wang, Wei-Guo Hu, Ji-Yuan Sun, Yan-Yan Hu, Jun-Jun Ma, Bao-Ming Yu

Min-Hua Zheng, Bo Feng, Jian-Wen Li, Ai-Guo Lu, Ming-Liang Wang, Wei-Guo Hu, Ji-Yuan Sun, Yan-Yan Hu, Jun-Jun Ma, Bao-Ming Yu, Department of General Surgery, Ruijin Hospital, Shanghai Minimally Invasive Surgery Center, Shanghai Institute of Digestive Surgery, Shanghai Second Medical University, Shanghai 200025, China
Supported by the Grant from Science and Technology Development of Shanghai, No. 00440
Correspondence to: Dr. Min-Hua Zheng, Department of General Surgery, Ruijin Hospital, Shanghai Second Medical University, Shanghai 200025, China. fengbo2022@163.com
Telephone: +86-21-64370045-664558 Fax: +86-21-64333548
Received: 2004-07-12 Accepted: 2004-09-04

Abstract

AIM: To evaluate the anti-tumor effects and possible involvement of anti-tumor immunity of electrochemotherapy (ECT) employing electroporation and bleomycin in human colon cancer xenografts in nude mice, and to establish the experimental basis for clinical application of ECT.

METHODS: Forty nude mice, inoculated subcutaneously human colon cancer cell line LoVo for 3 wk, were allocated randomly into four groups: B+E+ (ECT), B+E– (administration of bleomycin alone), B-E+ (administration of electric pulses alone), and B-E- (no treatment). Tumor volumes were measured daily. The animals were killed on the 7th d, the weights of xenografts were measured, and histologies of tumors were evaluated. Cytotoxicity of spleen natural killer (NK) and lymphokine-activated killer (LAK) cells was then assessed by lactic dehydrogenase release assay.

RESULTS: The mean tumor volume of group B+E+ was statistically different from the other three groups after the treatment (F = 36.80, P<0.01). There was one case of complete response, seven cases of partial response (PR) in group B+E+, one case of PR in group B+E- and group B-E+ respectively, and no response was observed in group B-E-. The difference of response between group B+E+ and the other three groups was statistically significant (χ^2 = 25.67, P<0.01). Histologically, extensive necrosis of tumor cells with considerable vascular damage and inflammatory cells infiltration were observed in group B+E+. There was no statistical difference between the cytotoxicity of NK and LAK cells in the four treatment groups.

CONCLUSION: ECT significantly enhances the chemosensitivity and effects of chemotherapy in human colon cancer xenografts in nude mice, and could be a kind of novel treatment modality for human colon cancer. The generation of T-cell-dependent, tumor-specific immunity might be involved in the process of ECT.

Key words: Electrochemotherapy; Colorectal neoplasm; Bleomycin; Nude mice; Anti-tumor immunity

Zheng MH, Feng B, Li JW, Lu AG, Wang ML, Hu WG, Sun JY, Hu YY, Ma JJ, Yu BM. Effects and possible anti-tumor immunity of electrochemotherapy with bleomycin on human colon cancer xenografts in nude mice. *World J Gastroenterol* 2005; 11(16): 2426-2430
http://www.wjgnet.com/1007-9327/11/2426.asp

INTRODUCTION

Colorectal cancer (CRC) is the second leading cause of malignancy not only in the Western world but also in China[1]. Despite advances in therapy, the 5-year survival rate is no more than 50-60%, mainly because of the frequency of hepatic involvement. And only 10-15% such hepatic metastasis can be curatively resected. Furthermore, there are a considerable number of patients who cannot undergo surgery even at an early stage of disease due to severe complications, such as chronic heart failure, chronic renal failure, and chronic obstructive pulmonary disease, *etc.* Conventional chemotherapy with 5-fluorouracil may be of some value in individual cases but can be limited by side effects when used systemically. Therefore, the introduction of effective chemotherapy against CRC is urgently needed, especially for patients who cannot undergo surgery and have recurrent disease.

Electrochemotherapy (ECT) could provide an innovative therapeutic approach for the treatment of CRC. The combination treatment, which involves the administration of a chemotherapeutic drug followed by the delivery of electric pulses to tumors was termed ECT[2]. The electric pulse electroporates the tumor cell membrane transiently and reversibly, allowing the chemotherapeutic agents greater access to its intracellular site of action and consistently provides improved responses relative to treatment with drugs alone. Although various anticancer drugs have been employed in ECT, the cytotoxic effect of bleomycin has reportedly been more significantly enhanced by electroporation than that of any other anticancer drug[3-5].

This experimental study was designed to evaluate the *in vivo* anti-tumor effects of ECT employing electroporation and bleomycin in human colon cancer xenografts in nude mice and cytotoxicity of spleen natural killer (NK) and lymphokine-activated killer (LAK) cells was further assessed to elucidate the possible anti-tumor immunity of ECT.

MATERIALS AND METHODS

Electropulse generator and electrodes

Electrical pulses were derived from a pulse generator (ECM 830; The BTX Division of Genetronics, USA). The output voltage from this generator is between 5 and 2 500 V, and pulses can be applied at a set voltage for a pulse length varying between 10 μs and 10 s. The electrode used in the study is BTX Tweezer Model 520 (Genetronics, USA) with a diameter of 7 mm and a pulse length between 10 μs and 99 ms.

Cell line and cell culture

LoVo, a metastatic human colon adenocarcinoma cell line, was obtained from American type culture collection (ATCC) and was maintained in RPMI-1640 (Gibco) supplemented with 2 mmol/L L-glutamine and 100 mL/L FCS at 37 ℃ in a humidified atmosphere containing 50 mL/L CO_2. For transplantation, the cells were more than 95% viable, as tested with the trypan blue exclusion dye method.

Tumor induction in nude mice

Male Balb/c (nu/nu) nude mice, aged 4-6-wk old and weighing 17-20 g, were purchased from animal center of Shanghai Institute of Cancer Research (Shanghai, China). Animals were housed and cared for according to the guidelines of specific pathogen free in Shanghai Second Medical University. LoVo cells resuspended in RPMI-1640 at a concentration of 1×10^7/mL and 100 μL of the cell suspension was inoculated subcutaneously into left front limb of the mice. Tumors were allowed to grow for 3 wk up to about 2-5 mm in longer diameter.

Treatment protocol of each group

A total of 40 nude mice in which human colon cancer xenograft was successfully established were allocated randomly into four groups (10 mice/group): (1) Group B+E+: ECT. After induction of general anesthesia by an intraperitoneal injection of 0.25% embutal, 50 μL bleomycin (Harbin, China) was injected into the tumor at the concentration of 1 000 μmol/L. Three minutes later, eight 100-μs pulses (field strength 900 V/cm) with a 10-ms interval were applied to the tumor; (2) Group B+E-: administration of bleomycin alone after anesthesia of the mice as described previously; (3) Group B-E+: administration of electric pulses alone with the same parameters described previously; (4) Group B-E- (no treatment): no treatment was applied to the mice except for the induction of anesthesia. Tumor size was measured by a caliper daily, and tumor volume was estimated according to the formula: $V = 0.5\times ab^2/2$, where a is the largest diameter and b is the smallest diameter. All animals of each group were killed on the 7th d, the weights of xenografts were measured. The volume of xenograft before and after the treatment were compared and response to the treatment was evaluated as follows[6]: complete response (CR): disappearance of the tumor; partial response (PR): reduction of the tumor volume by 50% or more; stable disease (Stab): reduction of the tumor volume by less than 50% or progression by less than 25%; progressive disease (Prog): increase in tumor volume by more than 25%. The efficacy of treatment was evaluated by comparing the mean post-therapy tumor volume of the four groups.

NK cell activity

Splenocytes (effector cells) were isolated from all mice by mechanical dissociation and lysing of erythrocytes. Splenocytes were fractionated by density centrifugation at 2 000 r/min for 20 min with Ficoll Hypaque and interface lymphocytes were obtained. YAC-1 cells (ATCC), a mouse lymphoma line sensitive to the cytotoxic activity of NK cells, were used as targets. YAC-1 cells were maintained in RPMI 1640 supplemented with 10% FCS. NK cell activity was determined in triplicate by lactic dehydrogenase (LDH) release assay. YAC-1 (1×10^5) were mixed with lymphocytes at final effector/target (E:T) ratios between 20:1 in 96-well U-bottom plates. The plates were lightly centrifuged at 500 r/min for 4 min and incubated for 4 h at 37 ℃ in 50 mL/L CO_2. The plates were then centrifuged at 500 r/min for 4 min, and 100-μL aliquots of supernatants were transferred from all wells to a fresh 96-well flat-bottom plate. One hundred microliters of LDH of substrate was added to each well and incubated for 20 min at room temperature. Fifty microliters of 1 mol/L HCl of stop solution was added, and the absorbance was recorded at 490 nm. The percentage of specific lysis was calculated using the formula: % cytotoxicity (NK) = (experimental LDH release-effector cell spontaneous LDH release-target cell spontaneous LDH release)/(target cell maximum LDH release-target cell spontaneous LDH release)×100%.

LAK cell activity

IL_2 was added into the remaining lymphocytes at a final concentration of 1 000 U/mL, then the lymphocytes were incubated for 72 h at 37 ℃ in 50 mL/L CO_2. LDH release assay described previously was used for measuring LAK cell activity. % cytotoxicity (LAK) = (experimental LDH release-effector cell spontaneous LDH release-target cell spontaneous LDH release)/(target cell maximum LDH release-target cell spontaneous LDH release)×100%.

Histological examination

On the 7th d of the treatment, mice were killed. The tumors were excised and fixed in 10% formaldehyde for 24 h, then embedded in paraffin. Sections were prepared for hematoxylin-eosin staining and histologic changes were evaluated by microscopy (40×).

Statistical analysis

The data is presented as the mean±SD. ANOVA was used to compare tumor volume and weight among the four study groups and Kruskal-Wallis test was used to compare the response rate among groups. Statistical analyses were performed using SPSS 11.0 software. $P<0.05$ was considered statistically significant.

RESULTS

Safety and side-effect of ECT

All mice tolerated the treatment well and no mice died of electroporation. Local swelling and medium necrosis were observed after the treatment in the mice of group B+E+, but not in those of group B-E+, group B+E- and group B-E-.

Tumor volume measurement before and after treatment

No significant difference was found among the four groups with respect to the mean tumor volume before treatment (Table 1). The tumor volume of group B+E+ on the 7th d of treatment was significantly reduced by 18.65±7.68 mm^3 while that of other three groups were significantly increased by 8.09±12.53, 10.36±4.41 and 13.88±2.44 mm^3 respectively (Figure 1). The tumor weight of group B+E+ was 14.48±6.65 mg, which was significantly less than that of other three groups. No significant difference was found among group B+E-, group B-E+, and group B-E- with respect to tumor volume and tumor weight (Table 1).

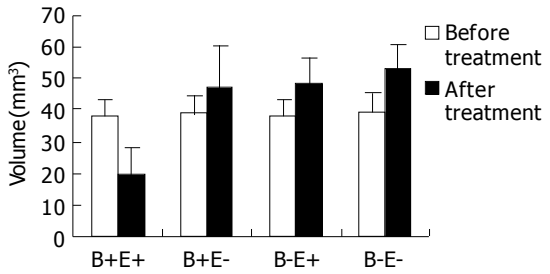

Figure 1 Mean tumor volume before and after treatment: group B-E-, no treatment; B+E-, administration of bleomycin alone; B-E+, administration of electric pulses alone; B+E+, ECT.

Tumor response

The response rates obtained after treatment are shown in Table 2. There was no statistically significant difference in the response rate among the first three groups (B-E-, B+E- and B+E+). In contrast, the response rate in group B+E+ differed significantly from that of each of the other group ($P<0.01$).

Total splenocytes and activity of NK cells and LAK cells

Total splenocytes and activity of NK cells and LAK cells of each group are shown in Table 3. There was no statistically significant difference between group B+E+ and other three groups (B-E-, B+E- and B-E+) in total splenocytes and activity of NK cells and LAK cells.

Table 1 Mean tumor volume and tumor weight before and after treatment

Group	Mean tumor volume		Tumor volume variance (mm^3)	Tumor weight after treatment (mg)
	Before (mm^3)	After (mm^3)		
B+E+	37.92±5.39	19.28±8.83[1]	–18.65±7.68[1]	14.48±6.65[1]
B+E–	38.84±5.47	46.93±13.23	8.09±12.53	35.31±10.01
B–E+	37.79±5.45	48.15±8.19	10.36±4.41	36.08±6.25
B–E–	39.32±6.30	53.20±7.22	13.88±2.44	39.99±5.41
F value	$F = 0.17$	$F = 25.22$	$F = 36.80$	$F = 25.32$
P value	$P = 0.917$	$P<0.01$	$P<0.01$	$P<0.01$

[1]B-E-, no treatment; B+E-, administration of bleomycin alone; B-E+, administration of electric pulses alone; B+E+, ECT.

Table 2 The response rates of the four groups after treatment

Group	CR (%)	PR (%)	Stab (%)	Prog (%)
B+E+	1 (10)	7 (70)	2 (20)	0 (0)
B+E–	0 (0)	1 (10)	2 (20)	7 (70)
B–E+	0 (0)	1 (10)	1 (10)	8 (80)
B–E–	0 (0)	0 (0)	0 (0)	10 (100)

B-E-, no treatment; B+E-, administration of bleomycin alone; B-E+, administration of electric pulses alone; B+E+, ECT ($\chi^2 = 25.67$, $P<0.01$).

Table 3 Total splenocytes and activity of NK cells and LAK cells of each group

Group	Total splenocytes (10^6)	Activity of NK cells	Activity of LAK cells
B+E+	110.8±10.62	18.49±2.73	23.51±2.41
B+E–	114.3±10.68	18.89±2.57	25.21±3.09
B–E+	116.4±10.32	18.68±2.86	25.32±2.90
B–E–	117.4±12.89	19.79±2.64	24.84±2.53

B-E-, no treatment; B+E-, administration of bleomycin alone; B-E+, administration of electric pulses alone; B+E+, ECT.

Histological analysis

Undamaged tumor cells and a few accompanying infiltrating cells were observed not only in the tumors of group B-E- but also in that of group B+E- and group B+E+. In contrast, there were massive necrotic area with a moderately intense mononuclear infiltration in the tumors of group B+E+ (Figure 2). The one CR was also confirmed histologically.

DISCUSSION

ECT is a new cancer therapy that utilizes electric pulses to augment the effectiveness of chemotherapeutic agents. Destabilization of the lipid bilayer of the cell membrane by the electric pulses transiently increases permeability. This provides intracellular access for any exogenous molecules including bleomycin which must be internalized by a cell to be effective. Thus, the combination becomes a potent anti-tumor treatment. The effectiveness of ECT on various types of cancer has been demonstrated not only *in vitro* but also in animal models, and several clinical trials of ECT have already been initiated[7-10]; however, the possible involvements of anti-tumor mechanisms, especially that of anti-tumor immunity, remain still unclear.

In current study, the mean tumor volume and tumor weight of group B+E+ on the 7th d of treatment was significantly less than those of other three groups ($P<0.01$), and bleomycin-mediated ECT produced a tumor response rate of 80% (10% CR and 70% PR) which was significantly higher than those of other three groups ($P<0.01$). These results concur with other experimental studies and demonstrate that the bleomycin-mediated ECT is effective and sensitive to human colon cancer xenografts in nude

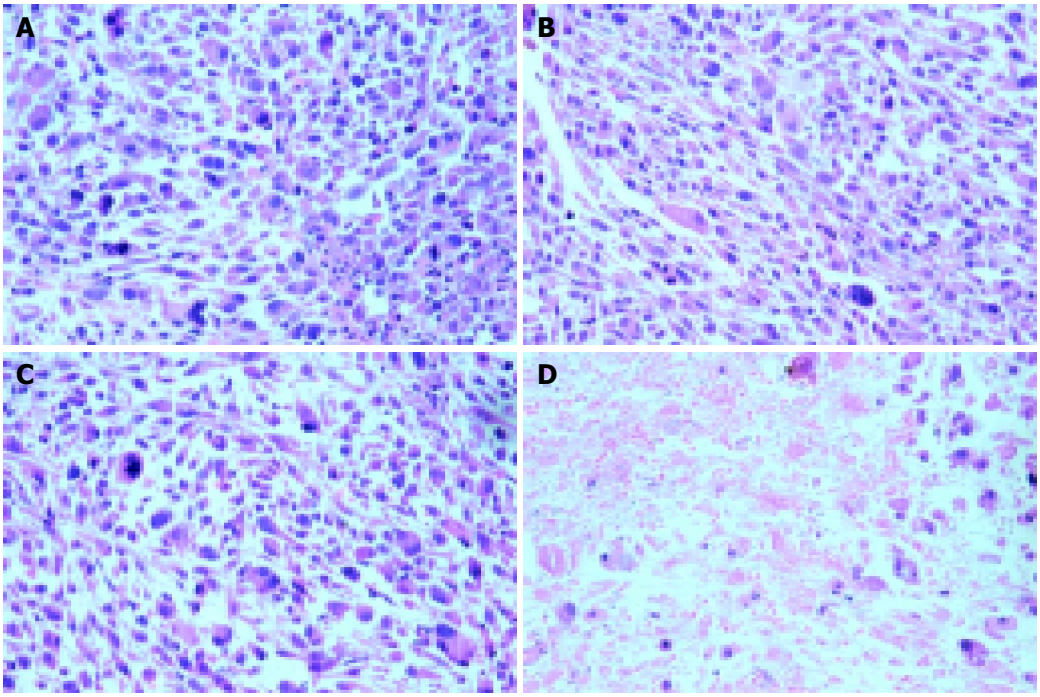

Figure 2 Histological examination of colon cancer xenografts on the 7th d after treatment (hematoxylin and eosin staining). **A:** (group B-E-), **B:** (group B-E+) and **C:** (group B+E-) contained markedly atypical cells arranged irregularly; **D**: (group B+E+) exhibited massive necrosis with a moderately intense mononuclear infiltration (40×).

mice. Furthermore, no mice died of electroporation in this study, which suggests that ECT using the voltage of 900 V/cm is safe and feasible.

Increased cytotoxicity of bleomycin by electroporation is the predominant mechanism involved in anti-tumor effectiveness of ECT. This notion is supported by the data demonstrating that exposure of tumor cells to electric pulses profoundly increased not only intracellular amounts of bleomycin but also intratumoral amounts of bleomycin several 100-fold[4,7,11]. Once inside the cell, bleomycin possesses a very potent intrinsic cytotoxicity, inducing single- and double-strand DNA breaks and cell cycle blockage[12]. Anti-vascular effect was also proposed as an additional mechanism involved in anti-tumor effectiveness of ECT[13]. Damage to endothelial cells caused by ECT may lead to obstruction of blood flow and ischemic death of tumor cells lining the obstructed blood vessel. It is supported by the observations that bleomycin-mediated ECT resulted in complete shut down of tumor blood flow observed 12 h after the treatment, and correlated with anti-tumor effectiveness and the extent of tumor necrosis[14]. Recently, ECT has been found to increase immune response to tumors[15-17] and the infiltration of inflammatory cells into tumor treated with bleomycin-mediated ECT was also reported[18]. However, its exact nature has yet to be defined.

NK cells recognize tumor cells without the need for immunization or pre-activation compared with T cells, which first require education by antigen-presenting cells[19,20]. Once activated, NK cells show increased cytolytic, secretory and proliferative functions. Activation of NK cells with high-dose IL-2 has been widely used and has been shown to mediate anti-tumor activity in experimental as well as clinical settings[21,22]. In current study, no statistically significant difference was found between group B+E+ and other three groups (B-E-, B+E- and B-E+) in total splenocytes and activity of NK cells and LAK cells, which demonstrated that non-specific immunity may not play an important role in the anti-tumor immunity of bleomycin-mediated ECT. Furthermore, it was reported that the induction of cytotoxic T lymphocytes against Colon 26 cells was observed in the spleens of mice with Colon 26 after treatment with ECT and bleomycin[16], and that the Balb/c mice inoculated subcutaneously with Colon 26 cells rejected inoculations of rechallenged Colon 26 cells after treatment of ECT and bleomycin, but not other kind of cancer cells[17]. Therefore, the generation of T-cell-dependent, tumor-specific protective immunity might be involved in the process of tumor nodule regression following ECT.

In conclusion, we have shown that *in vivo* ECT with bleomycin is effective in reducing or even eliminating subcutaneous human colon cancer xenografts in nude mice. Additional investigations are also required to define parameters such as the optimum duration of treatment, dose effects, and the volume of tumor that can be treated. Research is currently in progress in this area. If results are encouraging, a clinical trial could be initiated to determine whether ECT is a valid alternative to systemic chemotherapy for patients with nonresectable metastases of malignancies, especially for those with hepatic metastasis of CRC.

REFERENCES

1 **Jemal A**, Thomas A, Murray T, Thun M. Cancer statistics, 2002. *CA Cancer J Clin* 2002; **52**: 23-47

2 **Mir LM**, Orlowski S, Belehradek J, Paoletti C. Electrochemotherapy potentiation of antitumour effect of bleomycin by local electric pulses. *Eur J Cancer* 1991; **27**: 68-72

3 **Gehl J**, Skovsgaard T, Mir LM. Enhancement of cytotoxicity by electropermeabilization: an improved method for screening drugs. *Anticancer Drugs* 1998; **9**: 319-325
4 **Kuriyama S**, Matsumoto M, Mitoro A, Tsujinoue H, Nakatani T, Fukui H, Tsujii T. Electrochemotherapy for colorectal cancer with commonly used chemotherapeutic agents in a mouse model. *Dig Dis Sci* 2000; **45**: 1568-1577
5 **Rodriguez-Cuevas S**, Barroso-Bravo S, Almanza-Estrada J, Cristobal-Martinez L, Gonzalez-Rodriguez E. Electrochemotherapy in primary and metastatic skin tumors: phase II trial using intralesional bleomycin. *Arch Med Res* 2001; **32**: 273-276
6 **Chazal M**, Benchimol D, Baque P, Pierrefite V, Milano G, Bourgeon A. Treatment of hepatic metastases of colorectal cancer by electrochemotherapy: an experimental study in the rat. *Surgery* 1998; **124**: 536-540
7 **Kuriyama S**, Tsujinoue H, Toyokawa Y, Mitoro A, Nakatani T, Yoshiji H, Tsujimoto T, Fukui H. A potential approach for electrochemotherapy against colorectal carcinoma using a clinically available alternating current system with bipolar snare in a mouse model. *Scand J Gastroenterol* 2001; **36**: 297-302
8 **Mitsui K**, Kato K, Nakamura K, Yamada Y, Honda N, Fukatsu H, Yoshikawa K. Effective treatment of bladder tumor-bearing mice by direct delivery of bleomycin using electrochemotherapy. *Drug Deliv* 2002; **9**: 249-252
9 **Kitamura A**. Bleomycin-mediated electrochemotherapy in mouse NR-S1 carcinoma. *Cancer Chemother Pharmacol* 2003; **51**: 359-362
10 **Shimizu T**, Nikaido T, Gomyo H, Yoshimura Y, Horiuchi A, Isobe K, Ebara S, Takaoka K. Electrochemotherapy for digital chondrosarcoma. *J Orthop Sci* 2003; **8**: 248-251
11 **Jaroszeski MJ**, Dang V, Pottinger C, Hickey J, Gilbert R, Heller R. Toxicity of anticancer agents mediated by electroporation *in vitro*. *Anticancer Drugs* 2000; **11**: 201-208
12 **Mir LM**, Tounekti O, Orlowski S. Bleomycin: revival of an old drug. *Gen Pharmacol* 1996; **27**: 745-748
13 **Sersa G**, Cemazar M, Miklavcic D, Chaplin DJ. Tumor blood flow modifying effect of electrochemotherapy with bleomycin. *Anticancer Res* 1999; **19**: 4017-4022
14 **Sersa G**, Krzic M, Sentjurc M, Ivanusa T, Beravs K, Kotnik V, Coer A, Swartz HM, Cemazar M. Reduced blood flow and oxygenation in SA-1 tumours after electrochemotherapy with cisplatin. *Br J Cancer* 2002; **87**: 1047-1054
15 **Mir LM**, Roth C, Orlowski S, Quintin-Colonna F, Fradelizi D, Belehradek J, Kourilsky P. Systemic antitumor effects of electrochemotherapy combined with histoincompatible cells secreting interleukin-2. *J Immunother Emphasis Tumor Immunol* 1995; **17**: 30-38
16 **Kuriyama S**, Mitoro A, Tsujinoue H, Toyokawa Y, Nakatani T, Yoshiji H, Tsujimoto T, Okuda H, Nagao S, Fukui H. Electrochemotherapy can eradicate established colorectal carcinoma and leaves a systemic protective memory in mice. *Int J Oncol* 2000; **16**: 979-985
17 **Miyazaki S**, Gunji Y, Matsubara H, Shimada H, Uesato M, Suzuki T, Kouzu T, Ochiai T. Possible involvement of antitumor immunity in the eradication of colon 26 induced by low-voltage electrochemotherapy with bleomycin. *Surg Today* 2003; **33**: 39-44
18 **Jaroszeski MJ**, Coppola D, Pottinger C, Benson K, Gilbert RA, Heller R. Treatment of hepatocellular carcinoma in a rat model using electrochemotherapy. *Eur J Cancer* 2001; **37**: 422-430
19 **Smyth MJ**, Hayakawa Y, Takeda K, Yagita H. New aspects of natural-killer-cell surveillance and therapy of cancer. *Nat Rev Cancer* 2002; **2**: 850-861
20 **Colucci F**, Caligiuri MA, Di Santo JP. What does it take to make a natural killer? *Nat Rev Immunol* 2003; **3**: 413-425
21 **Sacchi M**, Vitolo D, Sedlmayr P, Rabinowich H, Johnson JT, Herberman RB, Whiteside TL. Induction of tumor regression in experimental model of human head and neck cancer by human A-LAK cells and IL-2. *Int J Cancer* 1991; **47**: 784-791
22 **Ueda Y**, Yamagishi H, Tanioka Y, Fujiwara H, Fuji N, Itoh T, Fujiki H, Yoshimura T, Oka T. Clinical application of adoptive immunotherapy and IL-2 for the treatment of advanced digestive tract cancer. *Hepatogastroenterology* 1999; **46 Suppl 1**: 1274-1279

Science Editor Guo SY **Language Editor** Elsevier HK

PO Box 2345, Beijing 100023, China
www.wjgnet.com
wjg@wjgnet.com

ELSEVIER

World J Gastroenterol 2005;11(16):2431-2437
World Journal of Gastroenterology ISSN 1007-9327

• *BASIC RESEARCH* •

Effect of norcantharidin on proliferation and invasion of human gallbladder carcinoma GBC-SD cells

Yue-Zu Fan, Jin-Ye Fu, Ze-Ming Zhao, Cun-Qiu Chen

Yue-Zu Fan, Ze-Ming Zhao, Cun-Qiu Chen, Department of General Surgery, Tongji Hospital of Tongji University, Shanghai 200065, China
Jin-Ye Fu, Department of Surgery, Pudong People Hospital, Shanghai 201200, China
Supported by the Scientific Foundation of Tongji University, China, No. KPB027
Correspondence to: Professor, Director Yue-Zu Fan, Department of General Surgery, Tongji Hospital of Tongji University, 389 Xincun Road, Shanghai 200065, China. fanyuezu_shtj@msn.com
Telephone: +86-21-56051080-1107 Fax: +86-21-56050502
Received: 2004-07-28 Accepted: 2004-09-04

Abstract

AIM: To investigate the effect of norcantharidin on proliferation and invasion of human gallbladder carcinoma GBC-SD cells *in vitro* and its anticancer mechanism.

METHODS: Human gallbladder carcinoma GBC-SD cells were cultured by cell culture technique. The growth and the invasiveness of GBC-SD cells *in vitro* were evaluated by the tetrazolium-based colorimetric assay and by the Matrigel experiment and the crossing-river test. Expression of PCNA, Ki-67, MMP_2 and $TIMP_2$ proteins of GBC-SD cells was determined by streptavidin–biotin complex method.

RESULTS: *In vitro* norcantharidin inhibited the growth and proliferation of GBC-SD cells in a dose- and time-dependent manner, with the IC_{50} value of 56.18 μg/mL at 48 h. Norcantharidin began to inhibit the invasion of GBC-SD cells at the concentration of 5 μg/mL, and the invasive action of GBC-SD cells was inhibited completely and their crossing-river time was prolonged significantly at 40 μg/mL. After treatment with norcantharidin, the expression of PCNA, Ki-67, and MMP_2 was significantly decreased. With the increase in $TIMP_2$ expression, the MMP_2 to $TIMP_2$ ratio was decreased significantly ($P<0.05$).

CONCLUSION: Norcantharidin inhibits the proliferation and growth of human gallbladder carcinoma cells *in vitro* at relatively low concentrations by inhibiting PCNA and Ki-67 expression. Its anti-invasive activity may be the result of decrease in MMP_2 to $TIMP_2$ ratio and reduced cell motility.

Key words: Norcantharidin; Gallbladder neoplasm; Cell culture; Proliferation; Invasion; Oncoprotein PCNA; Ki-67; MMP_2 and $TIMP_2$; Immunohistochemistry

Fan YZ, Fu JY, Zhao ZM, Chen CQ. Effect of norcantharidin on proliferation and invasion of human gallbladder carcinoma GBC-SD cells. *World J Gastroenterol* 2005; 11(16): 2431-2437
http://www.wjgnet.com/1007-9327/11/2431.asp

INTRODUCTION

Primary carcinoma of the gallbladder represents a highly lethal and aggressive malignant tumor because of its dormancy course, difficult diagnosis, early metastasis, strong invasion and poor prognosis[1,4]. The only potentially curative therapy for gallbladder carcinoma is surgical resection. Unfortunately, most patients with this type of cancer present with advanced and unresectable disease-only 10-30% of patients can be considered for surgery on presentation[1,3,5,7] and should be considered for palliative treatment such as chemotherapy[1,3,6,8,9] and radiotherapy[1,3,6,10,11]. However, reports of chemotherapy and radiotherapy in gallbladder carcinoma are disappointing, results are conflicting and most series have a small number of patients[1,3,6,8-11]. Obviously, there is an urgent need to identify new therapeutic agents for the treatment of gallbladder carcinoma *in vivo*. Many lines of evidence have shown that Chinese medicine contains many chemical compounds with anticancer effects. We reported the influence of norcantharidin (NCTD, a demethylated form of cantharidin, which is an active ingredient of Chinese medicine-Mylabris) on growth and apoptosis of GBC-SD cell lines of human gallbladder carcinoma[12,13]. In the present study, human gallbladder carcinoma GBC-SD cell lines were used to study the *in vitro* effect of NCTD on proliferation and invasion of human gallbladder carcinoma GBC-SD cells and its mechanism.

MATERIALS AND METHODS

Materials

GBC-SD cell lines of human gallbladder carcinoma were purchased from Shanghai Cell Institute Country Cell Bank. NCTD was purchased from Beijing Fourth Pharmaceutical Works, China. Matrigel invasion chamber, which is composed of a layer of artificial basement membrane matrix above PET membrane with 8.0-μm hole, were purchased from Becton Dickinson, USA. Rat monoclonal antibody proliferating cell nuclear antigen (PCNA) and Ki-67 were respectively purchased from Calbiochem Co. and Antibody Diagnostica Co.; Monoclonal MMP_2 antibody was purchased from Neomarker and $TIMP_2$ antibody from Boster. Bovine calf serum, RPMI-1640 medium, trypsin and D-Hanks' solution were all purchased from Gibco; MTT solution and DMSO

were purchased from Sigma; SABC kit and DAB are all purchased from Boster.

Methods

Cell cultures[12,13] GBC-SD cells of human gallbladder carcinoma were cultured in RPMI-1640 medium supplemented with 10% bovine calf serum in an incubator with 50 mL/L at 37 ℃. The medium was changed every 2 d. When the cells became confluent, namely a 95% plating efficiency, they were trypsinized with 0.25% trypsin. Then the cells were returned to culture at 37 ℃ in 50 mL/L CO_2 for 24 h, and they were washed twice with Hanks' balanced salt solution, and used in this experiment.

Inhibitory effect of NCTD on growth of GBC-SD cells The tetrazolium-based colorimetric assay (MTT) was used to evaluate the inhibitory effect of NCTD on growth of GBC-SD cells *in vitro*, namely the tumor cytotoxicity test[12,13]. After GBC-SD cells were cultured in a 96-well plate (3×10^5 cells·100 μL/well) in culture medium overnight, they were treated with various concentrations of NCTD in fresh culture medium at 37 ℃ for 24 h. The tumor cell cytotoxicity was determined by MTT. The optical densities (*A* values) at 540 nm were measured using an ELISA reader (DG3032, Shanghai). The A_{540} value of the experimental groups was divided by the A_{540} value of untreated controls and presented as a percentage of the cells. The inhibitory percent of various concentrations of NCTD on GBC-SD cells (%) = (1-A_{540} value in the experimental group/A_{540} value of control group) ×100%. Three separate experiments were performed. The concentration of drug giving 50% growth inhibition (IC_{50}) was calculated from the formula $LC_{50} = I_g^{-1}[X_m - I(\Sigma_p - 0.5)]$.

Matrigel invasion experiment of GBC-SD cells (1) Living GBC-SD cells were trypsinized with 0.25% trypsin and washed with fresh culture medium, suspended in the culture medium with 10% bovine calf serum (1×10^6 cells/mL). The tumor cell suspension was transferred to the above layer of the Matrigel invasion chamber (0.3 mL/every chamber), while 0.8 mL of RPMI-1640 medium with 10% bovine calf serum was only added to the bottom layer of the Matrigel invasion chamber. Then the cells were cultured in 50 mL/L CO_2 at 37 ℃ for 24 h; (2) The cells were treated without (untreated control group) or with various concentrations of NCTD (the six-concentration groups, every concentration ×3) in fresh culture medium (0.3 mL/every chamber), were cultured in an incubator with 50 mL/L at 37 ℃ for 72 h; (3) The passing-membrane cells were collected from the above layer of the Matrigel invasion chamber, centrifuged (200 r/min, 10 min), dyed by Trypan blue dye, and counted in a hemocytometer. Each experiment was performed thrice.

Crossing-river experiment of GBC-SD cells The suspension of GBC-SD cells (3×10^5 cells/mL) according to the above-mentioned confection method were fed (3 mL/well) into six-well culture plates and incubated in 50 mL/L at 37 ℃ for 24 h; (2) The cells were treated without (untreated control group) or with various concentrations of NCTD in fresh culture medium, and were again cultured in 50 mL/L at 37 ℃ for 84 h; (3) After being washed with PBS and one beeline as a river was then laid out on the well with 10 μL pipette tip, the cells of culture plate well were washed twice with PBS and cultured in the medium supplemented with 10% bovine calf serum in 50 mL/L at 37 ℃. Beeline mark on the well was observed every 2 h till the mark was filled with the cells. Three separate experiments were performed for each concentration/exposure time combination.

Immunohistochemistry assay of PCNA, Ki-67, MMP_2, $TIMP_2$ Expression of PCNA, Ki-67, MMP_2 and $TIMP_2$ proteins of GBC-SD cells was determined by streptavidin-biotin complex method (SABC). PCNA, Ki-67, MMP_2 and $TIMP_2$ antibodies were respectively used at a concentration of 1:100. Goat serum, biotinylated secondary antibody (goat anti-mouse IgG) and DAB are all purchased from Boster. For negative control, the slides were treated with PBS in place of primary antibody. Ten slides were made up per experimental group. More than 10 visual fields were observed or more than 500 cells were counted per slide. The positive index of PCNA represented expression of PCNA protein. The positive index of PCNA = number of PCNA-positive cells/1 000 cells. The positive index of Ki-67 represented expression of Ki-67 protein. The positive percentage of MMP_2 or $TIMP_2$ showed expression of MMP_2 or $TIMP_2$ protein.

Data statistical analysis All the statistical analyses were performed using SPSS 10.0 for Windows. $P<0.05$ or $F<0.05$ was considered to be of statistical significance.

RESULTS

Inhibitory effect of NCTD on growth of GBC-SD cells

Inhibitory effect of various concentrations of NCTD on GBC-SD cells The effect of NCTD on cell growth was examined at doses between 0 and 100 μg/mL. As shown in Figure 1, inhibitory effect of NCTD at low concentrations (5 μg/mL) on GBC-SD cells was not obvious; but as concentration increased, proliferation of GBC-SD cells was markedly inhibited by NCTD with 98.59% growth inhibition at 100 μg/mL concentration, in a dose-dependent manner. IC_{50} is 56.18 μg/mL.

Inhibitory effect of IC_{50} NCTD on GBC-SD cells at different time The effect of NCTD on cell growth was examined at times between 0 and 120 h. As shown in Figure 2, anti-proliferation effect of IC_{50} NCTD on GBC-SD cells began to show after being cultured for 6 h;

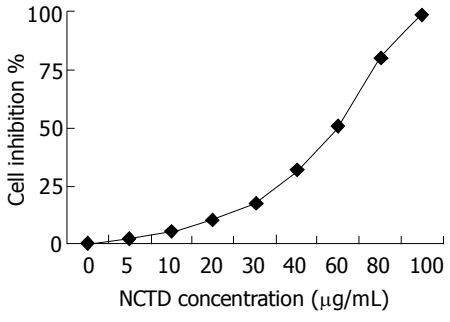

Figure 1 The dose-response curves of effect of NCTD on GBC-SD cells for 72 h. Inhibition of the growth of human gallbladder carcinoma GBC-SD cells by various concentrations of NCTD. Cell number was counted by the MTT method.

Table 1 Influence of different concentrations of NCTD on Matrigel invasion of GBC-SD cells

Group	NCTD (μg/mL)	*n*	Passing-membrane cells (% of control group)	Dead passing-membrane cells (% of control group)
Control	0	6	100.0	17.2±1.15
NCTD	5	6	62.0±5.08[b]	31.7±4.29[b]
	10	6	37.7±2.01[b]	59.7±1.15[b]
	20	6	18.0±1.79[b]	67.3±4.93[b]
	40	6	5.0±1.80[b]	95.2±4.88[b]

[b]$P<0.01$ *vs* control group.

Table 2 Influence of different concentration of NCTD on the crossing-river time of GBC-SD cells

Group	NCTD (μg/mL)	*n*	Crossing-river time (h)
Control	0	6	22.6±0.67
NCTD	5	6	28.2±1.00[b]
	10	6	33.4±0.71[b]
	20	6	45.0±0.68[b]
	30	6	58.8±0.72[b]
	40	6	>72[b]

[b]$P<0.01$ *vs* control group.

moreover, the inhibitory effect was markedly intensified as time prolonged with 52.18% growth inhibition for 48 h, in a time-dependent manner. So it was most obvious after 48 h.

Influence of NCTD on Matrigel invasion of GBC-SD cells *in vitro* As shown in Table 1, GBC-SD cells in untreated control group passed more of the membrane and had more invasive capability *in vitro*; NCTD began to inhibit the invasion of GBC-SD cells at the concentration of 5 μg/mL and as its concentration increased, their passing-membrane cells markedly decreased, the Trypan blue dyed cells, namely the dead passing-membrane cells obviously increased ($P<0.01$). At 40 μg/mL of NCTD, the invasive action of GBC-SD cells was inhibited completely. Its effect was also in a dose-dependent manner. The experiment showed that NCTD could inhibit obviously the *in vitro* invasive capability simulating human basement membrane of GBC-SD cells.

Influence of NCTD on the crossing-river test of GBC-SD cells As shown in Table 2, the crossing-river time of GBC-SD cells in various experiment groups was prolonged significantly after treatment with NCTD. When compared with control group, the crossing-river time was prolonged by 25% in 5 μg/mL NCTD group; 160% in 30 μg/mL NCTD group; GBC-SD cells did not still cross-river completely after 72 h in more than 40 μg/mL NCTD group. The crossing-river test indicated that NCTD could inhibit movement capability of GBC-SD cells *in vitro* markedly.

Influence of NCTD on expression of PCNA, Ki-67 proteins of GBC-SD cells The positive expression, with brown or yellow dye, of PCNA or Ki-67 occurred in cell nucleoli. GBC-SD cells in control group showed mostly the positive dye of PCNA and Ki-67 (Figures 3A and 4A), the positive index of PCNA and Ki-67 reached 0.932±0.031 and 0.964±0.092, respectively. After treatment with IC_{50} NCTD for 48 h, the positive cells of expression of PCNA and Ki-67 proteins decreased significantly, the dye of cell nucleoli became light and shallow (Figures 3B and 4B), the positive index of PCNA and Ki-67 came down 0.318±0.023 and 0.297±0.018 respectively, when compared with the control group (Table 3, $P<0.05$).

Influence of NCTD on expression of MMP_2, $TIMP_2$ proteins and $MMP_2/TIMP_2$ of GBC-SD cells The positive expression, with brown or yellow dye, of MMP_2 occurred in cytoplast, $TIMP_2$ in cytoplast or on nucleoli membrane. The positive expression of MMP_2, the negative expression of $TIMP_2$ was observed in most GBC-SD cells of control group (Figures 5A and 6A). After treatment with various concentrations of NCTD for 48 h and as its concentration increased, the positive cells of MMP_2 expression was decreased and the dye became light and race, the positive

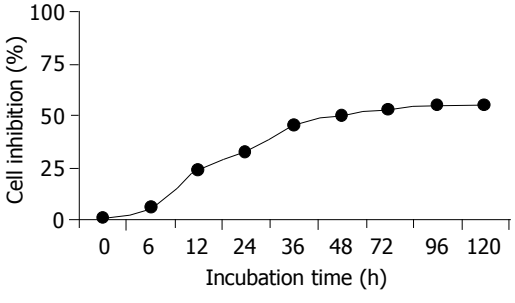

Figure 2 The inhibitory effect curves of IC_{50} NCTD on GBC-SD cells at different times. Cell number was counted by the MTT method.

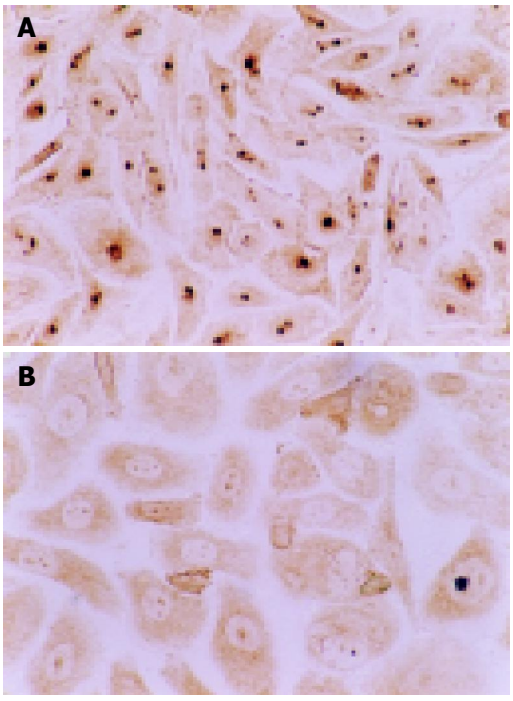

Figure 3 Positive expression occurred in cell nucleoli, with brown or yellow dye, of PCNA protein of GBC-SD cells (immunohistochemistry SABC method, ×200). **A:** The brown dye of PCNA was shown positively in most cells of the control group. **B:** In the experiment group with treatment of IC_{50} NCTD for 48 h, the positive cells of PCNA expression decreased significantly and the dye in cell nucleoli became light and shallow.

Table 3 Influence of NCTD on expression of PCNA, Ki-67 proteins of GBC-SD cells

Group	*n*	Positive index (mean±SD)	
		PCNA	Ki-67
Control	10	0.932±0.031	0.964±0.092
IC_{50} NCTD (56.18 μg/mL)	10	0.318±0.023[a]	0.297±0.018[a]

[a]P<0.05 *vs* control group.

Table 4 Influence of NCTD on expression of MMP_2, $TIMP_2$ proteins and the MMP_2 to $TIMP_2$ ratio of GBC-SD cells

Group	NCTD (μg/mL)	*n*	Percent of protein expression (%)		$MMP_2/TIMP_2$
			MMP_2	$TIMP_2$	
Control	0	10	62.82±3.20	13.42±1.27	4.68
NCTD	5	10	34.61±1.82[a]	30.79±2.15[a]	1.12[b]
	10	10	27.02±1.40[a]	34.22±2.97[a]	0.79[b]
	20	10	26.18±1.81[a]	35.60±2.04[a]	0.74[b]
	40	10	19.56±2.36[a]	29.54±2.33[a]	0.66[b]

[a]P<0.05 *vs* control group; [b]P<0.01 *vs* control group.

percentage of MMP_2 expression was reduced significantly; the positive cells and the positive percentage of $TIMP_2$ expression were all increased significantly; the MMP_2 to $TIMP_2$ ratio was decreased significantly (Figures 5B and 6B; Table 4, P<0.05).

DISCUSSION

Present treatment for primary carcinoma of the gallbladder

Primary carcinoma of the gallbladder is one of the malignant neoplasms with increasing incidence recently. As the special site of anatomy, the feature of biology and epidemiology of the disease, it is hitherto a poor prognostic disease with difficult diagnosis, early metastasis and dismal treatment result[1,4]. The only potentially curative therapy for the disease is still surgical resection. Unfortunately, most patients with this type of cancer present with advanced and unresectable disease-only 10-30% of patients can be considered for surgery on presentation, furthermore, only about 5% of patients were alive after 5 years since operation[1,3,5,7]. So, it is important that these patients should be considered for palliative, integrated treatment such as chemotherapy[1,3,6,8,9] and radiotherapy[1,3,6,10,11]. However, no specific chemoradiotherapy program for carcinoma of the gallbladder has emerged as the definitive acceptable standard of care, most series have small number of patients and there is much room for improvement[1,3,6,8-11]. With the deep research on the etiology, molecular biology of tumor and tumorigenesis, there is obviously an urgent need to identify new therapeutic agents for the treatment of gallbladder carcinoma.

Many lines of evidence have shown that Chinese medicine contains many chemical compounds with anticancer effects. We reported the effect of norcantharidin (NCTD) on growth and apoptosis of GBC-SD cell lines of human gallbladder carcinoma[12,13]. NCTD, the demethylated analog and the low-cytotoxic derivative of cantharidin, a 7-oxabicyclo[2.2.1] heptane-2, 3-dicarboxylic acid derivative, a natural toxin and the active ingredient extracted from Chinese medicine Mylabris. NCTD is synthesized from furan and maleic anhydride via the Diels-Alder reaction[14-17]. It has been reported that NCTD inhibit the proliferation and growth of a variety of human tumor cell lines *in vitro*, and are used to treat human cancers with stimulation of the bone marrow and increase of the peripheral leukocyte count[14,18-21]. There were, however, very few reports describing the effect of NCTD on human gallbladder carcinoma. In the present study, we investigated the *in vitro* effect of NCTD on proliferation and invasion of human gallbladder carcinoma GBC-SD cells and its mechanism.

Inhibitory effect of NCTD on proliferation, growth of GBC-SD cells and its mechanism

Modern oncology research has shown that genesis and development of tumor are obviously related with proliferation and apoptosis of the cells. Proliferation and apoptosis of normal cells comparatively maintain their balanceable condition. If cell apoptosis is arrested or cell proliferation exceeds its apoptosis, the cells grow predominately. This is a significant basis of genesis and development of tumor. One of the most important mechanisms, on which many anti-cancer agents inhibit the growth of tumor is inhibition of the proliferation of tumor cells or inducement of their apoptosis[21,22].

In this study, we investigated the effect of NCTD on proliferation of human gallbladder carcinoma GBC-SD cells and its anti-cancer mechanism. NCTD was shown obviously

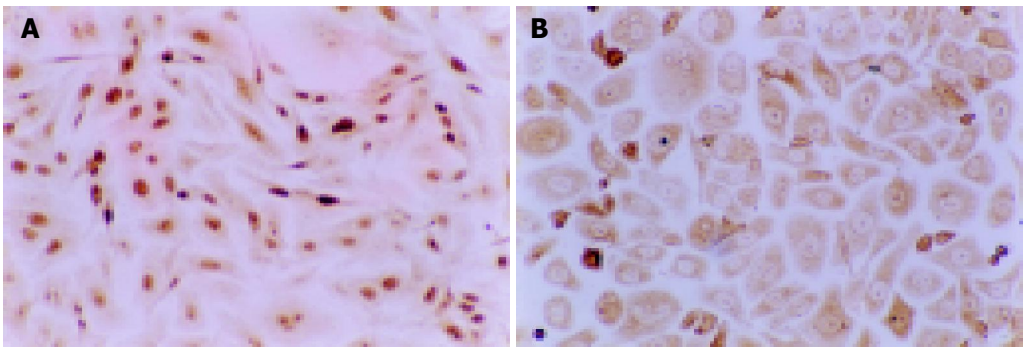

Figure 4 The positive expression occurred in cell nucleoli, with brown or yellow dye, of Ki-67 protein of GBC-SD cells (immunohistochemistry SABC method, ×100). **A:** The brown dye of Ki-67 was shown positively in most cells of the control group. **B:** In the experiment group with treatment of IC_{50} NCTD for 48 h, the positive cells of Ki-67 expression decreased significantly and the dye in cell nucleoli became light and shallow.

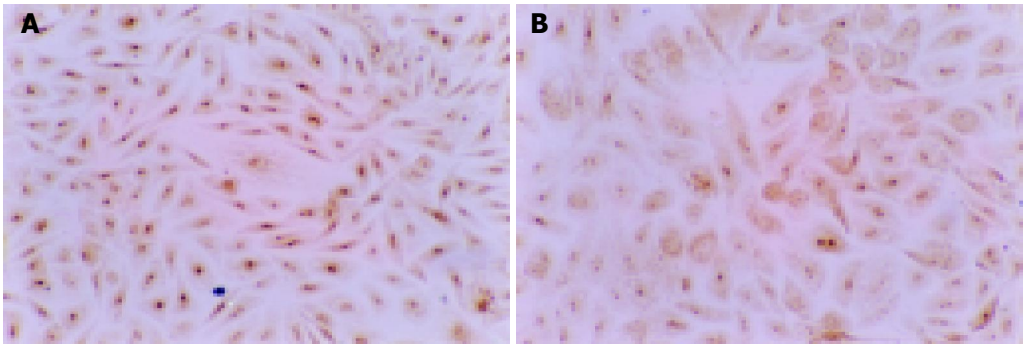

Figure 5 Positive expression with brown dye occurred in cytoplast of MMP_2 protein of GBC-SD cells (immunohistochemistry SABC method, ×100). **A:** The brown dye of MMP_2 was shown positively in most cells of the control group. **B:** In the experiment group with treatment of NCTD (5 μg/mL) for 48 h, the positive cells of MMP_2 expression decreased significantly and the dye in the cytoplast became light.

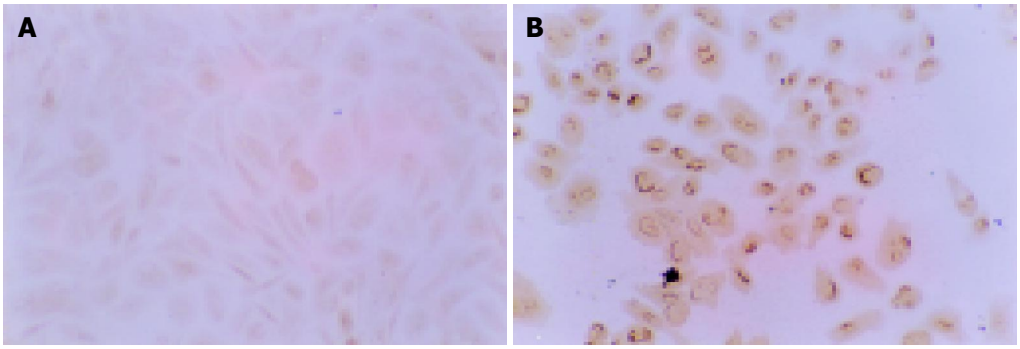

Figure 6 Positive expression with brown dye occurred on nucleoli membrane of $TIMP_2$ protein of GBC-SD cells (immunohistochemistry SABC method, ×100). **A:** The negative expression of $TIMP_2$ was observed in most GBC-SD cells of the control group. **B:** In the experiment group with treatment of NCTD (5 μg/mL) for 48 h, the positive cells of $TIMP_2$ expression were increased significantly and the dye on nucleoli membrane represent brown.

effective in inhibiting the proliferation of GBC-SD cells in a dose- and time-dependent manner. This is consistent with the foreign reports about the effect of NCTD on other tumor cells[22,23]. The reports demonstrated that NCTD is the inhibitor of protein phosphatase type 2A[24-26] and can inhibit the growth of human colon cancer HT29 cells, inhibit cell growth and arrest the cell cycle at G_2/M phase in K562 human myeloid leukemia cells, inhibit DNA synthesis in H L-60 cells and induce apoptosis in human tumor cells[23,27-29]. We reported that after treatment with NCTD, percentage of the G_2/M phase in human gallbladder carcinoma GBC-SD cells was increased, percentage of the S phase was decreased with the increased rate of cell apoptosis by flow cytometry; cell nuclear shrinkage, membrane budding and karyorrhexis in some GBC-SD cells were shown by light microscope; microvillus decreasing, cell apparatus including Golgi and mitochondria atrophy, and typical apoptosis cells were observed by electron microscope, and there was the morphological change of apoptosis of GBC-SD cells[12]. It was shown that the mechanisms, on which NCTD inhibit the proliferation and the growth of human gallbladder carcinoma GBC-SD cells might be correlated with the inhibition of cell proliferation, arresting of cell cycle, blockage of DNA synthesis, influence of cell metabolism and inducement of cell apoptosis[12].

PCNA and Ki-67, gene proteins of cell proliferation-related, are the markers for reflection of cell proliferation[30-33]. In this study, after treatment with IC_{50} NCTD for 48 h, the positive GBC-SD cells of expression of PCNA and Ki-67 proteins were decreased significantly; their positive indexes were also decreased significantly ($P<0.05$). It was shown that NCTD could influence the expression of the proliferation-related gene proteins, PCNA and Ki-67, of GBC-SD cells. This may be one of the mechanisms by which NCTD inhibit proliferation and growth of human gallbladder carcinoma GBC-SD cells.

Inhibitory effect of NCTD on invasion of GBC-SD cells and its mechanism

Tumor invasion, one of the essential characters of malignant neoplasm, is considered to be a dynamic, complex and multi-step process[34], but the essential step is the degradation of extracellular matrix (ECM) and basement membrane (BM)[34-37]. It was reported that matrix metalloproteinases (MMPs) are important for the degradation of ECM. MMPs hydrolyze specifically type IV, V, VII, X collagens and fibronectin, elastin, *etc*., which are all important components of ECM and BM, and are closely associated with the invasiveness and metastasis of tumor[34-37]. Tissue inhibitors of metalloproteinases (TIMPs), as the specific inhibitors of MMPs, have such ability to form tight-binding, non-covalent inhibitory complexes with multiple members of the MMP family that they inhibit MMP activity of ECM degradation and have anti-metastasis function[34-37]. The organic balance or homeostasis of MMPs to TIMPs ratio

is the decisive factor for the maintenance of ECM steadiness and integrity[38-40]. So, inhibition of cancer cell invasion, maintenance of ECM integrity and homeostasis of expression of MMP_S and $TIMP_S$ became one of the basic mechanisms of anti-cancer treatment for invasion and metastasis of tumor[41-43].

In the present study, The Matrigel experiment, the crossing-river test and immuno-histochemistry assay of MMP_2, $TIMP_2$ in human gallbladder carcinoma GBC-SD cells were shown that NCTD began to inhibit the *in vitro* invasion and movement of GBC-SD cells at the concentration of 5 μg/mL; and that after treatment with norcantharidin, the expression of MMP_2 was significantly decreased, with the increase in $TIMP_2$ expression the MMP_2 to $TIMP_2$ ratio were decreased significantly ($P<0.05$). Also, these changes were obviously related with the decrease of passing-membrane GBC-SD cells in the Matrigel experiment. NCTD could affect the expression of matrix dissolution-related gene proteins-MMP_2 and $TIMP_2$, and the ratio of $MMP_2/TIMP_2$, consequently, exert the inhibiting effect of invasion of GBC-SD cells. So, NCTD *in vitro* inhibits not only proliferation of human gallbladder carcinoma GBC-SD cells but also invasion and metastasis of the cells at relatively low concentrations. Its anti-invasive activity may be the result of decrease in MMP_2 to$TIMP_2$ ratio and reduced motility of the cells.

REFERENCES

1 **Misra S,** Chaturvedi A, Misra NC, Sharma ID. Carcinoma of the gallbladder. *Lancet Oncol* 2003; **4**: 167-176
2 **Bartlett DL.** Gallbladder cancer. *Semin Surg Oncol* 2000; **19**: 145-155
3 **Taner CB,** Nagorney DM, Donohue JH. Surgical treatment of gallbladder cancer. *J Gastrointest Surg* 2004; **8**: 83-89; discussion 89
4 **Ito H,** Matros E, Brooks DC, Osteen RT, Zinner MJ, Swanson RS, Ashley SW, Whang EE. Treatment outcomes associated with surgery for gallbladder cancer: a 20-year experience. *J Gastrointest Surg* 2004; **8**: 183-190
5 **Muratore A,** Polastri R, Capussotti L. Radical surgery for gallbladder cancer: current options. *Eur J Surg Oncol* 2000; **26**: 438-443
6 **Jarnagin WR,** Ruo L, Little SA, Klimstra D, D'Angelica M, DeMatteo RP, Wagman R, Blumgart LH, Fong Y. Patterns of initial disease recurrence after resection of gallbladder carcinoma and hilar cholangiocarcinoma: implications for adjuvant therapeutic strategies. *Cancer* 2003; **98**: 1689-1700
7 **Kondo S,** Nimura Y, Hayakawa N, Kamiya J, Nagino M, Uesaka K. Regional and para-aortic lymphadenectomy in radical surgery for advanced gallbladder carcinoma. *Br J Surg* 2000; **87**: 418-422
8 **Todoroki T.** Chemotherapy for gallbladder carcinoma-a surgeon's perspective. *Hepatogastroenterology* 2000; **47**: 948-955
9 **Ishii H,** Furuse J, Yonemoto N, Nagase M, Yoshino M, Sato T. Chemotherapy in the treatment of advanced gallbladder cancer. *Oncology* 2004; **66**: 138-142
10 **Houry S,** Barrier A, Huguier M. Irradiation therapy for gallbladder carcinoma: recent advances. *J Hepatobiliary Pancreat Surg* 2001; **8**: 518-524
11 **Kresl JJ,** Schild SE, Henning GT, Gunderson LL, Donohue J, Pitot H, Haddock MG, Nagorney D. Adjuvant external beam radiation therapy with concurrent chemotherapy in the management of gallbladder carcinoma. *Int J Radiat Oncol Biol Phys* 2002; **52**: 167-175
12 **Fan YZ,** Fu JY, Zhao ZM, Chun CQ. Influence of norcantharidin on proliferation and apoptosis of GBC-SD cell lines of human gallbladder carcinoma. *Shanghai Yixue* 2003; **26**(Suppl): 1-4
13 **Fan YZ,** Fu JY, Zhao ZM, Chen CQ. The *in vitro* effect of norcantharidin on proliferation and invasion of human gallbladder carcinoma GBC-SD cells and its mechanism. *Zhonghua Zhongliu Zazhi* 2004; **26**: 271-274
14 **Wang GS.** Medical uses of mylabris in ancient China and recent studies. *J Ethnopharmacol* 1989; **26**: 147-162
15 **Liu J,** Gao J, Liu X. Advances in the study of Cantharidin and its derivatives. *Zhongyaocai* 2003; **26**: 453-455
16 **Williams LA,** Moller W, Merisor E, Kraus W, Rosner H. *In vitro* anti-proliferation/ cytotoxic activity of cantharidin (Spanish Fly) and related derivatives. *West Indian Med J* 2003; **52**: 10-13
17 **Ho YP,** To KK, Au-Yeung SC, Wang X, Lin G, Han X. Potential new antitumor agents from an innovative combination of demethylcantharidin, a modified traditional Chinese medicine, with a platinum moiety. *J Med Chem* 2001; **44**: 2065-2068
18 **McCluskey A,** Ackland SP, Bowyer MC, Baldwin ML, Garner J, Walkom CC, Sakoff JA. Cantharidin analogues: synthesis and evaluation of growth inhibition in a panel of selected tumour cell lines. *Bioorg Chem* 2003; **31**: 68-79
19 **Mack P,** Ha XF, Cheng LY. Efficacy of intra-arterial norcantharidin in suppressing tumour 14C-labelled glucose oxidative metabolism in rat Morris hepatoma. *HPB Surg* 1996; **10**: 65-72
20 **Yang EB,** Tang WY, Zhang K, Cheng LY, Mack PO. Norcantharidin inhibits growth of human HepG2 cell-transplanted tumor in nude mice and prolongs host survival. *Cancer Lett* 1997; **117**: 93-98
21 **Yi SN,** Wass J, Vincent P, Iland H. Inhibitory effect of norcantharidin on K562 human myeloid leukemia cells *in vitro*. *Leuk Res* 1991; **15**: 883-886
22 **Kok SH,** Hong CY, Kuo MY, Lee CH, Lee JJ, Lou IU, Lee MS, Hsiao M, Lin SK. Comparisons of norcantharidin cytotoxic effects on oral cancer cells and normal buccal keratinocytes. *Oral Oncol* 2003; **39**: 19-26
23 **Chen YN,** Cheng CC, Chen JC, Tsauer W, Hsu SL. Norcantharidin-induced apoptosis is via the extracellular signal-regulated kinase and c-Jun-NH2-terminal kinase signaling pathways in human hepatoma HepG2 cells. *Br J Pharmacol* 2003; **140**: 461-470
24 **Liu XH,** Blazsek I, Comisso M, Legras S, Marion S, Quittet P, Anjo A, Wang GS, Misset JL. Effects of norcantharidin, a protein phosphatase type-2A inhibitor, on the growth of normal and malignant haemopoietic cells. *Eur J Cancer* 1995; **31**A: 953-963
25 **Hart ME,** Chamberlin AR, Walkom C, Sakoff JA, McCluskey A. Modified norcantharidins; synthesis, protein phosphatases 1 and 2A inhibition, and anticancer activity. *Bioorg Med Chem Lett* 2004; **14**: 1969-1973
26 **Baba Y,** Hirukawa N, Tanohira N, Sodeoka M. Structure-based design of a highly selective catalytic site-directed inhibitor of Ser/Thr protein phosphatase 2B (calcineurin). *J Am Chem Soc* 2003; **125**: 9740-9749
27 **Hong CY,** Huang SC, Lin SK, Lee JJ, Chueh LL, Lee CH, Lin JH, Hsiao M. Norcantharidin-induced post-G (2)/M apoptosis is dependent on wild-type p53 gene. *Biochem Biophys Res Commun* 2000; **276**: 278-285
28 **Chen YN,** Chen JC, Yin SC, Wang GS, Tsauer W, Hsu SF, Hsu SL. Effector mechanisms of norcantharidin-induced mitotic arrest and apoptosis in human hepatoma cells. *Int J Cancer* 2002; **100**: 158-165
29 **Peng F,** Wei YQ, Tian L, Yang L, Zhao X, Lu Y, Mao YQ, Kan B, Lei S, Wang GS, Jiang Y, Wang QR, Luo F, Zou LQ, Liu JY. Induction of apoptosis by norcantharidin in human colorectal carcinoma cell lines: involvement of the CD95 receptor/ligand. *J Cancer Res Clin Oncol* 2002; **128**: 223-230
30 **Hall PA,** Levison DA, Woods AL, Yu CC, Kellock DB, Watkins JA, Barnes DM, Gillett CE, Camplejohn R, Dover R. Proliferating cell nuclear antigen (PCNA) immunolocalization in paraffin sections: an index of cell proliferation with evidence

of deregulated expression in some neoplasms. *J Pathol* 1990; **162**: 285-294

31 **Takasaki Y,** Kogure T, Takeuchi K, Kaneda K, Yano T, Hirokawa K, Hirose S, Shirai T, Hashimoto H. Reactivity of anti-proliferating cell nuclear antigen (PCNA) murine monoclonal antibodies and human autoantibodies to the PCNA multiprotein complexes involved in cell proliferation. *J Immunol* 2001; **166**: 4780-4787

32 **Gerdes J,** Lemke H, Baisch H, Wacker HH, Schwab U, Stein H. Cell cycle analysis of a cell proliferation associated human nuclear antigen defined by the monoclonal antibody Ki-67. *J Immunol* 1984; **133**: 1710-1715

33 **Aoki T,** Tsukinoki K, Karakida K, Ota Y, Otsuru M, Kaneko A. Expression of cyclooxygenase-2, Bcl-2 and Ki-67 in pleomorphic adenoma with special reference to tumor proliferation and apoptosis. *Oral Oncol* 2004; **40**: 954-959

34 **Meyer T,** Hart IR. Mechanisms of tumour metastasis. *Eur J Cancer* 1998; **34**: 214-221

35 **Kleiner DE,** Stetler-Stevenson WG. Matrix metalloproteinases and metastasis. *Cancer Chemother Pharmacol* 1999; **43** Suppl: S42-S51

36 **Stamenkovic I.** Matrix metalloproteinases in tumor invasion and metastasis. *Semin Cancer Biol* 2000; **10**: 415-433

37 **Zhang JT,** Fan YZ. Matrix metalloproteinases (MMPs), tissue inhibitors of metalloproteinases (TIMPs) and their roles in invasion and metastasis of tumor. *Zhongliu* 2002; **22**: 161-163

38 **Gohji K,** Fujimoto N, Ohkawa J, Fujii A, Nakajima M. Imbalance between serum matrix metalloproteinase-2 and its inhibitor as a predictor of recurrence of urothelial cancer. *Br J Cancer* 1998; 77: 650-655

39 **Gohji K,** Fujimoto N, Fujii A, Komiyama T, Okawa J, Nakajima M. Prognostic significance of circulating matrix metalloproteinase-2 to tissue inhibitor of metalloproteinases-2 ratio in recurrence of urothelial cancer after complete resection. *Cancer Res* 1996; **56**: 3196-3198

40 **Zucker S,** Cao J, Chen WT. Critical appraisal of the use of matrix metalloproteinase inhibitors in cancer treatment. *Oncogene* 2000; **19**: 6642-6650

41 **Fan YZ,** Zhang JT. Significance of MMP-2/TIMP-2 in gallbladder carcinoma. *J Tumor Marker Oncol* 2001; **16**: 339

42 **Fan YZ,** Zhang JT. Study on the ratio of MMP-2/TIMP-2 in patients with carcinomas of the gallbladder and their clinical value. *Zhonghua Gandan Waike Zazhi* 2002; **8**: 630-631

43 **Zhang JT,** Fan YZ, Yang HC, Yang YQ. Expression and its significance of MMP-2 and TIMP-2 proteins in gallbladder carcinomas. *US Chin J Lymphol Oncol* 2003; **2**: 36-41

Science Editor Guo SY **Language Editor** Elsevier HK

PO Box 2345, Beijing 100023, China
www.wjgnet.com
wjg@wjgnet.com

ELSEVIER

World J Gastroenterol 2005;11(16):2438-2443
World Journal of Gastroenterology ISSN 1007-9327

• *BASIC RESEARCH* •

Effects of augmentation of liver regeneration recombinant plasmid on rat hepatic fibrosis

Qing Li, Dian-Wu Liu, Li-Mei Zhang, Bing Zhu, Yu-Tong He, Yong-Hong Xiao

Qing Li, Dian-Wu Liu, Li-Mei Zhang, Bing Zhu, Yu-Tong He, Yong-Hong Xiao, Department of Epidemiology, Hebei Medical University, Shijiazhuang 050017, Hebei Province, China
Supported by the Natural Science Foundation of Hebei Province, No. 302489
Correspondence to: Dr. Dian-Wu Liu, Department of Epidemiology, Hebei Medical University, 361 Zhongshan Donglu, Shijiazhuang 050017, Hebei Province, China. liudianw@hebmu.edu.cn
Fax: +86-311-6265531
Received: 2004-07-31 Accepted: 2004-09-24

Key words: Hepatic fibrosis; Rat; Augmentation of liver regeneration; Gene therapy; Tissue inhibitor of metalloproteinases-1

Li Q, Liu DW, Zhang LM, Zhu B, He YT, Xiao YH. Effects of augmentation of liver regeneration recombinant plasmid on rat hepatic fibrosis. *World J Gastroenterol* 2005; 11(16): 2438-2443
http://www.wjgnet.com/1007-9327/11/2438.asp

Abstract

AIM: To investigate the effects of eukaryotic expression of plasmid on augmentation of liver regeneration (ALR) in rat hepatic fibrosis and to explore their mechanisms.

METHODS: Ten rats were randomly selected from 50 Wistar rats as normal control group. The rest were administered intraperitoneally with porcine serum twice weekly. After 8 wk, they were randomly divided into: model control group, colchicine group (Col), first ALR group (ALR_1), second ALR group (ALR_2). Then colchicine ALR recombinant plasmid were used to treat them respectively. At the end of the 4th wk, rats were killed. Serum indicators were detected and histopathological changes were graded. Expression of type I, III, collagen and TIMP-1 were detected by immunohisto-chemistry and expression of TIMP-1 mRNA was detected by semi-quantified RT-PCR.

RESULTS: The histologic examination showed that the degree of the rat hepatic fibrosis in two ALR groups was lower than those in model control group. Compared with model group, ALR significantly reduced the serum levels of ALT, AST, HA, LN, PCIII and IV ($P<0.05$). Immunohistochemical staining showed that expression of type I, III, collagen and TIMP-1 in two ALR groups was ameliorated dramatically compared with model group (I collagen: 6.94±1.42, 5.80±1.66 and 10.83±3.58 in ALR_1, ALR_2 and model groups, respectively; III collagen: 7.18±1.95, 4.50±1.67 and 10.25±2.61, respectively; TIMP-1: 0.39±0.05, 0.20±0.06 and 0.53±0.12, respectively, $P<0.05$ or $P<0.01$). The expression level of TIMP-1 mRNA in the liver tissues was markedly decreased in two ALR groups compared with model group (TIMP-1 mRNA/β-actin: 0.89±0.08, 0.65±0.11 and 1.36±0.11 in ALR_1, ALR_2 and model groups respectively, $P<0.01$).

CONCLUSION: ALR recombinant plasmid has beneficial effects on rat hepatic fibrosis by enhancing regeneration of injured liver cells and inhibiting TIMP-1 expressions.

INTRODUCTION

Hepatic fibrosis is a common pathological process of chronic hepatic disease, which can lead to cirrhosis and increase the risk for hepatocellular carcinoma[1,2]. Advanced fibrosis and cirrhosis were generally considered to be irreversible conditions even after removal of the injurious agent[3]. Over the past 15 years, substantial progress has been made in understanding the cellular and molecular regulation of hepatic fibrosis. It is now clear that the accumulation of extracellular matrix (ECM) in fibrotic diseases of the liver is not a static or unidirectional event but a dynamic and regulated process that is amenable to interv-ention[4]. At present, the common sense is that cirrhosis could be prevented[5] and hepatic fibrosis could be reversed effectively when the right therapeutic strategy is applied[6]. With the development of the technology of gene therapy and deep study of the mechanism of hepatic fibrosis, the experimental gene therapy of hepatic fibrosis is becoming the main strategy on treating hepatic fibrosis[7-11].

Augmentation of liver regeneration (ALR) was originally cloned from liver tissue of neonatal rats by Hagiya[12] in 1994. Many studies have revealed that ALR appears to be an important regulator of liver regeneration and has trophic effects on regenerating liver and potent antihepatitis effects[13-16].

The present research is to observe the effects of ALR recombinant plasmid on rat hepatic fibrosis. We first established a rat model of immune hepatic fibrosis cirrhosis and then tested the therapeutic effects of ALR recombinant plasmid.

Colchicine has been used in liver diseases as an anti-fibrotic drug[17,18]. We use colchcine here as a positive control treatment.

MATERIALS AND METHODS

Construction of ALR recombinant plasmid

Restrictive enzymes *Eco*RI and *Hind*III were purchased

from Promega Corporation (USA); pcDNA3 vector was purchased from Invitrogen Company (USA). The *E. coli DH5a* was kindly provided by Dr. Yu-Huai Jin (Department of Microbiology of Hebei Medical University). pBV200-ALR plasmid was cloned and constructed by Zhang *et al*[16]. The primers were synthesized according to Hagiya's report[12] by Sangon Biological Technology Company (Shanghai, China). The forward: 5'-GCG AAG CTT ATG CGG ACC CAG AAG C-3', the reverse: 5'-GCT GAA TTC TTA GTC ACA GGA GCC CTT-3'. The full-length ALR cDNA was PCR amplified using the primers with pBV220-ALR as the DNA template. The amplified product and pcDNA3 vector DNA were digested respectively with *Hind*III and *Eco*RI and then incubated at 75 ℃ for 10 min. The ALR-pcDNA recombinant plasmid was constructed according to reference[19]. The ALR and pcDNA3 fragment with compatible cohesive terminal were connected in bacteriophage T_4 DNA ligation system at 14 ℃ overnight. The reaction contained *T_4 DNA ligase* 1 μL (3 u), 2´Ligation Buffer 5 μL, 120 μg ALR fragment and 100 μg pcDNA3 fragment, 5 μL ligation mixtures was added to 200 μL *E. coli DH5a*. Appropriate volume of transformed competent cell onto LB plate containing ampicillin (100 mg/L) was transferred at 37 ℃ overnight. Bacterial colonies containing ALR plasmid were identified with restriction enzymes *(Eco*RI*, Hind*III) and agarose gel electrophoresis.

Establishment of animal model

Fifty Wistar rats, male, weighing 180-200 g, were obtained from Experimental Animal Center of Hebei Medical University, China. The rats were housed (five per cage) in individual cages and subjected to 12 h-day/12 h-night cycle with free access to basic food and water. All animals were treated humanely according to the national guideline for the care of animals in the country.

Taking randomly 10 from 50 Wistar rats as normal control group (*N*, 10), which were treated with physiological saline. The rest were given an intraperitoneal injection of 0.5 mL of porcine serum according to reference[20], twice a wk for 8 wks. At the 8th wk, the liver pathology proved that the hepatic fibrosis had been established by randomly euthanizing two rats. Then administration of porcine serum was stopped. Those model rats were randomly divided into: model control group (M, 9), colchicine group (Col, 10), first ALR group (ALR_1, 9), which were given with porcine serum continuously until the end of experiment), second ALR group (ALR_2, 10) and the treatments were administered. The colchicine group was administered with colchicine orally at a dose of 0.14 mg/kg per d; two ALR groups were administered with pcDNA3-ALR recombinant plasmid through caudal vein at a dose of 0.2 mg/kg per wk; normal control group and model control group were administered with physiological saline of 0.5 mL through caudal vein per week. All the administrations lasted for 4 wk.

Collection of specimens

The rats were euthanized under ether anesthesia by exsanguinations via the abdominal aorta 7 d after the last administration for each group. Serum samples were collected from all rats and livers and spleen were excised.

Histologic grading

Liver tissues were fixed in formalin and embedded in paraffin. Hematoxylin and eosin (HE) staining and Masson staining were performed according to the standard procedure. Histologic grade of chronic hepatic fibrosis was determined by a semi-quantitative method based on the criteria described below: grade 0: normal liver, grade 1: few collagen fibrils extended from the central vein and portal tract, grade 2: collagen fibrils extension was apparent but had not yet encompassed the whole lobule, grade 3: collagen fibrils extended into and encompassed the whole lobule, grade 4: diffuse extension of collagen fibrils and pseudo-lobule was formed.

Two pathologists who had no knowledge of their sources and each other's assessment examined the stained slide independently.

Serum activities of AST and ALT were determined by the Laboratory Department of 4th Affiliated Hospital, Hebei Medical University, China. Serum hyaluronic acid (HA), laminin (LN), types III procollagen (PCIII) and IV collagen concentrations were measured radioimmunologically using a commercial kit (Shanghai Navy Medical Institute, Shanghai, China) according to the manufacturer's instructions.

Immunohistochemistry

Immunohischemistry kit and anti-mouse monoclonal antibodies of Tissue Inhibitors of Metalloproteinase-1 (TIMP-1) were purchased from Boster Biological Technology Ltd (Wuhan, China). Immunohistochemistry was performed according to the method previously described[21].

Semi-quantitative PCR

RNA isolation kits were purchased from Boster Biological Technology Ltd. (Wuhan, China). TIMP-1 mRNA primers were purchased from Sangon Biological Technology Company (Shanghai, China). Total RNA was extracted using an RNA isolation kit, and quantity and quality was detected on a spectrophotometer. Purified RNA 2 mg and primer Oligo (dT) were used for reverse transcription. The primers were: TIMP-1, 482 bp, forward: 5'-TTC GTG GGG ACA CCA GAA GTC-3', reverse: 5'-TAT CTG GGA CCG CAG GGA CTG-3'. β-actin, 234 bp, forward: 5'-GGA GAA GAT GAC CCA GAT CA-3', reverse: 5'-GAT CTT CAT GAG GTA GTC AG-3'. Amplification conditions included initial denaturation for 5 min at 94 ℃, 30 cycles of amplification with denaturation at 94 ℃ for 45 s, annealing at 61 ℃ for 45 s, and extension at 72 ℃ for 1 min. PCR products were analyzed by agarose gel electrophoresis (15 g/L) and visualized by ethidium bromide staining and ultraviolet illumination. Expression of TIMP-1 was scanned by Champ Gel Image Analysis System (Beijing Page Creation Science Company, Beijing, China). The obtained values were related to housekeeping gene β-actin, and the resulting relative ratios were analyzed statistically.

Statistical analysis

Data were analyzed with SPSS 11.5 software. Quantitative data were presented as mean±SD and compared using one way ANOVA procedure. Frequency data were compared using Ridit procedure.

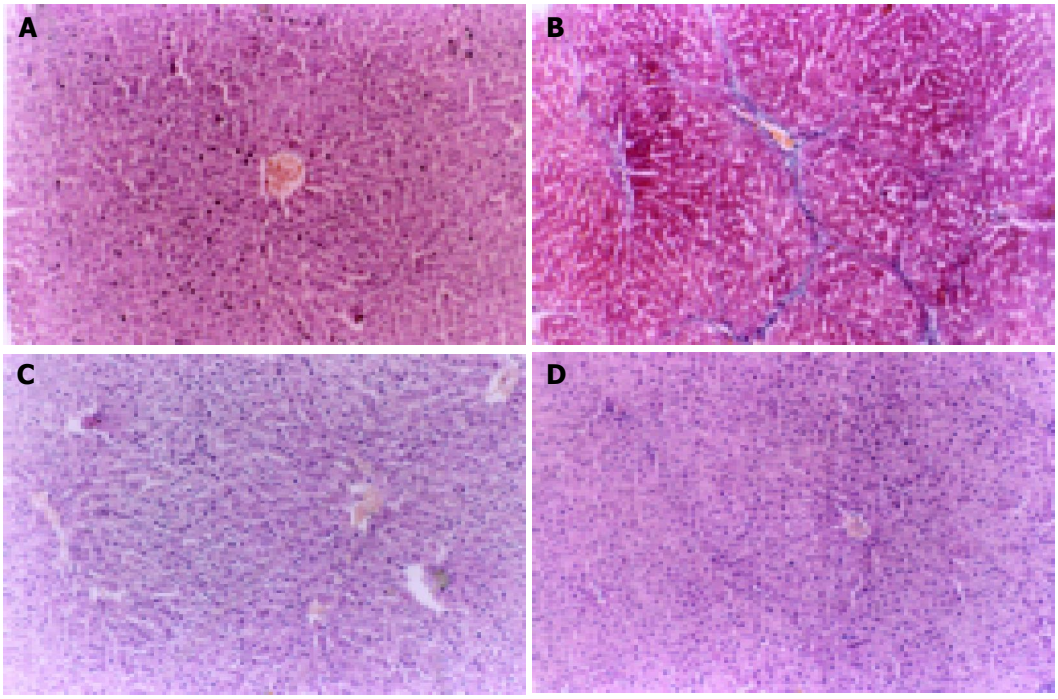

Figure 1 Histologic section of experimental groups (HE´200). **A**: Normal rat liver tissue, hepatic cords were well arranged; the structure of hepatic lobule was intact. **B**: Model rat liver tissue, collagen deposition extending from central veins, fibrotic septa and even pseudolobuli formation. **C**: ALR_1 group rat liver tissue, apparent amelioration of hepatocyte degeneration. **D**: ALR_2 group rat liver tissue, marked reduction in collagen deposition with no obvious pseudolobuli formation.

RESULTS

Histopathologic alterations

Control livers showed normal lobular architecture with central veins and radiating hepatic cords with irregular sinusoids, and a normal distribution of collagen with a variable amount in portal tracts and a thin rim around central veins (Figure 1A). Livers in model group showed disorderly hepatocyte cords, severe fatty degeneration, spotty or focal necrosis and infiltration of inflammatory cells and collagen deposition extending from central veins or portal tracts, with thick or thin fibrotic septa and even pseudolobuli formation (Figure 1B). Treatment with ALR resulted in apparent amelioration of hepatocyte degeneration, necrosis and infiltration of inflammatory cells and marked reduction in collagen deposition with no obvious pseudolobuli formation in ALR_1 group (Figure 1C) and ALR_2 group (Figure 1D). Statistical analysis presented significant differences between two ALR groups and model control group in histologic grading, indicating that fibrogenesis in two ALR groups was much less severe than that of model control group (Table 1).

Liver functions and serum fibrosis markers changes

Serum content of ALT, AST, in Col group and two ALR groups was slightly higher than that of normal control group, but significantly lower than that in model control group ($P<0.05$, Table 2).

Serum content of HA, LN, PCIII ($P<0.05$) and IV ($P<0.01$) in Col group and two ALR groups was significantly lower than that in model control group. Serum content of PCIII in ALR_2 group was also lower than that in Col group and in ALR_1 group ($P<0.05$, Table 3).

These data confirmed the histologic findings that ALR can inhibit hepatic fibrogenesis and improve liver function.

Table 1 Histological grading of hepatic fibrosis

Group	*n*	Grade 0	Grade 1	Grade 2	Grade 3	Grade 4
N	10	10	0	0	0	0
M[c]	9	0	0	0	4	5
Col[a]	10	0	3	3	2	2
ALR_1[a]	9	0	2	4	1	2
ALR_2[a]	10	1	3	3	2	1

[a]$P<0.05$ *vs* model control group; [c]$P<0.05$ *vs* normal control group.

Table 2 Serum content of ALT, AST (mean±SD)

Group	*n*	ALT(u/L)	AST(u/L)
N	10	69.88±10.16	134.25±21.63
M	9	108.67±16.69[c]	201.22±22.85[c]
Col	10	73.20±12.25[a]	182.10±48.11[a]
ALR_1	9	88.56±11.18[a]	165.33±22.21[a]
ALR_2	10	78.40±14.60[a]	160.90±23.99[a]

[a]$P<0.05$ *vs* model group; [c]$P<0.05$ *vs* normal control group.

Table 3 Serum content of HA, LN, PCIII and IV (mean±SD)

Group	*n*	HA (μg/L)	LN (μg/L)	PCIII (μg/L)	IV (μg/L)
N	10	338.67±48.24	33.71±14.53	10.17±2.78	36.80±15.04
M	9	435.91±40.31[c]	62.50±9.72[c]	18.13±7.11[c]	125.00±45.06[d]
Col	10	357.90±90.99[a]	40.98±13.74[a]	11.29±4.42[a]	37.78±8.89[b]
ALR_1	9	327.43±111.26[a]	36.56±10.01[a]	12.60±8.80[a]	41.29±23.86[b]
ALR_2	10	319.29±73.91[a]	36.04±8.89[a]	5.74±2.14[aeg]	38.38±16.36[b]

[a]$P<0.05$ *vs* model control group; [b]$P<0.01$ *vs* model control group; [c]$P<0.05$ *vs* normal control group; [d]$P<0.01$ *vs* normal control group; [e]$P<0.05$ *vs* Col group; [g]$P<0.05$ *vs* ALR_1 group.

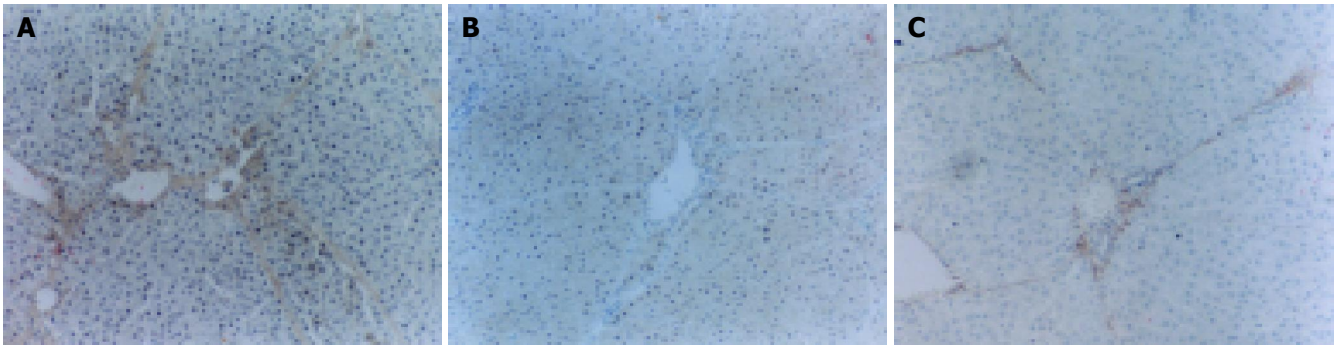

Figure 2 Immunohistochemistry section of TIMP-1 expressed (×200). **A**: Model rat liver tissue, positive staining was seen at interstitial cells, inflammatory cells, impaired hepatocytes as well as normal hepatocytes. **B**: ALR_1 group rat liver tissue, staining of TIMP-1 was decreased. **C**: ALR_2 group rat liver tissue, staining of TIMP-1 was markedly decreased.

Expression of I, III collagen and TIMP-1 by immunohistochemistry

ALR and colchicine can reduce the expression of I, III collagen and TIMP-1 in liver tissue.

Image analysis showed that positive staining index of I and III collagen in model group was the highest ($P<0.01$) and was evidently decreased in every treated groups ($P<0.01$).

Positive staining of TIMP-1 was found at central vein and Disse's areas but not at hepatocytes on sections of normal control group, whereas on sections of model control group, the positive staining was seen at interstitial cells, inflammatory cells, impaired hepatocytes as well as normal hepatocytes (Figure 2A). Fibrotic septa were only slightly stained.

Compared with model control group, the staining index of TIMP-1 in colchicine group, ALR_1 group (Figure 2B) and ALR_2 group (Figure 2C) was markedly decreased ($P<0.01$). The staining index of III collagen in ALR_2 group was lower than in ALR_1 group ($P<0.05$) and the staining index of TIMP-1 in ALR_2 group was also markedly lower than in colchicine group and in ALR_1 group ($P<0.01$, Table 4).

TIMP-1 mRNA was detected in normal rat liver, but the expression level was increased significantly in model control group. Compared with model group, the ratio of TIMP-1 mRNA to β-actin in two ALR groups and colchicine group was markedly decreased ($P<0.01$) and the ratio in ALR_2 group was markedly lower than in ALR_1 group ($P<0.01$, Table 4). Thus, the data suggested that ALR and colchicine could reduce the pathologic expression of TIMP-1 in hepatic fibrosis.

Table 4 Expression of I, III and IV collagen and TIMP-1 and level of TIMP-1 mRNA in relation to β-actin (mean±SD)

Group	*n*	I collagen	III collagen	TIMP-1	TIMP-1 mRNA/β-actin
N	10	3.23±1.02	2.92±1.13	0.16±0.06	0.49±0.09
M	9	10.83±3.58[d]	10.25±2.61[d]	0.53±0.12[d]	1.36±0.11[d]
Col	10	7.10±1.76[b]	5.81±1.86[b]	0.30±0.05[b]	0.77±0.16[b]
ALR_1	9	6.94±1.42[b]	7.18±1.95[a]	0.39±0.05[b]	0.89±0.08[b]
ALR_2	10	5.80±1.66[b]	4.50±1.67[bg]	0.20±0.06[bfh]	0.65±0.11[bh]

[a]$P<0.05$ *vs* model control group; [b]$P<0.01$ *vs* model control group; [d]$P<0.01$ *vs* normal control group; [f]$P<0.01$ *vs* Col group; [g]$P<0.05$ *vs* ALR_1 group; [h]$P<0.01$ *vs* ALR_1 group.

DISCUSSION

Ukei *et al*[10], found that hepatocyte growth factor (HGF) could promote the proliferation of hepatocytes as a potent mitogen and observably reverse the progression of hepatic fibrosis in rats, indicating that maybe ALR has an effect on hepatic fibrosis.

ALR is a novel cytokine which specifically stimulates hepatic cell proliferation and is able to rescue acute liver failure by inhibition of hepatic natural killer cell activity in acute liver injury[13]. Its complex mechanism might be involved in the synthesis or stability of the nuclear and mitochondrial transcripts that are present in actively regenerating cells. Many data have demonstrated that the administration of exogenous ALR protein can stimulate hepatocyte proliferation and reverse experimental hepatic fibrosis[13-15,21,22].

The present study demonstrated that ALR recombinant plasmid has potent effects for rat hepatic fibrosis based on both histologic examination and functional analysis. Its effects are even greater than the effects of colchicine in detecting the expression of TIMP-1. HA, LN, PCIII and IV have been found to be ideal serum markers of hepatic fibrosis. We detected that the serum content of HA, LN, PCIII and IV in two ALR group is decreased markedly compared with model group. In addition, ALR recombinant plasmid can reduce heightened ALT and AST, indicating that they can promote the repair of injured liver cell.

An ideal anim model should be very similar to the characteristics of human disease. Here the rats in ALR_1 group were stimulated continuously by pathogenic factor (administered intraperitoneally with porcine serum) until the end of the experiment. We think that the pathogenic stimulating would cease even if patients were administered with drugs in lots of cases. In the present study, model control group, two ALR groups represent respectively spontaneous resolution of hepatic fibrosis, therapy plus removing pathogeny (ALR_2 group) and therapy but not removing pathogeny (ALR_1 group). The therapeutic effects of ALR in ALR_2 group are more ideal than in ALR_1 group through detecting the expression of III collagen, TIMP-1 and TIMP-1 mRNA, which suggests that removing pathogeny can achieve more ideal effects for treating hepatic fibrosis.

Hepatic fibrosis is the process of excessive deposition of collagen and other ECM component. Some ECM deposition is necessary for wound healing to provide strength and

temporary structure to damaged tissue; however, if not limited, it can be pathologic[23]. The increase of ECM synthesis and decrease of ECM degradation will result in excess deposition of ECM in liver. The decrease of ECM degradation was the primary reason for the excess deposition of ECM in the late stage. The metalloproteinases (MMPs) played a leading role during the degradation of ECM[24-26]. MMPs were a group of zinc-ion dependent enzymes, which created conditions for further degradation of other proteinases through reducing the stability of helical structure of collagen and changing the secondary structure of substrates. TIMPs were a group of polypeptides with the ability of inhibiting the function of MMPs. Research work showed that TIMP can be divided into four classes: TIMP-1, TIMP-2, TIMP-3, and TIMP-4. However, only TIMP-1 and TIMP-2 could be detected in liver[27-29]. The expression of TIMP-1 was more obvious than that of TIMP-2. All these indicated that TIMP-1 did play an important role in the development of liver fibrosis and cirrhosis. At present, it was found that TIMP-1 in the injured liver increased early and obviously, and many researchers thought that TIMP-1 was a very important promoting factor in the process of hepatic fibrosis[30-32]. This has important implications for the future development of therapeutic antifibrotic strategies in the liver[31,32]. It may be the basic mechanism of reversing hepatic fibrosis and a leading strategy of treating hepatic fibrosis to suppress the expression of TIMP-1 mRNA.

In normal liver, the collagen types I, III account for about 80% of the total collagen of liver, while it rises up to more than 95% in fibrotic liver. The collagen type I covers about 60-70% of the total collagen of fibrotic liver, and type III is 20-30%[33,34]. Therefore, collagen I, III are regarded as the important parameters to reflect the metabolism of collagen, and thus we can judge the therapeutic effect of anti-fibrosis strategies[35,36]. The content of collagen I, III was lower in the ALR group than that in model group. At the same time, we found that TIMP-1 and TIMP-1 mRNA were expressed obviously in model group and TIMP-1 level in ALR groups were markedly decreased.

These data showed that ALR recombinant plasmid can increase the degradating capacity of collagen I, III, decrease the deposition of ECM and the expression of TIMP-1 in pathologic liver tissue and thus reverse the hepatic fibrosis induced by porcine serum administration. This may be the molecular mechanism of ALR. ALR gene therapy may be potentially useful for the treatment of patients with liver cirrhosis.

REFERENCES

1 **Miyazawa K,** Moriyama M, Mikuni M, Matsumura H, Aoki H, Shimizu T, Yamagami H, Kaneko M, Shioda A, Tanaka N, Arakawa Y. Analysis of background factors and evaluation of a population at high risk of hepatocellular carcinoma. *Intervirology* 2003; **46**: 150-156

2 **Nagao Y,** Fukuizumi K, Kumashiro R, Tanaka K, Sata M. The prognosis for life in an HCV hyperendemic area. *Gastroenterology* 2003; **125**: 628-629

3 **Lee HS,** Huang GT, Chen CH, Chiou LL, Lee CC, Yang PM, Chen DS, Sheu JC. Less reversal of liver fibrosis after prolonged carbon tetrachloride injection. *Hepatogastroenterology* 2001; **48**: 1312-1315

4 **Friedman SL.** Molecular regulation of hepatic fibrosis, an integrated cellular response to tissue injury. *J Biol Chem* 2000; **275**: 2247-2250

5 **Riley TR,** Bhatti AM. Preventive strategies in chronic liver disease: part II. Cirrhosis. *Am Fam Physician* 2001; **64**: 1735-1740

6 **Brenner DA.** Signal transduction during liver regeneration. *J Gastroenterol Hepatol* 1998; **13** Suppl: S93-S95

7 **Garcia-Banuelos J,** Siller-Lopez F, Miranda A, Aguilar LK, Aguilar-Cordova E, Armendariz-Borunda J. Cirrhotic rat livers with extensive fibrosis can be safely transduced with clinical-grade adenoviral vectors. Evidence of cirrhosis reversion. *Gene Ther* 2002; **9**: 127-134

8 **Salgado S,** Garcia J, Vera J, Siller F, Bueno M, Miranda A, Segura A, Grijalva G, Segura J, Orozco H, Hernandez-Pando R, Fafutis M, Aguilar LK, Aguilar-Cordova E, Armendariz-Borunda J. Liver cirrhosis is reverted by urokinase-type plasminogen activator gene therapy. *Mol Ther* 2000; **2**: 545-551

9 **Rudolph KL,** Chang S, Millard M, Schreiber-Agus N, DePinho RA. Inhibition of experimental liver cirrhosis in mice by telomerase gene delivery. *Science* 2000; **287**: 1253-1258

10 **Ueki T,** Kaneda Y, Tsutsui H, Nakanishi K, Sawa Y, Morishita R, Matsumoto K, Nakamura T, Takahashi H, Okamoto E, Fujimoto J. Hepatocyte growth factor gene therapy of liver cirrhosis in rats. *Nat Med* 1999; **5**: 226-230

11 **Ueno H,** Sakamoto T, Nakamura T, Qi Z, Astuchi N, Takeshita A, Shimizu K, Ohashi H. A soluble transforming growth factor beta receptor expressed in muscle prevents liver fibrogenesis and dysfunction in rats. *Hum Gene Ther* 2000; **11**: 33-42

12 **Hagiya M,** Francavilla A, Polimeno L, Ihara I, Sakai H, Seki T, Shimonishi M, Porter KA, Starzl TE. Cloning and sequence analysis of the rat augmenter of liver regeneration (ALR) gene: expression of biologically active recombinant ALR and demonstration of tissue distribution. *Proc Natl Acad Sci USA* 1994; **91**: 8142-8146

13 **Tanigawa K,** Sakaida I, Masuhara M, Hagiya M, Okita K. Augmenter of liver regeneration (ALR) may promote liver regeneration by reducing natural killer(NK) cell activity in human liver diseases. *J Gastroenterol* 2000; **35**: 112-119

14 **Polimeno L,** Capuano F, Marangi LC, Margiotta M, Lisowsky T, Ierardi E, Francavilla R, Francavilla A. The augmenter of liver regeneration induces mitochondrial gene expression in rat liver and enhances oxidative phosphorylation capacity of liver mitochondria. *Dig Liver Dis* 2000; **32**: 510-517

15 **Yang X,** Wang A, Zhou P, Wang Q, Wei H, Wu Z, He F. Protective effect of recombinant human augmenter of liver regeneration on CCl4-induced hepatitis in mice. *Chin Med J (Engl)* 1998; **111**: 625-629

16 **Zhang LM,** Liu DW, Yang J, Li Q. Construction of eukaryotic express plasmid of rat augmenter of liver regeneration gene and effect on acute hepatic failure in rats. *Hebei Yike Daxue Xuebao* 2004; **25**: 68-70

17 **Lee SJ,** Kim YG, Kang KW, Kim CW, Kim SG. Effects of colchicine on liver functions of cirrhotic rats: beneficial effects result from stellate cell inactivation and inhibition of TGF beta1 expression. *Chem Biol Interact* 2004; **147**: 9-21

18 **Das D,** Pemberton PW, Burrows PC, Gordon C, Smith A, McMahon RF, Warnes TW. Antioxidant properties of colchicine in acute carbon tetrachloride induced rat liver injury and its role in the resolution of established cirrhosis. *Biochim Biophys Acta* 2000; **1502**: 351-362

19 **Peng D,** Qian C, Sun Y, Barajas MA, Prieto J. Transduction of hepatocellular carcinoma (HCC) using recombinant adeno-associated virus (rAAV): *in vitro* and *in vivo* effects of genotoxic agents. *J Hepatol* 2000; **32**: 975-985

20 **Shiga A,** Shirota K, Nishita T, Nomura Y. Study on the pathogenesis of porcine serum-induced liver fibrosis in rats with special reference to the effects of hypertension. *J Vet Med Sci* 1998; **60**: 29-34

21 **Giorda R,** Hagiya M, Seki T, Shimonishi M, Sakai H, Michaelson J, Francavilla A, Starzl TE, Trucco M. Analysis of the structure and expression of the augmenter of liver regen-

eration (ALR) gene. *Mol Med* 1996; **2**: 97-108
22 **Polimeno L,** Margiotta M, Marangi L, Lisowsky T, Azzarone A, Ierardi E, Frassanito MA, Francavilla R, Francavilla A. Molecular mechanisms of augmenter of liver regeneration as immunoregulator: its effect on interferon-gamma expression in rat liver. *Dig Liver Dis* 2000; **32**: 217-225
23 **Vaillant B,** Chiaramonte MG, Cheever AW, Soloway PD, Wynn TA. Regulation of hepatic fibrosis and extracellular matrix genes by the th response: new insight into the role of tissue inhibitors of matrix metalloproteinases. *J Immunol* 2001; **167**: 7017-7026
24 **Herbst H,** Wege T, Milani S, Pellegrini G, Orzechowski HD, Bechstein WO, Neuhaus P, Gressner AM, Schuppan D. Tissue inhibitor of metalloproteinase-1 and -2 RNA expression in rat and human liver fibrosis. *Am J Pathol* 1997; **150**: 1647-1659
25 **Ulrich D,** Lichtenegger F, Eblenkamp M, Repper D, Pallua N. Matrix metalloproteinases, tissue inhibitors of metalloproteinases, aminoterminal propeptide of procollagen type III, and hyaluronan in sera and tissue of patients with capsular contracture after augmentation with Trilucent breast implants. *Plast Reconstr Surg* 2004; **114**: 229-236
26 **Li YL,** Sato M, Kojima N, Miura M, Senoo H. Regulatory role of extracellular matrix components in expression of matrix metalloproteinases in cultured hepatic stellate cells. *Cell Struct Funct* 1999; **24**: 255-261
27 **Alcolado R,** Arthur MJ, Iredale JP. Pathogenesis of liver fibrosis. *Clin Sci (Lond)* 1997; **92**: 103-112
28 **Iredale JP.** Tissue inhibitors of metalloproteinases in liver fibrosis. *Int J Biochem Cell Biol* 1997; **29**: 43-54
29 **Arthur MJ,** Iredale JP, Mann DA. Tissue inhibitors of metalloproteinases: role in liver fibrosis and alcoholic liver disease. *Alcohol Clin Exp Res* 1999; **23**: 940-943
30 **Flisiak R,** Maxwell P, Prokopowicz D, Timms PM, Panasiuk A. Plasma tissue inhibitor of metalloproteinases-1 and transforming growth factor beta 1-possible non-invasive biomarkers of hepatic fibrosis in patients with chronic B and C hepatitis. *Hepatogastroenterology* 2002; **49**: 1369-1372
31 **Yoshiji H,** Kuriyama S, Miyamoto Y, Thorgeirsson UP, Gomez DE, Kawata M, Yoshii J, Ikenaka Y, Noguchi R, Tsujinoue H, Nakatani T, Thorgeirsson SS, Fukui H. Tissue inhibitor of metalloproteinases-1 promotes liver fibrosis development in a transgenic mouse model. *Hepatology* 2000; **32**: 1248-1254
32 **Iredale JP**, Benyon RC, Pickering J, McCullen M, Northrop M, Pawley S, Hovell C, Arthur MJ. Mechanisms of spontaneous resolution of rat liver fibrosis. Hepatic stellate cell apoptosis and reduced hepatic expression of metalloproteinase inhibitors. *J Clin Invest* 1998; **102**: 538-549
33 **Louis H,** Le Moine A, Quertinmont E, Peny MO, Geerts A, Goldman M, Le Moine O, Deviere J. Repeated concanavalin A challenge in mice induces an interleukin 10-producing phenotype and liver fibrosis. *Hepatology* 2000; **31**: 381-390
34 **Kovalovich K,** DeAngelis RA, Li W, Furth EE, Ciliberto G, Taub R. Increased toxin-induced liver injury and fibrosis in interleukin-6-deficient mice. *Hepatology* 2000; **31**: 149-159
35 **Arthur MJ.** Collagenases and liver fibrosis. *J Hepatol* 1995; **22**: 43-48
36 **Arthur MJ.** Degradation of matrix proteins in liver fibrosis. *Pathol Res Pract* 1994; **190**: 825-833

Science Editor Guo SY **Language Editor** Elsevier HK

PO Box 2345, Beijing 100023, China
www.wjgnet.com
wjg@wjgnet.com

ELSEVIER

World J Gastroenterol 2005;11(16):2444-2449
World Journal of Gastroenterology ISSN 1007-9327

• *BASIC RESEARCH* •

Effects of pharmacological serum from normal and liver fibrotic rats on HSCs

Xi-Xian Yao, Tao Lv

Xi-Xian Yao, Tao Lv, Hebei Institute of Gastroenterology, Department of Digestive Disease, The Second Hospital of Hebei Medical University, Shijiazhuang 050000, Hebei Province, China
Correspondence to: Professor Xi-Xian Yao, Hebei Institute of Gastroenterology, Department of Digestive Disease, The Second Hospital of Hebei Medical University, No. 215, Hepingxi Road, Shijiazhuang 050000, Hebei Province, China. yaoxixian@163.com
Telephone: +86-311-7222831 Fax: +86-311-7061012
Received: 2004-02-27 Accepted: 2004-06-07

Abstract

AIM: To make drug sera of *Salvia miltiorrhiza* and Yigankang, both of which are Chinese herbs that activate bleeding and eliminate stasis, in normal rats and those with liver fibrosis, respectively. To investigate and compare the effects of the two different drug sera on the proliferation and activation of hepatic stellate cells (HSCs).

METHODS: Some rats were induced with liver fibrosis: 40% carbon tetrachloride (CCl_4) subcutaneous injection, twice a week for 9 wk. *Salvia miltiorrhiza*, Yigankang, colchicines and normal saline were administered into the stomachs of normal rats and those with liver fibrosis. Drug sera were extracted 5 d later. HSCs *in vitro* were cultivated in different drug sera for 24 h. The rates of proliferation and expression of α-smooth muscle actin (α-SMA) were detected by 3-(4,5-dimethylthiazol-2-yl)-2,5-diphenyltetrazolium bromide (MTT) and immunocytochemistry stain, respectively.

RESULTS: The drug sera from normal and liver fibrotic rats could be used to cultivate HSCs and to observe the effects of the corresponding components of herbs on HSCs. *Salvia miltiorrhiza* and Yigankang had better inhibitory effects on HSCs than colchicines (MTT: normal drug serum: *Salvia miltiorrhiza* 0.42±0.08, Yigankang 0.32±0.10 *vs* colchicines 0.45±0.12 pathological drug serum: *Salvia miltiorrhiza* 0.33±0.02, Yigankang 0.26±0.01 *vs* colchicines 0.41±0.09. $P<0.05$). The drug sera of *Salvia miltiorrhiza*, Yigankang from liver fibrotic rats had a stronger inhibitory effect than the same ones from normal rats (MTT: *Salvia miltiorrhiza*: normal drug serum 0.42±0.08 *vs* pathological drug serum 0.33±0.02. Yigankang: normal drug serum 0.32±0.10 *vs* pathological drug serum 0.26±0.01. $P<0.05$).

CONCLUSION: *Salvia miltiorrhiza* and Yigankang could inhibit the expression of α-SMA and the proliferation of HSCs. The drug sera from normal and liver fibrotic rats had different effects on HSCs, probably due to different metabolic processes, effective components and different quantities of drug contents in drug sera from rats with different states of liver.

Key words: Seropharmocological method; Hepatic stellate cell; α-Smooth muscle actin; Salvia; Yigankang

Yao XX, Lv T. Effects of pharmacological serum from normal and liver fibrotic rats on HSCs. *World J Gastroenterol* 2005; 11(16): 2444-2449
http://www.wjgnet.com/1007-9327/11/2444.asp

INTRODUCTION

The activation and proliferation of hepatic stellate cells (HSCs) is the major cellular basis for the formation of liver fibrosis[1,2]. No ideal Western medicine has been developed against liver fibrosis until now, otherwise, a series of blood-activating and stasis-eliminating Chinese medicine, such as *Salvia miltiorrhiza*, has a positive effect on the preventive treatment and inversion of liver fibrosis[3,4]. But it is difficult to clarify the working mechanism and real effective components of such Chinese medicine against fibrosis. A feasible way to solve this problem appeared when the seropharmacological method was advanced in 1984[5]. By traditional seropharmacological method, the drug sera are always extracted from normal rats which have been induced with drugs[6]. But it is the patients with hepatic diseases who take the corresponding drugs clinically. What is the difference between normal and pathologic livers during the metabolic process? The project has been carried out to find out if there exist differences in the working effects and effective components of the same drugs caused by different states of liver.

MATERIALS AND METHODS

Cell line

HSC cell line: CFSC is established and presented by Professor Greenwell, Marion Bessin Liver Research Center, Albert Einstein College of Medicine. The phenotype of CFSC is HSC which has been activated. They were obtained from CCl_4-cirrhotic liver of rats, after spontaneous immortalization in culture.

Materials

Eighty of clean, male Sprague-Dawley (SD) rats of 200-250 g

were from the Laboratory Animal Center of Hebei Medical University. RPMI-1640 culture medium, L-Glutamine, hydroxyethyl piperazine ethanesulfonic acid (HEPES), pancreatin, MTT, dimethyl sulfoxide (DMSO), antibody of α-SMA were all from Biological Technological Company. Carbon tetrachloride (CCl_4) and other materials were all analytically pure (AP). Chinese herbs were from Lerentang Chinese Medicine Drugstore.

Grouping

SD rats 80: 200-250 g, male, were randomized into eight groups, 10 in each group.

Group A: normal rats.

A1: *Salvia miltiorrhiza* A2: Yigankang A3: colchicines A4: normal control (normal saline).

Group B: liver fibrotic rats.

B1: *Salvia miltiorrhiza* B2: Yigankang B3: colchicine B4: fibrosis control (normal saline).

The rats in group A were all normal and healthy. The rats in groups A1-A4 were fed with corresponding drugs or normal saline. The rats in group B were all induced with liver fibrosis, then corresponding drugs or normal saline were fed.

Inducing liver fibrosis in rats

The rats in group B were induced with liver fibrosis by 40% CCl_4, subcutaneous injection, 4 mL/kg the first time, then 2 mL/kg, twice a week, for 9 wk.

Preparation of drug solution

Salvia miltiorrhiza and Yigankang were from Lerentang Drugstore of Hebei Province. They were decocted and concentrated. The solutions were sealed and kept in 4 ℃. The quantities of raw herbs in solution: *Salvia miltiorrhiza* 0.51 g/mL, Yigankang 0.72 g/mL. Colchicines (tablets) were dissolved in normal saline to form 0.04 mg/mL.

Preparation of drug serum

Corresponding drugs were poured into the stomachs of rats for 5 d. The quantity of drugs is 10 times that of the normal adults per kilogram per day, twice a day. Rats were fasted since the night of the 4th day. Blood was extracted from inferior vena cava 2 h after the drugs were given on the fifth morning. Then serum was obtained by centrifugation, 3 000 r/min, 4 ℃, for 20 min. The serum from the rats in the same group were mixed, then were inactivated at 56 ℃, for 30 min. The sera were stored at -70 ℃. Drug sera sterilized by filtration, were dissolved in 8% new calf serum (NCS)/RPMI-1640 cell culture medium to produce 10% drug serum-1640 culture medium, which was ready for use at -20 ℃.

Detection of the inhibitory rate of drug serum on HSC growth by MTT

Cell solutions were incubated on 96-well plate. When HSCs grew to 90%, they were cultivated in pure RPMI-1640 (no serum) overnight, so as to synchronize HSCs into the G_0 period. The next morning, corresponding groups of 10% drug serum-1640 media in the wells were changed. There were nine such holes for each kind of drug serum. The results were obtained from an average of nine numbers. A group of control was set at the same time. Twenty microliters of MTT was added after the drug serum was allowed to have worked for 24 h. Then DMSO was added 4 h later. Optical density (A) in all holes was measured. Then the inhibitory rate (IR) of all drug sera on the growth of HSCs were calculated. IR = $(A_{\text{experiment group}}-A_{\text{control group}})/A_{\text{control group}}\times 100\%$.

Detecting the expression of α-SMA in HSCs by immunocytochemistry stain

HSCs were transferred onto the bottle chip. HSCs were cultured in pure RPMI-1640 overnight when HSCs grew to 90% on the chip. There were three similar chips for each kind of drug serum. The chips were taken out after being cultivated in drug serum for 24 h. HSCs were fixated. Antibody of α-SMA was added on HSCs, then SP immunocytochemistry stain was performed. The rate of positive cells was obtained by analyzing the stain (using the analysis software from Huadong Normal University) under microscope (×200). Final results were obtained from the average.

Statistical analysis

SPSS 10.0 was used to perform F and χ^2 test and $P<0.05$ was regarded as statistically significant.

RESULTS

Obvious proliferation of fibers appeared in the liver when the rats in group B were modeled for 9 wk. There were inflammation necrosis and vacuole degeneration in the liver. No obvious changes appeared in the rat livers of group A. (Figure 1).

The experiment of pure sera from normal and fibrotic rats on HSCs *in vitro* for 48 h showed that the RPMI-1640 culture media with serum from normal and fibrotic rats could keep the growth of HSCs' normal. The effect of drug sera from normal and fibrotic rats on HSCs for 48 h showed that drug sera from three kinds of drugs could be used to cultivate HSCs *in vitro*, but HSCs' growth and differentiation were very slow. The typical phenotype of HSCs was disappearing gradually; synapses were getting fewer and smaller; and cell bodies expanded. All showed that

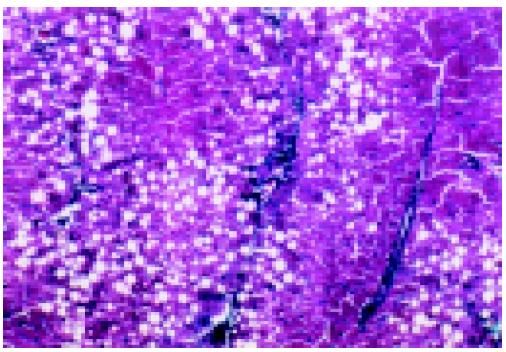

Figure 1 Liver fibrosis with inflammation necrosis and ballooning after CCl_4 injection for 9 wk (Masson, 100×).

Table 1 Inhibitory rate of drug sera on the proliferation of HSC (MTT)

Group	IR (%)	*A*	Group	IR (%)	*A*
A1	33.62±0.72[a]	0.42±0.08[a]	B1	47.42±0.17[c,e]	0.33±0.02[c,e]
A2	49.74±1.02[a]	0.32±0.10[a]	B2	58.12±1.04[c,e]	0.26±0.01[c,e]
A3	29.38±0.75	0.45±0.12	B3	34.66±0.78	0.41±0.09
A4	-	0.64±0.08	B4	-	0.62±0.11

[a]$P<0.05$ *vs* group A3 and A4 *A* (mean±SD); [c]$P<0.05$ *vs* group B3 and B4; [e]$P<0.05$ *vs* group A1 and A2, respectively; IR = $(A_{\text{experiment group}}-A_{\text{control group}}) \div A_{\text{control group}}\times 100\%$.

components in drug sera had worked on HSCs (Figure 2).

The detection of IR of drug sera on HSCs growth by MTT showed that *Salvia miltiorrhiza*, Yigankang inhibited the proliferation of HSCs more than colchicines ($P<0.05$). The drug sera from rats in groups B1 and B2 (sera of *Salvia miltiorrhiza*, Yigankang from fibrotic rats) had a stronger effect than that from A1 and A2 (sera of *Salvia miltiorrhiza*, Yigankang from normal rats) ($P<0.05$) (Table 1).

The detection of α-SMA in HSCs by SP immunocytochemistry stain showed that the drug sera of *Salvia miltiorrhiza* and Yigankang from normal and fibrotic rats could all inhibit the expression of α-SMA, compared with colchicines ($P<0.05$). The drug sera from B1 and B2 had a stronger effect than that from A1 and A2 ($P<0.05$) (Figure 3, Table 2).

Table 2 Effect of drug sera on the expression of α-SMA in HSC (%)

Group	αSMA	Group	αSMA
A1	41.72±1.48[a]	B1	37.13±2.42[c,e]
A2	37.00±0.45[a]	B2	32.13±1.46[c,e]
A3	48.13±1.08	B3	46.12±0.48
A4	64.10±2.85	B4	60.88±2.07

[a]$P<0.05$ *vs* group A3 and A4; [c]$P<0.05$ *vs* group B3 and B4; [e]$P<0.05$ *vs* group A1 and A2, respectively; α-SMA (number of positive HSCs ÷ number of all HSCs ×100%).

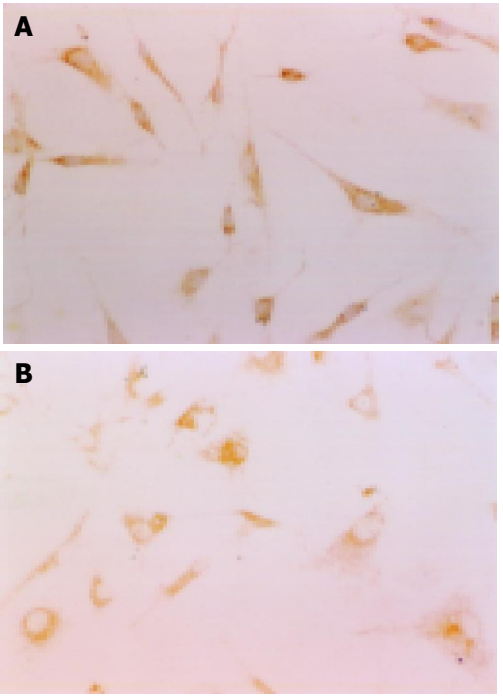

Figure 2 HSCs in the media of different sera (immunocytochemistry stain of α-SMA, 400×). **A**: HSCs in NCS/RPMI-1640, **B**: HSCs in drug sera/RPMI-1640: cells expanded and synapses became fewer and smaller.

DISCUSSION

Today, chronic hepatic diseases caused by hepatitis virus, and the following liver fibrosis, cirrhosis and a few of liver cancer are still a serious problem, which is harmful to people's health in China. Liver fibrosis is a necessary stage during the development of liver cirrhosis[7,8]. Therefore the preventive treatment and inversion of liver fibrosis is the key point to cure chronic hepatic diseases and to improve the prognosis. Now the researches mainly focus on how to inhibit and cut the initiative factor of fibrosis-the activation and proliferation of HSC[9]. No ideal Western drug and therapeutic method have emerged until now[10]. Otherwise, a few blood-activating and stasis-eliminating Chinese medicine, such as *Salvia miltiorrhiza*, Yigan Granule (Yigankang), show a positive effect in clinical and experimental studies[11,12]. Based on Yigan infusion, YigankangY is a new generation drug which was developed in recent years, and shows outstanding superiority in treating liver fibrosis (A recipe of Traditional Chinese Medicine, TCM, by Professor Xi-Xian Yao, who is a famous expert of gastrointestinal disease in China. The medicine has been commonly put into clinical use for 18 years, widely welcomed by sufferers because of its minimal side effects and excellent clinical efficiencies). But it is difficult to clarify the effective components of herbs which consist of complex parts. It is also a bottleneck that obstructs the development and application of new TCM. Chinese herbs come mostly from nature. They could be taken only after being dried and decocted under certain conditions. Also certain kinds of herbs do not have specific and exact structures like Western medicine, quite compressed to make complex prescriptions. Some nonpharmocological effect may occur if the herbs were added into the culture media of HSCs *in vitro* directly. Some drugs and drug precursors work through the effective substance which was produced after being transformed *in vivo*[13], or real effective components were physiologically active matters which were induced *in vivo* by the drugs. Such kind of drugs could be believed to be useless if they are added into the cell lines *in vitro* directly[14,15]. How to represent the effective components and the working mechanism of TCM by organic metabolism is the key problem.

The results of this research show that the drug sera of blood-activating and stasis-eliminating Chinese medicine such as *Salvia miltiorrhiza*, Yigankang (complex prescription)

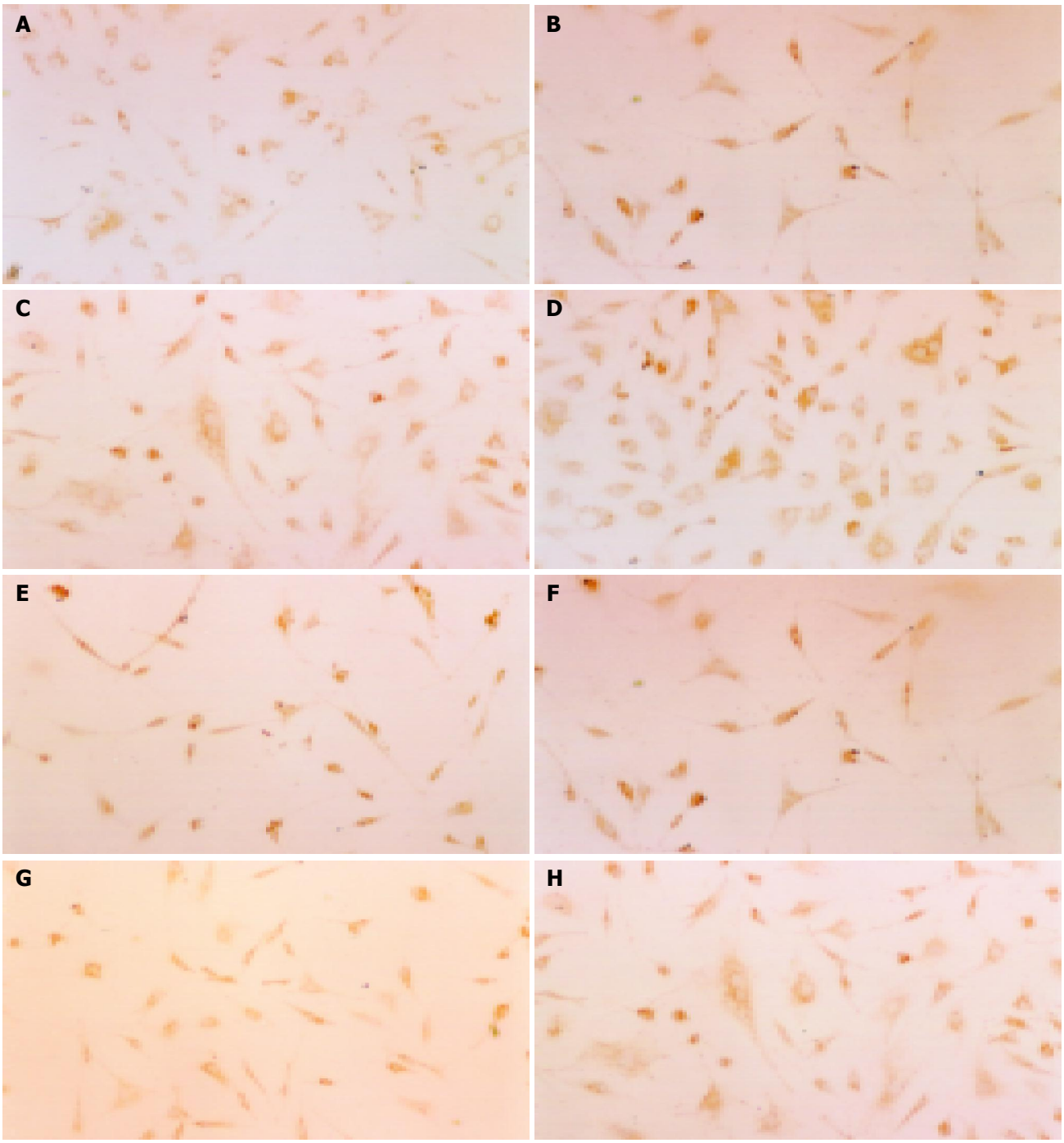

Figure 3 Immunocytochemistry stain of α-SMA in HSCs-positive cells: brown in plasm. When HSCs were inhibited, the number of HSCs decreased, while the expression of α-SMA increased, with cell bodies expanded and synapses fewer and smaller (200×). **A**: HSCs in normal serum of *Salvia miltiorrhiza*; **B**: HSCs in normal serum of Yigankang; **C**: HSCs in normal serum of colchicines; **D**: HSCs in normal serum of rats; **E**: HSCs in pathological serum of *Salvia miltiorrhiza*; **F**: HSCs in pathological serum of Yigankang; **G**: HSCs in pathological serum of colchicines; **H**: HSCs in pathological serum of fibrotic rats.

had an apparently inhibitory effect on HSC proliferation and the expression of α-SMA, which is the marker of the activation of HSCs[16,17]. The expressive rate of α-SMA on HSC of *Salvia miltiorrhiza*, Yigankang was 37.13%, 32.13%, respectively, which were lower than that of colchicines and normal saline (46.12%, 60.88%, respectively) obviously ($P<0.05$) (Table 2, Figure 3). The inhibitory rate of *Salvia miltiorrhiza* and Yigankang on HSC proliferation was 47.42%, 58.12%, respectively, which were higher than that of the control group ($P<0.05$) (Table 1). So it might be considered that some effective components were produced when *Salvia miltiorrhiza*, Yigankang was taken into the body and transformed after they were decocted. The effective components enter the liver and inhibit the activation and proliferation of HSC through certain mechanisms (such as inhibiting lipid peroxidation[18,19]). But the exact working components and their structures need further investigation.

In this experiment we mimicked the real condition of the usage of herbs clinically and in the manner of their disposal afterwards, the style of usage, the dosage and the metabolic process *in vivo*. The drug sera thus obtained contain the real working components which are produced

after the metabolic process *in vivo* and then enter the serum. To research the effect of the sera on the function and the phenotype of HSCs, we applied the sera to cell culture *in vitro* in order to clarify the working mechanism of TCM. This is the traditional "pharmacological method"[20]. At the same time we noticed that, usually it is patients with liver diseases that take the herbs clinically. Different (normal and pathological) conditions of liver, which is the biggest organ for biological metabolism, could lead to some difference in the conversion of the same drug. The final effective components in the sera and the effects may differ when the same drug is metabolized by the body with different states of liver. In traditional pharmacological method, healthy rats are the drug receivers, and drug serum resources. So the aim of the study is to improve the traditional seropharmacological method in order to make the drug serum provider animals resemble the real body condition of clinical drug users. So we could mimic the possible condition, possible process, the products of the herbs' metabolism *in vivo*, and patients' condition clinically to the greatest extent, more exact than traditional "pharmacological method". Thus we call it "modified seropharmacological method".

The results of the research showed that, the drug sera of *Salvia miltiorrhiza* and Yigankang from liver fibrotic rats have a stronger inhibitory effect on the activation and proliferation of HSCs than the corresponding serum from normal rats. At the same time, the drug serum of *Salvia miltiorrhiza* from fibrotic rats inhibits the proliferation of HSCs at the rate of 47.42%, which is higher than the drug serum of *Salvia miltiorrhiza* from normal rats: 33.62% ($P<0.05$) (Table 1). The expressive rates of α-SMA on HSCs in the sera of *Salvia miltiorrhiza* from fibrotic and normal rats are 37.13%, 41.72% ($P<0.05$) (Table 2, Figure 3). The drug sera of Yigankang from fibrotic and normal rats inhibited the proliferation of HSCs at the rate of 58.12%, 49.74% ($P<0.05$) (Table 1). The rate of expression of α-SMA in HSCs in the sera of Yigankang from fibrotic and normal rats were 32.13%, 37.00%, respectively ($P<0.05$) (Table 2, Figure 3). So we considered that the drug sera extracted from liver fibrosis could reflect the metabolic process better, products and working components of the TCM against liver fibrosis *in vivo* theologically, and this kind of drug serum could be applied in the experimental study of TCM against liver fibrosis. The effects of pathological drug sera from liver fibrotic rats were strengthened than those from normal rats (both *Salvia miltiorrhiza* and Yigankang), which may be related with the different drug effects caused by different functional status of livers. From the Chinese traditional theory of "diagnosis based on different symptoms and pathogenesis" in Chinese traditional medicine[21], TCM will work best only if the symptoms and etiology are best suited to the indication. Both *Salvia miltiorrhiza* and Yigankang, are blood-activating and stasis-eliminating herbs; undoubtedly they indicate liver fibrosis. Normal rats had no illness or symptoms, so the effects of blood-activating and stasis-eliminating are not obvious. So the blood-activating and stasis-eliminating herbs such as *Salvia miltiorrhiza* and Yigankang might have a better effect on fibrotic rats. We considered that different functional status of livers metabolized drugs differently, so there was a difference in metabolic effective components and their content.

The drug sera that come from pathological liver (fibrotic model) (pathological drug serum) inhibited the activation and proliferation of HSCs more strongly than those from normal rats. The following factors may work. (1) TCM has an advantage to doubly regulate the physiological functions. They have no obvious effect on the normal liver cells, but perform a better regulatory effect on pathological liver, thereby making an effective indication. (2) In liver fibrosis models caused by CCl_4, some responsive factors such as toxins and inhibitory cytokines induced by CCl_4 *in vivo* entered the serum, which cannot be inactivated by the pathological (fibrotic) liver may inhibit the HSC *in vitro*. The inhibitory effect of this kind of inhibitory cytokines may not be HSC specific, which is to say that, they could inhibit the activation and proliferation of many kinds of cells *in vivo* besides HSC. (3) The ability of the liver to transform and inactivate drugs decreases because the metabolic function of the fibrotic livers decreases generally. So it makes the concentration of the effective components higher, and prolong the working time, so as to inhibit HSCs more (Figure 3). Further researches needs to be performed to clarify the reason why drug sera from normal and fibrotic rats have different effects on HSC. For example, the rats could be modeled into liver fibrosis not by CCl_4 in order to know whether or not the effect caused by nonspecific factors induced by CCl_4 exists. Also we can optimize the conditions of serum inactivation so as to inactivate nonspecific factors. Or we can carry out the comparative study of pharmacokinetics after healthy volunteers and fibrotic patients take the same drugs, then compare the corresponding effective components in drug sera. Thus we can know the real reason why pathological drug sera work stronger, and modify the pharmocological method further.

Blood-activating and stasis-eliminating Chinese herbs such as *Salvia miltiorrhiza* and Yigankang have obvious effects on liver fibrosis[22,23]. But there is no ideal way to clarify the effective components among them. The value of this research lies in that we could get the real effective components of *Salvia miltiorrhiza* and Yigankang after they were metabolized by normal and fibrotic liver, which could provide reliable samples for analyzing the working components in the sera by HPLC, *etc*. Still there are difficulties in analyzing the sort, quantity and structure of effective components in the serum. It is also the key problem that needs to be solved in the study and development of new TCM. Making the drug sera of effective TCM against liver fibrosis by "modified seropharmacological methods", by analyzing the effective part may be a feasible way to get the working part in the drug sera which are effective against fibrosis. It is also an important direction for future development. It might be possible to analyze the components and structures of the effective parts in drug sera against liver fibrosis, by high volume gene microarray chips, *etc*. It is also one of the important tasks in the research of TCM in future.

REFERENCES

1 **Weiskirchen R**, Kneifel J, Weiskirchen S, van de Leur E, Kunz D, Gressner AM. Comparative evaluation of gene delivery devices in primary cultures of rat hepatic stellate cells

and rat myofibroblasts. *BMC Cell Biol* 2000; **1**: 4
2 **Vincent KJ**, Jones E, Arthur MJ, Smart DE, Trim J, Wright MC, Mann DA. Regulation of E-box DNA binding during *in vivo* and *in vitro* activation of rat and human hepatic stellate cells. *Gut* 2001; **49**: 713-719
3 **Zhang M**, Song G, Minuk GY. Effects of hepatic stimulator substance, herbal medicine, selenium/vitamin E, and ciprofloxacin on cirrhosis in the rat. *Gastroenterology* 1996; **110**: 1150-1155
4 **Nan JX**, Park EJ, Kang HC, Park PH, Kim JY, Sohn DH. Anti-fibrotic effects of a hot-water extract from Salvia miltiorrhiza roots on liver fibrosis induced by biliary obstruction in rats. *J Pharm Pharmacol* 2001; **53**: 197-204
5 **Zhang QH**, Zhong B, Chen KJ. Effect of concentrated xuefu zhuyu pill on proliferation of vascular smooth muscle cells in experimental atheriosclerosis rabbits observed by serologic pharmacological test. *Zhongguo Zhongxiyi Jiehe Zazhi* 1996; **16**: 156-159
6 **Xue DY**, Hong JH, Xu LM. Salianic-acid B inhibits MAPK signaling in activated rat hepatic stellate cells. *Zhonghua Ganzangbing Zazhi* 2004; **12**: 471-474
7 **Wu J**, Zern MA. Hepatic stellate cells: a target for the treatment of liver fibrosis. *J Gastroenterol* 2000; **35**: 665-672
8 **Lee KS**, Buck M, Houglum K, Chojkier M. Activation of hepatic stellate cells by TGF alpha and collagen type I is mediated by oxidative stress through c-myb expression. *J Clin Invest* 1995; **96**: 2461-2468
9 **Muhlbauer M**, Bosserhoff AK, Hartmann A, Thasler WE, Weiss TS, Herfarth H, Lock G, Scholmerich J, Hellerbrand C. A novel MCP-1 gene polymorphism is associated with hepatic MCP-1 expression and severity of HCV-related liver disease. *Gastroenterology* 2003; **125**: 1085-1093
10 **Shimizu I**. Antifibrogenic therapies in chronic HCV infection. *Curr Drug Targets Infect Disord* 2001; **1**: 227-240
11 **Yao XX**, Fu YL, Li XL. A multi-central study of effect of Yi–gan infusion on 324 cases of chronic hepatitis. *Hebei Yixueyuan Xuebao* 1989; **10**: 231-233
12 **Jiang SL**, Li XT, Yao XX. Efficacy of profhylaxis and treatment of Yigankang on rat with hepatic fibrosis. *Zhongguo Quanke Yixue* 2002; **5**: 525-527
13 **Zhao G**, Wang LT, Chen JJ. Effect of anti-fibrosis compound contained serum on procollagen Type I and IV, matrix metalloproteinase and its tissue inhibitor-1 gene expression in HSC-LI90 cell line. *Zhongguo Zhongxiyi Jiehe Zazhi* 2004; **24**: 47-50
14 **Yamashiki M**, Nishimura A, Nomoto M, Suzuki H, Kosaka Y. Herbal medicine 'Sho-saiko-to' induces tumour necrosis factor-alpha and granulocyte colony-stimulating factor *in vitro* in peripheral blood mononuclear cells of patients with hepatocellular carcinoma. *J Gastroenterol Hepatol* 1996; **11**: 137-142
15 **Kayano K**, Sakaida I, Uchida K, Okita K. Inhibitory effects of the herbal medicine Sho-saiko-to (TJ-9) on cell proliferation and procollagen gene expressions in cultured rat hepatic stellate cells. *J Hepatol* 1998; **29**: 642-649
16 **Dooley S**, Hamzavi J, Breitkopf K, Wiercinska E, Said HM, Lorenzen J, Ten Dijke P, Gressner AM. Smad7 prevents activation of hepatic stellate cells and liver fibrosis in rats. *Gastroenterology* 2003; **125**: 178-191
17 **Liu X**, Zhang Z, Yang L, Chen D, Wang Y. Inhibition of the activation and collagen production of cultured rat hepatic stellate cells by antisense oligonucleotides against transforming growth factor-beta 1 is enhanced by cationic liposome delivery. *Huaxi Yike Daxue Xuebao* 2000; **31**: 133-135, 142
18 **Shimizu I**. Impact of oestrogens on the progression of liver disease. *Liver Int* 2003; **23**: 63-69
19 **Kim KY**, Choi I, Kim SS. Progression of hepatic stellate cell activation is associated with the level of oxidative stress rather than cytokines during CCl4-induced fibrogenesis. *Mol Cells* 2000; **10**: 289-300
20 **Reichen J**. Liver function and pharmacological considerations in pathogenesis and treatment of portal hypertension. *Hepatology* 1990; **11**: 1066-1078
21 **Deng YQ**, Fan XF. Relationship between liver fibrosis criteria and syndrome-type of TCM in patients with non-alcoholic fatty liver. *Zhongguo Zhongxiyi Jiehe Zazhi* 2001; **21**: 652-653
22 **Yao XX**, Tang YW, Yao DM, Xiu HM. Effect of Yigan Decoction on the expression of type I, II, III collagen proteins in experimental hepatic in rats. *Shijie Huaren Xiaohua Zazhi* 2001; **9**: 263-267
23 **Tang YW**, Yao XX, Yao HS. Observation of ultrastructure and protective effect on Yigankang on liver cells on experimental liver fibrosis rats. *Zhongguo Zhongxiyi Jiehe Xiaohua Zazhi* 2002; **10**: 76-78

Science Editor Guo SY **Language Editor** Elsevier HK

PO Box 2345, Beijing 100023, China
www.wjgnet.com
wjg@wjgnet.com

ELSEVIER

World J Gastroenterol 2005;11(16):2450-2455
World Journal of Gastroenterology ISSN 1007-9327

• *CLINICAL RESEARCH* •

Risk-adjustment in hepatobiliarypancreatic surgery

Hemant M Kocher, Paris P Tekkis, Palepu Gopal, Ameet G Patel, Simon Cottam, Irving S Benjamin

Hemant M Kocher, Paris P Tekkis, Ameet G Patel, Irving S Benjamin, Academic Department of Surgery, King's College Hospital, Denmark Hill, London SE5 9RY, UK
Palepu Gopal, Simon Cottam, Department of Anaesthesia, King's College Hospital, Denmark Hill, London SE5 9RY, UK
Supported by the Agostino Trappani International Foundation, Naples (Hemant Kocher) and The Royal College of Surgeons of England (Paris Tekkis)
Correspondence to: Hemant Kocher MS, MD, FRCS, Department of Health National Clinician Scientist, Senior Lecturer Tumour Biology Laboratory, Cancer Research UK Clinical Centre, Queen Mary's School Of Medicine and Dentistry at Barts and The London, John Vane Science Centre, Charterhouse Square, London EC1M 6BQ, UK. hemant.kocher@cancer.org.uk
Telephone: +44-207-346-5163 Fax: +44-207-346-3575
Received: 2004-06-19 Accepted: 2004-08-22

Abstract

AIM: The present study evaluates the performance of the POSSUM, the American Society of Anesthetists (ASA), APACHE and Childs classification in predicting mortality and morbidity in hepatopancreaticobiliary (HPB) surgery. We describe especially the limitations and advantages of risk in stratifying the patients.

METHODS: We investigated 177 randomly chosen patients undergoing elective complex HPB surgery in a single institution with a total of 71 pre-operative and intra-operative risk factors. Primary endpoint was in-hospital mortality and morbidity. Ordered logistic regression analysis was used to identify individual predictors of operative morbidity and mortality.

RESULTS: The operative mortality in the series was 3.95%. This compared well with the p-POSSUM and APACHE predicted mortality of 4.31% and 4.29% respectively. Post-operative complications amounted to 45% with 24 (13.6%) patients having a major adverse event. On multivariate analysis the pre-operative POSSUM physiological score (OR = 1.18, P = 0.009) was superior in predicting complications compared to the ASA (P = 0.108), APACHE (P = 0.117) or Childs classification (P = 0.136). In addition, serum sodium, creatinine, international normalized ratio (INR), pulse rate, and intra-operative blood loss were independent risk factors. A combination of the POSSUM variables and INR offered the optimal combination of risk factors for risk prognostication in HPB surgery.

CONCLUSION: Morbidity for elective HPB surgery can be accurately predicted and applied in everyday surgical practice as an adjunct in the process of informed consent and for effective allocation of resources for intensive and high-dependency care facilities.

Key words: Hepatobiliarypancreatic surgery; Risk adjustment; Operative mortality; Operative morbidity; Regression models

Kocher HM, Tekkis PP, Gopal P, Patel AG, Cottam S, Benjamin IS. Risk-adjustment in hepatobiliarypancreatic surgery. *World J Gastroenterol* 2005; 11(16): 2450-2455
http://www.wjgnet.com/1007-9327/11/2450.asp

INTRODUCTION

Observed healthcare outcomes (mortality, length of hospital stay, quality of life) are increasingly relied upon for evaluating the quality of medical care. Expected outcomes represent predictions about what ought to happen to a particular patient, or group of patients, given pre-defined standards of care. Predictions are based on relevant prognostic factors including patient's age, disease severity and co-morbidity. Operative mortality and morbidity are objective measures of outcome that can be readily used for monitoring performance within a center or between centers. However, for this measure to be truly objective it must be adjusted for the patient-related risk factors (case-mix).

The Portsmouth Physiological and Operative Severity Score for enumeration of mortality and morbidity[1] (p-POSSUM) was developed as a modification of the original POSSUM equation which was described by Copeland *et al*[2], and has been widely applied to adjust for case-mix in general surgery. These scoring systems used a 12-factor, four-grade, physiological score and a 6-factor, four-grade, operative severity score, compensating for the type of procedure. Although the POSSUM scoring systems have been applied in patients undergoing general[3], colorectal[4] and vascular[5] surgery, recent reports have pointed out the limitations of applying the POSSUM scoring for example at the extremes of age in colorectal surgery[6] and in emergency vascular surgery[7].

Other types of risk scoring systems have been devised. The American Society of Anesthetists (ASA) grading system is a subjective pre-operative co-morbid index, which has been shown to be a good predictor of post-operative survival[8]. Specific to cirrhotic patients, the Child-Pugh grading system has been shown to be an adequate predictor of short-term and long-term survival[9]. Other systems such as APACHE II scoring system have also been used[10].

Hepatobiliarypancreatic surgical procedures are complex with difficult post-operative management. Many procedures of heterogeneous complexities are being carried out in the referral centers and in order to compare centers these factors may have to be taken into account. It requires a multi-disciplinary approach to patient management with a high dependence on the intensive care facilities. It is being

concentrated akin to cardiac and neurosurgery in large centers with a good throughput. Risk adjustment of patients undergoing complex procedure is imminently needed for a qualified informed consent and allocation of meager high-cost resources. The aim of the present study was to compare the POSSUM equation with other risk scoring systems along with other peri-operative variables in order to identify factors, which may affect the outcome of patients undergoing hepatobiliarypancreatic surgery.

MATERIALS AND METHODS

Data and variables

A team of surgeons, anesthetists and intensivists met to decide the risk factors and scoring systems, which may be valuable predictors for post-operative outcome in hepatopancreaticobiliary (HPB) surgery. Dedicated proformas comprised of (1) demographic details, (2) pre-operative assessment and clinical staging, (3) surgical treatment, (4) postoperative course and complications and (5) data points for various scoring systems [POSSUM, APACHE, ASA, Child-Pugh] and other possible factors for HPB surgery (these currently available and widely used risk stratification models were used as starting point, other factors such as temperature, transfusion requirement were chosen based on literature review as factors affecting outcome in HPB surgery), (6) anesthetic data included intra-operative routinely collected data on a central computerized system, which included pulse, blood pressure, oxygen saturation, core temperature, blood gas measurements, blood loss and intra-operative fluid management, (7) outcomes as defined below. Data were recorded on a Microsoft Access 2000 database (Microsoft Corporation, USA). The patient records underwent an extensive process of data editing to check for missing or out-range values and inconsistencies between data fields. Following rectification of these records, error-free data were entered into a master file. Primary outcome was in-hospital operative mortality, defined as death during the same hospital admission as the operation, regardless of cause and post-operative morbidity classified as minor (delays discharge), intermediate (requiring non-invasive intervention), major (life-threatening or requiring invasive intervention). In-hospital mortality was validated from case records, hospital mortuary registers and the hospital Patient Administration System. The patient and procedural risk factors included (1) age; (2) gender; (3) POSSUM pre-operative physiological score and operative severity score[2] ; (4) surgical procedure categorized according to the OPCS4 system, (5) APACHE variables, (6) cancer staging according to TNM classification of HPB malignancies where applicable; (7) Child-Pugh classification, (8) ASA grade, (9) other peri-operative variables such as clotting profile, type of previous surgery, intra-operative parameters as defined above.

Patient selection

Patients undergoing major elective hepatobiliarypancreatic surgery at King's College Hospital were included in the study. Prospective data on 77 consecutive patients were collected for the year March 2000-February 2001. Retrospective data (n = 100) were collected from case notes for the period 1991-1999. Patients were selected randomly from a central prospective database using a computer-generated random number sample. Case notes were then retrieved and other data in surgical and anesthetic computerized data were further added.

Statistical analysis

Unifactorial ordered logistic regression was used to identify risk factors related to in-hospital adverse events[11]. Morbidity and mortality were combined as a single ordinal variable comprising three possible outcomes: (1) no morbidity or mortality, (2) mild to intermediate morbidity, (3) major morbidity or mortality. Continuous variables such as POSSUM and APACHE were categorized into quartiles, representing groups increasing operative risk. Any variable whose univariate test had a P-value of <0.25 was considered as a candidate for the multivariate analysis. In order to maximize the information extracted from the predictor variables, we used a median imputation technique for substituting any incomplete data[12]. Multifactorial ordered logistic regression analysis was used to adjust for multiple risk factors and their interactions, entered into the model in a stepwise fashion. Internal validation was performed by comparing observed and predicted complication rates across the various subgroups of international normalized ratio (INR) values using the Hosmer-Lemeshow χ^2 test[13].

Software

The following statistical software packages were utilized: "Intercooled STATA 6.0 for Windows" (STATA Corporation, USA), "Statistical Package for the Social Sciences" version 11 for Windows (SPSS, Chicago, IL, USA).

RESULTS

A summary of the diagnosis and type of operative procedures are shown in Tables 1 and 2 respectively. The patient demographic characteristics and in-hospital operative mortality and morbidity are shown in Tables 3 and 4. The overall observed in-hospital operative mortality was 3.95% and morbidity was 45.2%.

Incomplete data for the 177 cases with 77 variables were 2% and were mainly for clotting profiles such as APTT

Table 1 Diagnosis

Organ	Number of patients (% of total)	Number of deaths (% mortality)
Hepatic	89 (50.3)	1 (1.1)
Liver primary	14 (7.9)	0
Colorectal secondaries	47 (26.6)	1 (2.1)
Other secondaries	5 (2.8)	0
Carcinoid tumors	10 (5.6)	0
Benign liver lesions	13 (7.3)	0
Biliary	63 (35.6)	4 (6.3)
Cholangiocarcinoma	24 (13.6)	4 (16.6)
Iatrogenic biliary strictures	24 (13.6)	0
Benign biliary strictures	15 (8.5)	0
Pancreatic	25 (14.1)	2 (8)
Pancreatic malignancy	18 (10.2)	2 (11)
Pancreatitis	7 (3.9)	0
Total	177 (100)	7 (3.95)

Table 2 Type of procedure and in-hospital mortality

Procedure	Number of patients (% of total)	Number of deaths (% mortality)
Right hepatectomy	29 (16.4)	1 (3.4)
Left hepatectomy	15 (8.5)	0
Extended right hepatectomy	16 (9)	2 (12.5)
Extended left hepatectomy	5 (2.8)	1 (20)
Segmental liver resection	28 (15.8)	0
Hepaticojejunostomy	47 (26.6)	0
Pancreaticoduodenectomy	22 (12.4)	3 (13.6)
Total pancreatectomy	2 (1.1)	0
Distal pancreatectomy	2 (1.1)	0
Others	11 (6.2)	0
Total	177 (100)	7 (3.95)

Table 4 Types of morbidity

System	Minor/intermediate[1]	Severe[1]
Respiratory	25 (14.1)	10 (5.6)
Gastrointestinal	23 (13.0)	12 (6.7)
Hematological	20 (11.3)	6 (3.4)
Wound	15 (8.5)	3 (1.7)
Intra-abdominal sepsis	15 (8.5)	2 (1.1)
Cardiac	9 (5.1)	3 (1.7)
Renal	8 (4.5)	3 (1.7)
Venous	2 (1.1)	2 (1.1)
Others	19 (10.7)	2 (1.1)
Total	56 (31.6)[1]	24 (13.6)[1]

[1]A given patient may have complications of varying grade in one or more systems.

and fibrinogen (0.5%), intra-operative hemodynamic and fluid balance parameters (1%) in the retrospective data set. Unadjusted odds ratios were calculated for each scoring system or factor's reference category as shown in Table 5. The POSSUM physiological score, the acute physiologic score of APACHE II, and ASA grade showed a significant association with postoperative morbidity particularly at the highest quartile. For example, patients with an APACHE score of 6-13 would be 2.9 times more likely to have a major adverse post-operative event in comparison with patients with an APACHE score of 0-1. The INR and intra-operative blood loss were the other discriminant risk factors of operative morbidity and mortality. Additional factors mentioned in Methods were tested but were found to be insignificant predictors of adverse outcomes in HPB surgery (results not shown). Adjusting for the type of other confounding variables, pancreaticoduodenectomy (Whipple's procedure) had the highest risk of operative morbidity (OR 2.27, 95%CI: 1.07-9.97) in comparison with the right hepatectomy, which was treated as the reference category.

The adjusted (multivariate ordered logistic regression) odds ratios and 95% CI for the POSSUM, INR, blood loss and type of operation are shown in Table 6.

Of the POSSUM physiologic score, the important factors were the serum sodium, creatinine and pulse rate.

Observed *vs* predicted probabilities of complications of all types or major complications are shown in Figure 1. There was no significant difference between observed and predicted operative morbidity rates across INR values ranging between 0.8 and 1.25. (Hosmer-Lemeshow χ^2 test = 7.762, degrees of freedom = 8, $P = 0.457$.) Similarly Figure 2 shows prediction curves for major and all complications based on the pre-operative POSSUM physiological score. Figures 3 and 4 show the probabilities of all complications and major complications respectively, based on the POSSUM physiological score and increasing values of INR.

Table 3 Patient characteristics and associated mortality and morbidity

Demographics	Number (% of total)
Age (median, range)	54.6 (19, 80)
Female patients	96 (54.2)
Length of stay (median, range)	
Hospital	15 (2-113)
ITU	0 (0–20)
HDU	0 (0–10)
Mortality (in-hospital)	7 (3.95)
Morbidity	
No morbidity	97 (54.8)
Minor/intermediate	56 (31.6)
Major	24 (13.6)

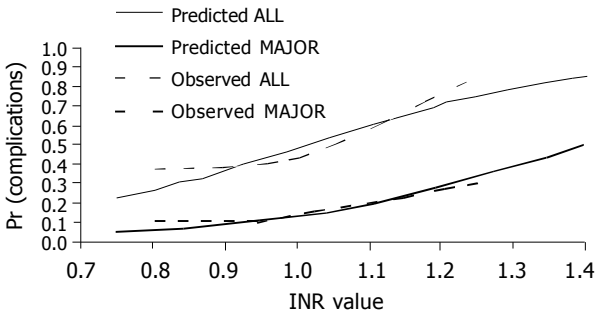

Figure 1 Observed *vs* predicted values of complications (all types or major only) with respect to INR values.

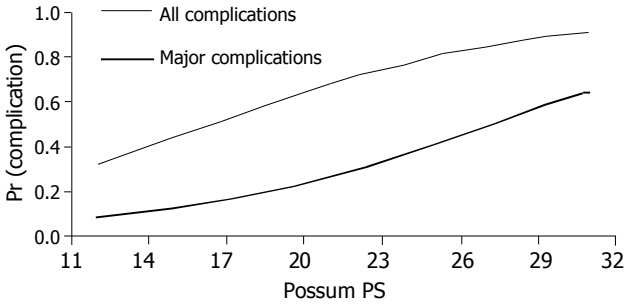

Figure 2 Prediction of possible complications (all types and major only) on the basis of POSSUM physiologic score in patients undergoing major elective HPB surgery.

DISCUSSION

Quality of care is multidimensional, it may be viewed from the patient's, the doctor's or healthcare provider's perspective and be assessed in terms of structure, process and outcomes

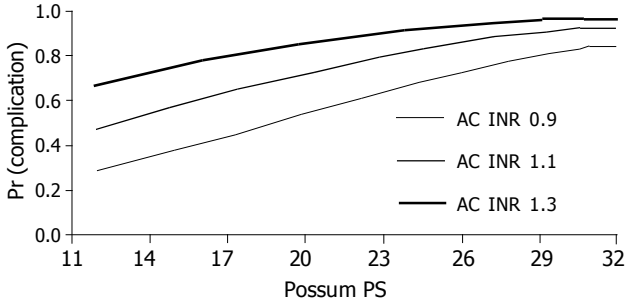

Figure 3 Prediction of all possible complications on the basis of POSSUM physiologic score and increasing values of INR in patients undergoing major elective HPB surgery.

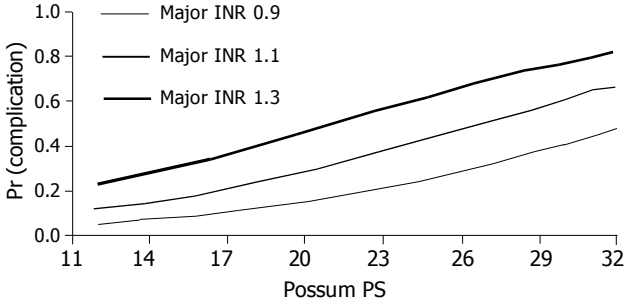

Figure 4 Prediction of possible major complications on the basis of POSSUM physiologic score and increasing values of INR in patients undergoing major elective HPB surgery.

of a healthcare delivery system[14,15]. The purpose of the present study was to identify and evaluate possible risk factors and scoring systems for HPB surgery.

Operative morality and morbidity are objective measures of healthcare, which can be easily measured[16]. Furthermore, major complications, which may be life threatening (major hemorrhage) or they may be requiring invasive treatment (percutaneous drainage of biliary tree or collection, or re-operation for intra-abdominal catastrophe). These have to be effectively managed in order to convert the near-misses to successes thereby maintaining low post-operative mortality. The management of major post-operative complications after major HPB surgery is multi-disciplinary requiring intensivists, interventional radiologists, endoscopists, hepatologists, anesthetists and dedicated ward and theatre staff not to mention high-cost technology. Thus, the major complications and mortality both have to be measured and risk adjusted in order to give a true picture of in-hospital and intra-hospital comparisons. Operative mortality and morbidity is expected to vary between hospitals. This variation is a function of differences in patient case-mix, random adverse events and differences in the process and structure of care[15]. Statistical analysis is intended to adjust for the case-mix as much as possible so that the remaining variation is more likely to be due to differences in the quality of care. The present study identifies the important factors associated with the adverse events in patients undergoing major HPB surgery.

Ordered logistic regression allowed us to order the types of complications in three groups of increasing severity of adverse outcome: no complications, minor/intermediate complications and major complications along with death[12]. Thus, the ordinal outcomes as mentioned above could be used to quantify the nature of complications and provide

Table 5 Analysis of the separate risk scoring systems by unifactorial ordered logistic regression using sampling quartiles for continuous variables

Risk score/factor	Group	Number of patients (% of total)	Minor/intermediate complications (%)	Major complications/ death (%)	Unadjusted odds ratio[1]	95%CI [1]
POSSUM	12-13	62 (35.0)	13 (21)	7 (11.3)	1	
Physiological	14-15	53 (29.9)	20 (37.7)	6 (11.3)	1.8	0.24, 3.77
Score[1,2]	16-17	31 (17.5)	13 (41.9)	3 (9.7)	1.9	0.81, 4.41
	18-31	31 (17.5)	10 (32.3)	8 (25.8)	3.12	1.32, 7.38
APACHE II	0-1	30 (16.9)	9 (30)	3 (10)	1	
Acute	2-3	66 (37.3)	20 (30.3)	6 (9.1)	0.97	0.41, 2.28
Physiological	4-5	49 (27.7)	14 (28.6)	7 (14.3)	1.18	0.48, 2.89
Score[1,3]	6-13	32 (18.1)	13 (40.6)	8 (25)	2.86	1.09, 7.5
ASA	1	47 (26.6)	12 (25.5)	3 (6.4)	1	
	2	77 (43.5)	27 (35.1)	8 (10.4)	1.73	0.15, 3.63
	3-4	31 (17.5)	17 (33.3)	12 (23.5)	3.16	1.41, 7.07
	Missing	2 (1.1)				
Child-Pugh	A	145 (81.9)	49 (33.8)	16 (11)	1	
	B	32 (18.1)	7 (21.9)	8 (25)	1.34	0.64, 2.94
	C	0				
INR	<0.9	45 (25.4)	13 (28.9)	4 (8.9)	1	
	0.9-1.1	119 (67.2)	36 (30.3)	16 (13.5)	1.32	0.67, 2.63
	>1.1	13 (7.3)	7 (53.9)	4 (30.7)	5.5	1.78, 17.5
Blood loss	<1	90 (50.9)	24 (26.7)	9 (10)	1	
	1-2	38 (21.5)	11 (29.0)	2 (5.3)	0.85	0.39, 1.85
-	>2	49 (27.7)	21 (43.0)	13 (26.0)	4.1	1.49, 11.13

[1]For illustration purposes all the scores (continuous variables) were grouped into meaningful quartiles. †Odds ratios and 95% confidence intervals (CI) calculated using unifactorial ordered logistic regression analysis. [2]Theoretical range of values for the physiological score of POSSUM is 12–96. [3]Theoretical range of values for the acute physiological score of APACHE II is 0-44.

Table 6 Multivariate ordered logistic regression analysis of risk factors for HPB surgery

Factor	Category	Estimate (b)	Adjusted OR	CI 95%
Physiological score-POSSUM	10^{-1} units increase		1.18	1.07, 1.31
INR[2]	10^{-2} units increase		1.47	1.12, 1.94
Blood loss	< 2 L		1	
	>2 L		4.1	1.49, 11.13
Procedure	Right hepatectomy		1	
	Pancreaticoduodenectomy		3.27	1.07, 9.97
Sub-factors of POSSUM[3]				
Serum sodium[1]	10^{-1} units increase		0.89	0.82, 0.97
Serum creatinine	10^{-1} units increase		1.01	1.00, 1.02
Pulse rate (bpm)	10^{-1} units increase		1.04	1.01, 1.06

[1]OR denotes that patients do worse with every unit decrease in sodium below the lower limit of normal range (130 mmol/L). [2]OR denotes that patients do worse with every 0.1 unit increase in INR above 1.1. [3]When the physiological score of the POSSUM variables are analyzed separately with multifactorial ordered logistic regression, the significant factors are sodium, creatinine and pulse rate which affect mortality and morbidity.

accurate and justifiable risk adjustment to take account of case-mix. Since the procedures in HPB surgery are mainly elective, the risk stratification is skewed towards fitter patients as compared to patients undergoing surgery for vascular or colorectal causes, where up to 40% of the workload may be emergency in nature; thus bringing in unfit patients. As can be seen from the physiologic scores for POSSUM, which ranged in this dataset from 12 to 31 as compared to a theoretical range of 12-96. Moreover more than 80% of patients had a pre-operative physiologic POSSUM score of less than 17. Similar scenario can be seen with the APACHE II acute physiologic score (80% below a score of 5) and ASA grading (around 80% ASA I or II). Also all the patients operated upon were either Child's A or B. Thus, we can observe a self-selection of fitter patients undergoing HPB surgery.

INR, intra-operative blood loss and type of procedure are other important risk factors, which may be important in predicting the outcome. Deranged INR in an elective situation represents established preoperative liver dysfunction.

Pancreaticoduodenectomy (PD) remains the single operation in the spectrum of major HPB operations, which has to be adjusted for whilst comparing outcomes from different units. Gastrointestinal and respiratory complications are higher in patients undergoing PD. This may artificially distort the outcomes of units performing higher or lower numbers of PD, making them appear worse or better respectively. Thus in these two aspects HPB surgery differs from other types of surgery. In addition, excessive intra-operative blood loss may make a particular patient remain in a high dependency unit for a longer duration than normal. However, this operator-dependent variable should be left out of the equation when comparing units, as it can be a surrogate marker for quality of surgery and the surgeon as a risk factor[17].

In addition, we have shown that it is possible to have demonstrable risk adjusted graphs (Figures 3 and 4), which can calculate risk predictions pre-operatively. This can make an informed consent a more objective procedure and justify the need for high dependency facilities in high risk patients for prolonged use.

The expected outcome for a population of patients can be calculated by summing the probabilities estimates of all patients in the population. Having calculated the expected outcome for a population of patients and adjusted for the patient-related risk factors, the observed to the expected outcomes can be compared. This can be done either as an O/E ratio[18] or as a mortality difference, i.e., the observed minus the expected outcomes (O-E difference)[19,20]. Such methodologies can be used as the basis of cross-sectional audits and for continuous or sequential monitoring of surgical performance within hospitals. Numerous studies have been done to develop audit tools for different specialities of surgery[21-30].

There are a number of limitations in this study. First, the sample size is small and it is a single hospital dataset. However, here we are attempting to identify the risk factors specific to HPB surgery. It needs to be validated across national datasets in order to develop a specific equation applicable to HPB surgery. Secondly, the number of pancreatic resections carried out as a proportion to the total number of operations is low and may affect the overall predictive power. If PD is incorporated as an independent risk factor, this shortcoming can be accounted for.

In conclusion the present study has demonstrated the uses and limitations of risk adjustment using the various scoring systems in HPB surgery. The availability of good quality data and validated models is fundamental for a continuous program of quality improvement. With adequate sample size the new risk scoring system can be devised and used for monitoring surgical outcomes between or within hospitals in order to meet the demands of professional and public scrutiny of outcomes in HPB surgery.

ACKNOWLEDGEMENTS

The present study was initiated by Hemant Kocher and Paris Tekkis. Irving Benjamin, Simon Cottam and Ameet Patel contributed to the proformas model and contributed patients. Data harvesting and aggregation was undertaken by Hemant Kocher, Paris Tekkis and Palepu Gopal. Data analysis and risk-modeling and 1st draft of this study was performed by Paris Tekkis and Hemant Kocher and edited by all investigators who contributed comments and corrections on the final draft. We thank the Agostino Trappani International Foundation, Naples for funding Hemant Kocher and The Royal College of Surgeons of England for funding Paris Tekkis. We are most grateful to Paul Bras, David Green and theater staff who have contributed data and supported the study.

REFERENCES

1 **Prytherch DR,** Whiteley MS, Higgins B, Weaver PC, Prout WG, Powell SJ. POSSUM and Portsmouth POSSUM for predicting mortality. Physiological and Operative Severity Score for the enUmeration of Mortality and morbidity. *Br J Surg* 1998; **85**: 1217-1220

2 **Copeland GP,** Jones D, Walters M. POSSUM: a scoring system for surgical audit. *Br J Surg* 1991; **78**: 355-360

3 **Copeland GP,** Sagar P, Brennan J, Roberts G, Ward J, Cornford

P, Millar A, Harris C. Risk-adjusted analysis of surgeon performance: a 1-year study. *Br J Surg* 1995; **82**: 408-411
4 **Tekkis PP,** Kocher HM, Bentley AJ, Cullen PT, South LM, Trotter GA, Ellul JP. Operative mortality rates among surgeons: comparison of POSSUM and p-POSSUM scoring systems in gastrointestinal surgery. *Dis Colon Rectum* 2000; **43**: 1528-1532, discusssion 1532-1534
5 **Midwinter MJ,** Tytherleigh M, Ashley S. Estimation of mortality and morbidity risk in vascular surgery using POSSUM and the Portsmouth predictor equation. *Br J Surg* 1999; **86**: 471-474
6 **Tekkis PP,** Kessaris N, Kocher HM, Poloniecki JD, Lyttle J, Windsor AC. Evaluation of POSSUM and P-POSSUM scoring systems in patients undergoing colorectal surgery. *Br J Surg* 2003; **90**: 340-345
7 **Lazarides MK,** Arvanitis DP, Drista H, Staramos DN, Dayantas JN. POSSUM and APACHE II scores do not predict the outcome of ruptured infrarenal aortic aneurysms. *Ann Vasc Surg* 1997; **11**: 155-158
8 **Belghiti J,** Hiramatsu K, Benoist S, Massault P, Sauvanet A, Farges O. Seven hundred forty-seven hepatectomies in the 1990s: an update to evaluate the actual risk of liver resection. *J Am Coll Surg* 2000; **191**: 38-46
9 **Pugh RN,** Murray-Lyon IM, Dawson JL, Pietroni MC, Williams R. Transection of the oesophagus for bleeding oesophageal varices. *Br J Surg* 1973; **60**: 646-649
10 **Gagner M,** Franco D, Vons C, Smadja C, Rossi RL, Braasch JW. Analysis of morbidity and mortality rates in right hepatectomy with the preoperative APACHE II score. *Surgery* 1991; **110**: 487-492
11 **Hosmer DW,** Lemeshow S. *Applied Logistic Regression*. 2nd ed. New York: John Wiley & Sons Inc; 2000
12 **Harrell FE,** Lee KL, Mark DB. Multivariable prognostic models: issues in developing models, evaluating assumptions and adequacy, and measuring and reducing errors. *Stat Med* 1996; **15**: 361-387
13 **Hosmer DW,** Lemeshow S. Goodness-of-fit testing for multiple logistic regression analysis when the estimated probabilities are small. *Biometrical J* 1988; **30**: 911-924
14 **Daley J,** Henderson WG, Khuri SF. Risk-adjusted surgical outcomes. *Annu Rev Med* 2001; **52**: 275-287
15 **Iezzoni LI.** Dimensions of risk. In: Iezzoni LI, editor. Risk adjustment for measuring healthcare outcomes. 2nd ed: Ann Arbor, MI: Health Administration Press 1997: 43-168
16 **Jacobson B,** Mindell J, McKee M. Hospital mortality league tables. *BMJ* 2003; **326**: 777-778
17 **Carter D.** The surgeon as a risk factor. *BMJ* 2003; **326**: 832-833
18 **Spiegelhalter DJ,** Myles JP, Jones DR, Abrams KR. Bayesian methods in health technology assessment: a review. *Health Technol Assess* 2000; **4**: 1-130
19 **Poloniecki J,** Valencia O, Littlejohns P. Cumulative risk adjusted mortality chart for detecting changes in death rate: observational study of heart surgery. *BMJ* 1998; **316**: 1697-1700
20 **Lovegrove J,** Valencia O, Treasure T, Sherlaw-Johnson C, Gallivan S. Monitoring the results of cardiac surgery by variable life-adjusted display. *Lancet* 1997; **350**: 1128-1130
21 **Tekkis PP,** McCulloch P, Poloniecki JD, Prytherch DR, Kessaris N, Steger AC. Risk-adjusted prediction of operative mortality in oesophagogastric surgery with O-POSSUM. *Br J Surg* 2004; **91**: 288-295
22 **Hadjianastassiou VG,** Tekkis PP, Poloniecki JD, Gavalas MC, Goldhill DR. Surgical mortality score: risk management tool for auditing surgical performance. *World J Surg* 2004; **28**: 193-200
23 **Tekkis PP,** Poloniecki JD, Thompson MR, Stamatakis JD. Operative mortality in colorectal cancer: prospective national study. *BMJ* 2003; **327**: 1196-1201
24 **McCulloch P,** Ward J, Tekkis PP. Mortality and morbidity in gastro-oesophageal cancer surgery: initial results of ASCOT multicentre prospective cohort study. *BMJ* 2003; **327**: 1192-1197
25 **Tekkis PP,** McCulloch P, Steger AC, Benjamin IS, Poloniecki JD. Mortality control charts for comparing performance of surgical units: validation study using hospital mortality data. *BMJ* 2003; **326**: 786-788
26 **Mohil RS,** Bhatnagar D, Bahadur L, Rajneesh DK, Magan M. POSSUM and P-POSSUM for risk-adjusted audit of patients undergoing emergency laparotomy. *Br J Surg* 2004; **91**: 500-503
27 **Bennett-Guerrero E,** Hyam JA, Shaefi S, Prytherch DR, Sutton GL, Weaver PC, Mythen MG, Grocott MP, Parides MK. Comparison of P-POSSUM risk-adjusted mortality rates after surgery between patients in the USA and the UK. *Br J Surg* 2003; **90**: 1593-1598
28 **Zafirellis KD,** Fountoulakis A, Dolan K, Dexter SP, Martin IG, Sue-Ling HM. Evaluation of POSSUM in patients with oesophageal cancer undergoing resection. *Br J Surg* 2002; **89**: 1150-1155
29 **Yii MK,** Ng KJ. Risk-adjusted surgical audit with the POSSUM scoring system in a developing country. Physiological and Operative Severity Score for the enUmeration of Mortality and morbidity. *Br J Surg* 2002; **89**: 110-113
30 **Tekkis PP,** Prytherch DR, Kocher HM, Senapati A, Poloniecki JD, Stamatakis JD, Windsor AC. Development of a dedicated risk-adjustment scoring system for colorectal surgery (colorectal POSSUM). *Br J Surg* 2004; **91**: 1174-1182

Science Editor Guo SY **Language Editor** Elsevier HK

PO Box 2345, Beijing 100023, China
www.wjgnet.com
wjg@wjgnet.com

ELSEVIER

World J Gastroenterol 2005;11(16):2456-2461
World Journal of Gastroenterology ISSN 1007-9327

• *CLINICAL RESEARCH* •

Risk factors of pancreatic leakage after pancreaticoduodenectomy

Yin-Mo Yang, Xiao-Dong Tian, Yan Zhuang, Wei-Min Wang, Yuan-Lian Wan, Yan-Ting Huang

Yin-Mo Yang, Xiao-Dong Tian, Yan Zhuang, Wei-Min Wang, Yuan-Lian Wan, Yan-Ting Huang, Department of Surgery, The First Teaching Hospital, Health Science Center, Beijing University, Beijing 100034, China
Correspondence to: Professor Yin-Mo Yang, Department of Surgery, The First Teaching Hospital, Health Science Center, Beijing University, Beijing 100034, China. yangyinmo@263.net
Telephone: +86-10-66171122
Received: 2004-06-19 Accepted: 2004-07-11

Abstract

AIM: To analyze the risk factors for pancreatic leakage after pancreaticoduodenectomy (PD) and to evaluate whether duct-to-mucosa pancreaticojejunostomy could reduce the risk of pancreatic leakage.

METHODS: Sixty-two patients who underwent PD at our hospital between January 2000 and November 2003 were reviewed retrospectively. The primary diseases of the patients included pancreas cancer, ampullary cancer, bile duct cancer, islet cell cancer, duodenal cancer, chronic pancreatitis, pancreatic cystadenoma, and gastric cancer. Standard PD was performed for 25 cases, PD with extended lymphadenectomy for 27 cases, pylorus-preserving PD for 10 cases. A duct-to-mucosa pancreaticojejunostomy was performed for patients with a hard pancreas and a dilated pancreatic duct, and a traditional end-to-end invagination pancreaticojejunostomy for patients with a soft pancreas and a non-dilated duct. Patients were divided into two groups according to the incidence of postoperative pancreaticojejunal anastomotic leakage: 10 cases with leakage and 52 cases without leakage. Seven preoperative and six intraoperative risk factors with the potential to affect the incidence of pancreatic leakage were analyzed with SPSS10.0 software. Logistic regression was then used to determine the effect of multiple factors on pancreatic leakage.

RESULTS: Of the 62 patients, 10 (16.13%) were identified as having pancreatic leakage after operation. Other major postoperative complications included delayed gastric emptying (eight patients), abdominal bleeding (four patients), abdominal abscess (three patients) and wound infection (two patients). The overall surgical morbidity was 43.5% (27/62). The hospital mortality in this series was 4.84% (3/62), and the mortality associated with pancreatic fistula was 10% (1/10). Sixteen cases underwent duct-to-mucosa pancreaticojejunostomy and 1 case (1/16, 6.25%) devel-oped postoperative pancreatic leakage, 46 cases underwent invagination pancreaticojejunostomy and 9 cases (9/46, 19.6%) developed postoperative pancreatic leakage. General risk factors including patient age, gender, history of jaundice, preoperative nutrition, pathological diagnosis and the length of postoperative stay were similar in the two groups. There was no statistical difference in the incidence of pancreatic leakage between the patients who received the prophylactic use of octreotide after surgery and the patients who did not undergo somatostatin therapy. Moreover, multivariate logistic regression analysis showed that none of the above factors seemed to be associated with pancreatic fistula. Two intraoperative risk factors, pancreatic duct size and texture of the remnant pancreas, were found to be significantly associated with pancreatic leakage. The incidence of pancreatic leakage was 4.88% in patients with a pancreatic duct size greater than or equal to 3 mm and was 38.1% in those with ducts smaller than 3 mm (P = 0.002). The pancreatic leakage rate was 2.94% in patients with a hard pancreas and was 32.1% in those with a soft pancreas (P = 0.004). Operative time, blood loss and type of resection were similar in the two patient groups. The incidence of pancreatic leakage was 6.25% (1/16) in patients with duct-to-mucosa anastomosis, and was 19.6% (9/46) in those with traditional invagination anastomosis. Although the difference of pancreatic leakage between the two groups was obvious, no statistical signific-ance was found. This may be due to the small number of patients with duct-to-mucosa anastomosis. By further analyzing with multivariate logistic regression, both pancreatic duct size and texture of the remnant pancreas were demonstrated to be independent risk factors (P = 0.007 and 0.017, OR = 11.87 and 15.45). Although anastomotic technique was not a significant factor, pancreatic leakage rate was much less in cases that underwent duct-to-mucosa pancreaticojejunostomy.

CONCLUSION: Pancreatic duct size and texture of the remnant pancreas are risk factors influencing pancreatic leakage after PD. Duct-to-mucosa pancreaticojejunostomy, as a safe and useful anastomotic technique, can reduce pancreatic leakage rate after PD.

Key words: Pancreaticoduodenectomy; Pancreatic leakage

Yang YM, Tian XD, Zhuang Y, Wang WM, Wan YL, Huang YT. Risk factors of pancreatic leakage after pancreaticoduodenectomy. *World J Gastroenterol* 2005; 11(16): 2456-2461
http://www.wjgnet.com/1007-9327/11/2456.asp

INTRODUCTION

Pancreaticoduodenectomy (PD) is one of the standard treatments for various benign and malignant diseases of the pancreatic head and periampullary region. Recently, the

operative mortality rate after PD has significantly declined, while the incidence of postoperative morbidity remains high, from 40% to 50%[1-5]. Pancreatic fistula is the major source of complications, and leakage rate varies from 0% to 25%, according to recent reports[6-8]. Abdominal abscess and hemorrhage are common sequelae of pancreatic anastomotic leakage, which have been associated with a mortality rate of 40% or more. Subsequently, pancreatic fistula has become one of the major complications discouraging surgeons from performing PD[2,6,7,9]. Recent literature suggests that many factors influence pancreatic leakage after PD, including sex, age, jaundice, operation time, intraoperative blood loss, pancreaticojejunal anastomotic technique, texture of the remnant pancreas, pancreatic duct size, use of somatostatin, and surgeon experience. However, no definite factor has yet been identified. Some authors have compared the incidence of pancreatic leakage with various techniques of anastomosis, such as invagination pancreaticojejunal anasto-mosis, duct-to-mucosa pancreaticojejunal anastomosis, pancreaticogastrostomy, pancreatic duct ligation, and their modifications. No conclusions though can be drawn to demonstrate which technique is best and suitable for any particular case. To analyze perioperative risk factors for pancreatic leakage after PD and to compare duct-to-mucosa with invagination pancreaticojejunal anastomosis, we reviewed retrospectively 62 cases that underwent PD at our hospital.

MATERIALS AND METHODS

Between January 2000 and November 2003, 62 patients underwent PD at our hospital, including 38 men and 24 women. Patients' age ranged from 33 to 77 years, with a mean age of 57.53 years. Before surgery, jaundice was found in 30 cases and 3 cases had hypoproteinemia. The diagnoses are shown in Table 1. All of the diseases were confirmed by pathologic examinations.

Table 1 Diseases and surgical techniques

Diseases	No. of patients (n = 62)	Surgical techniques	
		PD (n = 52)	PPPD (n = 10)
Pancreas cancer	29	26	3
Ampullary cancer	14	10	4
Bile duct cancer	13	12	1
Islet cell cancer	2	1	1
Duodenal cancer	1	1	0
Chronic pancreatitis	1	1	0
Pancreatic cystadenoma	1	0	1
Gastric cancer	1	1	0

PD: pancreaticoduodenectomy; PPPD: pylorus-preserving pancreaticoduodenectomy.

Surgical techniques

In the 62 cases, standard PD was performed for 25 patients, PD with extended lymphadenectomy for 27 patients, and PPPD for 10 patients. One patient with gastric cancer invading the peripancreas region underwent radical gastrostomy and PD with extended lymphadenectomy. In all cases, two drainage tubes were placed posterior to the biliary and pancreatic anastomoses.

The selection of various pancreaticojejunal anastomotic techniques was based on pancreatic duct size and texture of the remnant pancreas. A duct-to-mucosa pancreaticojejunostomy was performed for patients with a hard pancreas and a dilated pancreatic duct (diameter $\geqslant$3 mm) (Figure 1). Posterior suture was achieved with 3-0 silk sutures between the posterior capsular parenchyma of the pancreatic remnant and the seromuscular layer of the jejunum. At the site for anastomosis to the main pancreatic duct, a small opening was made on the antimesenteric side of the jejunal wall according to the site and diameter of the pancreatic duct. Then anastomosis between the pancreatic duct and jejunum (all layers) was performed with 6-0 Prolene interrupted sutures at intervals of approximately 1 mm, from the posterior layer to the anterior layer, with all knots out of the anastomosis. Next, suture of the anterior side of the anastomosis between the pancreatic capsular parenchyma and the jejunal seromuscular layer was made by the same technique as used for the posterior side. No pancreatic duct drainage was used in cases undergoing duct-to-mucosa anastomotic technique (Figure 2). A traditional end-to-end or end-to-side invagination pancreaticojejunostomy was performed for patients with a soft pancreas and a non-dilated duct. The pancreas remnant was invaginated into the jejunum by about 2 cm, and two-layer sutures were performed interruptedly, with an internal duct stent tube inserted in the pancreatic duct.

Prophylactic use of somatostatin after PD was based on the experience of the surgeon and satisfactory degree of the anastomosis. Octreotide was used for 5-7 d postoperatively, 0.3 mg per d by subcutaneous injection.

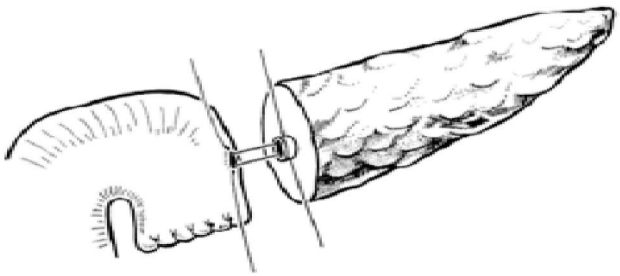

Figure 1 End-to-side duct-to-mucosa pancreaticojejunal anastomosis.

Study design and statistical analysis

Pancreaticojejunal anastomotic leakage was defined as: (1) discharge from the postpancreatic drain $\geqslant$50 mL/d after postoperative d 3, and (2) an amylase level of drainage fluid exceeding three times of the serum concentration.

Patients were divided into two groups according to the above criteria: 10 cases with postoperative pancreaticojejunal anastomotic leakage (leakage group) and 52 cases without leakage (nonleakage group). Seven general factors and six intraoperative clinical factors with the potential to affect the incidence of pancreaticojejunal anastomotic leakage were analyzed. Statistical computations were done with the SPSS10.0 software. Data were expressed as mean±SE, and percentage was used to express grouped data. The two groups were

first compared by the univariate statistical tests, *t*-test, rank sum test, χ^2 test or Fisher's exact test, when applicable (Tables 2 and 3). Logistic regression was then used to determine the effect of multiple factors on pancreatic leakage (Table 4). *P* less than 0.05 was considered statistically significant.

RESULTS

Complications

Of the 62 patients, 10 (16.1%) were identified as having pancreatic leakage after operation. Other major postoperative complications included delayed gastric emptying (eight patients), abdominal bleeding (four patients), abdominal abscess (three patients) and wound infection (two patients). Overall surgical morbidity was 43.5% (27/62). One patient died of massive abdominal hemorrhage associated with pancreatic fistula 10 d after operation, and two died of abdominal bleeding within 3 d after operation. The hospital mortality in this series was 4.84% (3/62), and the mortality associated with pancreatic fistula was 10% (1/10). One patient required reoperation because of abdominal bleeding, but no pancreaticojejunal anastomotic leakage was found in this patient.

Risk factors

General risk factors were compared for patients with or without pancreatic leakage (Table 2). Patient age, gender, history of jaundice, preoperative nutrition, pathological diagnosis and the length of postoperative stay were similar in the two groups. The incidence of pancreatic fistula was 20.7% (6/29) in the 29 patients who received the prophylactic use of octreotide treatment after surgery, compared to 12.1% (4/33) in the 33 patients who did not undergo somatostatin therapy, and no statistical difference was found in the two patient groups. Moreover, multivariate logistic regression analysis showed that none of these factors seemed to be associated with pancreatic fistula.

Two intraoperative risk factors were found to be significantly associated with pancreatic leakage: pancreatic duct size and texture of the remnant pancreas. The incidence of pancreatic leakage was 4.88% in patients with a pancreatic duct size greater than or equal to 3 mm, and was 38.1% in those with ducts smaller than 3 mm ($P = 0.002$). The pancreatic leakage rate was 2.94% in patients with a hard pancreas, and was 32.1% in those with a soft pancreas ($P = 0.004$). Operative time, blood loss and type of resection were similar in the two patient groups. The incidence of pancreatic leakage was 6.25% (1/16) in patients with duct-to-mucosa anastomosis, and was 19.6% (9/46) in those with traditional invagination anastomosis. Although the difference of pancreatic leakage between the two groups was obvious, no statistical significance was found. This may be due to the small number of patients with duct-to-mucosa anastomosis.

The three factors affecting pancreatic leakage were further analyzed by multivariate logistic regression. Both pancreatic duct size and texture of the remnant pancreas were demonstrated to be independent risk factors (Table 3). Patients with a small pancreatic duct or a soft pancreas were at high risk of pancreatic leakage.

Table 2 General risk factors for pancreatic leakage [*n* (%)]

Parameters	Leakage group (*n* = 12)	Nonleakage group (*n* = 45)	*P*
Age (yr)	59.8±10.04	57.1±11.37	0.487
Gender			0.166
Male	4 (10.5)[1]	34 (89.5)[1]	
Female	6 (25)[1]	18 (75)[1]	
History of jaundice			0.733
Yes	4 (13.3)[1]	26 (86.7)[1]	
No	6 (18.8)[1]	26 (81.2)[1]	
Preoperative serum-albumin			>0.95
Normal	10 (16.9)[1]	49 (83.1)[1]	
Low	0 (0)[1]	3 (100)[1]	
Pathology			0.312[2]
Pancreas cancer	3 (10.3)[1]	26 (89.7)[1]	
Ampullary cancer	3 (21.4)[1]	11 (78.6)[1]	
Bile duct cancer	3 (23.1)[1]	10 (76.9)[1]	
Islet cell tumor	1 (50)[1]	1 (50)[1]	
Duodenal cancer	0 (0)[1]	1 (100)[1]	
Chronic pancreatitis	0 (0)[1]	1 (100)[1]	
Pancreatic cystadenoma	0 (0)[1]	1 (100)[1]	
Gastric cancer	0 (0)	1 (100)	
Octreotide			0.493
Used	6 (20.7)[1]	23 (79.3)[1]	
Non-used	4 (12.1)[1]	29 (87.9)[1]	
Postoperative stay (d)	32.7±12.37	26.4±13.51	0.177

[1]Values in parentheses are percentages. [2]Pancreatic cancer *vs* non-pancreatic cancer.

Table 3 Intraoperative risk factors for pancreatic leakage [*n* (%)]

Parameters	Leakage group (*n* = 12)	Nonleakage group (*n* = 45)	*P*
Type of resection			0.629
PD	8 (15.1)[1]	45 (84.9)[1]	
PPPD	2 (22.2)[1]	7 (87.8)[1]	
Anastomotic technique			0.43
Duct-to-mucosa	1 (6.25)[1]	15 (93.75)[1]	
Invagination	9 (19.6)[1]	37 (80.4)[1]	
Pancreatic size (mm)			0.002
⩾3	2 (4.88)[1]	39 (95.12)[1]	
<3	8 (38.1)[1]	13 (61.9)[1]	
Pancreatic texture			0.004
Hard	1 (2.94)[1]	33 (97.06)[1]	
Soft	9 (32.1)[1]	19 (67.9)[1]	
Operative time (h)	7.05±2.40	6.34±2.02	0.325
Intraoperative blood loss (mL)[2]	400 (0, 1 250)	350 (0, 1 200)	0.352

[1]Values in parentheses are percentages. [2]Median (minimum, maximum).

Table 4 Multivariate logistic regression for pancreatic leakage

Parameters	*P*	Odds ratio	CI
Anastomotic technique			
Duct-to-mucosa	–	1	
Invagination	0.128	9.967	0.514-193.15
Pancreatic size (mm)			
⩾3	–	1	
<3	0.007	11.867	1.96-71.86
Pancreatic texture			
Hard	–	1	
Soft	0.017	15.445	1.629-146.46

CI: 95% confidence intervals.

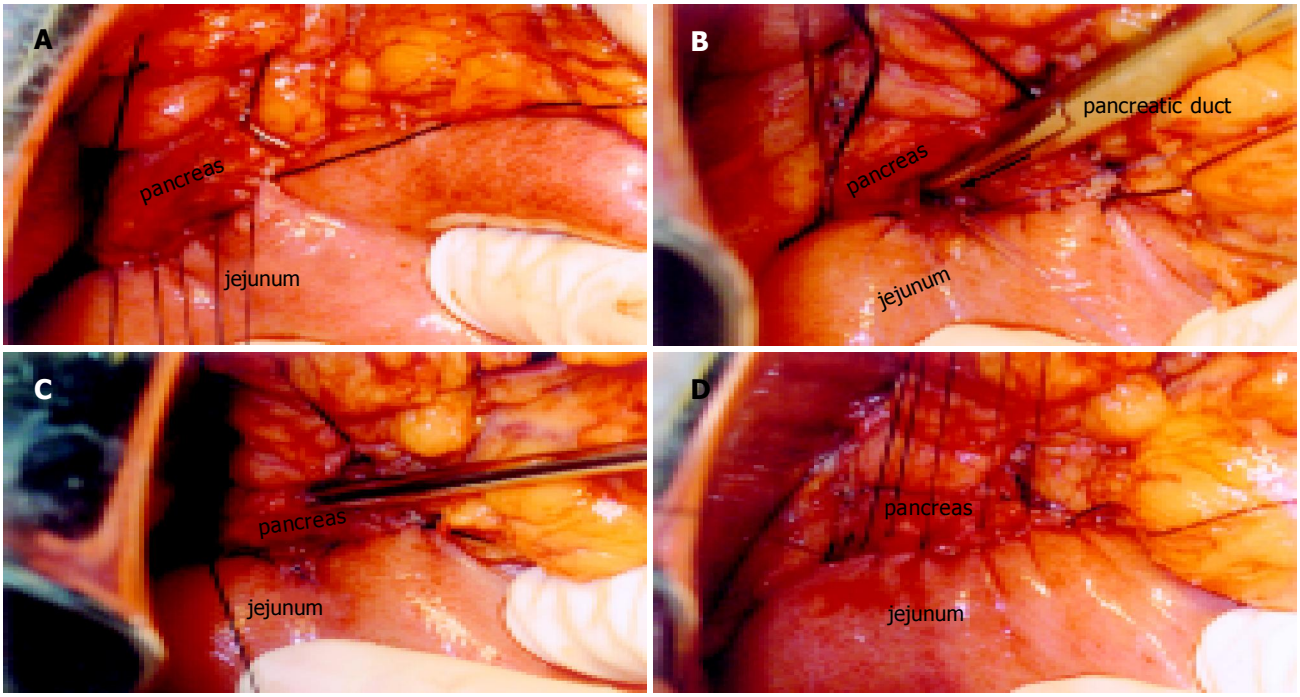

Figure 2 Duct-to-mucosa pancreaticojejunal anastomosis. **A**: Posterior suture with 3-0 silk sutures between posterior capsular parenchyma of the pancreatic remnant and the seromuscular layer of the jejunum. **B**: Posterior layer anastomosis with 6-0 Prolene interrupted sutures between the pancreatic duct and jejunum (all layers). **C**: Anterior layer anastomosis with 6-0 Prolene interrupted sutures between the pancreatic duct and jejunum. **D**: Anterior suture with 3-0 silk sutures between anterior interrupted sutures between the pancreatic duct and capsular parenchyma of the pancreatic remnant and the seromuscular layer of the jejunum.

Treatment and outcome

All the 10 patients who developed pancreatic leakage were diagnosed on the basis of the total amount and concentration of amylase in postpancreatic drainage exudate. One patient had abdominal massive hemorrhage, and two had abdominal abscess, the rest were successfully managed by conservative treatment. In five patients, a prolonged drainage duration for 4 wk after surgery was required. Octreotide was administered to five patients, including two with ineffective drains requiring another percutaneous drainage.

DISCUSSION

In recent years, PD has been used increasingly as a safe method of resection in patients with malignant and benign disorders of the pancreas and periampullary region. Although postoperative mortality has decreased significantly, the incidence of postoperative morbidity is still high. The overall surgical morbidity after PD was 43.5% (27/62), and the incidence of pancreatic leakage was 16.1% (10/62), similar to recent literature reports[6].

Risk factors for pancreatic anastomotic leakage after PD

Risk factors for pancreatic leakage include general factors (age, gender, jaundice, malnutrition), disease factors (pancreatic pathology, pancreatic texture, pancreatic duct size, pancreatic juice output) and procedure-related factors (operative time, resection type, anastomotic technique, intraoperative blood loss). In addition, surgeon experience has been shown to correlate with pancreatic anastomotic leakage rate, and prophylactic use of somatostatin has also been reported in recent literature to influence pancreatic leakage.

It has been widely accepted that a fibrotic pancreatic remnant in patients with chronic pancreatitis facilitates the pancreaticoenteric anastomosis, whereas a soft and friable pancreatic parenchyma makes the anastomosis difficult to perform. Yeo *et al*[10], found that there was a strong association between the pancreatic texture and pancreatic leakage. None of the 53 patients with hard pancreatic remnants developed pancreatic leakage, whereas 25% (19/75) of patients with soft pancreatic texture were complicated by pancreatic leakage. Hosotani *et al*[11], reviewed 161 patients who had undergone PD and reported a fistula rate of 11% (17/161), finding that pancreaticojejunostomy anastomotic technique, pancreatic texture and pancreatic duct size were substantial risk factors for pancreatic leakage after PD. In a study by Marcus *et al*[12], male sex was found to be a significant factor predisposing pancreatic fistula[15]. A recent study by Yeh *et al*[13], identified jaundice, creatinine clearance abnormality, and intraoperative blood loss as significant risk factors for leakage. Matsusue *et al*[14], found that advanced age (>70 years) was an adverse factor for pancreatic leakage.

Inhibition of exocrine pancreatic secretion may reduce the anastomotic fistula rate after PD. In recent years, more importance has been attached to prophylactic use of somatostatin after PD, but no consensus has been achieved. European studies found that prophylactic octreotide in pancreatic resection could reduce total morbidity rate or pancreatic fistula rate, though none of them demonstrated a decrease in the overall mortality rate[15-18]. In another report, a significantly lower pancreatic fistula rate was observed with the use of octreotide among patients who underwent distal pancreatectomy or local pancreatic resection, whereas no statistical difference was noted between octreotide and

placebo groups in patients who underwent PD[15]. Yeo *et al*[10], recently randomized 211 patients who underwent PD into saline control and octreotide groups. The pancreatic fistula rate in the octreotide group was 11%, and 9% in the control group. The authors concluded that prophylactic use of octreotide after PD could not reduce the pancreatic fistula rate[10]. Poon *et al*[19], studied the meta-analysis of six prospective randomized trials on the prophylactic use of octreotide in pancreatic resection and published them as full reports in the literature from January 1990 to December 2000. The meta-analysis did not show any beneficial effect of octreotide on pancreatic anastomotic leakage rate.

In this study, we analyzed 13 general or intraoperative factors. Two intraoperative factors were significantly associated with the risk of pancreatic leakage: pancreatic duct size and texture of the remnant pancreas. Multivariate analysis also revealed that the two factors turned out to be independent risk factors. Prophylactic use of octreotide after PD did not result in a decline of the pancreatic fistula rate.

Anastomotic techniques and pancreatic leakage

Management of the pancreatic remnant after PD is regarded as the key point to reduce pancreatic leakage. Various reconstruction techniques have been developed to diminish pancreatic fistulae, such as duct-to-mucosa pancreaticojejunostomy, invagination pancreaticojejunostomy, pancreaticogastrostomy, use of a transanastomotic stenting tube, and their modifications. Ligation or obliteration of the pancreatic duct has not been popularized as they abolish the pancreatic exocrine secretion, with still a high incidence of pancreatic leakage[20-22].

Reviewing various techniques of pancreaticojejunal anastomosis in the literatures published over the last decade, Poon *et al*[19], found that duct-to-mucosa anastomosis was a safer technique than invagination anastomosis. Marcus *et al*[12], found that duct-to-mucosa anastomosis was associated with a low pancreatic fistula rate in low-risk patients with a dilated pancreatic duct or a fibrotic pancreas, whereas end-to-end invagination technique was safer in high-risk patients with small ducts or a soft friable pancreas. Suzuki *et al*[23], selected various pancreaticojejunostomy techniques according to the pancreatic texture and duct size, and obtained an overall pancreatic leakage rate of 8% (4/50). All of the patients who developed pancreatic fistulae were all with a small duct and a soft pancreas. In that series, the incidence of pancreatic leakage rate was 6.25% in patients who underwent a duct-to-mucosa pancreaticojejunal anastomosis, compared to 19.6% in invagination group. The difference, of course, resulted from the variation of anastomotic techniques; while all of the patients who received the duct-to-mucosa anastomosis, on the other hand, were with a dilated pancreatic duct ($\geqslant$3 mm) or a soft pancreas. Therefore, both of the two factors might be associated with the discrepancy of the pancreatic leakage rate in the two groups.

There has been no conclusion as to whether a pancreatic duct stent for internal or external drainage can reduce the pancreatic leakage rate after PD. According to the authors who recommended it, a stent might help drain the pancreatic secretion juice from the anastomosis, and allow a more precise placement of sutures, thus protecting the pancreatic duct from injury and reducing fistula rate[24-27]. Some investigators found a few drawbacks to this method, such as accidental removal of the stent, obstruction or bending of the stenting tube, which might increase the incidence of pancreatic leakage. However, the overall pancreatic leakage rate in patients with a pancreatic stent was found to be similar to that in patients without a stent[28]. Therefore, as far as invagination anastomosis is concerned, it is safer to use an internal drainage stent for patients with a small pancreatic duct and a soft pancreas.

Appraisal of duct-to-mucosa pancreaticojejunal anastomosis

Duct-to-mucosa pancreaticojejunal anastomosis was first used by Cattel in 1943. This technique allows direct contact of the pancreatic duct with jejunal mucosa, preventing direct contact of pancreatic juice with the cut end of the pancreas and thus helping healing of the mucosa, protecting the anastomosis by embedding the pancreatic remnant under jejunal serosa. Therefore, duct-to-mucosa anastomosis is a theoretically more rational technique to avoid pancreatic fistulae. Since it is technically difficult to perform, duct-to-mucosa pancreaticojejunal anastomosis was previously recommended for patients with a dilated pancreatic duct, whereas in recent years this technique has been preferred regardless of the diameter of the pancreatic duct[11,29]. Hosotani *et al*[11], using multivariate analysis found that only pancreaticojejunal anastomosis technique turned out to be an independent risk factor and duct-to-mucosa anastomosis pancreaticojejunostomy reduced the risk of pancreatic leakage after PD (odds ratio = 4.15). In our hospital, invagination pancreaticojejunal anastomosis was performed for patients with either a dilated or a non-dilated pancreatic duct before 2000, with a consistent high pancreatic leakage rate. From 2000, duct-to-mucosa pancreaticojejunal anastomosis has been performed for patients with a dilated pancreatic duct, and the pancreaticojejunal anastomotic leakage rate has declined significantly when compared with previous invagination anastomosis, though no statistical difference was found in the present study.

Based on accumulated evidence so far, no conclusion could be drawn to appraise various anastomotic techniques, since most pertinent articles were retrospective studies. In prospective studies, most were not randomized controlled trials. On the other hand, anastomotic leakage rate is greatly related to the surgery technique and experience, which cannot be easily compared among different institutions. The need for a prospective randomized controlled trial by the same surgeons to evaluate various anastomotic techniques is highlighted. In conclusion, anastomotic techniques should be selected based on the status of the remnant pancreas intraoperatively: duct-to-mucosa anastomosis without a pancreatic duct stent for patients with a dilated pancreatic duct ($\geqslant$3 mm), and invagination anastomosis with an internal drainage stent for patients with a small pancreatic duct and a soft pancreas.

REFERENCES

1 **Neoptolemos JP,** Russell RC, Bramhall S, Theis B. Low mortality following resection for pancreatic and periampullary tumours in 1026 patients: UK survey of specialist pancreatic

units. UK Pancreatic Cancer Group. *Br J Surg* 1997; **84**: 1370-1376
2 **Bottger TC,** Junginger T. Factors influencing morbidity and mortality after pancreaticoduodenectomy: critical analysis of 221 resections. *World J Surg* 1999; **23**: 164-171; discussion 171-172
3 **Cameron JL,** Pitt HA, Yeo CJ, Lillemoe KD, Kaufman HS, Coleman J. One hundred and forty-five consecutive pancreaticoduodenectomies without mortality. *Ann Surg* 1993; **217**: 430-435; discussion 435-438
4 **Fernandez-del Castillo C,** Rattner DW, Warshaw AL. Standards for pancreatic resection in the 1990s. *Arch Surg* 1995; **130**: 295-299; discussion 299-300
5 **Jimenez RE,** Fernandez-del Castillo C, Rattner DW, Chang Y, Warshaw AL. Outcome of pancreaticoduodenectomy with pylorus preservation or with antrectomy in the treatment of chronic pancreatitis. *Ann Surg* 2000; **231**: 293-300
6 **Trede M,** Schwall G. The complications of pancreatectomy. *Ann Surg* 1988; **207**: 39-47
7 **Cullen JJ,** Sarr MG, Ilstrup DM. Pancreatic anastomotic leak after pancreaticoduodenectomy: incidence, significance, and management. *Am J Surg* 1994; **168**: 295-298
8 **Strasberg SM,** Drebin JA, Soper NJ. Evolution and current status of the Whipple procedure: an update for gastroenterologists. *Gastroenterology* 1997; **113**: 983-994
9 **van Berge Henegouwen MI,** De Wit LT, Van Gulik TM, Obertop H, Gouma DJ. Incidence, risk factors, and treatment of pancreatic leakage after pancreaticoduodenectomy: drainage versus resection of the pancreatic remnant. *J Am Coll Surg* 1997; **185**: 18-24
10 **Yeo CJ,** Cameron JL, Lillemoe KD, Sauter PK, Coleman J, Sohn TA, Campbell KA, Choti MA. Does prophylactic octreotide decrease the rates of pancreatic fistula and other complications after pancreaticoduodenectomy? Results of a prospective randomized placebo-controlled trial. *Ann Surg* 2000; **232**: 419-429
11 **Hosotani R**, Doi R, Imamura M. Duct-to-mucosa pancreaticojejunostomy reduces the risk of pancreatic leakage after pancreatoduodenectomy. *World J Surg* 2002; **26**: 99-104
12 **Marcus SG,** Cohen H, Ranson JH. Optimal management of the pancreatic remnant after pancreaticoduodenectomy. *Ann Surg* 1995; **221**: 635-645; discussion 645-648
13 **Yeh TS,** Jan YY, Jeng LB, Hwang TL, Wang CS, Chen SC, Chao TC, Chen MF. Pancreaticojejunal anastomotic leak after pancreaticoduodenectomy--multivariate analysis of perioperative risk factors. *J Surg Res* 1997; **67**: 119-125
14 **Matsusue S,** Takeda H, Nakamura Y, Nishimura S, Koizumi S. A prospective analysis of the factors influencing pancreaticojejunostomy performed using a single method, in 100 consecutive pancreaticoduodenectomies. *Surg Today* 1998; **28**: 719-726
15 **Montorsi M,** Zago M, Mosca F, Capussotti L, Zotti E, Ribotta G, Fegiz G, Fissi S, Roviaro G, Peracchia A. Efficacy of octreotide in the prevention of pancreatic fistula after elective pancreatic resections: a prospective, controlled, randomized clinical trial. *Surgery* 1995; **117**: 26-31
16 **Buchler M,** Friess H, Klempa I, Hermanek P, Sulkowski U, Becker H, Schafmayer A, Baca I, Lorenz D, Meister R. Role of octreotide in the prevention of postoperative complications following pancreatic resection. *Am J Surg* 1992; **163**: 125-130; discussion 130-131
17 **Friess H,** Beger HG, Sulkowski U, Becker H, Hofbauer B, Dennler HJ, Buchler MW. Randomized controlled multicentre study of the prevention of complications by octreotide in patients undergoing surgery for chronic pancreatitis. *Br J Surg* 1995; **82**: 1270-1273
18 **Pederzoli P,** Bassi C, Falconi M, Camboni MG. Efficacy of octreotide in the prevention of complications of elective pancreatic surgery. Italian Study Group. *Br J Surg* 1994; **81**: 265-269
19 **Poon RT,** Lo SH, Fong D, Fan ST, Wong J. Prevention of pancreatic anastomotic leakage after pancreaticoduodenectomy. *Am J Surg* 2002; **183**: 42-52
20 **Bartoli FG,** Arnone GB, Ravera G, Bachi V. Pancreatic fistula and relative mortality in malignant disease after pancreaticoduodenectomy. Review and statistical meta-analysis regarding 15 years of literature. *Anticancer Res* 1991; **11**: 1831-1848
21 **Marczell AP,** Stierer M. Partial pancreaticoduodenectomy (Whipple procedure) for pancreatic malignancy: occlusion of a non-anastomosed pancreatic stump with fibrin sealant. *HPB Surg* 1992; **5**: 251-259; discussion 259-260
22 **Di Carlo V,** Chiesa R, Pontiroli AE, Carlucci M, Staudacher C, Zerbi A, Cristallo M, Braga M, Pozza G. Pancreatoduodenectomy with occlusion of the residual stump by Neoprene injection. *World J Surg* 1989; **13**: 105-110; discussion 110-111
23 **Suzuki Y,** Fujino Y, Tanioka Y, Hiraoka K, Takada M, Ajiki T, Takeyama Y, Ku Y, Kuroda Y. Selection of pancreaticojejunostomy techniques according to pancreatic texture and duct size. *Arch Surg* 2002; **137**: 1044-1047; discussion 1048
24 **Hamanaka Y,** Suzuki T. Total pancreatic duct drainage for leakproof pancreatojejunostomy. *Surgery* 1994; **115**: 22-26
25 **Mok KT,** Wang BW, Liu SI. Management of pancreatic remnant with strategies according to the size of pancreatic duct after pancreaticoduodenectomy. *Br J Surg* 1999; **86**: 1018-1019
26 **Yoshimi F,** Ono H, Asato Y, Ohta T, Koizumi S, Amemiya R, Hasegawa H. Internal stenting of the hepaticojejunostomy and pancreaticojejunostomy in patients undergoing pancreatoduodenectomy to promote earlier discharge from hospital. *Surg Today* 1996; **26**: 665-667
27 **Roder JD,** Stein HJ, Bottcher KA, Busch R, Heidecke CD, Siewert JR. Stented versus nonstented pancreaticojejunostomy after pancreatoduodenectomy: a prospective study. *Ann Surg* 1999; **229**: 41-48
28 **Imaizumi T,** Harada N, Hatori T, Fukuda A, Takasaki K. Stenting is unnecessary in duct-to-mucosa pancreaticojejunostomy even in the normal pancreas. *Pancreatology* 2002; **2**: 116-121
29 **Howard JM.** Pancreatojejunostomy: leakage is a preventable complication of the Whipple resection. *J Am Coll Surg* 1997; **184**: 454-457

Science Editor Wang XL **Language Editor** Elsevier HK

PO Box 2345, Beijing 100023, China
www.wjgnet.com
wjg@wjgnet.com

ELSEVIER

World J Gastroenterol 2005;11(16):2462-2466
World Journal of Gastroenterology ISSN 1007-9327

• *CLINICAL RESEARCH*•

Characteristics and therapeutic efficacy of sulfasalazine in patients with mildly and moderately active ulcerative colitis

Qi-Kui Chen, Shi-Zheng Yuan, Zhuo-Fu Wen, Ying-Qiang Zhong, Cu-Jun Li, Hui-Sheng Wu, Can-Rong Mai, Peng-Yan Xie, Yu-Min Lu, Zhong-Lin Yu

Qi-Kui Chen, Shi-Zheng Yuan, Ying-Qiang Zhong, Department of Gastroenterology, The Second Affiliated Hospital, Sun Yat-Sen University, Guangzhou 510120, Guangdong Province, China
Zhuo-Fu Wen, The Third Affiliated Hospital, Sun Yat-Sen University, Guangzhou 510100, Guangdong Province, China
Cu-Jun Li, Department of Gastroenterology, The First Affiliated Hospital, Sun Yat-Sen University, Guangzhou 510089, Guangdong Province, China
Hui-Sheng Wu, Department of Gastroenterology, The First People's Hospital of Guangzhou City, Guangzhou 510033, Guangdong Province, China
Can-Rong Mai, Department of Gastroenterology, Peking Union Medical College Hospital, Beijing 100730, China
Peng-Yan Xie, Department of Gastroenterology, The First Hospital, Beijing University, Beijing 100034, China
Yu-Min Lu, Department of Gastroenterology, The Third Hospital, Beijing University, Beijing 100083, China
Zhong-Lin Yu, Department of Gastroenterology, Beijing Friendship Hospital, Capital University of Medical Science, Beijing 100050, China
Correspondence to: Dr. Qi-Kui Chen, Department of Gastroenterology, The Second Affiliated Hospital, Sun Yat-Sen University,107 West Yanjiang Road, Guangzhou 510120, Guangdong Province, China. qkchen@21cn.com
Telephone: +86-20-81332598 Fax: +86-20-81332244
Received: 2004-02-02 Accepted: 2004-02-24

Abstract

AIM: To investigate the characteristics and short-term efficacy of sulfasalazine (SASP) in patients with mildly and moderately active ulcerative colitis (UC).

METHODS: Two hundred and twenty-eight patients with mildly and moderately active UC were recruited, 106 patients in 1993-1995, and 122 patients in 2000-2002, they were assigned as the 1990s group (n = 106) and the 2000s group (n = 122), prospectively. The general characteristics, clinical manifestations, colonoscopic and histological data were compared between the two groups. The short-term efficacy and safety of SASP 3 g per d were evaluated.

RESULTS: Between 2000s and 1990s groups, the gender ratio of men to women was 1:1.18 and 1:1.04, 57.4% and 50.9% of the patients were between 30 and 49 years old. The gender ratio and age of UC patients were not significantly different. The total course of 50.0% and 37.1% of UC patients was less than 1 year (P<0.05), 10.6% and 31.2% of the cases had a duration of more than 5 years (P<0.05) in 2000s and 1990s groups, respectively. The most common clinical type was first episode in 2000s group and chronic relapse in 1990s group. The patients showed a higher frequency of abdominal pain and tenderness in 1990s group than in 2000s group. Erosions were found in 84.4% and 67.9% of patients in 2000s and 1990s groups (P<0.05). Rough and granular mucosa (67.9% *vs* 43.4%, P<0.05) and polyps (47.2% *vs* 32.8%, P<0.05) were identified in 1990s group more than in 2000s group. There were no significant differences in clinical, colonoscopic and histological classifications. After SASP (1 g thrice per d) treatment for 6 wk, the clinical, colonoscopic and histological remission rates were 71.8%, 21.8% and 16.4%, respectively. In 79 patients with clinical remission, 58.2% and 67.1% remained grade 1 in colonoscopic and histological findings, respectively. The overall effects in first episode type (complete remission in 10, 18.9%, partial remission in 28, 52.8%, and improvement in 9, 17.0%) were better than in chronic relapse type (complete remission in 3, 7.5%; partial remission in 16, 40.0%; and improvement in 15, 37.5%) and chronic persistent type (complete remission in 1, 5.9%; partial remission in 6, 35.3%; and improvement in 6, 35.3%) respectively (P<0.05). In 110 patients treated with SASP, 18 patients (16.4%) had adverse reactions. Except for two cases of urticaria and one case of WBC decrease, none of the patients had to stop the treatment because of severe adverse reactions.

CONCLUSION: Patients with mildly and moderately active UC in 2000s group had a shorter disease course, milder clinical manifestations, more first episode type and higher frequency of acute mucosal lesions in colonoscopy than in 1990s group. The patients in 1990s group had higher proportion of chronic relapse type and chronic mucosal change in colonoscopy than in 2000s group. The short-term efficacy of SASP could be mainly remission of clinical manifestations. But more than half of the patients still had light inflammation in colonoscopy and histology. The overall effects of SASP in first episode type were better than those in other types. SASP was a safe and effective drug to treat mildly and moderately active UC.

Key words: Sulfasalazine; Ulcerative colitis; Pharmacodynamics

Chen QK, Yuan SZ, Wen ZF, Zhong YQ, Li CJ, Wu HS, Mai CR, Xie PY, Lu YM, Yu ZL. Characteristics and therapeutic efficacy of sulfasalazine in patients with mildly and moderately active ulcerative colitis. *World J Gastroenterol* 2005; 11 (16): 2462-2466
http://www.wjgnet.com/1007-9327/11/2462.asp

INTRODUCTION

Ulcerative colitis (UC) is a common disease in countries of Northern America and Europe. The incidence and modality of UC might vary greatly across the world[1-7]. China is an area with relatively low incidence of UC. With the changes of lifestyle and environmental factors, patients with UC have increased persistently and UC has become one of the most common causes of chronic diarrhea. The aim of this study was to compare the differences of the general characteristics, clinical manifestations, colonoscopic and histological involvements between patients in 1993-1995 and in 2000-2002, and investigate short-term efficacy and safety of sulfasalazine (SASP) in patients with mildly and moderately active UC.

MATERIALS AND METHODS

Patients

Two hundred and twenty-eight patients with mildly and moderately active UC were collected according to the criteria of diagnosis and treatment issued by National Symposium of Chronic and Non-infectious Intestinal Diseases of Taiyuan in 1993[8]. All patients were diagnosed with colonoscopy. There were 108 male patients and 120 female patients. The mean age was 41.3±12.4 years (range 18-65 years).

Methods

The data of 228 patients were collected in The Second and First Affiliated Hospital of Sun Yat-Sen University; The First People's Hospital of Guangzhou City; Peking Union Medical College Hospital; First and Third Hospital of Peking University and Beijing Friendship Hospital of Capital University of Medical Science. One hundred and six patients were from 1993-1995, and 122 patients from 2000-2002, they were assigned as the 1990s group and the 2000s group, respectively. The general characteristics, clinical manifestations, laboratory results, colonoscopic and histological involvements were compared between the two groups. The stool bacterial culture and amebic examination were carried out for 3 d continuously to exclude bacterial and amebic infection. The patients had not received any medical treatment for UC 1 mo prior to enrollment.

The activity index (AI) of the diseases was quantified by the scoring system of Seo[9,10]: $AI = 60X_1+13X_2+0.5X_3-0.4X_4-1.5X_5+200$. In this system, X_1 = the extent of bloody stools ($X_1 = 0$, no bloody stool; $X_1 = 1$, obvious bloody stool), X_2 = times of stool per day, X_3 = ESK, X_4 = hemoglobin, X_5 = serum albumin. AI values below 150, values between 150 and 220, and values above 220 corresponded to grades 1-3 of clinical classification. The colonoscopic classification was graded according to the criteria by Baron[11]. In this system, 0 = normal mucosa, 1 = congestive edema and loss of vascular pattern of mucosa, 2 = mucosal friability and bleeding contacted, 3 = mucosal bleeding spontaneously, 4 = mucosal ulceration. The pathological diagnosis and classification were scored according to the criteria by Truelove and Richards[12]: 0 = no neutrophil infiltration in the lamina propria of mucosa, 1 = neutrophil infiltration (<10/HP), 2 = neutrophil infiltration (10-50/HP) with more than 50% of crypt involved, 3 = neutrophil infiltration (>50/HP) with crypt abscesses, 4 = acute inflammation and ulceration.

Therapeutic protocol

One hundred and ten patients were included in the therapeutic protocol of SASP (1 g, thrice a day) for 6 wk. The clinical types of 110 patients were first episode (n = 53), chronic relapse (n = 40) and chronic persistent (n = 17). Fifty-three patients were in 1990s group and 57 patients in 2000s group, respectively. The clinical remission meant the absence of clinical manifestations, less than twice of soft and shaped stool per day normalization of hemoglobin, ESR and serum albumin. The overall effects of UC patients treated with SASP were evaluated according to complete remission, partial remission, improvement and inefficiency. Complete remission meant that clinical and colonoscopic classifications became grade 0 and that histological classification was not more than 1 score. Partial remission showed that clinical classification was grade 0 and that colonoscopic and histological classifications were improved more than 1 score. Improvement meant that one of clinical or colonoscopic or histological classification was improved more than 1 score. Adverse reactions were recorded simultaneously.

Statistical analysis

All data were analyzed with SPSS 10.0/PC statistical package. The frequency was compared by the χ^2 test. The rank data were compared with Ridit test.

RESULTS

Patients' characteristics

Among 228 patients with mildly and moderately active UC, the gender ratio (M/F) was 1∶1.18 and 1∶1.04 in 2000s and 1990s groups (P>0.05), respectively. The distribution of age, course of the illness and clinical types of mildly and moderately active UC are shown in Tables 1 and 2.

Table 1 Distribution of age and course of the illness

Age and course		2000s group n (%)	1990s group n (%)
Age (yr)	<30	21 (17.2)	19 (17.9)
	30-	31 (25.4)	33 (31.1)
	40-	39 (32.0)	21 (19.8)
	50-	14 (11.5)	21 (19.8)
	60-	17 (13.9)	12 (11.3)
Total course of the illness (yr)	<1.0	61 (50.0)[a]	33 (31.7)
	1.0-	48 (39.3)	40 (37.7)
	5.0-	6 (4.9)[a]	18 (17.0)
	10.0-	7 (5.7)[a]	15 (17.0)
Course of present flare-up (yr)	<0.5	85 (69.7)	71 (67.0)
	0.5-	20 (16.4)	17 (16.0)
	1.0-	17 (13.9)	18 (17.0)

[a]P<0.05 *vs* 1990s group.

Clinical manifestations

The major clinical manifestations were abdominal discomfort

(59.8% *vs* 69.8, *P*>0.05), abdominal pain (57.4% *vs* 71.2%, *P*<0.05), tenesmus (40.0% *vs* 50.0%, *P*>0.05), abdominal tenderness (32.8% *vs* 46.2%, *P*<0.05), abdominal distention (28.7% *vs* 31.1%, *P*>0.05) between patients in 2000s and 1990s group. The changes of stool frequency and property are shown in Table 3.

Table 2 Clinical types of the illness

Type of the illness	2000s group *n* (%)	1990s group *n* (%)
First episode	62 (50.8)[a]	37 (34.9)
Chronic relapse	38 (31.0)[a]	60 (56.6)
Chronic persistent	22 (18.1)	9 (8.5)

[a]*P*<0.05 *vs* 1990s group.

Table 3 Frequency and property of stool

Frequency of stool and property		2000s group *n* (%)	1990s group *n* (%)
Frequency of stool	<21	53 (43.4)	40 (37.7)
(times per week)	21-	57 (46.2)	48 (45.5)
	42-	12 (9.8)	18 (17)
Property of stool	Nonmucous and bloody stool	36 (29.5)	27 (25.5)
	Slight mucous and bloody stool	43 (35.2)	30 (28.3)
	Slight mucous and bloody stool	43 (35.2)	49 (46.2)

Colonoscopic findings

The types of lesions of the patients included proctitis (29.5% *vs* 21.7%, *P*>0.05), left-sided colitis (48.4%% *vs* 61.3%, *P*>0.05), extensive colitis (18.9% *vs* 17.0%, *P*>0.05) and local colitis (3.3% *vs* 0%, *P*>0.05) in 2000s group and 1990s group, respectively. The colonoscopic findings were congestive edema (98.4% *vs* 98.1%, *P*>0.05), erosion (84.4% *vs* 67.9%,*P*<0.05), mucosal friability and bleeding contacted (90.2% *vs* 88.7%, *P*>0.05), rough and granular mucosa (43.4% *vs* 67.9%,*P*<0.05), ulceration (59.8% *vs* 48.1%, *P*>0.05), purulent secretion (20.5% *vs* 27.4%, *P*>0.05), spontaneous bleeding (72.1% *vs* 83%, *P*>0.05) and polyps (32.8% *vs* 47.2%, *P*<0.05) in 2000s group and 1990s group, respectively.

Clinical, colonoscopic and histological classifications

Clinical, colonoscopic and histological classifications at diagnosis are shown in Table 4. There were no significant differences in classifications between 2000s and 1990s groups.

Table 4 Clinical, colonoscopic and histological classifications

Classifications	Clinical *n* (%)		Colonoscopic *n* (%)		Histological *n* (%)	
	2000s group	1990s group	1990s group	2000s group	2000s group	1990s group
Grade 1	64 (52.5)	41 (38.7)	25 (20.5)	10 (9.4)	25 (20.5)	14 (13.3)
Rade 2	53 (43.4)	57 (53.8)	46 (37.7)	36 (34.0)	46 (37.7)	33 (31.1)
Grade 3	5 (4.1)	8 (7.5)	37 (30.3)	11 (10.4)	39 (32.)	40 (37.7)
Grade 4			14 (11.5)	49 (46.2)	12 (9.8)	19 (17)

Comparison of clinical, colonoscopic and histological classifications before and after treatment with SASP

The short-term efficacy of SASP in 110 patients with mildly and moderately active UC is shown in Table 5. In 79 patients of clinical remission, only 21 (26.6%) and 14 (17.7%) of cases were grade 0, most of the patients (58.2% and 67.1%) remained grade 1 by colonoscopic and histological examination.

Table 5 Comparison of clinical, colonoscopic and histological classifications before and after treatment with SASP in 110 patients

Classification	Clinical *n* (%)		Colonoscopic *n* (%)		Histological *n* (%)	
	Before	After	Before	After	Before	After
Grade 0	0	79 (71.8)	0	24 (21.8)	0	18 (16.4)
Grade 1	56 (50.9)	27 (24.6)	7 (6.4)	56 (50.9)	21 (19.1)	67 (60.9)
Grade≥2	54 (49.1)	4 (3.6)	103 (93.6)	30 (27.3)	89 (80.9)	25 (22.7)
P	<0.01		<0.01		<0.01	

Comparison of efficacy between UC patients with different types of the illness treated with SASP

The comparison of efficacy between the patients with different types of the illness treated with SASP is shown in Table 6. There were significant differences among first episode, chronic relapse and chronic persistent types (*P*<0.01).

Table 6 Comparison of efficacy in the patients with different types of the illness treated with SASP

The overall effects	First episode *n* (%)	Chronic relapse *n* (%)	Chronic persistent *n* (%)
Complete remission	10 (18.9)	3 (7.5)	1 (5.9)
Partial remission	28 (52.8)	16 (40.0)	6 (35.3)
Improvement	9 (17.0)	15 (37.5)	6 (35.3)
Inefficiency	6 (11.3)	6 (15.0)	4 (23.5)
P		<0.05	

Adverse reactions of SASP

In 110 patients treated with SASP, 18 of them (16.4%) had one or more than one kind of adverse reactions: two patients had urticaria, three fever, five dizziness, four nausea, six anorexia, one fatigue, one WBC decrease, four AST increase and three ALT increase. Except for the cases with urticaria and WBC decrease, none of the patients had to stop the treatment because of severe adverse reactions.

DISCUSSION

UC is a chronic inflammatory bowel disease (IBD) of unknown etiology. In European countries, the overall incidence was 10.4 per 100 000 between ages 15 and 64 years old[13]. UC was found mainly in male patients at ages of 25-34 years. The number of UC patients doubled every 10 years in countries of high prevalence. The incidence of UC may vary greatly across world[1,2,13,14]. The epidemiological investigation based on population was not reported in China. But the cases of UC reported were greatly increased over the last 10 years[15]. UC has become one common cause of

chronic diarrhea in China.

Although an accurate diagnosis of IBD and differentiation between UC and Crohn's disease are sometimes difficult even after thorough pathological study, severe UC is diagnosed easily[16]. Mildly and moderately active UC are difficult to identify because of non-specific clinical and colonoscopic findings. Varied geographical, climate, social, environmental, psychological and genetic factors may affect the incidence of UC[17-21]. China, a geographical area with the characteristics of the sub-tropics, has a lower prevalence of UC. There are few data on mildly and moderately active UC.

In this study, the gender ratio (M/F) was smaller in 2000s group than in 1990s group, but there was no significant difference. The peak age range was 30-49 years old, accounting for with 57.4% and 50.9% of the patients in 2000s group and 1990s group, respectively. It suggested that the susceptible populations could be middle-aged women. The total course of 50.0% and 37.1% of the patients was less than 1 year in 2000s group and 1990s group, but the total course of 10.6% and 37.1% of the patients was more than 5 years in 2000s group and 1990s group. There were more patients with abdominal pain and tenderness in 1990s group than in 2000s group. It suggested that the total course of UC might be shorter and that the extent of disease was lighter in 2000s group than in 1990s group. The clinical type of UC was mainly first episode in 2000s group and chronic relapse in 1990s group. It showed that UC patients were diagnosed earlier in recent years.

The patients with less than 21 times of stool per week accounted for 43.4% and 37.7%, but more patients (70.4% and 73.6%) were found to have bloody stool in 2000s group and 1990s group. The low frequent and mucous and bloody stool was characteristic of diarrhea of the patients with mildly and moderately active UC in this study. In clinical, colonoscopic and histological classifications, no significant differences were found in patients between 2000s and 1990s group.

Colonoscopic distribution of lesions in 2000s and 1990s group showed that 77.9% and 83.0% were found in leftside colon, and extensive colitis was found in 18.9% and 17.0% of the patients. Although mucosal edema and loss of vascular pattern were the most common colonoscopic findings, they had limited diagnostic values[22,23]. The frequency of mucosal erosions in 2000s group was higher than in 1990s group. However, more mucosal granularity and polyps were found in 1990s group than in 2000s group. The mucosal granularity and polyps were helpful to diagnose chronic relapse of UC. It showed that the patients had a higher proportion of chronic change in 1990s group than in 2000s group, and that the patients had a higher frequency of acute lesions in 2000s group than in 1990s group.

SASP is one of classic and commonly used medicine in treatment of mildly and moderately active UC[24,25]. In this study, short-term efficacy of SASP on mildly and moderately active UC showed obvious improvement of clinical manifestations, and relatively low remission of colonoscopic appearances and histological involvements. Light inflammatory changes were found in most of the patients, which corresponded to researches before. Therefore, the therapy of mildly and moderately active UC with SASP as with 5-aminosalicylic acid needs a long course[26-29].

Study showed that the overall effects of SASP on mildly and moderately active UC depended upon different clinical types of the illness. The overall effects of SASP in first episode type were better than those in chronic relapse type and in chronic persistent type. Because of its short-term efficacy, safety and inexpensiveness, SASP still is one of the common drugs for treatment of mildly and moderately active UC in China.

REFERENCES

1 **Yang SK,** Loftus EV, Sandborn WJ. Epidemiology of inflammatory bowel disease in Asia. *Inflamm Bowel Dis* 2001; **7**:260-270

2 **Stone MA,** Mayberry JF, Baker R. Prevalence and management of inflammatory bowel disease: a cross-sectional study from central England. *Eur J Gastroenterol Hepatol* 2003; **15**: 1275-1280

3 **Bernstein CN,** Blanchard JF, Rawsthorne P, Wajda A. Epidemiology of Crohn's disease and ulcerative colitis in a central Canadian province: a population-based study. *Am J Epidemiol* 1999; **149**: 916-924

4 **Probert CS,** Jayanthi V, Rampton DS, Mayberry JF. Epidemiology of inflammatory bowel disease in different ethnic and religious groups: limitations and aetiological clues. *Int J Colorectal Dis* 1996; **11**: 25-28

5 **Sonnenberg A.** Geographic variation in the incidence of and mortality from inflammatory bowel disease. *Dis Colon Rectum* 1986; **29**: 854-861

6 **Blanchard JF,** Bernstein CN, Wajda A, Rawsthorne P. Small-area variations and sociodemographic correlates for the incidence of Crohn's disease and ulcerative colitis. *Am J Epidemiol* 2001; **154**: 328-335

7 **Levenstein S,** Prantera C, Varvo V, Scribano ML, Andreoli A, Luzi C, Arca M, Berto E, Milite G, Marcheggiano A. Stress and exacerbation in ulcerative colitis: a prospective study of patients enrolled in remission. *Am J Gastroenterol* 2000; **95**: 1213-1220

8 National Symposium of Chronic and Non-infectious Intestinal Diseases. The criteria of diagnosis and treatment of inflammatory bowel disease. *Zhonghua Xiaohua Zazhi* 1993; **13**: 354

9 **Seo M,** Okada M, Yao T, Ueki M, Arima S, Okumura M. An index of disease activity in patients with ulcerative colitis. *Am J Gastroenterol* 1992; **87**: 971-976

10 **Seo M,** Okada M, Yao T, Okabe N, Maeda K, Oh K. Evaluation of disease activity in patients with moderately active ulcerative colitis: comparisons between a new activity index and Truelove and Witts' classification. *Am J Gastroenterol* 1995; **90**: 1759-1763

11 **Baron JH,** Connell AM, Lennard-Jones JE. Variation between observers in describing mucosal appearances in proctocolitis. *Br Med J* 1964; **1**: 89-92

12 **Truelove SC,** Richards WC. Biopsy studies in ulcerative colitis. *Br Med J* 1956; **1**: 1315-1318

13 **Shivananda S,** Lennard-Jones J, Logan R, Fear N, Price A, Carpenter L, van Blankenstein M. Incidence of inflammatory bowel disease across Europe: is there a difference between north and south? Results of the European Collaborative Study on Inflammatory Bowel Disease(EC-IBD). *Gut* 1996; **39**: 690-697

14 **Rutgeerts P.** A critical assessment of new therapies in inflammatory bowel disease. *J Gastroenterol Hepatol* 2002; **17** Suppl: S176-S185

15 **Jiang ZL,** Cui HF. Features of ulcerative colitis in China: an analysis 10218 cases. *Shijie Huaren Xiaohua Zazhi* 2001; **9**: 869-873

16 **Matsui T,** Yao T, Sakurai T, Yao K, Hirai F, Matake H, Tsuda S, Wada Y, Iwashita A, Kamachi S. Clinical features and pattern of indeterminate colitis: Crohn's disease with ulcer-

ative colitis-like clinical presentation. *J Gastroenterol* 2003; **38**: 647-655

17 **Farrokhyar F,** Swarbrick ET, Grace RH, Hellier MD, Gent AE, Irvine EJ. Low mortality in ulcerative colitis and Crohn's disease in three regional centers in England. *Am J Gastroenterol* 2001; **96**: 501-507

18 **Lewis** JD**,** Aberra FN, Lichtenstein GR, Bilker WB, Brensinger C, Strom BL. Seasonal variation in flares of inflammatory bowel disease. *Gastroenterology* 2004; **126**: 665-673

19 **Rubin GP,** Hungin AP, Chinn DJ, Dwarakanath D. Quality of life in patients with established inflammatory bowel disease: a UK general practice survey. *Aliment Pharmacol Ther* 2004; **19**: 529-535

20 **Jowett SL,** Seal CJ, Phillips E, Gregory W, Barton JR, Welfare MR. Dietary beliefs of people with ulcerative colitis and their effect on relapse and nutrient intake. *Clin Nutr* 2004; **23**: 161-170

21 **Halme L,** Turunen U, Helio T, Paavola P, Walle T, Miettinen A, Jarvinen H, Kontula K, Farkkila M. Familial and sporadic inflammatory bowel disease: comparison of clinical features and serological markers in a genetically homogeneous population. *Scand J Gastroenterol* 2002; **37**: 692-698

22 **Moum B,** Ekbom A, Vatn MH, Elgjo K. Change in the extent of colonoscopic and histological involvement in ulcerative colitis over time. *Am J Gastroenterol* 1999; **94**: 1564-1569

23 **Bitton A,** Peppercorn MA, Antonioli DA, Niles JL, Shah S, Bousvaros A, Ransil B, Wild G, Cohen A, Edwardes MD, Stevens AC. Clinical, biological, and histologic parameters as predictors of relapse in ulcerative colitis. *Gastroenterology* 2001; **120**: 13-20

24 **Sutherland LR,** May GR, Shaffer EA. Sulfasalazine revisited: a meta-analysis of 5-aminosalicylic acid in the treatment of ulcerative colitis. *Ann Intern Med* 1993 ; **118**: 540-549

25 **Muijsers RB,** Goa KL. Balsalazide: a review of its therapeutic use in mild-to-moderate ulcerative colitis. *Drugs* 2002; **62**: 1689-1705

26 **LaRosa D,** Rubin PH, Bodian C, Present DH. Maintenance oral sulfasalazine prolongs remission in ulcerative proctitis and proctosigmoiditis. *Am J Gastroenterol* 1991; **86**: 1456-1460

27 **Feagan BG.** Maintenance therapy for inflammatory bowel disease. *Am J Gastroenterol* 2003; **98**: S6-S17

28 **Green JR,** Swan CH, Gibson JA, Kerr GD, Swarbrick ET, Thornton PC. Patient-led variable dosing with balsalazide as long-term therapy for maintenance in ulcerative colitis: a 3-year prospective observational study. *Aliment Pharmacol Ther* 2004; **19**: 435-442

29 **Piodi LP,** Ulivieri FM, Cermesoni L, Cesana BM. Long-term intermittent treatment with low-dose 5-aminosalicylic enemas is efficacious for remission maintenance in ulcerative colitis. *Scand J Gastroenterol* 2004; **39**: 154-157

Science Editor Zhu LH **Language Editor** Elsevier HK

PO Box 2345, Beijing 100023, China
www.wjgnet.com
wjg@wjgnet.com

ELSEVIER

World J Gastroenterol 2005;11(16):2467-2471
World Journal of Gastroenterology ISSN 1007-9327

• *CLINICAL RESEARCH* •

Extended radical operation of pancreatic head cancer: Appraisal of its clinical significance

De-Qing Mu, Shu-You Peng, Guo-Feng Wang

De-Qing Mu, Shu-You Peng, Department of Surgery, Second Affiliated Hospital, Medical College of Zhejiang University, Hangzhou 310009, Zhejiang Province, China
Guo-Feng Wang, Department of Pathology, Second Affiliated Hospital, Medical College of Zhejiang University, Hangzhou 310009, Zhejiang Province, China
Correspondence to: De-Qing Mu, Department of Surgery, Second Affiliated Hospital, Medical College of Zhejiang University, Hangzhou 310009, Zhejiang Province, China. samier-1969@163.com
Telephone: +86-571-87783762
Received: 2003-03-04 Accepted: 2003-04-01

Abstract

AIM: To evaluate the significance of extended radical operation and its indications.

METHODS: Between January 1995 and December 1998, 56 inpatients with pancreatic head cancer received operation. Among them 35 patients (group 1) experienced the Whipple operation, and 21 patients (group 2) received the extended radical operation. The 1-, 2-, 3-year cumulative survival rates were used to evaluate the efficacy of the two operative procedures. Clinical stage (CS) was assessed retrospectively with the help of CT. The indications for extended radical operation were discussed.

RESULTS: There was no difference in hospital mortality and morbidity rates. Whereas the 1-, 2-, 3-year cumulative survival rates were 84.8%, 62.8%, 39.9% in the extended radical operation group, and were 70.8%, 47.6%, 17.2% in the Whipple operation group, there was a significant difference between the two groups ($P<0.001$, $P<0.001$, $P<0.001$, respectively). Most of the deaths within 3 years after operation were due to recurrence in the two groups. However, the 1-, 2-, 3-year cumulative rates of death due to local recurrence were decreased from 37.4% in patients that received the Whipple procedure to 23.8% in those who received by extended radical operation. Patients who survived for more than 3 years were only noted in those with CS1 in the Whipple procedure group and were founded in cases with CS1, CS2 and part of CS3 in the extended radical operation group.

CONCLUSION: The extended radical operation appears to benefit patients with pancreatic head carcinoma which was indicated in CS1, CS2 and part of CS3 without severe invasion.

Key words: Radical operation; Pancreatic head cancer

Mu DQ, Peng SY, Wang GF. Extended radical operation of pancreatic head cancer: Appraisal of its clinical significance. *World J Gastroenterol* 2005; 11(16): 2467-2471
http://www.wjgnet.com/1007-9327/11/2467.asp

INTRODUCTION

Although surgical resection is the only approach that can offer a possibility of cure for pancreatic cancer, however, the prognosis after curative resection continues to be the worst of the gastrointestinal neoplasms, there have been many controversies about whether extended radical resection is worthwhile or not compared with the Whipple procedure[1-3]. In the present study, an attempt was made to evaluate the effectiveness of extended radical operation in the treatment of pancreatic head cancer in comparison with the Whipple procedure and to discuss its indications.

MATERIALS AND METHODS

Patients

A total of 56 patients with pancreatic head carcinoma were admitted to our Department from January 1995 to December 1998. Among them 39 were males and 17 females with an average age of 57.8 years (range 46-71years). The patients did not receive any anticancer therapy before and after operation.

Methods

We performed the Whipple operation (Group I) and extended radical operation (Group II), respectively. In Group I, men/women were 2.2:1 with a median age of 57.3±4.6 years; in Group II men/women were 2.5:1 with a median age of 58.9±5 years. Lymphatic clearance in Group I was limited to that located directly adjacent to the pancreatic head. In the pancreas, the pancreatic resection line was on the left border of the superior mesenteric vein. In the subjects of Group II, the lymph node clearance was performed by dissection of N1 and N2 groups along with a proper clearance of N3 group and neighboring connective tissue clearance (Figures 1A and B). Among these nerve-plexuses resection around the retroperitoneum was conducted in 13 cases, resection and reconstruction of the portal-vein system were performed in 6 cases, and resection of the common hepatic artery or superior mesenteric artery was carried out in four patients. The resection line for pancreatic tissues was 1-2 cm from the left border of the aorta.

The clinical stage (CS) for all enrolled patients was assessed retrospectively by two independent and experienced examiners

according to the maximal tumor size (T), retropancreatic invasion (Rp), portal-vein invasion (PV), and arterial (hepatic, celiac, or superior mesenteric artery) invasion from preoperative diagnostic images such as computed tomography (CT) scan and abdominal selective angiogram. Based on assessments of these four factors on a four-grade scale, the disease was classified in one of the four CS, using the following criteria: T1 0-2 cm, T2 2.1-4 cm, T3 4.1-6 cm,T4 >6 cm; Rp0 normal retropancreatic tissue on CT scan, Rp1 slight speculation in retropancreatic tissue, Rp2 limited invasion, Rp3 severe invasion; PV0 normal appearance of portal-vein, PV1 mild irregularity or rigidity of portal-vein, PV2 moderate irregularity of portal-vein, PV3 severe irregularity or stenosis of the portal-vein; A0 normal appearance of the major arteries, A1 mild displacement or rigidity of the major arteries, A2 moderate displacement or irregularity of the major arteries, A3 stenosis of a major artery.

CS1 T1, Rpo, PVo,A0-1.CS2 T1-2, Rp1, PV1, A0-1.CS3 T2-3 Rp2, PV2, A1-2.CS4 T3-4, Rp2-3, PV2-3, A2-3

The maximal size was verified postoperatively and accessed with the same staging method as that used in CT image staging. Retroperitoneal invasion was divided into 'interstitial invasion' and lymph node involvement, interstitial invasion includes lymphatic vessel, neural, and soft tissue invasion. Presence or absence of vascular invasion was recorded as 'positive' or 'negative'. All findings of CT images were compared with pathological results. The resected specimens were in turn fixed in 40 g/L formaldehyde solution, sliced into 5 μm sections, stained with hematoxylin and eosin, and examined with light microscope.

All patients were followed up postoperation and surveyed every 6 mo by systemic medical check-up including determinations of plasma carcinoembryonic antigen and CA19-9, ultrasonography and CT to make sure whether and where cancer recurrence developed. The tumor relapse was grossly classified as local, distant, or both according to the site of recurrence. Local recurrence was defined as a recurrent tumor mass within the tumor bed, while the distant recurrence was classified as hepatic metastasis and peritoneal dissemination.

The cumulative survival rate was calculated by a life table method. Statistical analysis was performed by using t and χ^2 test. P value less than 0.05 was considered statistically significant.

RESULTS

Operative deaths were defined as those occurred within 30 d after operation. Hospital morbidity and mortality were 12.5% and 0% in group I and 14% and 0% in group II, respectively. There were no differences between the two groups. These data indicated that extended radical operation could be performed as safely as the Whipple procedure.

Clinical stages

4, 28, 3, 0 cases in group I and 2, 6, 9, 4 cases in group II respectively belong to CS1, CS2. CS3, and CS4. The distribution of cases based on the following factors such as maximum tumor size, retropancreatic invasion, and enterohepatic vascular invasion see Table 1.

There was no significant difference in the distribution of in CS1(T1; Rp0; PV0, A0-1) and CS2(T1-2 Rp1 PV1 A0-1) between the two groups. However, more CS3(T2-3, Rp2 PV2 A2) and CS4(T3-4 Rp2-3 PV2-3 A2) patients had extended radical operation performed on them.

Histopathological correlation

Tumor diameter ranged between 1.5 and 6.5 cm (mean 3.6 cm), in addition to pancreatic cancer coexisting with chronic pancreatitis ($n = 3$), pathological result were consensus with CT imaging. Histological assessment of Rp: negative pathological test for Rp0, Rp1 present with inflammatory adherence ($n = 4$) and microscopic metastasis in the form of tiny lymph nodes, lymphatics, and nerves invasion which were embedded in soft tissue ($n = 22$). Rp2 and Rp3 exhibited positive pathological outcomes. Rates of histologically proved metastasis to individual lymph nodes observed in our series were as follows: N1: N_{06}: 23.8% ($n = 5$), N_{08}: 14.4% ($n = 3$), $N_{012inferior}$: 33.3% ($n = 7$), N_{013}: 33.3% ($n = 7$), N_{014}: 28.6% ($n = 6$), N_{017}: 33.3% ($n = 7$), N2: N_{09}: 14.4% ($n = 3$), N_{011}: 19.1% ($n = 4$), $N_{012superior}$23.8% ($n = 5$), N_{016}:23.8% ($n = 5$); N3: N_{03}: 0%, N_{04}: 0%, N_{05}: 14.4% ($n = 3$), N_{07}: 13.3% ($n = 2$). All metastatic lymph nodes present with the shape of big,

Table 1 Case distribution in different CS of pancreatic cancer between two groups

Operative procedures (patients)	T				Rp				PV				A			
	T1	T2	T3	T4	Rp0	Rp1	Rp2	Rp3	PV0	PV1	PV2	PV3	A0	A1	A2	A3
Whipple	5	28	2	0	9	19	7	0	11	15	9	0	21	14	0	0
Extended	4	9	5	3	6	7	6	2	9	8	3	1	12	5	4	0

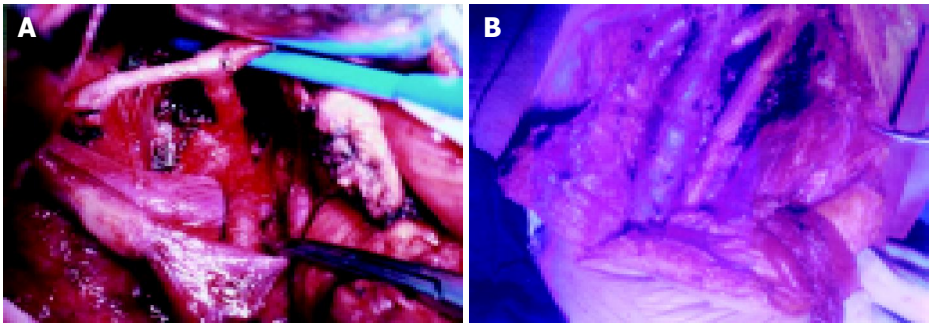

Figure 1 **A** and **B** exhibit the ranges of lymph node clearance and neighboring connective tissue dissection. N2 nodes were cleared with neighboring connective tissue. The major vessels including aorta, inferior vein, resection as well as resection and reconstruction of the portal vein were performed.

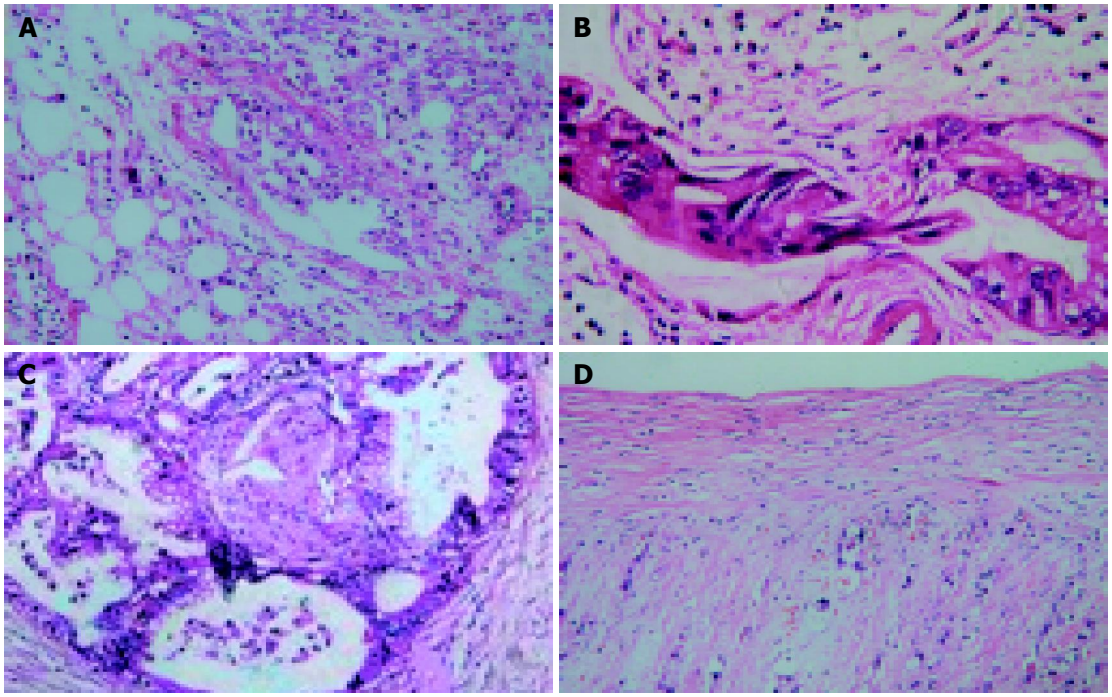

Figure 2 'Interstitial invasions' (**A,B:** connective tissue and lymphatic vessel invasion; **C:** nerve invasion); **D**: PV2 portal venous wall invasion.

middle, small as well as tiny nodus and themselves confluent types, metastatic frequency of lymph nodes was in turn tiny nodus (100%), small nodus (83%), middle nodus (79%), big nodus (66%). From the eight patients with PV2-3A2-3 that underwent vascular resection, correlation of CT findings with histopathological results was performed in 10 vessels (4SMVs, 2PVs, 3CHAs, 1SMAs). Histopathological invasion was found in 6 of 6 (100%) and 1 of 4 (25%) arteries. Figure 2 exhibited the histopathological results of CT findings present with T3Rp2PV2A2

Comparisons of survival rate of two surgical treatments were made, the follow-up period was more than 3 years for all patients. In group I, six cases were lost and seven cases died of other diseases within 3 years. The remaining 22 cases died of cancer recurrence, 18 died within 3 years (13 patients died of local recurrence, five patients died of distant metastasis). In group II, two patients were lost and three patients died of other diseases within 3 years, the remaining 16 patients died of recurrence, nine patients died within 3 years (five patients died of local recurrence, another four patients died of distant metastasis). Comparison of the cumulative rate of survival between the two groups showed that the 1-, 2-, and 3-year cumulative survival rates were 70.8%, 47.6%, 17.2% in group I and 84.8%, 62.8%, 39.9% in group II, respectively. There was a significant difference between the two groups.

The ratio of the number of 3-year survivors to the number of patients in each clinical subgroup is shown in Table 2.

The clinical tumor classification was compared between the two groups. A higher proportion of group I such as CS2 and CS3 died of local recurrence, but a significant difference is observed in CS3 (T2-3 Rp2 PV0-2 A0-1) in group II. The ratio of the number of local recurrence to the number of patients in each clinical subgroup is shown in Table 3.

The clinical tumor classification of patients who died of distant metastasis was compared between the two procedures. The ratio of the number of distant metastasis to the number of patients in each clinical subgroup is shown in Table 4.

Comparison of the cumulative rate of deaths due to total cancer recurrence between the two groups showed that 22 patients in group I and 9 patients in group II died of recurrence within 3 years after operation, the 3-year cumulative death rate was 51.4% in group I and 42.9% in

Table 2 Clinical settings in the patients surviving longer than 3 years

Operative procedures	T				Rp				PV				A			
(*n*)	T1	T2	T3	T4	Rp0	Rp1	Rp2	Rp3	PV0	PV1	PV2	PV3	A0	A1	A2	A3
Whipple	3	1	0	0	4	0	0	0	4	0	0	0	4	0	0	0
Extended	4	2	1	0	3	2	2	0	4	2	1	0	5	2	0	0

Table 3 Clinical settings in patients who died of local recurrence

Operative procedures	T				Rp				PV				A			
(*n*)	T1	T2	T3	T4	Rp0	Rp1	Rp2	Rp3	PV0	PV1	PV2	PV3	A0	A1	A2	A3
Whipple	4	8	1	-	2	6	5	-	2	7	4	-	5	8	-	-
Extended	0	1	1	3	0	0	2	3	0	0	3	2	0	1	4	0

Table 4 Clinical setting in the patients died of distant metastasis

Operative procedure	T				Rp				PV				A			
(*n*)	T1	T2	T3	T4	Rp0	Rp1	Rp2	Rp3	PV0	PV1	PV2	pV3	A0	A1	A2	A3
Whipple	0	3	2	-	0	2	3	-	0	1	4	-	0	5	-	-
Extended	0	0	2	2	0	0	3	1	0	0	3	1	0	0	4	0

group II. There was a significant difference between the two groups ($P<0.05$). Thirteen patients in group I and five patients in group II died of local recurrence, the 3 years cumulative death rate was 37.1% in group I and 23.8% in group II ($P<0.05$). Five patients in group I and four in group II died of distant metastasis, the 3 years cumulative death rate was 14.3% in group I and 19.0% in group II. These data showed that the extended radical operation could decrease deaths due to local recurrence, but could not reduce the death rate due to distant metastasis.

Finally, the cumulative survival rates were examined for their relations to CS as estimated retrospectively from preoperative assessments of images of the lesion by CT scan and abdominal selective angiography. As a result the cumulative survival rates (1-, 2- and 3-year) related to CS, were shown to be 100%, 71% and 57% for CS1; 71%, 47% and 26% for CS2; 46%, 12% and 7% for CS3; and 7%, 0% and 0% for CS4 patients. Thus 3-year survivors were noted to exist among CS1, CS2 and part of CS3 patients.

DISCUSSION

In this study, there were no differences in morbidity and mortality between patients performed by extended *vs* standard resection, but survival difference can be detected in patients with pancreatic cancer that underwent extended radical operation in comparison with those that underwent Whipple procedure. Although this was not a randomized trial and insignificant comparison of survival rate may be unreliable. Other prospective, randomized trials also have suggested that extended radical resection rather than the Whipple operation could provide survival advantages over patients with advanced pancreatic head cancer[4,5]. The reasons why extended lymphadenectomy should be performed are as follows. Lymph node studies conducted by us in the present study confirmed that patients who underwent the Whipple procedure have metastatic lymph nodes beyond the confines of the Whipple dissection. Pancreatic cancer cells had aggressively perineural invasion behaviors, even if there were no cancer cells at the margin of the pancreas at the time of surgery, the cancer cells may spread further to the noncancerous pancreas or retroperitoneum, where apparently provide a nidus for cancer recurrence after surgery[6,7]. A relationship between 'interstitial invasion' and lymph node metastases seems to exist. Nagai pointed out that the 'interstitial invasion' was almost invariably found in the regions where lymph node metastases were observed[8], Ishikawa further demonstrated that when metastatic lymph node was limited to the N1 region, due to 'interstitial invasion', microinvasion had already occurred in the N2 region[9]. Mao *et al*[10], stressed that spleenful lymphatic vessels in the retroperitoneal space might be a communicating channel, tumor cells not only spread from the N1 group to N2 group, but also bypass the N1 nodes to pass from the primary tumor to the N2 nodes via alternative routes, even if a metastasis was not found in the N1 nodes, N2 nodes were not necessarily free of tumor. Thus, the lymphatic vessels that are distributed throughout the capsule of the pancreas and the border between the pancreas and the retroperitonium act as routeways for tumor invasion into the peritoneal cavity. Many researchers deem that an extensive dissection of the retroperitoneum and extrapancreatic nerve pleux could lower local recurrence rate of pancreatic bed often involved by tumor extension[11-15]. Excision of regional blood vessels was usually precluded by the Whipple procedure, in the present study one patient with $PV2^{(+)}$ in group II could survive more than 3 years. Extended radical resection permitted elimination of potentially negative margins and sometimes long-term survival could be expected[16-18].

Extended radical resection required defined CS. In the present study, relation between evaluation of maximum of tumor, retroperitoneal invasion (Rp), arterial and venous invasion by CT imaging and histological correlation were performed. Tumor margin, in addition to a small number of pancreatic cancer coexisting with chronic pancreatitis, evaluation of the CT imaging were basically in accordance with pathological outcome. Retroperitoneal invasion in this study was divided into lymph node involvement and 'interstitial invasion'. Types of metastatic lymph node included large nodus, middle nodus, small and tiny nodus and their integrated types. Tiny nodus were often embedded in fatty tissue and difficulty detected by CT imaging, however, the presence of such occult microscopic metastatic lymph node involvement was found in about 50% of patients with pancreatic cancer[19,20]. Presence of microscopic metastasis in occult lymph nodes, peripancreatic lymphatics, and nerves has been demonstrated in at least 50% of pancreatic cancers[21,22]. Such a phenomenon is indiscernible by CT imaging, only was divided into Rp1 in our present study. Evaluation of involved vessel system and pathological outcome were performed, we found differences between arterial and venous systems, cancer cells were proved to be aggressive against PV2 and PV3, however, as for A2 in CT imaging, only one patient with $A2^{(+)}$ confirmed the presence of cancer cells in the arterial wall. Nakayama *et al*[23], point out that the cause of artery stenosis or wall irregularity was due to fibrotic tissue prolifer-ation associated with tumor circumference, atherosclerotic changes of the artery wall, neointimal proliferation, or nontu-morous thrombus secondary to perivascular fibrotic changes in response to tumor growth.

Extended radical resection may be beneficial to selected patients. In this study, the extended radical operation resulted in a 3-year survival primarily for the patients with CS1, CS2 and part of CS3 (T2Rp2PV2A1). The incidence in 3-year survivors among patients with CS3 in the extended radical operation was found. None occurred in patients that underwent the Whipple procedure in the same clinical setting. The clinical evidence thus clearly indicated the therapeutic benefits of extended radical operation. The 3-year survival rate of patients has been improved by extended radical operation that decreased local recurrence. The rate of recurrence for patients with CS1 and CS2 lesions generally was lower than that for those with CS3 and CS4, i.e., extended radical operation was able to control local recurrence in patients with CS1, CS2 and CS3 (T2 Rp2PV2 A1) disease. However, radical resection was not an effective treatment for CS3 (T3Rp2PV2 A2) and CS4 (T3Rp3 PV3 A2-3) diseases. In the present study, CS3 was divided into CS3a(T2 Rp2PV2 A1) and CS3b(T3Rp2PV2 A1-2), because there exists abundant lymphatic vessels inside the pancreas which communicate with each other, as the tumor size

enlarges, the chance of cancer cells invading lymphatic vessels and the rate of recurrence after resection increase. In Gebhardt' series, when carcinoma measuring up to 2.1-4 cm, invasion of the lymphatic vessel in 81% of the patients, however carcinomas measuring 4.1-6 cm, invasion of the lymphatic vessel in 100% of the patients[24]. Ishikawa demonstrated that when tumors were larger than T2, even extended radical could control local recurrence, and distant metastasis could be avoided[9]. In addition to local recurrence, distant metastasis occurred commonly in CS3-4 (T3-4 Rp2-3 PV2-3 A2-3) in which we can see that patients with large tumors (T3-4), deeply retropancreatic invasion (Rp3), and enterohepatic vascular invasions (PV3, A2-3) were at a higher risk for death due to distant metastasis. Patients with Rp3, cancer cells either as single cells or cell clumps were randomly allocated to the large area of loose connective tissue of the peritonium[25], in such a condition extended radical resection has been proven to be unable to obtain negative margin, even the negative margin with a few millimeters away from the tumor was obtained, avoidance of future metastasis could not be assured[26]. It is suggested that patients with higher CSs such as CS3-4 (T3-4 Rp3 PV3A2-3) might have cancer extension beyond the limit of surgical management, even wide lymph node dissection, resection of surrounding connective tissue, and en bloc resection of major vessels could not obtain R0 surgery (without cancer cells). The negative survival impact of R1 (residual tumor) surgery has been observed in many studies and was associated with high rates of local and regional recurrence[27]. Therefore, indicators of extended radical operation for pancreatic head cancer were CS1, CS2, and CS3 (T2Rp2PV2A1). It can be concluded that indication of extended radical operation is practically possible in CS1, CS2 and part of CS3 (T2-3Rp2PV2A1) but unrealistic in CS3-4(T3-4Rp2-3PV2-3A2-3).

REFERENCES

1 **Sasson AR,** Hoffman JP, Ross EA, Kagan SA, Pingpank JF, Eisenberg BL. En bloc resection for locally advanced cancer of the pancreas: is it worthwhile? *J Gastrointest Surg* 2002; **6**: 147-157; discussion 157-158

2 **Tsiotos GG,** Farnell MB, Sarr MG. Are the results of pancreatectomy for pancreatic cancer improving? *World J Surg* 1999; **23**: 913-919

3 **Kawarada Y,** Das BC, Naganuma T, Isaji S. Surgical treatment of pancreatic cancer. Does extended lymphadenectomy provide a better outcome? *J Hepatobiliary Pancreat Surg* 2001; **8**: 224-229

4 **Pedrazzoli S,** DiCarlo V, Dionigi R, Mosca F, Pederzoli P, Pasquali C, Kloppel G, Dhaene K, Michelassi F. Standard versus extended lymphadenectomy associated with pancreatoduodenectomy in the surgical treatment of adenocarcinoma of the head of the pancreas: a multicenter, prospective, randomized study. Lymphadenectomy Study Group. *Ann Surg* 1998; **228**: 508-517

5 **Popiela T,** Kedra B, Sierzega M. Does extended lymphadenectomy improve survival of pancreatic cancer patients? *Acta Chir Belg* 2002; **102**: 78-82

6 **Hirai I,** Kimura W, Ozawa K, Kudo S, Suto K, Kuzu H, Fuse A. Perineural invasion in pancreatic cancer. *Pancreas* 2002; **24**: 15-25

7 **Takahashi S,** Hasebe T, Oda T, Sasaki S, Kinoshita T, Konishi M, Ueda T, Ochiai T, Ochiai A. Extra-tumor perineural invasion predicts postoperative development of peritoneal dissemination in pancreatic ductal adenocarcinoma. *Anticancer Res* 2001; **21**: 1407-1412

8 **Nagai H,** Kuroda A, Morioka Y. Lymphatic and local spread of T1 and T2 pancreatic cancer. A study of autopsy material. *Ann Surg* 1986; **204**: 65-71

9 **Ishikawa O,** Ohhigashi H, Sasaki Y, Kabuto T, Fukuda I, Furukawa H, Imaoka S, Iwanaga T. Practical usefulness of lymphatic and connective tissue clearance for the carcinoma of the pancreas head. *Ann Surg* 1988; **208**: 215-220

10 **Mao C,** Domenico DR, Kim K, Hanson DJ, Howard JM. Observations on the developmental patterns and the consequences of pancreatic exocrine adenocarcinoma. Findings of 154 autopsies. *Arch Surg* 1995; **130**: 125-134

11 **Nagakawa T,** Konishi I, Ueno K, Ohta T, Akiyama T, Kayahara M, Miyazaki I. Surgical treatment of pancreatic cancer. The Japanese experience. *Int J Pancreatol* 1991; **9**: 135-143

12 **Nagakawa T,** Nagamori M, Futakami F, Tsukioka Y, Kayahara M, Ohta T, Ueno K, Miyazaki I. Results of extensive surgery for pancreatic carcinoma. *Cancer* 1996; **77**: 640-645

13 **Imaizumi T,** Hanyu F, Harada N, Hatori T, Fukuda A. Extended radical Whipple resection for cancer of the pancreatic head: operative procedure and results. *Dig Surg* 1998; **15**: 299-307

14 **Nagakawa T,** Konishi I, Ueno K, Ohta T, Kayahara M, Miyazaki I. Extended radical pancreatectomy for carcinoma of the head of the pancreas. *Hepatogastroenterology* 1998; **45**: 849-854

15 **Ishikawa O**, Ohigashi H, Yamada T, Sasaki Y, Imaoka S, Nakaizumi A, Uehara H, Tanaka S, Takenaka A. Radical resection for pancreatic cancer. *Acta Gastroenterol Belg* 2002; **65**: 166-170

16 **van Geenen RC,** ten Kate FJ, de Wit LT, van Gulik TM, Obertop H, Gouma DJ. Segmental resection and wedge excision of the portal or superior mesenteric vein during pancreatoduodenectomy. *Surgery* 2001; **129**: 158-163

17 **Nakao A,** Kaneko T, Takeda S, Inoue S, Harada A, Nomoto S, Ekmel T, Yamashita K, Hatsuno T. The role of extended radical operation for pancreatic cancer. *Hepatogastroenterology* 2001; **48**: 949-952

18 **Nakao A,** Takeda S, Sakai M, Kaneko T, Inoue S, Sugimoto H, Kanazumi N. Extended radical resection versus standard resection for pancreatic cancer: the rationale for extended radical resection. *Pancreas* 2004; **28**: 289-292

19 **Edis AJ,** Kiernan PD, Taylor WF. Attempted curative resection of ductal carcinoma of the pancreas: review of Mayo Clinic experience, 1951-1975. *Mayo Clin Proc* 1980; **55**: 531-536

20 **O'Brien PH,** Mincey KH. Analysis of pancreatoduodenectomy. *J Surg Oncol* 1985; **28**: 50-58

21 **Tsuchiya R,** Noda T, Harada N, Miyamoto T, Tomioka T, Yamamoto K, Yamaguchi T, Izawa K, Tsunoda T, Yoshino R. Collective review of small carcinomas of the pancreas. *Ann Surg* 1986; **203**: 77-81

22 **Tsuchiya R,** Oribe T, Noda T. Size of the tumor and other factors influencing prognosis of carcinoma of the head of the pancreas. *Am J Gastroenterol* 1985; **80**: 459-462

23 **Nakayama Y,** Yamashita Y, Kadota M, Takahashi M, Kanemitsu K, Hiraoka T, Hirota M, Ogawa M, Takeya M. Vascular encasement by pancreatic cancer: correlation of CT findings with surgical and pathologic results. *J Comput Assist Tomogr* 2001; **25**: 337-342

24 **Gebhardt C,** Meyer W, Reichel M, Wunsch PH. Prognostic factors in the operative treatment of ductal pancreatic carcinoma. *Langenbecks Arch Surg* 2000; **385**: 14-20

25 **Hiraoka T,** Uchino R, Kanemitsu K, Toyonaga M, Saitoh N, Nakamura I, Tashiro S, Miyauchi Y. Combination of intraoperative radiation with resection of cancer of the pancreas. *Int J Pancreatol* 1990; **7**: 201-207

26 **Kayahara M,** Nagakawa T, Ueno K, Ohta T, Takeda T, Miyazaki I. An evaluation of radical resection for pancreatic cancer based on the mode of recurrence as determined by autopsy and diagnostic imaging. *Cancer* 1993; **72**: 2118-2123

27 **Henne-Bruns D,** Vogel I, Luttges J, Kloppel G, Kremer B. Surgery for ductal adenocarcinoma of the pancreatic head: staging, complications, and survival after regional versus extended lymphadenectomy. *World J Surg* 2000; **24**: 595-601; discussion 601-602

Science Editor Wang XL **Language Editor** Elsevier HK

PO Box 2345, Beijing 100023, China
www.wjgnet.com
wjg@wjgnet.com

ELSEVIER

World J Gastroenterol 2005;11(16):2472-2476
World Journal of Gastroenterology ISSN 1007-9327

• *BRIEF REPORTS* •

Intrabiliary rupture: An algorithm in the treatment of controversial complication of hepatic hydatidosis

Kenan Erzurumlu, Adem Dervisoglu, Cafer Polat, Gokhan Senyurek, Ibrahim Yetim, Murat Hokelek

Kenan Erzurumlu, Adem Dervisoglu, Cafer Polat, Gokhan Senyurek, Ibrahim Yetim, Murat Hokelek, Department of Surgery, Medical School, Ondokuz Mayis University, Kurupelit, Samsun, Turkey
Correspondence to: Kenan Erzurumlu, MD, Professor, Department of Surgery, Medical School, Ondokuz Mayis University, 55139 Kurupelit, Samsun, Turkey. kerzurum@omu.edu.tr
Telephone: +90-362-4576000-2470 Fax: +90-362-4576029
Received: 2004-03-31 Accepted: 2004-05-13

Abstract

AIM: Intrabiliary rupture (IBR) is a common and serious compli-cation of hepatic hydatid cyst. The incidence varies from 1% to 25%. The treatment of IBR is still controversial. We aimed to design an algorithm for the treatment of hepatic hydatidosis with IBR by reviewing our cases.

METHODS: Eight cases of IBR were analyzed retrospectively. Patients were evaluated according to age, sex, clinical findings, cyst number and stage, abdominal ultrasonography and CT-scan, surgical methods, complica-tions, results and coincidental diseases.

RESULTS: Female/male ratio was 1/7. Mean age was 52.12±18.26 years (range 24-69 years). Right upper quadrant pain, flatulence, palpable hepatic mass were symptoms common in all patients. Cholestatic jaundice was found in four cases. In all patients, cyst evacuation and omento-plasty were performed, followed by either choledochod-uodenostomy, T-tube drainage, intracavitary suturing of the orifice, two cases in each. Whereas in two patients diagnosed post-operatively percutaneous drainage of biliary collection or ERCP and sphincteroplasty were added. Morbidity and hospital stay were higher in these cases.

CONCLUSION: When the diagnosis of IBR can be done pre-or intra-operatively, morbidity decreases. If a biliary fistula is seen post-operatively, endoscopic procedures such as ERCP, sphincteroplasty or nasobiliary drainage can be applied.

Key words: Intrabiliary rupture; Hepatic hydatidcyst

Erzurumlu K, Dervisoglu A, Polat C, Senyurek G, Yetim I, Hokelek M. Intrabiliary rupture: An algorithm in the treatment of controversial complication of hepatic hydatidosis. *World J Gastroenterol* 2005; 11(16): 2472-2476
http://www.wjgnet.com/1007-9327/11/2472.asp

INTRODUCTION

Intrabiliary rupture (IBR) is the most common and serious complication of hepatic hydatid cyst (HHC). It has also been reported as 'cystobiliary fistula' or 'cystobiliary communication' in the literature. The incidence varies from 1% to 25% although an incidence of 64.75% has been reported from a multicentric study in Tunisia[1-12].

Obstructive jaundice, fever, right-upper quadrant pain, nausea and vomiting, flatulence, palpable hepatic mass are the most commonly encountered symptoms in intrabiliary rupture[2,3,9].

Although there is some consensus on the medical and surgical treatment of hydatid cyst diseases, the treatment of intrabiliary rupture still remains controversial. Intracystic suturing of the orifice, T-tube drainage, double side drainage, cystobiliary disconnection, choledochoduodenostomy, choledochojejunostomy, endoscopic sphincterotomy and nasobiliary stent application have been used.

In this report, eight cases of intrabiliary rupture were presented and discussed in the light of literature review.

MATERIALS AND METHODS

In this study, eight cases of hepatic hydatid cyst with cystobiliary fistulae treated by our team between 1994 and 2003 were presented. They began to undergo intra-operative ultrasonography (US) in 1997.

All patients' records were reviewed and evaluated as to the age, sex, clinical findings, cyst number and stages according to Gharbi's classification, abdominal ultrasonography and CT-scan results, surgical methods, complications, results and coincidental diseases.

RESULTS

Patients' data

Between 1994 and 2003, a total of 70 cases of hepatic hydatidosis were treated surgically by our team, of these cases eight (11.42%) had cystobiliary fistulae, diagnosed either pre-, intra- or post-operatively. Female/male ratio was 1/7. Mean age was 52.12±18.26 years (range 24-69 years).

Right upper quadrant pain, flatulence, palpable hepatic mass were the symptoms present in all patients. Cholestatic jaundice was found in four cases.

Four patients had one, two patients had two and the

Table 1 Patients' characteristics (n = 8)

Mean age		52.12±18.26
Female/male		1/7
Symptoms		
Right upper quadrant pain, palpable hepatic mass, flatulence		8
Cholestatic jaundice		4
Number of cysts		
1		4
2		2
3 or more		2
Stages of cysts (According to Gharbi's classification)	Stage II	3
	Stage III	5
Choledochal image at US and CT-scan	dilated (= 2 cm)	3
	Normal	5

Table 2 Objectives of the cysts and diagnostic investigations

Patient number	ALT, AST, ALP levels	Bilirubin levels (total/conj mg/dL)
1	High	7/5
2	N	N
3	N	N
4	N	N
5	High	5/3
6	High	5/3
7	High	11/8
8	N	N

other two patients had three or more cysts. The majority of the cysts were in stage III (62.5 %) and stage II (37.5 %) (Table 1). Seven cases had their cysts in the right hepatic lobe, one in the left lobe. The cyst sizes were in the range of 2.5-15 cm. Table 1 summarizes the patients' data.

Four cases had obstructive jaundice. Total bilirubin was as high as 7 mg/dL. ALT, AST and ALP levels were thrice the normal levels. Four patients had no elevation at biochemical analysis (Table 2).

US and CT-scan showed choledochal dilatation of 2 cm in three patients. Biochemical tests of these cases were high.

Treatments of patients

Benzimidazole treatment was started 7-30 d before surgery (mean 14±8.45 d) and continued for 2-5 mo (mean 3.71±1.11 mo) after surgery, in a monthly cyclic protocol.

All cysts were treated by evacuation+omentoplasty+ drainage of the cystic cavity. The cystic cavities were disinfected by 1.7 mg/mL albendazole solution as described previously[13-15]. When choledochotomy was done, all contents in the common bile duct (CBD) were evacuated and biliary tracts were irrigated with 0.9% NaCl solution. Table 3 and Figure 1 show the treatment of intrabiliary rupture.

Evidence of obstructive jaundice with cystic contents in large common bile duct There were three such cases. Two of them were treated by choledochoduodenostomy. Cystic content and hemobilia were diagnosed in the CBD of the third case in which choledochus was evacuated and T-tube drainage was performed. The specific cause of hemobilia could not be determined.

Evidence of obstructive jaundice, invisible orifice, normal caliber choledochus There was only one such patient. Hyperbilir-ubinemia was 5 mg/dL. There was no bile staining of the cystic liquid. No pathological change was found at the inspection or palpation of the CBD, therefore no surgical procedure was performed for intrabiliary rupture. However, bile leakage in the range of 1 000 mL/d was diagnosed in the early post-operative period. Perihepatic biliary collection was also diagnosed later and drainage under US guidance was performed. Bile leakage subsequently regressed and stopped in 2 wk.

The cases with bile stained cystic liquid Two of the three such cases had visible orifices and were treated by suturing with nonabsorbable materials. At last one orifice could not be identified. Choledochotomy was done since it was suspected that there was cystic content in the CBD, but cystic content could not be seen. T-tube drainage was carried out. Biliary fistulae did not occur.

In a case of *unsuspected intrabiliary rupture,* a cyst, 10 cm in diameter was present in the right lobe. The cystic liquid was not stained by bile. Extrahepatic biliary system was found normal intra-operatively. No orifice could be identified because of difficult localization. A high output (1 000 mL/d) biliary fistula occurred on the first post-operative day and continued for a week. ERCP and sphincteroplasty were performed and the biliary fistula stopped at the 4th post-operative week.

T-tubes were removed on the 10th d in patients with a normal caliber choledoch, while the removal was delayed on the 20th d in patients with an enlarged choledoch with daughter vesicles and hemobilia.

Table 3 Diagnosis and treatment of cystobiliary fistulae

Patient number	Clinical and diagnostic characteristics of the patients	Treatment of common bile duct
1	Evidence of obstructive jaundice with cystic contents in large CBD	Choledochoduodenostomy
2	Bile stained cystic liquid and visible orifice	Suturing orifice
3	Bile stained cystic liquid and visible orifice	Suturing orifice
4	Bile in cystic liquid	T-tube drainage
5	Evidence of obstructive jaundice, invisible orifice, normal caliber choledochus (postop biliary leakage)	Percutaneous drainage under US guidance post-operatively
6	Evidence of obstructive jaundice with cystic contents in a large CBD	Choledochoduodenostomy
7	Evidence of obstructive jaundice, hemobilia, enlargement of the CBD with cystic content	T-tube drainage
8	No suspicion of intrabiliary rupture	ERCP and sphincteroplasty

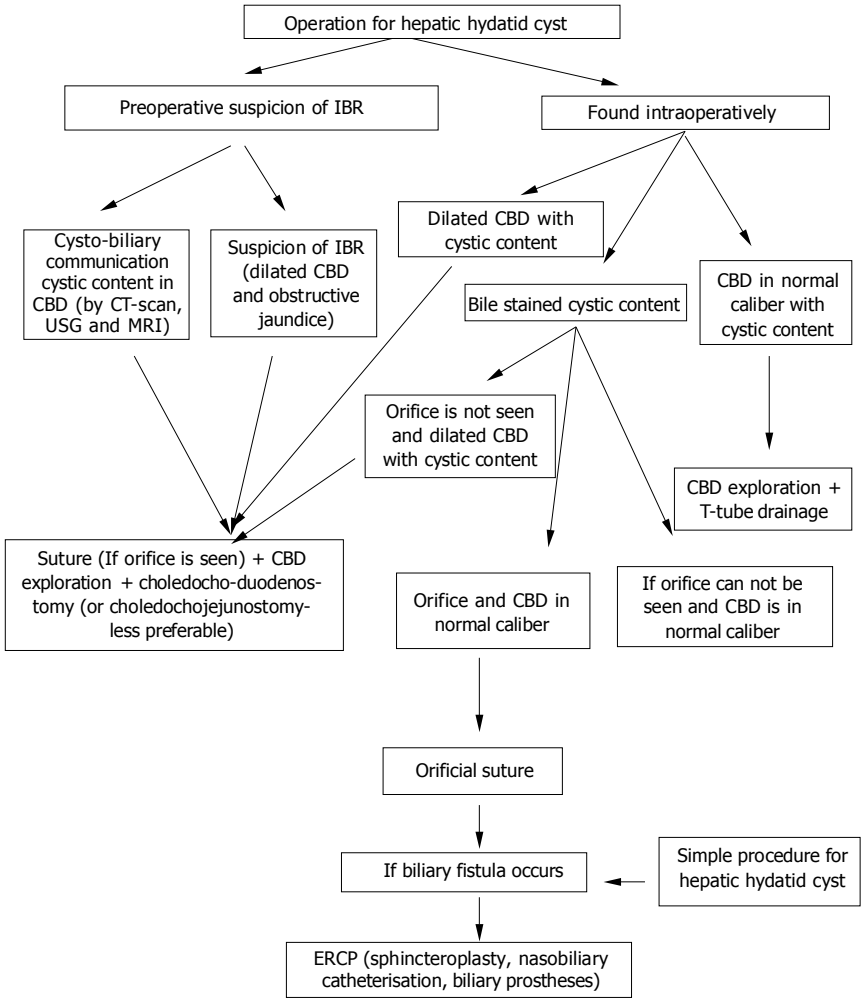

Figure 1 Algorithm in the management of intrabiliary rupture (IBR: intrabiliary rupture, CBD: common bile duct).

Four patients had coincidental diseases. Two of them had cholelithiasis (cholecystectomy was done). One of them had coronary disease. Another patient had coronary disease, hypertension and diabetes mellitus.Perihepatic biliary collection noted above was only a complication.

The mean length of hospital stay was 17±11.63 d (range 10-45 d). In one patient with prolonged biliary fistulae the hospital stay was 45 d. When this patient was excluded, the mean hospital stay was 13±2.94 d.

The mean follow-up period was 57.87±40.47 mo (range 3-120 mo). No morbidity or mortality was seen during this period.

DISCUSSION

Intrabiliary rupture is a common and serious complication of hepatic hydatidosis. It occurs especially in centrally localized and high stage cyst. High intracystic pressure up to 80 cm H_2O is a predisposing factor. The cyst rupture can occur in three clinical forms. Contained rupture occurs when the cyst contents are confined within the pericyst. Communicating rupture defines tearing of the pericyst and evacuation of cyst contents into the biliary tract or bronchioles. Direct rupture describes complete tear of the cyst wall and spillage of the cyst contents into the peritoneal or pleural cavity. Small cysto-biliary communications develop in 80-90% of all HHCs[16].

Furthermore, there are two different clinical settings associated with intrabiliary rupture: frank intrabiliary rupture and simple communication. In the former, the cyst content drains to biliary tract and causes cholestatic jaundice. In the latter simple communications are frequently overlooked and could cause biliary fistulae post-operatively[17]. If the cystobiliary opening was less than 5 mm, spontaneous drainage of the cystic content was uncommon and could be treated by suturing under the direct vision[18]. If the CBD diameter was larger than 5 mm, cystic content migration into the biliary tract would occur in 65% of the cases[19]. Vesicles, debris and purulent materials may be found in the biliary collection.

In all patients the most frequent symptoms were right upper quadrant pain and flatulence. Obstructive jaundice and fever have been recorded in 90% and 20% of the cases respectively. Nausea and vomiting were rare[2,3,9,20].

Diagnosis of IBR is difficult and can be established pre-, intra- and post-operatively. When obstructive jaundice is present, US, CT-scan, magnetic resonance imaging (MRI) and scintigraphic investigation can show the cyst and cystobiliary communications, but in patients with no jaundice, a correct diagnosis can be made in only 25%. Radiodiagnostic

evaluation can also demonstrate cystic content in the gall bladder[7] and the CBD[1,4,19,21]. On the other hand, cholelithiasis and choledocholithiasis are common (81-61.53%) coincidental diseases[6,7]. Laboratory and serological tests can also be helpful for diagnosis.

If obstructive jaundice was not present and cystobiliary connection could not be seen pre-operatively, three findings should raise suspicion of cystobiliary fistulas, namely bile-stained cystic fluid, visualized and sutured bile leak orifice intra-operatively; intra-operative observation of CBD enlargement or the presence of cyst content in the common bile duct; unexpected post-operative bile drainage from the cavity drains[8,22,23].

The orifice of bile leakage could be seen in 11.7-17.07% of the cases during the operation[3,23] while this was difficult in posteriorly localized cysts. In these cases, cholangiography could be done by a catheter pushed into the ductus cysticus or the cystobiliary fistula[3,4,8,22,23]. As an extreme procedure, puncture of choledochus and injection of radioopac solution or methylene blue are helpful to diagnose intrabiliary rupture or to see the orifice. Eleftheriadis[23] emphasized that choledochoscopy could also be helpful in the diagnosis of IBR.

When an intrabiliary rupture is diagnosed pre-or intra-operatively, there are alternative treatment modalities in addition to conventional surgery of hepatic hydatid cyst. Cystic evacuation, removal of germinative layer, disinfection of cystic cavity are necessary. If cystobiliary orifice is seen and no cystic content is observed in a normal caliber choledochus, suturing the orifice is sufficient to prevent the complications. Videolaparoscopical suturing of the orifice has been reported in literature[8].

When cystic content is observed in a normal caliber choledochus, choledochotomy+evacuation of cystic content and debris from biliary tree±irrigation with 0.9% NaCl solution and T-tube drainage are enough. If CBD enlargement is diagnosed with cystic content in it or in the gallbladder, choledochoduodenostomy is preferable. Some authors have reported the wide application of T-tube drainage in cases with high morbidity rates[3,4,6,7,9,22,24,25]. On the other hand, Roux and Y hepaticojejunostomy have been reported for the treatment of bile duct stricture associated intrabiliary rupture[20,26]. Open sphincteroplasty was also used in the last decades[25].

The presence of cholangitis has been reported as a risk factor. Even T-tube drainage itself could cause cholestatic icterus[3,17,27] and is also a source of infection[28]. Some authors have used cystojejunostomy albeit the risk that cystic content drainage into the biliary tract could result in obstructive jaundice and cholangitis[21,29].

When intrabiliary rupture was overlooked during the surgical treatment, biliary fistulae (up to 1 000 mL/d) were unavoidable and if this occurred ERCP would be necessary. Post-operative biliary fistula rate was about 20% in all cases[22,23,30,31].

In the cases of overlooked cystobiliary fistulae, transsphincteric evacuation of the CBD and sphincteroplasty could be applied. Nasobiliary drainage could also be done. Usually, the majority of biliary fistulae could be closed in a few weeks[2,8,27,30,32].

The usage of endoprostheses in biliary fistula was not common. This can be considered in either high output bile leakage or for intractable fistulae[31].

The morbidity and mortality rates of all patients were 19.44-43.03% and 1.8-4.5% respectively in literature. The most common causes of deaths were sepsis and hepatic failure[3,4,9,22,23].

Hospital stay was the longest in the T-tube group. The patients undergoing choledochoduodenostomy had longer hospital stay than those undergoing simple orifice suturing[3].

In conclusion, IBR has an algorithm in the diagnosis and treatment. If it is not detected pre- or intra-operatively, a biliary fistula is common, its morbidity and mortality rates are high. Detecting and suturing orifices in cystic wall are the best methods of treatment. When cystic content is found in choledochus or when biliary fistula occurs, more complex procedures are necessary.

REFERENCES

1 **Alper A,** Ariogul O, Emre A, Uras A, Okten A. Choledochoduodenostomy for intrabiliary rupture of hydatid cysts of liver. *Br J Surg* 1987; **74**: 243-245
2 **Atli M,** Kama NA, Yuksek YN, Doganay M, Gozalan U, Kologlu M, Daglar G. Intrabiliary rupture of a hepatic hydatid cyst: associated clinical factors and proper management. *Arch Surg* 2001; **136**: 1249-1255
3 **Bedirli A,** Sakrak O, Sozuer EM, Kerek M, Ince O. Surgical management of spontaneous intrabiliary rupture of hydatid liver cysts. *Surg Today* 2002; **32**: 594-597
4 **Daali M,** Fakir Y, Hssaida R, Hajji A, Hda A. Hydatid cysts of the liver opening in the biliary tract. Report of 64 cases. *Ann Chir* 2001; **126**: 242-245
5 **Dawson JL,** Stamatakis JD, Stringer MD, Williams R. Surgical treatment of hepatic hydatid disease. *Br J Surg* 1988; **75**: 946-950
6 **Lygidakis NJ.** Diagnosis and treatment of intrabiliary rupture of hydatid cyst of the liver. *Arch Surg* 1983; **118**: 1186-1189
7 **Marti-Bonmati L,** Menor F, Ballesta A. Hydatid cyst of the liver: rupture into the biliary tree. *AJR Am J Roentgenol* 1988; **150**: 1051-1053
8 **Masatsugu T,** Shimizu S, Noshiro H, Mizumoto K, Yamaguchi K, Chijiiwa K, Tanaka M. Liver cyst with biliary communication successfully treated with laparoscopic deroofing: a case report. *JSLS* 2003; **7**: 249-252
9 **Ulualp KM,** Aydemir I, Senturk H, Eyuboglu E, Cebeci H, Unal G, Unal H. Management of intrabiliary rupture of hydatid cyst of the liver. *World J Surg* 1995; **19**: 720-724; discussion 728
10 **Yilmaz E,** Gokok N. Hydatid disease of the liver: current surgical management. *Br J Clin Pract* 1990; **44**: 612-615
11 **Dugalic D,** Djukic V, Milicevic M, Stevovic D, Knezevic J, Pantic J. Operative procedures in the management of liver hydatidoses. *World J Surg* 1982; **6**: 115-118
12 **Dadoukis J,** Gamvros O, Aletras H. Intrabiliary rupture of the hydatid cyst of the liver. *World J Surg* 1984; **8**: 786-790
13 **Erzurumlu K,** Ozdemir M, Mihmanli M, Cevikbas U. The effect of intraoperative mebendazole-albendazole applications on the hepatobiliary system. *Eur Surg Res* 1995; **27**: 340-345
14 **Erzurumlu K,** Sahin M, Selcuk MB, Yildiz C, Kesim M. Intracystic application of mebendazole solution in the treatment of liver hydatid disease: Preliminary report of two cases. *Eur Surg Res* 1996; **28**: 466-470
15 **Erzurumlu K,** Hokelek M, Gonlusen L, Tas K, Amanvermez R. The effect of albendazole on the prevention of secondary hydatidosis. *Hepatogastroenterology* 2000; **47**: 247-250
16 **Lewall DB,** McCorkell SJ. Rupture of echinococcal cysts: diagnosis, classification, and clinical implications. *AJR Am J Roentgenol* 1986; **146**: 391-394
17 **Hankins JR.** Management of complicated hepatic hydatid

cysts. *Ann Surg* 1963; **158**: 1020-1034
18 **Ozmen MM,** Coskun F. New technique for finding the ruptured bile duct into the liver cysts: scope in the cave technique. *Surg Laparosc Endosc Percutan Tech* 2002; **12**: 187-189
19 **Zaouche A,** Haouet K, Jouini M, El Hachaichi A, Dziri C. Management of liver hydatid cysts with a large biliocystic fistula: multicenter retrospective study. Tunisian Surgical Association. *World J Surg* 2001; **25**: 28-39
20 **Jabbour N,** Shirazi SK, Genyk Y, Mateo R, Pak E, Cosenza DC, Peyre CG, Selby RR. Surgical management of complicated hydatid disease of the liver. *Am Surg* 2002; **68**: 984-988
21 **Barros JL.** Hydatid disease of the liver. *Am J Surg* 1978; **135**: 597-600
22 **Kayaalp C,** Bostanci B, Yol S, Akoglu M. Distribution of hydatid cysts into the liver with reference to cystobiliary communications and cavity-related complications. *Am J Surg* 2003; **185**: 175-179
23 **Eleftheriadis E,** Tzartinoglou E, Kotzampassi K, Aletras H. Choledochoscopy in intrabiliary rupture of hydatid cyst of the liver. *Surg Endosc* 1987; **1**: 199-200
24 **Moreno VF**, Lopez EV. Acute cholangitis caused by ruptured hydatid cyst. *Surgery* 1985; **97**: 249
25 **Vicente E,** Meneu JC, Hervas PL, Nuno J, Quijano Y, Devesa M, Moreno A, Blazquez L. Management of biliary duct confluence injuries produced by hepatic hydatidosis. *World J Surg* 2001; **25**: 1264-1269
26 **Akkiz H,** Akinoglu A, Colakoglu S, Demiryurek H, Yagmur O. Endoscopic management of biliary hydatid disease. *Can J Surg* 1996; **39**: 287-292
27 **Ovnat A,** Peiser J, Avinoah E, Barki Y, Charuzi I. Acute cholangitis caused by ruptured hydatid cyst. *Surgery* 1984; **95**: 497-500
28 **Giouleme O,** Nikolaidis N, Zezos P, Budas K, Katsinelos P, Vasiliadis T, Eugenidis N. Treatment of complications of hepatic hydatid disease by ERCP. *Gastrointest Endosc* 2001; **54**: 508-510
29 **de Aretxabala X,** Perez OL. The use of endoprostheses in biliary fistula of hydatid cyst. *Gastrointest Endosc* 1999; **49**: 797-799
30 **Dumas R,** Le Gall P, Hastier P, Buckley MJ, Conio M, Delmont JP. The role of endoscopic retrograde cholangiopancreatography in the management of hepatic hydatid disease. *Endoscopy* 1999; **31**: 242-247
31 **Rodriguez AN**, Sanchez del Rio AL, Alguacil LV, De Dios Vega JF, Fugarolas GM. Effectiveness of endoscopic sphincterotomy in complicated hepatic hydatid disease. *Gastrointest Endosc* 1998; **48**: 593-597
32 **Bilsel Y**, Bulut T, Yamaner S, Buyukuncu Y, Bugra D, Akyuz A, Sokucu N. ERCP in the diagnosis and management of complications after surgery for hepatic echinococcosis. *Gastrointest Endosc* 2003; **57**: 210-213

Science Editor Wang XL and Zhu LH **Language Editor** Elsevier HK

PO Box 2345, Beijing 100023, China
www.wjgnet.com
wjg@wjgnet.com

ELSEVIER

World J Gastroenterol 2005;11(16):2477-2481
World Journal of Gastroenterology ISSN 1007-9327

• *BRIEF REPORTS* •

Efficacy of omeprazole and amoxicillin with either clarithromycin or metronidazole on eradication of *Helicobacter pylori* in Chinese peptic ulcer patients

Wei-Hao Sun, Xi-Long Ou, Da-Zhong Cao, Qian Yu, Ting Yu, Jin-Ming Hu, Feng Zhu, Yun-Liang Sun, Xi-Ling Fu, Han Su

Wei-Hao Sun, Xi-Long Ou, Da-Zhong Cao, Qian Yu, Ting Yu, Feng Zhu, Yun-Liang Sun, Xi-Ling Fu, Han Su, Department of Gastroenterology, Zhongda Hospital of Southeast University, Nanjing 210009, Jiangsu Province, China
Jin-Ming Hu, Department of Digestive Endoscopy, Golmud Railway Hospital, Golmud 816000, Qinghai Province, China
Supported by the Scientific Research Foundation for Foreign-Returned Chinese Scholars, State Education Ministry, China
Correspondence to: Dr. Wei-Hao Sun, Department of Geriatrics, The First Affiliated Hospital of Nanjing Medical University, Nanjing 210009, Jiangsu Province, China
Telephone: +86-25-83718836-6044 Fax: +86-25-83783506
Received: 2004-02-02 Accepted: 2004-03-24

Abstract

AIM: One-week triple therapy with proton pump inhibitors, clarithromycin and amoxicillin has recently been proposed as the first-line treatment for *Helicobacter pylori* (*H pylori*) infection; however, data regarding the effects of this regimen in China are scarce. The aim of this prospective and randomized study was to compare the efficacy of clarithromycin and metronidazole when they were combined with omeprazole and amoxicillin on eradication of *H pylori* and ulcer healing in Chinese peptic ulcer patients.

METHODS: A total of 103 subjects with *H pylori*-positive peptic ulcer were randomly divided into two groups, and accepted triple therapy with omeprazole 20 mg, amoxicillin 1 000 mg and either clarithromycin 500 mg (OAC group, n = 58) or metronidazole 400 mg (OAM group, n = 45). All drugs were given twice daily for 7 d. Patients with active peptic ulcer were treated with omeprazole 20 mg daily for 2-4 wk after anti-*H pylori* therapy. Six to eight weeks after omeprazole therapy, all patients underwent endoscopies and four biopsies (two from the antrum and two others from the corpus of stomach) were taken for rapid urease test and histological analysis (with modified Giemsa staining) to examine *H pylori*. Successful eradication was defined as negative results from both examination methods.

RESULTS: One hundred patients completed the entire course of therapy and returned for follow-up. The eradication rate of *H pylori* for the per-protocol analysis was 89.3% (50/56) in OAC group and 84.1% (37/44) in OAM group. Based on the intention-to-treat analysis, the eradication rate of *H pylori* was 86.2% (50/58) in OAC group and 82.2% (37/45) in OAM group. There were no significant differences in eradication rates between the two groups on either analysis. The active ulcer-healing rate was 96.7% (29/30) in OAC group and 100% (21/21) in OAM group (per-protocol analysis, P>0.05). Six patients in OAC group (10.3%) and five in OAM group (11.1%) reported adverse events (P>0.05).

CONCLUSION: One-week triple therapy with omeprazole and amoxicillin in combination with either clarithromycin or metronidazole is effective for the eradication of *H pylori*. The therapeutic regimen comprising metronidazole with low cost, good compliance and mild adverse events may offer a good choice for the treatment of peptic ulcers associated with *H pylori* infection in China.

Key words: Omeprazole; Amoxicillin; *H pylori*

Sun WH, Ou XL, Cao DZ, Yu Q, Yu T, Hu JM, Zhu F, Sun YL, Fu XL, Su H. Efficacy of omeprazole and amoxicillin with either clarithromycin or metronidazole on eradication of *Helicobacter pylori* in Chinese peptic ulcer patients. *World J Gastroenterol* 2005; 11(16): 2477-2481
http://www.wjgnet.com/1007-9327/11/2477.asp

INTRODUCTION

Helicobacter pylori (*H pylori*) infects the stomachs of more than 50% of people worldwide, and is responsible for most peptic ulcer diseases, gastritis and gastric malignancies[1-4]. According to the Maastricht 2-2000 consensus report[5], eradication of *H pylori* infection is strongly recommended in duodenal and gastric ulcers, whether they are active or not. Cure of the infection not only promotes peptic ulcer healing but also reduces ulcer relapse. Recently, 1-wk triple therapy with a proton-pump inhibitor (PPI) and two antimicrobial agents (clarithromycin, amoxicillin, or metronidazole/tinidazole) has been shown to be one of the most effective regimens and is recommended as the first-line treatment of *H pylori* eradication due to its high cure rates and convenience[6-8]. However, as in many other infectious diseases, antibiotic resistance is the major cause of treatment failure. Metronidazole-resistant strains of *H pylori* have been reported to be increasing worldwide[9-11].

Although clarithromycin is an excellent drug for treating *H pylori* infection overseas[12,13], this drug has not

been widely used in China due to its high cost. Therefore, we evaluated the efficacy of 1-wk triple therapy with omeprazole, amoxicillin and clarithromycin (OAC) for *H pylori* eradication and active peptic ulcer healing in Chinese population. We also compared the results of OAC regimen with a conventional traditional triple therapy with omeprazole, amoxicillin and metronidazole (OAM).

MATERIALS AND METHODS

Patients

Patients with endoscopically-confirmed peptic ulcers (including scar stage), and biopsy-proven *H pylori* infection were enrolled into this prospective, randomized, investigator-blind, single-center study. Patients excluded from the study included patients with liver cirrhosis, renal failure, or other serious concomitant illnesses; alcoholics; patients were treated in the two months preceding study entry with antibiotics, bismuth preparations, proton pump inhibitors or H_2-receptor antagonists; patients with known allergy to the medications used; patients with a history of previous gastric surgery; pregnant women; and patients who previously underwent eradication therapy. These criteria were ascertained by means of a complete history, physical examination, appropriate hematological and biochemical tests. A total of 103 patients (85 men and 18 women) who were recruited prospectively in the gastroenterology unit at Affiliated Zhongda Hospital of Southeast University, fulfilled the criteria for admission to the study. All patients gave their fully informed written consent before entering the study. The study also received the approval of the Medical Ethics Committee of Southeast University.

Eradication methods

Patients were randomly divided into two groups, and accepted triple therapy with omeprazole 20 mg, amoxicillin 1 000 mg and either clarithromycin 500 mg (OAC group, $n = 58$) or metronidazole 400 mg (OAM group, $n = 45$). All drugs were given twice daily for 7 d. Patients with active peptic ulcer were treated with omeprazole 20 mg daily for 2-4 wk after anti-*H pylori* therapy. Each patient was asked to return at the end of antibiotic treatment for a structured clinical interview to assess adverse events and compliance.

Evaluation of eradication therapy

Six to eight weeks after omeprazole therapy, all patients underwent endoscopies and four biopsies (two from the antrum and another two from the corpus of the stomach) were taken for rapid urease test and histological analysis (with modified Giemsa staining) to examine *H pylori*. Successful eradication was defined as negative results from both examination methods. The healing of active ulcer was also evaluated during endoscopic examination.

Statistical analysis

The results of treatment were evaluated with per-protocol (PP) analysis (which included only patients who completed the study) and intention-to-treat (ITT) analysis (which included also patients who did not complete the study). The demographic and clinical characteristics of the two groups were compared by χ^2 test. The results of treatment were compared by χ^2 test or Fisher's exact test. $P<0.05$ was considered statistically significant.

RESULTS

Demographic and clinical characteristics

The demographic and clinical characteristics of the 103 patients in the two groups are shown in Table 1. No significant differences in demographic and clinical characteristics were found between the two groups.

Table 1 Baseline characteristics of patients in two groups

	OAC ($n = 58$)	OAM ($n = 45$)
Age (yr, mean±SD)	52±11	50±12
Sex (M/F)	48/10	37/8
Gastric ulcer, active	10	8
Gastric ulcer, scar	13	11
Duodenal ulcer, active	21	14
Duodenal ulcer, scar	14	12

Eradication rates of H pylori

Of the 103 patients enrolled in this study, 3 (2.9%) withdrew from the study because of drug-related adverse events. Of them, two patients (each from OAC group and OAM group) with skin rash and one from OAC group with diarrhea discontinued the treatment. As a result, 100 patients (97.1%, 56 patients in OAC group and 44 patients in OAM group) completed the entire course of therapy and returned for follow-up. The eradication rates based on PP or ITT analyses are shown in Table 2. There were no significant differences in eradication rates between the two groups.

Table 2 Eradication rates in two treatment groups

	OAC ($n = 58$)	OAM ($n = 45$)	χ^2	P
PP analysis (%)	50/56(89.3)	37/44(84.1)	0.59	0.44
ITT analysis (%)	50/58(86.2)	37/45(82.2)	0.31	0.58

Numbers in parentheses indicate percentages.

Healing rates of active peptic ulcer

The active ulcer-healing rate on PP analysis was 96.7% (29/30) in OAC group and 100% (21/21) in OAM group. There were no significant differences between the two groups ($\chi^2 = 0.71$, $P>0.05$).

Adverse events and compliance

Completed questionnaires about the adverse events and compliance were obtained from all the 103 patients. Adverse events were noticed (Table 3) in six patients in OAC group, and five patients in OAM group, with no statistically significant differences between the two groups ($\chi^2 = 0.02$, $P = 0.90$). The symptoms of adverse events were mild and did not necessitate any additional treatment in both groups. None of the other serious events such as hepatic or renal functional damages were found by means of biochemical

examination in the two groups. All patients, except for two who had acute allergic skin rashes and one who had diarrhea, were able to take the study medication completely for the full study period. Thus, 100 patients (97.1%) had an excellent compliance.

Table 3 Adverse events during treatment

	OAC (n = 58)	OAM (n = 45)
Skin rash	1	1
Diarrhea	1	1
Headache	2	0
Nausea	1	1
Anorexia	1	0
Metallic taste	0	2
Total (%)	6/58 (10.3)	5/45 (11.1)

DISCUSSION

Many authors have reported a correlation between *H pylori* infection and peptic ulcers[1,7,8]. Incidence of *H pylori* infection was higher in patients with gastroduodenal ulcers than in subjects without gastroduodenal disorders. The eradication of *H pylori* has been strongly recommended in all patients with peptic ulcer, including those with complications[5]. Eradication of *H pylori* could assure rapid symptom relief and accelerate ulcer healing[14], prevent ulcer relapse and reduce complications[7,8,15-18]. Furthermore, eradication of *H pylori* could also improve the healing of intractable ulcers[19-21]. However, the survival capabilities of *H pylori* in the stomach made it difficult to be eradicated, and effective treatment required multi-drug regimens consisting of two antibiotics (usually selected from clarithromycin, metronidazole, amoxicillin, and tetracycline) combined with PPI or bismuth compounds[5,22,23]. Although the optimal treatment of *H pylori* infection is still a matter of debate, the effectiveness of PPI based 1-wk triple therapy has now been well established and remains one of the first-line therapies of choice[6,14,24,25].

Clarithromycin is a new generation of macrolide antibiotic that inhibits bacterial protein synthesis. Its antibacterial spectrum is similar to that of erythromycin, but it is more acid-stable, better absorbed, and is thought to be an effective drug for treating *H pylori* infection[7,12,13]. Among several eradication regimens, PPI with clarithromycin and amoxicillin is thought to be one of the most effective treatments of *H pylori*. Amoxicillin resistance was rarely reported[26] but clarithromycin resistance has increased year after year[27], and eradication rates with clarithromycin-containing regimens decreased significantly[28]. The present study showed that the *H pylori* eradication rate in OAC group was 89.3% (50/56, PP analysis). The result is in accordance with previous reports from China and Spain[29,30]. However, in a study from Japan by Ogura *et al*[31], eradication was achieved in 39/40 (98%) by PP analysis in clarithromycin-based triple therapy for non-resistant *H pylori* infection. These results indicate that the therapeutic effect of clarithromycin for *H pylori* eradication is not quite consistent. It may be related to different resistance to clarithromycin of infecting *H pylori* strains in various countries and regions. Widespread use of antimicrobial drugs has resulted in a worldwide increase in the prevalence of antibiotic resistance in *H pylori*, 5-11% of clinical *H pylori* strains isolated in China are resistant to clarithromycin[32,33]. Although clarithromycin was not available in China before 1996, the other members of macrolides such as spiramycin, erythromycin and roxithromycin have been widely used over the past years for the treatment of respiratory infection, sexually transmitted diseases and other infectious diseases. Thus, *H pylori* is able to develop resistance to clarithromycin rapidly after contact with it, as cross-resistance exists between macrolides. Some studies have shown that clarithromycin resistance in *H pylori* substantially affected the success rate of eradication regimens containing clarithromycin[28]. In the present randomized study, there were no significant differences between OAC and OAM treatment groups in terms of *H pylori* eradication and ulcer healing, confirming that 1-wk triple therapy with omeprazole and amoxicillin in combination with either clarithromycin or metronidazole has the same effectiveness on eradicating the bacterium. Both eradication regimens were well tolerated and patient compliance was excellent. However, clarithromycin is too expensive to be widely used in China.

Antibacterial treatment of *H pylori* is difficult because of the very rapid development of resistance to antimicrobial agents, especially to nitroimidazoles, such as metronidazole and tinidazole, and clarithromycin[34]. The resistance of *H pylori* to metronidazole and clarithromycin strongly affected the success of regimens involving these drugs. The prevalence of resistance to these anti-microbial agents varied with gender, ethnic group and country of origin[34]. It was reported from Hong Kong (China) that almost 50% of pre-treatment strains of *H pylori* were resistant to metronidazole and over 10% to clarithromycin[33]. Metronidazole resistance has been shown to reduce *H pylori* eradication rates in the regimens containing amoxicillin and metronidazole[35,36]. Several studies have shown a significantly higher rate of metronidazole resistant *H pylori* among women[37-39], indicating that this drug can be widely used for pelvic inflammatory diseases in females[37]. In the current study, the number of men was absolutely more than that of women either in OAC or in OAM group. Whether the sex bias of patients was related to the better eradication in OAM group remains unknown. We did not test *in vitro* sensitivity to metronidazole and clarithromycin. Although Epsilometer (E) test has been recommended as the best and simplest method for routine testing of antibiotic sensitivity to *H pylori*, the technique is not yet widely available in China. On the other hand, the exact mechanism responsible for the development of *H pylori* resistance to metronidazole still remains obscure, antimicrobial effectiveness *in vivo* was poorly predicted by sensitivity *in vitro*[37]. This is largely because the current breakpoints, which are the *in vitro* concentrations defining the cut off between sensitive and resistant strains, do not correlate with levels required for eradication of infection from the gastric mucosa.

In the past, prevention of peptic ulcer recurrence was based on long term use of H_2-receptor antagonists or PPIs. Since *H pylori* was recognized, it has been well understood that eradicating the bacterium could significantly reduce the recurrence of peptic ulcer diseases[8,16-18]. In our study, the

ulcer relapse rate during the 12-mo follow-up was 66.7% (4/6) in *H pylori*-positive patients and none of the 24 *H pylori*-negative patients relapsed (data not shown). In conclusion, 1-wk triple therapy with omeprazole and amoxicillin in combination with either clarithromycin or metronidazole is equally effective for eradication of *H pylori* and ulcer healing. Clarithromycin is the most expensive antimicrobial drug used to treat *H pylori* infection. Metronidazole with lower cost, good compliance and mild adverse events may offer a good choice for the treatment of peptic ulcers associated with *H pylori* infection in China.

REFERENCES

1 **Marshall BJ,** Warren JR. Unidentified curved bacilli in the stomach of patients with gastritis and peptic ulceration. *Lancet* 1984; **1**: 1311-1315
2 **Blaser MJ.** Hypotheses on the pathogenesis and natural history of *Helicobacter pylori*-induced inflammation. *Gastroenterology* 1992; **102**: 720-727
3 **Forman D,** Newell DG, Fullerton F, Yarnell JW, Stacey AR, Wald N, Sitas F. Association between infection with *Helicobacter pylori* and risk of gastric cancer: evidence from a prospective investigation. *BMJ* 1991; **302**: 1302-1305
4 **Parsonnet J,** Hansen S, Rodriguez L, Gelb AB, Warnke RA, Jellum E, Orentreich N, Vogelman JH, Friedman GD. *Helicobacter pylori* infection and gastric lymphoma. *N Engl J Med* 1994; **330**: 1267-1271
5 **Malfertheiner P,** Megraud F, O'Morain C, Hungin AP, Jones R, Axon A, Graham DY, Tytgat G. Current concepts in the management of *Helicobacter pylori* infection-the Maastricht 2-2000 Consensus Report. *Aliment Pharmacol Ther* 2002; **16**: 167-180
6 **Lind T,** Veldhuyzen van Zanten S, Unge P, Spiller R, Bayerdorffer E, O'Morain C, Bardhan KD, Bradette M, Chiba N, Wrangstadh M, Cederberg C, Idstrom JP. Eradication of *Helicobacter pylori* using one-week triple therapies combining omeprazole with two antimicrobials: the MACH I Study. *Helicobacter* 1996; **1**: 138-144
7 **Malfertheiner P,** Kirchner T, Kist M, Leodolter A, Peitz U, Strobel S, Bohuschke M, Gatz G. *Helicobacter pylori* eradication and gastric ulcer healing-comparison of three pantoprazole-based triple therapies. *Aliment Pharmacol Ther* 2003; **17**: 1125-1135
8 **Hawkey CJ,** Atherton JC, Treichel HC, Thjodleifsson B, Ravic M. Safety and efficacy of 7-day rabeprazole-and omeprazole-based triple therapy regimens for the eradication of *Helicobacter pylori* in patients with documented peptic ulcer disease. *Aliment Pharmacol Ther* 2003; **17**: 1065-1074
9 **Noach LA,** Langenberg WL, Bertola MA, Dankert J, Tytgat GN. Impact of metronidazole resistance on the eradication of *Helicobacter pylori*. *Scand J Infect Dis* 1994; **26**: 321-327
10 **Forbes GM,** Collins BJ, McCullough CA, Coombs GW, Robins PD. Short duration therapy for *Helicobacter pylori* in Western Australia: the impact of metronidazole resistance. *Aust N Z J Med* 1998; **28**: 13-17
11 **Ling TK,** Cheng AF, Sung JJ, Yiu PY, Chung SS. An increase in *Helicobacter pylori* strains resistant to metronidazole: a five-year study. *Helicobacter* 1996; **1**: 57-61
12 **Isomoto H,** Furusu H, Morikawa T, Mizuta Y, Nishiyama T, Omagari K, Murase K, Inoue K, Murata I, Kohno S. 5-day vs. 7-day triple therapy with rabeprazole, clarithromycin and amoxicillin for *Helicobacter pylori* eradication. *Aliment Pharmacol Ther* 2000; **14**: 1619-1623
13 **Veldhuyzen Van Zanten S,** Machado S, Lee J. One-week triple therapy with esomeprazole, clarithromycin and metronidazole provides effective eradication of *Helicobacter pylori* infection. *Aliment Pharmacol Ther* 2003; **17**: 1381-1387
14 **Asaka M,** Sugiyama T, Kato M, Satoh K, Kuwayama H, Fukuda Y, Fujioka T, Takemoto T, Kimura K, Shimoyama T, Shimizu K, Kobayashi S. A multicenter, double-blind study on triple therapy with lansoprazole, amoxicillin and clarithromycin for eradication of *Helicobacter pylori* in Japanese peptic ulcer patients. *Helicobacter* 2001; **6**: 254-261
15 **Dayal VM,** Kumar P, Kamal J, Shahi SK, Agrawal BK. Triple-drug therapy of *Helicobacter pylori* infection in duodenal ulcer disease. *Indian J Gastroenterol* 1997; **16**: 46-48
16 **Hopkins RJ,** Girardi LS, Turney EA. Relationship between *Helicobacter pylori* eradication and reduced duodenal and gastric ulcer recurrence: a review. *Gastroenterology* 1996; **110**: 1244-1252
17 **Van der Hulst RW,** Rauws EA, Koycu B, Keller JJ, Bruno MJ, Tijssen JG, Tytgat GN. Prevention of ulcer recurrence after eradication of *Helicobacter pylori*: a prospective long-term follow-up study. *Gastroenterology* 1997; **113**: 1082-1086
18 **Seppala K,** Pikkarainen P, Sipponen P, Kivilaakso E, Gormsen MH. Cure of peptic gastric ulcer associated with eradication of *Helicobacter pylori*. Finnish Gastric Ulcer Study Group. *Gut* 1995; **36**: 834-837
19 **Avsar E,** Kalayci C, Tozun N, Lawrence R, Kiziltas S, Gultekin O, Ulusoy NB. Refractory duodenal ulcer healing and relapse: comparison of omeprazole with *Helicobacter pylori* eradication. *Eur J Gastroenterol Hepatol* 1996; **8**: 449-452
20 **Kihira K,** Sato K, Yoshida Y, Takimoto T, Taniguchi Y, Kimura K. The effect of the eradication of *H pylori* on the intractable ulcer. *Nihon Rinsho* 1993; **51**: 3285-3288
21 **Sugiyama T,** Asaka M. Eradication of *Helicobacter pylori* infection in patients with intractable gastric ulcer. *Aliment Pharmacol Ther* 2003; **18**: 544-545
22 **Burette A,** Glupczynski Y, Deprez C. Evaluation of various multidrug eradication regimens for *Helicobacter pylori*. *Eur J Gastroenterol Hepatol* 1992; **4**: 817-823
23 **Chiba N,** Rao BV, Rademaker JW, Hunt RH. Meta-analysis of the efficacy of antibiotic therapy in eradicating *Helicobacter pylori*. *Am J Gastroenterol* 1992; **87**: 1716-1727
24 **Zanten SJ,** Bradette M, Farley A, Leddin D, Lind T, Unge P, Bayerdorffer E, Spiller RC, O'Morain C, Sipponen P, Wrangstadh M, Zeijlon L, Sinclair P. The DU-MACH study: eradication of *Helicobacter pylori* and ulcer healing in patients with acute duodenal ulcer using omeprazole based triple therapy. *Aliment Pharmacol Ther* 1999; **13**: 289-295
25 **Malfertheiner P,** Bayerdorffer E, Diete U, Gil J, Lind T, Misiuna P, O'Morain C, Sipponen P, Spiller RC, Stasiewicz J, Treichel H, Ujszaszy L, Unge P, Zanten SJ, Zeijlon L. The GU-MACH study: the effect of 1-week omeprazole triple therapy on *Helicobacter pylori* infection in patients with gastric ulcer. *Aliment Pharmacol Ther* 1999; **13**: 703-712
26 **van Zwet AA,** Vandenbroucke-Grauls CM, Thijs JC, van der Wouden EJ, Gerrits MM, Kusters JG. Stable amoxicillin resistance in *Helicobacter pylori*. *Lancet* 1998; **352**: 1595
27 **Vakil N,** Hahn B, McSorley D. Clarithromycin-resistant *Helicobacter pylori* in patients with duodenal ulcer in the United States. *Am J Gastroenterol* 1998; **93**: 1432-1435
28 **Houben MH,** van de Beek D, Hensen EF, de Craen AJ, Rauws EA, Tytgat GN. A systematic review of *Helicobacter pylori* eradication therapy-the impact of antimicrobial resistance on eradication rates. *Aliment Pharmacol Ther* 1999; **13**: 1047-1055
29 **Chen S,** Chen Z, Bei L. Omeprazole, clarithromycin and amoxicillin therapy for *Helicobacter pylori* infection. *Zhonghua Neike Zazhi* 1996; **35**: 799-802
30 **Calvet X,** Lopez-Lorente M, Cubells M, Bare M, Galvez E, Molina E. Two-week dual vs. one-week triple therapy for cure of *Helicobacter pylori* infection in primary care: a multicentre, randomized trial. *Aliment Pharmacol Ther* 1999; **13**: 781-786
31 **Ogura K,** Yoshida H, Maeda S, Yamaji Y, Kawabe T, Okamoto M, Shiratori Y, Omata M. Clarithromycin-based triple therapy for non-resistant *Helicobacter pylori* infection. How long should it be given? *Scand J Gastroenterol* 2001; **36**: 584-588
32 **Pan ZJ,** Su WW, Tytgat GN, Dankert J, van der Ende A.

Assessment of clarithromycin-resistant *Helicobacter pylori* among patients in Shanghai and Guangzhou, China, by primer-mismatch PCR. *J Clin Microbiol* 2002; **40**: 259-261
33 **Wang WH,** Wong BC, Mukhopadhyay AK, Berg DE, Cho CH, Lai KC, Hu WH, Fung FM, Hui WM, Lam SK. High prevalence of *Helicobacter pylori* infection with dual resistance to metronidazole and clarithromycin in Hong Kong. *Aliment Pharmacol Ther* 2000; **14**: 901-910
34 **Harris A,** Misiewicz JJ. Treating *Helicobacter pylori*-the best is yet to come? *Gut* 1996; **39**: 781-783
35 **Lerang F**, Moum B, Haug JB, Tolas P, Breder O, Aubert E, Hoie O, Soberg T, Flaaten B, Farup P, Berge T. Highly effective twice-daily triple therapies for *Helicobacter pylori* infection and peptic ulcer disease: does *in vitro* metronidazole resistance have any clinical relevance? *Am J Gastroenterol* 1997; **92**: 248-253
36 **Veldhuyzen van Zanten S,** Hunt RH, Cockeram A, Schep G, Malatjalian D, Sidorov J, Matisko A, Jewell D. Adding once-daily omeprazole 20 mg to metronidazole/amoxicillin treatment for *Helicobacter pylori* gastritis: a randomized, double-blind trial showing the importance of metronidazole resistance. *Am J Gastroenterol* 1998; **93**: 5-10
37 **Graham DY,** de Boer WA, Tytgat GN. Choosing the best anti-*Helicobacter pylori* therapy: effect of antimicrobial resistance. *Am J Gastroenterol* 1996; **91**: 1072-1076
38 **Ching CK,** Leung KP, Yung RW, Lam SK, Wong BC, Lai KC, Lai CL. Prevalence of metronidazole resistant *Helicobacter pylori* strains among Chinese peptic ulcer disease patients and normal controls in Hong Kong. *Gut* 1996; **38**: 675-678
39 **Bell GD,** Powell K, Burridge SM, Pallecaros A, Jones PH, Gant PW, Harrison G, Trowell JE. Experience with 'triple' anti-*Helicobacter pylori* eradication therapy: side effects and the importance of testing the pre-treatment bacterial isolate for metronidazole resistance. *Aliment Pharmacol Ther* 1992; **6**: 427-435

Science Editor Zhu LH, Wang XL and Li WZ **Language Editor** Elsevier HK

PO Box 2345, Beijing 100023, China
www.wjgnet.com
wjg@wjgnet.com

ELSEVIER

World J Gastroenterol 2005;11(16):2482-2485
World Journal of Gastroenterology ISSN 1007-9327

• *BRIEF REPORTS* •

Expression of cellular FLICE-inhibitory protein and its association with p53 mutation in colon cancer

Xiao-Dong Zhou, Jie-Ping Yu, Hong-Xia Chen, Hong-Gang Yu, He-Sheng Luo

Xiao-Dong Zhou, Jie-Ping Yu, Hong-Gang Yu, He-Sheng Luo, Department of Gastroenterology, Renmin Hospital of Wuhan University, Wuhan 430060, Hubei Province, China
Hong-Xia Chen, Department of Gynecology and Obstetrics, Renmin Hospital of Wuhan University, Wuhan 430060, Hubei Province, China
Supported by the Scientific Research Foundation for Returned Overseas Chinese Scholars, State Education Ministry, China (2003)14
Co-first-authors: Xiao-Dong Zhou and Hong-Xia Chen
Correspondence to: Dr. Xiao-Dong Zhou, Department of Gastroenterology, Renmin Hospital of Wuhan University, Jiefang road 238, Wuhan 430060, Hubei Province, China. zhouxd7612@hotmail.com
Telephone: +86-1354-5110116 Fax: +86-27-88042292
Received: 2004-03-13 Accepted: 2004-04-07

Abstract

AIM: To investigate the expression of cellular FLICE (Fas associated death domain-like IL-1beta-converting enzyme)-inhibitory protein (c-FLIP) and its association with p53 mutation in colon cancer.

METHODS: Immunohistochemical staining of c-FLIP and mutant p53 by using specific antibodies was performed by the standard streptavidin-peroxidase technique for 45 colon cancer tissue samples with matched normal tissues. Semi-quantitative reverse transcriptional (RT)-PCR was used to measure c-FLIP mRNA levels. *t*-test statistical method was used in data analyses.

RESULTS: c-FLIP mRNA was expressed in all colon cancer tissues and its level (0.63±0.12) was significantly higher than that in normal tissues (0.38±0.10, $P<0.01$). Immunohistochemically, c-FLIP protein was also expressed in all colon cancers (45/45) and 71.1% (32/45) showed an intense immunostaining, in contrast, 93.3% (42/45) of normal colonic mucosa showed positive staining and none of them immunostained intensely. The quantity of c-FLIP protein was significantly higher in cancer tissues than in normal mucosa (7.04±1.20 *vs* 5.21±0.86, $P<0.01$). Positive staining of mutant p53 protein was found in 60% (27/45) colon cancers. c-FLIP mRNA level was decreased in p53 positive group compared with p53 negative cancer tissues (0.59±0.13 *vs* 0.69±0.14, $P<0.01$), but c-FLIP protein had a significantly higher level in p53 positive cancer tissues than in negative ones (7.57±1.30 *vs* 6.25±1.27, $P<0.01$).

CONCLUSION: c-FLIP is specially overexpressed in colon cancers and it might contribute to carcinogenesis of normal colonic mucosa. p53 may exert transcriptional upregulation effects on c-FLIP gene and more potent effects on promoting the degradation of c-FLIP protein.

Key words: Cellular FLICE; p53; Colon cancer

Zhou XD, Yu JP, Chen HX, Yu HG, Luo HS. Expression of cellular FLICE-inhibitory protein and its association with p53 mutation in colon cancer. *World J Gastroenterol* 2005; 11 (16): 2482-2485
http://www.wjgnet.com/1007-9327/11/2482.asp

INTRODUCTION

The development and progression of colorectal cancer involves unregulated epithelial cell proliferation associated with a series of accumulated genetic alterations. There is evidence that prolonged survival of such genetically unstable colonic epithelial cells, with their ultimate malignant transformation, is associated with progressive inhibition of apoptosis. Apoptosis is a morphologically distinct form of cell death, which is genetically regulated and, in addition to other roles, provides a vital protective mechanism against the development of neoplasia by removing cells with DNA damage. Inhibition of apoptosis thus confers a survival advantage on cell harboring genetic alterations and may promote acquisition of further mutations to cause neoplastic progression, and also contribute to the development of resistance to chemotherapy.

A new class of virus-encoded apoptosis inhibitory molecules, designated viral FLICE (Fas associated death domain-like IL-1beta-converting enzyme)-inhibitory protein (v-FLIP), was described previously[1-3]. These molecules are composed of two DEDs (death effect domain)[1]. Cellular homologs of v-FLIP have been identified by different groups and have been termed cellular FLICE-inhibitory protein (c-FLIP), CASH, Casper, CLARP, FLAME-1, I-FLICE, MRIT, and Usurpin. At mRNA level, c-FLIP exists as multiple splice variants, but at protein level only two endogenous forms, c-$FLIP_{long}$ (c-$FLIP_L$) and c-$FLIP_{short}$ (c-$FLIP_S$) could be detected so far[4-6]. c-$FLIP_L$ is a 55 ku protein and structurally similar to procaspase-8; it contains two DEDs and a caspase-like domain. This domain lacks residues that are important for its catalytic activity, most notably a cysteine residue within the active site. The short form of c-FLIP is a 28 ku protein and structurally resembles v-FLIP containing also two DEDs. Both c-FLIP species were found to be recruited

to the DISC (death inducing signaling complex)[6]. A number of studies support the notion that both forms of c-FLIP can prevent Fas/CD95 and other death receptors mediated apoptosis by interacting with either FADD (Fas associated death domain) and/or procaspase-8[2,4,7]. Overexpression of c-FLIP gene was found in many malignancies and played a pivotal role in apoptotic resistance of tumor cells and contributed to tumorigenesis eventually[8-10]. However, the exact *in vivo* expression status of c-FLIP and its association with p53 mutation in colon cancer have not been characterized until now. In the present study, we performed an expression analysis of c-FLIP at mRNA and protein levels to determine its prevalence in colonic carcinomas and its association with p53 mutation.

MATERIALS AND METHODS

Tissue specimens

Forty-five fresh colon cancer tissues with matched normal tissues from patients with disparate pathological stages were collected and fresh-frozen in liquid nitrogen after surgical resections performed at Renmin Hospital, Wuhan University (Wuhan, China) from 2000 to 2002. Of these, 26 were male and 19 were female. The mean age was 57 years (SD 24.1 years, range, 30-81 years). None of the patients had received chemo-, radio- or immuno-therapy before resection. Part of each specimen was routinely processed, fixed in 40 g/L buffered formalin, and embedded in paraffin for histopathological analysis (hematoxylin and eosin stain) and immunohistoc-hemical staining. All tissues were scored by two pathologists blinded to culture results and disease status. Among the 45 cases, 16 were well-differentiated adenocarcinomas, 27 were moderately differentiated carcinomas, and only 2 were poorly differentiated carcinomas.

Methods

Immunohistochemistry Immunohistochemistry streptavidin-peroxidase (S-P) technique was used to detect c-FLIP and mutant p53 protein. Affinity purified rabbit polyclonal anti-human c-FLIP specific IgG and mouse monoclonal anti-human p53 specific IgG recognizing mutant p53 were purchased from Santa Cruz Biotechnology and Neomarkers Biotechnical Company, respectively. Immunostaining S-P kit was purchased from Beijing Zhongshan Biotechnical Company. Immunohistochemistry was performed as follows: Formalin-fixed, paraffin-embedded tissue blocks were serially sectioned at 4 μm. Sections were deparaffinized in xylene and rehydrated before analysis. Endogenous peroxidase was quenched with 3.0% hydrogen peroxide in methanol for 10 min; antigen retrieval was performed by microwave for 15 min and tissue sections were then blocked for 20 min with normal rabbit serum. This was followed by incubation overnight at 4 ℃ with primary antibody at a dilution of 1:120 for c-FLIP or 1:100 for p53. Incubation with PBS instead of the primary antibody served as a negative control. Sections were washed thrice with PBS for 2 min each and incubated with second antibody for 30 min at room temperature. After washing thrice with PBS for 2 min each, sections were stained by a streptavidin-peroxidase detection system. Antibody binding was visualized using diaminobenzidine as chromogen and counterstained with hematoxylin.

The degree of c-FLIP staining was estimated by semi-quantitative evaluation and categorized by the extent and intensity of staining as follows: (1) The extent of positive cells was estimated as 0: positive staining cells <5%, 1: positive staining cells 5-25%, 2: positive staining cells 26-50%, 3: positive staining cells 51-75%, 4: positive staining cells >75%. (2) The intensity of staining was scored as 0: achromatic, 1: light yellow, 2: yellow, 3: brown. The percentage of positive tumor cells and staining intensity were multiplied to produce a weighted score for each case. Cases with weighted scores <1 were defined as negative; otherwise were defined as positive. p53 staining was graded into two grades: positive cells<5% was defined as negative and ⩾5% was defined as positive.

Semi-quantitative reverse transcriptional (RT)-PCR After homogenization, total RNAs were extracted from 45 fresh primary colon cancer tissues and paired normal colonic mucosa, using TRIzol reagent (Invitrogen, San Diego, CA). First strand cDNA was synthesized from 1 μg of total RNA using oligo-dT primer and Moloney murine leukemia virus reverse transcriptase (Promega, Southampton, UK) according to the instructions of the manufacturers. For PCR, the primer sequences and expected product sizes were as follows: c-FLIP$_{L/S}$, (sense) 5'-TGT TGC TAT AGA TGT GG-3' and (antisense) 5'- AAG GAT CCT TGA GAC TCT-3', 512 bp; and β-actin, (sense) 5'-TGA CGG GGT CAC CCA CAC TGT GCC-3', (antisense) 5'-CTG CAT CCT GTC GGC AAT GCC AG-3', 475 bp. The reaction was performed at 95 ℃ for 2 min, followed by 35 cycles of denaturing at 95 ℃ for 45 s, annealing at 55 ℃ for 45 s and extension at 72 ℃ for 1 min.

The PCR products were analyzed on 2% agarose gels and visualized by ethidium bromide staining. Quantitation of expression levels was achieved after adjustment for the expression levels of the housekeeping gene β-actin by densitometry (Bio-Rad, Hercules, CA, USA). The relative level of expression was then represented as the ratio of c-FLIP$_{L/S}$/β-actin in normal tissues and carcinomas.

Statistical analysis

The statistical software package SPSS 10.0 was used and data were presented as mean±SD. The prevalence of c-FLIP gene expression in cancers and normal tissues and its association with p53 mutation were compared by the Student's *t*-test. A *P* value less than 0.05 was considered to indicate statistical significance.

RESULTS

Expression of c-FLIP protein in colon

By immunohistochemistry, anti-c-FLIP pAb reacted with colonic mucosal epithelial cells of normal tissues and the majorities were light yellow or yellow micro-granules located in the cytoplasm and/or plasma membranes. In colon cancer, the positive staining showed yellow or brown coloration in the cytoplasm and/or plasma membranes (Figure 1). c-FLIP-positive and -negative areas were found within the same tissue, and the intensity of positive staining was also found

to vary within a case tested. After multiplying the weighted c-FLIP scores, the mean expression scores in normal mucosa ranged from 0 to 9 (5.21±0.86); none of them showed a brown immunostaining and 6.7% (3/45) showed negative reactivity. c-FLIP protein was constitutively expressed in all carcinomas (45/45) and the mean scores ranged from 1 to 12 (7.04±1.20); 71.1% (32/45) of them were brown immunostained. Moreover, its level was significantly higher than that of matched normal colonic mucosa (Table 1), (P<0.01).

Table 1 Expression of c-FLIP gene in colon cancer and matched normal tissues (mean±SD)

Group	Number	c-FLIP protein	P	c-FLIP mRNA	P
Normal tissue	45	5.21±0.86		0.38±0.10	
Cancer tissue	45	7.04 ±1.20	<0.01	0.63±0.12	<0.01

Expression of c-FLIP mRNA in colon

We examined mean expression levels of c-FLIP mRNA in 45 colonic carcinomas and their matched normal tissues, using a semi-quantitative RT-PCR assay. RT-PCR was controlled by equalization of input RNA for each sample and comparable amplification efficiencies were validated by the uniformity of control β-actin RT-PCR product yields. RT-PCR results showed that the adjacent non-tumor specimens and colon cancer specimens constitutively expressed c-FLIP mRNA (Figure 2), but the mean expression levels varied between these tissues. While the mean expression levels of c-FLIP mRNA (c-FLIP/β-actin) in 45 normal colonic tissues ranged from 0.14 to 0.58 (0.38±0.10), the levels in 45 carcinomas ranged from 0.40 to 0.83 (0.63±0.12) (Table 1). Mean c-FLIP mRNA expression in carcinoma was significantly higher than in normal colonic mucosa (P<0.01).

Expression of mutant p53 protein and its relationship with expression levels of c-FLIP gene in colon cancer tissues

Immunohistochemical results showed that mutant p53 was expressed in 60% (27/45) colon cancer tissues with positive staining in the nuclei of tumor cells (Figure 3). To determine the relationship between p53 protein and c-FLIP level, we compared the expression level of c-FLIP in p53 positive cancer group with that in p53 negative group. As a result (Table 2), c-FLIP mRNA level was decreased in p53 positive cancer group compared with p53 negative cancer tissues (0.59±0.13 *vs* 0.69±0.14, P<0.01), but c-FLIP protein had a significantly higher level in p53 positive cancer tissues than in negative ones (7.57±1.30 *vs* 6.25±1.27, P<0.01).

Table 2 Correlation between c-FLIP mRNA and protein and p53 mutation in colon cancer (mean±SD)

Group	Number	c-FLIP protein	P	c-FLIP mRNA	P
p53 positive	27	7.57±1.30		0.59±0.13	
p53 negative	18	6.25 ±1.27	<0.01	0.69±0.14	<0.01

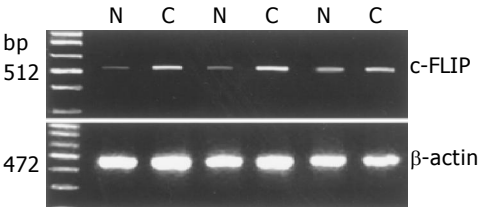

Figure 2 c-FLIP (cellular FLICE inhibitory protein) mRNA and β-actin mRNA expression in colon cancer tissue (lanes C) and matched normal mucosa (lanes N).

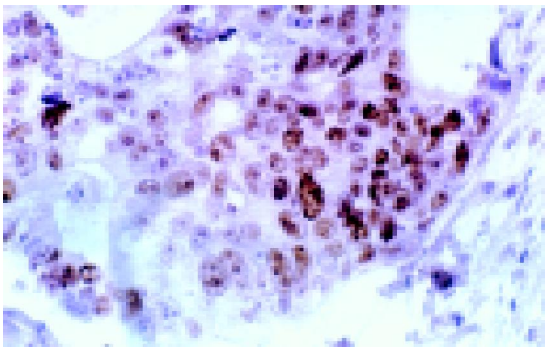

Figure 3 Immunohistochemical staining for mutant p53 in the nuclei of colon cancer cells (S-P ×400).

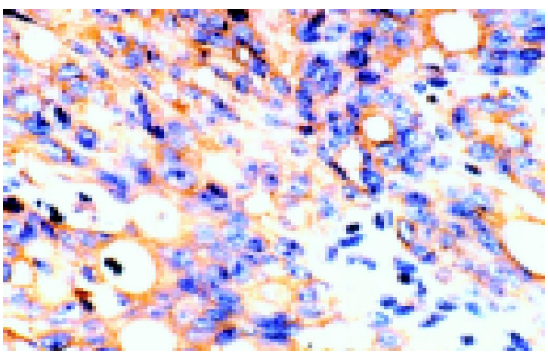

Figure 1 c-FLIP (cellular FLICE inhibitory protein) strongly positive staining. Membrane or cytoplasm of colon cancer cells was stained brown (S-P ×400).

DISCUSSION

In the last decade, basic cancer research has focused on the deregulation of apoptosis as a central event in the process of carcinogenesis and a number of studies showed a central role of apoptosis in tumorigenesis of colon cancer. Varied regulators of apoptosis including p53, survivin, Fas and nuclear factor-kappa B have been implicated in the development of colon cancer[11]. A novel anti-apoptotic gene, designated c-FLIP, has been demonstrated to be overexpressed in several human cancers, suggesting an important role of c-FLIP in cancer development[8-10]. However, the exact expression status of c-FLIP and its possible regulation mechanisms in colon cancer have not been determined.

In this study, we detected the expression level of c-FLIP gene in colon cancer by using immunohistochemistry and RT-PCR. The results showed that the expression of c-FLIP gene was frequently upregulated at both mRNA and

protein levels in colonic carcinoma compared with their normal counterparts, suggesting that increased expression of c-FLIP gene was a tumor specific phenomenon and overexpression of c-FLIP might contribute to tumorigenesis of colon cancer by abrogating death signals of tumor cells conducted by death receptors such as Fas, TNF-R, DR3, TRAIL-R, *etc*. Recently, Ryu *et al*[12], also reported that c-FLIP was specially overexpressed in colon cancer with the same positive rates of mRNA and protein as detected in our experiments, but the positive rate of c-FLIP protein in normal colonic mucosa was lower than the present research (89.6% *vs* 93.3%). We deduced that it was at least partially due to the different antibodies used to detect the protein level in immunostaining. The antibody used in the previous study was designed only to recognize the long form of c-FLIP (c-FLIP$_L$); however, the antibody used in our study was expected to recognize both forms of c-FLIP protein (c-FLIP$_L$ and c-FLIP$_S$), both of which were demonstrated to act as inhibitors of apoptosis[1,4,7].

Wild type (wt) p53 gene is a tumor suppressor gene, playing an important role in inducing cell cycle arrest and apoptosis. Wt p53 gene mutation is one of the most common genomic alterations in human neoplasia. Because of its short and unstable half-life, it cannot be detected by immunohistochemical examinations; mutant p53 gene product, a more stable protein product accumulated in cells having a loss of its normal function by extending its half-life, may inactivate the wt p53. As we all know, wt p53 is a well-known transcriptional activator of target gene and can induce apoptosis depending on the transcriptional regulation of apoptosis-related genes. Bartke *et al*, systematically analyzed mRNA level of about 60 apoptosis-related genes by means of RNAse protection assays and found that 15% of these genes were significantly regulated by wt p53. Furthermore, the transcriptional regulation of wt p53 target genes was based on a common principle, in which pro-apoptotic factors were upregulated and anti-apoptotic factors were repressed by p53. However, c-FLIP was found to be a remarkable exception as its mRNA was upregulated by wt p53 in colon cancer cell lines[13]. Still little is known about the relationship between p53 and c-FLIP *in vivo*. At the beginning of the current study, we supposed that c-FLIP mRNA and protein levels would be downregulated accompanied with p53 mutation. As a result, c-FLIP mRNA level decreased in mutant p53 positive cancer group, whereas c-FLIP protein level was significantly upregulated unexpectedly. It seems this is a contradictory result. We speculated other mechanisms might act on the regulation of c-FLIP protein level besides transcriptional upregulation mechanism. Fukazawa *et al*[14], have recently shown that wt p53 could enhance the degradation of FLIP via a ubiquitin-proteasome pathway resulting in sensitization of human colon cancer cells to apoptosis. Taken together, we deduced that wt p53 could also enhance the degradation of c-FLIP protein *in vivo* and this effect might be more potent than the transcriptional upregulation of c-FLIP gene. Thus, c-FLIP protein level elevated as a result of dramatically decreased degradation in spite of relatively moderate downregulation of c-FLIP mRNA when p53 mutated in colon cancer. Further studies are needed to validate it.

In summary, our data show that c-FLIP is overexpressed in colon cancer than in matched normal tissues and may promote the evasion of tumor cells from apoptosis that eventually contribute to carcinogenesis and/or progression of the tumor. p53 may exert transcriptional upregulation effects on c-FLIP gene *in vivo* and also a more potent effect on promoting the degradation of c-FLIP protein in the mean time.

REFERENCES

1 **Thome M,** Schneider P, Hofmann K, Fickenscher H, Meinl E, Neipel F, Mattmann C, Burns K, Bodmer JL, Schroter M, Scaffidi C, Krammer PH, Peter ME, Tschopp J. Viral FLICE-inhibitory proteins (FLIPs) prevent apoptosis induced by death receptors. *Nature* 1997; **386**: 517-521

2 **Hu S,** Vincenz C, Ni J, Gentz R, Dixit VM. I-FLICE, a novel inhibitor of tumor necrosis factor receptor-1- and CD-95-induced apoptosis. *J Biol Chem* 1997; **272**: 17255-17257

3 **Bertin J,** Armstrong RC, Ottilie S, Martin DA, Wang Y, Banks S, Wang GH, Senkevich TG, Alnemri ES, Moss B, Lenardo MJ, Tomaselli KJ, Cohen JI. Death effector domain-containing herpesvirus and poxvirus proteins inhibit both Fas- and TNFR1-induced apoptosis. *Proc Natl Acad Sci USA* 1997; **94**: 1172-1176

4 **Irmler M,** Thome M, Hahne M, Schneider P, Hofmann K, Steiner V, Bodmer JL, Schroter M, Burns K, Mattmann C, Rimoldi D, French LE, Tschopp J. Inhibition of death receptor signals by cellular FLIP. *Nature* 1997; **388**: 190-195

5 **Shu HB,** Halpin DR, Goeddel DV. Casper is a FADD- and caspase-related inducer of apoptosis. *Immunity* 1997; **6**: 751-763

6 **Scaffidi C,** Schmitz I, Krammer PH, Peter ME. The role of c-FLIP in modulation of CD95-induced apoptosis. *J Biol Chem*1999; **274**: 1541-1548

7 **Xiao C,** Yang BF, Asadi N, Beguinot F, Hao C. Tumor necrosis factor-related apoptosis-inducing ligand-induced death-inducing signaling complex and its modulation by c-FLIP and PED/PEA-15 in glioma cells. *J Biol Chem* 2002; **277**: 25020-25025

8 **Bullani RR,** Huard B, Viard-Leveugle I, Byers HR, Irmler M, Saurat JH, Tschopp J, French LE. Selective expression of FLIP in malignant melanocytic skin lesions. *J Invest Dermatol* 2001; **117**: 360-364

9 **Thomas RK,** Kallenborn A, Wickenhauser C, Schultze JL, Draube A, Vockerodt M, Re D, Diehl V, Wolf J. Constitutive expression of c-FLIP in Hodgkin and Reed-Sternberg cells. *Am J Pathol* 2002; **160**: 1521-1528

10 **Zhou XD,** Yu JP, Liu J, Luo HS, Chen HX, Yu HG. Overexpression of cellular FLICE-inhibitory protein (FLIP) in gastric adenocarcinoma. *Clin Sci (Lond)* 2004; **106**: 397-405

11 **Yu LL,** Yu JP, Ran ZX, Yu HG. Relationship between nuclear factor-kappa B, apoptosis and proliferation in colorectal neoplasia. *Shijie Huaren Xiaohua Zazhi* 2002; **10**: 309-312

12 **Ryu BK,** Lee MG, Chi SG, Kim YW, Park JH. Increased expression of cFLIP(L) in colonic adenocarcinoma. *J Pathol* 2001; **194**: 15-19

13 **Bartke T,** Siegmund D, Peters N, Reichwein M, Henkler F, Scheurich P, Wajant H. p53 upregulates cFLIP, inhibits transcription of NF-kappaB-regulated genes and induces caspase-8-independent cell death in DLD-1 cells. *Oncogene* 2001; **20**: 571-580

14 **Fukazawa T,** Fujiwara T, Uno F, Teraishi F, Kadowaki Y, Itoshima T, Takata Y, Kagawa S, Roth JA, Tschopp J, Tanaka N. Accelerated degradation of cellular FLIP protein through the ubiquitin-proteasome pathway in p53-mediated apoptosis of human cancer cells. *Oncogene* 2001; **20**: 5225-5231

Science Editor Zhu LH **Language Editor** Elsevier HK

PO Box 2345, Beijing 100023, China
www.wjgnet.com
wjg@wjgnet.com

ELSEVIER

World J Gastroenterol 2005;11(16):2486-2490
World Journal of Gastroenterology ISSN 1007-9327

• *BRIEF REPORTS* •

Correlation between CD4, CD8 cell infiltration in gastric mucosa, *Helicobacter pylori* infection and symptoms in patients with chronic gastritis

Ai-Ping Lu, Sheng-Sheng Zhang, Qing-Lin Zha, Da-Hong Ju, Hao Wu, Hong-Wei Jia, Cheng Xiao, Shao Li, Hui Jian

Ai-Ping Lu, Da-Hong Ju, Hao Wu, Hong-Wei Jia, Cheng Xiao, Institute of Basic Theory, China Academy of Traditional Chinese Medicine, Beijing 100700, China
Qing-Lin Zha, Jiangxi Traditional Chinese Medicine Institute, Nanchang 330066, Jiangxi Province, China
Sheng-Sheng Zhang, Beijing Traditional Chinese Medicine Hospital, Beijing 100007, China
Shao Li, Tsinghua University, Beijing 100028, China
Ai-Ping Lu, Hui Jian, National Pharmaceutical Engineer Center for Herbal Solid Preparation, Nanchang 330047, Jiangxi Province, China
Supported by the National Science Foundation, China, No. 90209002 and 90209032; Key Grant from National Administration of Traditional Chinese Medicine, No. 000-J-Z-02; Beijing Creative Human Resource Plan
Correspondence to: Dr. Ai-Ping Lu, Institute of Basic Theory, China Academy of Traditional Chinese Medicine, Dongzhimen, Beijing 100700, China. catcm@public.bta.net.cn
Telephone: +86-10-64067611 Fax: +86-10-64013896
Received: 2004-05-29 Accepted: 2004-06-29

Abstract

AIM: To evaluate the correlation between CD4, CD8 cell infiltration in gastric mucosa, *Helicobacter pylori* (*H pylori*) infection and symptoms or the assemblage of symptoms in cases with chronic gastritis.

METHODS: Biopsy samples at the gastric antrum were obtained from 62 patients with chronic gastritis. CD4 and CD8 cell infiltration was evaluated by immunohistochemical assays on frozen sections of the biopsy samples. Fifteen symptoms referring to digestion-related activity and non-digestion related activity were observed. The correlation between lymphocyte infiltration and each symptom or symptom assemblage was analyzed by logistic regression and *K*-mean cluster methods.

RESULTS: CD4 cell infiltrations in gastric mucosa were much more in patients with *H pylori* infection, while CD8 cell infiltrations were similar in patients with or without *H pylori* infection. Logistic regression analysis showed that the symptoms including heavy feeling in head or body ($t = 2.563$), and thirst ($t = 2.478$) were significantly related with CD4 cell infiltration in gastric mucosa ($P<0.05$), and cool limbs with aversion to cold were related with CD8 cell infiltration ($t = 2.872$, $P<0.05$). Further analysis showed that non-digestive related symptom assemblage could increase the predicted percentage of CD4 and CD8 cell infiltration in gastric mucosa, including lower CD4 infiltration by 12.5%, higher CD8 infiltration by 33.3%, and also non-*H pylori* infection by 23.6%. *K*-means cluster analysis of all symptoms and CD4 and CD8 cell infiltration in gastric mucosa showed a similar tendency to increase the predicted percentage of CD4, CD8 cell infiltration and *H pylori* infection.

CONCLUSION: Based on correlation between the gastric mucosa lymphocyte infiltration, *H pylori* infection and clinical symptoms, symptoms or symptomatic assemblages play an important role in making further classification of chronic gastritis, which might help find a more specific therapy for chronic gastritis.

Key words: Mucosal immune; *Helicobacter pylori* infection; Symptoms; Chronic gastritis

Lu AP, Zhang SS, Zha QL, Ju DH, Wu H, Jia HW, Xiao C, Li S, Jian H. Correlation between CD4, CD8 cell infiltration in gastric mucosa, *Helicobacter pylori* infection and symptoms in patients with chronic gastritis. *World J Gastroenterol* 2005; 11(16): 2486-2490
http://www.wjgnet.com/1007-9327/11/2486.asp

INTRODUCTION

The role of immune reactions in *Helicobacter pylori* (*H pylori*) infection and chronic gastritis is a research area of rapid progress[1,2]. It has been recognized that lamina propria lymphocytes are essential in gastric lesions induced by *H pylori* infection[3-5]. However, the correlation concerning *H pylori* infection and CD4 and CD8 lymphocytes in gastric mucosa is not well understood. Moreover, the lack of cognition for the complex manifestations of *chronic gastritis* is another nodus for the effect of subjective symptoms on the objective pathologic parameters, which may lead to a further diagnostic classification of chronic gastritis.

To further explore the correlation between the *H pylori* infection and CD4 and CD8 cell infiltration in gastric mucosa in patients with chronic gastritis, a clinical investigation was designed and a novel analytical method was proposed in this work. More importantly, the study based on the important role of subjective symptoms in disease identification in traditional Chinese medicine (TCM), took a different perspective in assessing the association between clinical subjective manifestations and objective parameters including *H pylori* infection, CD4 and CD8 cell infiltration in gastric mucosa.

MATERIALS AND METHODS

Patients

A total of 62 patients with chronic gastritis, who were diagnosed through gastroscopy and mucosal biopsy, were included in the present study. All patients were investigated by the Beijing Traditional Chinese Medicine Hospital in 2002. Among them, 29 were males and 33 were females, aged from 18 to 65 years with a mean age of 42 years. Gastric biopsies were histologically evaluated for chronic gastritis diagnosis according to the criteria of the visual analog scale in Sydney classification and grading of gastritis[6], and immunohistologically evaluated for CD4 and CD8 cell infiltrations[7].

Diagnosis of H pylori infection

Three specimens of gastric mucosa were obtained from each patient via endoscopy. Gastric mucosa was sampled from the area of greater curvature at gastric antrum, *H pylori* infection was determined by pathological staining with hematoxylin and eosin (HE) followed by Giemsato. Under a microscope, *H pylori* could be observed as a typical curve like S. It looked like a short bacillus or a globular body with a slight curve.

Detection of CD4 and CD8 cells in gastric mucosa

Gastric mucosa tissues were sampled by gastric mucosal biopsy from the antrum of each patient. Immunohistochemical assay was used to detect the infiltration of CD4 and CD8 cells in gastric mucosa frozen sections. The test kits were from Vector Laboratory (Vector Stain ABC Kits). Briefly, for the detection of CD4 and CD8 cells, the first antibodies were rabbit anti-human antibodies, and the second antibodies were goat anti-rabbit antibodies, and the samples were stained with DAB (Sigma, USA). Positive granules could be observed. The average of positive granules of three samples from Q-win DC100 image analysis was used for further statistical analysis.

Symptom observation

Fifteen common clinical symptoms based on TCM were observed as follows. Digestion-related symptoms included stomachache, distending fullness in stomach, abdomen, nausea or vomit, acid regurgitation and epigastric upset, diarrhea, hard stool, and constipation. Non-digestion related symptoms included weakness of body or faint limbs, lower spirit, heavy feeling in head or whole body, irritating, distending fullness in the chest, thirst, weak taste without thirst, cool limbs with aversion to cold. The symptoms observed on the day of biopsy were taken for the analysis.

Statistical analysis

SPSS 11.5 statistical package program was used for data analysis. The variables were processed by ANVOA analysis and logistic regression analysis, respectively. The clusters of CD4, CD8 cell infiltrations and symptoms were analyzed by *k*-means cluster method for further ANOVA and logistic regression analyses.

RESULTS

Table 1 shows that CD4 cell infiltrations in gastric mucosa was much more in the cases with *H pylori* infection, while CD8 cell infiltrations were similar in patients with or without *H pylori* infection (Figure 1). The results suggested that CD4 cell infiltrations were positively related with *H pylori* infection.

Table 1 Changes CD4 and CD8 cells in *H pylori* positive and negative cases (mean±SD)

HP infection	*n*	CD4	CD8
Positive	45	9 102.82±2 747.18[a]	6 285.67±3 308.74
Negative	17	6 255.33±3 284.88	6 992.91±3 524.89

[a]$P<0.05$ *vs* negative cases.

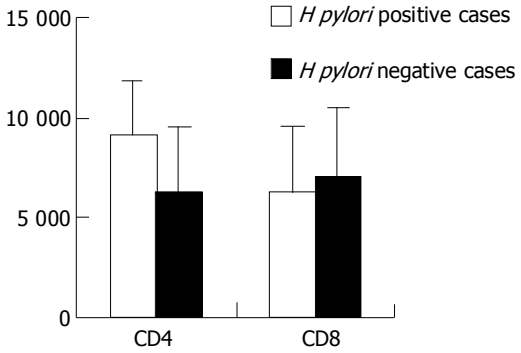

Figure 1 Difference of CD4 and CD8 cell infiltrations in gastric mucosa between *H pylori* positive and negative cases ($P<0.05$).

Table 2 shows the importance of each symptom in CD4 cell infiltrations in gastric mucosa (logistic regression). It demonstrated that the heavy feeling of head or body and thirst were significantly related with CD4 cell infiltrations ($P<0.05$).

Table 2 Correlation between symptoms and CD4 cell infiltrations

P	Symptom
$P = 0.01–0.05$	Heavy head or heavy body ($t = 2.563$), thirst ($t = 2.478$)
$P = 0.06–0.2$	Lower spirit, weakness of body or faint limbs, irritation
$P = 0.21–0.5$	Stomachache, hard stool, weak taste without thirst, distending fullness in chest, cool limbs with aversion to cold
$P>0.6$	Distending fullness in abdomen, diarrhea, constipation, acid regurgitation and epigastric upset, nausea or vomiting

Table 3 shows the importance of each symptom in CD8 cell infiltrations in gastric mucosa (logistic regression). It demonstrated that the cool limbs with aversion to cold were significantly related with CD8 cell infiltrations ($P<0.05$).

Referring to the results in Tables 2 and 3, the non-digestion related symptoms might have positive relations with CD4 and CD8 cell infiltrations in gastric mucosa. Thus, the symptoms were classified into two groups of digestion and non-digestion related symptoms based on the common clinical results, and then the data were analyzed with logistic

regression for the relationship between the assemblage of symptoms, clusters of CD4 or CD8 cell infiltrations, and *H pylori* infection (Tables 4 and 5).

Table 3 Correlation between symptoms and CD8 cell infiltrations

P	Symptom
P = 0.01–0.05	Cool limbs with aversion to cold (*t* = 2.872)
P = 0.06–0.2	Stomachache, nausea or vomiting
P = 0.21–0.5	Weakness of body or faint limbs
P>0.6	Heavy feeling of head or body, thirst, distending fullness in abdomen, diarrhea, constipation, acid regurgitation and epigastric upset, hard stool, weak taste without thirst, distending fullness in chest, lower spirit, irritation

Table 4 Effect of symptom assemblages on the predicted percentage of CD4 and CD8 cell infiltrations

Symptom	Cell level	Predicted percentage of CD4	Predicted percentage of CD8
Digestion related	Lower	62.5	89.2
	Higher	62.1	16.7
	Overall	62.3	60.7
Non-digestion related	Lower	75.0	83.8
	Higher	58.6	50.0
	Overall	67.2	70.5

Table 5 Effect of symptom assemblages on the predicted percentage of *H pylori* infection

Symptom	*H pylori* infection	Predicted percentage
Digestion related	Negative	17.6
	Positive	95.5
	Overall	73.8
Non-digestion related	Negative	41.2
	Positive	93.2
	Overall	78.7

Table 4 shows that the non-digestion related symptom assemblage could increase the predicted percentage of CD4 cell infiltrations. Lower CD4 infiltration was increased by 12.5%, higher CD4 infiltration was increased by 3.5% and the total increase was 5.1%. Table 4 also shows that the non-digestion related symptom assemblage could affect the predicted percentage of CD8 cell infiltrations. Higher CD8 infiltration was increased 33.3% and the total increase was 9.8%, and lower CD8 infiltration was decreased 5.4%. The results suggested that the non-digestion related symptom assemblage might have positive relations with CD4 and CD8 cell infiltrations in gastric mucosa.

Table 5 shows that the non-digestive related symptom assemblage could increase the predicted percentage of patients with or without *H pylori* infection. It was increased 23.6% in patients without *H pylori* infection and the total increase was 4.9%, and was similar in patients with *H pylori* infection.

In order to further explore the importance of symptom assemblages in CD4 and CD8 cell infiltrations in gastric mucosa, the cases were classified into two categories via *K*-mean cluster analysis according to the clinical manifestations, and then the relationship between the two categories of symptoms and CD4, CD8 cell infiltrations was analyzed by logistic regression method (Table 6).

Table 6 shows that the digestion related symptoms including distending fullness in abdomen, stomachache, diarrhea, regurgitation and epigastric upset were clustered into category 1, and the others including all non-digestion related symptoms were clustered into category 2. The symptom assemblage in category 2 could affect the predicted percentage of CD4 cell infiltration. Lower CD4 infiltration was increased 9.3%, higher CD4 infiltration was increased 17.3% and the total increase was 2.3%. Table 6 also shows that the symptom assemblage in category 2 could affect the predicted percentage of CD8 cell infiltration. Lower CD8 was decreased 9.9%, higher CD8 was increased 58.3% and the total increase was 11.4%. Table 6 also shows that the symptom assemblage in category 2 could affect the predicted percentage of *H pylori* infection. It was increased by 35.5% in patients without *H pylori* infection and the total increase was 3.3%, and was similar in patients with *H pylori* infection.

The results in Tables 4-6 further suggested that there might be a positive relationship between the subjective manifestations and the objective parameters (CD4 and CD8 cell infiltrations). To further explore their relationships in chronic gastritis, all cases were classified into two categories via *K*-mean cluster analysis based on the symptoms, CD4 and CD8 cell infiltrations, and then the symptom differences between the two clusters of patients were analyzed by ANOVA.

Table 7 shows the importance of each symptom in the two clusters. It showed that the weakness of body or faint limbs, lower spirit, hard stool, played a significant role in the cluster identification ($P<0.05$) while constipation, thirst, distending fullness in chest, nausea or vomiting, had a

Table 6 Effect of symptom assemblage based on *K*-mean cluster analysis on the predicted percentage of CD4 and CD8 infiltrations and *H pylori* infection

Symptom	Infiltration	Predicted percentage of CD4	Predicted percentage of CD8	*H pylori* infection	Predicted percentage
Category one[1]	Lower	78.1	100	Negative	0
	Higher	44.8	0	Positive	100
	Overall	62.3	60.7	Overall	72.1
Category two[1]	Lower	68.8	81.1	Negative	35.3
	Higher	62.1	58.3	Positive	90.9
	Overall	65.6	72.1	Overall	75.4

[1]Category one included distending fullness in abdomen, stomachache, diarrhea, regurgitation and epigastric upset, and category two had other symptoms.

potential role in the two cluster identification (P = 0.06-0.2).

The results in Table 7 were similar to those in Tables 2-6, and further suggested that the non-digestion related symptoms or symptom assemblage were positively related with CD4 and CD8 cell infiltrations.

Table 7 Difference of symptoms between the two clusters of cases based on the symptoms, CD4 and CD8 cell infiltrations

P	Symptom
P = 0.01–0.05	Weakness of body or faint limbs (F = 5.005), lower spirit (F = 5.750), hard stool (F = 5.835)
P = 0.06–0.2	Constipation, thirst, distending fullness in chest, nausea or vomiting
P = 0.21–0.5	Stomachache, diarrhea, weak taste without thirst, cool limbs with aversion to cold
P>0.6	Heavy feeling of head or body, distending fullness in abdomen, acid regurgitation and epigastric upset, irritation

DISCUSSION

Chronic gastritis is related to *H pylori* infection, which may cause immunological reactions in peripheral mononuclear cells. The activity and characteristics of peripheral mononuclear cells may differ in ulcer and non-ulcer patients infected with *H pylori*[3]. It has been reported that CD4 cells are sensitized *in vivo* and migrate to gastric mucosa where they induce gastritis in response to *H pylori* antigens, suggesting that CD4-dependent *H pylori* gastritis could lead to epithelial damage with proliferative and metaplastic responses[4,5,7]. The number of activated cytotoxic lamina propria lymphocytes was increased in gastric mucosa affected with acute gastric mucosal lesions, suggesting that lymphocytes are crucial in the pathogenesis of gastric lesions[8-10]. Yuceyar *et al*[11], found that there was no obvious alteration in total T and B lymphocytes and $CD4^+$ T, $CD8^+$ T lymphocytes and natural killer cells in chronic antral gastritis patients compared to normal persons, suggesting that there is no systemic alteration in the specific immune system in response to *H pylori* in patients with chronic antral gastritis[11]. Itoh *et al*[12], found that gastric T cells were differentiated to produce a large amount of IFN-gamma by a mechanism unrelated to *H pylori* infection. *H pylori* infection appeared to activate T cells to secrete even more IFN-γ, which might contribute to maintaining a perpetual inflammation in *H pylori*-infected stomach. Our results showed that CD4 cells in gastric mucosa were much more in patients with *H pylori* infection, while CD8 cells were similar in patients with or without *H pylori* infection (Table 1). However, the mechanism how CD4 cells affect gastric mucosal lesions remains unclear.

The clinical manifestations of CG patients are intricate. They are divergent due to the pathological changes of gastric mucosa, and are affected by environmental factors. However, the relationship between the divergent manifestations and pathological changes is not completely understood. The study on chronic gastritis has shown that proper assemblages of symptoms could improve the accuracy of *H pylori* infection classification, and improper assemblages could decrease the accuracy of *H pylori* infection classification. Our results in this paper showed that the symptoms including the heavy feeling of head or body and thirst were significantly related with CD4 cell distributions in gastric mucosa (P<0.05), and cool limbs with aversion to cold were related with CD8 cells (P<0.05). Also the symptoms including lower spirit, weakness of body or faint limbs and irritation were related with CD4 cell distributions (P = 0.06-0.2), while stomachache, nausea or vomiting were related with CD8 cells (P=0.06-0.2), suggesting that the different objective symptoms might play different roles in *H pylori* infection and lymphocyte infiltrations in gastric mucosa. Further logistic analysis showed that non-digestion related symptom assemblage could increase the predicted percentage of CD4 and CD8 cells in gastric mucosa, and the percentage of non-*H pylori* infection to some degree (Tables 2 and 3). Also the symptom assemblages classified with *K*-mean cluster analysis showed similar results in predicting the percentage of *H pylori* infection, lymphocyte infiltration (Tables 4 and 5). The results showed that the proper combination of symptoms might play a more important role in predicting the percentage of *H pylori* infection and lymphocyte infiltration. To further explore the contribution of symptom assemblages to CD4 and CD8 cell distributions in gastric mucosa, the cases were classified into two categories via *K*-mean cluster analysis according to the clinical manifestations, and then the relationship between the two categories of symptoms and CD4, CD8 cells was analyzed by logistic regression method. The results showed that digestion-related symptoms including distending fullness in abdomen, stomachache, diarrhea, regurgitation and epigastric upset were clustered into category 1, and the others including all non-digestion related symptoms were clustered into category 2. The symptom assemblage in category 2 could affect the predicted percentage of lymphocyte infiltration in gastric mucosa and *H pylori* infection (Table 6). Our further analysis on the two cluster symptoms via ANOVA showed that the symptoms, such as weakness of body or faint limbs, lower spirit, hard stool, played a significant role in classification of the two symptom assemblages (P<0.05), and the results further suggested that different symptoms might play different roles in *H pylori* infection and lymphocyte infiltration in gastric mucosa, and that the non-digestion related symptoms played a more important role in *H pylori* infection and lymphocyte infiltration in gastric mucosa.

Similar results on the positive relationship between subjective symptoms or symptom assemblages and objective parameter such as pathological changes and therapeutic effects, are described in detail in TCM. The identification of diseases (Zheng identification, or Zheng differentiation) in TCM depends on the information obtained from the interrogation, auscultation, inspection and pulse-feeling, and the major characteristics of the information are its subjectivity. The long history of TCM has proven that the subjective symptoms play a more important role in the diagnosis and treatment of diseases. Our results indicate that further studies on the relationship between subjective symptoms and objective parameters are needed.

In conclusion, the symptoms or symptomatic assemblages have a positive correlation with CD4, CD8 cells and *H pylori* infection, and might play an important role in making further classification of chronic gastritis, which might help to find a more specific therapy for different groups of chronic gastritis.

REFERENCES

1 **Aguilar GR**, Ayala G, Fierros-Zarate G. *Helicobacter pylori*: recent advances in the study of its pathogenicity and prevention. *Salud Publica Mex* 2001; **43**: 237-247

2 **Prinz C**, Schoniger M, Rad R, Becker I, Keiditsch E, Wagenpfeil S, Classen M, Rosch T, Schepp W, Gerhard M. Key importance of the *Helicobacter pylori* adherence factor blood group antigen binding adhesin during chronic gastric inflammation. *Cancer Res* 2001; **61**: 1903-1909

3 **Ohara T**, Arakawa T, Higuchi K, Kaneda K. Overexpression of co-stimulatory molecules in peripheral mononuclear cells of *Helicobacter pylori*-positive peptic ulcer patients: possible difference in host responsiveness compared with non-ulcer patients. *Eur J Gastroenterol Hepatol* 2001; **13**: 11-18

4 **Peterson RA**, Hoepf T, Eaton KA. Adoptive transfer of splenocytes in SCID mice implicates CD4+ T cells in apoptosis and epithelial proliferation associated with *Helicobacter pylori*-induced gastritis. *Comp Med* 2003; **53**: 498-509

5 **Riedel S**, Kraft M, Kucharzik T, Pauels HG, Tiemann M, Steinbuchel A, Domschke W, Lugering N. CD4+ Th1-cells predominate in low-grade B-cell lymphoma of gastric mucosa-associated lymphoid tissue (MALT type). *Scand J Gastroenterol* 2001; **36**: 1198-1203

6 **Dixon MF**, Genta RM, Yardley JH, Correa P. Classification and grading of gastritis. The updated Sydney System. International Workshop on the Histopathology of Gastritis, Houston 1994. *Am J Surg Pathol* 1996; **20**: 1161-1181

7 **Sommer F**, Faller G, Konturek P, Kirchner T, Hahn EG, Zeus J, Rollinghoff M, Lohoff M. Antrum- and corpus mucosa-infiltrating CD4(+) lymphocytes in *Helicobacter pylori* gastritis display a Th1 phenotype. *Infect Immun* 1998; **66**: 5543-5546

8 **Suzuki T**, Ito M, Hayasaki N, Ishihara A, Ando T, Ina K, Kusugami K. Cytotoxic molecules expressed by intraepithelial lymphocytes may be involved in the pathogenesis of acute gastric mucosal lesions. *J Gastroenterol* 2003; **38**: 216-221

9 **Nakagawa K**, Higuchi K, Arakawa T, Kobayashi K, Kaneda K. Phenotypical and morphological analyses of intraepithelial and lamina propria lymphocytes in normal and regenerating gastric mucosa of rats in comparison with those in intestinal mucosa. *Arch Histol Cytol* 2000; **63**: 159-167

10 **De Silva HD**, Van Driel IR, La Gruta N, Toh BH, Gleeson PA. CD4+ T cells, but not CD8+ T cells, are required for the development of experimental autoimmune gastritis. *Immunology* 1998; **93**: 405-408

11 **Yuceyar H**, Saruc M, Kokuludag A, Terzioglu E, Goksel G, Isisag A. The systemic cellular immune response in the *Helicobacter pylori*-associated duodenal ulcer and chronic antral gastritis. *Hepatogastroenterology* 2002; **49**: 1177-1179

12 **Itoh T**, Wakatsuki Y, Yoshida M, Usui T, Matsunaga Y, Kaneko S, Chiba T, Kita T. The vast majority of gastric T cells are polarized to produce T helper 1 type cytokines upon antigenic stimulation despite the absence of *Helicobacter pylori* infection. *J Gastroenterol* 1999; **34**: 560-570

Science Editor Wang XL **Language Editor** Elsevier HK

PO Box 2345, Beijing 100023, China
www.wjgnet.com
wjg@wjgnet.com

ELSEVIER

World J Gastroenterol 2005;11(16):2491-2496
World Journal of Gastroenterology ISSN 1007-9327

• *BRIEF REPORTS* •

Combined effects of Cantide and chemotherapeutic drugs on inhibition of tumor cells' growth *in vitro* and *in vivo*

Ying Yang, Qiu-Jun Lv, Qing-You Du, Bing-Hu Yang, Ru-Xian Lin, Sheng-Qi Wang

Ying Yang, Qiu-Jun Lv, Qing-You Du, Bing-Hu Yang, Ru-Xian Lin, Sheng-Qi Wang, Beijing Institution of Radiation Medicine, Beijing 100850, China
Ying Yang, Department of Biochemistry, National Institute for the Control of Pharmaceutical and Biological Product, Beijing 100050, China
Supported by the National Nature Science Foundation of China, No. 39870879, and Key Technologies R and D Program of China, No. 2002AA2Z3337
Co-first-authors: Ying Yang and Sheng-Qi Wang
Co-correspondents: Ying Yang and Sheng-Qi Wang
Correspondence to: Professor Sheng-Qi Wang, Beijing Institution of Radiation Medicine, Beijing 100850, China. sqwang@nic.bmi.ac.cn
Telephone: +86-10-66932211 Fax: +86-10-66932211
Received: 2004-03-31 Accepted: 2004-05-29

Abstract

AIM: To investigate the combination effect of hTERT antisense oligonucleotide "Cantide" and three chemotherapeutic drugs (cisplatin, 5-fluorouracil (5-FU) and adriamycin (ADM)) on inhibiting the proliferation of HepG2, BGC and A549 cell lines *in vitro*, and to investigate the efficacy of Cantide used in combination with cisplatin (DDP) *in vivo*.

METHODS: Cantide was transfected into these tumor cells by Lipofectin, and cell growth activity was calculated by microcytotoxicity assay. *In vivo* study, cells of HepG2 were implanted in Balb/c nude mice for 4 d. Then Cantide, DDP and Cantide+DDP were given intraperitoneally for 24 d respectively. The body weights of the tumor-bearing animals and their tumor mass were measured later to assess the effect of combination therapy in the nude mice. To evaluate the interaction of Cantide and these chemotherapeutic drugs, SAS software and Jin Zhengjun method were used.

RESULTS: Combination treatments with 0.1 μmol/L Cantide reduced the IC_{50} of DDP, 5-FU and ADM from 1.07, 4.15 and 0.29 μg/mL to 0.25, 1.52 and 0.12 μg/mL respectively. The inhibition ability of DDP, 5-FU and ADM respectively in combination with Cantide in these tumor cells was higher than that of these drugs alone ($P<0.0001$). And synergism ($Q \geqslant 1.15$) was observed at the lower concentration of DDP ($\leqslant$1 μg/mL), 5-FU ($\leqslant$10 μg/mL) and ADM ($\leqslant$0.1 μg/mL) with combination of Cantide. *In vivo*, combination treatment with Cantide and DDP produced the greater growth inhibition of human liver carcinoma cells HepG2 in nude mice (0.65±0.19 g tumor) compared with that when only one of these drugs was used (Cantide group: 1.05±0.16 g tumor, $P = 0.0009<0.001$; DDP group: 1.13±0.09 g tumor, $P = 0.0001<0.001$).

CONCLUSION: These findings indicate that Cantide may enhance therapeutic effectiveness of chemotherapeutic drugs over a wide range of tumor cells *in vitro*, and the combination use of Cantide and DDP can produce much higher inhibition rates, as compared with when either of these drugs was used only *in vivo*.

Key words: hTERT; Antisense oligonucleotide; Tumor; Chemotherapeutic drugs

Yang Y, Lv QJ, Du QY, Yang BH, Lin RX, Wang SQ. Combined effects of Cantide and chemotherapeutic drugs on inhibition of tumor cells' growth *in vitro* and *in vivo*. *World J Gastroenterol* 2005; 11(16): 2491-2496
http://www.wjgnet.com/1007-9327/11/2491.asp

INTRODUCTION

In some areas of the world, cancer has become or shortly will become the leading disease-related cause of death in human beings[1]. In contrast, there are still many inadequate medical treatments of cancer. The main curative therapies for cancer surgery and radiation can be only successful in general if the cancer is found at an early stage and is localized. Currently conventional chemotherapy for treatment of the advanced tumors, although quite effective, has been associated with toxicities to normal tissue and organs, which is still a major dose limited factor. And chemoresistance is another major obstacle for successful treatment of cancer[2]. So it is difficult to remove these tumor cell contaminants with the use of the conventional chemotherapy only. It is clear that new therapeutic options are necessary.

Recent progresses in identification and characterization of new molecular targets for cancer and the limited effectiveness of conventional treatment strategies have attracted considerable attention on the development of new types of anticancer drugs. These new drugs would be highly specific for malignant cells with minimized side effects due to well-defined mechanisms of action. Antisense oligodeoxynucleotides (ASODNs) are a new drug they are short, synthetic stretches of DNA which can hybridize with specific mRNA strands that correspond to target genes. By binding to the mRNA, ASODN prevents the sequence of the target gene from being converted into a protein, thereby blocking the action of the gene[3]. So ASODNs have been extensively considered

for the down regulation of oncogenes in cancer therapy[4]. And a more recent approach was the use of ASODNs in combination with conventional chemotherapy for potential anticancer therapy[5-7]. Combination therapy of ASODNs and cytotoxic drugs potentially has several advantages including lower doses of chemotherapeutic drugs, less side effects on normal cells and loss of chemoresistance. Hopefully the combination therapy will serve as a base for more effective elimination of tumor cells[8].

In our previous studies it was demonstrated that tumor cells treated with Cantide, an ASODN targeted to human telomerase reverse transcriptase (hTERT) mRNA, resulted in a relatively rapid decrease of tumor cells' growth *in vitro*. Cytotoxic effect of Cantide was also compared with the sense, random and mismatched ODNs as control sequences. Only Cantide has potent inhibitory effect on tumor cells proliferation[9]. *In vivo* treatment of HepG2 tumor xenografts with Cantide significantly retarded the growth of the tumors. In this study, to explore the potential of Cantide used in combination with chemotherapeutic drugs on inhibition of human tumor cells' growth, the cytotoxic interaction between Cantide and three chemotherapeutic drugs cisplatin (DDP), 5-fluorouracil (5-FU) and adriamycin (ADM) are analyzed *in vitro* and investigation of the efficacy of Cantide in combination with DDP *in vivo* is presented.

MATERIALS AND METHODS

Cell and culture condition

Human hepatocellular carcinoma cell (HepG2) was obtained from American Type Culture Collection. Human lung adenocarcinoma cells (A549) and human gastric cells (BGC823) were obtained from Chinese National Cancer Institute, Chinese Academy of Medical Science. HepG2 and BGC823 cells were cultured in DMEM (GIBCO BRL, Grand Island, NY, USA), supplemented with 10% FCS (GIBCO BRL), 100 U/mL penicillin and 100 U/mL streptomycin. A549 were cultured in RPMI-1640 (GIBCO BRL), supplemented with 10% FBS (GIBCO BRL), 100 U/mL penicillin and 100 U/mL streptomycin. Tumor cells were kept at 37 ℃ in a humidified atmosphere containing 50 mL/L CO_2.

Chemotherapeutic drugs

Cisplatin (DDP) was obtained from Qilu Pharmaceutical General Factory, China. 5-FU was obtained from Tianjin people's Pharmaceutical Factory, China. ADM was obtained from Hisun Pharmaceutical Co. Ltd, China.

Synthesis of Cantide

The antisense phosphorothioate oligodeoxynucleotides "Cantide" (5'-ACTCACTCAGGCCTCAGACT-3') was synthesized on solid supports using Oligo Pilot II DNA (Amersham-Pharmacia, USA) and purified by HPLC Prep 4000 (Waters Delta, USA) with SOURCE 15Q (Amersham-Pharmacia, USA).

Evaluation of the effect of Cantide used in combination with chemotherapeutic drugs on inhibiting proliferation of HepG2 cells

HepG2 cells were seeded at a density of 4×10^3 cells/well flat-bottomed plates (100 μL/well). After 24 h, culture medium was removed and the cells were washed with fresh FCS-free DMEM. In the above-mentioned medium, Cantide was delivered into these cells in the form of complex with Lipofectin (Invitrogen, USA) as described in the direction of Lipofectin. Using this method, three samples of concentrations (0.1, 0.2, 0.4 μmol/L) of Cantide were transfected into HepG2. After incubating for 6 h, 100 μL of cell culture medium with different chemotherapeutic drugs was replaced in each well. And five concentrations around the IC_{50} of each chemotherapeutic drugs (DDP: 0.25, 0.5, 1, 2, 4 μg/mL; 5-FU: 1.0, 2.5, 5, 10, 20 μg/mL; ADM: 0.025, 0.05, 0.1, 0.2, 0.4 μg/mL) were used. Each anticancer drugs' different concentrations was used in combination with Cantide's three concentrations (0.1, 0.2, 0.4 μmol/L) respectively, and each test group was tested thrice. At the same time, treatments with Cantide alone and either of the anticancer drugs were assayed, and treatments with cell culture medium without any drugs were used as control tests. After 72-h incubation, 20 μL of MTS (Promega, USA) was added in each well, followed by a 90-min incubation at 37 ℃. Inhibition rate (IR) of tumor cells proliferation was assessed according to absorption at 490 nm using a Victor 1420 Multilable Counter (WALLAC, USA).

Analysis of the antitumor profile of combination treatment with Cantide and chemotherapeutic drugs

Human hepatocellular carcinoma cells (HepG2), human lung adenocarcinoma cell lines (A549) and human gastric tumor cells (BGC823) were tested and results obtained are presented in this paper. A549 and BGC823 cells were treated as what was done with HepG2 cells (as described above), but the ranges of concentrations of anticancer drugs were different according to different cell lines.

Tumors and mice

Female 4-5-wk-old Balb/c nude mice were purchased from Center for Animals for Experiment, Chinese Academy of Medical Science. HepG2 tumor cells cultured *in vitro* and 6×10^6 cells were injected into the neck of the nude mice. Four days later, the tumor could be sensed by touch.

Treatment in vivo

The above-mentioned nude mice were divided into four groups (n = 7-8 mice/group). Cantide only group: Cantide was dissolved in saline and administered intraperitoneally (i.p.) 50 mg/kg daily for 24 consecutive days; DDP only group: DDP was dissolved in saline and administered intraperitoneally (i.p.) 1 mg/kg every other day for seven times totally; Combination treatment group: the nude mice were treated by Cantide plus DDP as described above; and negative control group (saline, i.p.). Tumor size was measured in two dimensions by calipers every 3 d, and the volume was calculated as length×width^2×0.52. The nude mice were then killed and the solid tumors were peeled off on the 27th d after treatment. Then their tumors were weighed and IR calculated.

Statistical analysis

The software package for statistical analyses was SAS 6.12,

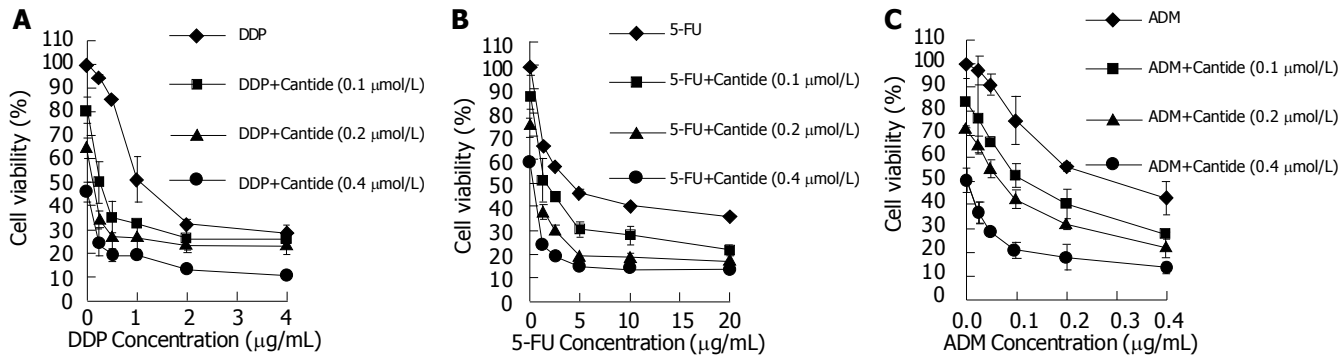

Figure 1 HepG2 cells' growth inhibited by Cantide, DDP(**A**), 5-FU(**B**) and ADM (**C**) only and at the indicated combinations on HepG2 cells. The dots represent the concentrations of chemotherapeutic drugs as 0 on the dose-response curves which means treatments with Cantide only. The cells were treated with Cantide complexed to Lipofectin for 6 h at 37 ℃. The medium was then replaced with media containing various concentrations of DDP, 5-FU and ADM. After 72 h of incubation, MTT assay was performed. Absorbance at 490 nm was normalized to the control, untreated cells to determine cell viability. Each value represents the mean±SD from triplicate determination.

and factorial design was used in the treatments *in vitro*, while *t* test was performed to assess potentially significant differences between individual groups of observations *in vivo*. In all tests, the significance of differences was accepted at $P<0.05$.

Analysis of the interaction between Cantide and anticancer drugs

To analyze the interaction between Cantide and the three anticancer drugs, Zheng-Jun Jin method[10] was used. This method provides a "Q" value, according to which the interaction between two drugs can be classified as antagonistic effect ($Q\leqslant 0.85$), additive effect ($0.85\leqslant Q<1.15$) or synergistic effect ($Q\geqslant 1.15$). And the formula is $Q = E_{a+b}/(E_a+E_b-E_a\times E_b)$, where E_{a+b}, E_a and E_b are average effect of combination treatment, effect of drug A only and effect of drug B only, respectively.

RESULTS

Cantide increases the cytotoxicity of DDP, 5-FU and ADM on HepG2

Cantide can decrease proliferation of HepG2 and increase HepG2 cells' sensitivity to anticancer treatment. For each experiment, dose-response curves of each single chemotherapeutic drug and its combination with Cantide at different doses were performed. Figure 1A shows that the drug concentration causing 50% growth inhibition (IC_{50}) of treatment of HepG2 cells with DDP only is 1.00 μg/mL, and IC_{50} of treatment of HepG2 cells with DDP in combination with Cantide (0.1 μmol/L) is 0.25 μg/mL. On the other hand, DDP can also increase the efficacy of Cantide. For example, 0.1 μmol/L Cantide used only (the dot which corresponds to 0 concentration of DDP on the dose-response curves) and when it was used in combination with 0.5 μg/mL DDP reduced the cell viability from 80% to 35%. Figure 1B indicates that combination treatment with 0.1 μmol/L Cantide reduced the IC_{50} of 5-FU from 4.15 to 1.52 μg/mL. And combination treatment with 0.1 μmol/L Cantide reduced the IC_{50} of ADM from 0.29 to 0.12 μg/mL (Figure 1C). The dose-response curves obtained from the combination experiments indicate that Cantide increased the cytotoxicity of DDP, 5-FU and ADM on HepG2 cells. And analysis with SAS software demonstrates statistically significant differences between any of the various single-drug treatments and combination treatment as indicated ($P<0.0001$).

Cantide synergistically interacts with chemotherapeutic drugs on HepG2

To investigate the nature of the interaction between Cantide and the anticancer drugs on HepG2 cells, Zheng-Jun Jin method[10] was used to analyze the cytotoxicity data for antagonism, additivity or synergy. Q values in Figure 2 indicate that the synergistic effects appeared for the combinations of Cantide with lower concentrations of anticancer drugs. Furthermore, Figure 2A shows that the combination treatments of DDP plus Cantide obtained better synergistic effects than those of other anti-drugs' combinations. The top Q value for combination treatment of Cantide and DDP was 2.08.

Inhibition effects of combination treatment with Cantide and chemotherapeutic drugs on different tumor cells

It was confirmed that the reduced cell growth rate in a variety of carcinoma cells upon treatment with single drug or the various combination treatments was due to the induction of cell death and cell viability calculated with microcytotoxicity assay (MTT) assays. As shown in Table 1, these values represent IC_{50} of chemotherapeutic drugs only and those of various combinations with Cantide on BGC and A549 cells. Values in first column with concentration treatments of Cantide are 0.0 (μmol/L) represent treatments with chemotherapeutic drugs only. And values in the next three columns represent IC_{50} of chemotherapeutic drugs in combination with Cantide. Similar results were obtained in cultures with BGC and A549 cells that combination treatments could decrease the IC_{50} of anticancer drugs.

Antitumor effects of Cantide used in combination with DDP on human liver tumor xenografts

On the 4th d after injecting HepG2 cell into these nude mice, the tumor could be sensed by touching and the volumes of tumors were approximately equal. Then these

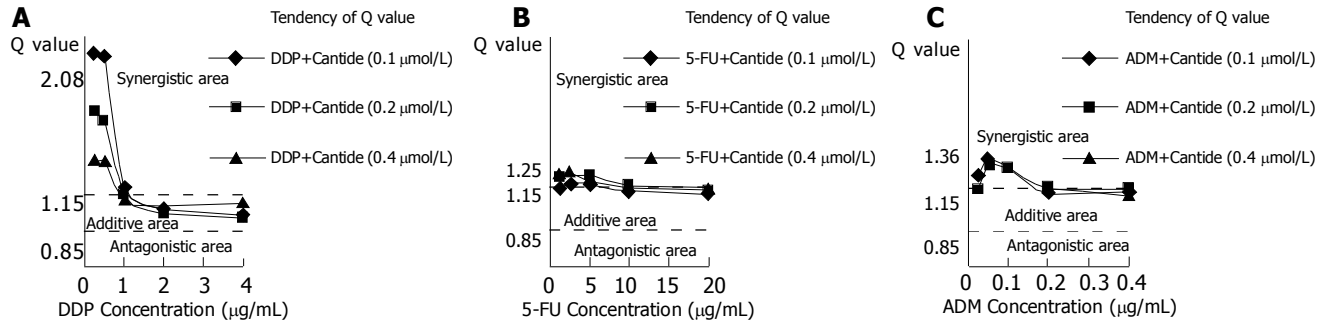

Figure 2 *Q* values for the combination treatments of Cantide with DDP (**A**), 5-FU (**B**) and ADM (**C**) tested on HepG2 cells. *Q* values were calculated from the dose-response curves shown in Figure 1 and analyzed with Zheng-Jun Jin method.

mice were divided into four treatment groups: DDP only, Cantide only, DDP+Cantide and control group. Six days later, the differences between the average tumor volume of the control group and each of those of the three treatment groups were statistically significant respectively (all $P<0.05$). And the tumor volume of combination therapy group increased less than that of any other treatment groups. Twelve days later, the volume of tumor in the combination treatment group was significantly smaller than those in the single drug therapy groups ($P<0.05$). When the test came to the end, the tumor volume of all groups were as follows: control, 1 995.21±342.77 mm^2; DDP 1 mg/kg, 1 107.07±222.66; Cantide 50 mg/kg, 1 022.88±284.70 mm^2; DDP 1 mg/kg+ Cantide 50 mg/kg, 729.86±128.04 mm^2 ($P<0.01$) (Figure 3). After these nude mice were killed, the solid tumors were peeled off to measure their weights and calculate the IR. The IR of combination therapy was 70.0% and it was significantly greater than the IR of the single drug therapy groups ($P<0.001$), where DDP and Cantide were 47.9% and 51.6% respectively (Table 2). And compared with single drug groups, the combination therapy had no significant side effect on nude mice.

Table 1 IC_{50} of chemotherapeutic drugs only or that of combination treatments (μg/mL)

Tumor cell lines	Chemotherapeutic drugs	Concentration of Cantide (μmol/L)			
		0.0	0.1	0.2	0.4
BGC	DDP	0.45	0.36	0.27	0.15
	5-FU	10.28	7.84	2.17	1.70
	ADM	0.60	0.43	0.38	0.11
A549	DDP	5.43	3.21	2.04	0.96
	5-FU	9.69	9.06	5.34	0.31
	ADM	0.76	0.71	0.60	0.43

Table 2 Tumor weights after treatment

Group	Tumor weight (g)	Inhibitory rate (%)
Control	2.17±0.31	0.0
Cantide	1.05±0.16	51.6
DDP	1.13±0.09	47.9
Cantide+DDP	0.65±0.19	70.0

Cantide+DDP group is significantly different from any group treated with a single drug: $P = 0.0009<0.001$ *vs* Cantide group; $P = 0.0001<0.001$ *vs* DDP group (*t* test). The results are expressed as mean±SD of 7–8 mice per group.

DISCUSSION

Telomerase is an RNA-dependent DNA polymerase that synthesizes telomeric DNA sequences and almost universally provides the molecular basis for unlimited proliferation potential. Since first discovered in *Tetrahymena thermophila* in 1985[11], telomerase activity was found to be absent in most normal human somatic cells but present in over 90% of cancerous cells and *in vitro* immortalized cells[12,13]. The holoenzyme consists of two essential components: one is a functional RNA component (hTR)[14,15], which serves as a template for telomeric DNA synthesis; the other is a catalytic protein (hTERT) with reverse transcriptase activity[16-19]. hTR is highly expressed in all tissues regardless of telomerase activity[20], with cancer cells generally having five-fold higher expression than normal cells. On the contrary, the expression (mRNA) of hTERT is estimated at less than 1-5 copies per cell and is closely associated with telomerase activity in cells. hTERT is generally repressed in normal cells and upregulated in immortal cells, suggesting that hTERT is the primary determinant for the enzyme activity [21,22]. Thus, inhibition of hTERT function is expected to be particularly effective on tumors. And there are some studies which prove that inhibition of telomerase could increase the sensitivity of DNA damaging drugs to tumor cells[23,24]. So, based on our previous studies[9], we investigated the ability of Cantide, an ASODN against hTERT mRNA, to sensitize carcinoma cells to hemotherapy and searched for antisense-drug combinations that could produce synergistic cytotoxicity.

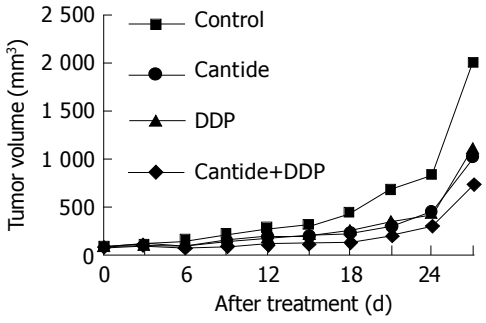

Figure 3 Tumor growth curves for Balb/c nude mice after treatment with DDP, Cantide or DDP+Cantide. Points for these groups represent the average values for 7-8 mice.

In this study, the cell lines HepG2, A549 and BGC were treated with Cantide, DDP, 5-FU or ADM only, or with different combinations of Cantide and chemotherapeutic drugs. As the example of HepG2 cells, the results showed that the inhibition ability of DDP, 5-FU and ADM respectively when used in combination with Cantide on HepG2 cells was higher than any of those when only one of the drugs was used ($P<0.0001$). And synergism ($Q \geqslant 1.15$) was observed for lower concentration of DDP ($\leqslant 1$ μg/mL), 5-FU ($\leqslant 10$ μg/mL) and ADM ($\leqslant 0.1$ μg/mL) for combination treatment with Cantide. In order to explore the inhibitory effects of combination treatments in different tumor cells further, the cell lines A549 and BGC were tested with the same methods as that for HepG2 cells. The data also demonstrated that combination treatment for these tumor cell lines with Cantide plus anticancer drugs synergistically induced greater growth inhibition of cancer cells when compared with treatment in which either one of the drugs was used. *In vivo* test, the results of the tumor growth delay assays were used for Cantide (50 mg/kg) only, DDP (1 mg/kg) only and Cantide (50 mg/kg)+DDP (1 mg/kg) in nude mice with intraperitoneal injection (i.p). The IR of tumor growth of combination therapy was significantly greater than that of any therapy using only one drug ($P<0.001$).

These findings could encourage further research in antisense therapy where Cantide is used in combination with chemotherapeutic drugs, and our conclusions are also supported by recent work of others showing the relationship between telomerase and chemotherapeutic drugs.

Cisplatin (DDP) is frequently prescribed for the treatment of a wide variety of neoplasms. It causes DNA strand break especially at guanine residues. Several possibilities exist as to how cisplatin might interfere with telomerase function[25]. One possibility is that the telomeric repeat sequence (TTAGGG)n could be cross-linked as G-Pt-G, A-Pt-G or G-Pt-T-Pt-G. Alternatively, interactions of cisplatin with essential sulfhydryl groups in the protein part of the enzyme are also possible. Furthermore, there is evidence that cisplatin might disable transcription of the telomerase-RNA encoding gene region, as the expression of human telomerase RNA component, measured using the hTR-specific TRC3 primers, was significantly decreased[26]. Since cisplatin's effect on telomerase activity is distinct from other cytotoxic drugs as described above, one might propose that inhibition of telomerase activity could, in part, contribute to cisplatin's remarkable efficacy against tumors and thus inhibition of telomerase activity might have therapeutic potential.

ADM promotes apoptotic cell death in a variety of experimental tumor cell lines[27]. It is found that ADM-induced DNA damage appears to preferentially target chromosome ends resulting in substantial telomere-related cytogenetic abnormalities, indicating that the observed senescence is due to telomere dysfunction[28].

5-FU, an inhibitor of thymidylate synthase, was shown to be more cytotoxic when used in combination with ASODN specific for thymidylate synthase mRNA. And Mitsui *et al* [29], found that some cancer cells exposed to 5-FU showed a diminished telomerase activity preceded by a time-dependent decrease in the mRNA expression of hTERT. Thus, therapeutic strategies involving applications of ASODN in combination with conventional cytotoxics appear promising for potential cancer therapy[30].

Although a critical and careful evaluation of telomere inhibitors in cancer chemotherapy *in vivo* is certainly required, and further studies on the mechanism of combination therapy are needed, our present data indicate that Cantide, the inhibitor of telomerase maintenance, may act to make cancers chemosensitize to DDP, 5-FU and ADM. Thus, it can encourage the development and evaluation of this therapeutic combination of drug applications.

REFERENCES

1 **Gibbs JB.** Mechanism-based target identification and drug discovery in cancer research. *Science* 2000; **287**: 1969-1973

2 **Benner E,** Bishop MR, Agarwal N, Iversen P, Joshi SS. Combination of antisense oligonucleotide and low-dose chemotherapy in hematological malignancies. *J Pharmacol Toxicol Methods* 1997; **37**: 229-235

3 **Jansen B,** Zangemeister-Wittke U. Antisense therapy for cancer-the time of truth. *Lancet Oncol* 2002; **3**: 672-683

4 **Akhtar S,** Hughes MD, Khan A, Bibby M, Hussain M, Nawaz Q, Double J, Sayyed P. The delivery of antisense therapeutics. *Adv Drug Deliv Rev* 2000; **44**: 3-21

5 **Gleave ME,** Zellweger T, Chi K, Miyake H, Kiyama S, July L, Leung S. Targeting anti-apoptotic genes upregulated by androgen withdrawal using antisense oligonucleotides to enhance androgen- and chemo-sensitivity in prostate cancer. *Invest New Drugs* 2002; **20**: 145-158

6 **van de Donk NW**, Kamphuis MM, van Dijk M, Borst HP, Bloem AC, Lokhorst HM. Chemosensitization of myeloma plasma cells by an antisense-mediated downregulation of Bcl-2 protein. *Leukemia* 2003; **17**: 211-219

7 **Miyake H,** Hara I, Kamidono S, Gleave ME. Novel therapeutic strategy for advanced prostate cancer using antisense oligodeoxynucleotides targeting anti-apoptotic genes upregulated after androgen withdrawal to delay androgen-independent progression and enhance chemosensitivity. *Int J Urol* 2001; **8**: 337-349

8 **Klasa RJ,** Bally MB, Ng R, Goldie JH, Gascoyne RD, Wong FM. Eradication of human non-Hodgkin's lymphoma in SCID mice by BCL-2 antisense oligonucleotides combined with low-dose cyclophosphamide. *Clin Cancer Res* 2000; **6**: 2492-2500

9 **Wang SQ,** Lin L, Chen ZB, Lin RX, Chen SH, Guan W, Wang XH. Effect of antisense oligonucleotides targeting telomerase catalytic subunit on tumor cell proliferation *in vitro*. *Chinese Sci Bulletin* 2002; **47**: 993-997

10 **Jin ZJ.** Addition in drug combination (author's transl). *Zhongguo Yaoli Xuebao* 1980; **1**: 70-76

11 **Greider CW,** Blackburn EH. Identification of a specific telomere terminal transferase activity in Tetrahymena extracts. *Cell* 1985; **43**: 405-413

12 **Kim NW,** Piatyszek MA, Prowse KR, Harley CB, West MD, Ho PL, Coviello GM, Wright WE, Weinrich SL, Shay JW. Specific association of human telomerase activity with immortal cells and cancer. *Science* 1994; **266**: 2011-2015

13 **Tatsumoto N,** Hiyama E, Murakami Y, Imamura Y, Shay JW, Matsuura Y, Yokoyama T. High telomerase activity is an independent prognostic indicator of poor outcome in colorectal cancer. *Clin Cancer Res* 2000; **6**: 2696-2701

14 **Feng J,** Funk WD, Wang SS, Weinrich SL, Avilion AA, Chiu CP, Adams RR, Chang E, Allsopp RC, Yu J. The RNA component of human telomerase. *Science* 1995; **269**: 1236-1241

15 **Ren X,** Gavory G, Li H, Ying L, Klenerman D, Balasubramanian S. Identification of a new RNA. RNA interaction site for human telomerase RNA (hTR): structural implications for hTR accumulation and a dyskeratosis congenita point mutation. *Nucleic Acids Res* 2003; **31**: 6509-6515

16 **Lai CK,** Mitchell JR, Collins K. RNA binding domain of

telomerase reverse transcriptase. *Mol Cell Biol* 2001; **21**: 990-1000

17 **Kilian A,** Bowtell DD, Abud HE, Hime GR, Venter DJ, Keese PK, Duncan EL, Reddel RR, Jefferson RA. Isolation of a candidate human telomerase catalytic subunit gene, which reveals complex splicing patterns in different cell types. *Hum Mol Genet* 1997; **6**: 2011-2019

18 **Lue NF,** Lin YC, Mian IS. A conserved *telomerase* motif within the catalytic domain of telomerase reverse transcriptase is specifically required for repeat addition processivity. *Mol Cell Biol* 2003; **23**: 8440-8449

19 **Horikawa I,** Barrett JC. Transcriptional regulation of the telomerase hTERT gene as a target for cellular and viral oncogenic mechanisms. *Carcinogenesis* 2003; **24**: 1167-1176

20 **Avilion AA,** Piatyszek MA, Gupta J, Shay JW, Bacchetti S, Greider CW. Human telomerase RNA and telomerase activity in immortal cell lines and tumor tissues. *Cancer Res* 1996; **56**: 645-650

21 **Yi X,** Tesmer VM, Savre-Train I, Shay JW, Wright WE. Both transcriptional and posttranscriptional mechanisms regulate human telomerase template RNA levels. *Mol Cell Biol* 1999; **19**: 3989-3997

22 **Kyo S,** Takakura M, Taira T, Kanaya T, Itoh H, Yutsudo M, Ariga H, Inoue M. Sp1 cooperates with c-Myc to activate transcription of the human telomerase reverse transcriptase gene (hTERT). *Nucleic Acids Res* 2000; **28**: 669-677

23 **Kondo Y,** Kondo S, Tanaka Y, Haqqi T, Barna BP, Cowell JK. Inhibition of telomerase increases the susceptibility of human malignant glioblastoma cells to cisplatin-induced apoptosis. *Oncogene* 1998; **16**: 2243-2248

24 **He D,** Zhang H. Antisense oligodeoxynucleotide of telomerase gene enhances cisplatin-induced apoptosis in acute myeloid leukemia and chronic myeloid leukemia cells. *Zhonghua Neine Zazhi* 2001; **40**: 654-656

25 **Cheng H,** Wu Z, Zheng J, Lu G, Yan J, Liu M, Huang D, Lin J. Inhibition on telomerase activity and cytotoxic effects by cisplatin in cultured human choroidal melanoma cells. *Yanke Xuebao* 2003; **19**: 54-59

26 **Burger AM,** Double JA, Newell DR. Inhibition of telomerase activity by cisplatin in human testicular cancer cells. *Eur J Cancer* 1997; **33**: 638-644

27 **Ladeda V,** Adam AP, Puricelli L, Bal de Kier Joffe E. Apoptotic cell death in mammary adenocarcinoma cells is prevented by soluble factors present in the target organ of metastasis. *Breast Cancer Res Treat* 2001; **69**: 39-51

28 **Elmore LW,** Rehder CW, Di X, McChesney PA, Jackson-Cook CK, Gewirtz DA, Holt SE. Adriamycin-induced senescence in breast tumor cells involves functional p53 and telomere dysfunction. *J Biol Chem* 2002; **277**: 35509-35515

29 **Mitsui A,** Kuwabara Y, Iwase H, Mitani M, Shinoda N, Sato A, Toyama T, Sugiura M, Suzuki T, Kato J, Fujii Y. Telomerase activity in esophageal squamous cell carcinoma: down-regulation by chemotherapeutic agent. *J Surg Oncol* 2002; **79**: 37-45

30 **Ciardiello F,** Caputo R, Troiani T, Borriello G, Kandimalla ER, Agrawal S, Mendelsohn J, Bianco AR, Tortora G. Antisense oligonucleotides targeting the epidermal growth factor receptor inhibit proliferation, induce apoptosis, and cooperate with cytotoxic drugs in human cancer cell lines. *Int J Cancer* 2001; **93**: 172-178

Science Editor Guo SY **Language Editor** Elsevier HK

PO Box 2345, Beijing 100023, China
www.wjgnet.com
wjg@wjgnet.com

ELSEVIER

World J Gastroenterol 2005;11(16):2497-2501
World Journal of Gastroenterology ISSN 1007-9327

• *BRIEF REPORTS* •

Effective siRNA targets screening for human telomerase reverse transcriptase

Yun Xia, Ru-Xian Lin, Su-Jun Zheng, Ying Yang, Xiao-Chen Bo, Dao-Yin Zhu, Sheng-Qi Wang

Yun Xia, Su-Jun Zheng, Ru-Xian Lin, Ying Yang, Xiao-Chen Bo, Sheng-Qi Wang, Beijing Institute of Radiation Medicine, Beijing 100850, China
Yun Xia, Dao-Yin Zhu, Department of Microbiology and Immunology, Chongqing Medical University, Chongqing 400016, China
Supported by the National Natural Science Foundation of China, No. 30371662
Correspondence to: Professor Sheng-Qi Wang, Beijing Institute of Radiation Medicine, No. 27 Taiping Road, Beijing 100850, China. sqwang@nic.bmi.ac.cn
Telephone: +86-10-66932211 Fax: +86-10-66932211
Received: 2004-03-20 Accepted: 2004-04-29

Abstract

AIM: To study the inhibitory effects of siRNAs targeting different hTERT sequences and to screen the effective siRNA sequence.

METHODS: Five double-stranded siRNAs targeting coding and non-coding regions of hTERT gene were designed and synthesized by T7 transcription system *in vitro*. siRNA4 sequence was screened by full length gene targeting technique and the rest of the siRNA sequences were selected randomly. After being purified by ethanol precipitation, the siRNAs were transfected to the human hepatocellular carcinoma cell (HepG2) by Lipofectamine 2000™. At 48-72 h after siRNAs transfection, MTT assay, RT-PCR and Western-blot were applied to evaluate the effects of siRNAs on cell growth, mRNA and protein expression level of hTERT gene, respectively.

RESULTS: Compared to the control cells, the cells treated with the five double-stranded siRNAs exhibited different degrees of inhibition of cell proliferation in a dose-dependent manner. siRNA2 and siRNA4, exhibited obvious effects of inhibiting hTERT mRNA and protein expression in HepG2 cells.

CONCLUSION: siRNAs targeting different hTERT sequences have significantly various inhibitory effects on hTERT gene expression. The siRNA sequence screened by full length gene targeting technique has comparable inhibitory effect with the rest siRNA sequences screened by random selection, suggesting that siRNAs and antisense oligonucleic acids may have the same effective target sites. Compared with chemical synthesis method, synthesizing double-stranded siRNA by T7 transcription system *in vitro* is a rapid, simple, and inexpensive method suitable for screening high-effect siRNA targeting site for specific gene.

Key words: siRNA targets; hTERT

Xia Y, Lin RX, Zheng SJ, Yang Y, Bo XC, Zhu DY, Wang SQ. Effective siRNA targets screening for human telomerase reverse transcriptase. *World J Gastroenterol* 2005; 11(16): 2497-2501
http://www.wjgnet.com/1007-9327/11/2497.asp

INTRODUCTION

Telomerase enzyme complex have two major subunits contributing to enzymatic activity: a structural RNA component (human telomerase RNA, hTER) that contains a template region that binds the TTAGGG repeats in telomerase and a catalytic subunit with reverse transcriptase activity (human telomerase reverse transcriptase, hTERT). Expression of hTERT is almost exclusively limited to cancer cells and recent research indicated that hTERT expression is a rate-limiting step in telomerase activity and carcinogenesis[1]. Inhibition of hTERT activity has potential significance in gene function research and cancer gene therapy.

RNA interference (RNAi) is a sequence-specific post-transcriptional gene silencing mechanism, which is triggered by double-stranded RNA (dsRNA), causing degradation of mRNAs homologous in sequence to the dsRNA and inhibiting specific gene expression effectively[2]. As for antisense DNA and ribozymes, various siRNAs directed at different sites of target gene exhibit obviously different suppression effects. Thus, siRNA faces the same challenges that confront other nucleic acid-based gene inactivation strategies: site selection[3]. In the present study, five siRNA sequences targeting at different sites of hTERT gene were designed by the method of random selection and full length gene targeting technique based on RNase digestion sensitivity. All of them were synthesized by T7 RNA polymerase *in vitro* and the inhibitory effects were evaluated on cell proliferation, hTERT mRNA and protein expression, respectively.

MATERIALS AND METHODS

Selection of the target sequence of siRNA

The principle of random selection of siRNA target sites was described previously[4]. In the totally five siRNA sequences, siRNA4 was selected by full length gene targeting technique established by our laboratory, the rest were selected by

Table 1 siRNA sequences targeting hTERT gene

Number	Position in hTERT mRNA	Sense sequence(5′-3′)	GC content (%)
1	2319-2329 (coding region)	AAGGC ACT GTT CAG CGT GCTC	57
2	2653-2673 (coding region)	AAGGC CTT CAA GAG CCA CGTC	57
3	1801-1821 (coding region)	AAGGT GCA AAG CAT TGG AATC	38
4	3652-3672 (non-coding region)	AAGGG CTG AGT GTC CAG CACA	57
5	3865-3885 (non-coding region)	AAGGA CCC TGG GAG CTC TGGG	67

random selection method. All siRNA sequences were done blast-research in GenBank to confirm that only hTERT gene was targeted. The information of the five siRNAs is summarized in Table 1.

Synthesis of DNA template for transcription in vitro

For *in vitro* transcription to produce 21-nt siRNA, four strands of 43-nt DNA template oligonucleotides were synthesized as:

P1: 5'T7 promoter Sense sequence (19 nt of AA down-stream) TT 3'
P2: 5'T7 promoter Antisense sequence TT 3'

P3 was complementary with P1; P4 was complementary with P2. T7 promoter sequence was: 5'-GGTAATACGAC-TCACTATAGGG-3'. The underlined G was the initiating site of transcription. The 43nt DNA oligomers were synthesized by an applied biosystems 391 DNA synthesizer and purified by PAGE.

siRNA synthesis

DNA template strands P1 and P3, were mixed in equimolar amounts, heated for 5 min at 95 ℃, then gradually cooled down to room temperature in annealing buffer to form the double-stranded DNA S1. P2 and P4 were treated the same way to form the double-stranded DNA S2. Transcription *in vitro* was carried out in two separate tubes by using the RiboMax™ Large Scale RNA Production System-T7 Kit (Promega) according to the manufacturer's instructions to obtain two single-stranded RNAs. The two complementary single-stranded RNAs were mixed and incubated at 37 ℃ overnight to form double-stranded RNA. Then the product was treated with DNase and single-stranded specific RNase T1 for 30 min at 37 ℃ to digest DNA template, unpaired single-stranded RNA and the 5' overhung GGG in double-stranded RNA was cleaved. The double-stranded RNA was then purified by ethanol precipitation and resolved with Nuclease-Free water. The product was the siRNA for transfection with 3' end overhung UU bases. RNAs were quantified by DU640 Nucleic Acid Analyzer (Beckman Coulter) and stored at -20 ℃.

Cell culture

The human hepatocellular carcinoma cell HepG2 (American Type Culture Collection, Rockville, MD) were maintained in DMEM medium containing 10% heat-inactivated fetal calf serum (Gibco Brl) and incubated at 37 ℃, 5% CO_2 atmosphere in a humidified incubator. Cells were regularly passaged to maintain exponential growth.

Transfection and MTT assay

The day before transfection, cells were seeded at a density of 5×10^3 cells/well in 96-well flat-bottomed plates (0.1 mL/well) and cultured for about 24 h at 37 ℃, 5% CO_2 atmosphere. When the cells reached 40-50% confluence, they were transfected with siRNAs complexed with Lipofectamine™ 2000 (Invitrogen) according to manufacturer's instructions in triplicate for each concentration. After an incubation for 48 h at 37 ℃, 20 μL MTS agent (Promega) was added to each well followed by another 90 min incubation at 37 ℃. Absorption was measured at 490-nm (Victor 1420 Multilabel Counter, Wallac) and inhibitory rates on cell proliferation was evaluated using the following formula:

$$\text{Inhibitory rate} = \frac{A_{\text{control}}-A_{\text{sample}}}{A_{\text{control}}-A_{\text{blank}}} \times 100\%$$

A_{control}: Absorption of cells treated with Lipofectamine ™2000 only; $A_{\text{sample:}}$ Absorption of cell treated with siRNA and Lipofectamine™2000; A_{blank}: Absorption of DMEM.

Analysis of hTERT mRNA level by RT-PCR

Totally 1.0×10^5 cells were seeded in a six-well plate. After 24 h incubation, cell confluence was about 50%. siRNAs were mixed with Lipofectamine™2000 and transfected to HepG2 cells with the final concentration 100 nmol/L. After an incubation for 48 h at 37 ℃, total RNA was isolated by TRIzol (Invitrogen) using a single-step phenol-extraction method. The cDNA strand was synthesized from 2 μg of RNA by using Superscriptase II (Invitrogen) according to the manufacturer's instructions. PCR primers were as follows: hTERT, 5'-TCTACCGGAAGAGTGTCTGGA-GCAA-3' (forward) and 5'-GCTCCCACGACGTAGTC-CATGTTCA-3' (reversed); amplicon, 202 bp; β_2-microglobulin 5'TTCAGGTTTACTCACGTCATCC-3' (forward), and 5'-CCAAATGCGGCATCTTCAAACCC-3' (reversed); amplicon, 317 bp. PCR reaction for hTERT and β_2-microglobulin was performed according to a method described earlier. PCR products were run on a 2.0% agarose gel and visualized by ethidium bromide staining. The intensities of DNA bands were measured by scanning the gel with Gel Doc 1000 (Bio-Rad). Inhibition of hTERT mRNA was calculated by relative intensity ratio hTERT/β_2-microglobulin according to the following formula:

$$\text{Inhibitory rate (\%)} = (1-A_{\text{sample}}\times A_{0\text{control}}/A_{\text{control}}\times A_{0\,\text{sample}})\times 100$$

A_{sample}: the intensity of hTERT PCR product in cells treated with 100 nM siRNA, $A_{0\text{control}}$: the intensity of β_2-microglobulin product in cells treated with Lipofectamine™

2000 alone, $A_{control}$: the intensity of β_2-microglobulin product in cells treated with 100 nmol/L siRNA, $A_{0sample}$: the intensity of hTERT PCR product in cells treated with Lipofectamine™2000 alone.

hTERT protein expression level by Western blot

Cells treated with 100 nmol/L siRNAs were harvested 72 h after transfection and lysed in a lysis buffer (RIPA-PICT, Roche) for 30 min on ice. A total of 40 μg of protein extracted from each transfected cell population was separated on 8% acrylamide gels using standard SDS-PAGE techniques and then transferred to Hybond-polyvinylidene difluoride membrane (Amersham Biosciences). The membrane was blocked overnight at 4 ℃ and then probed with 1∶2 000 diluted anti-hTERT specific antibody (Alpha Diagnostic) for 1 h at room temperature. The membrane was washed thrice for 15 min each with TBST buffer, incubated with 1∶2 000 diluted HRP-conjugated secondary antibody (Sigma) for 1 h at room temperature, washed four times for 15 min each with TBST buffer. Finally, membrane was incubated with ECL-PLUS reagent (Amersham Biosciences) for 5 min at room temperature to develop the bands, which were scanned by Typhoon 9410 Variable Mode Imager (Amersham Pharmacia). β-Actin was used as control for loading equal amount of protein in each gel. The inhibition rate was calculated in the same manner as RT-PCR.

RESULTS

siRNAs inhibited HepG2 cell growth

All of the five siRNAs showed inhibitory effects on HepG2 cell growth in a dose-dependent manner (Figure 1). siRNA2 had the highest inhibitory effect at a dose of 160 nmol/L (43.1%) and siRNA4 had better inhibitory effects at doses 10-80 nmol/L compared with the other siRNAs, it was very close to the inhibitory rate of siRNA2 at a dose 160 nmol/L (39.6%). These results suggested that siRNA targeting hTERT gene could effectively suppress HepG2 cell growth.

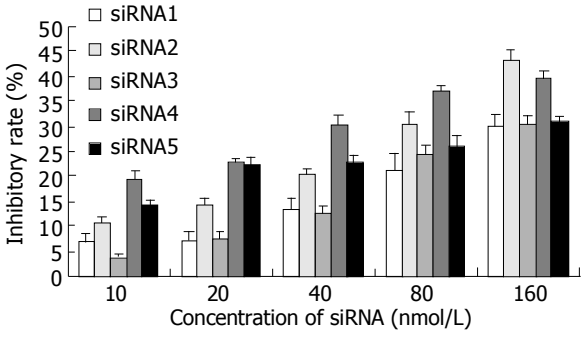

Figure 1 Inhibitory effects of different siRNA on HepG2 cell growth. HepG2 cells were transfected with siRNA and 48 h after transfection, MTT assays were tested for cell viability. The results were expressed as mean±SD from three determinants.

siRNA down-regulated hTERT mRNA expression

In order to detect whether siRNA could inhibit hTERT gene expression, the mRNA level of hTERT was determined by semi-quantitative RT-PCR. A 202-bp DNA fragment for hTERT gene and a 317-bp DNA fragment for β_2-microglobulin gene were amplified by RT-PCR with specific primers, respectively. The result of RT-PCR showed that hTERT mRNA expression level was decreased after 48-h treatment with 100 nmol/L siRNAs when compared to the control cell except siRNA3 (Figure 2A). Normalized to the levels of β_2-microglobulin, the relative inhibitory rates of siRNA1-siRNA5 were 48.3%, 43.7%, 8.3%, 70.7%, 32.7%, respectively (Figure 2B).

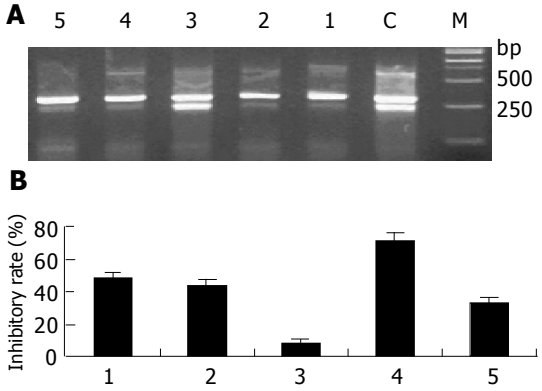

Figure 2 Inhibition of hTERT mRNA expression in HepG2 cells after 48-h transfection with 100 nmol/L siRNA. **A**: Electrophoresis of PCR products of hTERT gene and β_2-microglobulin gene in HepG2 cells. Lanes 1-5: HepG2 cells treated with 100 nmol/L siRNA1-siRNA5; Lane C: Cells treated with Lipofectamine™2000 only; Lane M: Molecular marker; **B**: Quantitation of inhibitory percentage of hTERT mRNA in siRNA treated cells. Each level of PCR product of hTERT gene was quantitated and normalized to the level of β_2-microglobulin. The results were expressed as mean±SD from three independent experiments.

siRNAs down-regulated hTERT protein expression

Western-blot analysis was performed to determine the effects of siRNAs treatment on hTERT protein level in HepG2 cells. A 130 ku band for hTERT protein was scanned and normalized to β-actin protein (Figure 3A). The relative inhibitory percentage of hTERT protein expression in the cells treated with 100 nmol/L siRNA1-siRNA5 was 33.0%, 82.5%, 43.0%, 61.5%, 36.5%, respectively (Figure 3B).

DISCUSSION

Short interfering RNAs (siRNAs) are powerful sequence-specific reagents designed to knockdown the expression of target genes in cultured mammalian cells through a process known as RNA interference (RNAi). Although the mechanism underlying RNAi activity has not been completely elucidated, RNAi has already become a powerful reverse genetic method for suppressing the expression of a target gene. Recent studies have demonstrated that 21 nt-siRNA duplexes are long enough to induce gene-specific suppression, but short enough to evade the host interferon response in cultured mammalian cells[5].The duplexes of 21 nt RNAs with symmetric 2-nt 3' overhangs are the most efficient mediators of mRNA degradation[6]. Especially, 2-nt 3' overhangs in

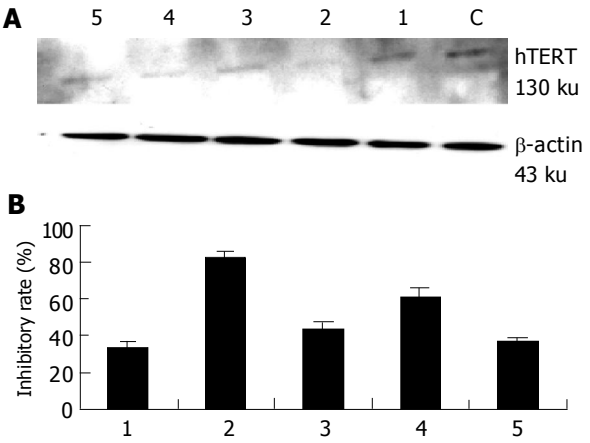

Figure 3 Inhibition of hTERT protein expression in HepG2 cells after 72-h transfection with 100 nmol/L siRNA. **A**: Western-blot analysis of hTERT protein expression in HepG2 cells. Lanes 1-5: HepG2 cells treated with 100 nmol/L siRNA1-siRNA5; Lane **C**: Cells treated with Lipofectamine™2000 only; **B**: Inhibitory percentage of hTERT protein in siRNA treated cells compared to the cells treated with Lipofectamine™2000 alone. Each level of hTERT protein was quantitated and normalized to the level of β-actin. Inhibitory rates were calculated by comparison to cells treated with Lipofectamine™2000 alone and results were expressed as mean±SD from two independent experiments.

antisense strand of siRNA are crucial for inducing RNAi in mammalian cells[7]. In the present study, four strands of 43 nt DNA template oligonucleotides were designed for synthesizing two single-stranded RNAs *in vitro* by using T7 RNA polymerase. The two complementary single-stranded RNAs could form 24 nt duplexes RNA with symmetric UU 3' overhangs and GGG 5' overhangs through Watson-Crik hybridization. GGG 5' overhangs in RNA duplexes were cleaved by single-stranded specific RNase T1 and the product was 21 nt siRNA for transfection with symmetric UU 3' overhangs.

In mammalian cells, it has recently been reported that siRNA efficacy is highly dependent upon target position, that is, the secondary structure of target RNA is an important determinant of activity for siRNA[8]. Currently selection of the targeted region is largely empirical. At the moment, there are no reliable ways to predict or identify the "ideal" sequence for an siRNA. Generally, the mRNA sequences of the desired gene were scanned randomly for AA sequences, then the AA and the downstream 19 nt were recorded and compared to an appropriate genome database to eliminate any with significant homology to other genes. Those sequences are the potential siRNA target sites[6]. Since siRNA, like antisense oligonucleotides, through an antisense mechanism results in loss of target RNA, it is reasonable to deduce that the degree of RNase H sensitivity of a given probe reflects the accessibility of the chosen site and could predict how well the siRNA will perform[9]. In this study, the results of MTT showed that the inhibition efficacy of siRNA4 was better than the others at concentrations of 10, 20, 40, and 80 nmol/L and close to siRNA2 at a concentration of 160 nmol/L. The robust inhibition of hTERT mRNA and protein expression was observed in siRNA4 and siRNA2, respectively. From the above results, we proved that siRNA2 and siRNA4 had better activity than the other three. As siRNA4 targeted the same sequence screened by the full length gene targeting technique, it is suggested that if a site is available for hybridization to an RNase H inducible oligonucleotide, then it is also available for hybridization and cleavage by the siRNA complex.

Many of the siRNAs reported to date are designed to target coding sequences, typically selected sequences located 100-200 bases away from the translation initiation sequence AUG, avoiding 5' or 3' untranslated regions[10]. Recently it has been reported that siRNA located at 3' untranslated region successfully inhibited the expression of target gene[11]. In our study, siRNA2 screened by random selection was located in hTERT translated region and exhibited inhibitory activity on hTERT gene expression. However, siRNA4 screened by the full length gene targeting technique was located in 3' untranslated region and exhibited similar activity compared with siRNA2. So it is more reasonable to select target sequences along with the full length mRNA of interested gene than to only select in the coding region.

In our previous study, a series of antisense oligonucleotides were designed based upon hTERT mRNA secondary structure. One of them, named cantide, has been demonstrated having robust inhibitory effects on tumor cell growth[12] and hTERT gene expression[5]. In this study, various siRNAs were introduced to HepG2 cells by liposome-mediated transfection and exhibited specific inhibitory effects on cell growth and hTERT gene expression. Compared to cantide, active siRNA exerted similar effects at much lower concentration. This result suggests that RNAi may be a promising gene-based therapy for cancer treatment[13].

Although, until recently, the siRNA produced by transcription or chemical synthesis *in vitro* only achieved a transient effect by using classic method such as liposome-mediated transfection[14], preparing siRNA by T7 transcription system *in vitro* is a rapid, simple and low-costing strategy suitable for screening the effective target sites[15]. In this research, five siRNAs targeting different sites of hTERT mRNA were designed and synthesized rapidly by T7 transcription system *in vitro* and two of them had high activity of gene-specific silencing effect. Our results suggest that siRNAs synthesized from a DNA template is a useful and effective way to specifically silence gene expression.

REFERENCES

1 **Kyo S,** Inoue M. Complex regulatory mechanisms of telomerase activity in normal and cancer cells: how can we apply them for cancer therapy? *Oncogene* 2002; **21**: 688-697
2 **Brummelkamp TR,** Bernards R, Agami R. A system for stable expression of short interfering RNAs in mammalian cells. *Science* 2002; **296**: 550-553
3 **Leirdal M,** Sioud M. Gene silencing in mammalian cells by preformed small RNA duplexes. *Biochem Biophys Res Commun* 2002; **295**: 744-748
4 **Yu JY,** DeRuiter SL, Turner DL. RNA interference by expression of short-interfering RNAs and hairpin RNAs in mammalian cells. *Proc Natl Acad Sci USA* 2002; **99**: 6047-6052
5 **Elbashir SM,** Harborth J, Lendeckel W, Yalcin A, Weber K, Tuschl T. Duplexes of 21-nucleotide RNAs mediate RNA interference in cultured mammalian cells. *Nature* 2001; **411**: 494-498
6 **Elbashir SM,** Harborth J, Weber K, Tuschl T. Analysis of gene function in somatic mammalian cells using small inter-

fering RNAs. *Methods* 2002; **26**: 199-213
7 **Hohjoh H.** RNA interference(RNA(i)) induction with various types of synthetic oligonucleotide duplexes in cultured human cells. *FEBS Lett* 2002; **521**: 195-199
8 **Holen T,** Amarzguioui M, Wiiger MT, Babaie E, Prydz H. Positional effects of short interfering RNAs targeting the human coagulation trigger Tissue Factor. *Nucleic Acids Res* 2002; **30**: 1757-1766
9 **Shi Y.** Mammalian RNAi for the masses. *Trends Genet* 2003; **19**: 9-12
10 **Sui G,** Soohoo C, Affar el B, Gay F, Shi Y, Forrester WC, Shi Y. A DNA vector-based RNAi technology to suppress gene expression in mammalian cells. *Proc Natl Acad Sci USA* 2002; **99**: 5515-5520
11 **McManus MT,** Petersen CP, Haines BB, Chen J, Sharp PA. Gene silencing using micro-RNA designed hairpins. *RNA* 2002; **8**: 842-850
12 **Wang SQ,** Lin L, Chen ZD, Lin RX, Chen SH, Guan W, Wang XH. Effect of antisense oliginucleotides targeting telomerase catalytic subunit on tumor cell proliferation *in vitro*. *Chinese Sci Bulletin* 2002; **47**: 993-997
13 **Wall NR,** Shi Y. Small RNA: can RNA interference be exploited for therapy? *Lancet* 2003; **362**: 1401-1403
14 **Tuschl T.** Expanding small RNA interference. *Nat Biotechnol* 2002; **20**: 446-448
15 **Leirdal M,** Sioud M. Gene silencing in mammalian cells by preformed small RNA duplexes. *Biochem Biophys Res Commun* 2002; **295**: 744-748

Science Editor Zhu LH **Language Editor** Elsevier HK

PO Box 2345, Beijing 100023, China
www.wjgnet.com
wjg@wjgnet.com

ELSEVIER

World J Gastroenterol 2005;11(16):2502-2507
World Journal of Gastroenterology ISSN 1007-9327

• *BRIEF REPORTS* •

Effects of dendritic cells from cord blood CD34$^+$ cells on human hepatocarcinoma cell line BEL-7402 *in vitro* and in SCID mice

Zhong-Jing Su, Hai-Bin Chen, Jin-Kun Zhang, Lan Xu

Zhong-Jing Su, Hai-Bin Chen, Jin-Kun Zhang, Cancer Pathology Laboratory, Department of Histology and Embryology, Shantou University Medical College, Shantou 515041, Guangdong Province, China
Lan Xu, Department of Obstetrics and Gynecology, The First Affiliated Hospital of Shantou University Medical College, Shantou 515041, Guangdong Province, China
Correspondence to: Professor Jin-Kun Zhang, Cancer Pathology Laboratory, Department of Histology and Embryology, Shantou University Medical College, Shantou 515041, Guangdong Province, China. jkzhang@stu.edu.cn
Telephone: +86-754-8900443 Fax: +86-754-8557562
Received: 2004-03-03 Accepted: 2004-04-13

Abstract

AIM: To develop a cancer vaccine of dendritic cells derived from human cord blood CD34$^+$ cells and to investigate its cytotoxicity on human hepatocarcinoma cells *in vitro* and in sever combined immunodeficiency (SCID) mice.

METHODS: Lymphocytes from cord blood or peripheral blood were primed by DCs, which were derived from cord blood and pulsed with whole tumor cell lysates. Nonradiative neutral red uptake assay was adopted to detect the cytotoxicity of primed lymphocytes on human hepatocarcinoma cell line BEL-7402 *in vitro*. The anti-tumor effect of primed lymphocytes *in vivo* was detected in SCID mice, including therapeutic effect and vaccination effect.

RESULTS: The cytotoxicity of DC vaccine primed lymphocytes from cord blood or peripheral blood on human hepatocarcinoma cell line BEL-7402 was significantly higher than that of unprimed lymphocytes *in vitro* (44.09% *vs* 14.69%, 47.92% *vs* 19.44%, $P<0.01$). There was no significant difference between the cytotoxicity of primed lymphocytes from cord blood and peripheral blood ($P>0.05$). The tumor growth rate and tumor size were smaller in SCID mice treated or vaccinated with primed lymphocytes than those with unprimed lymphocytes. SCID mice vaccinated with primed lymphocytes had a lower tumor incidence (80% *vs* 100%, $P<0.05$) and delayed tumor latent period compared with mice vaccinated with unprimed lymphocytes (11 d *vs* 7 d, $P<0.01$).

CONCLUSION: Vaccine of cord blood derived-DCs has an inhibitory activity on growth of human hepatocarcinoma cells *in vitro* and in SCID mice. The results also implicate the potential role of cord blood derived-DC vaccine in clinical tumor immunotherapy.

Key words: Dendritic cells; Hepatocarcinoma

Su ZJ, Chen HB, Zhang JK, Xu L. Effects of dendritic cells from cord blood CD34$^+$ cells on human hepatocarcinoma cell line BEL-7402 *in vitro* and in SCID mice. *World J Gastroenterol* 2005; 11(16): 2502-2507
http://www.wjgnet.com/1007-9327/11/2502.asp

INTRODUCTION

Hepatocarcinoma is a major malignant cancer in Asian and southern African countries. Resection, chemotherapy and alcohol injection are potentially curative for only small, local tumors. Unfortunately, the diseases of most patients have developed to the advanced stage at diagnosis. In China, the mortality of hepatocarcinoma ranks second among malignant tumors, only behind that of lung cancer in urban areas and stomach cancer in rural areas[1].

Dendritic cells (DCs) express abundant MHC molecules and costimulatory molecules, and are professional antigen presenting cells (APC). Immature DCs can uptake antigens through macropinocytosis, phagocytosis and receptor-mediated endocytosis and have a poor ability to activate lymphocytes. After capturing antigens, immature DCs come into mature stage and migrate from peripheral areas to lymph nodes, where they present antigens to lymphocytes and activate the immune response. For their potent ability to present antigens and activate lymphocytes, DCs are considered as the natural adjuvant for immune response[2,3]. Not surprisingly, tumor cells could escape from host immune surveillance when there is a functional failure of DCs, and the fact is that the number of mature DCs with normal functions was decreased in local tumor tissue and peripheral blood of tumor patients[4,5]. Based on these, DC-based experiments have been developed for tumor immunotherapy in the past decade. Our laboratory once found that DCs from mice spleen fused with hepatocarcinoma cells that manifested antitumor effects *in vivo*. There are also reports on DCs from human peripheral blood generating specific T cell responses and eliciting tumor regression[6,7]. However, getting a great deal of peripheral blood or other tissues from tumor patients to produce DCs *in vitro* is not practical in clinics. Since peripheral blood DCs are derived from bone marrow CD34$^+$ multipotential hematopoietic stem cells *in vivo*, Ferrari *et al*[8], adopted chemotherapy combined with granulocyte colony-stimulating factors to mobilize bone marrow CD34$^+$ cells into peripheral blood of cancer patients, and they found with such results that there was an increase of CD34$^+$ cells in peripheral blood,

but the number of DCs was not significantly increased, and the subset of DCs changed, i.e., the ratio of DC1/DC2 reversed, implicating that the differentiation of DCs in cancer patients was dysfunctional.

In cord blood, the percentage of $CD34^+$ cells is slightly lower than in bone marrow, but the percentage of $CD34^+/CD38^-$ cells is higher. Compared with $CD34^+/CD38^+$ cells, $CD34^+/CD38^-$ cells are early stem cells and more sensitive to stimulation of cytokines[9,10]. In addition, harvesting cord blood is a slightly invasive procedure. Here, we investigated the anti-tumor effects of DCs from human cord blood $CD34^+$ cells on human hepatocarcinoma cell line BEL-7402 *in vitro* and in sever combined immunodeficiency (SCID) mice.

MATERIALS AND METHODS

Tumor cell line and animals

Human hepatocellular carcinoma cell line BEL-7402 (Shanghai Institute of Cell Biology, Chinese Academy of Sciences) was cultured in RPMI 1640 (GIBCO BRL, USA) containing 10% heat-inactivated newborn calf serum (NCS, GIBCO BRL, USA), 100 U/mL penicillin and 100 μg/mL streptomycin at 37 ℃ in a humidified atmosphere containing 50 mL/L CO_2. SCID mice (6-8-wk old) were purchased from Animal Center of Sun Yat-Sen University Medical College (Guangzhou, China), bred in a specific-pathogen-free laboratory at Shantou University Medical College Affiliated Tumor Hospital. All animal procedures were performed in accordance with recommendations for the proper use and care of laboratory animals.

Preparing DCs from human cord blood

Normal human umbilical cord blood was obtained from Department of Obstetrics of the First Affiliated Hospital of Shantou University Medical College. Fresh cord blood samples were diluted 1∶4 in PBS (pH 7.4). After Ficoll-Hypaque (1.077 g/mL, Tianjin Hematology Institute, China) centrifugation (400 r/min for 35 min at 20 ℃), mononuclear cells were collected from the interface and washed twice in PBS (200 r/min for 10 min at 20 ℃).

Cord blood $CD34^+$ hematopoietic stem cells were labeled with a $CD34^+$ progenitor cell isolation kit (Miltenyi Biotec, Germany) and separated from cord blood mononuclear cells by Mini magnetic cell sorting (Mini MACS, Miltenyi Biotec, Germany) according to the protocol. DCs were induced from cord blood $CD34^+$ hematopoietic stem cells as previously described[11]. Briefly, $CD34^+$ cells were adjusted to the concentration of 3×10^4/mL and cultured at 37 ℃ in a humidified 50 mL/L CO_2 atmosphere in RPMI 1640 containing 10% NCS, 100 U/mL penicillin, 100 μg/mL streptomycin and supplemented with 100 μg/mL recombined human granulocyte-macrophage colony-stimulating factor (rhGM-CSF, Biotinge Co., China), 50 U/mL recombined human tumor necrosis factor-α (TNF-α, PeproTech EC Ltd Co., UK). For every 2 d, half of the medium was replaced with fresh complete medium supplemented with 100 μg/mL rhGM-CSF, 50 U/mL TNF-α for a total period of 2 wk. The differentiation process of DCs was observed under a phase contrast microscope (Olympus, Japan).

Pulsing DCs with whole tumor cell lysates

Human hepatocarcinoma cell line BEL-7402 was trypsinized and washed twice in PBS, then lysed by ultrasonication (Misonix, USA). The cell lysates were monitored by light microscopy. After being cultured with GM-CSF and TNF-α for 14 d, cord blood-derived DCs were collected and incubated with whole cell lysates of BEL-7402 at a ratio of three tumor cells equivalent to one DC (i.e., 3∶1) in RPMI 1640 containing 10% NCS. After 12 h of incubation, pulsed DCs were washed twice in PBS and resuspended in RPMI 1640.

Priming lymphocytes in vitro with pulsed DCs

Human peripheral blood (from healthy volunteers of our laboratory) or cord blood (from Department of Obstetrics of the First Affiliated Hospital of Shantou University Medical College) mononuclear cells were isolated with Ficoll-Hypaque by density gradient centrifugation and cultured in RPMI 1640 complete medium. After being incubated for 4 h, non-adherent cells were harvested as lymphocytes.

Cord blood derived-whole tumor cell lysate pulsed-DCs were added to lymphocytes from peripheral blood or cord blood at a responder-to-stimulator ratio of 20∶1 in RPMI 1640 containing 10% NCS and 80 U/mL recombined human interleukin-2 (rhIL-2, Biotinge Co., China). After being cultured for 5 d, cells were harvested as primed lymphocytes.

Neutral red uptake assay

Human hepatocarcinoma cell line BEL-7402 was seeded into 96-well cell culture plates (Costar, USA) at a concentration of 0.4×10^4/200 μL per well. After 24-h incubation, the culture medium was removed and the cell number was counted. Then fresh medium containing DC-primed lymphocytes from peripheral blood, DC-primed lymphocytes from cord blood, unprimed lymphocytes from peripheral blood, unprimed lymphocytes from cord blood were added as effector cells in PB-DLC group, CB-DLC group, PB-LC group and CB-LC group respectively, at an effector-to-target ratio of 10∶1, three wells for every group. In control group, no effector cells were added. Forty-eight hours after the effector cells were added, the medium was replaced by 100 μL neutral red (30 μg/mL). After incubation for another 1 h, the neutral red was removed. Cultures were carefully washed twice with PBS and the neutral red in tumor cells was extracted with 100 μL solution of 1% hydrochloric acid/ethanol. Neutral red absorbance value (A value) of tumor cells at wavelength 570 nm was detected with a 3550-UV microplate reader (Bio-Rad, USA). Each assay was performed in quadruplicate. The results were presented as mean±SD. Cytolytic activities of the effector cells were calculated as (1-A value of experimental group/A value of control group)×100%.

Treatment or vaccination with primed lymphocytes in SCID mice

Tumor cells and SCID mice were prepared as described above. To study the therapeutic effect of DC-primed lymphocytes on hepatoma *in vivo*, a human hepatoma model was established in SCID mice by subcutaneous (s.c.) injection

of viable BEL-7402 of logarithmic stage (2×10^6 cells in 100 μL PBS for each mouse) at the right flank. Subsequently, the tumor-bearing mice in Tr-DLC group and Tr-LC group (5 mice/group) were injected s.c. at the left flank with 1×10^7 DC-primed lymphocytes or with unprimed lymphocytes from peripheral blood respectively, twice at 3-d intervals.

To study the protective effect of DC-primed lymphocytes on human hepatocarcinoma cells *in vivo*, SCID mice in Im-DLC group and Im-LC group (5 mice/group) were first vaccinated with 1×10^7 DC-primed lymphocytes or with unprimed lymphocytes respectively, twice at 3-d intervals. Four days after the second vaccination, the mice in Im-DLC group and Im-LC group were both challenged with human hepatocarcinoma BEL-7402 cells of logarithmic stage (2×10^6 cells in 100 μL PBS for each mouse).

In control group, SCID mice were just injected s.c. with human hepatocarcinoma BEL-7402 cells (2×10^6) at the right flank. After tumor cell injection, tumor incidence and tumor latent period of all mice were recorded. The widest diameter (*a*) and narrowest diameter (*b*) of the tumor *in vivo* were measured twice a week with calipers. Tumor volume was calculated according to the formula $V = ab^2/2$[12]. After 32 d of tumor cell injection, all the mice were killed and tumor volume was measured *ex vivo*.

Statistical analysis

Data were analyzed with SPSS11.0 statistical software. Tumor volumes were statistically analyzed after evolution. The significant difference between groups was determined by one-way ANOVA test. Two-sided $P<0.05$ was considered statistically significant. No mouse was excluded from this study.

RESULTS

Generation of DCs from cord blood CD34$^+$ cells

$CD34^+$ cells from cord blood were round and regular with a diameter of about 7-8 μm. Under the stimulation of rhGM-CSF 100 μg/mL and rhTNF-α 50 U/mL, the cell number increased and cell clones formed. At the same time the cells stretched out cytoplasmic projections. During the later period of culture, DCs shed from the clones to the medium. On day 14, the total number of cells increased about 20-fold. Under a phase contrast microscope, we found that after being pulsed with BEL-7402 cell lysates at a ratio of 3:1, human cord blood-derived DCs displayed more pronounced dendritic processes (Figure 1).

Cytotoxicity of DC-primed lymphocytes in vitro

Lymphocytes were primed by tumor cell lysate pulsed-DCs at a responder-to-stimulator ratio of 20:1 for 5 d. As shown in Table 1, the neutral red absorbance value of viable tumor cells in PB-DLC group and CB-DLC group was significantly lower than that in PB-LC and CB-LC groups ($P<0.01$). There was no significant difference in *A* value between PB-DLC group and CB-DLC group ($P>0.05$). According to *A* value, the cytotoxicity of primed lymphocytes from peripheral blood or cord blood was 47.92% and 44.09% respectively, while the cytotoxicity of unprimed lymphocytes was 19.44% and 14.69%.

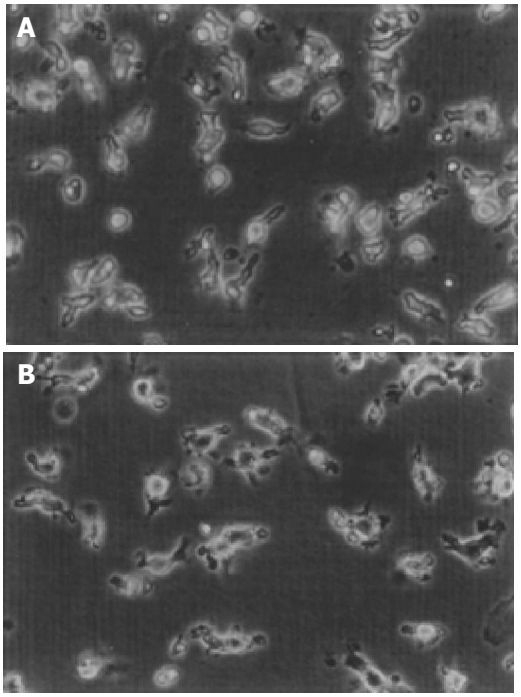

Figure 1 Morphology of DCs. **A**: Morphology of DCs derived from cord blood at d 14 was irregular and with cytoplasm projections. **B**: After being pulsed with whole tumor cell lysates, the dendritic processes of DCs being more typical (phase contrast microscope, 20×5.5).

Table 1 Neutral red absorbance value (*A* value) of human hepatocarcinoma BEL-7402 cells and cytotoxicity of effector cells in different groups (mean±SD)

Group	*A*	Cytotoxicity (%)
Control	0.1286±0.0165	
CB-LC	0.1097±0.0276[a]	14.69
PB-LC	0.1036±0.0291[a]	19.44
CB-DLC	0.0719±0.0118[b,d]	44.09
PB-DLC	0.0670±0.0145[b,f]	47.92

[a]$P<0.05$ *vs* control group, [b]$P<0.01$ *vs* control group, [d]$P<0.01$ *vs* CB-LC group, [f]$P<0.01$ *vs* PB-LC group.

Therapeutic effect of DC-primed lymphocytes in SCID mice

To evaluate whether DCs derived from cord blood had therapeutic effects on hepatoma cells *in vivo*, treatment experiments were performed in SCID mice. All SCID mice developed tumors within 7 d after injection of 2×10^6 hepatocarcinoma BEL-7402 cells. In tumor-bearing mice treated with DC-primed lymphocytes, both the tumor growth rate *in vivo* (Figure 2) and the tumor volume measured *ex vivo* on the 32nd d after tumor cell injection (Figure 3) were smaller than those in mice treated with unprimed lymphocytes ($P<0.05$). There was no significant difference between mice treated with unprimed lymphocytes and mice in control group ($P>0.05$) (Figures 2 and 3).

Protective effect of primed lymphocytes in SCID mice

To evaluate whether DCs derived from cord blood exerted protective effects in SCID mice against human hepatoma cells *in vivo*, vaccination experiments were performed. All mice (5/5) vaccinated with unprimed lymphocytes developed

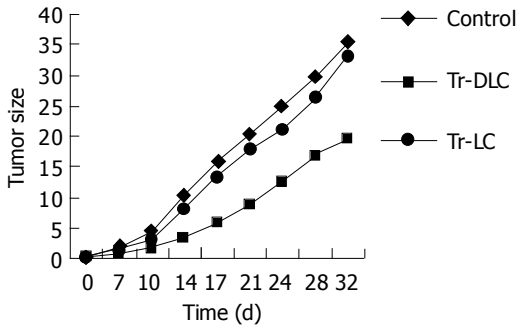

Figure 2 Growth curves of human hepatocarcinoma BEL-7402 cells in SCID mice treated with DC-primed lymphocytes (Tr-DLC), unprimed lymphocytes (Tr-LC) and in control group respectively.

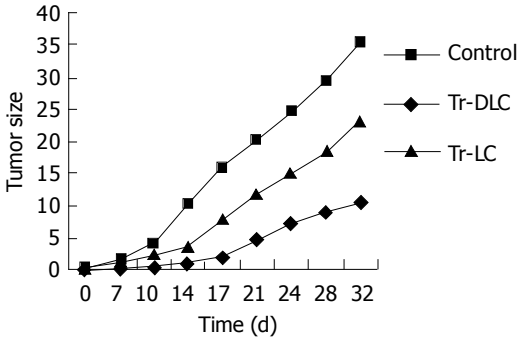

Figure 4 Growth curves of human hepatocarcinoma cell BEL-7402 in SCID mice vaccinated with DC-primed lymphocytes (Im-DLC), unprimed lymphocytes (Im-LC) and in control group respectively.

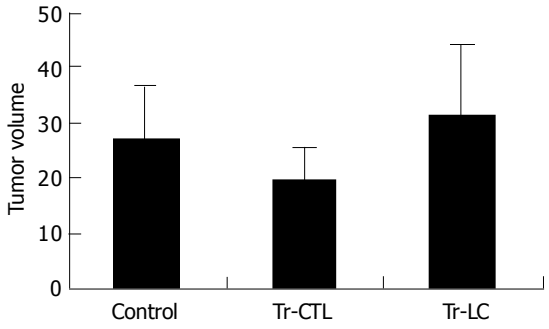

Figure 3 All mice were killed after 32 d of tumor cell injection and tumor volumes measured *ex vivo* and presented as mean±SD after evolution (5 mice/group).

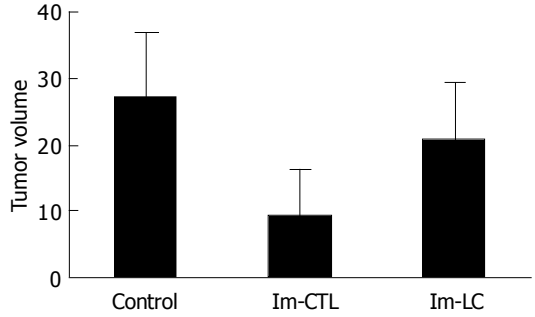

Figure 5 All mice were killed after 32 d of tumor cell challenge and tumor volumes were measured *ex vivo* and presented as mean±SD after evolution (5 mice/group).

tumors within 7 d after injection of 2×10^6 hepatocarcinoma cells. On day 32 after tumor challenge, 80% (4/5) mice vaccinated with DC-primed lymphocytes developed tumors and the tumor latent period was about 11-14 d. Tumor growth rate *in vivo* (Figure 4) and tumor volume measured *ex vivo* on the 32nd d after tumor cell challenge (Figure 5) both decreased in mice vaccinated with DC-primed lymphocytes compared with mice vaccinated with unprimed lymphocytes and mice in control group ($P<0.05$).

DISCUSSION

In this study, $CD34^+$ cells were isolated from cord blood mononuclear cells by Mini MACS. With the stimulation of rhGM-CSF and rhTNF-α, cord blood-derived $CD34^+$ cells could proliferate, and the cell number and formation of cell clones were increased. In this experiment, the number of total cells increased about 20-fold after being cultured for 14 d with cytokines. During proliferation, cells differentiated into DCs and displayed cell projections. Caux *et al*[11], reported that cord blood $CD34^+$ cells differentiated into DCs in two different ways with the stimulation of GM-CSF and TNF-α. After being cocultured with cytokines for 5-7 d, there were two kinds of cell phenotypes, one was $CD14^+$, the other was $CD1a^+$. On the 12-14th d of culture, they both differentiated into DCs.

After being pulsed with whole tumor cell lysates, cord blood-derived DCs manifested more processes, which were similar to the morphological changes of Langerhans cells from skin stretching out typical dendrites after being cultured for several days *in vitro*. Researchers also found that formation of cell dendrites was related to the expression of cell skeleton 55 ku fascin-actin bundling protein[13]. Fascin and CD83 were also the phenotypic characteristics of mature DCs[14,15]. We considered that the typical dendrites might be the morphological characteristics of mature DCs.

Since neutral red can stain viable cells and is rejected by dead cells, we adopted the nonradiative neutral red uptake assay in this study to detect the absorbance value of tumor cells, and then the cytolytic activity of effector cells on tumor cells was calculated according to the absorbance value. The results in Table 1 indicated that the cytotoxicity of primed lymphocytes was significantly higher than that of unprimed lymphocytes from peripheral blood *in vitro*, so were primed lymphocytes and unprimed lymphocytes from cord blood. Cord blood lymphocytes mainly consist of $CD45RA^+$ naive cells[16]. Our finding in this study that there was no significant difference between the cytolytic activity of primed lymphocytes from cord and peripheral blood suggested that DCs from cord blood respectively could activate naive lymphocytes as well as memory lymphocytes, which was consistent with previous reports[17].

The potent effect of DCs on activating resting lymphocytes was associated with its surface molecules and cell skeleton. One of these molecules attracting the attention of many

researchers is DC-SIGN (DC-specific ICAM-3 grabbing nonintegrin), which is the receptor of HIV and mycobacteria, more importantly, also the high affinitive receptor of intercellular adhesion molecule (ICAM)-3 expressed on lymphocytes[18-20]. DC-SIGN can promote DCs to contact with lymphocytes through combination with ICAM-3, even without the existence of antigens. Moreover, the contact of DCs with lymphocytes and formation of immunosynapse are necessary for DCs presenting antigens and activating lymphocytes. Cell skeleton protein fascin not only takes part in maintaining cell morphology and developing cell dendrites but also plays an important role in the active skeleton rearrangement and formation of immunosynapse[14,21]. Mosialos *et al*[22], and Kupfer and Singer[23] reported that DCs were the only leukocytes that could express fascin and the only APC that could make an active rearrangement of its skeleton during the formation of immunosynapse. It is possible that the DC-specific DC-SIGN and the ability of skeleton rearrangement are associated with its specific ability to activate resting lymphocytes.

In this study, we adopted SCID mice, which lacked T and B lymphocytes genetically, to study the antitumor effect of DC primed lymphocytes *in vivo*. The sections stained with HE showed that spleen cells of SCID mice were scattered with no obvious splenic corpuscle or periarterial lymphatic sheath (picture not shown). This indicated that SCID mice in this experiment had no "immune leak", so there was no host immune response to injected cells. In SCID mice treated with DC-primed lymphocytes, the rate of tumor growth was slower than that of mice in control group, suggesting that DC vaccine can inhibit tumor growth *in vivo*. While in mice vaccinated with DC-primed lymphocytes, and challenged with human hepatocarcinoma cells, though still some mice developed tumors, tumor incidence was significantly decreased, implicating the antitumor effect of DC vaccine *in vivo*. The reason why the tumor volume in mice treated with unprimed lymphocytes was greater than that in control group may be the heterogeneity of individuals. After all, the difference between these two groups was not significant ($P>0.05$).

The rejection of tumor cells *in vivo* depends on effector T cells. In the results of our experiments, tumor cell lysates pulsed-DC vaccine manifested some therapeutic and protective effects against tumor cells *in vivo*. The use of tumor cell lysates as a source of antigens to pulse DCs has several advantages. First, it mimics the physiologic process by which a growing tumor induces an immune response. Second, there is also a possibility that DCs pulsed with whole tumor cell lysates could present a broader range of epitopes of tumor antigens and activate polyclone subpopulations of T cells compared to a single peptide or antigen-pulsed DCs. Third, it is not necessary to characterize and isolate tumor molecular antigens. The preparation of such a DC vaccine pulsed with whole tumor cell lysates is relative facile. One disadvantage of this approach, however, is the potential danger of evoking autoimmune reactivity to self or normal tissues. Anti-dsDNA and anti-nuclear antibodies were found existing in animal experiments after vaccinated with whole tumor antigen-pulsed DCs[24,25]. In clinic, fortunately, no unbearable side effects have been reported except for rare vitiligo in melanoma patients treated with whole tumor antigen-pulsed DCs[26]. Many clinic experiments have also proved that DC vaccine is safe for patients. We wish this preliminary study can provide some evidence for advanced study of cord blood-derived DC vaccine and its application in clinics for tumor patients.

ACKNOWLEDGEMENTS

We thank Miss Jiong-Yu Chen and Professor De-Rui Li of Affiliated Tumor Hospital, Professor Kang-Sheng Li of Department of Immunology and staff of Department of Obstetrics and Gynecology in First Affiliated Hospital of Shantou University Medical College, for their assistance and support to this work.

REFERENCES

1 **Zhang S,** Li L, Lu F. Mortality of primary liver cancer in China from 1990 through 1992. *Zhonghua Zhongliu Zazhi* 1999; **21:** 245-249
2 **Steinman RM,** Dhodapkar M. Active immunization against cancer with dendritic cells: the near future. *Int J Cancer* 2001; **94:** 459-473
3 **Mellman I,** Steinman RM. Dendritic cells: specialized and regulated antigen processing machines. *Cell* 2001; **106:** 255-258
4 **Schwaab T,** Weiss JE, Schned AR, Barth RJ. Dendritic cell infiltration in colon cancer. *J Immunother* 2001; **24:** 130-137
5 **Ratta M,** Fagnoni F, Curti A, Vescovini R, Sansoni P, Oliviero B, Fogli M, Ferri E, Della-Cuna GR, Tura S, Baccarani M, Lemoli RM. Dendritic cells are functionally defective in multiple myeloma: the role of interleukin-6. *Blood* 2002; **100:** 230-237
6 **Geiger JD,** Hutchinson RJ, Hohenkirk LF, McKenna EA, Yanik GA, Levine JE, Chang AE, Braun TM, Mule JJ. Vaccination of pediatric solid tumor patients with tumor lysate-pulsed dendritic cells can expand specific T cells and mediate tumor regression. *Cancer Res* 2001; **61:** 8513-8519
7 **Geiger J,** Hutchinson R, Hohenkirk L, McKenna E, Chang A, Mule J. Treatment of solid tumours in children with tumour-lysate-pulsed dendritic cells. *Lancet* 2000; **356:** 1163-1165
8 **Ferrari S,** Rovati B, Porta C, Alessandrino PE, Bertolini A, Collova E, Riccardi A, Danova M. Lack of dendritic cell mobilization into the peripheral blood of cancer patients following standard- or high-dose chemotherapy plus granulocyte-colony stimulating factor. *Cancer Immunol Immunother* 2003; **52:** 359-366
9 **Ueda T,** Yoshida M, Yoshino H, Kobayashi K, Kawahata M, Ebihara Y, Ito M, Asano S, Nakahata T, Tsuji K. Hematopoietic capability of CD34+ cord blood cells: a comparison with CD34+ adult bone marrow cells. *Int J Hematol* 2001; **73:** 457-462
10 **Gigant C,** Latger-Cannard V, Bensoussan D, Feugier P, Bordigoni P, Stoltz JF. Quantitative expression of adhesion molecules on granulocyte colony-stimulating factor-mobilized peripheral blood, bone marrow, and cord blood CD34+ cells. *J Hematother Stem Cell Res* 2001; **10:** 807-814
11 **Caux C,** Vanbervliet B, Massacrier C, Dezutter-Dambuyant C, de-Saint-Vis B, Jacquet C, Yoneda K, Imamura S, Schmitt D, Banchereau J. CD34+ hematopoietic progenitors from human cord blood differentiate along two independent dendritic cell pathways in response to GM-CSF+TNF alpha. *J Exp Med* 1996; **184:** 695-706
12 **Carlsson G,** Gullberg B, Hafstrom L. Estimation of liver tumor volume using different formulas-an experimental study in rats. *J Cancer Res Clin Oncol* 1983; **105:** 20-23
13 **Ross R,** Ross XL, Schwing J, Langin T, Reske-Kunz AB. The actin-bundling protein fascin is involved in the formation of dendritic processes in maturing epidermal Langerhans cells. *J*

Immunol 1998; **160:** 3776-3782
14 **Al-Alwan MM,** Rowden G, Lee TD, West KA. Fascin is involved in the antigen presentation activity of mature dendritic cells. *J Immunol* 2001; **166:** 338-345
15 **Thurnher M,** Papesh C, Ramoner R, Gastl G, Bock G, Radmayr C, Klocker H, Bartsch G. *In vitro* generation of CD83+ human blood dendritic cells for active tumor immunotherapy. *Exp Hematol* 1997; **25:** 232-237
16 **D'Arena G,** Musto P, Cascavilla N, Di Giorgio G, Fusilli S, Zendoli F, Carotenuto M. Flow cytometric characterization of human umbilical cord blood lymphocytes: immunophenotypic features. *Haematologica* 1998; **83:** 197-203
17 **Caux C,** Massacrier C, Dezutter-Dambuyant C, Vanbervliet B, Jacquet C, Schmitt D, Banchereau J. Human dendritic Langerhans cells generated *in vitro* from CD34+ progenitors can prime naive CD4+ T cells and process soluble antigen. *J Immunol* 1995; **155:** 5427-5435
18 **Geijtenbeek TB,** Kwon DS, Torensma R, van Vliet SJ, van Duijnhoven GC, Middel J, Cornelissen IL, Nottet HS, KewalRamani VN, Littman DR, Figdor CG, van-Kooyk Y. DC-SIGN, a dendritic cell-specific HIV-1-binding protein that enhances trans-infection of T cells. *Cell* 2000; **100:** 587-597
19 **Geijtenbeek TB,** Torensma R, van-Vliet SJ, van Duijnhoven GC, Adema GJ, van-Kooyk Y, Figdor CG. Identification of DC-SIGN, a novel dendritic cell-specific ICAM-3 receptor that supports primary immune responses. *Cell* 2000; **100:** 575-585
20 **Tailleux L,** Schwartz O, Herrmann JL, Pivert E, Jackson M, Amara A, Legres L, Dreher D, Nicod LP, Gluckman JC, Lagrange PH, Gicquel B, Neyrolles O. DC-SIGN is the major Mycobacterium tuberculosis receptor on human dendritic cells. *J Exp Med* 2003; **197:** 121-127
21 **Al-Alwan MM,** Rowden G, Lee TD, West KA. The dendritic cell cytoskeleton is critical for the formation of the immunological synapse. *J Immunol* 2001; **166:** 1452-1456
22 **Mosialos G,** Birkenbach M, Ayehunie S, Matsumura F, Pinkus GS, Kieff E, Langhoff E. Circulating human dendritic cells differentially express high levels of a 55-kd actin-bundling protein. *Am J Pathol* 1996; **148:** 593-600
23 **Kupfer A,** Singer SJ. The specific interaction of helper T cells and antigen-presenting B cells. IV. Membrane and cytoskeletal reorganizations in the bound T cell as a function of antigen dose. *J Exp Med* 1989; **170:** 1697-1713
24 **Ludewig B,** Ochsenbein AF, Odermatt B, Paulin D, Hengartner H, Zinkernagel RM. Immunotherapy with dendritic cells directed against tumor antigens shared with normal host cells results in severe autoimmune disease. *J Exp Med* 2000; **191:** 795-804
25 **Bondanza A,** Zimmermann VS, Dell'Antonio G, Dal-Cin E, Capobianco A, Sabbadini MG, Manfredi AA, Rovere-Querini P. Cutting edge: dissociation between autoimmune response and clinical disease after vaccination with dendritic cells. *J Immunol* 2003; **170:** 24-27
26 **Rosenberg SA**, White DE. Vitiligo in patients with melanoma: normal tissue antigens can be targets for cancer immunotherapy. *J Immunother Emphasis Tumor Immunol* 1996; **19:** 81-84

Science Editor Zhu LH, Li WZ and Wang XL **Language Editor** Elsevier HK

PO Box 2345, Beijing 100023, China
www.wjgnet.com
wjg@wjgnet.com

ELSEVIER

World J Gastroenterol 2005;11(16):2508-2512
World Journal of Gastroenterology ISSN 1007-9327

• *BRIEF REPORTS* •

Profiling of differentially expressed chemotactic-related genes in MCP-1 treated macrophage cell line using human cDNA arrays

Guang-Xing Bian, Hong Miao, Lei Qiu, Dong-Mei Cao, Bao-Yu Guo

Guang-Xing Bian, Hong Miao, Lei Qiu, Bao-Yu Guo, Department of Biochemical Pharmacy, School of Pharmacy, Second Military Medical University, Shanghai 200433, China
Dong-Mei Cao, Department of Pathology and Physiology, College of Basic Medical Sciences, Second Military Medical University, Shanghai 200433, China
Correspondence to: Professor Bao-Yu Guo, Department of Biochemical Pharmacy, School of Pharmacy, Second Military Medical University, Shanghai 200433, China. byguo1632000@yahoo.com.cn
Telephone: +86-21-25070398
Received: 2003-10-24 Accepted: 2004-04-13

Abstract

AIM: To study the global gene expression of chemotactic genes in macrophage line U937 treated with human monocyte chemoattractant protein-1 (MCP-1) through the use of ExpreeChip™HO_2 cDNA array.

METHODS: Total RNA was extracted from MCP-1 treated macrophage line U937 and normal U937 cells, reversely transcribed to cDNA, and then screened in parallel with HO_2 human cDNA array chip. The scanned result was additionally validated using RT-PCR.

RESULTS: The result of cDNA array showed that one chemotactic-related gene was up-regulated more than two-fold (RANTES) and seven chemotactic-related genes were down-regulated more than two-fold (CCR1, CCR5, ccl16, GROβ, GROγ, IL-8 and granulocyte chemotactic protein 2) in MCP-1 treated U937 cells at mRNA level. RT-PCR analysis of four of these differentially expressed genes gave results consistent with cDNA array findings.

CONCLUSION: MCP-1 could influence some chemokine and receptor expressions in macrophages *in vitro*. MCP-1 mainly down-regulates the expression of chemotactic genes influencing neutrophilic granulocyte expression (GROβ, GROγ, IL-8 and granulocyte chemotactic protein 2), and the mRNA level of CCR5, which plays a critical role in many disorders and illnesses.

Key words: MCP-1; ExpreeChip™HO_2

Bian GX, Miao H, Qiu L, Cao DM, Guo BY. Profiling of differentially expressed chemotactic-related genes in MCP-1 treated macrophage cell line using human cDNA arrays. *World J Gastroenterol* 2005; 11(16): 2508-2512
http://www.wjgnet.com/1007-9327/11/2508.asp

INTRODUCTION

Chemokines are small secreted proteins that function as potent activators and chemoattractants for leukocyte subpopulations and some nonhemopoietic cells. Most chemokines elicit their effects through interactions with seven-transmembrane-domain, G-protein-coupled receptors. The size of this family has grown considerably and now includes dozens of members[1]. According to the position of conserved cysteine residues in their primary sequence, the chemokine superfamily is divided into four subfamilies (C-X-C, C-C, C, and C-X_3-C) which attract specific subsets of leukocytes[2]. Chemokine expression secondary to stimulation with proinflammatory cytokines has been reported in many types of diseases[3].

Monocyte chemoattractant protein-1 (MCP-1) was first purified from conditioned medium of baboon aortic smooth muscle cells in culture on the basis of its ability to attract monocytes, but not neutrophils, *in vitro*. It is a potent chemoattractant for monocytes *in vitro*, with an ED50 similar to that of IL-8 for neutrophils (500 pmol/L). MCP-1 induces the expression of integrins required for chemotaxis, and has also been reported to attract NK cells as well as T lymphocytes[4-6].

Recently, the function of chemokines has extended far beyond leukocyte physiology. For example, MCP-1 was found to play a pathogenic role in many diseases. Its expression could be detected in human atheromatous plaques and in aortic walls of primates fed with high-cholesterol diets, consistent with a model of atherogenesis in which MCP-1 in the vessel walls attracted monocytes that eventually became foam cells[7]. Similarly, the presence of inflammatory cells in the joints of patients with rheumatoid arthritis has been explained by IL-8 and MCP-1 in synovial fluids[8]. This expression was also documented in glomerulonephritis, asthma, inflammatory bowel disease, and allogeneic transplant rejection[6,9].

The ligand-binding repertoires of different chemokine receptors significantly overlap, so do the sets of receptors expressed by different leukocytes and other target cells, this further adds to the versatility of the chemokine system. There are high complexities among the conditions of chemokine expressions and binding to receptors. For example, among the known CC chemokines, MCP-1, MCP-2, MCP-3, MCP-4, MCP-5, macrophage inflammatory protein (MIP)-1α, MIP-1β, I309, and HCC-1, all have monocyte chemoattractant activities in vitro. Furthermore, monocytes express at least three cloned CC chemokine receptors, namely CCR1, CCR2, and CCR5, and even though MCP-1 binds to only CCR2 with a high affinity, CCR2 also binds to

MCP-3 and MCP-5[4,6]. The cDNA array technology has been demonstrated as a very useful tool for identifying differentially expressed genes. In order to study the regulation of MCP-1 on other chemokines and their receptors, we studied the potential regulation function of MCP-1 on the expression of chemotactic-related genes in macrophages.

MATERIALS AND METHODS

Materials

huMCP-1 was purchased from Dingguo Biotech Corp.[10]. Human macrophage line U937 was reserved by our study group. FCS, chloroform, isopropanol, DEPC, TRIzol were purchased from Huashun Corp.

Cell culture and huMCP-1 treatment

Macrophage line U937 was incubated in 10 mL RPMI1640 medium containing 10% FCS. When cell count reached 0.5-1×10^6/mL, cells were centrifuged and the supernates were discarded. The cells were resuspended with the same volume of RPMI1640 medium containing huMCP-1 (10 mg/mL) and incubated overnight.

Human cDNA array, probe, hybridization, and data analysis

Culture cells were washed with cooled PBS (pH 7.2) twice, then lysed by TRIzol, extracted with chloroform, precipitated with isopropanol, and washed with 80% ethanol. The deposits were dehydrated by vacuum, then solubilized by Nes buffer. mRNA was purified by an Oligotex mRNA mini kit, then the control mRNA of cells was labeled with cy5-dUTP and the mRNA of stimulated cells was labeled with cy3-dUTP, deposited by ethanol and solubilized in 20 μL hybridization buffer (5× SSC+0.2% SDS). ExpreeChip™HO_2 was made by MERGEN Corp. The chip and probe were degenerated for 5 min at 95 ℃, then hybridized for 15-17 h at 60 ℃, washed with 2× SSC+0.2% SDS and 0.1%× SSC +0.2% SDS, 0.1%× SSC, and dried at room temperature. The chip was scanned by ScanArray3000, then the result was analyzed by ImaGene3.0. The criteria of gene expression changes were cy3/cy5≥2, or cy3/cy5≤0.5.

Semiquantitative RT-PCR

cDNA was generated using 1 μg of total RNA from the two U937 cell lines (normal and MCP-1 treated) as templates in a 20-μL reaction mixture, and reverse transcription was carried out at 42 ℃ for 1 h followed by at 95 ℃ for 10 min using the preamplification system (GIBCOL). cDNA (2 μL) was amplified in a 25 μL PCR reaction mixture containing 2× PCR buffer (10 mmol/L Tris-HCl, pH 8.3, 50 mmol/L KCl), 1.9 or 2.4 mmol/L of $MgCl_2$, 0.5 μmol/L of primers, 0.18 mmol/L of deoxynucleotide triphosphate, and 1 unit Taq DNA polymerase (TaKaRa). The conditions of hot-start PCR reaction were as follows: at 95 ℃ for 10 min followed by 25-35 cycles of denaturation at 94 ℃ for 1 min, annealing at 60 ℃ for 1 min (for primers of β-actin, GROβ, GROγ and IL-8) or at 50 ℃ for 1 min (for primers of regulated upon activation, normal T cell expressed and secreted, RANTES), and extension at 72 ℃ for 1 min. The final step of extension was at 72 ℃ for 10 min. PCR reagents were purchased from Takara. All of the primers were synthesized by Genecore Corp., Shanghai. The cycle number was optimized for each gene-specific primer pair to ensure the amplification in a linear range, and the results were semiquantitative. PCR products (5 μL) were visualized by electrophoresis on a 2% agarose gel stained with ethidium bromide.

RESULTS

Identification of differentially expressed chemotactic-related genes in U937 cells by the human ExpreeChip™HO_2 chip

ExpreeChip™HO_2 (invoice: 0102-003) used in this study was made by MERGEN Corp. The chip contained 10 ng of each gene-specific cDNA from 1 152 known genes and 9 housekeeping genes. Several plasmid and bacteriophage DNAs and blank spots were also included as negative and blank controls to confirm hybridization specificity. A complete list of the genes with array positions and GenBank accession numbers of the chip used here could be accessed at the website. Genes were considered to be up-regulated when the intensity ratio between expressions in the MCP-1 treated U937 cell lines compared with normal cell lines was two-fold. Genes were labeled as down-regulated when the ratio between normal and MCP-1 treated cell lines was two-fold. The analysis of scatter diagrams is seen in Figure 1, using EC cells as system controls.

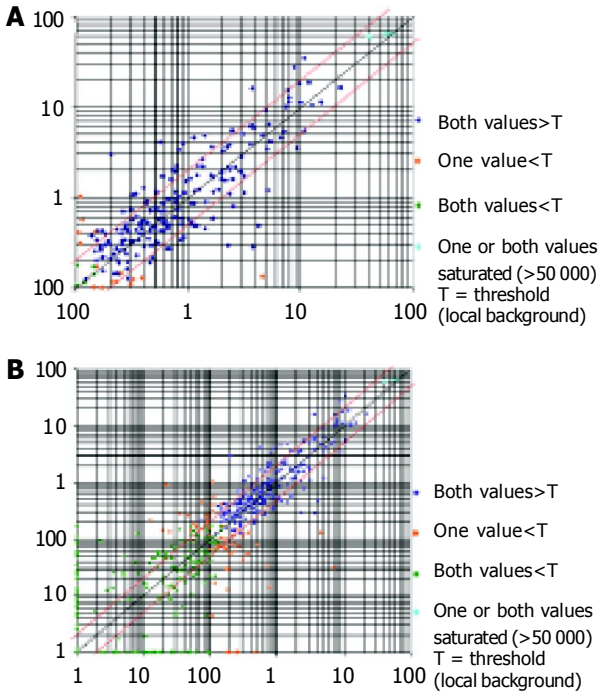

Figure 1 Chip result analysis of EC cells (**A**) and U937 cell line (**B**). The x-axis is the relative intensity of cy3 signal, and y-axis is the relative intensity of cy5 signal. The ratio x/y≥R2 shows that the gene expression was up-regulated, and x/y≤0.5 shows that the gene was down-regulated.

Results of chip detection

The membranes carrying 1 152 cDNA probes of defined human genes, and their accession numbers, names, and the scanned data were given below. Among the 1 152 genes,

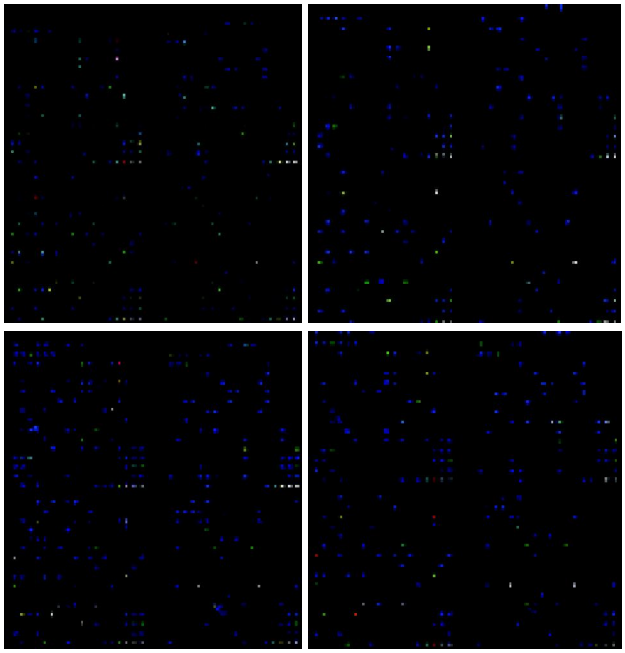

Figure 2 U937 mRNA expression analysis using Mergen cDNA arrays. These maps revealed a number of genes that were significantly expressed in controls and MCP-1 treated cells, with an expression ratio above 2 (the red color dot, more red color dots indicate more highly expressed genes) or below 0.5 (the blue color dot, more blue color dots indicate meagerly expressed genes). Results were the mean from two separate experiments and were arranged in order of decreasing relative expression after treated with MCP-1 compared with untreated controls. A correlation analysis of the results from the two separate experiments showed that the findings were highly reproducible, because r = 0.897 for the 25 genes with the highest relative mRNA expression after MCP-1 treatment.

110 were up-regulated, 91 were down-regulated (Figure 2). We searched for chemokine genes and chemokine receptor genes to study the gene expression changes in chemokine superfamily (Tables 1 and 2). Gene names shown in bold designate that genes with mRNA expression were also analyzed by RT-PCR (Figure 3).

Confirmation of differentially expressed chemotactic-related genes by semiquantitative RT-PCR

The semiquantitative RT-PCR results showed that RANTES genes were up-regulated, whereas GROβ, GROγ and IL-8 were down-regulated in MCP-1 treated cell lines (Figure 3) .These results were similar to those detected by Human ExpreeChip^{TM}HO$_2$ chip (Tables 1 and 2).

Table 1 Expression of chemokine receptor genes in U937 cell line

Sample/ Control	Control/ Sample	Unigene symbol	Gene description
0.1	1.0	CCR1	Chemokine (C-C motif) receptor 1
1.0	19.2	CCR2	Chemokine (C-C motif) receptor 2
0.7	1.3	CCR3	Chemokine (C-C motif) receptor 3
0.6	1.6	CCR3	Chemokine (C-C motif) receptor 3
1.0	1.0	CCR4	Chemokine (C-C motif) receptor 4
0.1	7.3	CCR5	Chemokine (C-C motif) receptor 5
1.0	1.0	CCR6	Chemokine (C-C motif) receptor 6
1.0	1.0	CCR7	Chemokine (C-C motif) receptor 7
1.0	1.0	CCR8	Chemokine (C-C motif) receptor 8
1.0	1.0	CCRL2	Chemokine (C-C motif) receptor-like 2
1.4	0.7	CXCR4	Chemokine (C-X-C motif), receptor 4 (fusin)

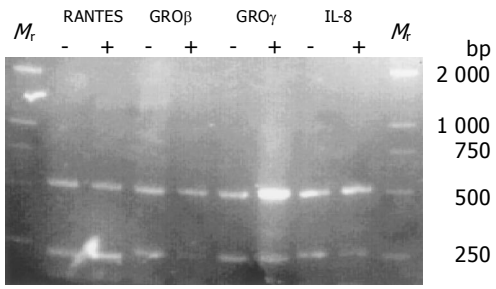

Figure 3 Primers and amplification of RT-PCR analysis. The full names of the genes and their accession numbers are given in bold in Tables 1 and 2. Sense and anti-sense primers were used to detect mRNA expression of the indicated genes by RT-PCR. The last two columns give the quantity of total RNA added to each RT-PCR reaction and the number of PCR cycles for PCR amplification used for RT-PCR analysis in MCP-1 treated U937 cells (+, MCP-1 treated). The same RT-PCR conditions were used for U937 cells (-, controls). β-actin was used as a quantitative control (sense: 5'-GGCATCCTCACCCTGAAGTA-3'; antisense: 5'-CCATCTCTTGCTCGAAGTCC-3'; 60 ℃; 496 bp; 1 μg; 30 cycles), RANTES (sense: 5'-CCCTCACCATCATCCTCACT-3'; antisense: 5'-TCCTTCGAGTGACAAACACG-3'; 50 ℃; 186 bp; 1 μg; 30 cycles), GROβ (sense: 5'-ATTCGGGGCAGAAAGAGAAC-3'; antisense: 5'-ACCCCTTTTATGCATGGTTG-3'; 60 ℃; 207 bp; 1 μg; 35 cycles), GROγ (sense: 5'-GAATTTGGGGCAGAAAATGA-3'; antisense: 5'-CGAACCCTTTTTATGCATGG-3'; 60 ℃; 227 bp; 1 μg; 30 cycles) and IL-8 (sense: 5'-AAGGAACCATCTCACTGTGTGTAAAC-3'; antisense: 5';-TTAGCACTCCTTGGCAAACTG-3'; 60 ℃; 247 bp; 1 μg; 25 cycles).

DISCUSSION

MCP-1 is a CC chemokine that attracts monocytes, memory T lymphocytes, and natural killer cells. The interaction of MCP-1 with its receptor is essential for monocyte activation and induction of chemotaxis during an inflammatory response. Because of its target cell specificity, MCP-1 has been postulated to play a pathogenic role in a variety of diseases characterized by mononuclear cell infiltration, including atherosclerosis, rheumatoid arthritis, and multiple sclerosis[6,11]. MCP-1 may exert these effects by influencing the expression of other chemokines, which is hard to be demonstrated for the complexity of the chemokine network. Genechip is a high-throughput method to evaluate hundreds of genes at one time, so it is the best method to investigate this complex process and the relationship between MCP-1 and other chemokines and receptors.

Although U937 cell line may differ in some aspects from human blood macrophages, it expresses functional chemokines and cytokines as human blood macrophages. The major advantage of using U937 cells is the homogeneity of the cell line, allowing comparison of findings between different experiments. For this reason, we used U937 cells in the present study to examine macrophage responses to MCP-1, even though they were not absolutely identical to human peripheral macrophages.

In the present study, we specifically examined the global gene expression of chemokines and their receptors, and demonstrated that MCP-1 could strongly down-regulate the expression level of the CXC subfamily chemokines: IL-8, GROβ, GROγ and granulocyte chemotactic protein 2. MCP-1 also could up-regulate the expression level of RANTES (CC subfamily), down-regulate the expression level of CCL16 (CC subfamily). It had no effect on the expression of XCL2 (C subfamily) and fractalkine (the only member of CX3C subfamily). In chemokine receptors, it could down-regulate the expression level of CCR2 and CCR5.

Table 2 Expression of chemokine genes in U937 cell line

Sample/Control	Control/Sample	Unigene symbol	Gene description
1.6	0.6	SCYA3	Small inducible cytokine A3 (homologous to mouse Mip-1a)
2.6	0.4	SCYA5	Small inducible cytokine A5 (RANTES)
1.0	1.0	SCYA17	Small inducible cytokine subfamily A (Cys-Cys), member 17
1.0	1.0	SCYA11	Small inducible cytokine subfamily A (Cys-Cys), member 11 (eotaxin)
1.0	1.0	SCYA13	Small inducible cytokine subfamily A (Cys-Cys), member 13
1.0	1.0	SCYA14	Small inducible cytokine subfamily A (Cys-Cys), member 14
0.4	2.8	SCYA16	Small inducible cytokine subfamily A (Cys-Cys), member 16
1.0	1.0	SCYA18	Small inducible cytokine subfamily A (Cys-Cys), member 18, pulmonary and activation-regulated
1.0	1.0	SCYA19	Small inducible cytokine subfamily A (Cys-Cys), member 19
1.0	1.0	SCYA20	Small inducible cytokine subfamily A (Cys-Cys), member 20
1.0	1.0	SCYA21	Small inducible cytokine subfamily A (Cys-Cys), member 21
1.0	1.0	SCYA22	Small inducible cytokine subfamily A (Cys-Cys), member 22
1.0	1.0	SCYA23	Small inducible cytokine subfamily A (Cys-Cys), member 23
1.0	1.0	SCYA25	Small inducible cytokine subfamily A (Cys-Cys), member 25
0.0	469.8	GRO2	GROβ (melanoma growth stimulating activity, beta)
0.0	47.6	GRO3	GROγ (melanoma growth stimulating activity, gamma)
0.0	34.5	IL8	Interleukin 8
1.0	1.0	SCYB11	Small inducible cytokine subfamily B (Cys-X-Cys), member 11
1.0	1.0	SCYB5	Small inducible cytokine subfamily B (Cys-X-Cys), member 5 (epithelial-derived neutrophil-activating peptide 78)
0.0	261.6	SCYB6	Small inducible cytokine subfamily B (Cys-X-Cys), member 6 (granulocyte chemotactic protein 2)
1.0	1.0	SCYC2	Small inducible cytokine subfamily C, member 2
1.0	1.0	SCYD1	Small inducible cytokine subfamily D (Cys-X3-Cys), member 1 (fractalkine, neurotactin)

IL-8, GROβ, GROγ and granulocyte chemoattractant protein-2 are all members of the CXC chemokine family. The GRO proteins are about 90% identical in amino acid sequence. IL-8 and granulocyte chemoattractant protein-2 are about 40-50% identical to each other and to any of the GRO proteins. The CXC subfamily can be further subdivided into ELR^+ and ELR groups, based on the presence or absence of the sequence motif glutamic acid-leucine-arginine (ELR) N-terminal to the first cysteine. They are all ELR^+ CXC chemokines. All ELR^+ CXC chemokines are powerful activators of neutrophils and induce chemotaxis, shape change, a rise in intracellular free calcium levels, exocytosis, and respiratory burst *in vitro* and neutrophil accumulation *in vivo*, whereas the ELR CXC chemokines are not neutrophil chemoattractants[12-14]. Our findings suggest that MCP-1, which activated and chemoattracted monocytes and macrophages, could depress the infiltration of neutrophils in inflammation by rendering macrophages to express less neutrophil chemokines. Many disorders begin as neutrophils infiltrate at the inflammatory location, and further develop as monocytes or macrophages infiltrate, MCP-1 then may be one of the regulating factors of such changes.

RANTES was isolated in a T- *vs* B-lymphocyte differential screen, and found to be inducible by mitogens or antigens in a variety of T-cell lines and circulating lymphocytes. *In vitro*, RANTES was nearly as a potent chemoattractant for monocytes as MCP-1, but was much less effective in stimulating exocytosis. In endothelial cell-free assays, RANTES attracted CD4+, CD45R0+ T lymphocytes, but in transendothelial systems it attracted CD8+ cells as well as CD4+, and was the most potent CC chemokine for CD8+ chemoattraction. The first hint about a connection between chemokines and HIV-1 came from the finding that RANTES could prevent infection by macrophage-tropic, nonsyncytium-inducing strains of HIV-1[15].

In vitro ligand binding experiments suggested that the sole cloned receptor of MCP-1 was CCR2. CCR2 responded to MCP-1, MCP-3 and MCP-5, but maximum responses were only obtained to MCP-1. CCR5 could interact with RANTES, MIP-1, or MCP-2 under physiological conditions[16,17]. CCR5 could also act as a co-receptor in HIV-1-mediated infection of CD4-positive lymphocytes and microglia. In addition, the ligands for CCR5 could inhibit infection with certain strains of HIV-1, and decreased susceptibility to HIV-1 infection has been linked with mutations in CCR5 gene[18,19]. CCR5 was also involved in a diverse array of inflammatory diseases[11,20,21]. Our findings suggested that MCP-1 might influence the process of these diseases, although the mechanism is not clear. Detailed data need to be further explored.

In summary, MCP-1 can influence the expression of some chemokines and receptors in macrophages *in vitro*. MCP-1 can also down-regulate the mRNA level of CCR5, which plays a critical role in many disorders and illnesses. MCP-1 can also greatly change other cytokines of the immune system, such as IL-18, TNF, IFN. Our findings disclose some relationship among MCP-1 and other chemokine-related members, shedding new light on the mechanism of the function of MCP-1 and the pathogenesis of related diseases.

REFERENCES

1 **Rossi D,** Zlotnik A. The biology of chemokines and their receptors. *Annu Rev Immunol* 2000; **18**: 217-242
2 **Baggiolini M.** Chemokines and leukocyte traffic. *Nature* 1998;

392: 565-568

3 **Zlotnik A,** Yoshie O. Chemokines: a new classification system and their role in immunity. *Immunity* 2000; **12**: 121-127

4 **Zhang L,** Khayat A, Cheng H, Graves DT. The pattern of monocyte recruitment in tumors is modulated by MCP-1 expression and influences the rate of tumor growth. *Lab Invest* 1997; **76**: 579-590

5 **Valente AJ,** Rozek MM, Sprague EA, Schwartz CJ. Mechanisms in intimal monocyte-macrophage recruitment. A special role for monocyte chemotactic protein-1. *Circulation* 1992; **86**: III20-III25

6 **Martinet N,** Beck G, Bernard V, Plenat F, Vaillant P, Schooneman F, Vignaud JM, Martinet Y. Mechanism for the recruitment of macrophages to cancer site: *In vivo* concentration gradient of monocyte chemotactic activity. *Cancer* 1992; **70**: 854-860

7 **Lu B,** Rutledge BJ, Gu L, Fiorillo J, Lukacs NW, Kunkel SL, North R, Gerard C, Rollins BJ. Abnormalities in monocyte recruitment and cytokine expression in monocyte chemoattractant protein 1-deficient mice. *J Exp Med* 1998; **187**: 601-608

8 **Corrigall VM,** Arastu M, Khan S, Shah C, Fife M, Smeets T, Tak PP, Panayi GS. Functional IL-2 receptor beta (CD122) and gamma (CD132) chains are expressed by fibroblast-like synoviocytes: activation by IL-2 stimulates monocyte chemoattractant protein-1 production. *J Immunol* 2001; **166**: 4141-4147

9 **Koch AE,** Kunkel SL, Harlow LA, Johnson B, Evanoff HL, Haines GK, Burdick MD, Pope RM, Strieter RM. Enhanced production of monocyte chemoattractant protein-1 in rheumatoid arthritis. *J Clin Invest* 1992; **90**: 772-779

10 **Xie L,** Guo J, Qian X, Chen W. Multiple types of chemokines expressed in mouse thymic stromal cell lines. *Zhongguo Yixue Kexueyuan Xuebao* 2000; **22**: 498-501

11 **Gu L,** Tseng S, Horner RM, Tam C, Loda M, Rollins BJ. Control of TH_2 polarization by the chemokine monocyte chemoattractant protein-1. *Nature* 2000; **404**: 407-411

12 **King AG,** Horowitz D, Dillon SB, Levin R, Farese AM, MacVittie TJ, Pelus LM. Rapid mobilization of murine hematopoietic stem cells with enhanced engraftment properties and evaluation of hematopoietic progenitor cell mobilization in rhesus monkeys by a single injection of SB-251353, a specific truncated form of the human CXC chemokine GRObeta. *Blood* 2001; **97**: 1534-1542

13 **Wang D,** Richmond A. Nuclear factor-kappa B activation by the CXC chemokine melanoma growth-stimulatory activity/growth-regulated protein involves the MEKK1/p38 mitogen-activated protein kinase pathway. *J Biol Chem* 2001; **276**: 3650-3659

14 **Miura M,** Fu X, Zhang QW, Remick DG, Fairchild RL. Neutralization of Gro alpha and macrophage inflammatory protein-2 attenuates renal ischemia/reperfusion injury. *Am J Pathol* 2001; **159**: 2137-2145

15 **Fischer FR,** Luo Y, Luo M, Santambrogio L, Dorf ME. RANTES-induced chemokine cascade in dendritic cells. *J Immunol* 2001; **167**: 1637-1643

16 **Oppermann M,** Mack M, Proudfoot AE, Olbrich H. Differential effects of CC chemokines on CC chemokine receptor 5 (CCR5) phosphorylation and identification of phosphorylation sites on the CCR5 carboxyl terminus. *J Biol Chem* 1999; **274**: 8875-8885

17 **Dean M,** Carrington M, Winkler C, Huttley GA, Smith MW, Allikmets R, Goedert JJ, Buchbinder SP, Vittinghoff E, Gomperts E, Donfield S, Vlahov D, Kaslow R, Saah A, Rinaldo C, Detels R, O'Brien SJ. Genetic restriction of HIV-1 infection and progression to AIDS by a deletion allele of the CKR5 structural gene. Hemophilia Growth and Development Study, Multicenter AIDS Cohort Study, Multicenter Hemophilia Cohort Study, San Francisco City Cohort, ALIVE Study. *Science* 1996; **273**: 1856-1862

18 **Raport CJ,** Gosling J, Schweickart VL, Gray PW, Charo IF. Molecular cloning and functional characterization of a novel human CC chemokine receptor (CCR5) for RANTES, MIP-1beta, and MIP-1alpha. *J Biol Chem* 1996; **271**: 17161-17166

19 **Samson M,** Labbe O, Mollereau C, Vassart G, Parmentier M. Molecular cloning and functional expression of a new human CC-chemokine receptor gene. *Biochemistry* 1996; **35**: 3362-3367

20 **Alkhatib G,** Combadiere C, Broder CC, Feng Y, Kennedy PE, Murphy PM, Berger EA. CC CKR5: a RANTES, MIP-1alpha, MIP-1beta receptor as a fusion cofactor for macrophage-tropic HIV-1. *Science* 1996; **272**: 1955-1958

21 **Vielhauer V,** Anders HJ, Mack M, Cihak J, Strutz F, Stangassinger M, Luckow B, Grone HJ, Schlondorff D. Obstructive nephropathy in the mouse: progressive fibrosis correlates with tubulointerstitial chemokine expression and accumulation of CC chemokine receptor 2- and 5-positive leukocytes. *J Am Soc Nephrol* 2001; **12**: 1173–1187

Science Editor Zhu LH and Wang XL **Language Editor** Elsevier HK

PO Box 2345, Beijing 100023, China
www.wjgnet.com
wjg@wjgnet.com

ELSEVIER

World J Gastroenterol 2005;11(16):2513-2517
World Journal of Gastroenterology ISSN 1007-9327

• *BRIEF REPORTS* •

A randomized controlled trial of laparoscopic versus open cholecystectomy in patients with cirrhotic portal hypertension

Wu Ji, Ling-Tang Li, Zhi-Ming Wang, Zhu-Fu Quan, Xun-Ru Chen, Jie-Shou Li

Wu Ji, Ling-Tang Li, Zhi-Ming Wang, Zhu-Fu Quan, Jie-Shou Li, Research Institute of General Surgery, Nanjing General Hospital of Nanjing PLA Command Area, Nanjing 210002, Jiangsu Province, China
Xun-Ru Chen, Department of Hepatobiliary Surgery, Kunming General Hospital of Chengdu PLA Command Area, Kunming 650032, Yunnan Province, China
Correspondence to: Professor Jie-Shou Li, Research Institute of General Surgery, Nanjing General Hospital of Nanjing PLA Command Area, 305 Eastern Zhongshan Road, Nanjing 210002, Jiangsu Province, China. lijiesou@public1.ptt.js.cn
Telephone: +86-25-80860065 Fax: +86-25-4803956
Received: 2003-03-05 Accepted: 2004-05-13

Abstract

AIM: To evaluate the characters, risks and benefits of laparoscopic cholecystectomy (LC) in cirrhotic portal hypertension (CPH) patients.

METHODS: Altogether 80 patients with symptomatic gallbladder disease and CPH, including 41 Child class A, 32 Child class B and 7 Child class C, were randomly divided into open cholecystectomy (OC) group (38 patients) and LC group (42 patients). The cohorts were well-matched for number, age, sex, Child classification and types of disease. Data of the two groups were collected and analyzed.

RESULTS: In LC group, LC was successfully performed in 36 cases, and 2 patients were converted to OC for difficulty in managing bleeding under laparoscope and dense adhesion of Calot's triangle. The rate of conversion was 5.3%. The surgical duration was 62.6±15.2 min. The operative blood loss was 75.5±15.5 mL. The time to resume diet was 18.3±6.5 h. Seven postoperative complications occurred in five patients (13.2%). All patients were dismissed after an average of 4.6±2.4 d. In OC group, the operation time was 60.5±17.5 min. The operative blood loss was 112.5±23.5 mL. The time to resume diet was 44.2±10.5 h. Fifteen postoperative complications occurred in 12 patients (30.0%). All patients were dismissed after an average of 7.5±3.5 d. There was no significant difference in operation time between OC and LC group. But LC offered several advantages over OC, including fewer blood loss and lower postoperative complication rate, shorter time to resume diet and shorter length of hospitalization in patients with CPH.

CONCLUSION: Though LC for patients with CPH is difficult, it is feasible, relatively safe, and superior to OC. It is important to know the technical characters of the operation, and pay more attention to the meticulous perioperative managements.

Key words: LC; CPH; OC

Ji W, Li LT, Wang ZM, Quan ZF, Chen XR, Li JS. A randomized controlled trial of laparoscopic versus open cholecystectomy in patients with cirrhotic portal hypertension. *World J Gastroenterol* 2005; 11(16): 2513-2517
http://www.wjgnet.com/1007-9327/11/2513.asp

INTRODUCTION

The advantages of laparoscopic cholecystectomy (LC) have been extensively published, and LC has become the "golden standard" in treating benign gallbladder diseases[1-4]. When LC began in the early 1990s, cirrhosis and pregnancy, previous abdominal surgery, obesity, acute cholecystitis were considered absolute contraindications for performance of the laparoscopic technique. Growing experience has allowed the use of LC in more complex procedures, such as in cirrhotic patients[5,6]. In recent years, several studies have reported good results and suggested liberal use of LC in patients with symptomatic gallbladder disease and cirrhosis[7-10]. However, its feasibility, benefits and successful use in patients with cirrhotic portal hypertension (CPH) are meagerly well-documented. Based on our previous studies on the influence of LC on the hepatic function and our experience with LC for cirrhotic patients, we have successively performed LC in patients with CPH. The present study is a retrospective analysis comparing the results of OC and LC in patients with symptomatic gallbladder disease and CPH.

MATERIALS AND METHODS

Eligibility of patients

Altogether 80 patients, including 65 male and 15 female, aged 52.3±12.2 years, were all diagnosed as symptomatic gallbladder disease and CPH. The diagnosis was mainly according to the disease history and ultrasound, spiral CT and esophageal barium swallow examination results, combined with laparoscopic examination results of the typical modular lesions in liver lobes. Clinical signs included megaspleen (62 cases), widened portal vein (diameter over 14 mm) (52 cases), ascites (27 cases), varices of esophagus and gastric fundus veins (31 cases). Seventy-one patients were hepatic cirrhosis (hepatitis B in 58 and hepatitis C in

13). Nine other patients had alcoholic cirrhosis. The Child-Pugh classification system was used to assess the severity of CPH. On preoperative assessment, 41 patients were classified as Child class A, 32 were Child class B and 7 were Child class C. Significant comorbidity was present in 25 (31.3%) patients, including cardiac disease (12 cases), respiratory compromise (10 cases), diabetes mellitus (6 cases), and renal impairment (3 cases). Nine (11.3%) patients had disease in more than two organ systems. No previous upper abdominal operation had been conducted in these patients. Randomization was done before operation by use of sealed envelopes. Patients were randomly divided into OC group (42 cases) and LC group (38 cases). The patients' characteristics of the two groups are listed in Table 1. These two groups were well-matched for number, age, sex, Child classification and types of disease. The study was approved by the local hospital ethics committee. Written informed consent to participate in the study was obtained from all patients.

Table 1 Comparison of patients' characteristics between two groups

	LC group (n = 38)	OC group (n = 42)	P
Age (yr)	50.2±11.6	53.8±14.2	0.606
Sex			0.943
Male	31	34	
Female	7	8	
Child classification			0.432
A	19	22	
B	15	17	
C	4	3	
Type of disease			0.761
Gallbladder polypus	3	2	
Gallbladder stones	35	40	

Methods

Patients underwent standard preoperative workup, including conventional blood tests, chest radiograph, electrocardiogram, ultrasonography, spiral CT scan, and/or esophageal barium swallow examination. No special preparation before operation was needed for Child class A cases. Hepatic function protection and supporting, ascites controlling and portal vein pressure reduction were considered individually for most Child class B and C cases. If the patient had class C cirrhosis, attempts were made to improve the patient's hepatic function to near class B level. Only after that, surgical operations arranged were allowed for a safer elective operation.

The patients were put in the supine position under general anesthesia with intratracheal intubation. A standard four ports laparoscopic procedure was performed for all LC cases by using two 5-mm and 10-mm ports after pneumoperitoneum was established using a Veress needle. The intraabdominal CO_2 pressure was controlled at about 1.33 kPa. The OC was completed with a 10-14 cm subxiphoid incision. A silicon drain was placed in the operation field for all patients, which was usually pulled out in 24-72 h after operation.

The patients inhaled oxygen after returning to the ICU ward. Changes of vital signs were monitored for 24-48 h. Fluid infusion, anti-inflammation, hemorrhage prevention, liver function protection and analgesics treatments were prescribed. Data on these two groups were collected and analyzed.

Statistical method

SPSS10.0 statistics software was used to establish the database. Statistical comparisons between OC and LC groups were made with Student's t test for categorical variables. Statistical significance was defined as $P<0.05$.

RESULTS

In LC group, LC was successfully performed in 36 of 38 cases, including three laparoscopic subtotal cholecystectomies. Two conversions to OC were necessary. One was due to difficulty in managing bleeding in the gallbladder bed under laparoscope and another for dense adhesion of Calot's triangle. The rate of conversion was 5.3%. The mean operative time was 62.6±15.2 min. The operative blood loss was 75.5±15.5 mL. The mean time to resume diet was 18.3±6.5 h. Seven postoperative complications occurred in five patients (13.2%). They were tracker infection (one case), respiratory system infection (one case), urinary system infection (one case), upper gastrointestinal bleeding (one case), mild hepatic encephalopathy (one case) and ascites aggravation (two cases). All patients were cured and dismissed after 4.6±2.4 d.

While in OC group, the mean operative time was 60.5±17.5 min. The operative blood loss was 112.5±23.5 mL. The mean time to resume diet was 44.2±10.5 h. Fifteen postoperative complications occurred in 12 patients (30.0%). They were wound infection (two cases), respiratory system infection (four cases), urinary system infection (two cases), mild hepatic encephalopathy (two cases) and ascites worsening (five cases). All patients were cured and dismissed after 7.5±3.5 d.

Comparison of perioperative parameters of two groups is listed in Table 2. There was no significant difference in operative time between the two groups. But LC offered several advantages over OC, including fewer blood loss and lower postoperative complication rate, shorter time to

Table 2 Comparison of perioperative parameters of two groups

Group	Operative time (min)	Blood loss (mL)	Time to resume diet (h)	Postoperative complication rate (%)	Length of hospitalization after operation (d)
LC group (n = 38)	62.6±15.2	75.5±17.5	18.3±6.5	13.2	4.6±2.4
OC group (n = 40)	60.5±17.5	112.5±23.5[b]	44.2±10.5[b]	30.0[b]	7.5±3.5[a]

[a]$P<0.05$, [b]$P<0.01$ *vs* LC.

resume diet and shorter hospital stay in patients with CPH.

DISCUSSION

In a review of 4 895 postmortem records, Bouchier[11] found that the frequency of gallbladder stone in patients with cirrhosis was 29.4%, more than twice the noncirrhotic frequency. Factors implicated in the higher incidence of gallbladder disease in these patients include: hypersplenism, increased levels of estrogen, and increased intravascular hemolysis with a reduction in gallbladder emptying and motility. Though there is no definite data on the frequency of gallbladder diseases in patients with CPH, it is estimated that the frequency might be 2-5 times higher than the noncirrhotic's. Most of these patients remain asymptomatic. Nevertheless, the management of symptomatic gallbladder diseases in patients with CPH has remained problematic. In the early 1980s, OC in cirrhotic patients was associated with a postoperative mortality ranging from 7% to 26%. The increased risks led to reluctance to undertake elective cholecystectomy in patients with cirrhosis and symptomatic gallbladder disease. By the late 1980s, better surgical results had been published for cirrhotic patients who underwent elective cholecystectomy[12]. OC was subsequently considered as an acceptable therapeutic option in cirrhotic patients with relatively normal hepatic function. Since the introduction of LC in 1990s, the question of whether cirrhotic patients might benefit from this less invasive approach has arisen[13,14]. It is well known that LC allows for shorter hospital stay and operative time, faster operative rehabilitation, and reduced wound complications for noncirrhotic patients when compared with OC. Several recent studies have also demonstrated that LC in Child A and B cirrhosis was safer and better tolerated than OC[15-18]. Cholecystectomy for patients with CPH is more complicated than that for cirrhotic cases. Excessive blood loss, postoperative liver failure, and sepsis were the most prominent problems for these special patients[19]. There have been few reports with limited cases of OC for patients with CPH. The results were relatively acceptable. But there has been no such report of LC for patients with CPH.

In our previous series studies, we have observed that laparoscopic surgery had obvious influence on the hepatic function. We have also demonstrated in our animal experiments that ischemia-reperfusion injury caused by pneumoperitonium played an important role in liver impairment. Methods to diminish this injury, for example, lowering pneumoperitonium pressure, shortening operation time, perioperative liver function protection and supporting were also proposed thereafter. We have carefully performed more than 200 LCs in cirrhotic patients since 1999. Based on the clinical and experimental experience, we tried LC in patients with CPH since 2001. This study was designed to prospectively compare the characters, risks and benefits of LC and OC in patients with CPH. We found that there was no significant difference in surgical duration between LC and OC groups. But LC offered several advantages over OC, including less amount of intraoperative hemorrhage and lower postoperative complication rate, reduced time to resume diet and hospital stay after operation. The results of our present study confirm that LC is a relatively feasible and safe operative approach, and it is superior to OC for patients with CPH. We speculate that LC can offer the following advantages for patients with CPH: (1) LC is a minimally invasive operation, which has little influence on patients, and ensures a quicker recovery. So it can improve the patient's tolerability for cholecystectomy, and thus extend the indication for cholecystectomy for patients with CPH[20,21]. (2) Ascitic infection which occurs frequently after OC, can result in intra-abdominal sepsis and death. Access to the sterile peritoneal cavity by millimetric (5 and 10 mm) channels may have an important role in the prevention of inadvertent bacterial seeding and contamination of the ascites. (3) Laparoscopy has the ability of magnification, which is helpful to make observation of minute organ structures more clearly. It is also beneficial to the observation of dilated and twisted portal vein branches in the operation field and congested gallbladder bed, thus can effectively avoid meaningless injury of blood vessel and the following bleeding. (4) LC is reported to have fewer postoperative complications, such as wound infection, incisional hernia and respiratory, urinary system infection. Reduction of these common complications is especially important for patients with CPH[22]. (5) Many patients with CPH also had various hepatitis virus infection. During laparoscopic surgical operation, the surgeon did not directly touch the patient's blood and viscera, so that the possibility of iatrogenic infections could be reduced. (6) Some patients with CPH may accept liver transplantation in the future. LC, without opening abdominal cavity, offers the potential for fewer right upper quadrant adhesions postoperatively. This will benefit liver transplantation.

LC still has shortages and our management measures to overcome them for patients with CPH included: (1) During LC, CO_2 pneumoperitonium can cause ischemia-reperfusion injury to the internal organs, such as liver and kidney. This may aggravate the damage of the hepatic function. Since this injury was positively correlated with the pressure of pneumoperitonium[23-25], we routinely establish the pneumoperitonium with a lower flow of CO_2, maintain the intra-abdominal pressure at about 1.33 kPa, and gradually relieve the pneumoperitonium after LC. We think these can reduce further damage to hepatic function. It has been reported that gasless pneumoperitonium can avoid ischemia-reperfusion injury to the internal organs. But we have no such experience. It may be worth trying. (2) It may not be as direct and convenient for LC in managing bleeding under laparoscope, especially when extensive bleeding and permeating bleeding occurred. We think it is critical for operators to proficiently master laparoscopic techniques as compression, electronic coagulation, and transfix. On the other hand, complete preparation of various laparoscopic apparatus is suggested. (3) Sometimes CPH can lead to atrophy-hypertrophy and displacement of liver lobes. This may cause inconvenient exposure of operative field under laparoscope. Adjustment of the tracker location is usually needed in this situation.

The results of this series indicated that LC for patients with CPH in the management of symptomatic gallbladder diseases is feasible and relatively safe. Nevertheless, the

procedure is still complicated and highly difficult which associates with significant morbidity compared with that of patients without cirrhosis[26]. LC for patients with CPH should be performed by experienced laparoscopic surgeons. We think that more attention should be paid to the following aspects: (1) Functions of important organs, such as liver, kidney, heart, lung, should be carefully checked before the operation to make clear patients' general status. Individual preoperative preparation should be conducted mainly based on patients' Child classification. Generally, no special preparation was needed for Child class A cases. Special individual measures should be taken to improve the patient's liver function for class B and C cases. For the patients with class C cirrhosis, attempts should be made to improve the patients' hepatic function to near class B, then surgical operation was arranged. Attempts which we have made included hepatic function protection, control of ascites, nutritional support, coagulation function amelioration and portal vein pressure reduction to allow for a safer elective operation. Correction of coagulopathy with platelets or fresh frozen plasma before surgery is advised, and availability of these products intraoperatively is essential. (2) Bleeding complications are significantly more common in patients with CPH. Several technical modifications should be made[27]. At the commencement of the laparoscopic procedure, special care should be taken during trocar insertion to avoid injury to dilated abdominal wall veins. The subxiphoid 5-mm port was placed more to the right of the midline to completely avoid the falciform ligament and its accompanying umbilical vein. Portal hypertension with large venous collaterals in the liver hilum provides a major challenge in the surgical management of the biliary tract[28]. This pathology is a major source of intraoperative and postoperative complications. We believe that meticulous care be taken to maintain hemostasis. Extreme caution with constant control of hemostasis was the hallmark of the procedure. Blunt dissection was avoided to minimize bleeding once the cystic duct was identified and divided and all tissues were clipped/ligated and cut. A variety of techniques other than unipolar electrocautery, including argon beam coagulation, ultrasonic dissection, and thrombin spray are available for use[29,30]. In a few cases, involving large collateral veins around the gallbladder, when severe bleeding is likely from large varices, subtotal cholecystectomy could be performed to prevent massive blood loss from the gallbladder bed[31,32]. This technique avoids dissection in the hepatic hilum. In our patient population, this maneuver was necessary in three patients. Surgeons should be aware of this procedure to lessen the risk of excessive blood loss during LC. All access ports were checked internally for bleeding just before completion of the procedure. Drainage of the operative field was performed routinely for all patients in this study, which was pulled out in 24-48 h after operation. This is helpful for postoperative observation and management. (3) In recent reports, conversion rates during LC ranged from 0% to 9%[33]. In this study, the rate of conversion to OC was 5.3%, which was similar to published data for LC conversion in a noncirrhotic patient population. A low threshold for conversion from LC to OC should be maintained. Conversion is not a complication, but a means to prevent more serious problems. Absolute indications for conversion include bleeding not readily controlled laparoscopically and an inability to recognize the anatomy properly[34,35]. The surgeon should not be reluctant to convert immediately to OC when there is uncertainty about the safety and efficiency of the operative procedure.

Our study has demonstrated the feasibility and advantages of LC in well-compensated patients with CPH. In the hands of an experienced surgical team, LC should be the procedure of choice in the treatment of gallbladder disease in these patients. We believe that along with further understanding of LC technique characteristics in patients with CPH, continuous improvements in the perioperative management, the expansive application of new surgical operation apparatus (such as ultrasound knife), as well as improvement of operator's technical skills, more and more patients with CPH will benefit from LC in the near future.

REFERENCES

1 **Neri V,** Ambrosi A, Di Lauro G, Fersini A, Valentino TP. Difficult cholecystectomies: validity of the laparoscopic approach. *JSLS* 2003; **7:** 329-333
2 **Curet MJ,** Contreras M, Weber DM, Albrecht R. Laparoscopic cholecystectomy. *Surg Endosc* 2002; **16:** 453-457
3 **Fernando R.** Laparoscopic cholecystectomy. *World J Surg* 2002; **26:** 1401; author reply 1401-1402
4 **Johnston SM,** Kidney S, Sweeney KJ, Zaki A, Tanner WA, Keane FV. Changing trends in the management of gallstone disease. *Surg Endosc* 2003; **17:** 781-786
5 **Yerdel MA,** Tsuge H, Mimura H, Sakagami K, Mori M, Orita K. Laparoscopic cholecystectomy in cirrhotic patients: expanding indications. *Surg Laparosc Endosc* 1993; **3:** 180-183
6 **Puggioni A,** Wong LL. A metaanalysis of laparoscopic cholecystectomy in patients with cirrhosis. *J Am Coll Surg* 2003; **197:** 921-926
7 **Poggio JL,** Rowland CM, Gores GJ, Nagorney DM, Donohue JH. A comparison of laparoscopic and open cholecystectomy in patients with compensated cirrhosis and symptomatic gallstone disease. *Surgery* 2000; **127:** 405-411
8 **Leone N,** Garino M, De Paolis P, Pellicano R, Fronda GR, Rizzetto M. Laparoscopic cholecystectomy in cirrhotic patients. *Dig Surg* 2001; **18:** 449-452
9 **Dalvi AN,** Deshpande AA, Doctor NH, Maydeo A, Bapat RD. Laparoscopic cholecystectomy in patient with portal cavernoma and portal hypertension. *Indian J Gastroenterol* 2001; **20:** 32-33
10 **Yeh CN,** Chen MF, Jan YY. Laparoscopic cholecystectomy in 226 cirrhotic patients. Experience of a single center in Taiwan. *Surg Endosc* 2002; **16:** 1583-1587
11 **Bouchier IA.** Postmortem study of the frequency of gallstones in patients with cirrhosis of the liver. *Gut* 1969; **10:** 705-710
12 **Sirinek KR,** Burk RR, Brown M, Levine BA. Improving survival in patients with cirrhosis undergoing major abdominal operations. *Arch Surg* 1987; **122:** 271-273
13 **Lacy AM,** Balaguer C, Andrade E, Garcia-Valdecasas JC, Grande L, Fuster J, Bosch J, Visa J. Laparoscopic cholecystectomy in cirrhotic patients. Indication or contradiction? *Surg Endosc* 1995; **9:** 407-408
14 **Morino M,** Cavuoti G, Miglietta C, Giraudo G, Simone P. Laparoscopic cholecystectomy in cirrhosis: contraindication or privileged indication? *Surg Laparosc Endosc Percutan Tech* 2000; **10:** 360-363
15 **Yerdel MA,** Koksoy C, Aras N, Orita K. Laparoscopic versus open cholecystectomy in cirrhotic patients: a prospective study. *Surg Laparosc Endosc* 1997; **7:** 483-486
16 **Urban L,** Eason GA, ReMine S, Bogard B, Magisano J, Raj P,

Pratt D, Brown T. Laparoscopic cholecystectomy in patients with early cirrhosis. *Curr Surg* 2001; **58:** 312-315
17 **Jan YY,** Chen MF. Laparoscopic cholecystectomy in cirrhotic patients. *Hepatogastroenterology* 1997; **44:** 1584-1587
18 **Friel CM,** Stack J, Forse A, Babineau TJ. Laparoscopic cholecystectomy in patients with hepatic cirrhosis: a five-year experience. *J Gastrointest Surg* 1999; **3:** 286-291
19 **Isam SM,** Ismail AA, Mohamed I, Suliman FS. Laparoscopic cholecystectomy in patients with bilharzial portal hypertension. *JSLS* 2000; **4:** 155-157
20 **Lausten SB,** El-Sefi T, Marwan I, Ibrahim TM, Jensen LS, Grofte T, Andreasen F, Vilstrup H, Raouf AA, Helmy A, Jensen SL. Postoperative hepatic catabolic stress response in patients with cirrhosis and chronic hepatitis. *World J Surg* 2000; **24:** 365-371
21 **Fuchs KH.** Minimally invasive surgery. *Endoscopy* 2002; **34:** 154-159
22 **Thompson MH,** Benger JR. Cholecystectomy, conversion and complications. *HPB Surg* 2000; **11:** 373-378
23 **Tunon MJ,** Gonzalez P, Jorquera F, Llorente A, Gonzalo-Orden M, Gonzalez-Gallego J. Liver blood flow changes during laparoscopic surgery in pigs. A study of hepatic indocyanine green removal. *Surg Endosc* 1999; **13:** 668-672
24 **Tuech JJ,** Pessaux P, Regenet N, Rouge C, Bergamaschi R, Arnaud JP. Laparoscopic cholecystectomy in cirrhotic patients. *Surg Laparosc Endosc Percutan Tech* 2002; **12:** 227-231
25 **Ozmen MM,** Kessaf Aslar A, Besler HT, Cinel I. Does splanchnic ischemia occur during laparoscopic cholecystectomy? *Surg Endosc* 2002; **16:** 468-471
26 **Kao LS,** Aaron BC, Dellinger EP. Trials and tribulations: current challenges in conducting clinical trials. *Arch Surg* 2003; **138:** 59-62
27 **Ota A,** Kano N, Kusanagi H, Yamada S, Garg A. Techniques for difficult cases of laparoscopic cholecystectomy. *J Hepatobiliary Pancreat Surg* 2003; **10:** 172-175
28 **Li JH,** Zheng CZ, Ke CW, Yin K. Management of aberrant bile duct during laparoscopic cholecystectomy. *Hepatobiliary Pancreat Dis Int* 2002; **1:** 438-441
29 **Power C,** Maguire D, McAnena OJ, Calleary J. Use of the ultrasonic dissecting scalpel in laparoscopic cholecystectomy. *Surg Endosc* 2000; **14:** 1070-1073
30 **Glavic Z,** Begic L, Rozman R. A new device for the detection and recognition of blood vessels in laparoscopic surgery. *Surg Endosc* 2002; **16:** 1197-1200
31 **Chowbey PK,** Sharma A, Khullar R, Mann V, Baijal M, Vashistha A. Laparoscopic subtotal cholecystectomy: a review of 56 procedures. *J Laparoendosc Adv Surg Tech A* 2000; **10:** 31-34
32 **Rosenberg J,** Bisgaard T. The difficult gallbladder: technical tips for laparoscopic cholecystectomy. *Surg Laparosc Endosc Percutan Tech* 2000; **10:** 249-252
33 **Capizzi FD,** Fogli L, Brulatti M, Boschi S, Di Domenico M, Papa V, Patrizi P. Conversion rate in laparoscopic cholecystectomy: evolution from 1993 and current state. *J Laparoendosc Adv Surg Tech A* 2003; **13:** 89-91
34 **Rosen M,** Brody F, Ponsky J. Predictive factors for conversion of laparoscopic cholecystectomy. *Am J Surg* 2002; **184:** 254-258
35 **Bingener-Casey J,** Richards ML, Strodel WE, Schwesinger WH, Sirinek KR. Reasons for conversion from laparoscopic to open cholecystectomy: a 10-year review. *J Gastrointest Surg* 2002; **6:** 800-805

Science Editor Zhu LH **Language Editor** Elsevier HK

PO Box 2345, Beijing 100023, China
www.wjgnet.com
wjg@wjgnet.com

ELSEVIER

World J Gastroenterol 2005;11(16):2518-2521
World Journal of Gastroenterology ISSN 1007-9327

• *BRIEF REPORTS* •

Effect of anti-tuberculosis therapy on liver function of pulmonary tuberculosis patients infected with hepatitis B virus

Lei Pan, Zhan-Sheng Jia, Lin Chen, En-Qing Fu, Guang-Yu Li

Lei Pan, Zhan-Sheng Jia, Guang-Yu Li, Center of Infectious Diseases, Tangdu Hospital, Fourth Military Medical University, Xi'an 710038, Shaanxi Province, China
Lin Chen, En-Qing Fu, Respiratory Department, Tangdu Hospital, Fourth Military Medical University, Xi'an 710038, Shaanxi Province, China
Correspondence to: Lei Pan, PhD, Center of Infectious Diseases, Tangdu Hospital, Fourth Military Medical University, Xi'an 710038, Shaanxi Province, China. panlei0225@sina.com
Telephone: +86-29-83528137 Fax: +86-29-83537377
Received: 2004-02-11 Accepted: 2004-02-21

Abstract

AIM: To observe the effect of anti-tuberculosis therapy on liver function of pulmonary tuberculosis patients with hepatitis B virus (HBV) infection, and to compare the differences of liver function by two treatments of anti-tuberculosis.

METHODS: Forty-seven TB patients with HBV infection and 170 TB patients without HBV infection were divided into HPBE(S) and HLAMKO treatment groups. Liver function tests before and after the treatments were performed once in 2 wk or monthly, and their clinical manifestations were recorded.

RESULTS: The rate of hepatotoxicity occurred in 26 (59%) TB patients with HBV during anti-TB treatment, higher than that in 40 (24%) TB patients without HBV. Hepatotoxicity occurred in 66 out of 217 patients, and the incidence of liver dysfunction was 46.1% in HPBE(S) group, significantly higher than that in HLAMKO group (12.7%) ($P<0.01$).

CONCLUSION: TB patients with HBV should choose HLAMKO treatment because of fewer hepatotoxicity.

Key words: Anti-tuberculosis; HBV

Pan L, Jia ZS, Chen L, Fu EQ, Li GY. Effect of anti-tuberculosis therapy on liver function of pulmonary tuberculosis patients infected with hepatitis B virus. *World J Gastroenterol* 2005; 11(16): 2518-2521
http://www.wjgnet.com/1007-9327/11/2518.asp

INTRODUCTION

In recent years, the occurrence of tuberculosis has been increasing obviously[1,2], and many tubercle bacilli are resistant to anti-tuberculosis drugs, so the combination of anti-tuberculosis drugs has become essential. At present, most commonly used anti-TB drugs are more or less hepatotoxic, especially when several anti-TB drugs are used in combination. Liver dysfunction caused by anti-TB drugs often results in interruption of anti-TB therapy and acute hepatic failure, which even threatens patient's life[3,4]. In China, a large number of people are carrying hepatitis B virus (HBV), so tuberculosis patients are very commonly infected with HBV. When these patients are treated by anti-TB medicines, is it easier to show liver dysfunction because of infection with HBV[5-9]? We analyzed the effect of anti-TB therapy on liver function of patients with pulmonary tuberculosis infected with HBV and compared the hepatotoxicity of an anti-TB plan (HPBES, including isonicazide, rifampicin, pyrazinamide, ethambutol, streptomycin) with that of another anti-TB plan-HLAMKO (including isonicazide, rifabutin, amikacin, ofloxacin, levofloxacin). We suggest that physicians should be careful to use anti-TB medicines for pulmonary tuberculosis patients with HBV infection and choose anti-TB medicines, which cause less liver damage.

MATERIALS AND METHODS

Subjects

Forty-seven patients carrying HBV for 3-15 years were all inpatients (1996-2001). Of them 28 were men and 19 were women aged 20-67 years. Their liver function was normal when they suffered from pulmonary tuberculosis. We also analyzed 170 outpatients and inpatients (including 108 men and 62 women) with pulmonary tuberculosis, but without carrying HBV. All patients were diagnosed as pulmonary tuberculosis by chest X-ray, medical history, antacid bacillus in phlegm and TB-PCR[10]. All patients were not infected with other hepatitis viruses and had no alcoholic liver ailment or other chronic liver ailment. The values of ALT were all below 60 U/L before anti-TB therapy, and these patients did not drink alcohol during the period of therapy. All patients were matched with the diagnostic standard set up in 1988[11], including 118 cases of pulmonary TB types II and III, 83 cases of tuberculosis pleurisy (type IV), 4 cases of tuberculosis pericarditis (type V), 7 cases of tracheal-bronchial TB, 5 cases of thoracic wall TB.

Methods of treatment

Patients were divided into two groups, HPBES group: isonicazide 0.3 g, once a day; rifampicin 0.45 g once a day, pyrazinamide 1.0 g once a day, ethambutol 1.0 g once a day and/or streptomycin 0.75 g once a day; and HLAMKO

group: isonicazide 0.3 g once a day, rifabutin 0.6 g once a week, amikacin 0.2 g VD, twice a day, ofloxacin 0.2 g VD, twice a day or levofloxacin 0.2 g VD, twice a day. The general conditions of the two groups were not distinguishable ($P>0.05$). All patients were treated till the disappearance of symptoms, smaller focal lesions on breast X-ray film, negative antacid bacilli in phlegm. The curative effects were graded as effectiveness: disappearance or improvement of symptoms and smaller focal lesions on breast X-ray film, remission: improved symptoms and unchanged focal lesions on breast X-ray film, inefficiency-without improvement of clinical symptoms and breast X-ray film.

Parameters detected

Patients' liver functions were detected by automatic biochemical analytic apparatus when the patients had empty stomachs. Anti-HAV, anti-HBV, anti-HCV, anti-HDV, anti-HEV were detected by ELISA. Liver function of the patients was examined repeatedly every 2 wk till 2 months after therapy, then every month. When ALT was above 1 336 IU/L 2-3 mo after therapy, we defined it as liver dysfunction. However, if it was below 3 340 IU/L, we still continued the anti-TB therapy and added some liver protecting and ALT decreasing medicines including febuprol, biphenydimethylesterate, *etc*. But if liver dysfunction was serious (ALT >3 340 IU/L) and the patients had clinical symptoms and the effect of treatment was not good, then we stopped using anti-TB drugs.

Statistical analysis

Data were expressed as mean±SD and the comparison between groups was analyzed by χ^2 test or t test.

RESULTS

Clinical characteristics of patients with hepatic damage

Of the 217 patients, ALT kept abnormal (>1 336 IU/L) in 66 patients (30%) for more than 4 wk during the course of anti-TB therapy. Abnormal ALT appeared 2 mo after anti-TB therapy in 48 patients, and 17 patients had symptoms including fatigue, decreased appetite, dizziness, nausea, *etc*. Of the 115 patients using HPBES therapy plan, 53 patients (46%) had abnormal liver function. Of the 102 patients using HLAMKO therapy plan, 13 patients (13%) had hepatic damage ($P<0.01$, Table 1). One 48-year-old male patient had acute hepatic necrosis 1 wk after the HPBES therapy plan and died.

Table 1 Liver dysfunction of 66 patients after anti-TB treatment (mean±SD)

	HPBE (S) (n = 53)	HLAMKO (n = 13)	Total (n = 66)
Age (yr)	43±10	46±13	44±12
Sex (M/F)	38/15	9/4	47/19
T-Bil (μmol/L)	26 (6–202)	22 (8–112)	25 (6–202)
Albumin (g/L)	41±5.2	44±6.4	41±6.1
Globulin (g/L)	30±4.8	31±6.2	30±5.7
AST (IU/L)	2 271±37	2 134±42	2 204±41
ALT (IU/L)	2 538±64	2 688±79	2 622±75

Changes of liver function in HBV carriers

Of the 47 HBV carriers without symptoms and physical signs of hepatitis, 20 patients were positive for HBeAg, and 26 patients (59%) had liver dysfunction after anti-TB treatment, only 24% (40/170) of non-HBV carriers had liver dysfunction ($P<0.01$), but there was no significant difference in liver dysfunction between the positive and negative HBeAg groups. In the 47 pulmonary tuberculosis patients carrying HBV, the percent of the HPBES group with hepatic damage was 80% (8/10), but that of the HLAMKO group with hepatic damage was 30.4% (3/10) ($P<0.01$). The percent of liver dysfunction in non-HBV carriers receiving HLAMKO plan was 7.6% (Table 2).

Table 2 Effect of HBV on liver function after anti-TB treatment (%)

Group	HPBE(S) (%)	HLAMKO (%)
HBV carriers	19/24 (79.2)[b]	7/23 (30)[b]
$HBeAg^+$	8/10 (80)[d]	3/10 (30)
$HBeAg^-$	11/14 (79)	4/13 (31)
Noncarriers	34/91 (37)	6/79 (8)

[b]$P<0.01$ *vs* noncarriers, [d]$P<0.01$ *vs* HPBE(S).

Comparison between the two therapy plans

One hundred and fifteen patients used the HPBES plan. The time of treatment was 32±10 d. The treatment was effective for 64% (74/115), alleviative for 28% (32/115), inefficient for 7% (9/115) patients. Fifty-nine patients had serious side effects (hepatic damage mainly), and 15 (25%) stopped the therapy because of it.

One hundred and two patients used the HLAMKO plan. The time of treatment was 35±10 d. The treatment was effective for 63% (65/102), alleviative for 36% (37/102), inefficient for 3% (3/102) patients. Seventeen patients had side effects, 2 (11%) stopped the therapy because of rash, and 13 had liver dysfunction, but completed anti-TB treatment.

The time of treatment and the curative effect between the two plans were not significantly different ($P>0.05$). The number of patients stopping anti-TB treatment because of side effects in HPBES group was much more than that in HLAMKO group. Most of the side effects were hepatic damage.

DISCUSSION

Hepatic damage caused by drugs is a common side effect of anti-TB treatment. One reason is hepatotoxicity of drugs. Enzymes for drug metabolism in hepatocyte microsomes may have congenital defect, malformation, low activity, or be inhibited by drugs, so drugs or drug metabolites are very toxic to hepatocytes. The other reason is hypersensitivity by drugs. The drugs as a hapten cause allergic reaction by immune mechanism leading to the single ALT increase in clinical situation. Commonly used anti-TB drugs, such as isonicazide, rifampicin, pyrazinamide, ethambutol, *etc*., are all hepatotoxic, especially when rifampicin and pyrazinamide

are used in combination[12]. Isonicazide causes hepatic damage either by the toxicity of or hypersensitivity induced by its metabolite-acehydrazide. Rifampicin may accelerate the metabolism of isonicazide as a strong enzyme inducer resulting in the increase of acehydrazide. Acehydrazide combines with biomacromolecules in liver leading to hepatocellular damage usually seen in aged patients with excessive drinking, malnutrition or a liver ailment. Pyrazinamide's hepatotoxicity is dose-dependent and the general dose rarely causes hepatic damage. Isonicazide and rifampicin are the first line anti-TB medicines because of their strong bactericidal effects. However, rifabutin, amikacin, ofloxacin, levofloxacin, *etc.*, in the HLAMKO treatment plan have not been reported with obvious hepatotoxicity[13,14]. We found that the incidence of liver dysfunction was significantly higher in regimen HPBE(S) (46.1%) compared with HLAMKO (12.7%) ($P<0.01$). We think that HLAMKO treatment plan is superior regarding its fewer hepatotoxicities.

There are many risk factors of hepatic damage during the course of anti-TB treatment, such as the type of tuberculosis, recurred tuberculosis, HBV infection, alcohol drinking, age, nutrition status, heredity, individual difference and immune status, *etc.* Scholars outside China reported that most of hepatocytes in HBV carriers without clinical symptoms had changes in histology and spot necrosis in some hepatocytes. One researcher took liver biopsy from 25 pulmonary tuberculosis patients with HBV infection during the course of anti-TB treatment and discovered that all the patients with liver dysfunction suffered from viral hepatitis, even liver cirrhosis. Hepatic damage of the patients with pulmonary tuberculosis during the course of anti-TB treatment was related to HBV infection and pre-existing pathologic changes in liver. Anti-TB medicines only aggravated pre-existing hepatic damage[15,16]. So, HBV infection or pre-existing liver ailment might be an important risk factor[17,18]. Hepatotoxicity caused by anti-TB medicines was liable to happen in the first 2-3 mo of aggressive anti-TB treatment. Hepatic damage of the patients with positive HBV was caused by viral damage overlapped by medicine damage[4]. In our study, the rate of hepatotoxicity in 26 (59%) TB patients with HBV infection during anti-TB treatment was higher than that in 40 (24%) patients without HBV, and the incidence of liver dysfunction was significantly higher in regimen HPBE(S) (80%) with HBV infection compared with HLAMKO (30%) ($P<0.01$). However, the percent of liver dysfunction in non-HBV carriers accepting HLAMKO plan was 7.6%. So, TB patients with HBV infection should choose HLAMKO with fewer liver hepatotoxicity, and we should pay great attention to associated risk factors of hepatic damage.

Hepatotoxicity caused by anti-TB medicines usually happened in the first 2-3 mo of anti-TB treatment. In our study, 66 out of 217 patients had hepatic damage which happened in 21 patients within 1 mo, in 45 patients within 2 mo. We should inform the patients the possible side effects and get co-operation of the patients and choose the treatment plan with efficiency and the least side effects. Furthermore, we should monitor liver function of the patients. If the patients suffered from hepatic damage during the course of anti-TB treatment, it should be stopped, but some scholars did not agree with drug withdrawal[8], as it could increase the tolerance of TB. Some data demonstrated that tuberculosis patients with HBV receiving anti-TB treatment and liver protecting treatment simultaneously did not suffer from hepatic damage and jaundice. So, we used liver protectors when the patients' ALT was above 80 IU/L because the liver protecting drugs could relieve the liver dysfunction caused by anti-TB medicines by getting rid of the toxin in liver and improving the repair and regeneration of liver cell membranes. After using liver protecting drugs, we monitored liver function every week. If liver function did not improve, we adjusted liver protecting drugs and continued to observe the patients for 2-3 wk, if still liver function did not improve, we might stop isonicazide, rifampicin or pyrazinamide.

Pulmonary tuberculosis patients with HBV were more sensitive to hepatotoxic drugs because of pre-existing hepatic damage and liver function of these patients improved more slowly. The hepatitis induced by hepatotoxic drugs still kept for some time after anti-TB treatment ended, we should still monitor liver function and give proper treatment after completion of anti-TB treatment.

It is important to pay attention to the risk factors, such as liver disease family history, excessive drinking, age, HBV-HCV carrier, *etc.*, and prevent the hepatic damage caused by anti-TB medicines. We should observe the patients more carefully and monitor liver function every 1-2 wk in the early course of anti-TB treatment. We must adjust anti-TB treatment plan and choose slight hepatotoxic drugs and use liver protecting drugs in patients with HBV infection, therefore, we may decrease the incidence of hepatitis induced by drugs and increase the cure rate of tuberculosis.

REFERENCES

1 **Zhu LZ.** The treatment of MDR-TB. *Zhonghua Jiehe He Huxi Zazhi* 2000; **23:** 77-78
2 **Raviglione MC,** Pio A. Evolution of WHO policies for tuberculosis control, 1948-2001. *Lancet* 2002; **359:** 775-780
3 **Chen L,** Jia ZS, Yao QM. Analysis of clinical characteristics of 59 old pulmonary tuberculosis patients. *Disi Junyi Daxue Xuebao* 2000; **21:** 872-874
4 **Wong WM,** Wu PC, Yuen MF, Cheng CC, Yew WW, Wong PC, Tam CM, Leung CC, Lai CL. Antituberculosis drug-related liver dysfunction in chronic hepatitis B infection. *Hepatology* 2000; **31:** 201-206
5 **Sadaphal P,** Astemborski J, Graham NM, Sheely L, Bonds M, Madison A, Vlahov D, Thomas DL, Sterling TR. Isoniazid preventive therapy, hepatitis C virus infection, and hepatotoxicity among injection drug users infected with Mycobacterium tuberculosis. *Clin Infect Dis* 2001; **33:** 1687-1691
6 **Pozniak A.** Mycobacterial diseases and HIV. *J HIV Ther* 2002; **7:** 13-16
7 **Colebunders R,** Lambert ML. Management of co-infection with HIV and TB. *BMJ* 2002; **324:** 802-803
8 **Tahaoglu K,** Atac G, Sevim T, Tarun T, Yazicioglu O, Horzum G, Gemci I, Ongel A, Kapakli N, Aksoy E. The management of anti-tuberculosis drug-induced hepatotoxicity. *Int J Tuberc Lung Dis* 2001; **5:** 65-69
9 **Saigal S,** Agarwal SR, Nandeesh HP, Sarin SK. Safety of an ofloxacin-based antitubercular regimen for the treatment of tuberculosis in patients with underlying chronic liver disease: a preliminary report. *J Gastroenterol Hepatol* 2001; **16:** 1028-1032
10 **Zou JX,** Liou MX, Qi WM, Guo TC, Jin FG. Polymerase chain

reaction and intensified kinyoun in diagnosis of L-form tubercle bacillus infection. *Disi Junyi Daxue Xuebao* 2000; **21:** 198-199
11 **Zhang PY.** Diagnosis and treatment of tuberculosis. *Zhonghua Jiehe He Huxi Zazhi* 2001; **24:** 70-74
12 **Yew WW,** Chau CH, Wong PC, Lee J, Wong CF, Cheung SW, Chan CY, Cheng AF. Ciprofloxacin in the management of pulmonary tuberculosis in the face of hepatic dysfunction. *Drugs Exp Clin Res* 1995; **21:** 79-83
13 **Yew WW,** Lee J, Wong PC, Kwan SY. Tolerance of ofloxacin in the treatment of pulmonary tuberculosis in presence of hepatic dysfunction. *Int J Clin Pharmacol Res* 1992; **12:** 173-178
14 **Schaberg T,** Rebhan K, Lode H. Risk factors for side-effects of isoniazid, rifampin and pyrazinamide in patients hospitalized for pulmonary tuberculosis. *Eur Respir J* 1996; **9:** 2026-2030
15 **Qu YW,** Guo Y, Zhao GD, He HZ, Liu Y. The mechanism and prevention of hepatic damage caused by anti-TB drug. *Zhongguo Fanglao Zazhi* 2001; **23:** 56-57
16 **van den Brande P,** van Steenbergen W, Vervoort G, Demedts M. Aging and hepatotoxicity of isoniazid and rifampin in pulmonary tuberculosis. *Am J Respir Crit Care Med* 1995; **152:** 1705-1708
17 **Lu Y,** Zhu LZ, Duan LS. The anti-TB effects of fluoroquinolone. *Zhonghua Jiehe He Huxi Zazhi* 1999; **22:** 693-695
18 **Mitchell I,** Wendon J, Fitt S, Williams R. Anti-tuberculous therapy and acute liver failure. *Lancet* 1995; **345:** 555-556

Science Editor Wang XL, Zhu LH and Guo SY **Language Editor** Elsevier HK

PO Box 2345, Beijing 100023, China
www.wjgnet.com
wjg@wjgnet.com

ELSEVIER

World J Gastroenterol 2005;11(16):2522-2525
World Journal of Gastroenterology ISSN 1007-9327

• *BRIEF REPORTS* •

Evaluation of CMU-1 preservation solutions using an isolated perfused rat liver model

Ying Cheng, Yong-Feng Liu, Dong-Hua Cheng, Bai-Feng Li, Ning Zhao

Ying Cheng, Yong-Feng Liu, Dong-Hua Cheng, Bai-Feng Li, Ning Zhao, Organ Transplant Unit, The First Affiliated Hospital, China Medical University, Shenyang 110001, Liaoning Province, China
Correspondence to: Dr. Ying Cheng, Organ Transplant Unit, The First Affiliated Hospital, China Medical University, Shenyang 110001, Liaoning Province, China. chengying75@sina.com
Telephone: +86-24-23256666-6452
Received: 2004-04-04 Accepted: 2004-05-13

Abstract

AIM: CMU-1 is a new preservation solution with a low potassium concentration as well as low viscosity that is highly effective in reducing preservation injury. The purpose of this experiment is to compare the protective effect of CMU-1 solution with that of UW during cold preservation and normothermic reperfusion.

METHODS: Wistar rats were divided into two groups according to different preservation solution: CMU-1 group and UW group. After 6, 12 and 24 h cold storage of rat liver in different preservation solutions, the isolated perfused rat liver model was applied to reperfuse the liver for 120 min normothermically (37 ℃) with Krebs-Henseleit solution, meanwhile the pH value of the preservation solution was measured. The perfusate was sampled for the evaluation of alanine aminotransferase (ALT) and lactate dehydrogenase (LDH). At the end of the reperfusion, all of the bile product was collected, energy metabolic substrate and histological examination were performed.

RESULTS: After preserving for 6 h, pH value of both groups did not change; after 12 h, both decreased but with no significant difference. After 24 h, pH value in UW solution group significantly decreased. The total adenine nucleotides level and AEC in liver tissue decreased with preservation time, but they were higher in CMU-1 group. And the amount of bile product after perfusion for 120 min in CMU-1 group was much more than that in UW group. However, there were no significant differences in ALT and LDH levels between two groups. Histology showed no difference.

CONCLUSION: The preservation effect of CMU-1 solution is similar with that of UW solution. However, CMU-1 solution shows some advantages over UW solution in energy metabolism, preventing intracellular acidosis and bile product.

Key words: CMU-1; IPRL; ALT

Cheng Y, Liu YF, Cheng DH, Li BF, Zhao N. Evaluation of CMU-1 preservation solutions using an isolated perfused rat liver model. *World J Gastroenterol* 2005; 11(16): 2522-2525
http://www.wjgnet.com/1007-9327/11/2522.asp

INTRODUCTION

For liver transplantation, hypothermic storage with the University of Wisconsin (UW) solution has been regarded as the golden standard[1]. This preservation solution efficiently prevents organ damage and allows prolonged storage of human livers[2], but its high viscosity results in less optimal perfusion and its high potassium concentration requires a pre-flush of liver grafts before reflow in the recipient. The CMU-1, a new preservation solution, was developed by China Medical University for hypothermic graft preservation. In this study, we investigated the preservative effect of CMU-1 solution using an isolated perfused rat liver model.

MATERIALS AND METHODS

Materials

The male Wistar rats (BW 250±20 g, provided by the Animal Center of China Medical University) were divided into groups as following: UW group: After 6 h (T6, $n = 6$), 12 h (T12, $n = 6$), 24 h (T24, $n = 6$) cold storage (40 ℃) in UW solution, the liver was reperfused by Krebs-Henseleit solution (370 ℃) oxygenated with 95% O_2 and 50 mL/L CO_2 for 120 min. CMU-1 group: The treatment was the same as that of the UW group except that the preservation solution was CMU-1 solution instead of the UW solution. The compositions of the UW and CMU-1 solution are listed in Table 1.

Table 1 Composition of UW and CMU-1 solutions

Substrate (mmol/L)	UW	CMU-1
Na^+	30	125
K^+	125	25
$H_2PO_4^-$	25	25
Lactobionate	100	100
Raffinose	30	25
Hydroxyl-ethyl-starch	50 g/L	–
Dextran-40	–	50 g/L
Histidine	–	60
Adenosine	5	–
Allopurinol	1	–
Glutathione	3	–
Insulin	100 IU/L	–
Dexamethasone	8	–
pH	7.4±0.2	7.4±0.2
Osmolarity	320 mosm/L	340 mosm/L
Viscosity	7.5 mpas	5.2 mpas

Methods

The rat livers were procured by Kamamda method and flushed in situ via portal vein by 50 mL 4 ℃ cold storage solution (UW or CMU-1) containing heparin (10 units/100 g) at the height of 40 cm by gravity[3]. The common bile duct was cannulized by a catheter. The liver was preserved in UW or CMU-1 solution for 6, 12 and 24 h. At the end of the preservation, the preservative solution was collected to measure the pH value to evaluate solution buffer capacity. Subsequently, the livers were placed in a perfusion cabinet at 37 ℃, and reperfused with 200 mL recirculating Krebs-Henseleit solution (containing 5% bovine albumin serum and 20 μmol/L sodium taurocholate). The perfusate pressure was 20 cm H_2O and the flow was measured by a monitor as 6-8 mL/min. The perfusate was saturated with O_2:CO_2 (95%:5%)[4,5]. The perfusate samples of 3 mL was collected at 0, 30, 60 and 120 min of reperfusion for determination of ALT and lactate dehydrogenase (LDH) by auto-analysis system.

At the end of each experiment, histological examination was performed in biopsies obtained from the left lateral lobe of livers. For determination of value of ATP, ADP and AMP in liver tissue by high performance liquid chromatography (HPLC), biopsies of 50 mm was taken, chilled in liquid nitrogen and stored at -70 ℃. The value of total adenine nucleotides (TAN) and adenine concentration evaluate (ACE) were calculated as follows: TAN = ATP +ADP+AMP, ACE = (ATP+0.5ADP)/TAN. At the end of perfusion, the bile was collected through the catheter.

Statistical analysis

Results were expressed as mean±SD. The data were analyzed with SPSS10.0; *P* values below 0.05 were considered statistically significant.

RESULTS

Energy material level in liver tissue

With the prolonged preservation time, the level of TAN and AEC decreased. While those of the CMU-1 group reduced more slowly than UW group, and after cold storage, the levels of TAN and ACE in CMU-1 group were significantly higher than those in UW group (Table 2, $P<0.05$).

Table 2 Value of TAN and AEC after perfusate for 120 min

Group	Time (h)	TAN	AEC
UW	6	15.14±2.13	0.56±0.04
	12	14.31±2.10	0.45±0.03
	24	13.44±1.08	0.43±0.02
CMU-1	6	16.15±2.41[a]	0.59±0.03[g]
	12	15.44±1.80[c]	0.51±0.01[i]
	24	14.54±1.89[e]	0.48±0.02[k]

[a]$P<0.05$ CMU-1 *vs* UW group; [c]$P<0.05$ CMU-1 *vs* UW group; [e]$P<0.05$ CMU-1 *vs* UW group; [g]$P<0.05$ CMU-1 *vs* UW group; [i]$P<0.05$ CMU-1 *vs* UW group; [k]$P<0.05$ CMU-1 *vs* UW group.

Bile product after reperfusion

The yellow bile was seen in the common bile duct catheter when the reperfusion began. The result of bile product after 120 min normothermic reperfusion is shown in Table 3. Before 6 h cold storage, no difference was found between the two groups. After 12 and 24 h cold storage, CMU-1 group was significantly higher than that in UW group (Table 3, $P<0.05$).

Table 3 Bile flow after perfusion for 120 min (mL/kg)

Group	6 h	12 h	24 h
UW	244±12	197±3	134±5
CMU-1	249±11	201±4[a]	144±7[c]

[a]$P<0.05$ CMU-1 *vs* UW group; [c]$P<0.05$ CMU-1 *vs* UW group.

ALT and LDH values of the perfusion solution

The ALT and LDH values of CMU-1 group in three preservation intervals were similar to those of UW group. There was no significant difference between the two groups (Tables 4 and 5, $P>0.05$).

Table 4 The value of ALT in the three intervals (IU/L)

Group	0	30	60	120 min
UW				
6 h	17.1±1.2	65.4±2.0	88.7±1.5	321.9±2.7
12 h	28.3±3.5	80.5±1.6	122.1±2.1	408.7±5.6
24 h	52±3.0	108.7±2.5	403.7±3.1	506.7±6.3
CMU-1				
6 h	17.8±2.1	66.1±1.1	87.4±1.8	319.1±5.4
12 h	31.5±1.9	79.9±2.5	125.4±2.9	419.3±6.3
4 h	48.8±1.8	110.3±2.6	398.9±4.1	510.3±4.9

Table 5 Value of LDH in the three intervals (IU/L)

Group	0	30	60	120 min
UW				
6 h	228.5±5.6	378.9±4.7	499.1±10.4	805.2±11.5
12 h	380.2±4.2	480.7±6.7	600.3±11.1	900±13.1
24 h	487.5±3.8	579.6±7.3	1 102±3.5	1 209±12.8
CMU-1				
6 h	218.5±7.4	381.6±5.7	502.4±8.6	811.3±15.6
12 h	407.2±9.1	465.7±3.9	589.7±6.9	904.6±13.9
24 h	478.5±4.3	580.7±2.9	1 109±7.9	1 302±14.2

Histology

After 24 h cold storage, the hepatic lobule structure of the UW group and CMU-1 group was still intact, but some sinusoidal regions became slightly narrow for swelling hepatocytes. The hepatic cords were still clear. The sinusoidal endothelium were normal with mild swelling and rounding. Histology showed no significant difference between the two groups.

The pH value of preservation solution

After 6 h cold storage there was little change in the pH values of the two solutions. After 12 h, the values of UW and CMU-1 solution was reduced to 7.32±0.03 and 7.35±0.02, respectively, there were no significant differences between the two groups. While after 24 h, the value of UW solution

was 7.0±0.03, but the value of CMU-1 solution remained 7.3±0.02. There was a significant difference between the two groups after being preserved for 24 h.

DISCUSSION

Though UW solution is considered as the standard preservation solution for liver, it still has some shortcomings such as high potassium, high viscosity, poor buffering capacity and so on. CMU-1 solution developed by China Medical University is a kind of hypernatrium solution. The main features are the following: (1) CMU-1 solution is a high-sodium, low-potassium solution that can avoid endothelial injury of the blood vessel during reperfusion. Liver preservation in high sodium solution would reduce damage to sinusoidal endothelial cells and hepatocytes[6]. It was hypothesized that Kupffer cells should be less activated and reperfusion injury reduced with the rat liver in cold storage of high-sodium solution[7-9]. (2) It has a potent buffer system-histidine along with the phosphate, which is effective in preventing the tissue from acidosis. Histidine as an impermeable anion can effectively prevent cells from swelling. (3) The colloid in CMU-1 solution is Dextran-40 instead of HES. The viscosity of the solution reduced from 7.5 to 5.2 mPas. Dextran-40 can prevent red cells congregate, protect endothelial cells and improve the liver microcirculation during preservation and reperfusion[10].

Under ischemic preservation conditions, production of ATP is reduced[11]. Depletion of ATP sources can result in disruption of cell homeostasis, as evidenced by the inability to keep the Na^+-K^+ pump, consequently, water moves intracellularly due to the high osmotic gradient resulting in cell swelling. In this condition, the extracelluar osmotic and electric charge gradients formed mainly by the impermeable anion (histidine and raffinose) and colloid (Dextran-40) in the preservation solution can effectively prevent water move intracellularly[12]. Furthermore, in hypothermic preservation condition, the Na^+-K^+ATPase on the hepatocelluar membrane is still active, and its activity is related to the intracellular concentration of Na^+ and extracellular concentration of K^+[13]. In the hypernatrium solution, the active Na^+-K^+ATPase can keep the balance of the ion and cellular activity. High potassium not only damages the blood vessel, but also inhibits the activity of the Na^+-K^+ATPase and delay the graft recovery after reperfusion[14]. Therefore, the hypernatrium solution can protect the hepatocytes and sinusoid endothelial cells effectively, while avoiding high potassium injury.

The ATP level in liver tissue is in direct proportion to the survival rate after transplantation[15]. In this study, the levels of TAN and ACE in CMU-1 group were significantly higher than those of the UW group after preservation, as a result of the bile flow, which is the sensitive index of liver function. These results may be related to the histidine, which can act as the metabolic substrate during the preservation[16].

As a neutral amino acid, the isoelectric point of histidine is 7.59, which is similar to the pH value of the preservation solution, so it acts as a potent buffer system to prevent acidosis[17,18]. The results of pH value in CMU-1 and UW solutions after 24 h cold storage demonstrated that the CMU-1 solution has potent buffer capacity and can effectively prevent intracellular acidosis.

Common parameters in the assessment of I/R injury in the liver are the release of ALT and LDH into the blood or perfusate. These enzymes are released only after the cell membrane has been injured, and the late phenomenon of I/R injury which indicates the damage of hepatocytes. In this study we found that there was no obvious difference between CMU-1 and UW groups in the three intervals. The results of ALT and LDH showed that the damage to the hepatocytes was similar, and CMU-1 and UW solution had the same liver protection effect after 24-h cold storage, as indicated by histology.

Bile production during reperfusion is a commonly applied marker of liver function and is determined by microcirculatory perfusion and the quality of hepatocytes[19]. It is reported that intracellular ATP level is highly correlated to bile production in the early reperfusion phase after transplantation of hypothermically stored rat livers[20]. In this study, no differences in bile production during 120-min reperfusion could be demonstrated between the differently preserved groups before 6-h cold storage, but after 12-h cold storage, the difference between CMU-1 group and UW group appeared. Especially after 24-h cold storage, the difference became more obvious. This result was correlated with the changes of TAN and ACE.

From the above results, we concluded that CMU-1 and UW solutions have the same rat liver protective effect. In the view of liver energy metabolism, preventing intracellular acidosis and bile production, the CMU-1 solution is superior to UW solution.

REFERENCES

1 **Spiegel HU,** Schleimer K, Freise H, Diller R, Drews G, Kranz D. Organ preservation with EC, HTK, and UW, solution in orthotopic rat liver transplantation. Part II. Morphological study. *J Invest Surg* 1999; **12**: 195-203

2 **Sumimoto K,** Matsura T, Oku JI, Fukuda Y, Yamada K, Dohi K. Protective effect of UW solution on postischemic injury in rat liver: suppression of reduction in hepatic antioxidants during reperfusion. *Transplantation* 1996; **62**: 1391-1398

3 **Delriviere L,** Gibbs P, Kobayashi E, Goto S, Kamada N, Gianello P. Detailed modified technique for safer harvesting and preparation of liver graft in the rat. *Microsurgery* 1996; **17**: 690-696

4 **Froomes PR,** Sachinidis J, Ghabrial H, Tochon-Danguy H, Scott A, Ching MS, Morgan DJ, Angus PW. A novel method for determining hepatic sinusoidal oxygen permeability in the isolated perfused rat liver using [15O]O2. *Nucl Med Biol* 2003; **30**: 93-100

5 **Ohwada S,** Sunose Y, Aiba M, Tsutsumi H, Iwazaki S, Totsuka O, Matsumoto K, Takeyoshi I, Morishita Y. Advantages of Celsior solution in graft preservation from non-heart-beating donors in a canine liver transplantation model. *J Surg Res* 2002; **102**: 71-76

6 **Hauet T,** Han Z, Doucet C, Ramella-Virieux S, Hadj Aissa A, Carretier M, Papadopoulos V. A modified University of Wisconsin preservation solution with high-NA+low-K+content reduces reperfusion injury of the pig kidney graft. *Transplantation* 2003; **76**: 18-27

7 **Tian YH,** Redaelli C, Schilling MK. High- or low-potassium solutions for the storage of abdominal and thoracic organs. *Langenbecks Arch Surg* 2000; **385**: 213-217

8 **Carini R,** Bellomo G, Benedetti A, Fulceri R, Gamberucci A, Parola M, Dianzani MU, Albano E. Alteration of Na+homeostasis as a critical step in the development of irreversible hepatocyte

injury after adenosine triphosphate depletion. *Hepatology* 1995; **21**: 1089-1098

9 **Ben Abdennebi H,** Steghens JP, Margonari J, Ramella-Virieux S, Barbieux A, Boillot O. High-Na+low-K+UW cold storage solution reduces reperfusion injuries of the rat liver graft. *Transpl Int* 1998; **11**: 223-230

10 **Ar'Rajab A**, Ahren B, Sundberg R, Bengmark S. A new dextran 40-based solution for liver preservation. *Transplantation* 1992; **53**: 742-745

11 **Holecek M,** Safranek R, Rysava R, Kadlcikova J, Sprongl L. Acute effects of acidosis on protein and amino acid metabolism in perfused rat liver. *Int J Exp Pathol* 2003; **84**: 185-190

12 **Kozlova I,** Khalid Y, Roomans GM. Preservation of mouse liver tissue during cold storage in experimental solutions assessed by x-ray microanalysis. *Liver Transpl* 2003; **9**: 268-278

13 **Li XL,** Liu YF, Wang FS, Liang J, Zhao N, He SG. Effect of varapamil and Na/K channel blockers on energy metabolism of human hepatocytes during low temperature preservation. *Zhonghua Qiguan Yizhi Zazhi* 2001; **22**: 266-269

14 **Li GC,** Liu YF, Liang J, Li XL, He SG. The states of Na^+, K^+ channel of human livers cells during cold preservation at 0-4 ℃. *Chin J Organ Transplant* 2002; **23**: 101-103

15 **So PW,** Fuller BJ. Enhanced energy metabolism during cold hypoxic organ preservation: studies on rat liver after pyruvate supplementation. *Cryobiology* 2003; **46**: 295-300

16 **Holecek M,** Rysava R, Safranek R, Kadlcikova J, Sprongl L. Acute effects of decreased glutamine supply on protein and amino acid metabolism in hepatic tissue: a study using isolated perfused rat liver. *Metabolism* 2003; **52**: 1062-1067

17 **Canelo R,** Hakim NS, Ringe B. Experience with hystidine tryptophan ketoglutarate versus University Wisconsin preservation solutions in transplantation. *Int Surg* 2003; **88**: 145-151

18 **Kloppel K,** Gerlach J, Neuhaus P. The effect of buffers in liver preservation solutions on hepatocytes in a model of *in vitro* preservation and reoxygenation. *Langenbecks Arch Chir* 1994; **379**: 264-270

19 **Misra S,** Varticovski L, Arias IM. Mechanisms by which cAMP increases bile acid secretion in rat liver and canalicular membrane vesicles. *Am J Physiol Gastrointest Liver Physiol* 2003; **285**: G316-G324

20 **Kamiike W,** Nakahara M, Nakao K, Koseki M, Nishida T, Kawashima Y, Watanabe F, Tagawa K. Correlation between cellular ATP level and bile excretion in the rat liver. *Transplantation* 1985; **39**: 50-55

Science Editor Zhang JZ **Language Editor** Elsevier HK

PO Box 2345, Beijing 100023, China
www.wjgnet.com
wjg@wjgnet.com

ELSEVIER

World J Gastroenterol 2005;11(16):2526-2529
World Journal of Gastroenterology ISSN 1007-9327

• *BRIEF REPORTS* •

Systemic chemo-immunotherapy for advanced-stage hepatocellular carcinoma

Xiao-Yu Yin, Ming-De Lü, Li-Jian Liang, Jia-Ming Lai, Dong-Ming Li, Ming Kuang

Xiao-Yu Yin, Ming-De Lü, Li-Jian Liang, Jia-Ming Lai, Dong-Ming Li, Ming Kuang, Department of Hepatobiliary Surgery, The First Affiliated Hospital, Sun Yat-Sen University, Guangzhou 510080, Guangdong Province, China
Correspondence to: Dr. Xiao-Yu Yin, Department of Hepatobiliary Surgery, The First Affiliated Hospital, Sun Yat-Sen University, Guangzhou 510080, Guangdong Province, China. yinxy@21cn.com
Telephone: +86-20-87765183 Fax: +86-20-87765183
Received: 2004-05-27 Accepted: 2004-06-28

Abstract

AIM: To evaluate the therapeutic efficacy of systemic chemo-immunotherapy for advanced hepatocellular carcinoma (HCC).

METHODS: Twenty-six patients with advanced HCC were treated by using systemic chemo-immunotherapy (PIAF regimen), which consisted of cisplatin (20 mg/m^2) intravenously daily for 4 consecutive day, doxorubicin (40 mg/m^2) intravenously on day 1, 5-fluorouracil (400 mg/m^2) intravenously daily for 4 consecutive day, and human recombinant α-interferon-2a (5 Mu/m^2) subcutaneous injection daily for 4 consecutive day. The treatment was repeated every 3 wk, with a maximum of six cycles.

RESULTS: A total of 90 cycles of PIAF treatment were administered, with a mean number of 3.9 cycles per patient. Eight patients received six cycles of treatment (group A), and the remaining 18 were subjected to two to five cycles (group B). There were 0 complete response, 4 partial responses, 9 static diseases and 13 progressive diseases, with a disease control rate of 50% (13/26). The 1-year survival rate was 24.3%, with a median survival time of 6.0 mo. Group A had a remarkably better survival as compared with group B, the 1- and 2-year survival rates were 62.5% *vs* 6.1% and 32.3% *vs* 0%, and a median survival time was 12.5 mo *vs* 5.0 mo (P = 0.001).

CONCLUSION: Systemic chemo-immunotherapy using PIAF regimen represented an effective treatment and could improve the survival rate and prolong the survival time in selected patients with advanced HCC.

Key words: Chemotherapy; Immunotherapy; Advanced-stage hepatocellular carcinoma

Yin XY, Lü MD, Liang LJ, Lai JM, Li DM, Kuang M. Systemic chemo-immunotherapy for advanced-stage hepatocellular carcinoma. *World J Gastroenterol* 2005; 11(16): 2526-2529
http://www.wjgnet.com/1007-9327/11/2526.asp

INTRODUCTION

Hepatocellular carcinoma (HCC) is one of the leading causes of death from malignancies worldwide[1]. Surgical resection offers the best hope of long-term survival[2,3]. However, only 9-37% of patients are candidates for surgical intervention due to advanced stage of the disease and/or impaired hepatic functional reserve[4,6].

Unresectable HCCs have been commonly treated by transcatheter arterial chemoembolization (TACE)[7-10] or image-guided local ablative therapies, including ethanol injection, radiofrequency ablation and microwave ablation[11-13]. However, their management, especially those with portal tumor thrombi or distant metastasis, still remains a major challenge. Systemic chemotherapy has been used as an alternative modality in clinical settings, unfortunately, its therapeutic efficacy appears disappointed[14].

Alpha-interferon (α-INF) is one kind of pleiotropic cytokines secreted by dendritic cells, macrophages and other hematopoietic cells in response to viral/bacterial infection[15]. In addition to its antiviral capacity, it has an anti-proliferative effect and a direct anti-tumoral activity[16-20]. Furthermore, it can enhance anti-tumoral effects of 5-fluorouracil (5-FU)[21-23]. Recently, a combined systemic chemo-immunotherapy consisting of α-INF, 5-FU, doxorubicin and cisplatin (known as PIAF regimen) was jointly designed by Chinese University of Hong Kong and the M.D. Anderson Cancer Center of United States, and has been shown to yield some remarkable outcomes for inoperable HCC[24,25].

In the present study, we evaluated the therapeutic efficacy of systemic chemo-immunotherapy for advanced-stage HCC.

MATERIALS AND METHODS

Study subjects and clinicopathological data

A total of 26 patients with advanced-stage HCC were treated by using systemic chemo-immunotherapy (PIAF regimen) at our hospital between June 2000 and July 2003. The entry criteria included: age between 18 and 70 years, absence of cardiovascular and renal diseases, unresectability of tumors, good general status with Karnofsky performance score >80%, serum total bilirubin <51.3 μmol/L and absence of massive or intractable ascites, endogenous creatinine clearance rate >50 mL/min, white blood cell count >3×10^9/L

and platelet count >100×10^9/L. Informed consent for treatment was obtained from each patient.

There were 23 males and 3 females, with a mean age of 46±10 years (range, 27 and 66 years). Twelve of them (46%) were primarily-treated cases, and the remaining 14 patients (54%) were recurrent cases after liver resection, with a time interval from initial hepatectomy of less than 1 year in 12 and more than 1 year in 2. Twenty-four of them (92.3%) were sero-positive for HBsAg. In pretreatment liver function status, 21 patients (80.8%) had grade A and 5 (19.2%) had grade B in Child-Pugh classification. Eighteen of them (69.2%) had an elevated serum alpha-fetoprotein (AFP) level of over 500 μg/L prior to treatment, with an average level of 32 104±18 819 μg/L (range, 1 000 and 62 273 μg/L).

Twenty-three out of 26 patients had intrahepatic tumors, including nodular type in 14, massive type in 5 and diffuse type in 4, with a mean dimension of 8.1±5.3 cm (range, between 1.0 and 16.4 cm). Portal trunk/major branch tumor thrombi were presented in 12 patients, superior mesenteric venous tumor thrombi in 1 and inferior vena cava tumor thrombi in 1. Nine patients had lung metastatic lesions, two had bone metastasis and one adrenal gland metastasis. According to UICC staging system, 1 patient had stage III, 16 had stage IVa and 9 stage IVb.

Administration of systemic chemo-immunotherapy

The PIAF regimen was illustrated in Table 1. One cycle of the treatment lasted for 4 d. Prior to initiation of the treatment, a bolus of 3 mg granisetron (Kytril) was given intravenously to relieve the adverse effects of nausea and vomiting. Non-steroid anti-inflammatory analgesics were used to relieve the fever caused by administration of α-INF-2a. The treatment was repeated at an interval of 3 wk, with a maximum number of six cycles. If the patients had white blood cell count <3×10^9/L prior to any cycle of treatment, granulocyte-macrophage colony-stimulating factor was administered and treatment was temporarily delayed until white blood cell count >3×10^9/L.

Table 1 Composition of the PIAF regimen

Drugs	Dose (mg/m^2 body surface/d)	Route of administration	Days of use
Cisplatin	20	IV drip	Days 1-4
Doxorubicin	40	IV injection	Day 1
5-FU	400	IV drip	Days 1-4
α-INF[1]	5 MU/m^2 body surface/d	S.C. injection	Days 1-4

[1]Human recombinant α-INF-2a (Shanghai Roche Co.). Abbreviations: IV: intravenous; S.C.: subcutaneous; MU: million unit.

Monitoring of adverse effects

Complete blood cell count, liver function test and renal function test were carried out before and after each cycle of treatment. Any side effect that occurred during the treatment was recorded.

Assessment of therapeutic efficacy

Before treatment, ultrasound investigation, computerized tomography scanning and chest X-ray examination were done to evaluate the size and extent of tumors. These imaging studies were repeated once after each of two to three cycles. In patients with pretreatment elevated AFP level, serum AFP was titrated before and after each cycle of treatment.

The therapeutic efficacy was evaluated as follows. Complete response (CR) was defined as complete disappearance of all known tumor nodules on imaging studies and normalization of serum AFP level for at least 4 wk. Partial response (PR) was defined as no less than 50% reduction in the size of the largest tumor nodule for at least 4 wk without presence of new lesions or progression of lesions. Static disease (SD) was defined as less than 50% reduction, or no more than 25% increase, in the size of the largest tumor nodule for at least 4 wk. Progressive disease (PD) was defined as more than 25% increase in the size of the largest tumor nodule for at least 4 wk or presence of new lesions.

Statistical analysis

The results were expressed as mean±SD. Statistical analysis was performed by using commercially-available SPSS software package version 10.0. Student's t test and χ^2 test were used to compare the differences of nominal and numerical variables between groups, respectively. Survival rate was calculated by using Kaplan-Meier method and log-rank method was used to compare its difference between groups. A two-tailed $P<0.05$ was considered statistically significant.

RESULTS

A total of 90 cycles of PIAF treatment were administered in 26 patients, with a mean number of 3.9±1.6 cycles per patient. Eight patients completed six cycles of treatment (group A), and the remaining 18 received two to five cycles (group B). The reasons why the patients were treated with less than six cycles included tumor progression in nine, intolerance to the treatment in six, death from massive upper gastrointestinal tract bleeding in two and death from heart disease in one. There were no significant differences in clinicopathological features between groups A and B (Table 2).

Table 2 Comparison of clinicopathological features between groups A and B

	Group A (n = 8)	Group B (n = 18)
Gender (male:female)	7:1	16:2
Age (yr)	46±9	45±10
HBsAg (positive:negative)	7:1	17:1
Liver function (grade A:B)	7:1	14:4
AFP (>500 μg/L:<500 μg/L)	6:2	12:6
Primarily-treated: Recurrent	2:6	10:8
Tumor staging (III:IVa:IVb)	0:5:3	1:11:6

No CR was achieved in 26 patients. There were 4 PR (Figure 1), 9 SD and 13 PD. Both PR and SD indicated that the disease was brought under control, and the disease control rate was 50% (13/26).

In adverse effects, bone marrow suppression was the most common, including leukopenia in 14 patients, thrombocytopenia

in 4 and erythrocytopenia in 2. The other side effects consisted of vomiting in 11, alopecia in 11, drug fever in 4, renal insufficiency in 2 and diarrhea in 2.

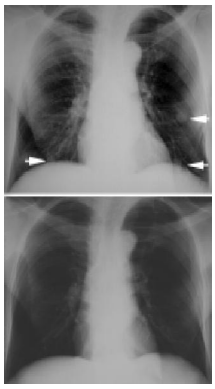

Figure 1 Bilateral lung metastases (arrowhead on the above panel) in a 47-year-old male patient with HCC, at 3.5 mo after hepatectomy and after six cycles of PIAF treatment (the below panel).

The mean follow-up time was 8.4±7.2 mo (range, 3 and 32.0 mo). Twenty-three patients were dead during follow-up. The death causes included tumor progression and/or liver function failure in 20, massive upper gastrointestinal bleeding in 2 and heart disease in 1. The remaining three were still alive. The 1-year survival rate was 24.3%, with a median survival time of 6.0 mo (Figure 2). Group A had a remarkably better survival in comparison with group B. The 1- and 2-year survival rates were 62.5% and 32.3% *vs* 6.1% and 0%, the median survival time was 12.5 mo *vs* 5.0 mo (log rank = 10.73, $P = 0.001$, Figure 3).

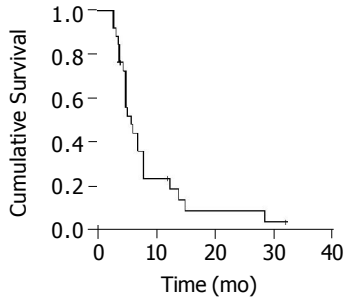

Figure 2 Survival curve after PIAF treatment.

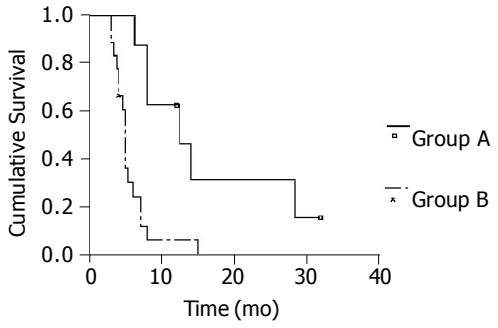

Figure 3 Comparison of post-treatment survival between groups A and B.

DISCUSSION

The management of advanced-stage HCC still remains a major challenge. Though TACE has been extensively used, there still exist some controversies about its therapeutic efficacy. Of the seven published randomized control trials comparing TACE with symptomatic treatment for advanced HCC, two showed a remarkable 2-year survival benefit of TACE, two indicated a likely trend, and the remaining three revealed no survival benefit of TACE[26]. Other image-guide percutaneous therapeutic modalities, such as ethanol injection, microwave ablation and radiofrequency ablation, were basically unsuitable for advanced diseases, especially for those with portal tumor thrombi and/or distant metastasis.

Systemic chemotherapy has been used as an alternative approach for advanced HCC, but it has been usually associated with a poor prognosis. A meta-analysis revealed that systemic monotherapy using adriamycin or 5-FU did not yield any survival benefit for patients with unresectable HCC[14].

Human recombinant α-INF is an immuno-modulatory cytokine. It has been widely used as an immunotherapeutic agent against various malignancies, including malignant melanoma[17], lymphoid malignancies[18], metastatic endocrine tumors[19], renal cell carcinoma[20,27] and leukemia[28] in clinical settings. Recently, Kaneko *et al*[16], demonstrated that α-INF could inhibit matrix metalloproteinase activity, thus yielding remarkable anti-proliferative and anti-metastatic effects on human liver cancer cells. PIAF chemo-immunotherapy represents one kind of combined regimens. It consists of three chemotherapeutic agents with different anti-tumoral mechanisms, thus helping enhance the tumoricidal efficacy and minimize the adverse effects. Moreover, the regimen takes advantages of synergistic anti-tumoral effects between α-INF and 5-FU. Recently, Leung *et al*[25], employed PIAF regimen to treat a series of 149 patients with unresectable HCC, 18.1% of them were in UICC stage I or II, 14.8% in stage III and 69.1% in stage IV. A PR rate of 14.8% and a median survival time of 7.2 mo were reported.

In the present series, the vast majority of patients had a late-stage disease, with presence of portal trunk tumor thrombi and/or extrahepatic metastasis in over 80%. According to UICC classification, over 96% of them were in stage IV. Such a late-staged disease was usually associated with a median survival time of no more than 3-4 mo. PIAF treatment brought the disease under control in 50% of patients, and yielded a 1-year survival rate of 24.3%, with a median survival time of 6.0 mo. Furthermore, the patients who completed six therapeutic cycles had a much better prognosis. The 1- and 2-year survival rates reached up to 62.5% and 32.3%, respectively, with a median survival time of 12.5 mo. In terms of therapeutic toxicity, bone marrow suppression took place at the greatest frequency, but was usually mild and transient. The treatment seemed to be well tolerant in most patients. Our results clearly indicate that PIAF treatment represents an effective treatment, and can improve the survival rate and prolong the survival time in selected patients with advanced HCC.

ACKNOWLEDGMENTS

The authors thank Dr. Z. Sheng Guo, an assistant professor

from Division of Surgical Oncology, University of Pittsburgh Cancer Institute, USA, for his critical reading of the manuscript.

REFERENCES

1 **Llovet JM,** Burroughs A, Bruix J. Hepatocellular carcinoma. *Lancet* 2003; **362**: 1907-1917
2 **Poon RT,** Fan ST, Lo CM, Ng IO, Liu CL, Lam CM, Wong J. Improving survival results after resection of hepatocellular carcinoma: a prospective study of 377 patients over 10 years. *Ann Surg* 2001; **234**: 63-70
3 **Ercolani G,** Grazi GL, Ravaioli M, Del Gaudio M, Gardini A, Cescon M, Varotti G, Cetta F, Cavallari A. Liver resection for hepatocellular carcinoma on cirrhosis: univariate and multivariate analysis of risk factors for intrahepatic recurrence. *Ann Surg* 2003; **237**: 536-543
4 **Poon RT,** Fan ST, Tsang FH, Wong J. Locoregional therapies for hepatocellular carcinoma: a critical review from the surgeon's perspective. *Ann Surg* 2002; **235**: 466-486
5 **Lau WY,** Leung TW, Yu SC, Ho SK. Percutaneous local ablative therapy for hepatocellular carcinoma: a review and look into the future. *Ann Surg* 2003; **237**: 171-179
6 **Yu AS,** Keeffe EB. Management of hepatocellular carcinoma. *Rev Gastroenterol Disord* 2003; **3**: 8-24
7 **Vogl TJ,** Trapp M, Schroeder H, Mack M, Schuster A, Schmitt J, Neuhaus P, Felix R. Transarterial chemoembolization for hepatocellular carcinoma: volumetric and morphologic CT criteria for assessment of prognosis and therapeutic success-results from a liver transplantation center. *Radiology* 2000; **214**: 349-357
8 **O'Suilleabhain CB,** Poon RT, Yong JL, Ooi GC, Tso WK, Fan ST. Factors predictive of 5-year survival after transarterial chemoembolization for inoperable hepatocellular carcinoma. *Br J Surg* 2003; **90**: 325-331
9 **Llovet JM,** Real MI, Montana X, Planas R, Coll S, Aponte J, Ayuso C, Sala M, Muchart J, Sola R, Rodes J, Bruix J. Arterial embolisation or chemoembolisation versus symptomatic treatment in patients with unresectable hepatocellular carcinoma: a randomised controlled trial. *Lancet* 2002; **359**: 1734-1739
10 **Lo CM,** Ngan H, Tso WK, Liu CL, Lam CM, Poon RT, Fan ST, Wong J. Randomized controlled trial of transarterial lipiodol chemoembolization for unresectable hepatocellular carcinoma. *Hepatology* 2002; **35**: 1164-1171
11 **Iannitti DA,** Dupuy DE, Mayo-Smith WW, Murphy B. Hepatic radiofrequency ablation. *Arch Surg* 2002; **137**: 422-426; discussion 427
12 **Lu MD,** Chen JW, Xie XY, Liu L, Huang XQ, Liang LJ, Huang JF. Hepatocellular carcinoma: US-guided percutaneous microwave coagulation therapy. *Radiology* 2001; **221**: 167-172
13 **Komorizono Y,** Oketani M, Sako K, Yamasaki N, Shibatou T, Maeda M, Kohara K, Shigenobu S, Ishibashi K, Arima T. Risk factors for local recurrence of small hepatocellular carcinoma tumors after a single session, single application of percutaneous radiofrequency ablation. *Cancer* 2003; **97**: 1253-1262
14 **Treiber G.** Systemic treatment of hepatocellular carcinoma. *Dig Dis* 2001; **19**: 311-323
15 **Hertzog PJ,** O'Neill LA, Hamilton JA. The interferon in TLR signaling: more than just antiviral. *Trends Immunol* 2003; **24**: 534-539
16 **Kaneko F,** Saito H, Saito Y, Wakabayashi K, Nakamoto N, Tada S, Suzuki H, Tsunematsu S, Kumagai N, Ishii H. Down-regulation of matrix-invasive potential of human liver cancer cells by type I interferon and a histone deacetylase inhibitor sodium butyrate. *Int J Oncol* 2004; **24**: 837-845
17 **Hancock BW,** Harris S, Wheatley K, Gore M. Adjuvant interferon-alpha in malignant melanoma: current status. *Cancer Treat Rev* 2000; **26**: 81-89
18 **Tsimberidou AM,** Giles F, Romaguera J, Duvic M, Kurzrock R. Activity of interferon-alpha and isotretinoin in patients with advanced, refractory lymphoid malignancies. *Cancer* 2004; **100**: 574-580
19 **Faiss S,** Pape UF, Bohmig M, Dorffel Y, Mansmann U, Golder W, Riecken EO, Wiedenmann B. Prospective, randomized, multicenter trial on the antiproliferative effect of lanreotide, interferon alfa, and their combination for therapy of metastatic neuroendocrine gastroenteropancreatic tumors-the International Lanreotide and Interferon Alfa Study Group. *J Clin Oncol* 2003; **21**: 2689-2696
20 **Donskov F,** Marcussen N, Hokland M, Fisker R, Madsen HH, von der Maase H. *In vivo* assessment of the antiproliferative properties of interferon-alpha during immunotherapy: Ki-67 (MIB-1) in patients with metastatic renal cell carcinoma. *Br J Cancer* 2004; **90**: 626-631
21 **Choi EA,** Lei H, Maron DJ, Mick R, Barsoum J, Yu QC, Fraker DL, Wilson JM, Spitz FR. Combined 5-fluorouracil/systemic interferon-beta gene therapy results in long-term survival in mice with established colorectal liver metastases. *Clin Cancer Res* 2004; **10**: 1535-1544
22 **Longley DB,** Harkin DP, Johnston PG. 5-fluorouracil: mechanisms of action and clinical strategies. *Nat Rev Cancer* 2003; **3**: 330-338
23 **Mitchell MS.** Combinations of anticancer drugs and immunotherapy. *Cancer Immunol Immunother* 2003; **52**: 686-692
24 **Lau WY,** Leung TW, Lai BS, Liew CT, Ho SK, Yu SC, Tang AM. Preoperative systemic chemoimmunotherapy and sequential resection for unresectable hepatocellular carcinoma. *Ann Surg* 2001; **233**: 236-241
25 **Leung TW,** Tang AM, Zee B, Yu SC, Lai PB, Lau WY, Johnson PJ. Factors predicting response and survival in 149 patients with unresectable hepatocellular carcinoma treated by combination cisplatin, interferon-alpha, doxorubicin and 5-fluorouracil chemotherapy. *Cancer* 2002; **94**: 421-427
26 **Llovet JM,** Bruix J. *Systematic* review of randomized trials for unresectable hepatocellular carcinoma: Chemoembolization improves survival. *Hepatology* 2003; **37**: 429-442
27 **Atzpodien J,** Royston P, Wandert T, Reitz M. Metastatic renal carcinoma comprehensive prognostic system. *Br J Cancer* 2003; **88**: 348-353
28 **Delannoy A,** Cazin B, Thomas X, Bouabdallah R, Boiron JM, Huguet F, Straetmans N, Zerazhi H, Vernant JP, Dombret H, Bilhou-Nabera C, Charrin C, Boucheix C, Sebban C, Lheritier V, Fiere D. Treatment of acute lymphoblastic leukemia in the elderly: an evaluation of interferon alpha given as a single agent after complete remission. *Leuk Lymphoma* 2002; **43**: 75-81

Science Editor Wang XL and Li WZ **Language Editor** Elsevier HK

PO Box 2345, Beijing 100023, China
www.wjgnet.com
wjg@wjgnet.com

ELSEVIER

World J Gastroenterol 2005;11(16):2530
World Journal of Gastroenterology ISSN 1007-9327

Acknowledgements to Reviewers of *World Journal of Gastroenterology*

Many reviewers have contributed their expertise and time to the peer review, a critical process to ensure the quality of *World Journal of Gastroenterology*. The editors and authors of the articles submitted to the journal are grateful to the following reviewers for evaluating the articles (including those were published and those were rejected in this issue) during the last editing period of time.

Ke-Ji Chen, Professor
Xiyuan Hospital, Chinese Tranditional Medicine University, Beijing 100091, China

Zong-Jie Cui, Professor
Institute of Cell Biology, Beijing Normal University, Beijing 100875, China

Da-Jun Deng, Professor
Department of Cancer Etiology, Peking University School of Oncology, 1 Da-Hong-Luo-Chang Street, Western District, Beijing 100034, China

Er-Dan Dong, Professor
Department of Life Science, Division of Basic Research in Clinic Medicine, National Natural Science Foundation of China, 83 Shuanqing Road, Haidian District, Beijng 100085, China

Xue-Gong Fan, Professor
Xiangya Hospital, Changsha 410008, China

Jin Gu, Professor
Peking University School of Oncology, Beijing Cancer Hospital, Beijing 100036, China

Shao-Heng He, Professor
Medical College of Shantou University, 22 Xinling Rd, Shantou, Guangdong, Shantou 515031, China

Zhi-Qiang Huang, Professor
Abdominal Surgery Institute of General Hospital of PLA, Fuxing Road, Beijing 100853, China

Lenard Michael Lichtenberger, Professor
Department of Integrative Biology and Pharmacology, The Univ. of Texas Medical School, Integrative Biology & Pharmacology, The Univ. of Texas Medical School, 6431 Fannin Street, Houston TX 77030, United States

Ai-Ping Lu, Professor
China Academy of Traditional Chinese Medicine, Dongzhimen Nei, 18 Beixincang, Beijing 100700, China

Robin G Lorenz, Associate Professor
Department of Pathology, University of Alabama at Birmingham, 845 19th Street South BBRB 730, Birmingham, AL 35294-2170, United States

You-Yong Lu, Professor
Beijing Molecular Oncology Laboratory, Peking University School of Oncology and Beijing Institute for Cancer Reaearch, #1, Da-Hong-Luo-Chang Street, Western District, Beijing 100034, China

Yu-Gang Song, Professor
Department of Training, The First Military Medicine University, The First Military Medicine University, Guangzhou 510515, China

Qin Su, Professor
Department of Pathology, Cancer Hospital and Cancer Institute, Chinese Academy of Medical Sciences and Peking Medical College, PO Box 2258, Beijing 100021, China

Frank Ivor Tovey, M.D.
Department of Surgery, University College London, 5 Crossborough Hill, Basingstoke RG21 4AG, United Kingdom

Zhao-You Tang, Professor
Liver Cancer Institute of Fudan University, 136 Yi Xue Yuan Road, Zhongshan Hospital, Shanghai 200032, China

Jonas Valantinas, M.D.
Professor of Gastroenterology, Vilnius University Hospital, Santariskiu 2, Vilnius LT-2600, Lithuania

Anton Vavrecka, M.D.
Clinic Of Gastroenterology, SZU, NSP SV.CAM, Antolska 11, Bratislava 85107, Slovakia

Meng-Chao Wu, M.D.
Eastern Hepatobillary Surgery Hospital, 225 Changhai Road, Shanghai 200438, China

Xian-Zhong Wu, M.D.
Tianjin Institute of Acute Abdominal Diseases, Nankai District, Tianjin 300100, China

Chun-Yang Wen, M.D.
Department of Molecular Pathology, Atomic Bomb Disease Institute, Nagasaki University Graduate School of Biomedical Sciences. 1-12-4 Sakamoto, Nagasaki 852-8523, Japan

Jia-Yu Xu, Professor
Shanghai Second Medical University, Rui Jin Hospital, 197 Rui Jin Er Road, Shanghai 200025, China

Mu-Jun Zhao, M.D.
Institute of Biochemistry and Cell Biology, Chinese Academy of Sciences, 320 Yueyang Road, Shanghai 200031, China

PO Box 2345, Beijing 100023, China
www.wjgnet.com
wjg@wjgnet.com

ELSEVIER

World J Gastroenterol 2005;11(16):Appendix 1
World Journal of Gastroenterology ISSN 1007-9327

Meetings

Major meetings coming up

Digestive Disease Week
106th Annual Meeting of AGA, The American Gastroenterology Association
May 14-19, 2005
www.ddw.org/
Chicago, Illinois

13th World Congress of Gastroenterology
September 10-14, 2005
www.wcog2005.org/
Montreal, Canada

13th United European Gastroenterology Week, UEGW
October 15-20, 2005
www.uegf.org/
Copenhagen, Denmark

American College of Gastroenterology Annual Scientific Meeting
October 28-November 2, 2005
www.acg.gi.org/
Honolulu Convention Center, Honolulu, Hawaii

Events and Meetings in the upcoming 6 months

EASL 2005 the 40th annual meeting
April 13–17, 2005
www.easl.ch/easl2005/
Paris, France

World Congress on Gastrointestinal Cancer
June 15–18, 2005
Barcelona

Digestive Disease Week *DDW 106th Annual Meeting*
May 15–18, 2005
www.ddw.org
Chicago, Illinois

Events and meetings in 2005

Canadian Digestive Disease Week Conference
February 26-March 6, 2005
www.cag-acg.org
Banff, AB

2005 World Congress of Gastroenterology
September 12–14, 2005
Montreal, Canada

International Colorectal Disease Symposium 2005
February 3–5, 2005
Hong Kong

13th UEGW meeting *United European Gastroenterology Week*
October 15–20, 2005
www.webasistent.cz/guarant/uegw2005/
Copenhagen-Malmoe

7th International Workshop on Therapeutic Endoscopy
September 10–12, 2005
www.alfamedical.com
Theodor Bilharz Research Institute

EASL 2005 the 40th annual meeting
April 13–17, 2005
www.easl.ch/easl2005/
Paris, France

Pediatric Gastroenterology, Hepatology and Nutrition
March 13, 2005
Jakarta, Indonesia

21st annual international congress *of Pakistan society of Gastroenterology & GI Endoscopy*
March 25–27, 2005
www.psgc2005.com
Peshawar

8th Congress of the Asian Society of HepatoBiliary Pancreatic Surgery
February 10–13, 2005
Mandaluyong, Philippines

APDW 2005 - Asia Pacific Digestive Week 2005
September 25–28, 2005
www.apdw2005.org
Seoul, Korea

World Congress on Gastrointestinal Cancer
June 15–18, 2005
Barcelona

British Society of Gastroenterology Conference (BSG)
March 14–17, 2005
www.bsg.org.uk
Birmingham

Digestive Disease Week *DDW 106th Annual Meeting*
May 15–18, 2005
www.ddw.org
Chicago, Illinois

70th ACG Annual Scientific Meeting and Postgraduate Course
October 28-November 2, 2005
Honolulu Convention Center, Honolulu, Hawaii

Events and Meetings in 2006

EASL 2006 - THE 41ST ANNUAL MEETING
April 26–30, 2006
Vienna, Austria

Canadian Digestive Disease Week Conference
March 4–12, 2006
www.cag-acg.org
Quebec City

XXX pan-american congress of digestive diseases *XXX congreso panamericano de anfermedades digestivas*
November 25-December 1, 2006
www.gastro.org.mx
Cancun

World Congress on Gastrointestinal Cancer
June 14–17, 2006
Barcelona, Spain

7th World Congress of the International Hepato-Pancreato-Biliary Association
September 3–7, 2006
www.edinburgh.org/conference
Edinburgh

71st ACG Annual Scientific Meeting and Postgraduate Course
October 20–25, 2006
Venetian Hotel, Las Vegas, Neveda

PO Box 2345, Beijing 100023, China
www.wjgnet.com
wjg@wjgnet.com

ELSEVIER

World J Gastroenterol 2005;11(16):Appendix 2-3
World Journal of Gastroenterology ISSN 1007-9327

Instructions to authors

GENERAL INFORMATION

World Journal of Gastroenterology (*WJG,* ISSN 1007-9327 CN 14-1219/R) is a weekly journal of more than 48 000 circulation, published on the 7th, 14th, 21st and 28th of every month.

Original Research, Clinical Trials, Reviews, Comments, and Case Reports in esophageal cancer, gastric cancer, colon cancer, liver cancer, viral liver diseases, *etc*., from all over the world are welcome on the condition that they have not been published previously and have not been submitted simultaneously elsewhere.

Published jointly by
The WJG Press and Elsevier Inc.

SUBMISSION OF MANUSCRIPTS

Manuscripts should be typed double-spaced on A4 (297×210 mm) white paper with outer margins of 2.5 cm. Number all pages consecutively, and start each of the following sections on a new page: Title Page , Abstract, Introduction, Materials and Methods, Results, Discussion, Acknowledgements, References, Tables, Figures and Figure Legends. Neither the Editors nor the Publisher is responsible for the opinions expressed by contributors. Manuscripts formally accepted for publication become the permanent property of The WJG Press and Elsevier Inc., and may not be reproduced by any means, in whole or in part without the written permission of both the Authors and the Publisher. We reserve the right to put onto our website and copy-edit accepted manuscripts. Authors should also follow the guidelines for the care and use of laboratory animals of their institution or national animal welfare committee.

Authors should retain one copy of the text, tables, photographs and illustrations, as rejected manuscripts will not be returned to the author(s) and the editors will not be responsible for the loss or damage to photographs and illustrations.

Online submission
Online submission is strongly advised. Manuscripts should be submitted through the Online Submission System at: http://www.wjgnet.com/index.jsp. Authors are highly recommended to consult the ONLINE INSTRUCTIONS TO AUTHORS (http://www.wjgnet.com/wjg/help/instructions.jsp) before attempting to submit online. Authors encountering problems with the Online Submission System may send an email describing the problem to wjg@wjgnet.com for assistance. If you submit manuscript online, do not make a postal contribution. A repeated online submission for the same manuscript is strictly prohibited.

Postal submission
Send 3 duplicate hard copies of the full-text manuscript typed double-spaced on A4(297×210 mm) white paper together with any original photographs or illustrations and a 3.5 inch computer diskette or CD-ROM containing an electronic copy of the manuscript including all the figures, graphs and tables in native Microsoft Word format or *.rtf format to:

World Journal of Gastroenterology
Apartment 1066 Yishou Garden,
58 North Langxinzhuang Road,
PO Box 2345, Beijing 100023, China
E-mail: wjg@wjgnet.com
http: //www.wjgnet.com

MANUSCRIPT PREPARATION

All contributions should be written in English. All articles must be submitted using a word-processing software. All submissions must be typed in 1.5 line spacing and in word size 12 with ample margins. The letter font is Tahoma. For authors originating from China, one copy of the Chinese translation of the manuscript is also required (excluding references). Style should conform to our house format. Required information for each of the manuscript sections is as follows:

Title page
Full manuscript title, running title, all author(s) name(s), affiliations, institution(s) and/or department(s) where the work was accomplished, disclosure of any financial support for the research, and the name, full address, telephone and fax numbers and email address of the corresponding author should be involved. Titles should be concise and informative (removing all unnecessary words), emphasize what is NEW, and avoid abbreviations. A short running title of less than 40 letters should be provided. List the author(s)' name(s) as follows: initials and/or first name, middle name or initial(s) and full family name.

Abstract
An informative, structured abstract of no more than 250 words should accompany each manuscript. Abstracts for original contributions should be structured into the following sections: AIM: Only the purpose should be included. METHODS: The materials, techniques, instruments and equipments, and the experimental procedures should be included. RESULTS: The observatory and experimental results, including data, effects, outcome, *etc*. should be included. Authors should present *P* value where necessary, and the significant data should accompany. CONCLUSION: Accurate view and the value of the results should be included.

The format of structured abstracts is at: http://www.wjgnet.com/wjg/help/11.doc

Key words
Please list 3-10 key words that could reflect content of the study.

Text
For most article types, the main text should be structured into the following sections: INTRODUCTION, MATERIALS AND METHODS, RESULTS and DISCUSSION, and should include appropriate Figures and Tables. Data should be presented in the body text or Figures and Tables, not both.

Illustrations
Figures should be numbered as 1, 2, 3 and so on, and mentioned clearly in the main text. Provide a brief title for each figure on a separate page. No detailed legend should be involved under the figures. This part should add into the text where the figures are applicable. Digital images: black and white photographs should be scanned and saved in TIFF format at a resolution of 300 dpi; color images should be saved as CMYK (print files) and not RGB (screen-viewing files). Place each photograph in a separate file. Print images: supply images of size no smaller than 126×76 mm printed on smooth surface paper; label the image by writing the Figure number and orientation using an arrow. Photomicrographs: indicate the original magnification and stain in the legend. Digital Drawings: supply files in EPS if created by Freehand and Illustrator, or TIFF from Photoshop. EPS files must be accompanied by a version in native file format for editing purposes. Scans of existing line drawings should be scanned at a resolution of 1200 dpi and as close as possible to the size at which they will appear when printed, not smaller. Please use uniform legends for the same subjects. For example: Figure 1 Pathological changes of atrophic gastritis after treatment. A: ...; B: ...;C: ...; D: ...; E: ...; F: ...; G: ...

Tables
Three-line tables should be numbered as 1, 2, 3 and so on, and mentioned clearly in the main text. Provide a brief title for each table. No detailed legend should be involved under the tables. This part should add into the text where the tables are applicable. The information should complement but not duplicate that contained in the text. Use one horizontal line under the title, a second under the column heads, and a third below the Table, above any footnotes. Vertical and italic lines should be omitted.

Notes in tables and illustrations
Data which is not statistically significant should not be noted. $^{a}P<0.05$, $^{b}P<0.01$ ($P>0.05$ should not be noted). If there are other series of *P* values, $^{c}P<0.05$ and $^{d}P<0.01$ are used; Third series of *P* values can be expressed as $^{e}P<0.05$ and $^{f}P<0.01$. Other notes in tables or under

illustrations should be expressed as ^1F, ^2F, ^3F; or some other symbols with a superscript (Arabic numerals) in the upper left corner. In a multi-curve illustration, each curve should be labeled with ●, ○, ■, □, ▲, △, *etc*. in a certain sequence.

Acknowledgments

Brief acknowledgments of persons who have made genuine contributions to the manuscripts and who endorse the data and conclusions are included. Authors are responsible for obtaining written permission to use any copyrighted text and/or illustrations.

References

Cited references should mainly be drawn from journals covered in the Science Citation Index (http://www.isinet.com) and/or Index Medicus (http://www.ncbi.nlm.nih.gov/PubMed) databases. Mention all references in the text, tables and figure legends, and set off by consecutive, superscripted Arabic numerals. References should be numbered consecutively in the order in which they appear in the text. Abbreviate journal title names according to the Index Medicus style (http://www.ncbi.nlm.nih.gov/entrez/query.fcgi?db=journals). Unpublished observations and personal communications are not listed as references. The style and punctuation of the references conform to ISO standard and the Vancouver style (5th edition); see examples below. Reference lists not conforming to this style could lead to delayed or even rejected publication status. Examples:

Standard jounal article (list all authors and include the PubMed ID [PMID] where applicable)

1 **Das KM,** Farag SA. Current medical therapy of inflammatory bowel disease. *World J Gastroenterol* 2000; 6: 483-489 [PMID: 11819634]
2 **Pan BR**, Hodgson HJF, Kalsi J. Hyperglobulinemia in chronic liver disease: Relationships between *in vitro* immunoglobulin synthesis, short lived suppressor cell activity and serum immunoglobulin levels. *Clin Exp Immunol* 1984; 55: 546-551 [PMID: 6231144]
3 **Lin GZ,** Wang XZ, Wang P, Lin J, Yang FD. Immunologic effect of Jianpi Yishen decoction in treatment of Pixu-diarrhoea. *Shijie Huaren Xiaohua Zazhi* 1999; 7: 285-287 [CMFAID:1082371101835979]

Books and other monographs (list all authors)

4 **Sherlock S,** Dooley J. Diseases of the liver and billiary system. 9th ed. Oxford: Blackwell Sci Pub, 1993: 258-296

Chapter in a book (list all authors)

5 **Lam SK.** Academic investigator's perspectives of medical treatment for peptic ulcer. In: Swabb EA, Azabo S. Ulcer disease: investigation and basis for therapy. New York: Marcel Dekker, 1991: 431-450

Electronic journal (list all authors)

6 **Morse SS.** Factors in the emergence of infectious diseases. Emerg Infect Dis serial online, 1995-01-03, cited 1996-06-05; 1(1):24 screens. Available from: URL: http//www.cdc.gov/ncidod/EID/eid.htm

PMID requirement

From the full reference list, please submit a separate list of those references embodied in PubMed, keeping the same order as in the full reference list, with the following information only: (1) abbreviated journal name and citation (e.g. *World J Gastroenterol* 2003;9(11): 2400-2403; (2) article title (e.g. Epidemiology of gastroenterologic cancer in Henan Province, China; (3) full author list (e.g. Lu JB, Sun XB, Dai DX, Zhu SK, Chang QL, Liu SZ, Duan WJ; (4) PMID (e.g. 14606064). Provide the full abstracts of these references, as quoted from PubMed on a 3.5 inch disk or CD-ROM in Microsoft Word format and send by post to The *WJG* Press. For those references taken from journals not indexed by *Index Medicus*, a printed copy of the first page of the full reference should be submitted. Attach these references to the end of the manuscript in their order of appearance in the text.

Inappropriate references

Authors should always cite references that are relevant to their article, and avoid any inappropriate references. Inappropriate references include those that are linked with a hyphen and the difference between the two numbers at two sides of the hyphen is more than 5. For example, [1-6], [2-14] and [1,3,4-10,22] are all considered as inappropriate references. Authors should not cite their own unrelated published articles.

Statistical data

Present as mean±SD and mean±SE.

Statistical expression

Express *t* test as *t*(in italics), *F* test as *F*(in italics), chi square test as χ^2 (in Greek), related coefficient as *r*(in italics), degree of freedom as γ(in Greek), sample number as *n*(in italics), and probability as *P*(in italics).

Units

Use SI units. For example: body mass, m(B) = 78 kg; blood pressure, p (B)=16.2/12.3 kPa; incubation time, t(incubation)=96 h, blood glucose concentration, c(glucose) 6.4±2.1 mmol/L; blood CEA mass concentration, p(CEA) = 8.6 24.5 μg/L; CO_2 volume fraction, 50 mL/L CO_2 not 5% CO_2; likewise for 40 g/L formaldehyde, not 10% formalin; and mass fraction, 8 ng/g, *etc*. Arabic numerals such as 23,243,641 should be read 23 243 641.

The format about how to accurately write common units and quantum is at: http://www.wjgnet.com/wjg/help/15.doc

Abbreviations

Standard abbreviations should be defined in the abstract and on first mention in the text. In general, terms should not be abbreviated unless they are used repeatedly and the abbreviation is helpful to the reader. Permissible abbreviations are listed in Units, Symbols and Abbreviations: A Guide for Biological and Medical Editors and Authors (Ed. Baron DN, 1988) published by The Royal Society of Medicine, London. Certain commonly used abbreviations, such as DNA, RNA, HIV, LD50, PCR, HBV, ECG, WBC, RBC, CT, ESR, CSF, IgG, ELISA, PBS, ATP, EDTA, mAb, can be used directly without further mention.

Italicization

Quantities: *t* time or temperature, *c* concentration, *A* area, *l* length, *m* mass, *V* volume.
Genotypes: *gyr*A, *arg* 1, *c myc*, *c fos*, *etc*.
Restriction enzymes: *Eco*RI, *Hin*dI, *Bam*HI, *Kbo* I, *Kpn* I, *etc*.
Biology: *Helicobacter pylori, H pylori, E coli, etc*.

SUBMISSION OF THE REVISED MANUSCRIPTS AFTER ACCEPTED

Please revise your article according to the revision policies of *WJG*. The revised version including manuscript and high-resolution image figures (if any) should be copied on a floppy or compact disk. Author should send the revised manuscript, along with printed high-resolution color or black and white photos, copyright transfer letter, the final check list for authors, and responses to reviewers by a courier (such as EMS) (submission of revised manuscript by e-mail or on the WJG Editorial Office Online System is NOT available at present).

Language evaluation

The language of a manuscript will be graded before sending for revision. (1) Grade A: priority publishing; (2) Grade B: minor language polishing; (3) Grade C: a great deal of language polishing; (4) Grade D: rejected. The revised articles should be in grade B or grade A.

Copyright assignment form

It is the policy of WJG to acquire copyright in all contributions. Papers accepted for publication become the copyright of WJG and authors will be asked to sign a transfer of copyright form. All authors must read and agree to the conditions outlined in the Copyright Assignment Form (which can be downloaded from http://www.wjgnet.com/wjg/help/9.doc).

Final check list for authors

The format is at: http://www.wjgnet.com/wjg/help/13.doc

Responses to reviewers

Please revise your article according to the comments/suggestions of reviewers. The format for responses to the reviewers' comments is at: http://www.wjgnet.com/wjg/help/10.doc

Proof of financial support

For paper supported by a foundation, authors should provide a copy of the document and serial number of the foundation.

Publication fee

Authors of accepted articles must pay publication fee.

PO Box 2345, Beijing 100023, China
www.wjgnet.com
wjg@wjgnet.com

ELSEVIER

World J Gastroenterol 2005;11(16):Appendix 4
World Journal of Gastroenterology ISSN 1007-9327

World Journal of Gastroenterology standard of quantities and units

Number	Nonstandard	Standard	Notice
1	4 days	4 d	In figures, tables and numerical narration
2	4 days	four days	In text narration
3	day	d	After Arabic numerals
4	Four d	Four days	At the beginning of a sentence
5	2 hours	2 h	After Arabic numerals
6	2 hs	2 h	After Arabic numerals
7	hr, hrs,	h	After Arabic numerals
8	10 seconds	10 s	After Arabic numerals
9	10 year	10 years	In text narration
10	Ten yr	Ten years	At the beginning of a sentence
11	0,1,2 years	0,1,2 yr	In figures and tables
12	0,1,2 year	0,1,2 yr	In figures and tables
13	4 weeks	4 wk	
14	Four wk	Four weeks	At the beginning of a sentence
15	2 months	2 mo	In figures and tables
16	Two mo	Two months	At the beginning of a sentence
17	10 minutes	10 min	
18	Ten min	Ten minutes	At the beginning of a sentence
19	50% (*V/V*)	500 mL/L	
20	50% (m/*V*)	500 g/L	
21	1 M	1 mol/L	
22	10 μM	10 μmol/L	
23	1N HCl	1 mol/L HCl	
24	1N H_2SO_4	0.5 mol/L H_2SO_4	
25	4rd edition	4^{th} edition	
26	15 year experience	15- year experience	
27	18.5 kDa	18.5 ku,18 500u or M_r18 500	
28	25 $g.kg^{-1}/d^{-1}$	25 g/(kg·d) or 25 g/kg per day	
29	6900	6 900	
30	1000 rpm	1 000 r/min	
31	sec	s	After Arabic numerals
32	1 pg $\cdot L^{-1}$	1 pg/L	
33	10 kilograms	10 kg	
34	13 000 rpm	13 000 *g*	High speed; *g* should be in italic and suitable conversion.
35	1000 *g*	1 000 r/min	Low speed. *g* cannot be used.
36	Gene bank	GenBank	International classified genetic materials collection bank
37	Ten L	Ten liters	At the beginning of a sentence
38	Ten mL	Ten milliliters	At the beginning of a sentence
39	umol	μmol	
40	30 sec	30 s	
41	1 g/dl	10 g/L	10-fold conversion
42	OD_{260}	A_{260}	"OD" has been abandoned.
43	One g/L	One microgram per liter	At the beginning of a sentence
44	*A*260 nm	A_{260}nm	*A* should be in italic.
	^bP<0.05	^aP<0.05	In Table, no note is needed if there is no significance in statistics: ^aP<0.05, ^bP<0.01 (no note if P>0.05). If there is a second set of P value in the same table, ^cP<0.05 and ^dP<0.01 are used for a third set: ^eP<0.05, ^fP<0.01.
45	**F*=9.87, §*F*=25.9, #*F*=67.4	^1F=9.87,^2F=25.9, ^3F=67.4	Notices in or under a table
46	KM	km	kilometer
47	CM	cm	centimeter
48	MM	mm	millimeter
49	Kg, KG	kg	kilogram
50	Gm, gr	g	gram
51	nt	N	newton
52	l	L	liter
53	db	dB	decibel
54	rpm	r/min	rotation per minute
55	bq	Bq	becquerel, a unit symbol
56	amp	A	ampere
57	coul	C	coulomb
58	HZ	Hz	
59	w	W	watt
60	KPa	kPa	kilo-pascal
61	p	Pa	pascal
62	ev	EV	volt (electronic unit)
63	Jonle	J	joule
64	J/mmol	kJ/mol	kilojoule per mole
65	10×10×10cm^3	10 cm×10 cm×10 cm	
66	N·km	KN·m	moment
67	$\bar{x}\pm s$	mean±SD	In figures, tables or text narration
68	Mean±SEM	mean±SE	In figures, tables or text narration
69	*im*	im	intramuscular injection
70	*iv*	iv	intravenous injection
71	Wang et al	Wang *et al.*	
72	EcoRI	*Eco*RI	*Eco* in italic and RI in positive. Restriction endonuclease has its prescript form of writing.
73	Ecoli	*E.coli*	Bacteria and other biologic terms have their specific expression.
74	Hp	*H pylori*	
75	Iga	*Iga*	writing form of genes
76	*igA*	IgA	writing form of proteins
77	-70 kDa	~70 ku	